NASA/TP—2016-218348

Ice Accretions and Full-Scale Iced Aerodynamic Performance Data for a Two-Dimensional NACA 23012 Airfoil

Harold E. Addy, Jr., Andy P. Broeren, and Mark G. Potapczuk
Glenn Research Center, Cleveland, Ohio

Sam Lee
Vantage Partners, Brook Park, Ohio

Didier Guffond and Emmanuel Montreuil
Office National d'Etudes et Recherches Aérospatiales, Châtillon, France

Frederic Moens
Office National d'Etudes et Recherches Aérospatiales, Meudon, France

April 2016

NASA STI Program . . . in Profile

Since its founding, NASA has been dedicated to the advancement of aeronautics and space science. The NASA Scientific and Technical Information (STI) Program plays a key part in helping NASA maintain this important role.

The NASA STI Program operates under the auspices of the Agency Chief Information Officer. It collects, organizes, provides for archiving, and disseminates NASA's STI. The NASA STI Program provides access to the NASA Technical Report Server—Registered (NTRS Reg) and NASA Technical Report Server—Public (NTRS) thus providing one of the largest collections of aeronautical and space science STI in the world. Results are published in both non-NASA channels and by NASA in the NASA STI Report Series, which includes the following report types:

- TECHNICAL PUBLICATION. Reports of completed research or a major significant phase of research that present the results of NASA programs and include extensive data or theoretical analysis. Includes compilations of significant scientific and technical data and information deemed to be of continuing reference value. NASA counter-part of peer-reviewed formal professional papers, but has less stringent limitations on manuscript length and extent of graphic presentations.

- TECHNICAL MEMORANDUM. Scientific and technical findings that are preliminary or of specialized interest, e.g., "quick-release" reports, working papers, and bibliographies that contain minimal annotation. Does not contain extensive analysis.

- CONTRACTOR REPORT. Scientific and technical findings by NASA-sponsored contractors and grantees.

- CONFERENCE PUBLICATION. Collected papers from scientific and technical conferences, symposia, seminars, or other meetings sponsored or co-sponsored by NASA.

- SPECIAL PUBLICATION. Scientific, technical, or historical information from NASA programs, projects, and missions, often concerned with subjects having substantial public interest.

- TECHNICAL TRANSLATION. English-language translations of foreign scientific and technical material pertinent to NASA's mission.

For more information about the NASA STI program, see the following:

- Access the NASA STI program home page at http://www.sti.nasa.gov

- E-mail your question to help@sti.nasa.gov

- Fax your question to the NASA STI Information Desk at 757-864-6500

- Telephone the NASA STI Information Desk at 757-864-9658

- Write to:
  NASA STI Program
  Mail Stop 148
  NASA Langley Research Center
  Hampton, VA 23681-2199

NASA/TP—2016-218348

Ice Accretions and Full-Scale Iced Aerodynamic Performance Data for a Two-Dimensional NACA 23012 Airfoil

Harold E. Addy, Jr., Andy P. Broeren, and Mark G. Potapczuk
Glenn Research Center, Cleveland, Ohio

Sam Lee
Vantage Partners, Brook Park, Ohio

Didier Guffond and Emmanuel Montreuil
Office National d'Etudes et Recherches Aérospatiales, Châtillon, France

Frederic Moens
Office National d'Etudes et Recherches Aérospatiales, Meudon, France

National Aeronautics and
Space Administration

Glenn Research Center
Cleveland, Ohio 44135

April 2016

Acknowledgments

The authors would like to acknowledge the outstanding technical support provided by Mr. David W. Sheldon, Mr. Robert F. Ide, and the staff at NASA's Icing Research Tunnel and by M. Jean-Claude Traineau, M. Philippe Desplas, M. Denis CassouDeSalle, and the staff at ONERA's F1 Pressurized, Subsonic Wind Tunnel during the wind tunnel tests described herein.

Level of Review: This material has been technically reviewed by a committee of peers.

Available from

NASA STI Program
Mail Stop 148
NASA Langley Research Center
Hampton, VA 23681-2199

National Technical Information Service
5285 Port Royal Road
Springfield, VA 22161
703-605-6000

This report is available in electronic form at http://www.sti.nasa.gov/ and http://ntrs.nasa.gov/

Contents

Ice Accretions and Full-Scale Iced Aerodynamic Performance Data for a Two-Dimensional NACA 23012 Airfoil

Harold E. Addy, Jr., Andy P. Broeren, and Mark G. Potapczuk
National Aeronautics and Space Administration
Glenn Research Center
Cleveland, Ohio 44135

Sam Lee
Vantage Partners
Brook Park, Ohio 44142

Didier Guffond and Emmanuel Montreuil
Office National d'Etudes et Recherches Aérospatiales
92322 Châtillon, France

and

Frederic Moens
Office National d'Etudes et Recherches Aérospatiales
92190 Meudon, France

Summary

This report documents the data collected during the large wind tunnel campaigns conducted as part of the SUNSET project (StUdies oN Scaling EffecTs due to ice) also known as the Ice-Accretion Aerodynamics Simulation study: a joint effort by NASA, the Office National d'Etudes et Recherches Aérospatiales (ONERA), and the University of Illinois. These data form a benchmark database of full-scale ice accretions and corresponding ice-contaminated aerodynamic performance data for a two-dimensional (2D) NACA 23012 airfoil. The wider research effort also included an analysis of ice-contaminated aerodynamics that categorized ice accretions by aerodynamic effects and an investigation of subscale, low-Reynolds-number ice-contaminated aerodynamics for the NACA 23012 airfoil. The low-Reynolds-number investigation included an analysis of the geometric fidelity needed to reliably assess aerodynamic effects of airfoil icing using artificial ice shapes.

Included herein are records of the ice accreted during campaigns in NASA Glenn Research Center's Icing Research Tunnel (IRT). Two different 2D NACA 23012 airfoil models were used during these campaigns; an 18-in. (45.7-cm) chord (subscale) model and a 72-in. (182.9-cm) chord (full-scale) model. The aircraft icing conditions used during these campaigns were selected from the Federal Aviation Administration's (FAA's) Code of Federal Regulations (CFR) Part 25 Appendix C icing envelopes. The records include the test conditions, photographs of the ice accreted, tracings of the ice, and ice depth measurements. Model coordinates and pressure tap locations are also presented.

Also included herein are the data recorded during a wind tunnel campaign conducted in the F1 Subsonic Pressurized Wind Tunnel of ONERA. The F1 tunnel is a pressured, high-Reynolds-number facility that could accommodate the full-scale (72-in. (182.9-cm) chord) 2D NACA 23012 model. Molds were made of the ice accreted during selected test runs of the full-scale model in the IRT. From these molds, castings were made that closely replicated the features of the accreted ice. The castings were then mounted on the full-scale model in the F1 tunnel, and aerodynamic performance measurements were made using model surface pressure taps, the facility force balance system, and a large wake rake designed specifically for these tests. Tests were run over a range of Reynolds and Mach numbers. For each run, the model was rotated over a range of angles-of-attack that included airfoil stall.

The benchmark data collected during these campaigns were, and continue to be, used for various purposes. The full-scale data form a unique, ice-accretion and associated aerodynamic performance dataset that can be used as a reference when addressing concerns regarding the use of subscale ice-accretion data to assess full-scale icing effects. Further, the data may be used in the development or enhancement of both ice-accretion prediction codes and computational fluid dynamic codes when applied to study the effects of icing. Finally, as was done in the wider study, the data may be used to help determine the level of geometric fidelity needed for artificial ice used to assess aerodynamic degradation due to aircraft icing. The structured, multifaceted approach used in this research effort provides a unique perspective on the aerodynamic effects of aircraft icing.

The data presented in this report are available in electronic form upon formal approval by proper NASA and ONERA

authorities. Contact the Icing Branch Chief at the NASA Glenn Research Center in Cleveland, Ohio, for further information.

Wherever practical, both U.S. customary and SI units are presented in this report. The IRT and the models were designed using U.S. customary units, so that system is shown as primary in those instances with SI as equivalents. The F1 tunnel was designed using SI units, so that system is shown as primary in those instances with the U.S. customary equivalents.

A list of symbols and acronyms used in this report is presented in Appendix A to aid the reader.

Research Objectives

This research had several objectives. They included both the establishment of benchmark databases of ice accretions and ice-accretion aerodynamic effects as well as the development of knowledge bases about the effects of ice accretions and ice-accretion features on aerodynamics. More specifically, these research objectives were to

- Establish a database of ice accretions on a large-scale, two-dimensional (2D) airfoil
- Establish a database of geometrically similar ice accretions on a small-scale, 2D airfoil
- Develop a database and knowledge base of the effects of ice accretions on the aerodynamics of a large-scale, 2D airfoil
- Provide guidance on the level of ice-accretion geometry fidelity needed for accurate simulation of the aerodynamic effects of aircraft inflight icing

The databases themselves constitute an important point of reference for the further development and validation of both computational ice-accretion codes as well as computational fluid dynamics (CFD) codes that are employed to help determine the effects of icing on aerodynamics. The knowledge base provides a reference of full-scale model ice accretions and associated higher Reynolds number effects for icing studies performed with small-scale model ice accretions at low Reynolds numbers. Moreover, the knowledge base provides a measure of the degree to which ice accretion features must be accurately simulated in an artificial ice shape to yield truly representative aerodynamic effects.

The primary purpose of this report is to present the complete datasets collected from the ice accretion tests and from the large-scale aerodynamic performance testing. Analysis of the performance data in this research is described in Reference 1.

Motivation

A variety of studies regarding the aerodynamic effects of ice accreted on smaller scale, 2D models at lower Reynolds numbers have been conducted. Questions persisted, however, about the extension of those results to larger scale models at higher Reynolds numbers for two primary reasons. First, a smaller scale model accretes ice differently than does a larger scale model when exposed to the same icing conditions, even if the two models are geometrically similar. This is primarily because the two models have different water droplet collection efficiencies. The shape, amount, and sometimes even the character of ice accretion features can be vastly different. Second, much of the aerodynamic performance data that are available for these smaller scale models with ice shape contamination have been obtained at low Reynolds numbers. The extension of those results to higher, more flight-typical Reynolds numbers has been questioned. Some higher Reynolds number, ice-contaminated, aerodynamic performance data for smaller scale models are available; however, concerns have been raised about the ice shapes not being similar to those that would accrete on a larger scale model, thereby possibly yielding results that were not representative of larger scale model, high-Reynolds-number scenarios.

Data from larger scale, higher Reynolds number aerodynamic performance tests of icing effects are limited for several reasons. First, flight testing of aircraft with ice contamination, either natural or artificial, is both expensive and hazardous. Second, existing icing tunnels are too small to conduct thorough aerodynamic performance evaluations of icing effects on larger scale models. Finally, conducting icing-effects studies in a large, aerodynamic wind tunnel involves a multistep process that is time consuming and expensive. In this last instance, ice is first accreted on a larger scale model in a large icing tunnel. Molds of these ice accretions are then made which preserve most, if not all, of the intricate features of the ice. From these molds, castings are made, producing accurate representations of the ice. The castings are subsequently mounted on the larger scale model and tested in a large aerodynamic tunnel. A great deal of labor is involved in making the molds and then the castings.

This research program was undertaken to address the lack of data and first-hand knowledge of the aerodynamic effects of ice accreted on a larger scale model at flight Reynolds numbers as well as to gain insight into how to relate smaller scale, low-Reynolds-number ice-contaminated test results to flight. Larger, full-scale models were specifically designed and constructed for ice accretion testing and for the higher Reynolds number aerodynamic performance effects testing. These cases formed the reference cases for the study. The addition of the corresponding smaller, subscale model, ice accretion and low-Reynolds-number testing allowed a unique opportunity to examine the applicability of that kind of data to higher Reynolds number results. By combining capabilities and sharing costs, the partner organizations were able to undertake the extensive research involved in this project.

The ultimate goal of this research is to establish methods to accurately evaluate the aerodynamic effects of icing on an aircraft flying in natural icing conditions using ground-based testing and computational tools. This is a longer term goal that will require the assessment and simulation of icing effects on swept wings and on wings of very large scale. This longer range goal is beyond the scope of this current research effort. This program, however, was developed with such a long-range goal in mind.

Approach

The data presented in this report are part of the aforementioned wider study that is described in a series of reports (Refs. 2 to 8). That wider study employed a seven-phase approach to the research. The phases were

1. Classification of ice accretions
2. Subscale ice accretion tests
3. Subscale aerodynamic performance tests
4. Full-scale ice accretion tests
5. Full-scale aerodynamic performance tests
6. Subscale ice-simulation validation aerodynamic performance tests
7. Establishment of a subscale ice-contaminated-airfoil aerodynamic simulation method

The data in this report are results from three of the phases and constitute the large-wind-tunnel campaigns involved in the research. Those three phases were (2) Subscale ice accretion tests, (4) Full-scale ice accretion tests, and (5) Full-scale aerodynamic tests. These data have value beyond the scope of this research program, particularly in the development and validation of both ice-accretion and CFD codes.

The three large-wind-tunnel campaigns consisted of two campaigns in the NASA Icing Research Tunnel (IRT) and one in the Office National d'Etudes et Recherches Aérospatiales (ONERA) F1 Subsonic Pressurized Wind Tunnel. The IRT campaigns will be described first followed by the F1 campaign.

Facility Descriptions

Two wind tunnels were used to produce the results presented in this report. They are described is this section.

Icing Research Tunnel (IRT)

The NASA IRT at Glenn Research Center in Cleveland, Ohio, is an atmospheric, closed-loop, refrigerated wind tunnel capable of generating an icing cloud for aircraft icing research and development (Refs. 9 and 10). Air temperature in the tunnel can be controlled from –40 to 40 °F (–40 to 4.4 °C). The tunnel is capable of airspeeds up to 350 kn (empty). The test section is 6 ft (1.8 m) high by 9 ft (2.7 m) wide by about 20 ft (6.1 m) long. An air-atomizing water spray system located in the settling chamber upstream of the test section generates the cloud. The cloud can be controlled to produce icing conditions over a range of droplet size and liquid water content (*LWC*) values. The droplets produced form a spectrum of sizes that is Gaussian in nature and is described by a median volumetric diameter (*MVD*) (Ref. 11). The IRT can produce clouds with *MVD* values ranging from 15 to 235 µm. The *LWC* (Ref. 11) of the cloud is dependent upon airspeed, but can generally range from about 0.3 to 2.5 g/m^3.

The IRT produces an icing cloud in the test section that is relatively uniform over an area that is approximately 4 ft (1.2 m) high and 5 ft (1.5 m) wide for the icing conditions used in this study (Ref. 12). The cloud is considered uniform if its variations in *LWC* fall within ±20 percent. The temperature of the air in the test section varies less than 1.8 °F (1.0 °C) from the set point and over the area of the uniform cloud (Ref. 13).

F1 Pressurized, Subsonic Wind Tunnel (F1)

The ONERA F1 facility at Le Fauga-Mauzac, France, is a pressurized, closed-loop, subsonic wind tunnel (Refs. 14 and 15). The test section is 4.5 m (14.8 ft) wide by 3.5 m (11.5 ft) high by 11 m (36.1 ft) long. It can be pressurized to 3.85 bar and produce Mach numbers up to a maximum of 0.36 and Reynolds numbers up to a maximum of 8 million based on a characteristic length of one-tenth of the square root of the cross-sectional area.

Model Descriptions

Three different test articles were used to obtain the data contained in this report. All three were 2D NACA 23012 models. Two were built to fit in NASA's IRT; one had an 18-in. (45.7 cm) chord and the other had a 72-in. (182.9-cm) chord. The third was built to fit in the ONERA's F1 tunnel. It had a 72-in. (182.9-cm) chord.

IRT Subscale Model

The model used for the subscale ice accretion tests in the NASA IRT was a single-element, 2D NACA 23012 with a chord length of 18 in. (45.7 cm). It was made of solid aluminum and spanned the 6 ft (1.8 m) from floor to ceiling of the IRT. It was designed with a removable leading edge in order to facilitate the manufacture of high-fidelity 3D replications of the ice for subsequent performance testing in a dry, aerodynamic tunnel. The removable leading edge was a 2.0-ft- (0.6-m-) long section of the leading edge centered at model midspan. Three such removable leading edges were made for the campaign. A of the model installed in the IRT is shown in Figure 1(a). A

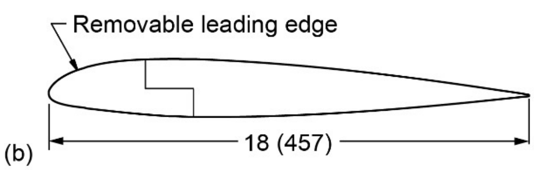

Figure 1.—IRT subscale model for ice accretion testing. (a) Photo. (b) Cross section. Dimensions are in inches (millimeters).

diagram of a cross section of the model with the removable leading edge depicted is shown in Figure 1(b). Model coordinates are given in Appendix B.

The model also had a chordwise row of pressure taps located 19-7/8 in. (50.5 cm) from the floor along the span of the model. These pressure taps were used to aerodynamically align the model in the tunnel. Pressure tap coordinates are listed in Appendix C. A thermocouple was affixed to the model at midchord near the tunnel floor to ensure it reached and maintained the proper temperature for a given test run.

IRT Full-Scale Model

The IRT full-scale model was also a 2D, single-element NACA 23012 airfoil with the same nondimensional coordinates as the subscale IRT model. It also spanned the 6.0 ft (1.8 m) from floor to ceiling of the IRT. The chord length of the full-scale model was 6.0 ft (1.8 m), four times the chord length of the subscale model. The full-scale model was also machined from solid aluminum and had a removable leading-edge section centered at midspan for use in manufacturing high-fidelity artificial ice shapes. For reasons that will be discussed in the following section, the full-scale removable leading-edge span was limited to 15 in. (38.1 cm). Three removable leading edges were also made for this model. A photograph of this model installed in the IRT test section is shown in Figure 2(a). A cross-sectional diagram depicting the removable leading edge is shown in Figure 2(b).

This model also had a chordwise row of pressure taps to facilitate aerodynamic alignment. This row of taps was located 20 in. (50.8 cm) above the tunnel floor on the model. Pressure tap coordinates for this model are given in Appendix C. A thermocouple was also affixed to the model at approximately midspan and near the tunnel floor to ensure the model reached and maintained proper temperature for the icing tests.

F1 Full-Scale Model

Like the IRT models, the F1 full-scale model was a 2D, single-element NACA 23012 airfoil with the same nondimensional coordinates as given in Appendix B. It was also machined out of solid aluminum. Like the IRT full-scale model, it had a chord length of 6.0 ft (1.8 m). It spanned the 3.5 m (11.5 ft) from floor to ceiling of the F1 tunnel. A photograph of the model installed in the F1 tunnel is shown in Figure 3(a).

The F1 model had two full-span removable leading edges. One was a clean leading edge that was used for measuring the baseline aerodynamic performance of the model. The other, the ice leading edge, was designed to allow attachment of artificial ice castings made from molds of ice accreted on the full-scale model in the IRT. A cross-sectional sketch of the model and two leading edges, along with a photo of one of the artificial ice castings, is shown in Figure 3(b). Both the clean leading edge and the ice leading edge spanned the entire length of the model, but were made in two spanwise sections to facilitate changeover while the model was installed in the test section in the tunnel. One section was 10.73 ft (3.3 m) long, and the other was 0.73 ft (0.2 m) long.

The F1 model had both chordwise and spanwise rows of pressure taps. The chordwise row was located 5.0 ft (1.5 m) above the floor of the F1 test section. The spanwise rows were

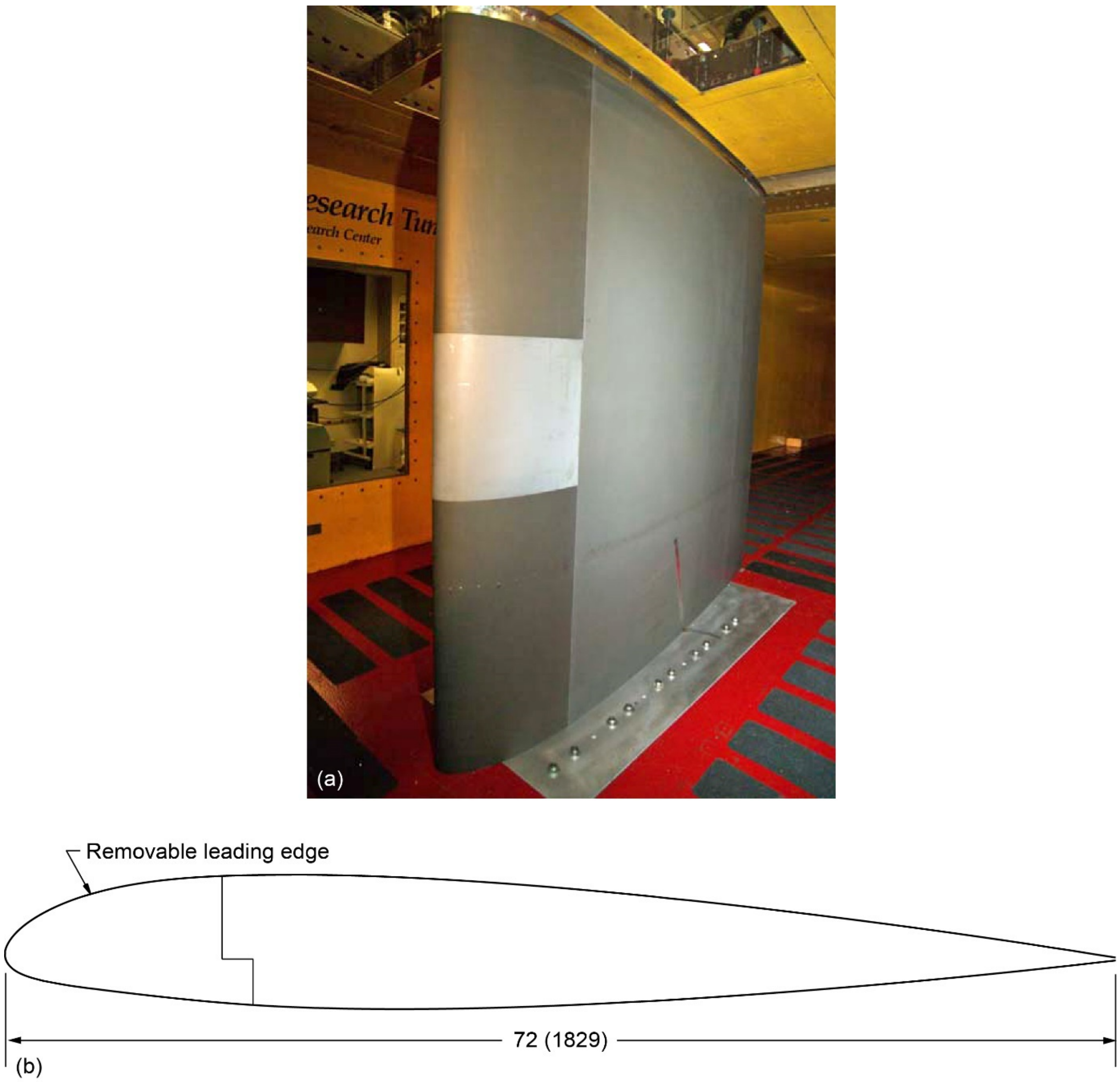

Figure 2.—IRT full-scale model for ice accretion testing. (a) Photo. (b) Cross section. Dimensions are in inches (millimeters).

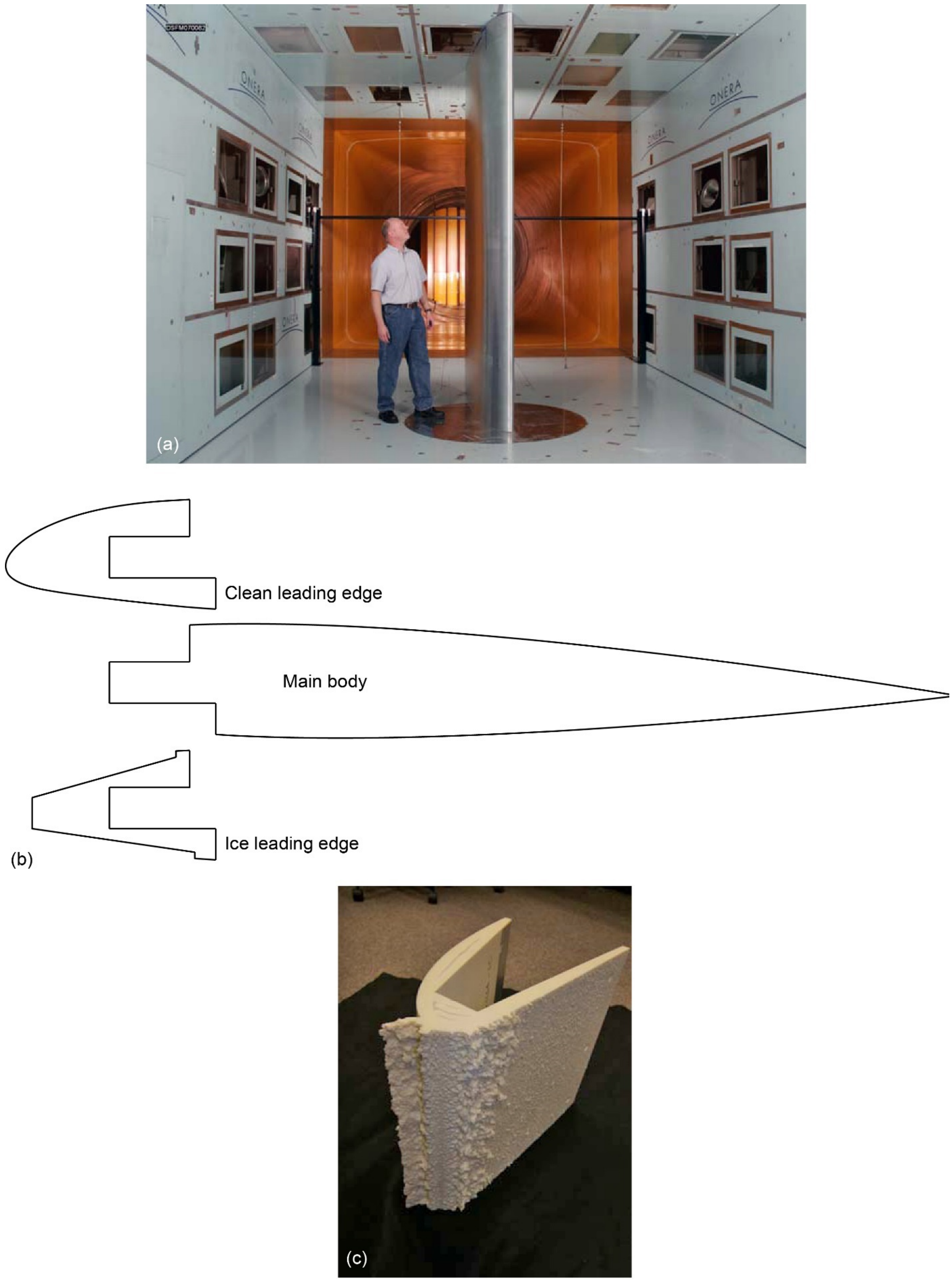

Figure 3.—F1 full-scale model for aerodynamic testing. (a) Photo. (b) Cross section. (c) Artificial ice casting.

located at 70 percent chord on the upper surface and toward each end of the model. All pressure tap locations for this model are given in Appendix C.

The artificial ice castings used in the F1 tests were made from ice accreted on the removable leading-edge section of the full-scale IRT model. The removable leading edge of the IRT full-scale model was limited to 1.25 ft (0.38 m) for two major reasons. First, the weight of a larger removable leading edge would have made it very difficult to remove from the model without damaging the accreted ice. Second, molds of ice must have some flexibility in order to remove them from the ice casting once it has been poured and has set up in the mold. The flexibility, though, means that large molds do not support their own weight well, and the resulting casting is distorted. Multiple castings were, therefore, required to cover the entire 11.46 ft (3.5 m) span of the two-dimensional F1 model. The original mold made of accreted ice is often damaged when removing it from the casting. Therefore, a second mold, called a production mold, is made from the original casting, typically called the master casting. The production mold is of a more durable material than the original mold because the master casting is more durable than the accreted ice, which would be damaged by the production molding process. The multiple castings required for the F1 model were then made from the production mold. Eleven such castings were used to cover the span of the F1 model. Chordwise pressure taps were installed in 1 of these 11 castings for each ice shape at the same spanwise location as the row of chordwise pressure taps on the main part of the model. Coordinates for the locations of the pressure taps in the castings are also given in Appendix C.

Test Descriptions

Descriptions of the test campaigns conducted in the two wind tunnels are described in this section.

IRT Tests

Two test campaigns were completed in the NASA IRT at Glenn Research Center: one with the subscale NACA 23012 model and one with the full-scale NACA 23012 model. As discussed previously, the primary objective of these tests was to obtain ice shapes for investigating aerodynamic performance effects. Several flight scenarios where a turboprop commuter aircraft might encounter icing conditions were used as a baseline for setting icing conditions in the IRT. The icing conditions were limited to those described in the Federal Aviation Administration's (FAA's) Code of Federal Regulations, 14 CFR Part 25 Appendix C, for this program. The goal of the overall study, however, was to obtain ice shapes representative of four different ice shape categories based upon types of aerodynamic effects: (1) horn ice, (2) streamwise ice, (3) spanwise ridge ice, and (4) initial roughness ice. The determination of these categories was part of the initial investigation of this program and is described in detail in Reference 2. The test matrices for both the subscale and the full-scale IRT campaigns are given in Appendix D of this report.

IRT Test Procedure

The procedure for each test point in the test matrices consisted of several steps. The tunnel was cooled and the model angle-of-attack (*AoA*) was adjusted to the desired setting. The tunnel air speed and temperature were set to their desired values, and the model was allowed to come to temperature. The tunnel's cloud was turned on, and the model was exposed to icing conditions for the predetermined length of time. Once the total exposure time was met, the cloud was turned off and the tunnel's airspeed was brought to idle. The test section was then opened, and researchers entered the tunnel to take photographs of the ice accreted on the model. The ice was then cut using a warmed metal plate. This allowed a cardboard template cut to the shape of the airfoil leading edge to be inserted into the ice so that its profile could be traced with a pencil. Typically, three tracings of the ice were made: one at the model (tunnel) centerline and one each at the locations of maximum and minimum ice accretion within the area of uniform icing cloud in the tunnel. Measurements of the thickness of the ice at each cut were also made. For the runs where a mold was made, only two cuts and tracings of the ice were made, one at each end of the removable leading edge so that the combination of ice and leading edge could be removed from the model. The omission of the centerline cut for these runs also left the ice intact for the mold. For the test runs where the desired ice accretion was an initial roughness shape, no tracings were made because the ice was too thin to trace. Tracings were digitized by hand using a digitizing tablet after the tests were completed. Photographs, digitized tracings, and ice thickness measurements are shown for each test point in Appendixes E and F for the subscale and full-scale IRT tests, respectively.

Molds were made of select ice accretions throughout each of the icing test campaigns. The ice accretions were selected to obtain ice shapes representative of each of the four categories discussed earlier. Test conditions were sometimes adjusted slightly to obtain the desired ice shapes. Mold materials were prepared before the tests each day as described in Reference 16. When a desired ice accretion was selected for the molding process, the removable leading edge, with the accreted ice, was unbolted and pulled away from the model. It was then mounted in a box, and mold material was poured in around the ice and leading edge. The assembly was then placed in a cold room where the mold material was allowed to cure for 6 to 8 hr. After curing, the mold boxes were disassembled so that the molds could be removed. The removable leading edges and mold boxes were then readied for the next tunnel run.

With the exception of the spanwise ridge ice accretion, the ice was accreted on both the subscale and full-scale airfoil models without ice protection to obtain ice representative of three of the four different ice shape categories identified in the first phase of the research. Spanwise ridge ice is a type of ice that might form on an aircraft wing in conjunction with the operation of its ice protection while flying in extreme icing conditions, such as in a cloud of either unusually high *LWC* or *MVD*. In these conditions, ice can form on a wing downstream of the ice-protected leading edge; either by warm water flowing back to a cold surface or by a high number of large droplets impinging aft of the protected area. In these cases, a forward-facing thickness of ice (a ridge) forms that is some distance aft of the leading edge of the wing and is oriented along the length (span) of it. The shape and placement of the spanwise ridge ice accretion give it unique aerodynamic characteristics. To generate a representative spanwise ridge ice accretion in the IRT, a thin, electric-foil heater was affixed to a removable leading edge of both the subscale and full-scale models to simulate the presence of a thermal ice protection system. Heater installation and operation were adjusted to obtain the desired spanwise ridge ice shape. Once the desired spanwise ridge ice accretion had been achieved, both the icing conditions and the heater operation were repeated for the mold run. Thermal analysis of heater operation during the generation of these spanwise ridge ice shapes was beyond the scope of this investigation.

F1 Tests

One aerodynamic performance test campaign was completed in the ONERA F1 facility at Le Fauga-Mauzac, France. A total of six ice shapes were selected from the full-scale ice accretion tests conducted in the IRT for the F1 Pressurized, Subsonic Wind Tunnel (F1) campaign: one horn shape, one spanwise ridge shape, two streamwise shapes, and two initial ice roughnesses. With the clean leading edge and a set of runs with boundary layer trips attached to the clean leading edge, there were a total of eight model configurations tested during the F1 campaign.

Aerodynamic performance measurements were made in the F1 tunnel using a force balance, surface pressure, and wake rake systems. The external force balance was mounted in a turntable in the floor of the F1 tunnel. The model was mounted vertically, in a cantilevered fashion, from the floor turntable. A mechanical stop-pin was used at the ceiling to prevent the model and force balance system from being overloaded.

As noted earlier, the model had two sets of surface pressure taps. One was oriented in the chordwise direction near the center of the model; at 60 in. (152.4 cm) above the tunnel floor. The other set was oriented in the spanwise direction on the upper surface of the model, at 70 percent of the chord length. Each artificial ice shape also had a chordwise row of pressure taps in line with the chordwise row on the main body of the model. All pressure tap locations on the model are given in Appendix C.

The tunnel also had surface pressure taps located on both walls and the ceiling of the test section (Ref 17). Each of the two walls had three axially oriented rows of taps: one at 7.7 cm (3.0 in.) above tunnel centerline, one 90.4 cm (35.6 in.) above centerline, and one 7.5 cm (29.5 in.) below centerline. The ceiling also had three rows of taps: one at –75.0 cm (–29.5 in.), one at –1.0 cm (–0.39 in.), and one at +73.0 cm (+28.7 in.) with respect to model chord. Each axial row had 15 pressure taps spaced 50.0 cm (19.7 in.) apart. The rows started at 350 cm (137.8 in.) upstream of the turntable center and ended the same distance downstream.

A wake rake was designed and built specifically for the F1 tests conducted as part of this program. It spanned 4.36 m (14.3 ft) of the 4.5 m (14.8 ft) width of the tunnel and was supported at each end by structural supports mounted to the floor. It was located at a height of 192.5 cm (75.8 in.) from the tunnel floor. The rake probe tips were located 1-1/2 chord lengths downstream of the trailing edge of the model. There were 102 total pressure probes spaced 2.0 cm (0.8 in.) apart and 21 static pressure probes spaced 10.0 cm (3.9 in.) apart. Both sets of probes were centered at the horizontal centerline of the tunnel. Two sets of guy-wires were used to stabilize the rake. The wires were anchored to the ceiling and floor at approximately 112.0 cm (44.3 in.) from each end of the rake. A photo of the wake rake is shown in Figure 4.

Figure 4.—F1 wake rake.

F1 Test Procedure

Each of the eight model configurations described above was run over a series of seven Mach and Reynolds number combinations. These Mach and Reynolds number combinations for each model configuration are given in Tables D.3 to D.18 in Appendix D of this report. The Lot number for each test point is also shown in the tables. For the F1 tests, the Lot number is used to designate a set of data recorded during the run. Some variation in the Reynolds and Mach numbers from the intended set point was encountered due to constraints in tunnel operation. The ranges over which the Reynolds and Mach numbers varied for each set point is noted in the test matrices found in those tables in Appendix D of this report.

At each combination of Reynolds number and Mach number, the model was rotated through a range of *AoA*s. Aerodynamic performance data were recorded over the range of *AoA*s such that performance curves could be generated. These data were obtained in two different ways: continuous sweep and fixed pitch. In the continuous-sweep method, the model was continuously rotated at a rate of 0.1° *AoA* per second from a low value (0° or lower *AoA*) through stall or until model loading reached a limit, whichever occurred first. In fact, the model load limit was only reached for one combination of Reynolds and Mach numbers for one configuration: the low-Mach-number, high-Reynolds-number setpoint for the clean configuration. For the fixed-pitch method, the model's *AoA* was set at several discrete values where data were collected over several recording scans. The scans of data for each *AoA* were then processed and averaged to give performance values at each discrete *AoA*. For the continuous-pitch runs, there is typically one Lot number for each combination of Mach and Reynolds numbers. For the fixed-pitch runs, there is one Lot number for each *AoA* at each combination of Mach and Reynolds numbers.

F1 Measurement Accuracy

The uncertainties of the aerodynamic measurements made in the F1 tunnel are listed in Table I (Ref. 17). The values given in the table are absolute uncertainties. At lower values of the aerodynamic measurements, the uncertainties, in terms of a relative value, become more significant. In a pressure tunnel such as the F1 where the range over which pressures might need to be measured is relatively large, the measurements made at lower pressures have a higher relative uncertainty. At lower Mach numbers, pressure transducers are often measuring in the lower part of their range, leading to higher relative uncertainty values. This can be seen in some of the wake rake pressure plots at low Mach number.

TABLE I.—ABSOLUTE UNCERTAINTIES OF AERODYNAMIC PERFORMANCE PARAMETERS MEASURED DURING ICING STUDIES IN ONERA F1 TUNNEL

Angle of attack (deg)	±0.02
Lift coefficient, balance	±0.010
Pitching moment coefficient, balance	±0.0007
Pressure coefficient	±0.015
Lift coefficient, surface pressures	±0.0070
Pitching moment coefficient, surface pressures	±0.0024
Drag coefficient, wake rake	±0.00048

Corrections

Wind tunnel wall corrections were applied to the lift, drag, pitching moment, and model surface pressure coefficients and to the *AoA* according to the widely accepted methods as described in Barlow, Rae, and Pope (Ref. 18) and Allen and Vincenti (Ref. 19). Another correction procedure was investigated, considering the pressure signature at the tunnel walls and the wake rake drag data. This procedure was derived from one used at the Nationaal Lucht-en Ruimtevaartlaboratorium High Speed Tunnel (NLR–HST), with some adaptations to the F1 setup. A detailed analysis of this tunnel wall correction procedure was done by Moens (Ref. 20). It was found that both procedures led to similar results over a wide part of the *AoA* range. Some slight differences were found to exist at the maximum lift coefficient in a region where the theoretical assumptions of both models are questionable. The corrected data provided in this report correspond to the former procedure, using the following equations:

$$\sigma = \frac{\pi^2}{48\left(1-\mathrm{M}^2\right)}\left(\frac{c}{h}\right)^2 \tag{1}$$

$$\tau = \frac{1}{4}\left(\frac{c}{h}\right) \tag{2}$$

$$\varepsilon_{\mathrm{sb}} = \frac{2-\mathrm{M}^2}{\left(1-\mathrm{M}^2\right)^{1/2}}\Lambda\sigma \tag{3}$$

where $\Lambda = 0.25$ (from Fig. 9.17 in Ref. 18).

$$\varepsilon_{\mathrm{wb}} = \frac{\left(2-\mathrm{M}^2\right)\left(1+0.4\mathrm{M}^2\right)}{1-\mathrm{M}^2}\tau C_{\mathrm{d,wake}} \tag{4}$$

$$\alpha_{\mathrm{cor,bal}} = \alpha + \frac{90\sigma}{\pi^2}\left(1-\mathrm{M}^2\right)^{1/2}\left(C_{\mathrm{l,bal}} + 4C_{\mathrm{m,bal}}\right) \tag{5}$$

$$\alpha_{\text{cor,psi}} = \alpha + \frac{90\sigma}{\pi^2}\left(1-\text{M}^2\right)^{1/2}\left(C_{\text{l,psi}} + 4C_{\text{m,psi}}\right) \tag{6}$$

$$C_{\text{l,bal,cor}} = C_{\text{l,bal}}\left(1-\sigma-\varepsilon_{\text{sb}}-\varepsilon_{\text{wb}}\right) \tag{7}$$

$$C_{\text{l,psi,cor}} = C_{\text{l,psi}}\left(1-\sigma-\varepsilon_{\text{sb}}-\varepsilon_{\text{wb}}\right) \tag{8}$$

$$C_{\text{d,wake,cor}} = C_{\text{d,wake}}\left(1-\frac{3-0.6\text{M}^2}{2-\text{M}^2}\varepsilon_{\text{sb}}-\varepsilon_{\text{wb}}\right) \tag{9}$$

$$C_{\text{m,bal,cor}} = C_{\text{m,bal}}\left(1-\varepsilon_{\text{sb}}-\varepsilon_{\text{wb}}\right) + \frac{C_{\text{l,bal}}}{4} \tag{10}$$

$$C_{\text{m,psi,cor}} = C_{\text{m,psi}}\left(1-\varepsilon_{\text{sb}}-\varepsilon_{\text{wb}}\right) + \frac{C_{\text{l,psi}}}{4} \tag{11}$$

$$C_{\text{p,cor}} = \frac{C_{\text{p}}}{\left(1+\varepsilon_{\text{sb}}+\varepsilon_{\text{wb}}\right)^2} \tag{12}$$

where

σ	model chord-to-test-section height parameter, with compressibility correction
M	Mach number
c	chord length
h	test-section height
τ	model chord-to-test-section height parameter
ε_{sb}	solid blockage correction factor
Λ	airfoil geometry parameter
ε_{wb}	wake blockage correction factor
$C_{\text{d,wake}}$	measured drag coefficient from wake-survey data
$\alpha_{\text{cor,bal}}$	corrected angle of attack, using force-balance data for corrections
α	measured angle of attack
$C_{\text{l,bal}}$	measured lift coefficient from force-balance data
$C_{\text{m,bal}}$	measured quarter-chord pitching moment coefficient from force-balance data
$\alpha_{\text{cor,psi}}$	corrected angle of attack, using force surface-pressure data for corrections
$C_{\text{l,psi}}$	measured lift coefficient from surface-pressure data
$C_{\text{m,psi}}$	measured quarter-chord pitching moment coefficient from surface-pressure data
$C_{\text{l,bal,cor}}$	corrected lift coefficient from force-balance data
$C_{\text{l,psi,cor}}$	corrected lift coefficient from surface-pressure data
$C_{\text{d,wake,cor}}$	corrected drag coefficient from wake-survey data
$C_{\text{m,bal,cor}}$	corrected quarter-chord pitching moment coefficient from force-balance data
$C_{\text{m,psi,cor}}$	corrected quarter-chord pitching moment coefficient from surface-pressure data
$C_{\text{p,cor}}$	corrected surface-pressure coefficient
C_{p}	measured surface-pressure coefficient

F1 Test Results

Results from the full-scale tests at the F1 tunnel are shown in Appendix G. The data are grouped by model configuration. For each configuration, complete sets of data are shown for each combination of Mach and Reynolds numbers. Lift, drag, and pitching moment coefficients as a function of *AoA* are shown first. Data from both the continuous-sweep and the fixed-pitch methods are shown. For the continuous-sweep method, the data are shown in one-half-degree *AoA* increments. Each of these data points is an average of five consecutive scans: the scan at the *AoA* shown, the two prior, and the two after. The lift and pitching moment performance data shown for the clean model and the model with trip strips have been calculated from the model surface pressure measurements. For all of the model configurations with artificial ice shapes, the lift and pitching moment performance data shown are from the force balance measurements. In general, the performance data agree well between the force balance and model surface pressure measurements. Ice-contaminated models, however, tend to experience a higher level of unsteady flow. Because the force balance measurements could be better filtered for the unsteady effects than the pressure tap measurements, the data from the force balance measurements are shown for the model configurations with artificial ice shapes. For reference purposes, data from the clean model continuous pitch test runs are co-plotted along with the performance for each of the other model configurations. All drag coefficient data shown are calculated from the wake rake pressure measurement.

The model surface pressure coefficients, wall surface pressure coefficients, ceiling surface pressure coefficients, and wake rake pressure data presented are from the fixed-pitch data collection method only. These data are shown for each *AoA* at which the fixed-pitch data were recorded. Side wall surface pressure data are designated either “pressure” or “suction,” corresponding to the side of the model that wall was facing. For these wall pressure coefficient data, the three wall taps furthest downstream of the lower two rows of taps were affected by the presence of the wake rake vertical supports. These data were, therefore, not shown in the plots. Similarly for the ceiling pressure coefficient data, several of the taps in the row closest to the model chord were covered by the model itself. These data were also not shown in the plots. No corrections have been applied to either the wall or ceiling surface pressure data.

Concluding Remarks

The data presented in this report are from an extensive research and testing program to investigate the aerodynamic performance effects of ice accretions on a full-scale model and to establish methods to faithfully simulate those results on a subscale model at lower Mach and Reynolds numbers. The database herein forms a benchmark for computational fluid dynamic simulation and ice accretion code development and validation. The knowledge base formed and described in interim reports of the research provides extensive insight in to the aerodynamic effects of icing, the degree to which ice features need to be faithfully simulated for accurate aerodynamic simulation, Mach and Reynolds number effects in ice-contaminated aerodynamics, and the applicability and limitations of subscale ice-contaminated aerodynamics testing. It also provides a means to evaluate the degree of geometric similarity needed in the ice simulation to obtain representative results to an acceptable level of uncertainty.

Glenn Research Center
National Aeronautics and Space Administration
Cleveland, Ohio, April 28, 2016

Appendix A.—Nomenclature

2D	two dimensional
3D	three dimensional
AoA	angle of attack
b	model span length
c	model chord length
C_{d}	drag coefficient
$C_{\mathrm{d,wake}}$	measured drag coefficient from wake-survey data
$C_{\mathrm{d,wake,cor}}$	corrected drag coefficient from wake-survey data
C_{l}	lift coefficient
$C_{\mathrm{l,bal}}$	measured lift coefficient from force-balance data
$C_{\mathrm{l,bal,cor}}$	corrected lift coefficient from force-balance data
$C_{\mathrm{l,psi}}$	measured lift coefficient from surface-pressure data
$C_{\mathrm{l,psi,cor}}$	corrected lift coefficient from surface-pressure data
C_{m}	moment coefficient
$C_{\mathrm{m,bal}}$	measured quarter-chord pitching moment coefficient from force-balance data
$C_{\mathrm{m,bal,cor}}$	corrected quarter-chord pitching moment coefficient from force-balance data
$C_{\mathrm{m,psi}}$	measured quarter-chord pitching moment coefficient from surface-pressure data
$C_{\mathrm{m,psi,cor}}$	corrected quarter-chord pitching moment coefficient from surface-pressure data
C_{p}	measured surface-pressure coefficient
$C_{\mathrm{p,cor}}$	corrected surface-pressure coefficient
CFD	computational fluid dynamics
CFR	Code of Federal Regulations
F1	ONERA Subsonic Pressurized Wind Tunnel
h	test-section height
FAA	Federal Aviation Administration
IRT	NASA Icing Research Tunnel
LWC	liquid water content
M	Mach number
MVD	median volumetric diameter
NLR–HST	Nationaal Lucht-en Ruimtevaartlaboratorium High Speed Tunnel
ONERA	Office National d’Etudes et Recherches Aérospatiales
Re	Reynolds number
T_{s}	static temperature
T_{t}	total temperature
V	air speed
α	measured angle of attack
$\alpha_{\mathrm{cor,bal}}$	corrected angle of attack, using force-balance data for corrections
$\alpha_{\mathrm{cor,psi}}$	corrected angle of attack, using force surface-pressure data for corrections
$\varepsilon_{\mathrm{sb}}$	solid blockage correction factor
$\varepsilon_{\mathrm{wb}}$	wake blockage correction factor
Λ	airfoil geometry parameter
σ	model chord-to-test-section height parameter, with compressibility correction
τ	model chord-to-test-section height parameter

Appendix B.—NACA 23012 Model Coordinates

TABLE B.1.—NACA 23012 AIRFOIL COORDINATES

x/c	*y/c*	*x/c*	*y/c*	*x/c*	*y/c*	*x/c*	*y/c*
1.00000	0.00126	0.29422	0.07561	0.00219	–0.00444	0.31988	–0.04491
0.98045	0.00441	0.28047	0.07582	0.00383	–0.00646	0.33443	–0.04506
0.96089	0.00750	0.26700	0.07594	0.00582	–0.00833	0.34924	–0.04512
0.94133	0.01053	0.25381	0.07597	0.00815	–0.01009	0.36430	–0.04510
0.92180	0.01349	0.24090	0.07590	0.01083	–0.01172	0.37961	–0.04500
0.90230	0.01639	0.22828	0.07573	0.01383	–0.01324	0.39516	–0.04482
0.88283	0.01923	0.21597	0.07547	0.01715	–0.01465	0.41094	–0.04456
0.86341	0.02201	0.20395	0.07512	0.02079	–0.01597	0.42696	–0.04422
0.84403	0.02473	0.19218	0.07467	0.02475	–0.01721	0.44319	–0.04381
0.82472	0.02739	0.18060	0.07411	0.02900	–0.01837	0.45964	–0.04332
0.80548	0.02999	0.16924	0.07342	0.03356	–0.01946	0.47630	–0.04275
0.78631	0.03253	0.15812	0.07257	0.03841	–0.02050	0.49317	–0.04211
0.76721	0.03501	0.14724	0.07156	0.04355	–0.02149	0.51023	–0.04141
0.74821	0.03743	0.13665	0.07038	0.04899	–0.02245	0.52748	–0.04063
0.72931	0.03979	0.12634	0.06901	0.05471	–0.02338	0.54491	–0.03978
0.71050	0.04209	0.11635	0.06746	0.06073	–0.02428	0.56252	–0.03886
0.69181	0.04433	0.10669	0.06573	0.06704	–0.02518	0.58030	–0.03788
0.67324	0.04650	0.09738	0.06381	0.07364	–0.02608	0.59824	–0.03683
0.65479	0.04861	0.08843	0.06172	0.08055	–0.02698	0.61634	–0.03572
0.63647	0.05065	0.07987	0.05946	0.08776	–0.02789	0.63459	–0.03455
0.61829	0.05263	0.07169	0.05705	0.09528	–0.02881	0.65298	–0.03332
0.60026	0.05453	0.06393	0.05449	0.10312	–0.02976	0.67150	–0.03203
0.58238	0.05637	0.05658	0.05181	0.11129	–0.03072	0.69016	–0.03068
0.56466	0.05814	0.04966	0.04901	0.11980	–0.03171	0.70893	–0.02927
0.54711	0.05983	0.04317	0.04612	0.12866	–0.03272	0.72781	–0.02780
0.52973	0.06145	0.03713	0.04316	0.13788	–0.03375	0.74681	–0.02628
0.51253	0.06299	0.03154	0.04013	0.14748	–0.03479	0.76589	–0.02470
0.49552	0.06445	0.02639	0.03706	0.15745	–0.03585	0.78508	–0.02306
0.47870	0.06583	0.02170	0.03397	0.16782	–0.03690	0.80434	–0.02137
0.46208	0.06713	0.01747	0.03087	0.17860	–0.03794	0.82368	–0.01962
0.44567	0.06834	0.01368	0.02778	0.18979	–0.03895	0.84310	–0.01782
0.42947	0.06948	0.01035	0.02471	0.20141	–0.03991	0.86257	–0.01596
0.41348	0.07052	0.00747	0.02169	0.21340	–0.04079	0.88209	–0.01404
0.39773	0.07148	0.00503	0.01871	0.22569	–0.04159	0.90167	–0.01206
0.38220	0.07234	0.00304	0.01579	0.23829	–0.04231	0.92128	–0.01003
0.36691	0.07312	0.00148	0.01295	0.25118	–0.04295	0.94093	–0.00793
0.35187	0.07380	0.00035	0.01019	0.26436	–0.04351	0.96059	–0.00577
0.33707	0.07439	–0.00036	0.00751	0.27782	–0.04398	0.98028	–0.00355
0.32252	0.07489	–0.00052	0.00241	0.29157	–0.04438	1.00000	–0.00126
0.30824	0.07530	0.00091	–0.00229	0.30559	–0.04468		

Appendix C.—Model Pressure Tap Locations

IRT Models

TABLE C.1.—PRESSURE TAP LOCATIONS FOR IRT SUBSCALE 18-in. (45.7-cm) CHORD, NACA 23012 MODEL

Tap no.	*x*/*c*	*y*/*c*	*x*, in.	*y*, in.	*x*, mm	*y*, mm
1	0.90000	–0.01223	16.2000	–0.220	411.48	–5.59
2	0.80000	–0.02175	14.4000	–0.392	365.76	–9.95
3	0.70000	–0.02994	12.6000	–0.539	320.04	–13.69
4	0.60000	–0.03673	10.8000	–0.661	274.32	–16.79
5	0.50000	–0.04183	9.0000	–0.753	228.60	–19.12
6	0.40000	–0.04474	7.2000	–0.805	182.88	–20.45
7	0.30000	–0.04456	5.4000	–0.802	137.16	–20.37
8	0.25000	–0.04290	4.5000	–0.772	114.30	–19.61
9	0.20000	–0.03979	3.6000	–0.716	91.44	–18.19
10	0.15000	–0.03507	2.7000	–0.631	68.58	–16.03
11	0.12500	–0.03231	2.2500	–0.582	57.15	–14.77
12	0.10000	–0.02938	1.8000	–0.529	45.72	–13.43
13	0.07500	–0.02626	1.3500	–0.473	34.29	–12.00
14	0.05000	–0.02261	0.9000	–0.407	22.86	–10.34
15	0.04000	–0.02081	0.7200	–0.375	18.29	–9.51
16	0.03000	–0.01861	0.5400	–0.335	13.72	–8.51
17	0.02000	–0.01569	0.3600	–0.282	9.14	–7.17
18	0.01000	–0.01121	0.1800	–0.202	4.57	–5.13
19	0.00500	–0.00756	0.0900	–0.136	2.29	–3.46
20	0.00000	0.00000	0.0000	0.000	0.00	0.00
21	0.00250	0.01866	0.0450	0.336	1.14	8.53
22	0.01000	0.02434	0.1800	0.438	4.57	11.13
23	0.01500	0.02885	0.2700	0.519	6.86	13.19
24	0.02000	0.03272	0.3600	0.589	9.14	14.96
25	0.02500	0.03614	0.4500	0.651	11.43	16.52
26	0.03000	0.03921	0.5400	0.706	13.72	17.93
27	0.04000	0.04456	0.7200	0.802	18.29	20.37
28	0.05000	0.04915	0.9000	0.885	22.86	22.47
29	0.07500	0.05802	1.3500	1.044	34.29	26.53
30	0.10000	0.06435	1.8000	1.158	45.72	29.42
31	0.12500	0.06880	2.2500	1.238	57.15	31.46
32	0.15000	0.07182	2.7000	1.293	68.58	32.84
33	0.20000	0.07497	3.6000	1.349	91.44	34.28
34	0.25000	0.07595	4.5000	1.367	114.30	34.72
35	0.30000	0.07552	5.4000	1.359	137.16	34.53
36	0.35000	0.07388	6.3000	1.330	160.02	33.78
37	0.40000	0.07134	7.2000	1.284	182.88	32.62
38	0.45000	0.06802	8.1000	1.224	205.74	31.10
39	0.50000	0.06406	9.0000	1.153	228.60	29.29
40	0.55000	0.05955	9.9000	1.072	251.46	27.23
41	0.60000	0.05456	10.8000	0.982	274.32	24.95
42	0.65000	0.04914	11.7000	0.885	297.18	22.47
43	0.70000	0.04335	12.6000	0.780	320.04	19.82
44	0.75000	0.03720	13.5000	0.670	342.90	17.01
45	0.80000	0.03071	14.4000	0.553	365.76	14.04
46	0.85000	0.02389	15.3000	0.430	388.62	10.92
47	0.90000	0.01673	16.2000	0.301	411.48	7.65
48	0.95000	0.00919	17.1000	0.165	434.34	4.20

TABLE C.2.—PRESSURE TAP LOCATIONS FOR IRT FULL-SCALE 72-in. (182.9-cm) CHORD, NACA 23012 MODEL

Tap no.	x/c	y/c	x, in.	y, in.	x, mm	y, mm
1	1.0000	0.0000	72.000	0.000	1828.80	0.00
2	0.9750	0.0053	70.200	0.378	1783.08	9.60
3	0.9500	0.0092	68.400	0.662	1737.36	16.81
4	0.9250	0.0130	66.600	0.936	1691.64	23.77
5	0.9000	0.0167	64.800	1.204	1645.92	30.58
6	0.8500	0.0239	61.200	1.720	1554.48	43.69
7	0.8000	0.0307	57.600	2.212	1463.04	56.18
8	0.7500	0.0372	54.000	2.679	1371.60	68.05
9	0.7000	0.0433	50.400	3.121	1280.16	79.27
10	0.6500	0.0492	46.800	3.539	1188.72	89.89
11	0.6000	0.0546	43.200	3.928	1097.28	99.77
12	0.5500	0.0596	39.600	4.288	1005.84	108.92
13	0.5000	0.0641	36.000	4.613	914.40	117.17
14	0.4500	0.0680	32.400	4.898	822.96	124.41
15	0.4000	0.0713	28.800	5.137	731.52	130.48
16	0.3600	0.0734	25.920	5.288	658.37	134.32
17	0.3200	0.0750	23.040	5.398	585.22	137.11
18	0.2800	0.0758	20.160	5.460	512.06	138.68
19	0.2400	0.0759	17.280	5.464	438.91	138.79
20	0.2100	0.0753	15.120	5.422	384.05	137.72
21	0.1800	0.0741	12.960	5.334	329.18	135.48
22	0.1500	0.0718	10.800	5.172	274.32	131.37
23	0.1200	0.0681	8.640	4.900	219.46	124.46
24	0.0900	0.0621	6.480	4.471	164.59	113.56
25	0.0653	0.0549	4.698	3.950	119.33	100.33
26	0.0400	0.0446	2.880	3.210	73.15	81.53
27	0.0200	0.0328	1.440	2.359	36.58	59.92
28	0.0100	0.0244	0.720	1.754	18.29	44.55
29	0.0041	0.0173	0.293	1.246	7.44	31.65
30	0.0001	0.0091	0.004	0.654	0.10	16.61
31	0.0000	0.0000	0.000	0.000	0.00	0.00
32	0.0040	–0.0066	0.288	–0.478	7.32	–12.14
33	0.0100	–0.0113	0.720	–0.810	18.29	–20.57
34	0.0200	–0.0157	1.440	–1.130	36.58	–28.70
35	0.0350	–0.0198	2.520	–1.424	64.01	–36.17
36	0.0550	–0.0234	3.960	–1.686	100.58	–42.82
37	0.0750	–0.0263	5.400	–1.890	137.16	–48.01
38	0.1000	–0.0294	7.200	–2.116	182.88	–53.75
39	0.1500	–0.0351	10.800	–2.525	274.32	–64.14
40	0.2000	–0.0398	14.400	–2.865	365.76	–72.77
41	0.2500	–0.0429	18.000	–3.089	457.20	–78.46
42	0.3000	–0.0446	21.600	–3.209	548.64	–81.51
43	0.3500	–0.0451	25.200	–3.249	640.08	–82.52
44	0.4000	–0.0448	28.800	–3.222	731.52	–81.84
45	0.4500	–0.0436	32.400	–3.140	822.96	–79.76
46	0.5500	–0.0395	39.600	–2.845	1005.84	–72.26
47	0.6500	–0.0335	46.800	–2.414	1188.72	–61.32
48	0.7500	–0.0260	54.000	–1.873	1371.60	–47.57
49	0.8500	–0.0172	61.200	–1.236	1554.48	–31.39
50	0.9500	–0.0069	68.400	–0.500	1737.36	–12.70

F1 Model

TABLE C.3.—PRESSURE TAP LOCATIONS FOR F1 NACA 23012 MODEL: CLEAN MODEL

Surface	Tap no.	*x*/*c*	*y*/*c*	*z*/*b*	*x*, in.	*y*, in.	*z*, in.	*x*, mm	*y*, mm	*z*, mm
(a) Chordwise row										
Lower	1	1.000000	–0.000358	0.436839	72.000	–0.026	60.057	1828.20	–0.65	1525.44
	2	0.949453	–0.006999	0.436158	68.361	–0.504	59.963	1735.79	–12.80	1523.06
	3	0.900032	–0.012228	0.436599	64.802	–0.880	60.024	1645.44	–22.36	1524.60
	4	0.849651	–0.017198	0.436640	61.175	–1.238	60.029	1553.33	–31.44	1524.74
	5	0.799649	–0.021788	0.437475	57.575	–1.569	60.144	1461.92	–39.83	1527.66
	6	0.749978	–0.026018	0.436610	53.998	–1.873	60.025	1371.11	–47.57	1524.64
	7	0.700663	–0.029894	0.436470	50.448	–2.152	60.006	1280.95	–54.65	1524.15
	8	0.649840	–0.033534	0.436575	46.788	–2.414	60.020	1188.04	–61.31	1524.52
	9	0.599772	–0.036742	0.436756	43.184	–2.645	60.045	1096.50	–67.17	1525.15
	10	0.549335	–0.039553	0.436423	39.552	–2.848	59.999	1004.29	–72.31	1523.99
	11	0.499718	–0.041849	0.436453	35.980	–3.013	60.003	913.59	–76.51	1524.09
	12	0.450108	–0.043609	0.436528	32.408	–3.140	60.014	822.89	–79.73	1524.35
	13	0.399989	–0.044746	0.436546	28.799	–3.222	60.016	731.26	–81.80	1524.41
	14	0.349252	–0.045117	0.436541	25.146	–3.248	60.016	638.50	–82.48	1524.40
	15	0.299216	–0.044556	0.436178	21.544	–3.208	59.966	547.03	–81.46	1523.13
	16	0.249900	–0.042893	0.436492	17.993	–3.088	60.009	456.87	–78.42	1524.23
Removable leading edge	17	0.200162	–0.039807	0.436497	14.412	–2.866	60.010	365.94	–72.78	1524.24
	18	0.150094	–0.035076	0.436378	10.807	–2.525	59.993	274.40	–64.13	1523.83
	19	0.100215	–0.029408	0.436269	7.216	–2.117	59.978	183.21	–53.76	1523.45
	20	0.075167	–0.026279	0.435994	5.412	–1.892	59.941	137.42	–48.04	1522.49
	21	0.050393	–0.022682	0.435994	3.628	–1.633	59.940	92.13	–41.47	1522.49
	22	0.029649	–0.018532	0.436510	2.135	–1.334	60.011	54.20	–33.88	1524.29
	23	0.018844	–0.015291	0.436153	1.357	–1.101	59.962	34.45	–27.95	1523.04
	24	0.008148	–0.010084	0.435472	0.587	–0.726	59.869	14.90	–18.44	1520.66
	25	0.002618	–0.005033	0.435365	0.189	–0.362	59.854	4.79	–9.20	1520.29
	26	0.000071	–0.000228	0.436229	0.005	–0.016	59.973	0.13	–0.42	1523.31
	27	–0.000633	0.005197	0.436395	–0.046	0.374	59.996	–1.16	9.50	1523.89
	28	0.000538	0.010725	0.436345	0.039	0.772	59.989	0.98	19.61	1523.71
	29	0.003108	0.015908	0.436345	0.224	1.145	59.989	5.68	29.08	1523.71
	30	0.006009	0.019961	0.436406	0.433	1.437	59.997	10.99	36.49	1523.93
	31	0.010252	0.024614	0.436346	0.738	1.772	59.989	18.74	45.00	1523.72
	32	0.014368	0.028366	0.436267	1.035	2.042	59.978	26.27	51.86	1523.44
	33	0.019984	0.032748	0.436280	1.439	2.358	59.980	36.53	59.87	1523.49
	34	0.029792	0.039121	0.436332	2.145	2.817	59.987	54.47	71.52	1523.67
	35	0.040508	0.044848	0.436448	2.917	3.229	60.003	74.06	81.99	1524.07
	36	0.050523	0.049377	0.436485	3.638	3.555	60.008	92.37	90.27	1524.20
	37	0.060780	0.053375	0.436512	4.376	3.843	60.012	111.12	97.58	1524.29
	38	0.080207	0.059555	0.436320	5.775	4.288	59.985	146.63	108.88	1523.63
	39	0.100078	0.064390	0.436442	7.206	4.636	60.002	182.96	117.72	1524.05
	40	0.120291	0.068100	0.436395	8.661	4.903	59.996	219.92	124.50	1523.89
	41	0.139699	0.070740	0.436308	10.058	5.093	59.984	255.40	129.33	1523.58
	42	0.161164	0.072822	0.436310	11.604	5.243	59.984	294.64	133.13	1523.59
	43	0.181168	0.074143	0.437415	13.044	5.338	60.136	331.21	135.55	1527.45

TABLE C.3.—Concluded. PRESSURE TAP LOCATIONS FOR F1 NACA 23012 MODEL: CLEAN MODEL

Surface	Tap no.	x/c	y/c	z/b	x, in.	y, in.	z, in.	x, mm	y, mm	z, mm
Upper	44	0.200463	0.075000	0.436542	14.433	5.400	60.016	366.49	137.11	1524.40
	45	0.220415	0.075578	0.436637	15.870	5.442	60.029	402.96	138.17	1524.73
	46	0.241198	0.075899	0.436793	17.366	5.465	60.050	440.96	138.76	1525.28
	47	0.260589	0.075966	0.436765	18.762	5.470	60.046	476.41	138.88	1525.18
	48	0.280101	0.075827	0.436558	20.167	5.460	60.018	512.08	138.63	1524.46
	49	0.299747	0.075495	0.436580	21.582	5.436	60.021	548.00	138.02	1524.53
	50	0.320199	0.074964	0.436556	23.054	5.397	60.018	585.39	137.05	1524.45
	51	0.340077	0.074282	0.436471	24.486	5.348	60.006	621.73	135.80	1524.15
	52	0.360039	0.073441	0.436429	25.923	5.288	60.000	658.22	134.27	1524.01
	53	0.379808	0.072468	0.436376	27.346	5.218	59.993	694.37	132.49	1523.82
	54	0.400032	0.071340	0.436447	28.802	5.136	60.003	731.34	130.42	1524.07
	55	0.419183	0.070155	0.436560	30.181	5.051	60.018	766.35	128.26	1524.46
	56	0.439982	0.068749	0.436512	31.679	4.950	60.012	804.38	125.69	1524.30
	57	0.459681	0.067310	0.436677	33.097	4.846	60.034	840.39	123.06	1524.87
	58	0.479972	0.065727	0.436628	34.558	4.732	60.028	877.48	120.16	1524.70
	59	0.500643	0.064015	0.435801	36.046	4.609	59.914	915.28	117.03	1521.82
	60	0.518759	0.062435	0.436823	37.351	4.495	60.054	948.40	114.14	1525.38
	61	0.540170	0.060482	0.436476	38.892	4.355	60.007	987.54	110.57	1524.17
	62	0.560303	0.058563	0.436813	40.342	4.217	60.053	1024.35	107.06	1525.35
	63	0.580485	0.056563	0.436320	41.795	4.073	59.985	1061.24	103.41	1523.63
	64	0.600351	0.054524	0.436143	43.225	3.926	59.961	1097.56	99.68	1523.01
	65	0.639920	0.050270	0.436922	46.074	3.619	60.068	1169.90	91.90	1525.73
	66	0.679950	0.045719	0.436582	48.956	3.292	60.021	1243.08	83.58	1524.54
	67	0.720134	0.040919	0.436464	51.850	2.946	60.005	1316.55	74.81	1524.13
	68	0.760150	0.035915	0.436490	54.731	2.586	60.009	1389.71	65.66	1524.22
	69	0.800202	0.030692	0.436501	57.615	2.210	60.010	1462.93	56.11	1524.26
	70	0.850191	0.023871	0.436508	61.214	1.719	60.011	1554.32	43.64	1524.28
	71	0.899308	0.016831	0.436459	64.750	1.212	60.004	1644.11	30.77	1524.11
	72	0.949720	0.009239	0.435792	68.380	0.665	59.913	1736.28	16.89	1521.78
(b) Spanwise row										
Upper	73	0.700231	0.043324	0.022051	50.417	3.119	3.032	1280.16	79.20	77.0
	74	0.699839	0.043371	0.043571	50.388	3.123	5.990	1279.45	79.29	152.1
	75	0.699932	0.043360	0.065497	50.395	3.122	9.004	1279.62	79.27	228.7
	76	0.699423	0.043420	0.087124	50.358	3.126	11.978	1278.68	79.38	304.2
	77	0.700744	0.043263	0.116363	50.454	3.115	15.998	1281.10	79.09	406.3
	78	0.700061	0.043344	0.145621	50.404	3.121	20.020	1279.85	79.24	508.5
	79	0.700236	0.043323	0.174820	50.417	3.119	24.034	1280.17	79.20	610.5
	80	0.698772	0.043498	0.217917	50.312	3.132	29.959	1277.49	79.52	761.0
	81	0.700571	0.043283	0.262344	50.441	3.116	36.067	1280.78	79.13	916.1
	82	0.700262	0.043320	0.305944	50.419	3.119	42.061	1280.22	79.20	1068.4
	83	0.700345	0.043310	0.694142	50.425	3.118	95.431	1280.37	79.18	2423.9
	84	0.700209	0.043327	0.737883	50.415	3.120	101.444	1280.12	79.21	2576.7
	85	0.700058	0.043345	0.781435	50.404	3.121	107.432	1279.85	79.24	2728.8
	86	0.700517	0.043290	0.825281	50.437	3.117	113.460	1280.69	79.14	2881.9
	87	0.699998	0.043352	0.854412	50.400	3.121	117.465	1279.74	79.26	2983.6
	88	0.700356	0.043309	0.883596	50.426	3.118	121.477	1280.39	79.18	3085.5
	89	0.700428	0.043300	0.912702	50.431	3.118	125.478	1280.52	79.16	3187.1
	90	0.700207	0.043327	0.934588	50.415	3.120	128.487	1280.12	79.21	3263.6
	91	0.700718	0.043266	0.956310	50.452	3.115	131.473	1281.05	79.10	3339.4
	92	0.700282	0.043318	0.978547	50.420	3.119	134.531	1280.25	79.19	3417.1

TABLE C.4.—PRESSURE TAP LOCATIONS FOR F1 NACA 23012 MODEL: ICE SHAPE EG1164, CHORDWISE ROW

Surface	Tap no.	*x*/*c*	*y*/*c*	*z*/*b*	*x*, in.	*y*, in.	*z*, in.	*x*, mm	*y*, mm	*z*, mm
Removable leading edge	17	0.195005	–0.039517	0.436427	14.040	–2.845	60.000	356.63	–72.27	1524.0
	18	0.149990	–0.034943	0.436427	10.799	–2.516	60.000	274.30	–63.90	1524.0
	19	0.109991	–0.030460	0.436427	7.919	–2.193	60.000	201.15	–55.71	1524.0
	20	0.069972	–0.025641	0.436427	5.038	–1.846	60.000	127.97	–46.89	1524.0
	21	0.039475	–0.021390	0.436427	2.842	–1.540	60.000	72.19	–39.12	1524.0
	22	0.030549	–0.024686	0.436427	2.200	–1.777	60.000	55.87	–45.15	1524.0
	23	0.028026	–0.021060	0.434187	2.018	–1.516	59.692	51.25	–38.52	1516.2
	24	0.023797	–0.022508	0.436427	1.713	–1.621	60.000	43.52	–41.16	1524.0
	25	0.019247	–0.017919	0.436427	1.386	–1.290	60.000	35.20	–32.77	1524.0
	26	0.007081	–0.018019	0.436427	0.510	–1.297	60.000	12.95	–32.95	1524.0
	27	0.003830	–0.010571	0.436427	0.276	–0.761	60.000	7.00	–19.33	1524.0
	28	–0.000686	–0.003863	0.436427	–0.049	–0.278	60.000	–1.25	–7.07	1524.0
	29	–0.007741	0.001039	0.437300	–0.557	0.075	60.120	–14.16	1.90	1527.0
	30	–0.005374	0.008287	0.435991	–0.387	0.597	59.940	–9.83	15.15	1522.5
	31	–0.009980	0.013909	0.436864	–0.719	1.001	60.060	–18.25	25.44	1525.5
	32	–0.017845	0.017401	0.436427	–1.285	1.253	60.000	–32.63	31.82	1524.0
	33	0.002359	0.013926	0.436427	0.170	1.003	60.000	4.31	25.47	1524.0
	34	0.009898	0.023620	0.436427	0.713	1.701	60.000	18.10	43.20	1524.0
	35	0.019976	0.032109	0.436427	1.438	2.312	60.000	36.53	58.72	1524.0
	36	0.029967	0.038915	0.436427	2.158	2.802	60.000	54.80	71.17	1524.0
	37	0.039980	0.044258	0.436427	2.879	3.187	60.000	73.12	80.94	1524.0
	38	0.049992	0.048891	0.436427	3.599	3.520	60.000	91.43	89.41	1524.0
	39	0.060006	0.052839	0.436427	4.320	3.804	60.000	109.74	96.63	1524.0
	40	0.079985	0.059289	0.436427	5.759	4.269	60.000	146.28	108.43	1524.0
	41	0.099996	0.064100	0.436427	7.200	4.615	60.000	182.87	117.23	1524.0
	42	0.119999	0.067655	0.436427	8.640	4.871	60.000	219.45	123.73	1524.0
	43	0.139996	0.070459	0.436427	10.080	5.073	60.000	256.02	128.86	1524.0
	101	0.159999	0.072575	0.436427	11.520	5.225	60.000	292.61	132.72	1524.0
	102	0.175000	0.073851	0.436427	12.600	5.317	60.000	320.04	135.06	1524.0

TABLE C.5.—PRESSURE TAP LOCATIONS FOR F1 NACA 23012 MODEL: ICE SHAPE EG1162, CHORDWISE ROW

Surface	Tap no.	*x*/*c*	*y*/*c*	*z*/*b*	*x*, in.	*y*, in.	*z*, in.	*x*, mm	*y*, mm	*z*, mm
Removable leading edge	17	0.195000	–0.039009	0.436427	14.040	–2.809	60.000	356.62	–71.34	1524.0
	18	0.150000	–0.034353	0.436427	10.800	–2.473	60.000	274.32	–62.82	1524.0
	19	0.108333	–0.029758	0.436427	7.800	–2.143	60.000	198.12	–54.42	1524.0
	20	0.075000	–0.025846	0.436427	5.400	–1.861	60.000	137.16	–47.27	1524.0
	21	0.050000	–0.022446	0.436427	3.600	–1.616	60.000	91.44	–41.05	1524.0
	22	0.028308	–0.018889	0.436427	2.038	–1.360	60.000	51.77	–34.54	1524.0
	23	0.019352	–0.016481	0.436427	1.393	–1.187	60.000	35.39	–30.14	1524.0
	24	0.011971	–0.015238	0.436427	0.862	–1.097	60.000	21.89	–27.87	1524.0
	25	0.005000	–0.012456	0.436427	0.360	–0.897	60.000	9.14	–22.78	1524.0
	26	0.000000	–0.009740	0.436427	0.000	–0.701	60.000	0.00	–17.81	1524.0
	27	–0.005000	–0.005713	0.436427	–0.360	–0.411	60.000	–9.14	–10.45	1524.0
	28	–0.009162	–0.001112	0.436427	–0.660	–0.080	60.000	–16.76	–2.03	1524.0
	29	–0.010000	0.004778	0.436427	–0.720	0.344	60.000	–18.29	8.74	1524.0
	30	–0.007999	0.009863	0.436427	–0.576	0.710	60.000	–14.63	18.04	1524.0
	31	–0.005000	0.015321	0.436427	–0.360	1.103	60.000	–9.14	28.02	1524.0
	32	0.000056	0.020899	0.436427	0.004	1.505	60.000	0.10	38.22	1524.0
	33	0.005000	0.026049	0.436427	0.360	1.876	60.000	9.14	47.64	1524.0
	34	0.010000	0.029436	0.436427	0.720	2.119	60.000	18.29	53.83	1524.0
	35	0.015000	0.032885	0.436427	1.080	2.368	60.000	27.43	60.14	1524.0
	36	0.020372	0.036039	0.436427	1.467	2.595	60.000	37.26	65.91	1524.0
	37	0.028971	0.040779	0.436427	2.086	2.936	60.000	52.98	74.58	1524.0
	38	0.040000	0.045836	0.436427	2.880	3.300	60.000	73.15	83.82	1524.0
	39	0.050000	0.049953	0.436427	3.600	3.597	60.000	91.44	91.35	1524.0
	40	0.060000	0.053729	0.436427	4.320	3.868	60.000	109.73	98.26	1524.0
	41	0.080000	0.059820	0.436427	5.760	4.307	60.000	146.30	109.40	1524.0
	42	0.100000	0.064581	0.436427	7.200	4.650	60.000	182.88	118.11	1524.0
	43	0.120000	0.067937	0.436427	8.640	4.891	60.000	219.46	124.24	1524.0
	101	0.140000	0.070676	0.436427	10.080	5.089	60.000	256.03	129.25	1524.0
	102	0.160000	0.072786	0.436427	11.520	5.241	60.000	292.61	133.11	1524.0
	103	0.175000	0.074103	0.436427	12.600	5.335	60.000	320.04	135.52	1524.0

TABLE C.6.—PRESSURE TAP LOCATIONS FOR F1 NACA 23012 MODEL: ICE SHAPE EG1126, CHORDWISE ROW

Surface	Tap no.	*x*/*c*	*y*/*c*	*z*/*b*	*x*, in.	*y*, in.	*z*, in.	*x*, mm	*y*, mm	*z*, mm
Removable leading edge ↓	17	0.194992	–0.039814	0.436427	14.039	–2.867	60.000	356.60	–72.81	1524.00
	18	0.150008	–0.034844	0.436427	10.801	–2.509	60.000	274.34	–63.72	1524.00
	19	0.108339	–0.030230	0.436427	7.800	–2.177	60.000	198.13	–55.28	1524.00
	20	0.074970	–0.026334	0.436427	5.398	–1.896	60.000	137.10	–48.16	1524.00
	21	0.049923	–0.022895	0.436427	3.594	–1.648	60.000	91.30	–41.87	1524.00
	22	0.029227	–0.019032	0.436427	2.104	–1.370	60.000	53.45	–34.81	1524.00
	23	0.019182	–0.016224	0.436427	1.381	–1.168	60.000	35.08	–29.67	1524.00
	24	0.011530	–0.013282	0.436427	0.830	–0.956	60.000	21.09	–24.29	1524.00
	25	0.005831	–0.010180	0.436427	0.420	–0.733	60.000	10.66	–18.62	1524.00
	26	0.001644	–0.005675	0.436427	0.118	–0.409	60.000	3.01	–10.38	1524.00
	27	–0.000831	–0.000705	0.436427	–0.060	–0.051	60.000	–1.52	–1.29	1524.00
	28	–0.001408	0.004444	0.436427	–0.101	0.320	60.000	–2.57	8.13	1524.00
	29	–0.000744	0.009170	0.436427	–0.054	0.660	60.000	–1.36	16.77	1524.00
	30	0.000956	0.013801	0.436427	0.069	0.994	60.000	1.75	25.24	1524.00
	31	0.003488	0.017423	0.436427	0.251	1.254	60.000	6.38	31.86	1524.00
	32	0.006699	0.021686	0.436427	0.482	1.561	60.000	12.25	39.66	1524.00
	33	0.010625	0.024972	0.436427	0.765	1.798	60.000	19.43	45.67	1524.00
	34	0.014732	0.028634	0.436427	1.061	2.062	60.000	26.94	52.37	1524.00
	35	0.020428	0.032949	0.436427	1.471	2.372	60.000	37.36	60.26	1524.00
	36	0.030251	0.039281	0.436427	2.178	2.828	60.000	55.32	71.84	1524.00
	37	0.040185	0.044455	0.436427	2.893	3.201	60.000	73.49	81.30	1524.00
	38	0.050125	0.048934	0.436427	3.609	3.523	60.000	91.67	89.49	1524.00
	39	0.060214	0.052753	0.436427	4.335	3.798	60.000	110.12	96.47	1524.00
	40	0.080133	0.059168	0.436427	5.770	4.260	60.000	146.55	108.21	1524.00
	41	0.100082	0.063981	0.436427	7.206	4.607	60.000	183.03	117.01	1524.00
	42	0.120048	0.067668	0.436427	8.643	4.872	60.000	219.54	123.75	1524.00
	43	0.140044	0.070467	0.436427	10.083	5.074	60.000	256.11	128.87	1524.00
	101	0.160031	0.072630	0.436427	11.522	5.229	60.000	292.66	132.83	1524.00
	102	0.175013	0.074027	0.436427	12.601	5.330	60.000	320.06	135.38	1524.00

TABLE C.7.—PRESSURE TAP LOCATIONS FOR F1 NACA 23012 MODEL: ICE SHAPE EG1159, CHORDWISE ROW

Surface	Tap no.	x/c	y/c	z/b	x, in.	y, in.	z, in.	x, mm	y, mm	z, mm
Removable leading edge	17	0.195000	–0.039 651	0.436427	14.040	–2.855	60.000	356.62	–72.51	1524.0
	18	0.170000	–0.036797	0.436427	12.240	–2.649	60.000	310.90	–67.30	1524.0
	19	0.150000	–0.034731	0.436587	10.800	–2.501	60.022	274.32	–63.52	1524.6
	20	0.127580	–0.032850	0.436427	9.186	–2.365	60.000	233.32	–60.08	1524.0
	21	0.118031	–0.032606	0.437445	8.498	–2.348	60.140	215.86	–59.63	1527.6
	22	0.107611	–0.035434	0.436427	7.748	–2.551	60.000	196.80	–64.80	1524.0
	23	0.102335	–0.029786	0.436427	7.368	–2.145	60.000	187.15	–54.47	1524.0
	24	0.095153	–0.027734	0.436427	6.851	–1.997	60.000	174.02	–50.72	1524.0
	25	0.076012	–0.025660	0.436427	5.473	–1.848	60.000	139.01	–46.93	1524.0
	26	0.053969	–0.022696	0.436427	3.886	–1.634	60.000	98.70	–41.51	1524.0
	27	0.032151	–0.018725	0.436427	2.315	–1.348	60.000	58.80	–34.24	1524.0
	28	0.021302	–0.015659	0.436427	1.534	–1.127	60.000	38.96	–28.64	1524.0
	29	0.012655	–0.012367	0.436427	0.911	–0.890	60.000	23.14	–22.62	1524.0
	30	0.005730	–0.007883	0.436427	0.413	–0.568	60.000	10.48	–14.42	1524.0
	31	0.000772	–0.001282	0.436427	0.056	–0.092	60.000	1.41	–2.34	1524.0
	32	–0.000304	0.006847	0.436427	–0.022	0.493	60.000	–0.56	12.52	1524.0
	33	0.002484	0.014646	0.436427	0.179	1.055	60.000	4.54	26.78	1524.0
	34	0.008106	0.022520	0.436427	0.584	1.621	60.000	14.82	41.18	1524.0
	35	0.016324	0.030212	0.436427	1.175	2.175	60.000	29.85	55.25	1524.0
	36	0.024160	0.035698	0.436427	1.739	2.570	60.000	44.18	65.28	1524.0
	37	0.031322	0.039864	0.436427	2.255	2.870	60.000	57.28	72.90	1524.0
	38	0.037411	0.043110	0.436427	2.694	3.104	60.000	68.42	78.84	1524.0
	39	0.043611	0.045980	0.436427	3.140	3.311	60.000	79.76	84.09	1524.0
	40	0.048795	0.049268	0.436427	3.513	3.547	60.000	89.24	90.10	1524.0
	41	0.044035	0.057644	0.436427	3.171	4.150	60.000	80.53	105.42	1524.0
	42	0.044244	0.060759	0.437045	3.186	4.375	60.085	80.91	111.12	1526.2
	43	0.060000	0.053924	0.435809	4.320	3.883	59.915	109.73	98.62	1521.8
	101	0.070000	0.056589	0.436427	5.040	4.074	60.000	128.02	103.49	1524.0
	102	0.080000	0.059704	0.436704	5.760	4.299	60.038	146.30	109.19	1525.0
	103	0.090000	0.062270	0.436856	6.480	4.483	60.059	164.59	113.88	1525.5
	104	0.100000	0.064411	0.436856	7.200	4.638	60.059	182.88	117.80	1525.5
	105	0.110000	0.066143	0.436427	7.920	4.762	60.000	201.17	120.96	1524.0
	106	0.120000	0.067665	0.436427	8.640	4.872	60.000	219.46	123.75	1524.0
	107	0.140000	0.070380	0.436427	10.080	5.067	60.000	256.03	128.71	1524.0
	108	0.160000	0.072540	0.436427	11.520	5.223	60.000	292.61	132.66	1524.0
	109	0.175000	0.073853	0.436427	12.600	5.317	60.000	320.04	135.06	1524.0

TABLE C.8.—PRESSURE TAP LOCATIONS FOR F1 NACA 23012 MODEL: ICE SHAPE EG1125, CHORDWISE ROW

Surface	Tap no.	*x*/*c*	*y*/*c*	*z*/*b*	*x*, in.	*y*, in.	*z*, in.	*x*, mm	*y*, mm	*z*, mm
Removable leading edge	17	0.195000	–0.039569	0.436427	14.040	–2.849	60.000	356.62	–72.36	1524.0
	18	0.150000	–0.034415	0.436427	10.800	–2.478	60.000	274.32	–62.94	1524.0
	19	0.108333	–0.029675	0.436427	7.800	–2.137	60.000	198.12	–54.27	1524.0
	20	0.075000	–0.025478	0.436427	5.400	–1.834	60.000	137.16	–46.59	1524.0
	21	0.050000	–0.021830	0.436427	3.600	–1.572	60.000	91.44	–39.92	1524.0
	22	0.030000	–0.017950	0.436427	2.160	–1.292	60.000	54.86	–32.83	1524.0
	23	0.019832	–0.015303	0.436427	1.428	–1.102	60.000	36.27	–27.99	1524.0
	24	0.009722	–0.011920	0.436427	0.700	–0.858	60.000	17.78	–21.80	1524.0
	25	0.003001	–0.009511	0.435809	0.216	–0.685	59.915	5.49	–17.39	1521.8
	26	–0.004231	–0.005423	0.437045	–0.305	–0.390	60.085	–7.74	–9.92	1526.2
	27	–0.008713	0.000263	0.437045	–0.627	0.019	60.085	–15.93	0.48	1526.2
	28	–0.007442	0.008811	0.437045	–0.536	0.634	60.085	–13.61	16.11	1526.2
	29	–0.002336	0.013758	0.436427	–0.168	0.991	60.000	–4.27	25.16	1524.0
	30	0.003486	0.018993	0.436245	0.251	1.367	59.975	6.38	34.73	1523.4
	31	0.007976	0.023645	0.436427	0.574	1.702	60.000	14.59	43.24	1524.0
	32	0.013605	0.028862	0.436427	0.980	2.078	60.000	24.88	52.78	1524.0
	33	0.020000	0.033827	0.436427	1.440	2.436	60.000	36.58	61.86	1524.0
	34	0.030000	0.040181	0.436427	2.160	2.893	60.000	54.86	73.48	1524.0
	35	0.040000	0.045437	0.436427	2.880	3.271	60.000	73.15	83.10	1524.0
	36	0.050000	0.049838	0.436427	3.600	3.588	60.000	91.44	91.14	1524.0
	37	0.060000	0.053761	0.436427	4.320	3.871	60.000	109.73	98.32	1524.0
	38	0.080000	0.059923	0.436427	5.760	4.314	60.000	146.30	109.59	1524.0
	39	0.100000	0.064650	0.436427	7.200	4.655	60.000	182.88	118.23	1524.0
	40	0.120000	0.068298	0.436427	8.640	4.917	60.000	219.46	124.90	1524.0
	41	0.140000	0.070944	0.436427	10.080	5.108	60.000	256.03	129.74	1524.0
	42	0.160000	0.073057	0.436427	11.520	5.260	60.000	292.61	133.61	1524.0
	43	0.175000	0.074258	0.436427	12.600	5.347	60.000	320.04	135.80	1524.0

TABLE C.9.—PRESSURE TAP LOCATIONS FOR F1 NACA 23012 MODEL: ICE SHAPE EG1134, CHORDWISE ROW

Surface	Tap no.	*x*/*c*	*y*/*c*	*z*/*b*	*x*, in.	*y*, in.	*z*, in.	*x*, mm	*y*, mm	*z*, mm
Removable leading edge ↓	17	0.195009	–0.039737	0.436427	14.041	–2.861	60.000	356.63	–72.67	1524.00
	18	0.149992	–0.034916	0.436427	10.799	–2.514	60.000	274.31	–63.85	1524.00
	19	0.108339	–0.030228	0.436427	7.800	–2.176	60.000	198.13	–55.28	1524.00
	20	0.075039	–0.026056	0.436427	5.403	–1.876	60.000	137.23	–47.65	1524.00
	21	0.050078	–0.022414	0.436427	3.606	–1.614	60.000	91.58	–40.99	1524.00
	22	0.030437	–0.018880	0.436427	2.191	–1.359	60.000	55.66	–34.53	1524.00
	23	0.023336	–0.017082	0.436427	1.680	–1.230	60.000	42.68	–31.24	1524.00
	24	0.014289	–0.013887	0.436427	1.029	–1.000	60.000	26.13	–25.40	1524.00
	25	0.006806	–0.010363	0.436427	0.490	–0.746	60.000	12.45	–18.95	1524.00
	26	0.001751	–0.006514	0.436427	0.126	–0.469	60.000	3.20	–11.91	1524.00
	27	–0.002172	–0.000837	0.436427	–0.156	–0.060	60.000	–3.97	–1.53	1524.00
	28	–0.002927	0.005025	0.436427	–0.211	0.362	60.000	–5.35	9.19	1524.00
	29	–0.001904	0.009904	0.436427	–0.137	0.713	60.000	–3.48	18.11	1524.00
	30	0.001379	0.015966	0.436427	0.099	1.150	60.000	2.52	29.20	1524.00
	31	0.004846	0.020382	0.436427	0.349	1.468	60.000	8.86	37.28	1524.00
	32	0.008899	0.024700	0.436427	0.641	1.778	60.000	16.28	45.17	1524.00
	33	0.013671	0.028886	0.436427	0.984	2.080	60.000	25.00	52.83	1524.00
	34	0.019680	0.033198	0.436427	1.417	2.390	60.000	35.99	60.71	1524.00
	35	0.029751	0.039591	0.436427	2.142	2.851	60.000	54.41	72.40	1524.00
	36	0.039883	0.044734	0.436427	2.872	3.221	60.000	72.94	81.81	1524.00
	37	0.049888	0.049166	0.436427	3.592	3.540	60.000	91.24	89.91	1524.00
	38	0.059812	0.053212	0.436427	4.306	3.831	60.000	109.38	97.31	1524.00
	39	0.079864	0.059624	0.436427	5.750	4.293	60.000	146.06	109.04	1524.00
	40	0.099925	0.064315	0.436427	7.195	4.631	60.000	182.74	117.62	1524.00
	41	0.119950	0.067959	0.436427	8.636	4.893	60.000	219.36	124.28	1524.00
	42	0.139960	0.070836	0.436427	10.077	5.100	60.000	255.96	129.55	1524.00
	43	0.159975	0.072984	0.436427	11.518	5.255	60.000	292.56	133.47	1524.00
	101	0.174990	0.074204	0.436427	12.599	5.343	60.000	320.02	135.70	1524.00

Appendix D.—Test Matrices

IRT Test Matrices

TABLE D.1.—IRT 18-in. (457-m) CHORD, SUBSCALE MODEL TESTS

Run	*V*, kt	*AoA*, deg.	*MVD*, µm	*LWC*, g/m³	T_t, °F (°C)	T_s, °F (°C)	Exposure time, min.	Ice shape type and run notes
ED0711	250	2.0	15.4	0.67	20.0 (–6.7)	5.2 (–14.9)	10.0	Horn
ED0712	250	2.0	15.4	0.67	24.0 (–4.4)	9.8 (–12.3)	10.0	Horn
ED0713	175	5.3	15.0	0.64	24.0 (–4.4)	16.8 (–8.5)	10.0	Horn
ED0714	175	5.3	15.0	0.64	28.0 (–2.2)	20.8 (–6.2)	10.0	Horn
ED0715	175	5.3	15.0	0.64	30.0 (–1.1)	22.8 (–5.1)	10.0	Horn
ED0716	175	5.3	15.0	0.64	28.0 (–2.2)	20.8 (–6.2)	10.0	Horn, repeat 714
ED0717	175	5.3	15.0	0.64	28.0 (–2.2)	20.8 (–6.2)	10.0	Horn, repeat 716, mold
ED0718	175	5.3	15.0	0.64	28.0 (–2.2)	20.8 (–6.2)	5.0	Horn
ED0719	175	5.3	15.0	0.64	28.0 (–2.2)	20.8 (–6.2)	2.0	Roughness
ED0720	175	5.3	15.0	0.64	28.0 (–2.2)	20.8 (–6.2)	0.5	Roughness
ED0721	175	5.3	15.0	0.64	28.0 (–2.2)	20.8 (–6.2)	5.0	Horn, repeat 718, mold
ED0722	175	5.3	15.0	0.64	28.0 (–2.2)	20.8 (–6.2)	1.0	Roughness
ED0723	175	5.3	15.0	0.64	28.0 (–2.2)	20.8 (–6.2)	0.5	Roughness, repeat 720, mold
ED0724	250	2.0	15.0	0.33	8.0 (–13.3)	–7.1 (–21.7)	10.0	Streamwise
ED0725	250	2.0	15.0	0.33	8.0 (–13.3)	–7.1 (–21.7)	5.0	Streamwise
ED0726	250	2.0	15.0	0.33	8.0 (–13.3)	–7.1 (–21.7)	5.0	Streamwise, repeat 725, mold
ED0727	175	5.3	15.0	0.30	0.0 (–17.8)	–7.4 (–21.8)	10.0	Streamwise
ED0728	175	5.3	15.0	0.30	0.0 (–17.8)	–7.4 (–21.8)	5.0	Streamwise
ED0729	175	5.3	15.0	0.30	0.0 (–17.8)	–7.4 (–21.8)	1.0	Roughness
ED0730	175	5.3	15.0	0.30	0.0 (–17.8)	–7.4 (–21.8)	5.0	Streamwise, repeat 728, mold
ED0731	175	5.3	15.0	0.30	0.0 (–17.8)	–7.4 (–21.8)	2.0	Roughness
ED0732	250	2.0	15.4	0.67	28.0 (–2.2)	11.0 (–10.5)	5.0	Horn
ED0733	200	2.0	15.4	0.75	28.0 (–2.2)	18.5 (–7.5)	5.0	Horn
ED0734	200	2.0	17.6	1.06	28.0 (–2.2)	18.5 (–7.5)	5.0	Horn
ED0735	200	2.0	15.4	0.75	28.0 (–2.2)	18.5 (–7.5)	5.0	Horn, repeat 733, mold
ED0736	175	5.3	15.0	0.64	28.0 (–2.2)	20.8 (–6.2)	0.5	Roughness, repeat 720
ED0737	175	5.3	15.0	0.64	24.0 (–4.4)	16.8 (–8.5)	10.0	Horn, repeat 713, mold
ED0738	250	2.0	15.0	0.33	8.0 (–13.3)	–7.1 (–21.7)	5.0	Streamwise, repeat 725
ED0739	175	5.3	15.0	0.30	0.0 (–17.8)	–7.4 (–21.8)	1.0	Roughness, repeat 729
ED0740	250	2.0	15.4	0.67	24.0 (–4.4)	9.8 (–12.3)	10.5	Spanwise ridge
ED0741	175	0.0	15.0	0.64	24.0 (–4.4)	16.8 (–8.5)	15.0	Spanwise ridge
ED0742	175	0.0	15.0	0.64	24.0 (–4.4)	16.8 (–8.5)	10.0	Spanwise ridge
ED0743	175	0.0	15.0	0.64	15.0 (–9.4)	7.8 (–13.5)	5.0	Spanwise ridge
ED0744	175	5.3	15.0	0.64	28.0 (–2.2)	20.8 (–6.2)	0.5	Roughness, repeat 720
ED0745	200	2.0	15.4	0.75	28.0 (–2.2)	18.5 (–7.5)	2.0	Roughness
ED0746	200	2.0	15.4	0.75	28.0 (–2.2)	18.5 (–7.5)	0.5	Roughness

TABLE D.1.—Concluded. IRT 18-in. (457-m) CHORD, SUBSCALE MODEL TESTS

Run	*V*, kt	*AoA*, deg.	*MVD*, µm	*LWC*, g/m^3	T_t, °F (°C)	T_s, °F (°C)	Exposure time, min.	Ice shape type and run notes
ED0747	250	2.0	15.4	0.67	28.0 (–2.2)	22.0 (–10.5)	0.5	Roughness
ED0748	175	5.3	15.0	0.30	0.0 (–17.8)	–7.4 (–21.8)	1.0	Roughness, repeat 729, mold
ED0749	175	0.0	15.0	0.64	24.0 (–4.4)	16.8 (–8.5)	5.0	Spanwise ridge
ED0750	175	0.0	15.0	0.64	24.0 (–4.4)	16.8 (–8.5)	5.0	Spanwise ridge, repeat 749
ED0751	175	0.0	15.0	0.64	24.0 (–4.4)	16.8 (–8.5)	5.0	Spanwise ridge, repeat 749, mold
ED0752	250	2.0	15.0	0.33	8.0 (–13.3)	–7.1 (–21.7)	1.0	Roughness
ED0753	200	2.0	15.0	0.39	8.0 (–13.3)	–1.3 (–18.5)	1.0	Roughness
ED0754	200	2.0	30.0	0.40	8.0 (–13.3)	–1.3 (–18.5)	5.0	Streamwise
ED0755	175	5.3	30.0	0.44	0.0 (–17.8)	–7.4 (–21.8)	5.0	Streamwise
ED0756	200	2.0	30.0	0.40	0.0 (–17.8)	–9.6 (–23.1)	5.0	Streamwise, mold
ED0757	200	2.0	15.0	0.33	0.0 (–17.8)	–9.6 (–23.1)	10.0	Streamwise, mold
ED0758	175	0.0	15.0	0.64	24.0 (–4.4)	16.8 (–8.5)	5.0	Spanwise ridge
ED0759	175	0.9	15.0	0.64	24.0 (–4.4)	16.8 (–8.5)	5.0	Spanwise ridge
ED0760	175	0.9	15.0	0.64	24.0 (–4.4)	16.8 (–8.5)	5.0	Spanwise ridge, repeat 759, mold
ED0761	200	2.0	15.4	0.75	28.0 (–2.2)	18.5 (–7.5)	5.0	Horn, repeat 735
ED0762	200	2.0	15.4	0.75	28.0 (–2.2)	18.5 (–7.5)	0.5	Roughness, repeat 746, mold
ED0763	175	5.3	15.0	0.64	28.0 (–2.2)	20.8 (–6.2)	5.0	Horn/repeat 718
ED0764	175	5.3	15.0	0.64	28.0 (–2.2)	20.8 (–6.2)	2.0	Roughness, repeat 719, mold
ED0765	175	1.0	15.0	0.64	24.0 (–4.4)	16.8 (–8.5)	5.0	Spanwise ridge
ED0766	175	1.0	15.0	0.64	24.0 (–4.4)	16.8 (–8.5)	5.0	Spanwise ridge, repeat 765, mold
ED0767	175	5.3	15.0	0.64	24.0 (–4.4)	16.8 (–8.5)	10.0	Horn, repeat 713 and 737
ED0768	175	5.3	15.0	0.64	28.0 (–2.2)	20.8 (–6.2)	2.0	Roughness, repeat 719 and 764
ED0769	200	2.0	15.4	0.75	28.0 (–2.2)	18.5 (–7.5)	0.5	Roughness, repeat 746 and 762
ED0770	200	2.0	30.0	0.40	0.0 (–17.8)	–9.6 (–23.1)	5.0	Streamwise, repeat 756
ED0771	200	2.0	15.0	0.33	0.0 (–17.8)	–9.6 (–23.1)	10.0	Streamwise, repeat 757
ED0772	175	5.3	15.0	0.30	0.0 (–17.8)	–7.4 (–21.8)	5.0	Streamwise, repeat 728 and 730
ED0773	200	2.0	15.4	0.75	28.0 (–2.2)	18.5 (–7.5)	10.0	Horn/mold

TABLE D.2.—IRT 72-in.- (1829-mm-) CHORD, FULL-SCALE MODEL TESTS

Run	*V*, kt	*AoA*, deg.	*MVD*, μm	*LWC*, g/m^3	T_t, °F (°C)	T_s, °F (°C)	Exposure time, min.	Ice shape type and run notes
EG1109	175	5.0	20.0	0.50	20.0 (–6.7)	12.8 (–10.7)	22.5	Horn
EG1110	175	5.0	20.0	0.50	24.0 (–4.4)	16.8 (–8.4)	22.5	Horn
EG1111	175	5.0	20.0	0.50	28.0 (–2.2)	20.8 (–6.2)	22.5	Horn
EG1112	200	2.0	20.0	0.50	28.0 (–2.2)	18.7 (–7.4)	22.5	Horn
EG1113	200	2.0	20.0	0.50	28.0 (–2.2)	18.7 (–7.4)	22.5	Horn, repeat 1112
EG1114	200	2.0	20.0	0.50	28.0 (–2.2)	18.7 (–7.4)	22.5	Horn, repeat 1112, mold
EG1115	175	5.0	20.0	0.60	28.0 (–2.2)	20.8 (–6.2)	22.5	Horn
EG1116	175	5.0	20.0	0.60	30.0 (–1.1)	22.7 (–5.2)	22.5	Horn
EG1117	200	2.0	20.0	0.50	28.0 (–2.2)	18.7 (–7.4)	2.0	Roughness
EG1118	200	2.0	20.0	0.50	28.0 (–2.2)	18.7 (–7.4)	1.0	Roughness
EG1119	175	5.0	20.0	0.60	28.0 (–2.2)	20.8 (–6.2)	2.0	Roughness
EG1120	200	2.0	20.0	0.30	4.0 (–15.6)	–5.3 (–20.7)	10.0	Streamwise
EG1121	200	2.0	40.0	0.55	4.0 (–15.6)	–5.3 (–20.7)	10.0	Streamwise
EG1122	200	2.0	15.0	0.30	4.0 (–15.6)	–5.3 (–20.7)	10.0	Streamwise
EG1123	200	2.0	15.0	0.30	4.0 (–15.6)	–5.3 (–20.7)	20.0	Streamwise
EG1124	200	5.0	15.0	0.30	4.0 (–15.6)	–5.3 (–20.7)	20.0	Streamwise
EG1125	200	2.0	15.0	0.30	4.0 (–15.6)	–5.3 (–20.7)	20.0	Streamwise, repeat 1123, mold
EG1126	200	2.0	20.0	0.50	28.0 (–2.2)	18.7 (–7.4)	2.0	Roughness, repeat 1117, mold
EG1127	175	5.0	20.0	0.70	28.0 (–2.2)	20.8 (–6.2)	22.5	Horn
EG1128	175	5.0	20.0	0.85	28.0 (–2.2)	20.8 (–6.2)	22.5	Horn
EG1129	200	2.0	20.0	0.50	28.0 (–2.2)	18.7 (–7.4)	22.5	Horn, repeat 1112 and 1113
EG1130	175	5.0	20.0	0.85	28.0 (–2.2)	20.8 (–6.2)	22.5	Horn, repeat 1128, mold
EG1131	200	2.0	15.0	0.30	4.0 (–15.6)	–5.3 (–20.7)	2.0	Roughness
EG1132	200	2.0	15.0	0.30	4.0 (–15.6)	–5.3 (–20.7)	4.0	Roughness
EG1133	200	2.0	40.0	0.55	4.0 (–15.6)	–5.3 (–20.7)	2.0	Roughness
EG1134	200	2.0	40.0	0.55	4.0 (–15.6)	–5.3 (–20.7)	2.0	Roughness, repeat 1133, mold
EG1135	200	2.0	15.0	0.30	4.0 (–15.6)	–5.3 (–20.7)	20.0	Streamwise, repeat 1123 and 1125
EG1136	200	2.0	40.0	0.55	4.0 (–15.6)	–5.3 (–20.7)	5.0	Streamwise
EG1137	200	5.0	15.0	0.30	4.0 (–15.6)	–5.3 (–20.7)	20.0	Streamwise, repeat 1124, mold
EG1138	175	5.0	20.0	0.85	28.0 (–2.2)	20.8 (–6.2)	22.5	Horn, repeat 1128 and 1130
EG1139	175	5.0	20.0	0.85	28.0 (–2.2)	20.8 (–6.2)	11.25	Horn
EG1140	200	2.0	20.0	0.50	28.0 (–2.2)	18.7 (–7.4)	2.0	Roughness, repeat 1117, 1126
EG1141	200	2.0	30.0	0.45	4.0 (–15.6)	–5.3 (–20.7)	10.0	Streamwise
EG1142	200	2.0	20.0	0.50	20.0 (–6.7)	10.7 (–11.8)	15.0	Spanwise ridge
EG1143	200	0.0	20.0	0.50	20.0 (–6.7)	10.7 (–11.8)	15.0	Spanwise ridge
EG1144	200	1.0	20.0	0.50	20.0 (–6.7)	10.7 (–11.8)	15.0	Spanwise ridge
EG1145	200	1.5	20.0	0.50	20.0 (–6.7)	10.7 (–11.8)	15.0	Spanwise ridge
EG1146	200	1.5	20.0	0.50	20.0 (–6.7)	10.7 (–11.8)	15.0	Spanwise ridge[a]
EG1147	200	0/2/1.5	20.0	0.50	20.0 (–6.7)	10.7 (–11.8)	15.0	Spanwise ridge[b]
EG1148	200	1.5	20.0	0.50	20.0 (–6.7)	10.7 (–11.8)	15.0	Spanwise ridge[a]

[a]Multiple runs at the same icing conditions were at various heater settings and resulted in varying spanwise ridge ice accretions.

[b]5 min at each *AoA*.

TABLE D.2.—Concluded. IRT 72-in.- (1829-mm-) CHORD, FULL-SCALE MODEL TESTS

Run	V, kt	AoA, deg.	MVD, µm	LWC, g/m^3	T_t, °F (°C)	T_s, °F (°C)	Exposure time, min.	Ice shape type and run notes
EG1149	150	1.5	20.0	0.62	20.0 (–6.7)	14.7 (–9.6)	15.0	Spanwise ridge
EG1150	150	1.5	20.0	0.81	20.0 (–6.7)	14.7 (–9.6)	15.0	Spanwise ridge
EG1151	150	1.5	20.0	0.81	20.0 (–6.7)	14.7 (–9.6)	15.0	Spanwise ridge[a]
EG1152	150	1.5	20.0	0.81	20.0 (–6.7)	14.7 (–9.6)	20.0	Spanwise ridge[a]
EG1153	150	1.5	20.0	0.81	20.0 (–6.7)	14.7 (–9.6)	15.0	Spanwise ridge, mold
EG1154	150	–1.5	20.0	0.81	24.0 (–4.4)	18.4 (–7.6)	15.0	Spanwise ridge
EG1155	150	1.5	20.0	0.81	20.0 (–6.7)	14.7 (–9.6)	17.5	Spanwise ridge
EG1156	150	1.5	20.0	0.81	20.0 (–6.7)	14.7 (–9.6)	17.5	Spanwise ridge[a]
EG1157	150	1.5	20.0	0.81	20.0 (–6.7)	14.7 (–9.6)	17.5	Spanwise ridge[a]
EG1158	150	1.5	20.0	0.81	20.0 (–6.7)	14.7 (–9.6)	17.5	Spanwise ridge[a]
EG1159	150	1.5	20.0	0.81	20.0 (–6.7)	14.7 (–9.6)	15.0	Spanwise ridge, repeat 1151, mold
EG1160	175	2.0	30.0	0.50	–5 (–20.6)	–12.2 (–24.6)	10.0	Streamwise
EG1161	150	2.0	30.0	0.55	–8 (–22.2)	–13.3 (–25.2)	10.0	Streamwise
EG1162	150	2.0	30.0	0.55	–8 (–22.2)	–13.3 (–25.2)	10.0	Streamwise, repeat 1161, mold
EG1163	175	5.0	15.0	0.64	28.0 (–2.2)	20.8 (–6.2)	10.0	Horn
EG1164	175	5.0	20.0	0.85	28.0 (–2.2)	20.8 (–6.2)	11.25	Horn, repeat 1139, mold

[a]Multiple runs at the same icing conditions were at various heater settings and resulted in varying spanwise ridge ice accretions.

[b]5 min at each *AoA*.

F1 Test Matrices

Clean Model

TABLE D.3.—CONTINUOUS-*AoA* SWEEP TESTS BY LOT NUMBER

[Sweep rate: 0.1 deg/s.]

Re×10[6]	M		
	0.10	0.20–0.21	0.29
4.6	392	----	-----
8.0–9.1	325	405	-----
12.0–12.3	308	357	472
15.9	----	338[a]	----

[a]Model pin contact near stall.

TABLE D.4.—FIXED-PITCH TESTS BY LOT NUMBER

Re×10[6]	*AoA*, deg				
	–5	0	5	10	15
(a) M = 0.10					
4.6–4.7	395	418	399	401	403
8.1	328	330	332	334	336
12.2–12.3	311	313	315	317	319
(b) M = 0.20–0.21					
9.1	408	410	412	414	----
11.9–12.0	372	376	378	380	382
15.9	341	343	345	347	----
(c) M = 0.28–0.29					
12.1–12.2	475	477	479	481	----

Clean Model With Trip Strips

TABLE D.5.—CONTINUOUS-*AoA* SWEEP TESTS BY LOT NUMBER

[Sweep rate: 0.1 deg/s.]

Re×10[6]	M		
	0.10	0.20–0.21	0.29
4.5	610	----	----
8.0–9.0	532	628	----
12.0–12.2	510	576	646
15.9	----	558[a]	----

[a]Model pin contact near stall.

TABLE D.6.—FIXED PITCH TESTS BY LOT NUMBER

Re×10[6]	*AoA*, deg				
	–5	0	5	10	15
(a) M = 0.10					
4.5	613	615	617	619	621
8.0	535	537	539	541	543
12.0–12.2	513	515	517	519	521
(b) M = 0.20–0.21					
9.0	631	633	635	637	639
11.9–12.0	579	581	583	585	587
15.9–16.0	561	563	565	567	569[a]
(c) M = 0.29					
12.2–12.3	649	651	653	655	-----

[a]Model pin contact near stall.

Horn Ice, Run EG1164

TABLE D.7.—CONTINUOUS-*AoA* SWEEP TESTS BY LOT NUMBER

[Sweep rate: 0.1 deg/s.]

Re×10^6	M		
	0.10	0.20–0.21	0.29
4.5	763	-----	-----
8.3–9.0	726	772	-----
12.2	701	749	781
15.9	-----	736	-----

TABLE D.8.—FIXED PITCH TESTS BY LOT NUMBER

Re×10^6	*AoA*, deg					
	–4	0	4	6	8	10
(a) M = 0.10						
4.5	765	766	767	768	769	770
8.2–8.3	728	729	731	732	733	734
11.9–12.1	704	706	708	710	712	714
(b) M = 0.20–0.21						
8.8–9.0	774	775	776	777	778	779
12.0–12.2	751	752	753	754	755	756
15.6–16.0	738	739	740	741	742	743
(c) M = 0.29						
12.1–12.2	783	784	785	786	787	-----

Streamwise Ice 1, Run EG1162

TABLE D.9.—CONTINUOUS-*AoA* SWEEP TESTS BY LOT NUMBER

[Sweep rate: 0.1 deg/s.]

Re×10^6	M		
	0.10	0.20–0.21	0.29
4.5	861	-----	-----
8.5–9.0	816	870	-----
12.1–12.2	801	839	879
16.0	-----	825	-----

TABLE D.10.—FIXED PITCH TESTS BY LOT NUMBER

Re×10^6	*AoA*, deg					
	–4	0	4	8	10	12
(a) M = 0.10						
4.5	863	864	865	866	867	868
8.4	818	819	820	821	822	823
12.2–12.3	803	804	805	806	807	808
(b) M = 0.20–0.21						
8.9–9.0	872	873	874	875	876	877
12.0–12.2	841	842	843	844	845	846
15.7–15.9	827	828	829	830	831	832
(c) M = 0.28–0.29						
12.1–12.2	881	882	883	884	885	-----

Roughness Ice 1, Run EG1126

TABLE D.11.—CONTINUOUS-*AoA* SWEEP TESTS BY LOT NUMBER

[Sweep rate: 0.1 deg/s.]

Re×10^6	M		
	0.10–0.11	0.20	0.29
4.5	985	-----	------
8.6–8.8	945	994	------
12.1	919	970	1003
15.9	-----	954	------

TABLE D.12.—FIXED PITCH TESTS BY LOT NUMBER

Re×10^6	*AoA*, deg					
	–4	0	4	8	10	11
(a) M = 0.10–0.11						
4.6	987	988	989	990	991	992
8.6–8.7	947	948	949	950	951	952
12.1–12.2	921	922	923	924	925	926
(b) M = 0.20–0.21						
8.8	996	997	998	999	1000	1001
12.1	972	973	974	975	976	977
15.9–16.0	956	957	958	959	960	961
(c) M = 0.29						
12.1–12.2	1005	1006	1007	1008	1009	-----

Spanwise Ridge Ice, Run EG1159

TABLE D.13.—CONTINUOUS-*AoA* SWEEP TESTS BY LOT NUMBER

[Sweep rate: 0.1 deg/s.]

Re×10^6	M		
	0.10–0.11	0.20	0.29
4.6	1124	------	------
8.4–8.7	1079	1135	------
12.1–12.2	1060	1106	1145
16.0	------	1090	------

TABLE D.14.—FIXED PITCH TESTS BY LOT NUMBER

Re×10^6	*AoA*, deg				
	–4	0	2	4	5
(a) M = 0.10–0.11					
4.6	1118	1119	1120	1121	1122
8.4	1073	1074	1075	1076	1077
12.1–12.2	1054	1055	1056	1057	1058
(b) M = 0.20–0.21					
8.6–8.7	1129	1130	1131	1132	1133
12.1–12.3	1100	1101	1102	1103	1104
15.8–16.0	1084	1085	1086	1087	1088
(c) M = 0.29					
12.0–12.2	1140	1141	1142	1143	------

Streamwise Ice 2, Run EG1125

TABLE D.15.—CONTINUOUS-*AoA* SWEEP TESTS BY LOT NUMBER
[Sweep rate: 0.1 deg/s.]

Re×10[6]	M		
	0.10	0.21	0.29
4.5	1359	------	------
8.2–8.9	1220	1290	------
12.1–12.2	1338	1253	1301
16.0	------	1232	------

TABLE D.16.—FIXED PITCH TESTS BY LOT NUMBER

Re×10[6]	*AoA*, deg					
	–4	0	4	8	10	11
(a) M = 0.10						
4.5	1352	1353	1354	1355	1356	1357
8.2–8.3	1213	1234	1215	1216	1217	1218
12.1–12.2	1331	1332	1333	1334	1335	1336
(b) M = 0.20–0.21						
8.9–9.0	1283	1284	1285	1286	1287	1288
12.1	1246	1247	1248	1249	1250	1251
15.9–16.0	1225	1226	1227	1228	1229	1230
(c) M = 0.29						
12.2	1295	1296	1297	1298	1299	------

Roughness Ice 2, Run EG1134

TABLE D.17.—CONTINUOUS-*AoA* SWEEP TESTS BY LOT NUMBER
[Sweep rate: 0.1 deg/s.]

Re×10[6]	M		
	0.10–0.11	0.21	0.29
4.6	1482	------	------
8.3–9.0	1429	1494	------
12.2	1398	1464	1505
15.8	------	1441	------

TABLE D.18.—FIXED PITCH TESTS BY LOT NUMBER

Re×10[6]	*AoA*, deg					
	–4	0	4	8	10	12
(a) M = 0.10–0.11						
4.6	1475	1476	1477	1478	1479	1480
8.3–8.4	1421	1423	1424	1425	1426	1427
12.1–12.3	1390	1403	1404	1405	1395	1396
(b) M = 0.20–0.21						
9.0	1487	1488	1489	1490	1491	1492
12.2–12.3	1456	1457	1458	1459	1461	1462
15.9–16.0	1434	1435	1436	1437	1438	1439
(c) M = 0.29						
12.1–12.2	1499	1500	1501	1502	1503	------

Appendix E.—Icing Research Tunnel Chord Subscale Model Test Results

Aerodynamic Test of Clean Model

V = 200 kt Re = 2.9×10^6
T_t = 21.0 °C M = 0.30
T_s = 15.6 °C

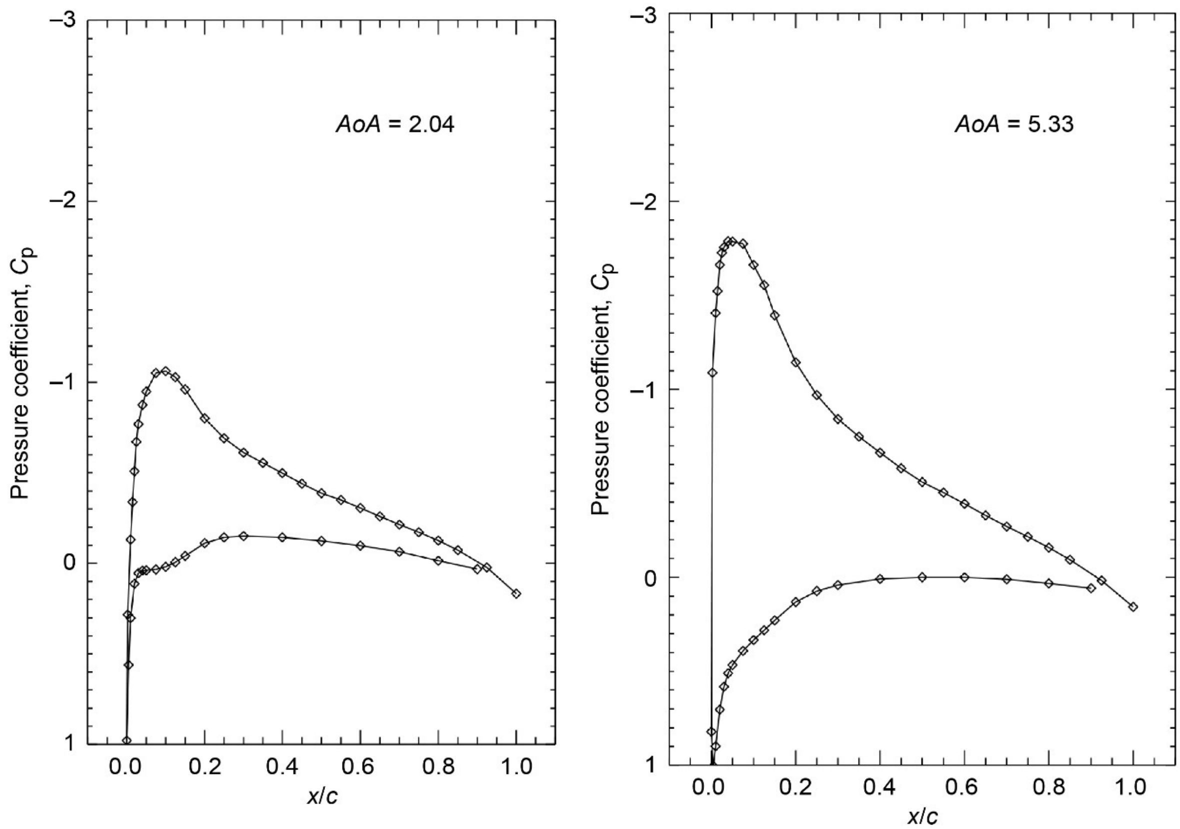

Aerodynamic Test of Clean Model

Appendix E.—IRT Subscale Model Tests

Run ED0711

V = 250 kt
T_t = –6.7 °C
T_s = –14.9 °C

AoA = 2.0°
LWC = 0.67 g/m^3
MVD = 15.4 μm
Exposure time = 10 min

Measured ice thickness

Station	Upper max, in.	Stag. line, in.	Lower max, in.
29.5	-	1.28	-
36	-	1.49	-
45.5	-	1.59	-

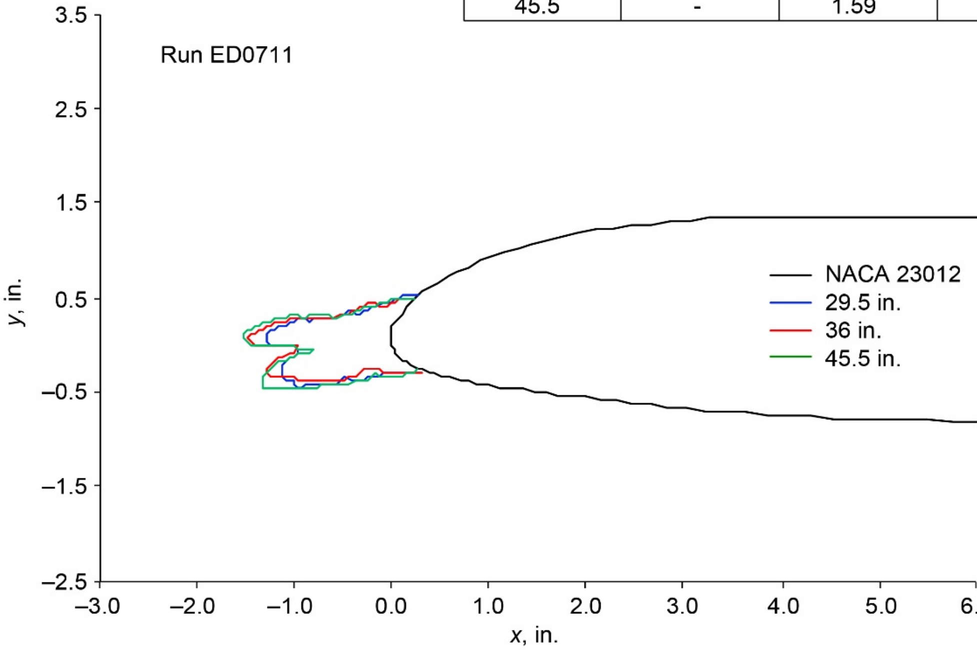

Pressure surface

Leading edge

Suction surface

Run ED0711

Appendix E.—IRT Subscale Model Tests

Run ED0712

V = 250 kt
T_t = –4.4 °C
T_s = –12.6 °C

AoA = 2.0°
LWC = 0.67 g/m^3
MVD = 15.4 µm
Exposure time = 10 min

Measured ice thickness*

Station	Upper max, in.	Stag. line, in.	Lower max, in.
30	1.35	0.57	1.19
-	-	-	-
-	-	-	-

*Ice broke off upper surface horn.

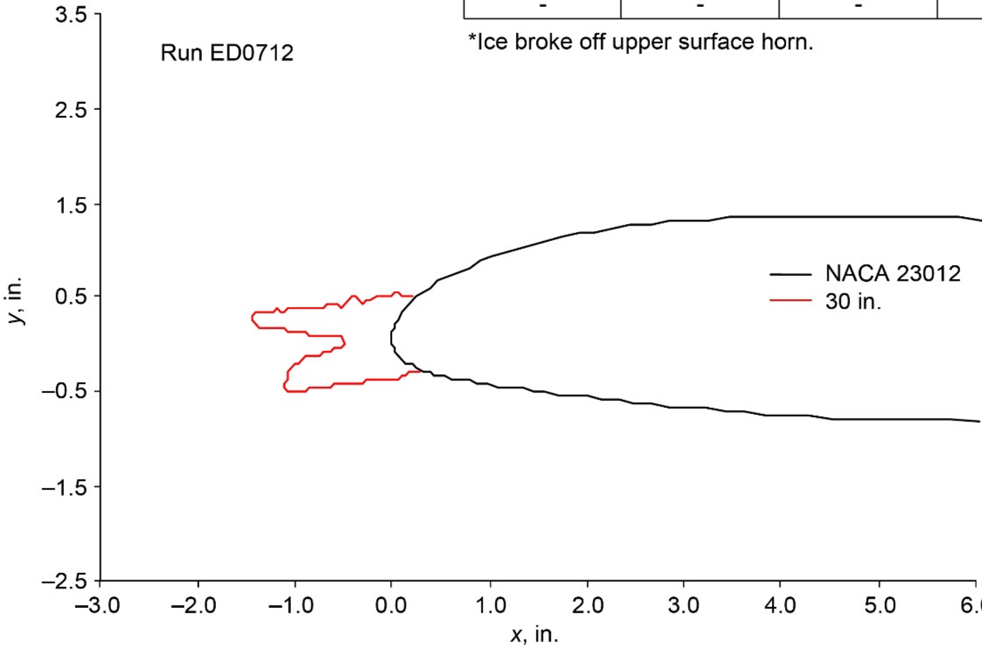

Pressure surface

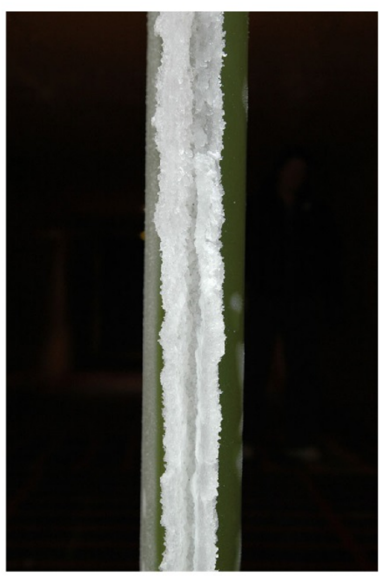

Leading edge

Suction surface

Run ED0712

Appendix E.—IRT Subscale Model Tests

Run ED0713

V = 175 kt	AoA = 5.0°
T_t = –4.4 °C	LWC = 0.64 g/m^3
T_s = –8.5 °C	MVD = 15.4 μm
	Exposure time = 10 min

Measured ice thickness

Station	Upper max, in.	Stag. line, in.	Lower max, in.
27.75	1.07	0.48	0.68
36	1.00	0.47	0.62
45	1.27	0.46	0.79

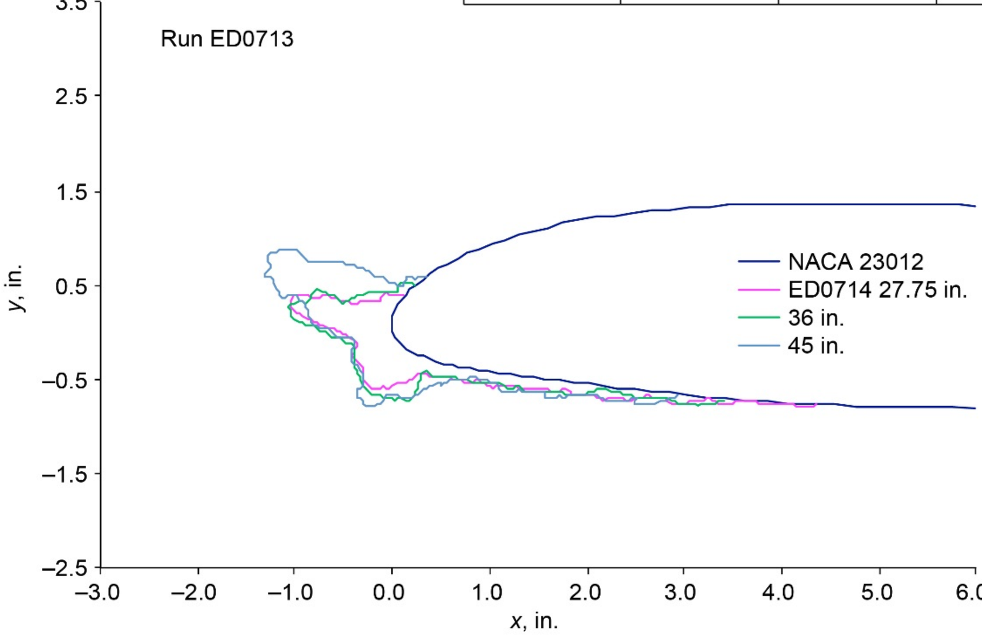

Pressure surface

Leading edge

Suction surface

Run ED0713

Appendix E.—IRT Subscale Model Tests

Run ED0714

V = 175 kt
T_t = –2.2 °C
T_s = –6.2 °C

AoA = 5.3°
LWC = 0.64 g/m^3
MVD = 15 µm
Exposure time = 10 min

Measured ice thickness

Station	Upper max, in.	Stag. line, in.	Lower max, in.
24.75	0.95	0.28	0.58
36	0.98	0.26	0.59
44	1.11	0.27	0.60

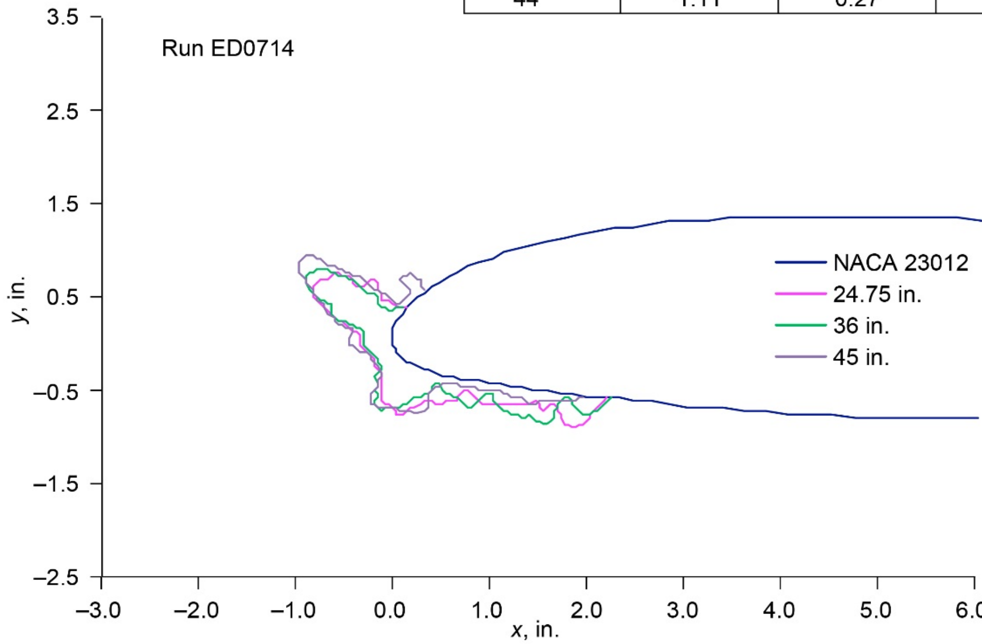

Pressure surface

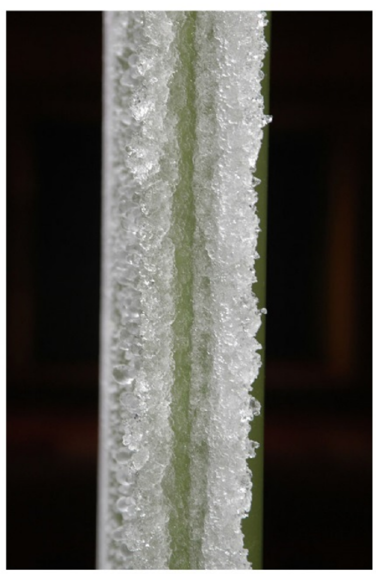

Leading edge

Suction surface

Run ED0714

Appendix E.—IRT Subscale Model Tests

Run ED0715

V = 175 kt
T_t = –1.1 °C
T_s = –5.1 °C

AoA = 5.0°
LWC = 0.64 g/m^3
MVD = 15 μm
Exposure time = 10 min

Measured ice thickness

Station	Upper max, in.	Stag. line, in.	Lower max, in.
28	0.93	0.14	0.59
36	0.82	0.17	0.52
41.5	1.08	0.18	0.92

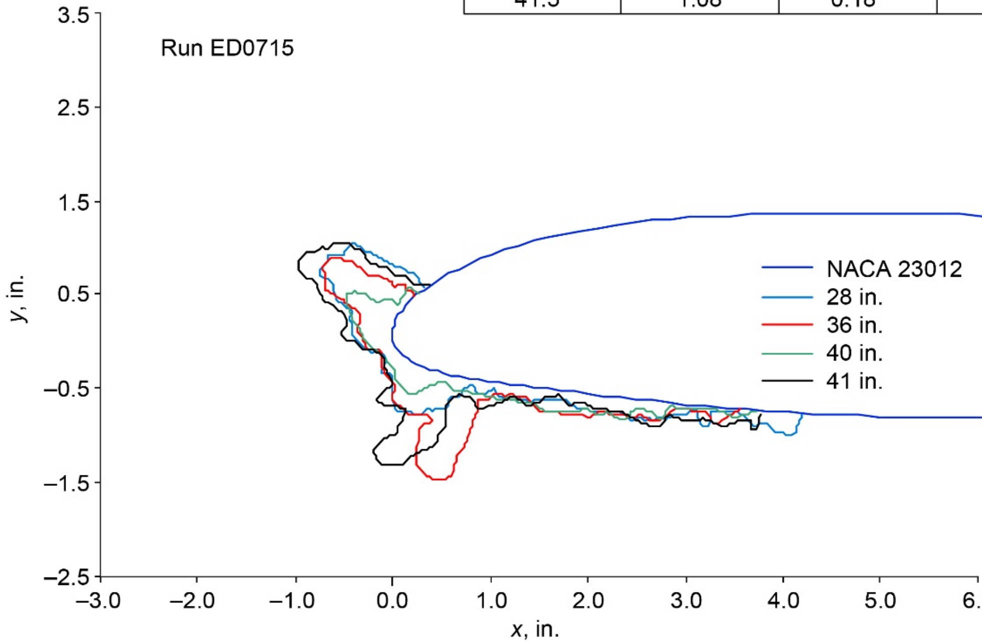

Pressure surface

Leading edge

Suction surface

Run ED0715

Appendix E.—IRT Subscale Model Tests

Run ED0716

V = 175 kt
T_t = –2.2 °C
T_s = –6.2 °C

AoA = 5.0°
LWC = 0.64 g/m^3
MVD = 15.0 µm
Exposure time = 10.0 min

Measured ice thickness

Station	Upper max, in.	Stag. line, in.	Lower max, in.
24.5	0.98	0.25	0.57
-	-	-	-
47.75	1.04	0.26	0.60

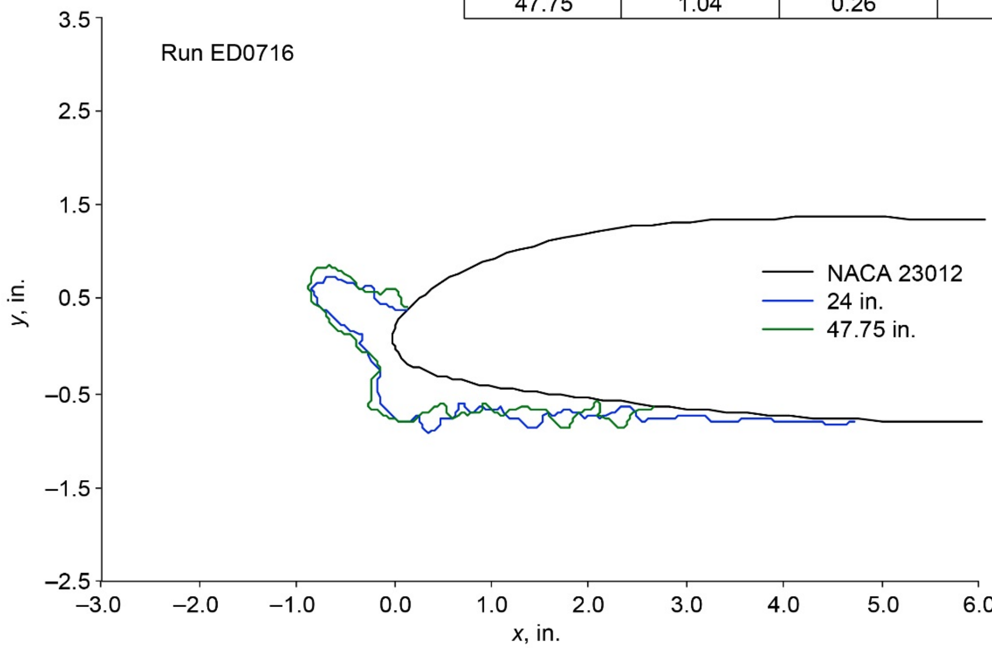

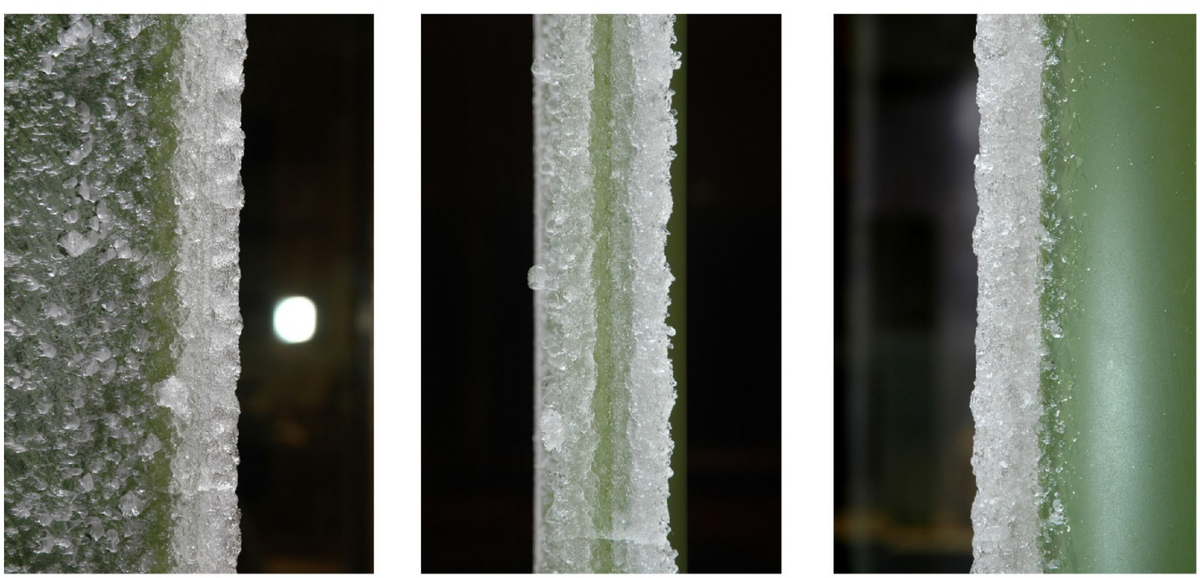

Pressure surface Leading edge Suction surface

Run ED0716

Appendix E.—IRT Subscale Model Tests

Run ED0717

V = 175 kt
T_t = –2.2 °C
T_s = –6.2 °C

AoA = 5.0°
LWC = 0.64 g/m^3
MVD = 15.0 µm
Exposure time = 10.0 min

Measured ice thickness

Station	Upper max, in.	Stag. line, in.	Lower max, in.
24	0.95	0.27	0.67
-	-	-	-
48	1.01	-	0.43

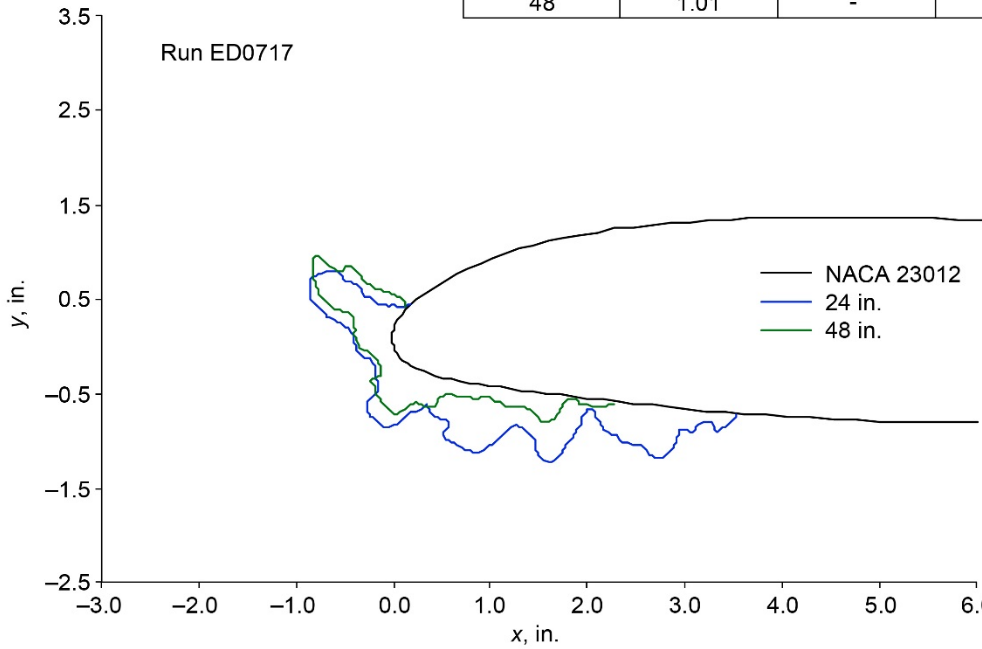

Pressure surface

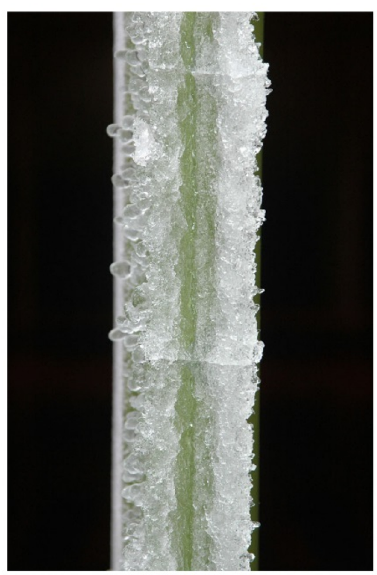

Leading edge

Suction surface

Run ED0717

Appendix E.—IRT Subscale Model Tests

Run ED0718

V = 17.5 kt
T_t = –2.2 °C
T_s = –6.2 °C

AoA = 5.0°
LWC = 0.64 g/m^3
MVD = 15.0 µm
Exposure time = 5.0 min

Measured ice thickness

Station	Upper max, in.	Stag. line, in.	Lower max, in.
36	0.61	0.15	0.28
40.5	0.57	0.15	0.30
43.5	0.65	0.15	0.33

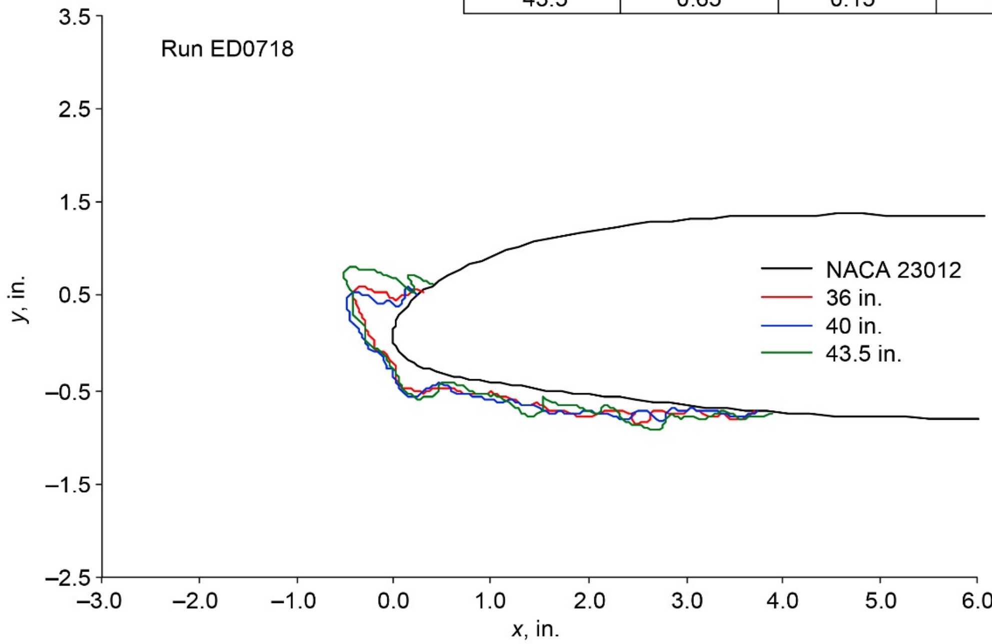

Pressure surface

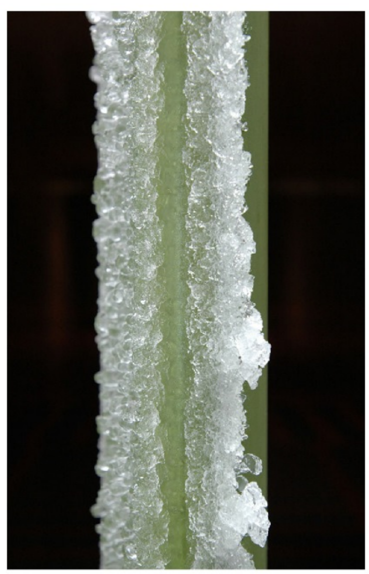

Leading edge

Suction surface

Run ED0718

Appendix E.—IRT Subscale Model Tests

Run ED0719

V = 175 kt
T_t = –2.2 °C
T_s = –6.2 °C

AoA = 5.0°
LWC = 0.64 g/m^3
MVD = 15.0 µm
Exposure time = 2.0 min

Measured ice thickness

Station	Upper max, in.	Stag. line, in.	Lower max, in.
-	-	-	-
36	0.16	0.08	0.14
-	-	-	-

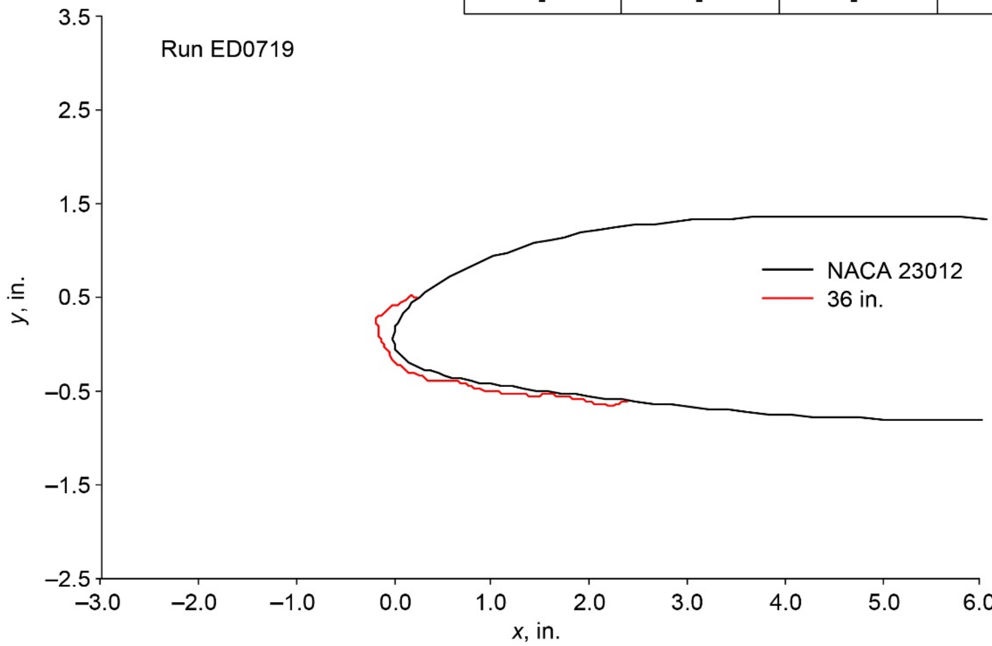

Pressure surface

Leading edge

Suction surface

Run ED0719

Appendix E.—IRT Subscale Model Tests

Run ED0720

V = 175 kt
T_t = –2.2 °C
T_s = –6.2 °C

AoA = 5.0°
LWC = 0.64 g/m^3
MVD = 15.0 µm
Exposure time = 0.5 min

Run ED0720

No tracings

Measured ice thickness*

Station	Upper max, in.	Stag. line, in.	Lower max, in.
-	-	-	-
-	-	-	-
-	-	-	-

*Not measureable.

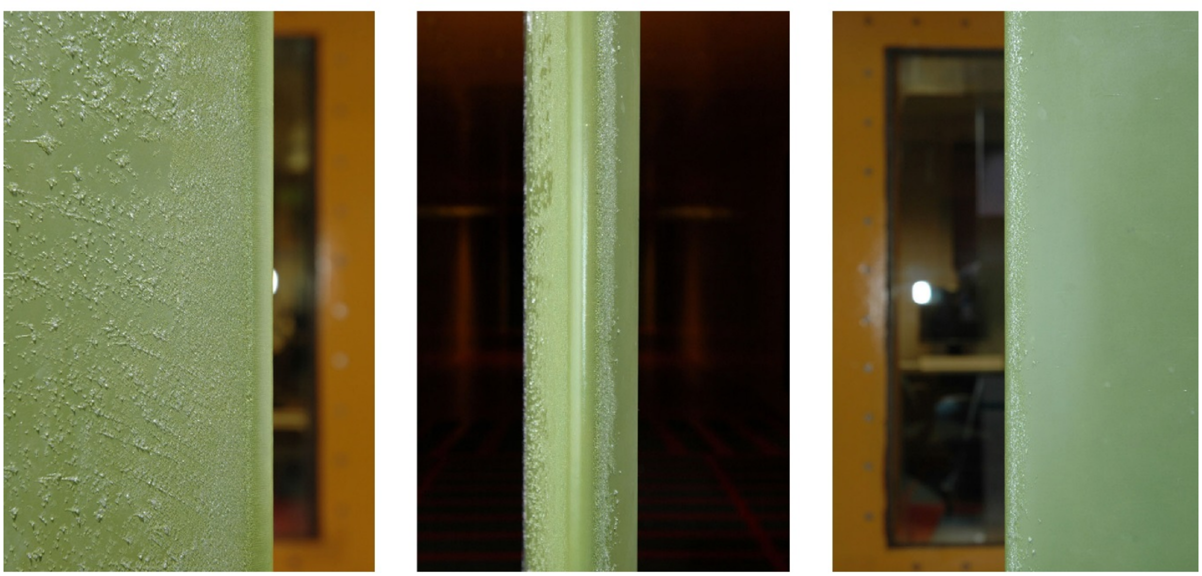

Pressure surface Leading edge Suction surface

Run ED0720

Appendix E.—IRT Subscale Model Tests

Run ED0721

V = 175 kt
T_t = –2.2 °C
T_s = –6.2 °C

AoA = 5.0°
LWC = 0.64 g/m^3
MVD = 15.0 µm
Exposure time = 5.0 min

Measured ice thickness

Station	Upper max, in.	Stag. line, in.	Lower max, in.
24	0.53	0.18	0.32
-	-	-	-
48	0.55	0	0.43

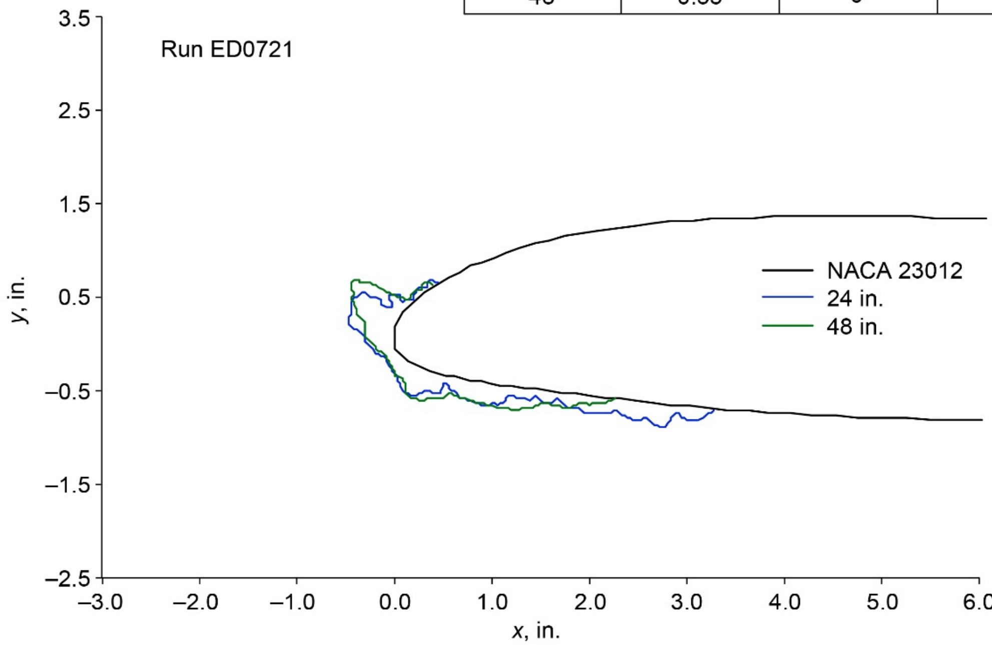

Pressure surface

Leading edge

Suction surface

Run ED0721

Appendix E.—IRT Subscale Model Tests

Run ED0722

V = 175 kt
T_t = –2.2 °C
T_s = –6.2 °C

AoA = 5.0°
LWC = 0.64 g/m^3
MVD = 15.0 µm
Exposure time = 1.0 min

Measured ice thickness

Station	Upper max, in.	Stag. line, in.	Lower max, in.
-	-	-	-
36	0.11	0.05	0.08
-	-	-	-

Run ED0722

No tracings


Pressure surface


Leading edge

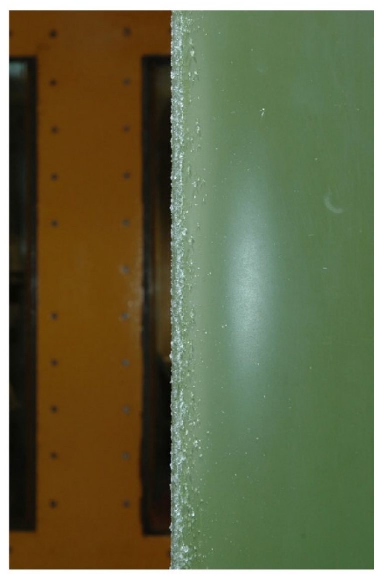
Suction surface

Run ED0722

Appendix E.—IRT Subscale Model Tests

Run ED0723

V = 175 kt
T_t = –2.2 °C
T_s = –6.2°F

AoA = 5.0°
LWC = 0.64 g/m^3
MVD = 15.0 µm
Exposure time = 0.5 min

Measured ice thickness

Station	Upper max, in.	Stag. line, in.	Lower max, in.
24	0.04	0.04	0.02
-	-	-	-
-	-	-	-

Run ED0723

No tracings

Pressure surface

Leading edge

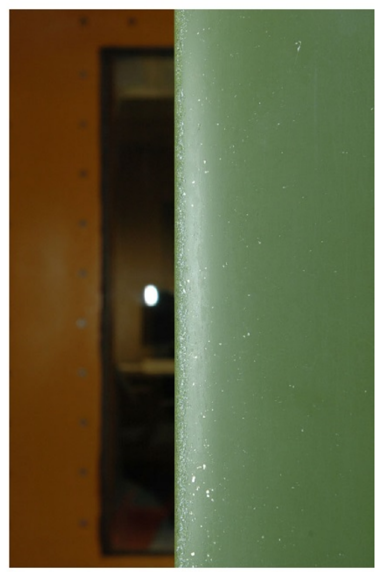

Suction surface

Run ED0723

Appendix E.—IRT Subscale Model Tests

Run ED0724

V = 250 kt
T_t = –13.3 °C
T_s = –21.7 °C

AoA = 2.0°
LWC = 0.33 g/m^3
MVD = 15.0 µm
Exposure time = 10.0 min

Measured ice thickness

Station	Upper max, in.	Stag. line, in.	Lower max, in.
-	-	-	-
36	-	0.69	-
43.125	-	0.86	-

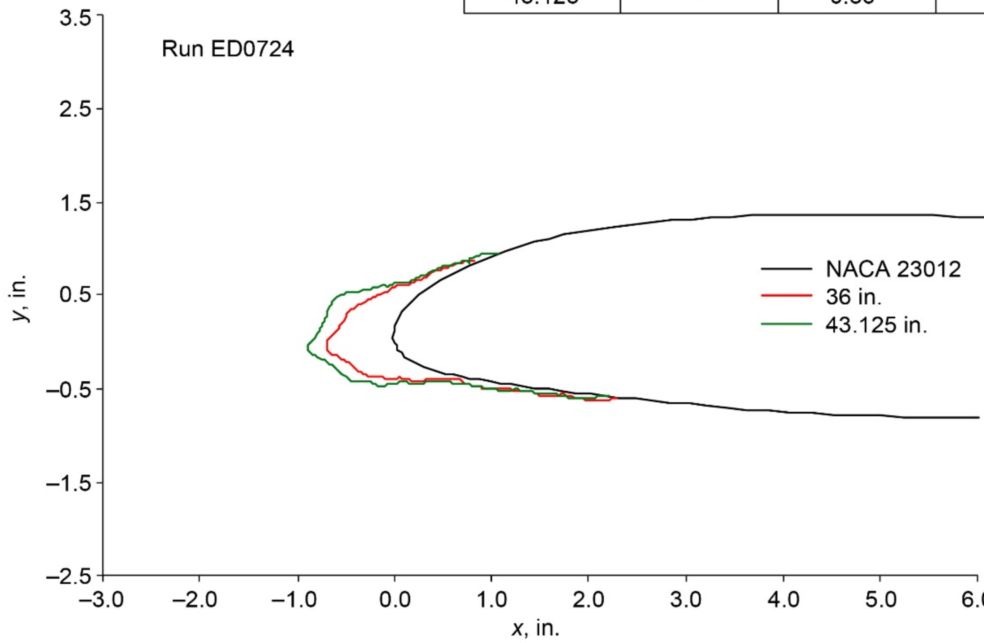

Pressure surface

Leading edge

Suction surface

Run ED0724

Run ED0725

V = 250 kt
T_t = –13.3 °C
T_s = –21.7 °C

AoA = 2.0°
LWC = 0.33 g/m^3
MVD = 15.0 µm
Exposure time = 5.0 min

Measured ice thickness

Station	Upper max, in.	Stag. line, in.	Lower max, in.
24	-	0.30	-
-	-	-	-
48	-	0.33	-

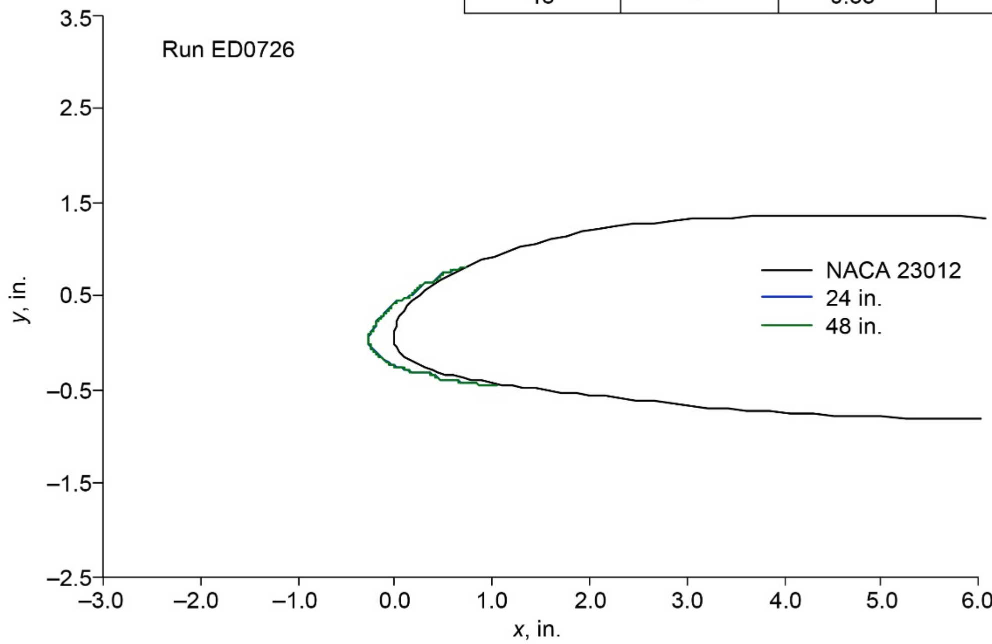

Pressure surface   Leading edge   Suction surface

Figure E18–Run # ED0726

Run ED0725

Appendix E.—IRT Subscale Model Tests

Run ED0726

V = 250 kt
T_t = –13.3 °C
T_s = –21.7 °C

AoA = 2.0°
LWC = 0.33 g/m^3
MVD = 15.0 µm
Exposure time = 5.0 min

Measured ice thickness

Station	Upper max, in.	Stag. line, in.	Lower max, in.
24	-	0.30	-
-	-	-	-
48	-	0.33	-

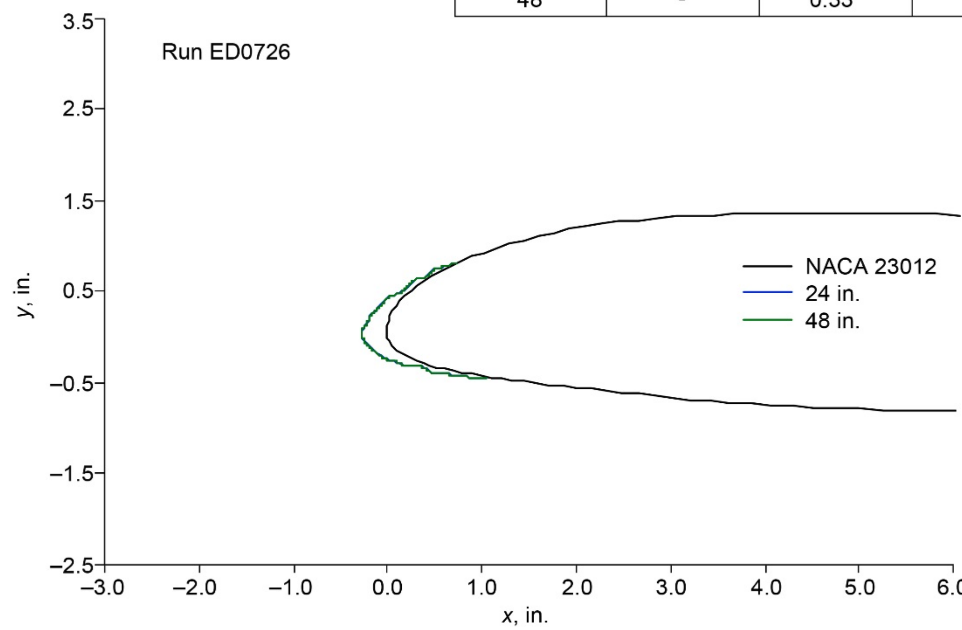

Pressure surface Leading edge Suction surface

Run ED0726

Appendix E.—IRT Subscale Model Tests

Run ED0727

V = 175 kt
T_t = –17.8 °C
T_s = –21.8 °C

AoA = 5.0°
LWC = 0.30 g/m^3
MVD = 15.0 µm
Exposure time = 10.0 min

Measured ice thickness

Station	Upper max, in.	Stag. line, in.	Lower max, in.
-	-	-	-
36	-	0.41	-
43	-	0.49	-

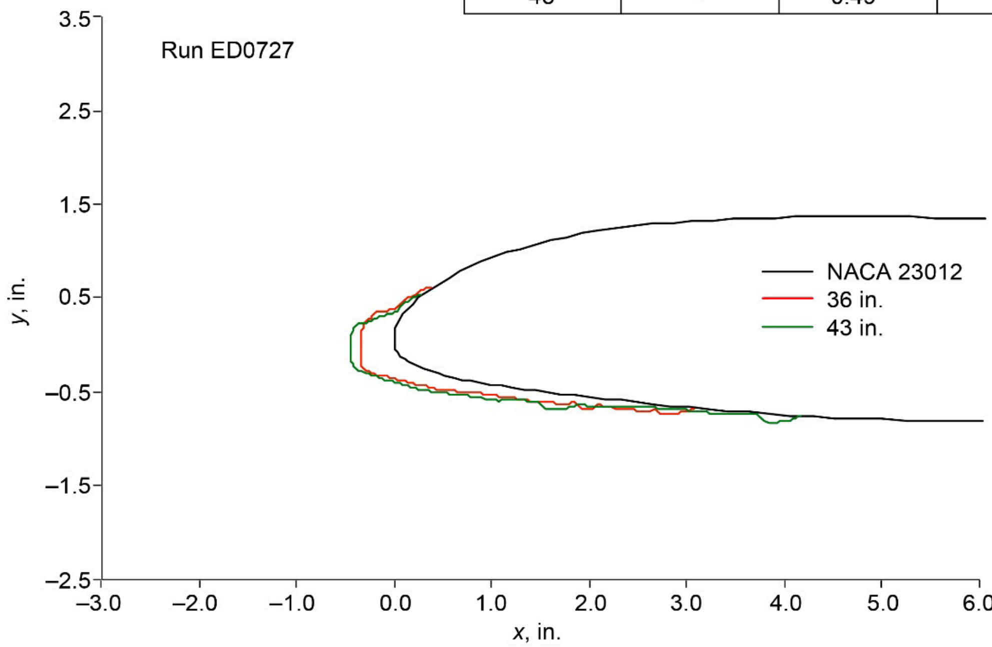

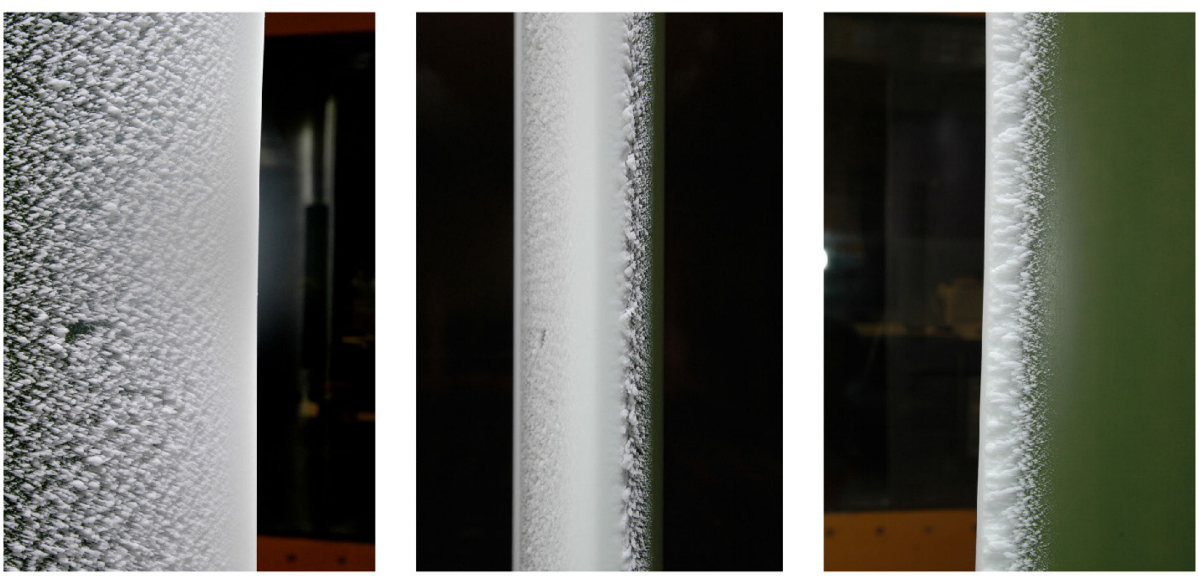

Pressure surface Leading edge Suction surface

Run ED0727

Appendix E.—IRT Subscale Model Tests

Run ED0728

V = 175 kt
T_t = –17.8 °C
T_s = –21.8 °C

AoA = 5.0°
LWC = 0.30 g/m^3
MVD = 15.0 µm
Exposure time = 5.0 min

Measured ice thickness

Station	Upper max, in.	Stag. line, in.	Lower max, in.
-	-	-	-
36	-	0.21	-
-	-	-	-

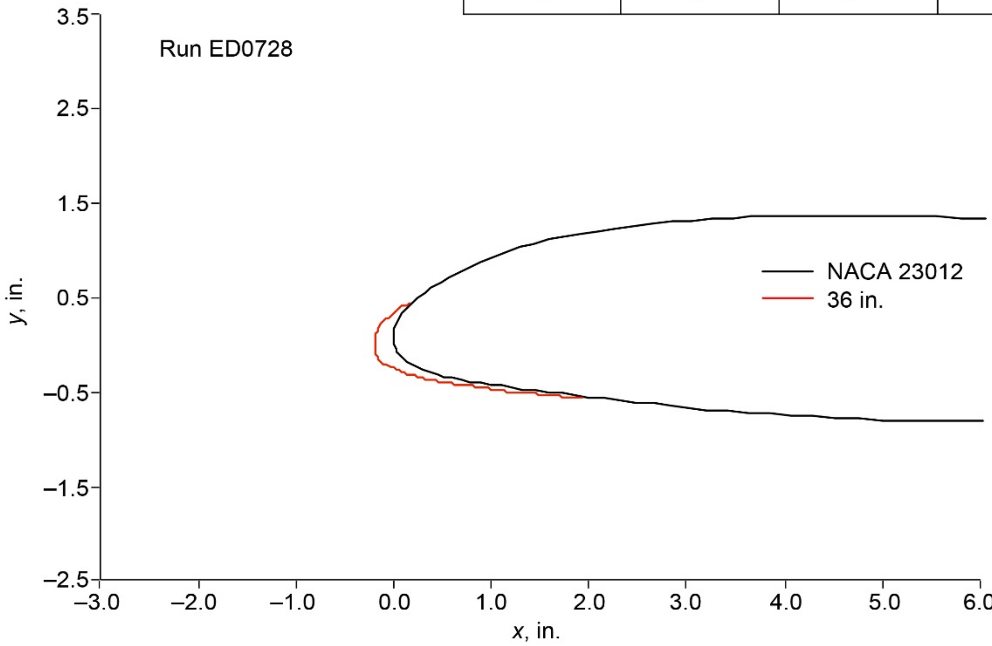


Pressure surface

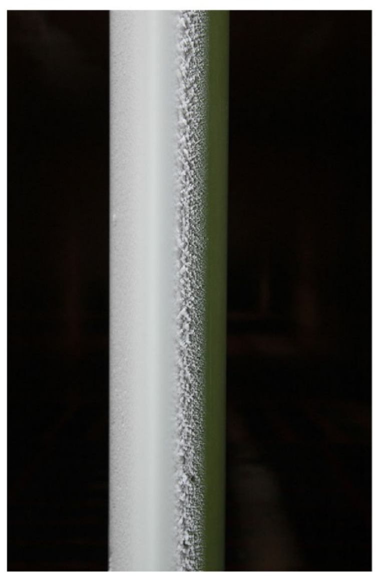
Leading edge


Suction surface

Run ED0728

Appendix E.—IRT Subscale Model Tests

Run ED0729

V = 175 kt
T_t = –17.8 °C
T_s = –21.8 °C

AoA = 5.0°
LWC = 0.30 g/m^3
MVD = 15.0 μm
Exposure time = 1.0 min

Measured ice thickness

Station	Upper max, in.	Stag. line, in.	Lower max, in.
-	-	-	-
36	0.02	0.05	0.01
-	-	-	-

Run ED0729

No tracings

Pressure surface Leading edge Suction surface

Run ED0729

Appendix E.—IRT Subscale Model Tests

Run ED0730

V = 175 kt
T_t = –17.8 °C
T_s = –21.8 °C

AoA = 5.0°
LWC = 0.30 g/m^3
MVD = 15.0 µm
Exposure time = 5.0 min

Measured ice thickness

Station	Upper max, in.	Stag. line, in.	Lower max, in.
24	-	0.17	-
-	-	-	-
48	-	0.19	-

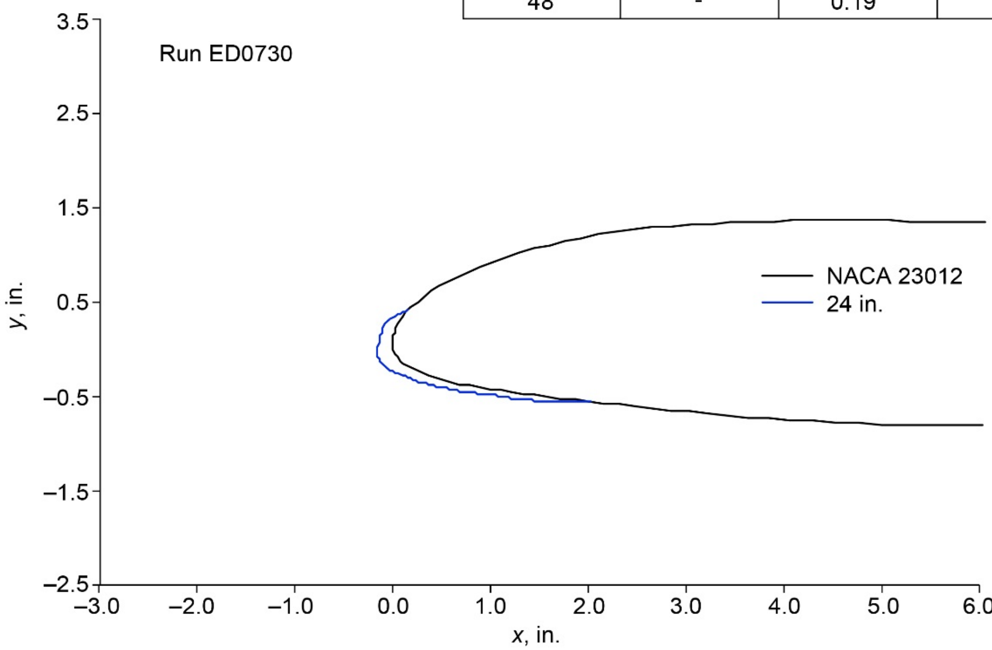

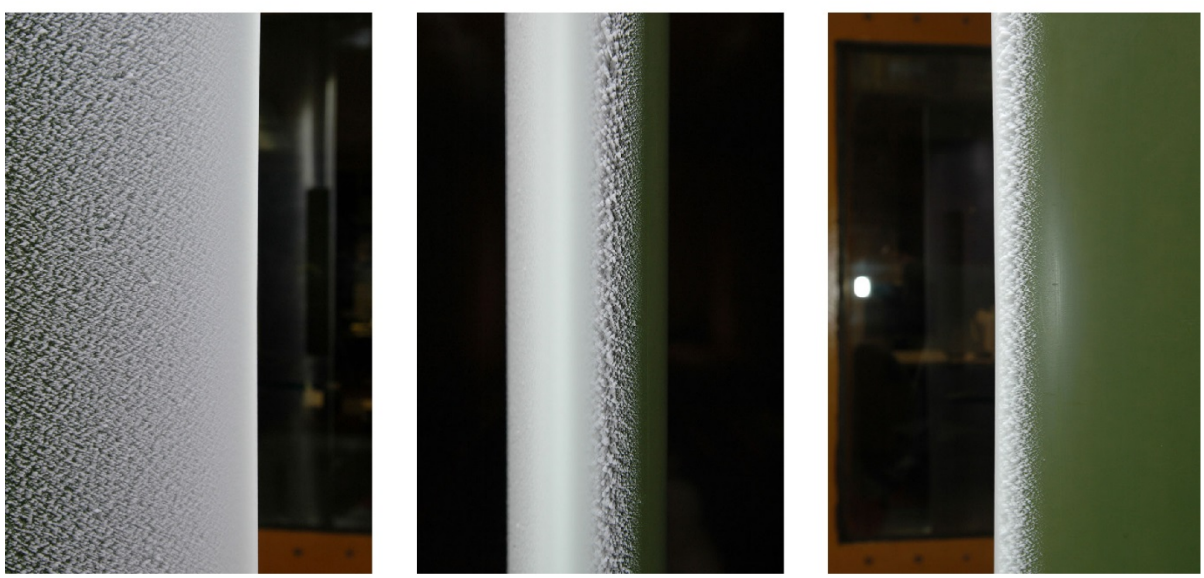

Pressure surface Leading edge Suction surface

Run ED0730

Appendix E.—IRT Subscale Model Tests

Run ED0731

V = 175 kt
T_t = –17.8 °C
T_s = –21.8 °C

AoA = 5.0°
LWC = 0.30 g/m^3
MVD = 15.0 µm
Exposure time = 2.0 min

Measured ice thickness

Station	Upper max, in.	Stag. line, in.	Lower max, in.
-	-	-	-
36	0.05	0.08	0.02
-	-	-	-

Run ED0731

No tracings

Pressure surface

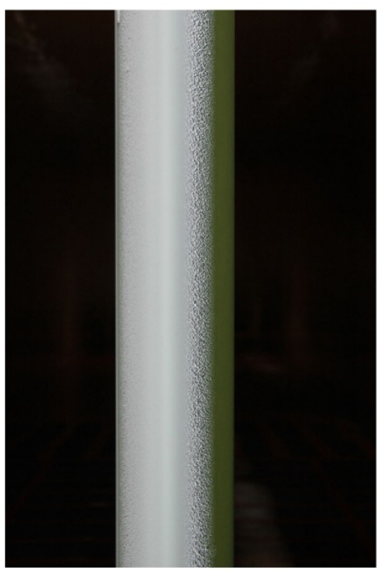

Leading edge

Suction surface

Run ED0731

Appendix E.—IRT Subscale Model Tests

Run ED0732

V = 250 kt
T_t = –2.2 °C
T_s = –10.5 °C

AoA = 2.0°
LWC = 0.67 g/m^3
MVD = 15.4 µm
Exposure time = 5.0 min

Measured ice thickness

Station	Upper max, in.	Stag. line, in.	Lower max, in.
27.75	0.85	0.16	0.65
36	1.04	0.15	0.85
-	-	-	-

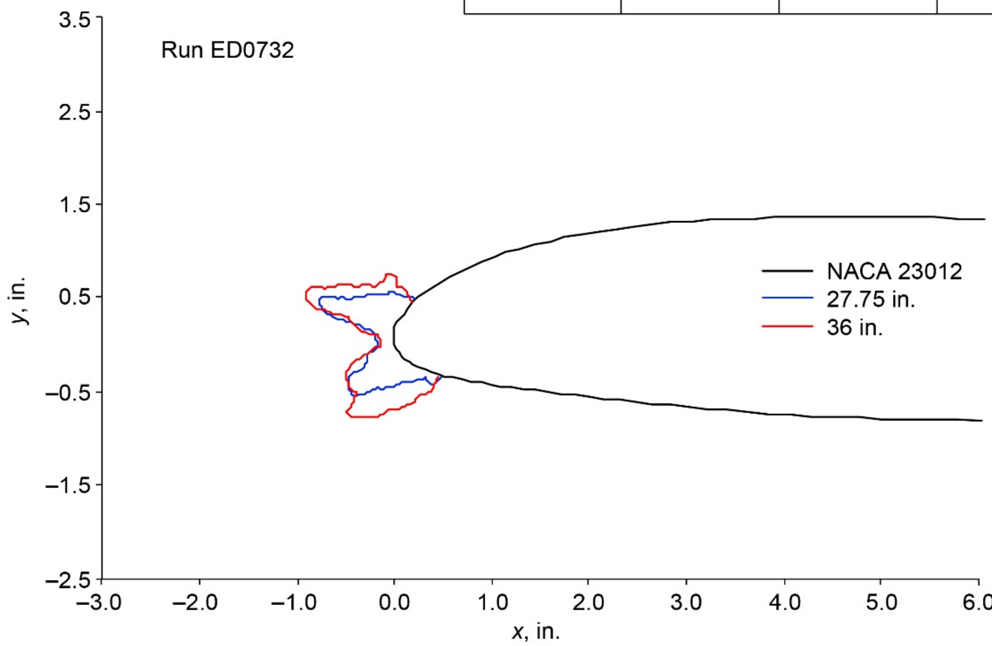

Pressure surface

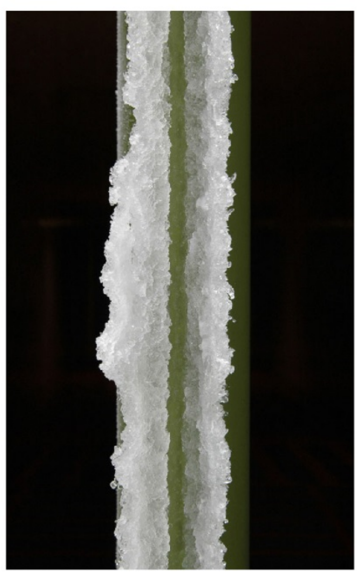

Leading edge

Suction surface

Run ED0732

Appendix E.—IRT Subscale Model Tests

Run ED0733

V = 200 kt
T_t = –2.2 °C
T_s = –7.5 °C

AoA = 2.0°
LWC = 0.75 g/m^3
MVD = 15.4 µm
Exposure time = 5.0 min

Measured ice thickness

Station	Upper max, in.	Stag. line, in.	Lower max, in.
29	0.76	0.15	0.54
36	0.77	0.16	0.65
45.25	1.05	0.14	0.64

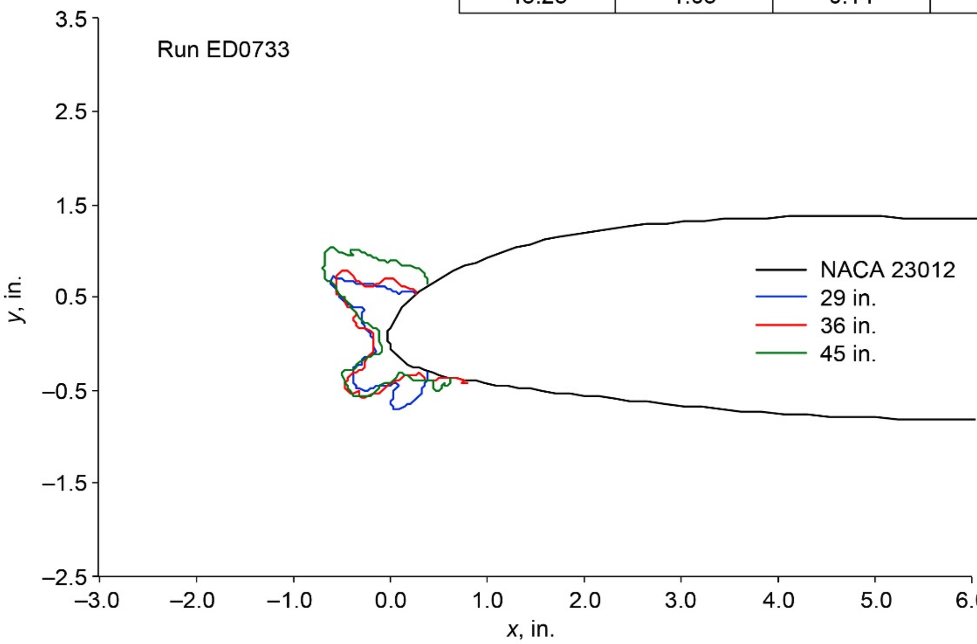

Pressure surface Leading edge Suction surface

Run ED0733

Appendix E.—IRT Subscale Model Tests

Run ED0734

V = 200 kt
T_t = –2.2 °C
T_s = –7.5 °C

AoA = 2.0°
LWC = 1.06 g/m^3
MVD = 17.6 μm
Exposure time = 5.0 min

Measured ice thickness

Station	Upper max, in.	Stag. line, in.	Lower max, in.
25.75	0.75	0.14	0.60
36	0.93	0.15	0.68
38.75	0.99	0.13	0.70

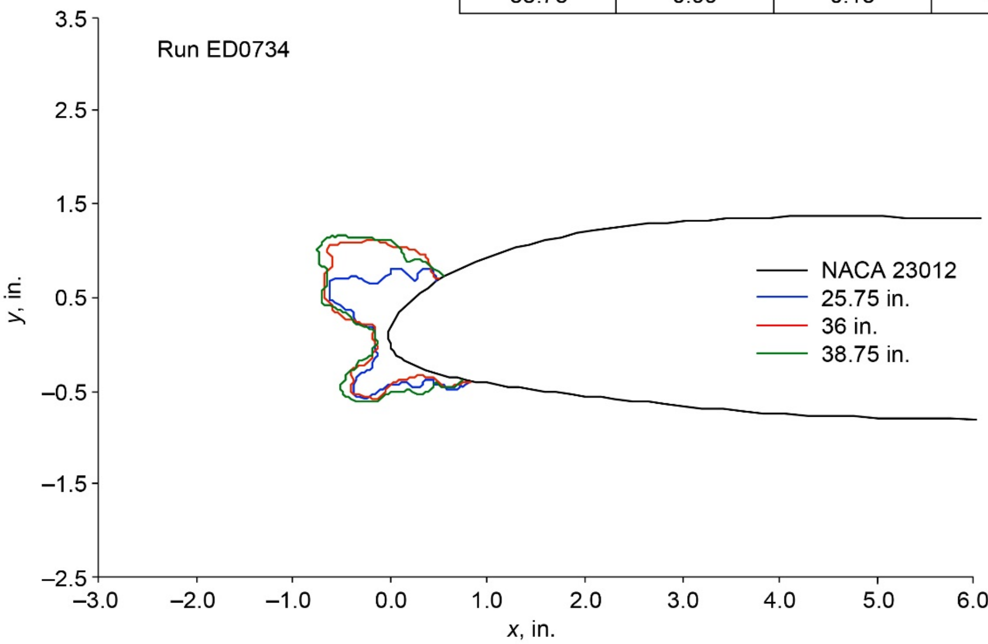

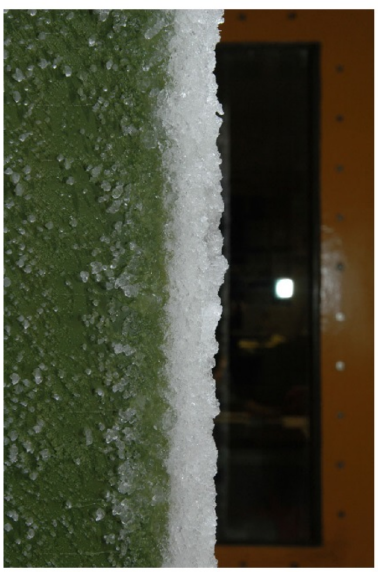

Pressure surface

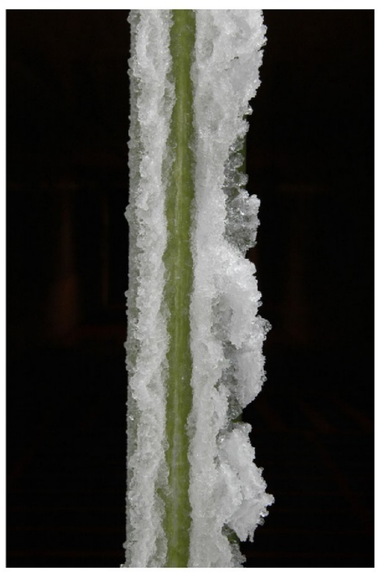

Leading edge

Suction surface

Run ED0734

Appendix E.—IRT Subscale Model Tests

Run ED0735

V = 200 kt
T_t = –2.2 °C
T_s = –7.5 °C

AoA = 2.0°
LWC = 0.75 g/m^3
MVD = 15.4 µm
Exposure time = 5.0 min

Measured ice thickness

Station	Upper max, in.	Stag. line, in.	Lower max, in.
24	0.88	0.15	0.62
-	-	-	-
48	0.79	0.15	0.56

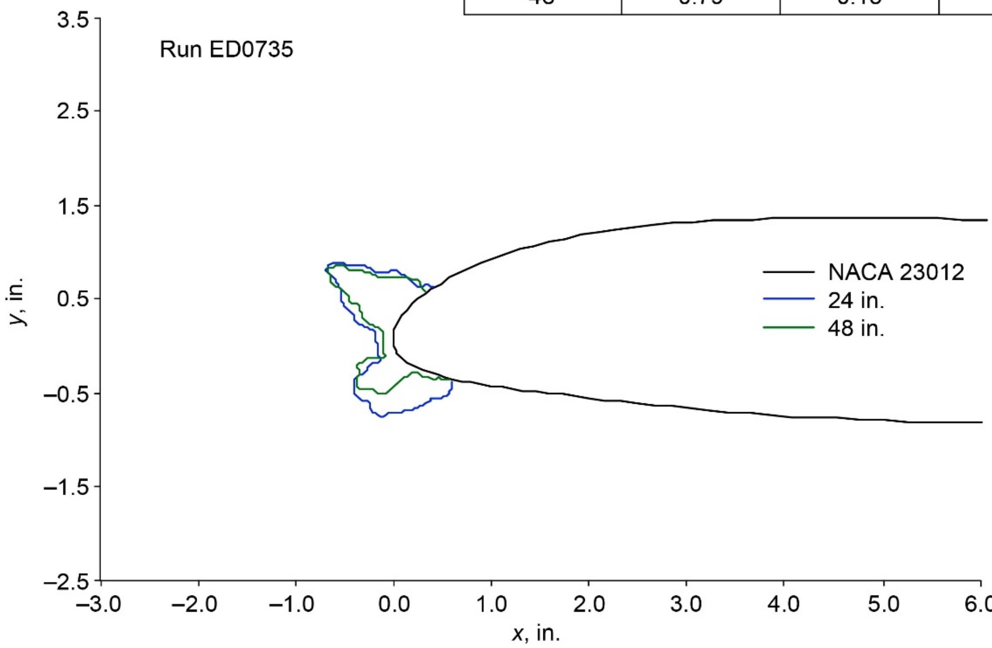

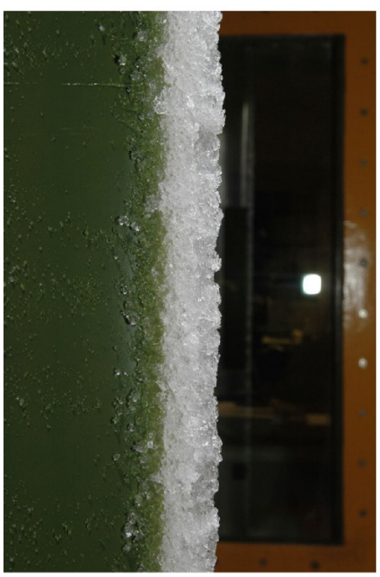

Pressure surface

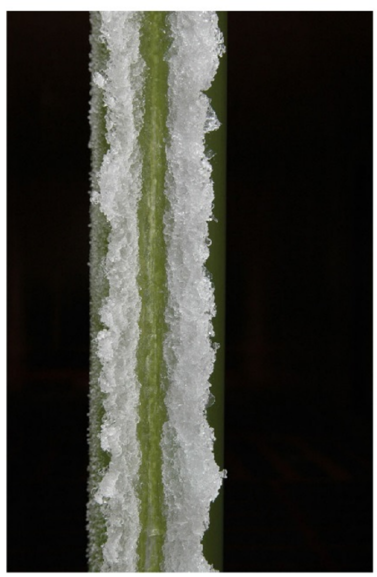

Leading edge

Suction surface

Run ED0735

Appendix E.—IRT Subscale Model Tests

Run ED0736

V = 200 kt
T_t = –2.2 °C
T_s = –6.2 °C

AoA = 5.0°
LWC = 0.64 g/m^3
MVD = 15.0 µm
Exposure time = 0.5 min

Measured ice thickness

Station	Upper max, in.	Stag. line, in.	Lower max, in.
-	-	-	-
36	0.04	0.03	0.01
-	-	-	-

Run ED0736

No tracings


Pressure surface


Leading edge


Suction surface

Run ED0736

Appendix E.—IRT Subscale Model Tests

Run ED0737

V = 175 kt
T_t = –4.4 °C
T_s = –8.5 °C

AoA = 5.0°
LWC = 0.64 g/m^3
MVD = 15.0 µm
Exposure time = 10.0 min

Measured ice thickness

Station	Upper max, in.	Stag. line, in.	Lower max, in.
24	1.12	0.44	0.72
-	-	-	-
48	1.18	-	0.80

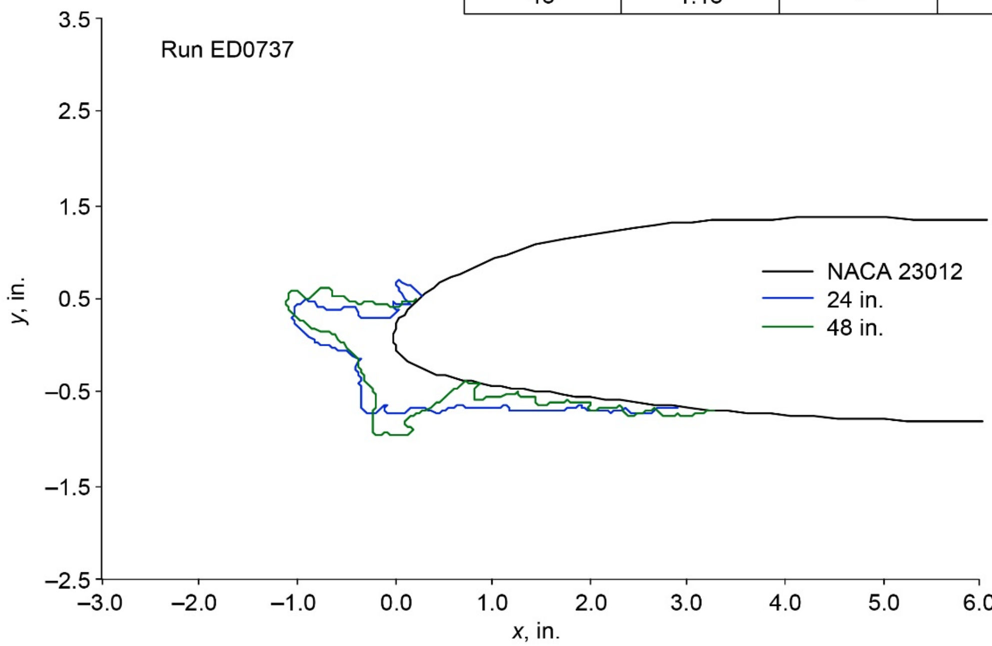


Pressure surface


Leading edge


Suction surface

Run ED0737

Appendix E.—IRT Subscale Model Tests

Run ED0738

V = 250 kt
T_t = –13.3 °C
T_s = –21.7 °C

AoA = 2.0°
LWC = 0.33 g/m^3
MVD = 15.0 µm
Exposure time = 5.0 min

Measured ice thickness

Station	Upper max, in.	Stag. line, in.	Lower max, in.
-	-	-	-
36	-	0.35	-
43.5	-	0.36	-

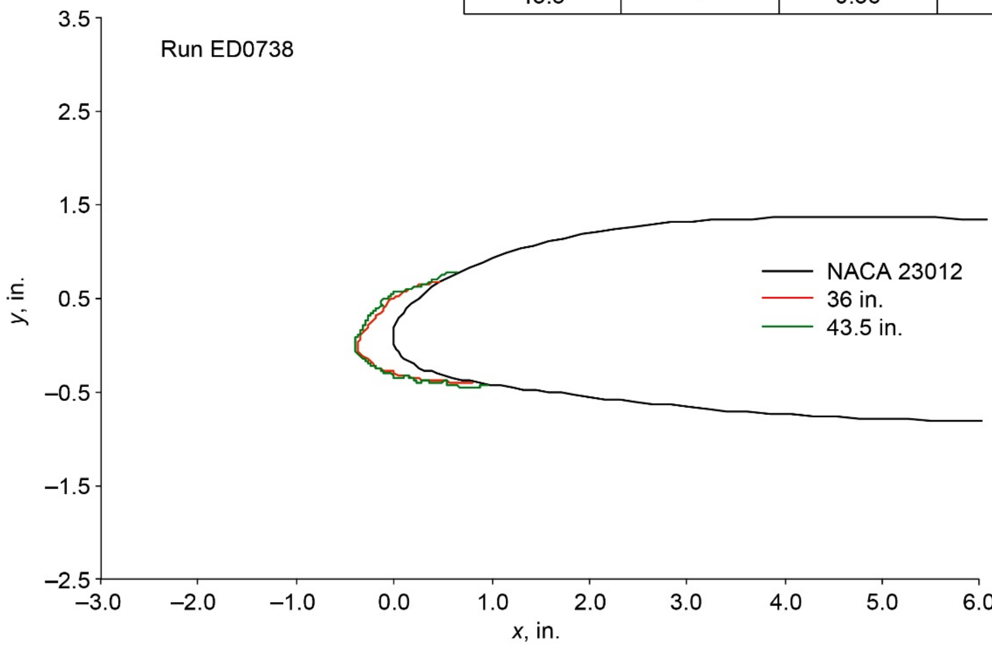


Pressure surface


Leading edge


Suction surface

Run ED0738

Run ED0739

V = 175 kt
T_t = –17.8 °C
T_s = –21.8 °C

AoA = 5.0°
LWC = 0.30 g/m^3
MVD = 15.0 µm
Exposure time = 1.0 min

Measured ice thickness

Station	Upper max, in.	Stag. line, in.	Lower max, in.
-	-	-	-
-	-	-	-
-	-	-	-

Run ED0739

No tracings

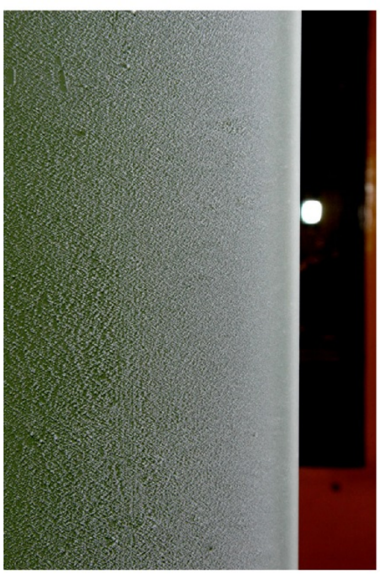

Pressure surface

Leading edge

Suction surface

Run ED0740

V = 250 kt
T_t = –4.4 °C
T_s = –12.3 °C

AoA = 2.0°
LWC = 0.67 g/m^3
MVD = 15.4 µm
Exposure time = 10.5 min

Measured ice thickness

Station	Upper max, in.	Stag. line, in.	Lower max, in.
-	-	-	-
-	-	-	-
-	-	-	-

Run ED0740

No tracings

Pressure surface

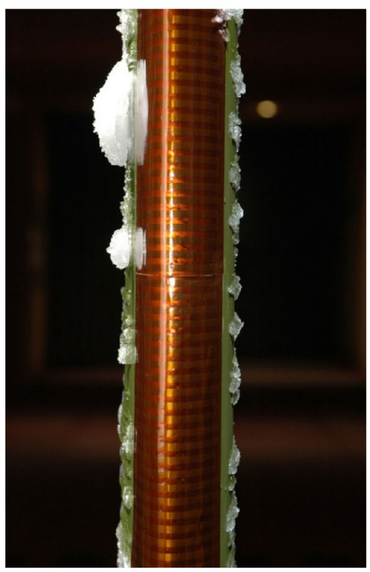

Leading edge

Suction surface

Run ED0740

Appendix E.—IRT Subscale Model Tests

Run ED0741

V = 175 kt
T_t = –4.4 °C
T_s = –8.5 °C

AoA = 0.0°
LWC = 0.64 g/m^3
MVD = 15.0 µm
Exposure time = 15.0 min

Measured ice thickness

Station	Upper max, in.	Stag. line, in.	Lower max, in.
-	-	-	-
36	0.79	0	0.27
-	-	-	-

Run ED0741

No tracings

Pressure surface

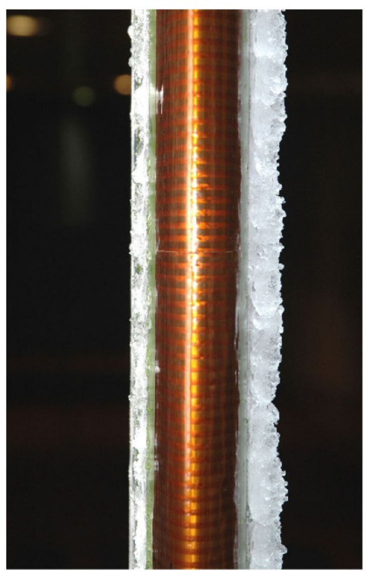

Leading edge

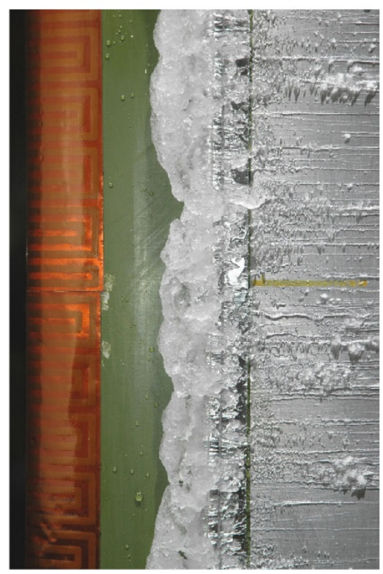

Suction surface

Run ED0741

Appendix E.—IRT Subscale Model Tests

Run ED0742

V = 175 kt
T_t = –4.4 °C
T_s = –8.5 °C

AoA = 0.0°
LWC = 0.64 g/m^3
MVD = 15.0 µm
Exposure time = 10.0 min

Measured ice thickness

Station	Upper max, in.	Stag. line, in.	Lower max, in.
-	-	-	-
36	0.57	0	0.60
-	-	-	-

Run ED0742

No tracings

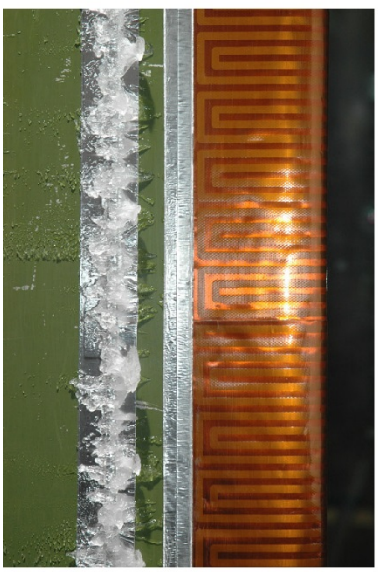

Pressure surface

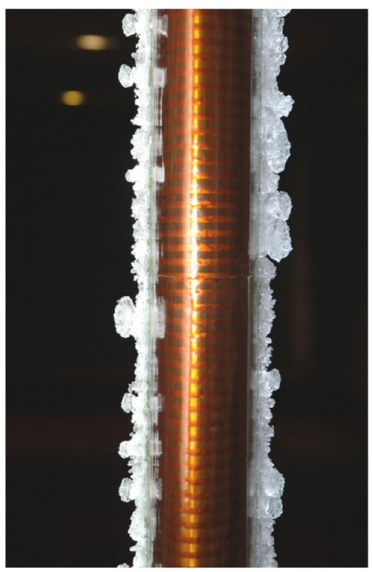

Leading edge

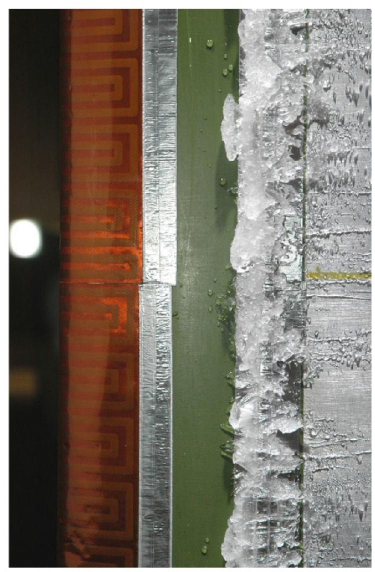

Suction surface

Run ED0742

Appendix E.—IRT Subscale Model Tests

Run ED0743

V = 175 kt
T_t = –9.4 °C
T_s = –13.5 °C

AoA = 0.0°
LWC = 0.64 g/m^3
MVD = 15.0 µm
Exposure time = 5.0 min

Measured ice thickness

Station	Upper max, in.	Stag. line, in.	Lower max, in.
-	-	-	-
36	0.17	0	0.18
-	-	-	-

Run ED0743

No tracings

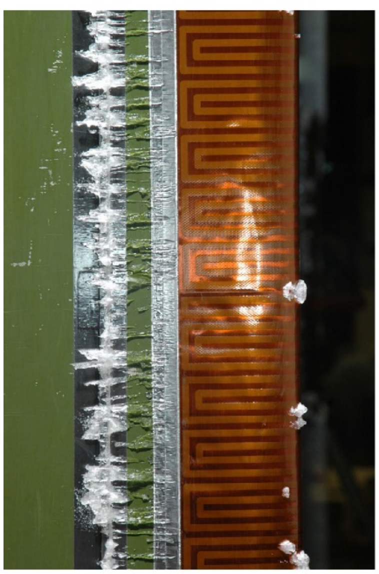

Pressure surface

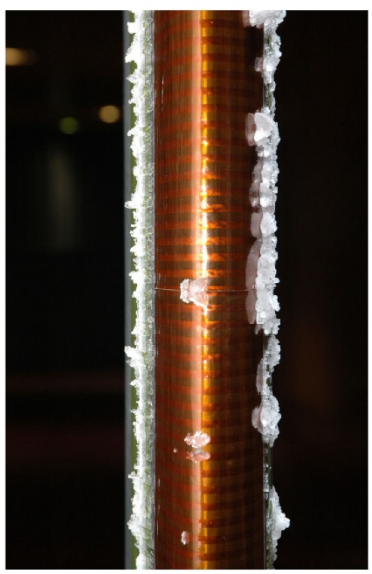

Leading edge

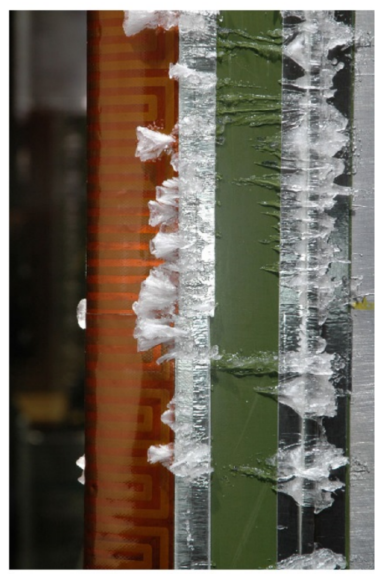

Suction surface

Run ED0743

Appendix E.—IRT Subscale Model Tests

Run ED0744

V = 175 kt
T_t = –2.2 °C
T_s = –6.2 °C

AoA = 5.0°
LWC = 0.64 g/m^3
MVD = 15.0 μm
Exposure time = 0.5 min

Measured ice thickness

Station	Upper max, in.	Stag. line, in.	Lower max, in.
-	-	-	-
-	-	-	-
49	0.02	0.01	0.01

Run ED0744

No tracings

Pressure surface

Leading edge

Suction surface

Run ED0744

Appendix E.—IRT Subscale Model Tests

Run ED0745

V = 200 kt
T_t = –2.2 °C
T_s = –7.5 °C

AoA = 2.0°
LWC = 0.75 g/m^3
MVD = 15.4 μm
Exposure time = 2.0 min

Measured ice thickness

Station	Upper max, in.	Stag. line, in.	Lower max, in.
24.75	0.25	0.08	0.26
36	0.35	0.08	0.25
41.5	0.40	0.07	0.24

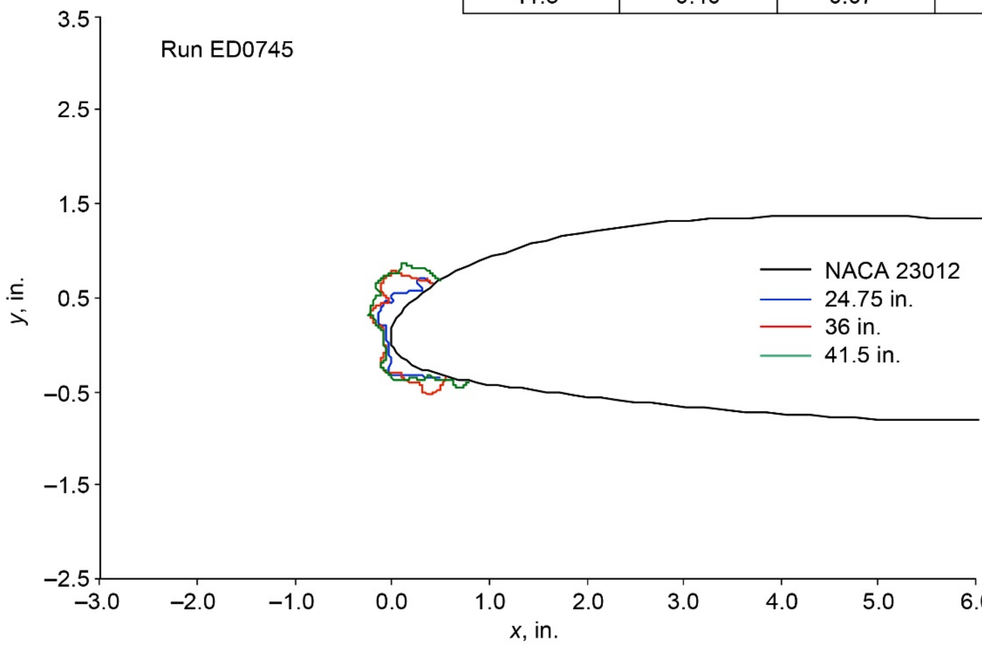

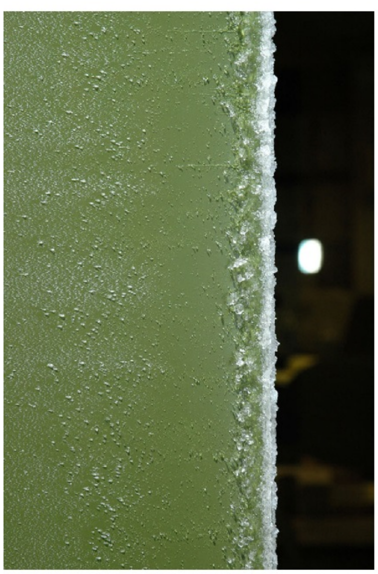

Pressure surface

Leading edge

Suction surface

Run ED0745

Appendix E.—IRT Subscale Model Tests

Run ED0746

V = 200 kt
T_t = –2.2 °C
T_s = –7.5 °C

AoA = 2.0°
LWC = 0.75 g/m^3
MVD = 15.4 µm
Exposure time = 0.5 min

Measured ice thickness

Station	Upper max, in.	Stag. line, in.	Lower max, in.
-	-	-	-
36	0.05	0.03	0.07
-	-	-	-

Run ED0746

No tracings

Pressure surface

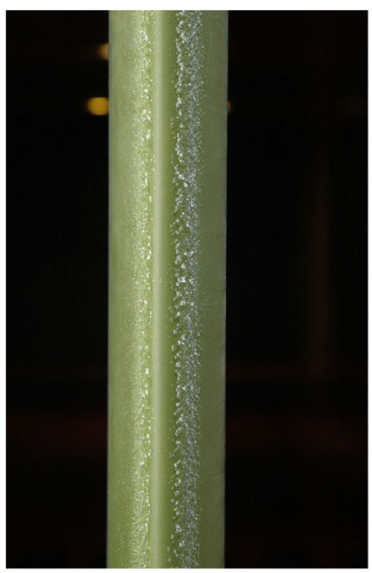

Leading edge

Suction surface

Run ED0746

Appendix E.—IRT Subscale Model Tests

Run ED0747

V = 250 kt
T_t = –2.2 °C
T_s = –10.5 °C

AoA = 2.0°
LWC = 0.67 g/m^3
MVD = 15.4 µm
Exposure time = 0.5 min

Measured ice thickness

Station	Upper max, in.	Stag. line, in.	Lower max, in.
-	-	-	-
36	0.09	0.04	0.06
-	-	-	-

Run ED0747

No tracings

Pressure surface

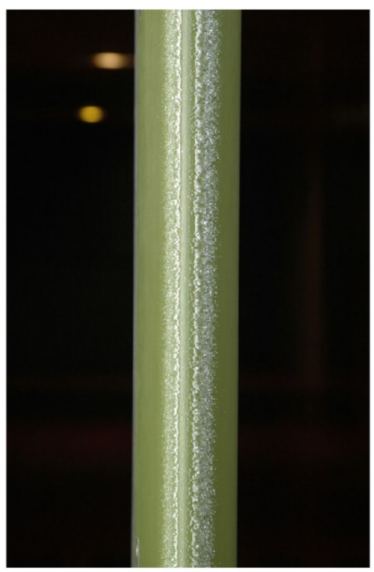

Leading edge

Suction surface

Run ED0747

Appendix E.—IRT Subscale Model Tests

Run ED0748

V = 175 kt
T_t = –17.8 °C
T_s = –21.8 °C

AoA = 5.0°
LWC = 0.30 g/m^3
MVD = 15.0 µm
Exposure time = 1.0 min

Measured ice thickness

Station	Upper max, in.	Stag. line, in.	Lower max, in.
24	<0.01	0.04	<0.01
-	-	-	-
-	-	-	-

Run ED0748

No tracings

Pressure surface

Leading edge

Suction surface

Run ED0748

Appendix E.—IRT Subscale Model Tests

Run ED0749

V = 175 kt
T_t = –4.4 °C
T_s = –8.5 °C

AoA = 0.0°
LWC = 0.64 g/m^3
MVD = 15.0 µm
Exposure time = 5.0 min

Measured ice thickness

Station	Upper max, in.	Stag. line, in.	Lower max, in.
-	-	-	-
36	0.08	0	0.11
-	-	-	-

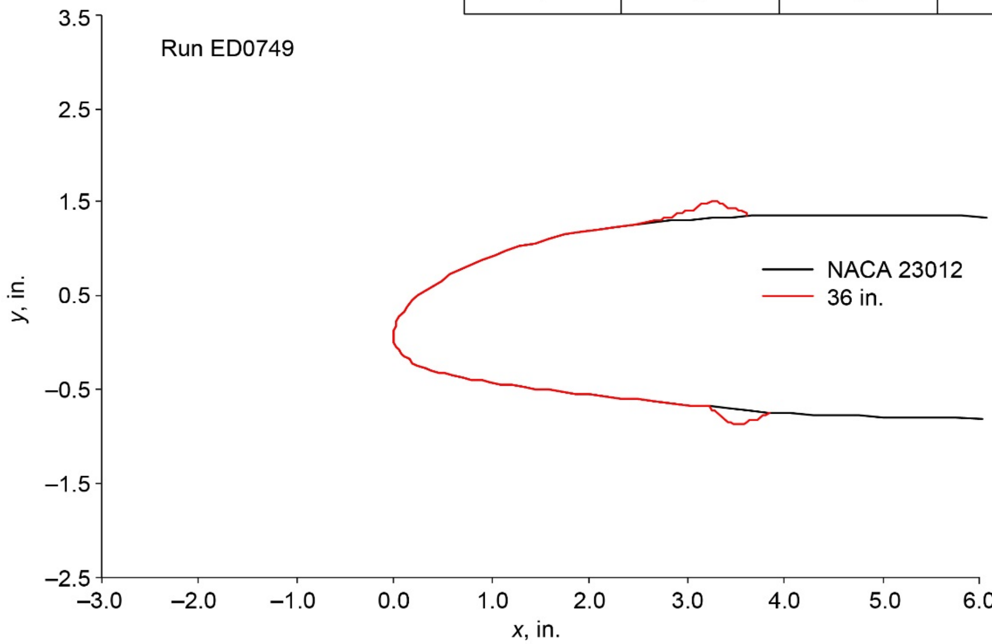

Pressure surface

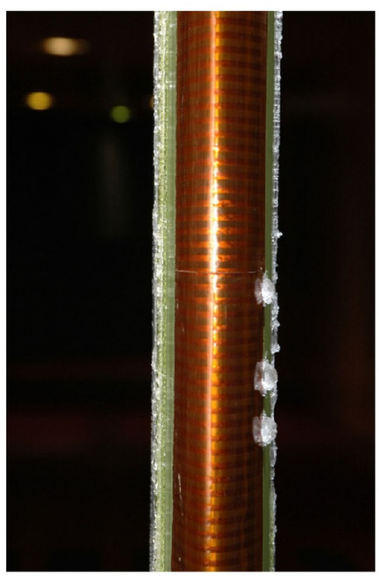

Leading edge

Suction surface

Run ED0749

Appendix E.—IRT Subscale Model Tests

Run ED0750

V = 175 kt
T_t = –4.4 °C
T_s = –8.5 °C

AoA = 0.0°
LWC = 0.64 g/m^3
MVD = 15.0 µm
Exposure time = 5.0 min

Measured ice thickness

Station	Upper max, in.	Stag. line, in.	Lower max, in.
-	-	-	-
36	0.10	0	0.13
-	-	-	-

Run ED0750

No tracings

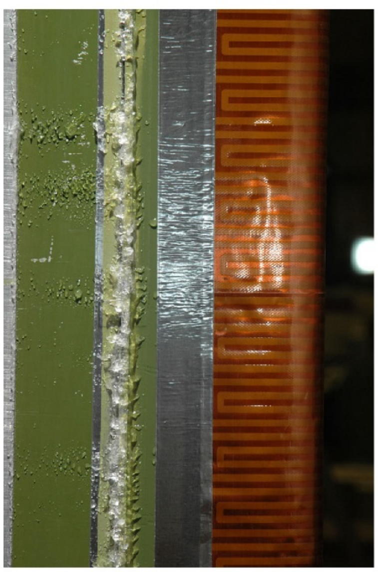
Pressure surface


Leading edge

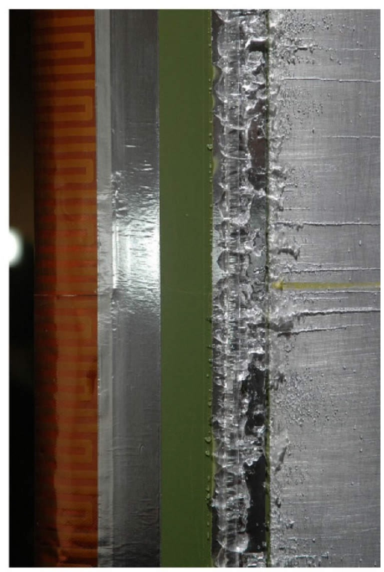
Suction surface

Run ED0750

Appendix E.—IRT Subscale Model Tests

Run ED0751

V = 175 kt
T_t = –4.4 °C
T_s = –8.5 °C

AoA = 0.0°
LWC = 0.64 g/m^3
MVD = 15.0 µm
Exposure time = 5.0 min

Measured ice thickness

Station	Upper max, in.	Stag. line, in.	Lower max, in.
-	-	-	-
36	0.12	0	0.20
-	-	-	-

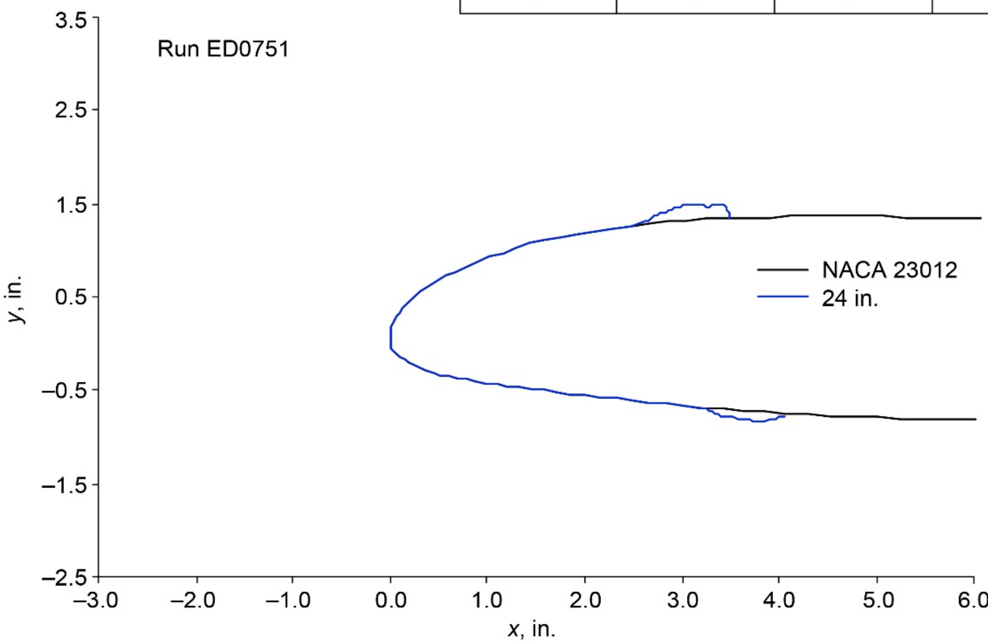

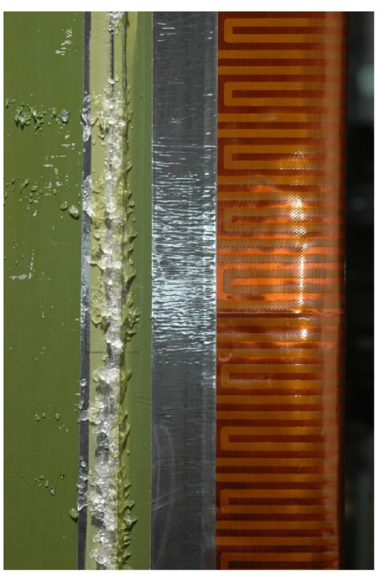

Pressure surface

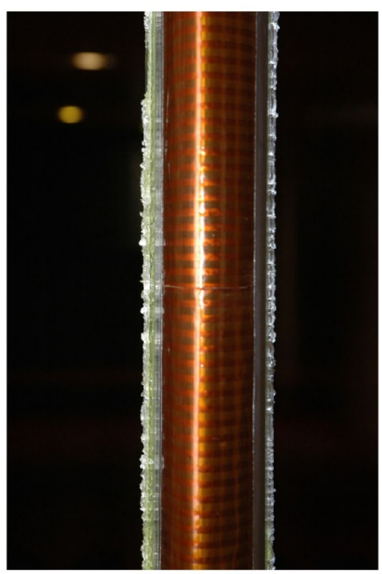

Leading edge

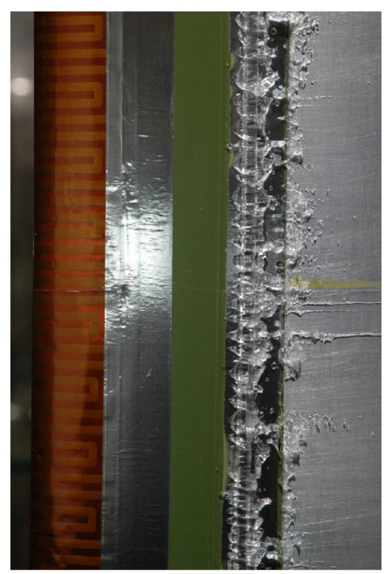

Suction surface

Run ED0751

Appendix E.—IRT Subscale Model Tests

Run ED0752

V = 250 kt
T_t = –13.3 °C
T_s = –21.7 °C

AoA = 2.0°
LWC = 0.33 g/m^3
MVD = 15.0 µm
Exposure time = 1.0 min

Run ED0752

Measured ice thickness*

Station	Upper max, in.	Stag. line, in.	Lower max, in.
-	-	-	-
-	-	-	-
-	-	-	-

*No tracings or ice thickness measurements made.

Pressure surface

Leading edge

Suction surface

Run ED0752

Appendix E.—IRT Subscale Model Tests

Run ED0753

V = 200 kt
T_t = 13.3 °C
T_s = –18.5 °C

AoA = 2.0°
LWC = 0.39 g/m^3
MVD = 15.0 µm
Exposure time = 1.0 min

Measured ice thickness

Station	Upper max, in.	Stag. line, in.	Lower max, in.
-	-	-	-
36	0.02	0.09	0.02
-	-	-	-

Run ED0753

No tracings

Pressure surface

Leading edge

Suction surface

Run ED0753

Appendix E.—IRT Subscale Model Tests

Run ED0754

V = 200 kt
T_t = –13.3 °C
T_s = –18.5 °C

AoA = 2.0°
LWC = 0.40 g/m^3
MVD = 30.0 µm
Exposure time = 5.0 min

Measured ice thickness

Station	Upper max, in.	Stag. line, in.	Lower max, in.
-	-	-	-
36	0.31	0.48	0.13
42.75	0.33	0.53	0.17

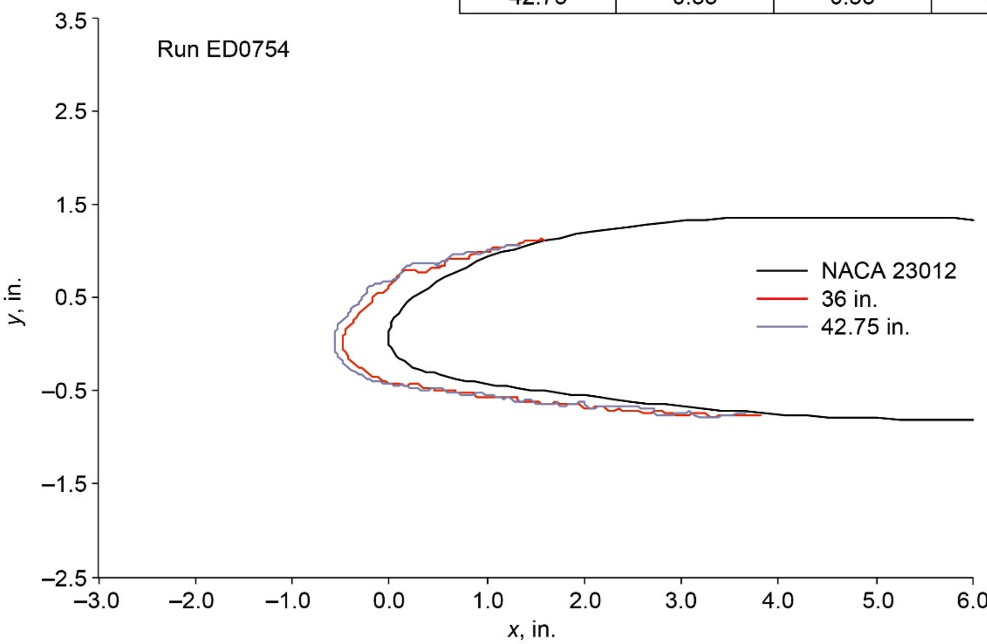

Pressure surface

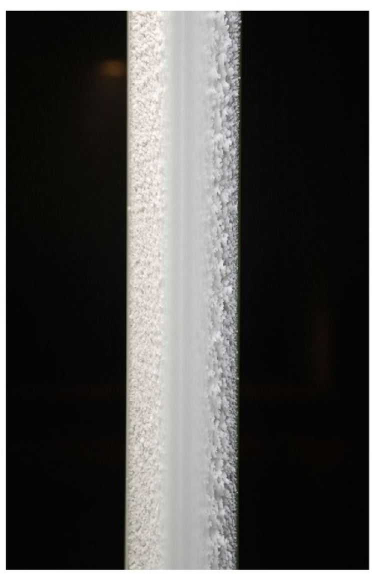

Leading edge

Suction surface

Run ED0754

Appendix E.—IRT Subscale Model Tests

Run ED0755

V = 175 kt
T_t = –17.8 °C
T_s = –22 °C

AoA = 5.3°
LWC = 0.44 g/m^3
MVD = 30.0 μm
Exposure time = 5.0 min

Measured ice thickness

Station	Upper max, in.	Stag. line, in.	Lower max, in.
-	-	-	-
36	0.26	0.43	0.15
43	0.22	0.49	0.16

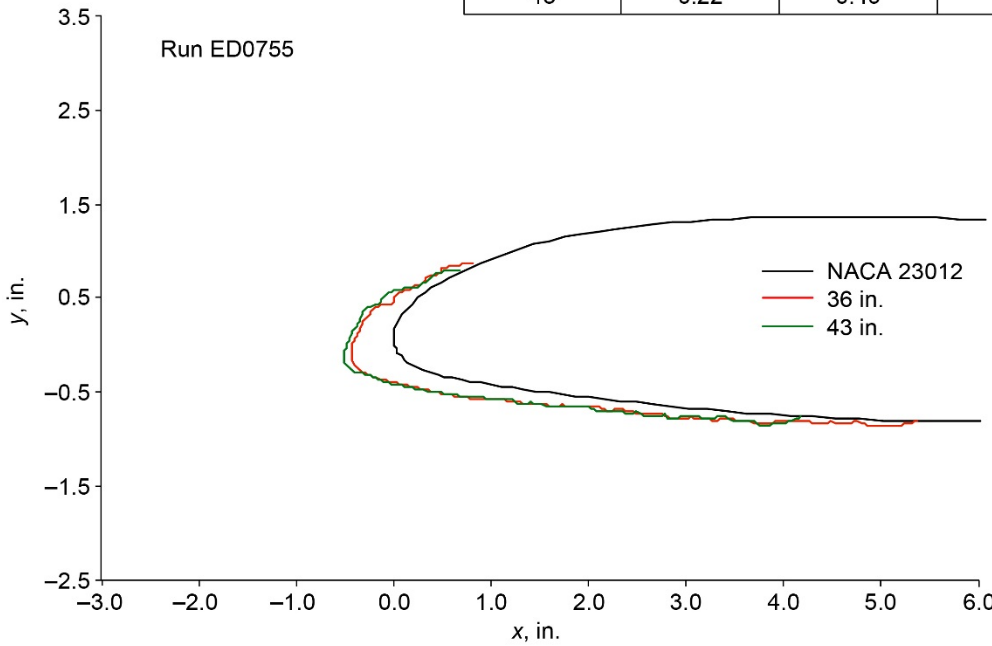

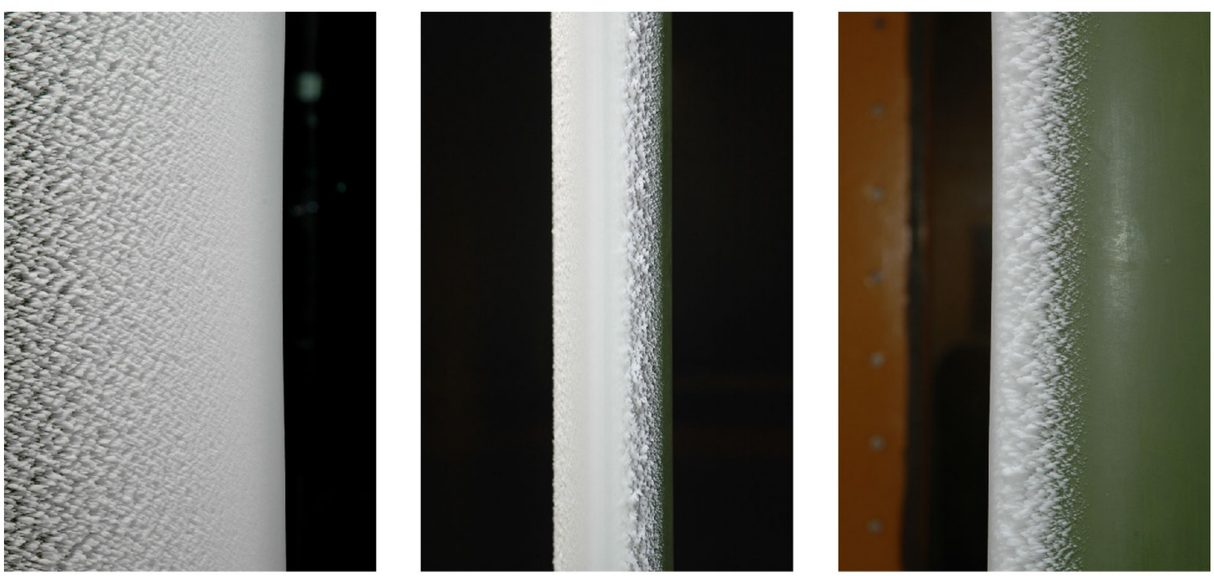

Pressure surface Leading edge Suction surface

Run ED0755

Appendix E.—IRT Subscale Model Tests

Run ED0756

V = 200 kt
T_t = –17.8 °C
T_s = –23.1 °C

AoA = 2.0°
LWC = 0.40 g/m^3
MVD = 30.0 µm
Exposure time = 5.0 min

Measured ice thickness

Station	Upper max, in.	Stag. line, in.	Lower max, in.
24	0.18	0.39	0.10
-	-	-	-
48	0.20	0.42	0.13

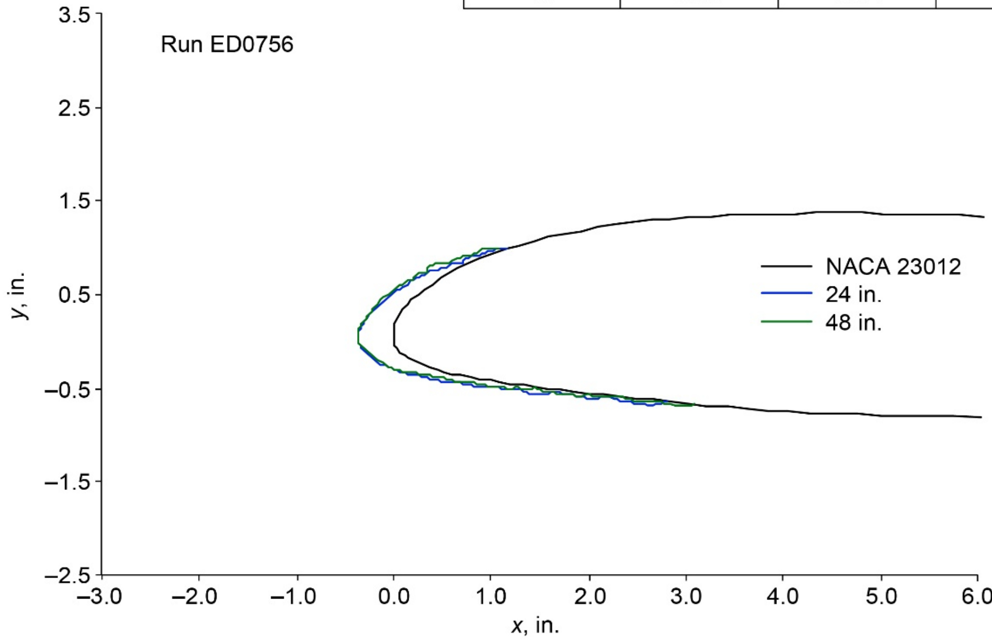

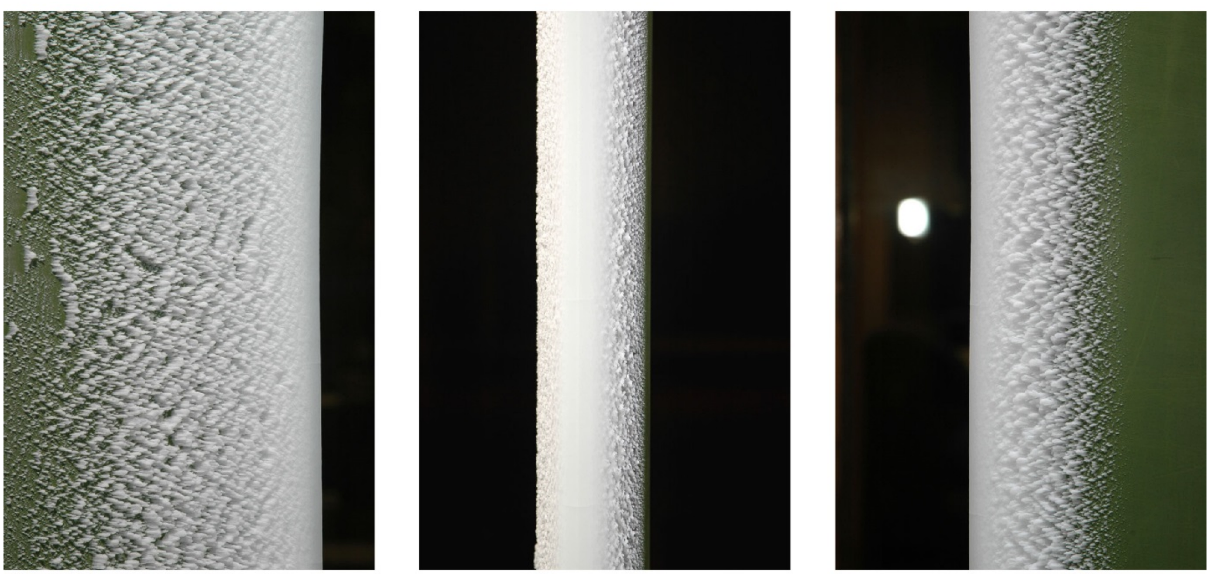

Pressure surface Leading edge Suction surface

Run ED0756

Appendix E.—IRT Subscale Model Tests

Run ED0757

V = 200 kt
T_t = –17.8 °C
T_s = –23.1 °C

AoA = 2.0°
LWC = 0.33 g/m^3
MVD = 15.0 µm
Exposure time = 10.0 min

Measured ice thickness

Station	Upper max, in.	Stag. line, in.	Lower max, in.
24	-	0.57	-
-	-	-	-
48	-	0.68	-

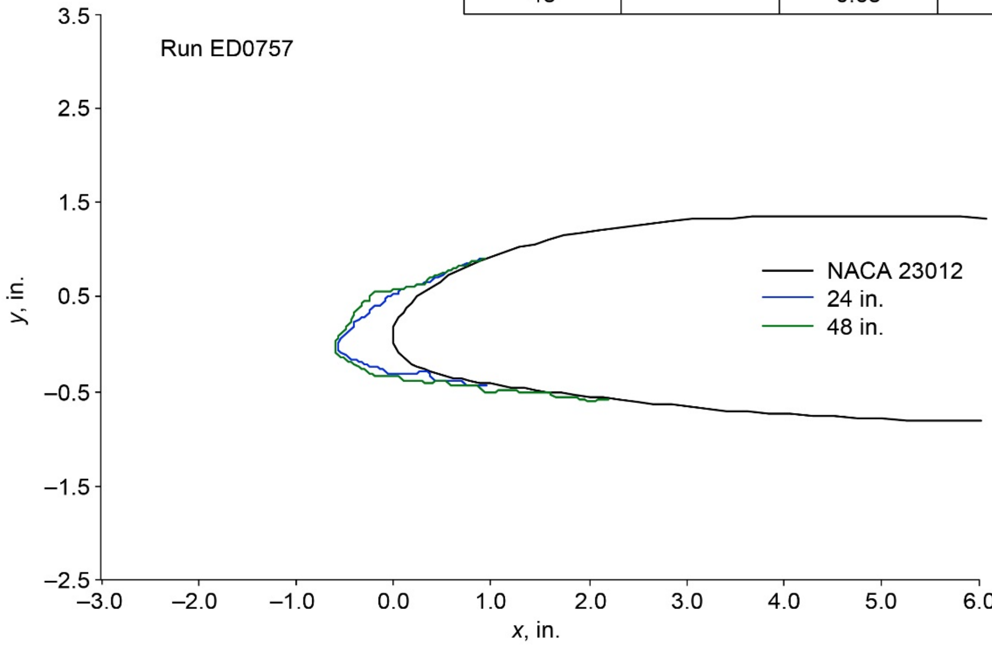

Pressure surface

Leading edge

Suction surface

Run ED0757

Appendix E.—IRT Subscale Model Tests

Run ED0758

V = 175 kt
T_t = –4.4 °C
T_s = –8.5 °C

AoA = 0.0°
LWC = 0.64 g/m^3
MVD = 15.0 µm
Exposure time = 5.0 min

Measured ice thickness

Station	Upper max, in.	Stag. line, in.	Lower max, in.
-	-	-	-
36	0.17	0	0.20
-	-	-	-

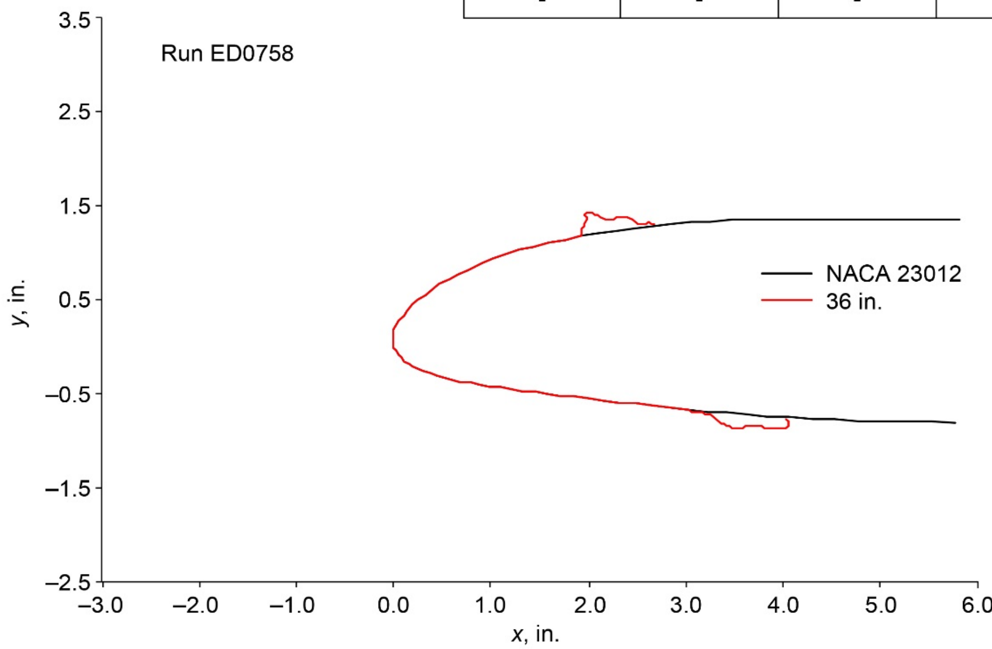

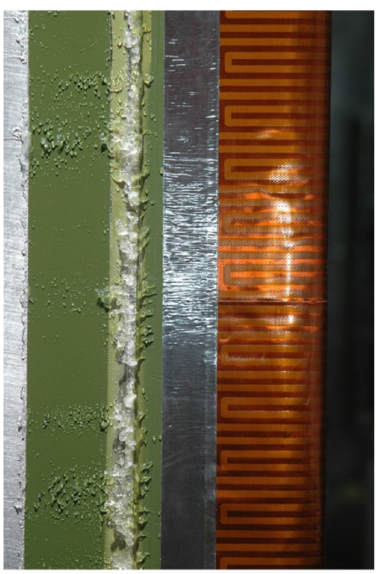
Pressure surface


Leading edge

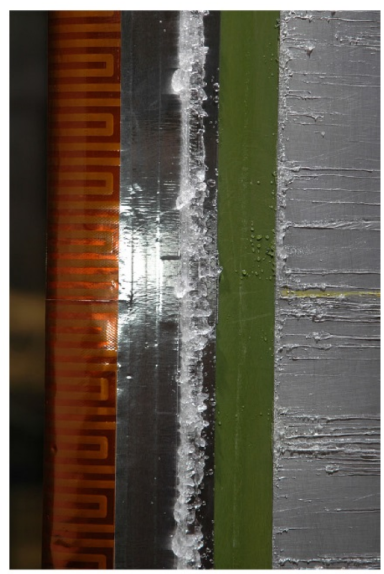
Suction surface

Run ED0758

Appendix E.—IRT Subscale Model Tests

Run ED0759

V = 175 kt
T_t = –4.4 °C
T_s = –8.5 °C

AoA = 0.9°
LWC = 0.64 g/m^3
MVD = 15.0 µm
Exposure time = 5.0 min

Measured ice thickness

Station	Upper max, in.	Stag. line, in.	Lower max, in.
-	-	-	-
36	0.12	0	0.44
-	-	-	-

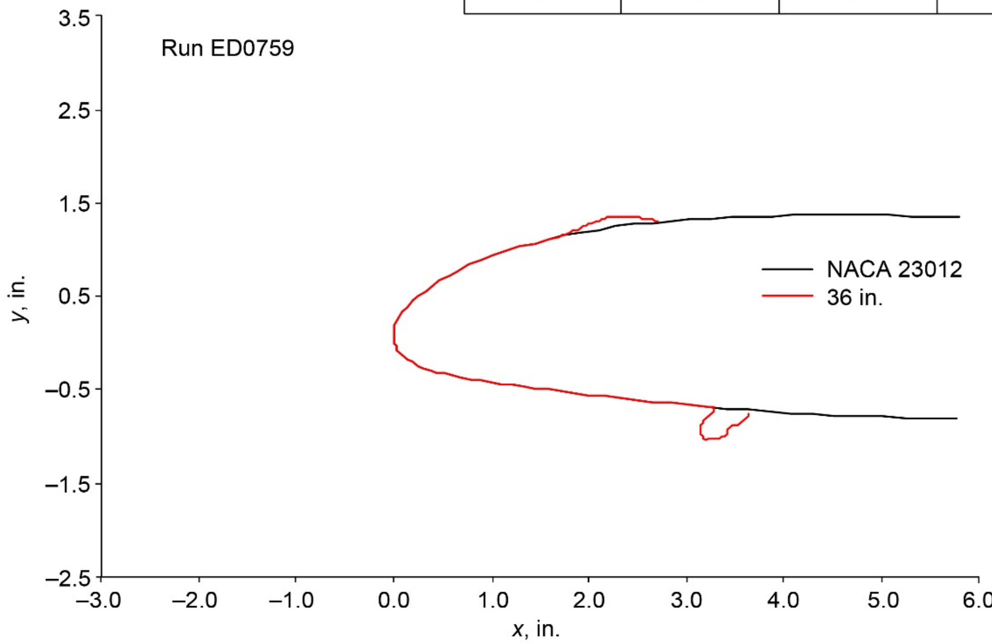

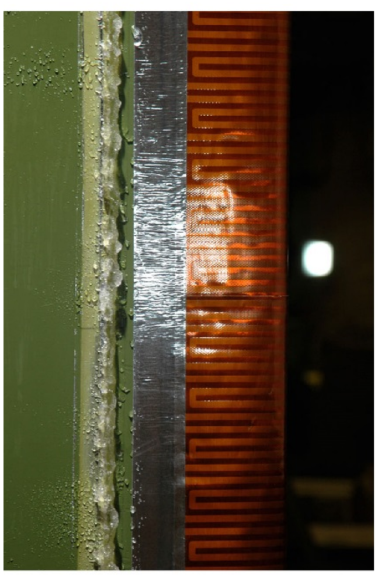

Pressure surface

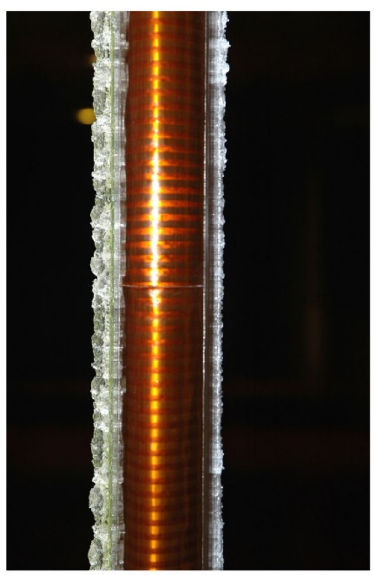

Leading edge

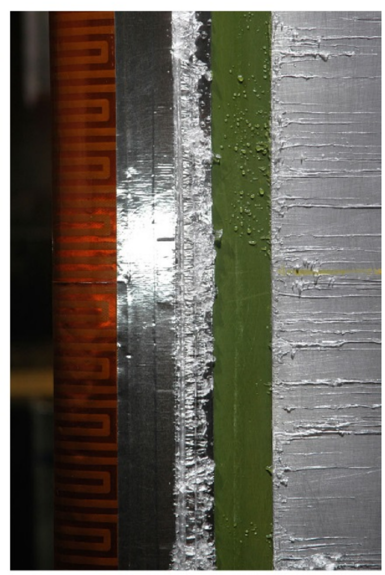

Suction surface

Run ED0759

Appendix E.—IRT Subscale Model Tests

Run ED0760

V = 175 kt
T_t = –4.4 °C
T_s = –8.5 °C

AoA = 0.9°
LWC = 0.64 g/m^3
MVD = 15.0 µm
Exposure time = 5.0 min

Measured ice thickness

Station	Upper max, in.	Stag. line, in.	Lower max, in.
-	-	-	-
36	0.12	0	0.44
-	-	-	-

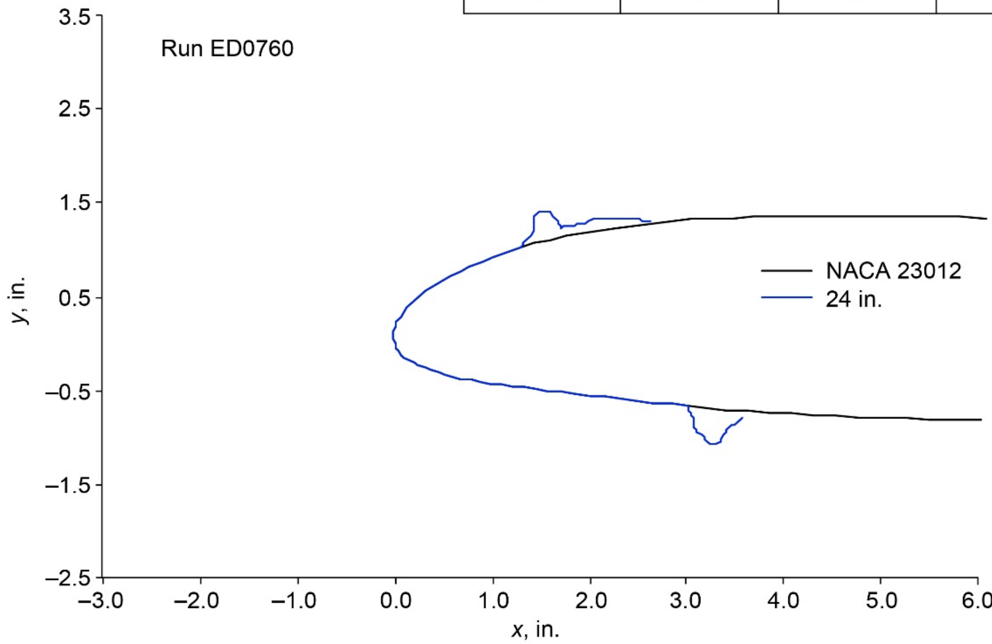

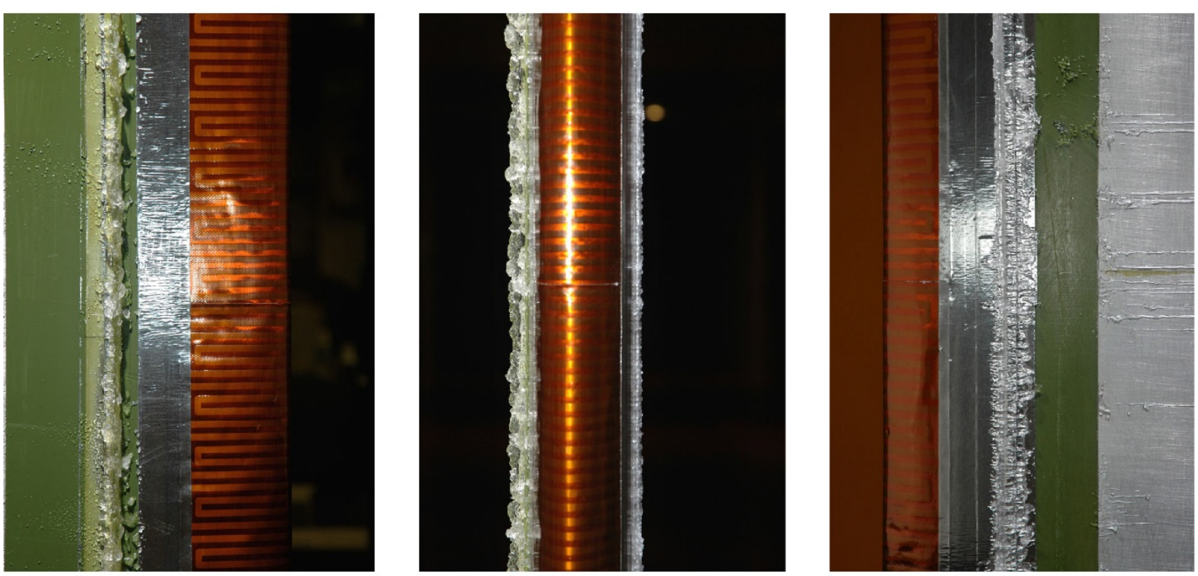

Pressure surface

Leading edge

Suction surface

Run ED0760

Appendix E.—IRT Subscale Model Tests

Run ED0761

V = 200 kt
T_t = –2.2 °C
T_s = –7.5 °C

AoA = 2.0°
LWC = 0.75 g/m^3
MVD = 15.4 μm
Exposure time = 5.0 min

Measured ice thickness

Station	Upper max, in.	Stag. line, in.	Lower max, in.
24	0.9	0.14	0.65
-	-	-	-
48	0.86	0.14	0.55

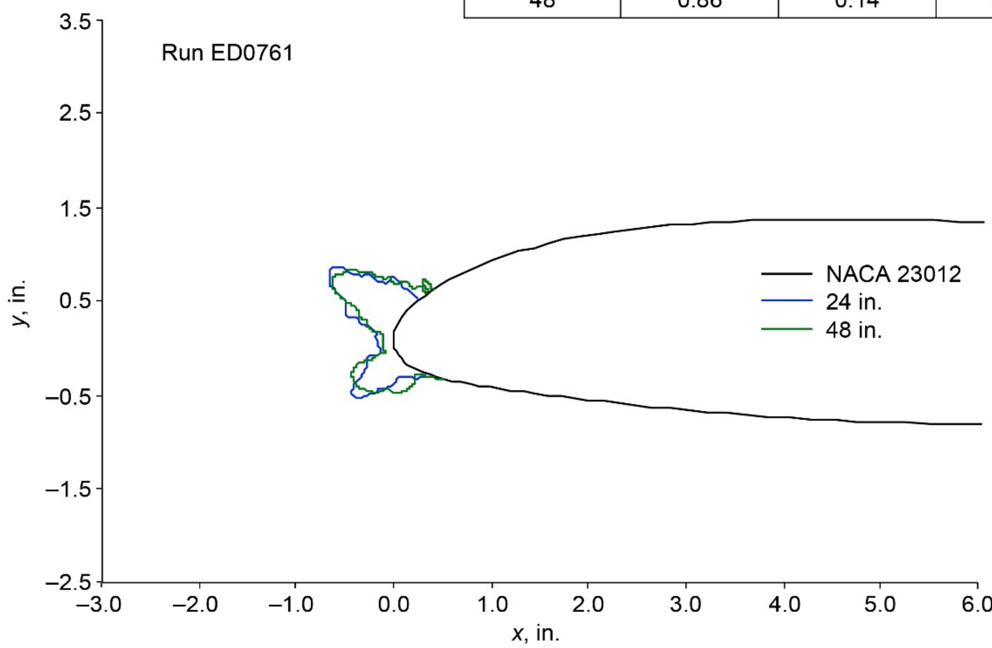


Pressure surface

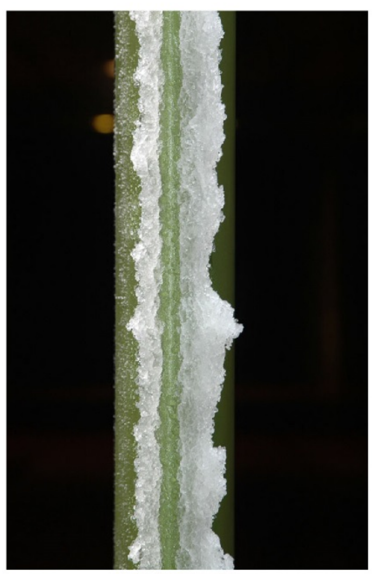
Leading edge


Suction surface

Run ED0761

Appendix E.—IRT Subscale Model Tests

Run ED0762

V = 200 kt
T_t = –2.2 °C
T_s = –7.5 °F

AoA = 2.0°
LWC = 0.75 g/m^3
MVD = 15.4 μm
Exposure time = 0.5 min

Measured ice thickness

Station	Upper max, in.	Stag. line, in.	Lower max, in.
23.5	0.06	0.02	0.03
-	-	-	-
48.5	0.06	0.02	0.03

Run ED0762

No tracings

Pressure surface

Leading edge

Suction surface

Run ED0762

Appendix E.—IRT Subscale Model Tests

Run ED0763

V = 175 kt
T_t = –2.2 °C
T_s = –6.2 °C

AoA = 5.0°
LWC = 0.64 g/m^3
MVD = 15.0 µm
Exposure time = 5.0 min

Measured ice thickness

Station	Upper max, in.	Stag. line, in.	Lower max, in.
24	0.54	0.15	0.28
-	-	-	-
48	0.62	0.14	0.36

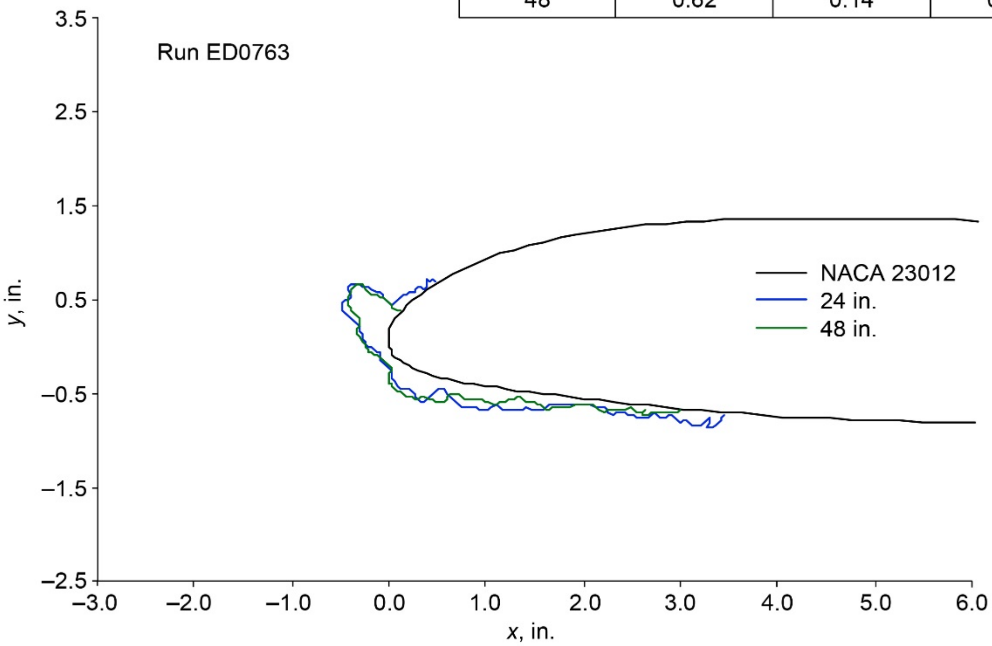


Pressure surface

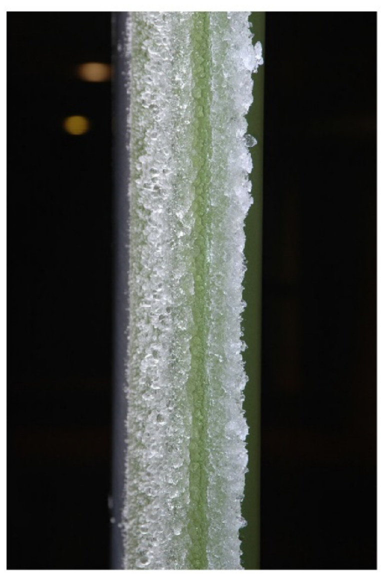
Leading edge


Suction surface

Run ED0763

Appendix E.—IRT Subscale Model Tests

Run ED0764

V = 175 kt
T_t = –2.2 °C
T_s = –6.2 °C

AoA = 5.0°
LWC = 0.64 g/m^3
MVD = 15.0 µm
Exposure time = 2.0 min

Measured ice thickness

Station	Upper max, in.	Stag. line, in.	Lower max, in.
24	0.23	0.09	0.11
-	-	-	-
-	-	-	-

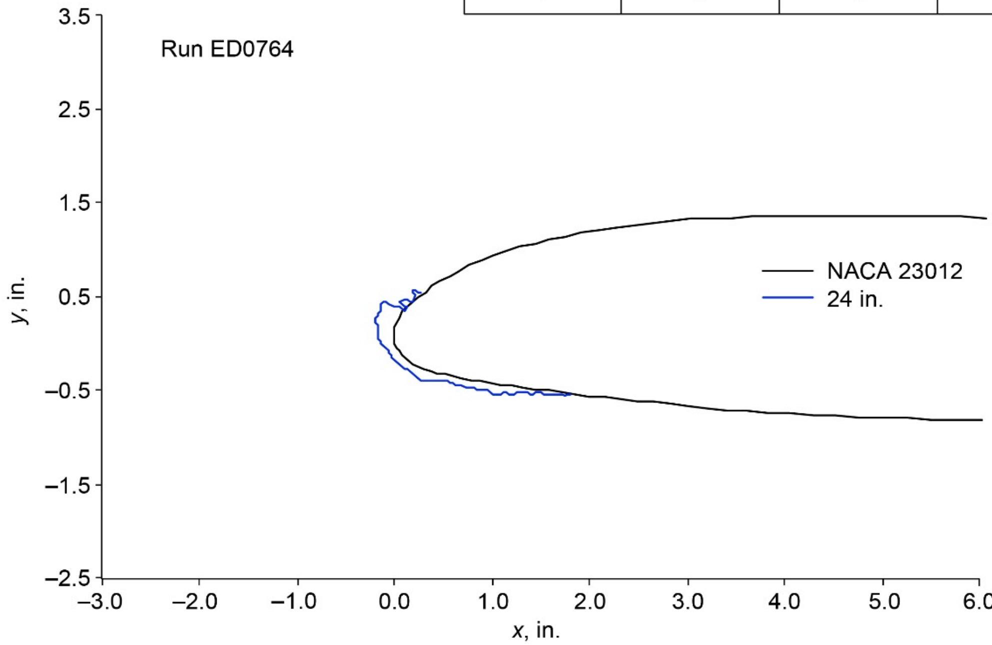

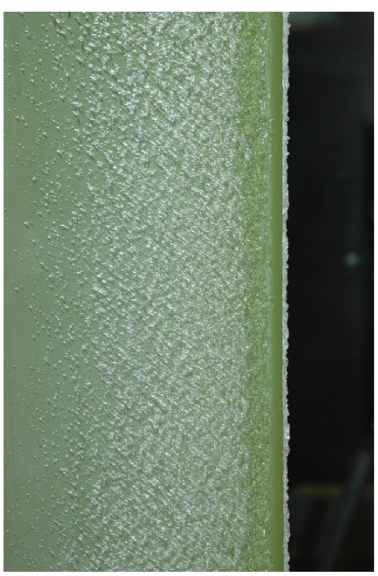

Pressure surface

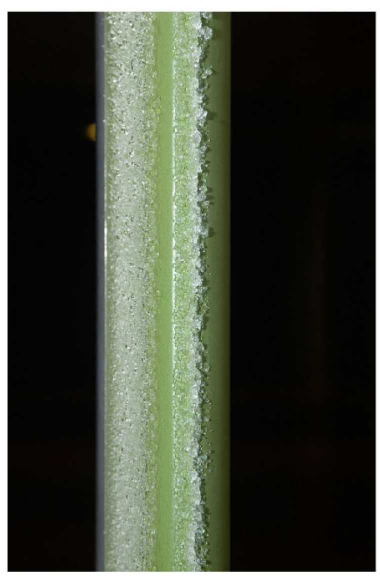

Leading edge

Suction surface

Run ED0764

Appendix E.—IRT Subscale Model Tests

Run ED0765

V = 175 kt
T_t = –4.4 °C
T_s = –8.5 °C

AoA = 1.0°
LWC = 0.64 g/m^3
MVD = 15.0 µm
Exposure time = 5.0 min

Measured ice thickness

Station	Upper max, in.	Stag. line, in.	Lower max, in.
-	-	-	-
36	0.06	0	0.08
-	-	-	-

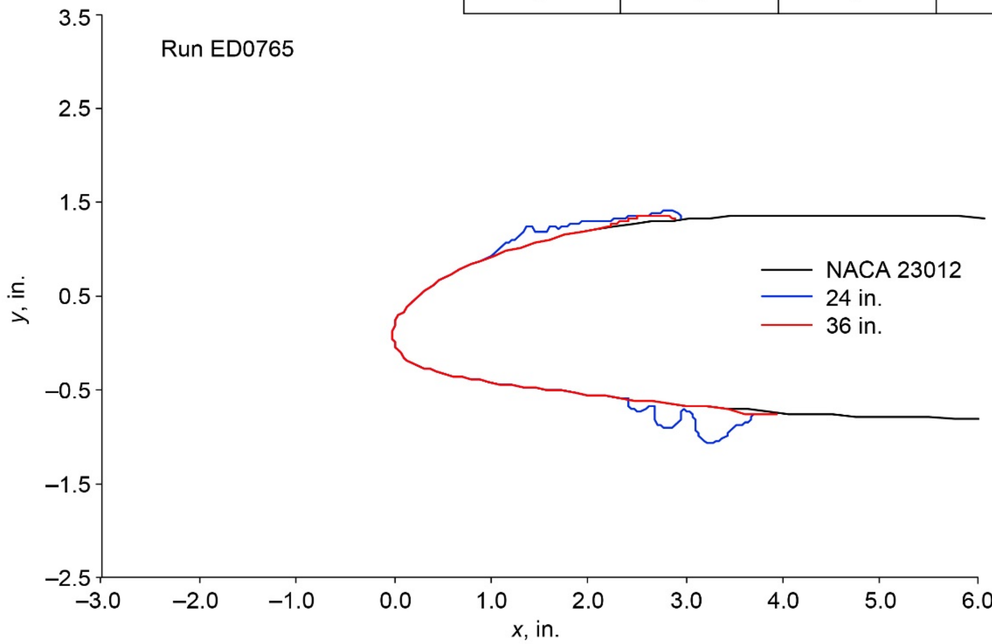

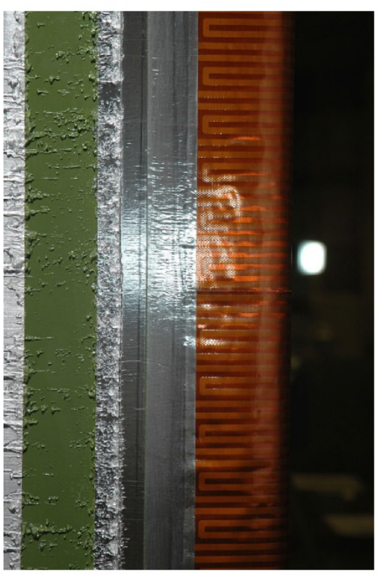

Pressure surface

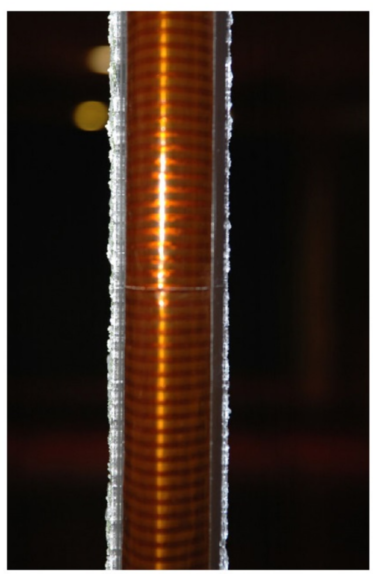

Leading edge

Suction surface

Run ED0765

Appendix E.—IRT Subscale Model Tests

Run ED0766

V = 175 kt
T_t = –4.4 °C
T_s = –8.5 °C

AoA = 1.0°
LWC = 0.64 g/m^3
MVD = 15.0 µm
Exposure time = 5.0 min

Measured ice thickness

Station	Upper max, in.	Stag. line, in.	Lower max, in.
24	0.11	0	0.42
-	-	-	-
-	-	-	-

Run ED0766

No tracings

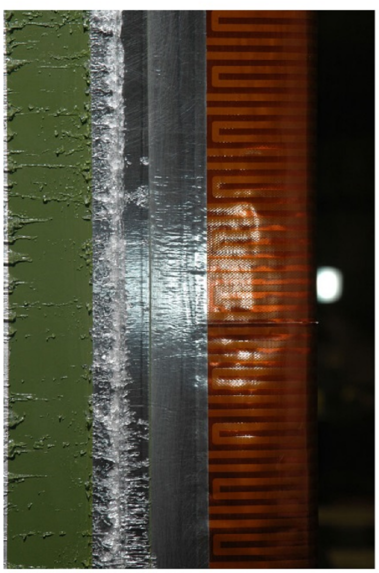

Pressure surface

Leading edge

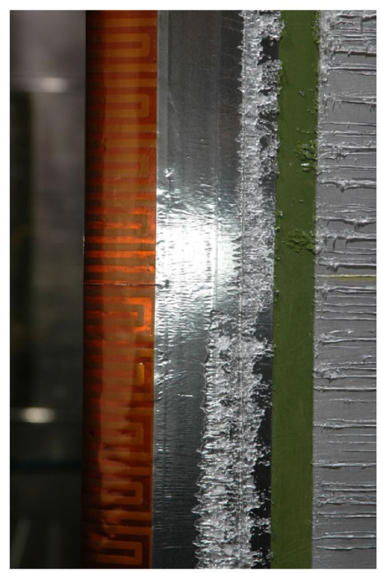

Suction surface

Run ED0766

Appendix E.—IRT Subscale Model Tests

Run ED0767

V = 175 kt
T_t = –4.4 °C
T_s = –8.4 °C

AoA = 5.0°
LWC = 0.64 g/m^3
MVD = 15.0 µm
Exposure time = 10.0 min

Measured ice thickness

Station	Upper max, in.	Stag. line, in.	Lower max, in.
24	1.09	0.42	0.80
-	-	-	-
48	1.14	0.44	0.75

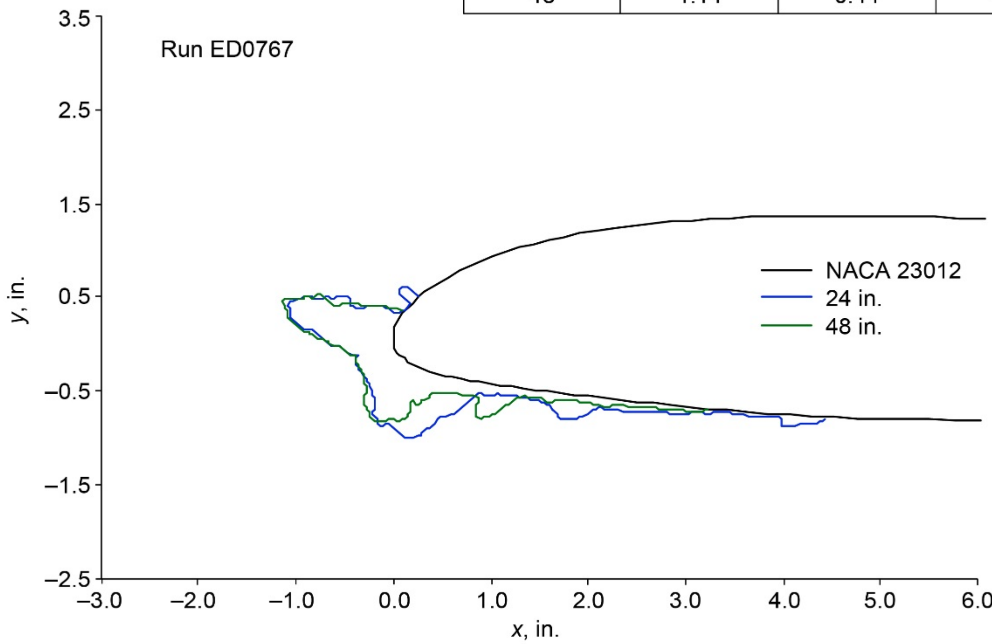

Pressure surface

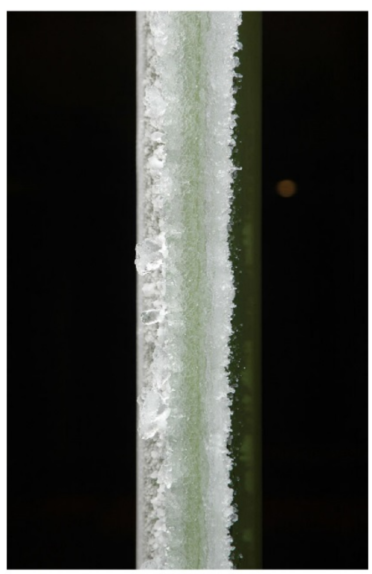

Leading edge

Suction surface

Run ED0767

Appendix E.—IRT Subscale Model Tests

Run ED0768

V = 175 kt
T_t = –2.2 °C
T_s = –6.2 °C

AoA = 5.0°
LWC = 0.64 g/m^3
MVD = 15.0 µm
Exposure time = 2.0 min

Measured ice thickness

Station	Upper max, in.	Stag. line, in.	Lower max, in.
-	-	-	-
36	0.23	0.08	0.13
-	-	-	-

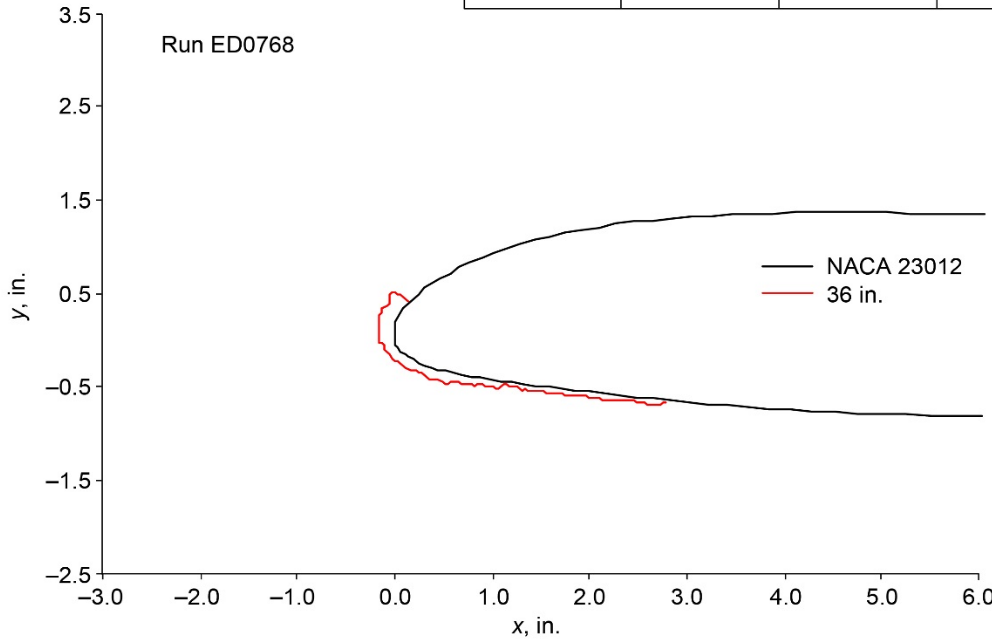

Pressure surface

Leading edge

Suction surface

Run ED0768

Appendix E.—IRT Subscale Model Tests

Run ED0769

V = 200 kt
T_t = –2.2 °C
T_s = –7.5 °C

AoA = 2.0°
LWC = 0.75 g/m^3
MVD = 15.4 µm
Exposure time = 0.5 min

Measured ice thickness

Station	Upper max, in.	Stag. line, in.	Lower max, in.
-	-	-	-
36	0.07	0.04	0.03
-	-	-	-

Run ED0769

No tracings

Pressure surface

Leading edge

Suction surface

Run ED0769

Appendix E.—IRT Subscale Model Tests

Run ED0770

V = 200 kt
T_t = –17.8 °C
T_s = –23.1 °C

AoA = 2.0°
LWC = 0.40 g/m^3
MVD = 30.0 µm
Exposure time = 5.0 min

Measured ice thickness

Station	Upper max, in.	Stag. line, in.	Lower max, in.
-	-	-	-
36	0.20	0.47	0.12
43.875	0.25	0.56	0.14

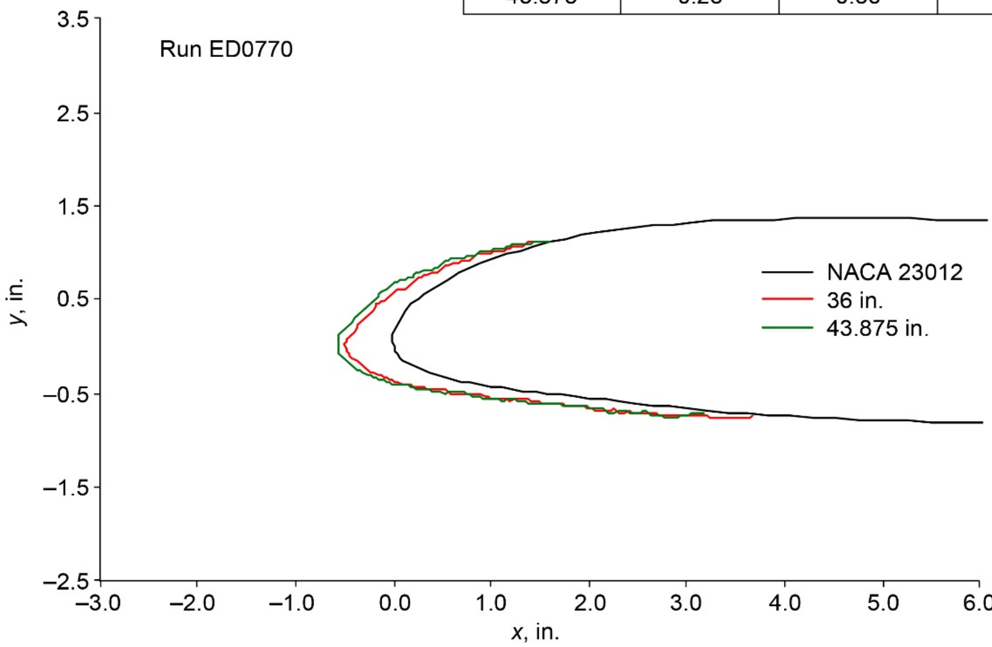

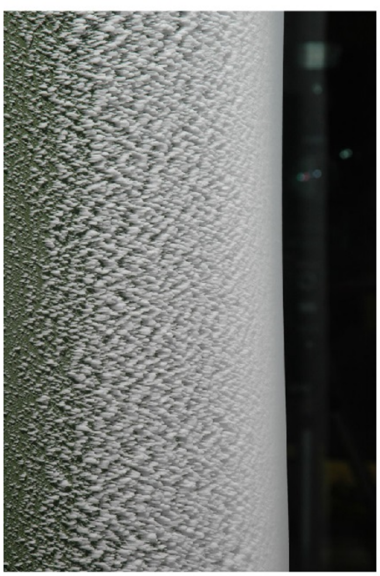
Pressure surface


Leading edge


Suction surface

Run ED0770

Appendix E.—IRT Subscale Model Tests

Run ED0771

V = 200 kt
T_t = –17.8 °C
T_s = –23.1 °C

AoA = 2.0°
LWC = 0.33 g/m^3
MVD = 15.0 µm
Exposure time = 10.0 min

Measured ice thickness

Station	Upper max, in.	Stag. line, in.	Lower max, in.
-	-	-	-
36	-	0.66	-
43	-	0.81	-

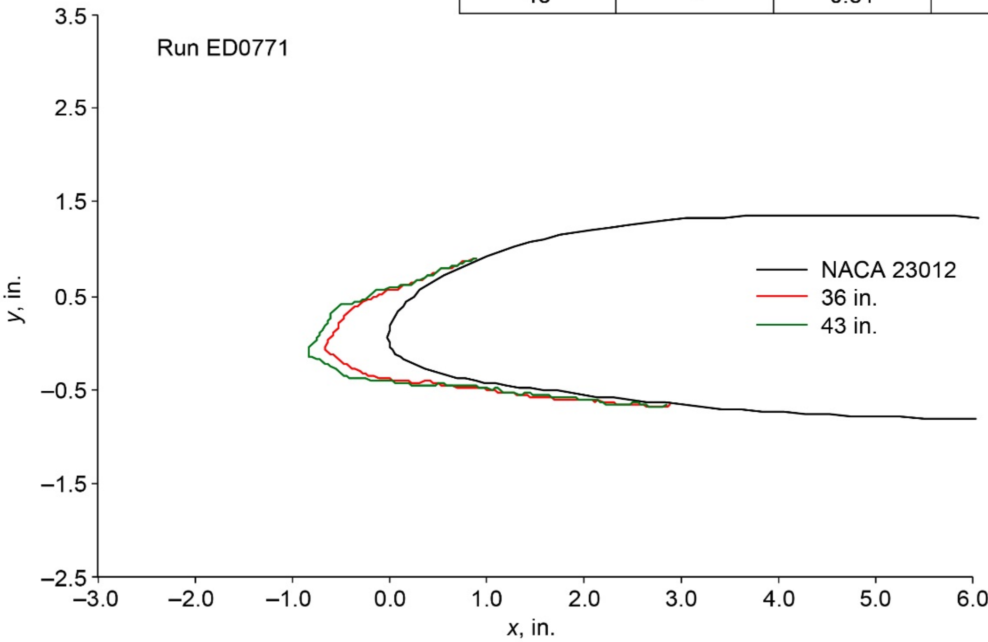

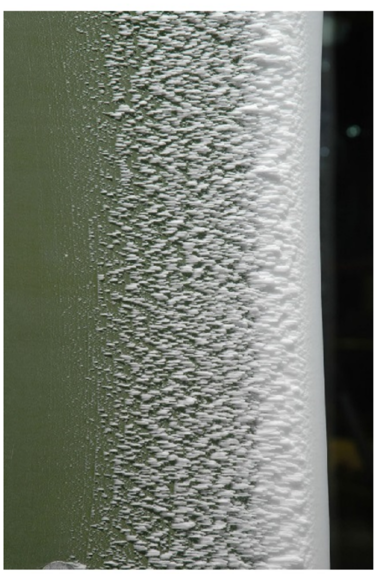

Pressure surface

Leading edge

Suction surface

Run ED0771

Appendix E.—IRT Subscale Model Tests

Run ED0772

V = 175 kt
T_t = –17.8 °C
T_s = –21.8 °C

AoA = 5.0°
LWC = 0.30 g/m^3
MVD = 15.0 µm
Exposure time = 5.0 min

Measured ice thickness

Station	Upper max, in.	Stag. line, in.	Lower max, in.
-	-	-	-
36	-	0.21	-
43.875	-	0.25	-

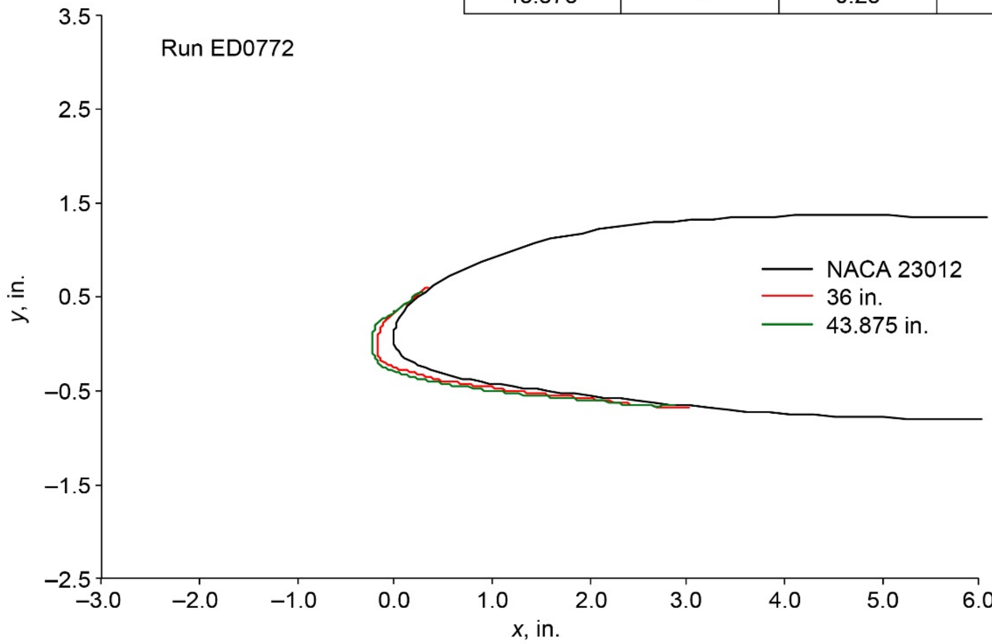

Pressure surface

Leading edge

Suction surface

Run ED0772

Appendix E.—IRT Subscale Model Tests

Run ED0773

V = 200 kt
T_t = –2.2 °C
T_s = –7.5 °C

AoA = 2.0°
LWC = 0.75 g/m^3
MVD = 15.4 μm
Exposure time = 10.0 min

Measured ice thickness

Station	Upper max, in.	Stag. line, in.	Lower max, in.
24	1.69	0.25	1.20
-	-	-	-
48	1.74	0.21	1.27

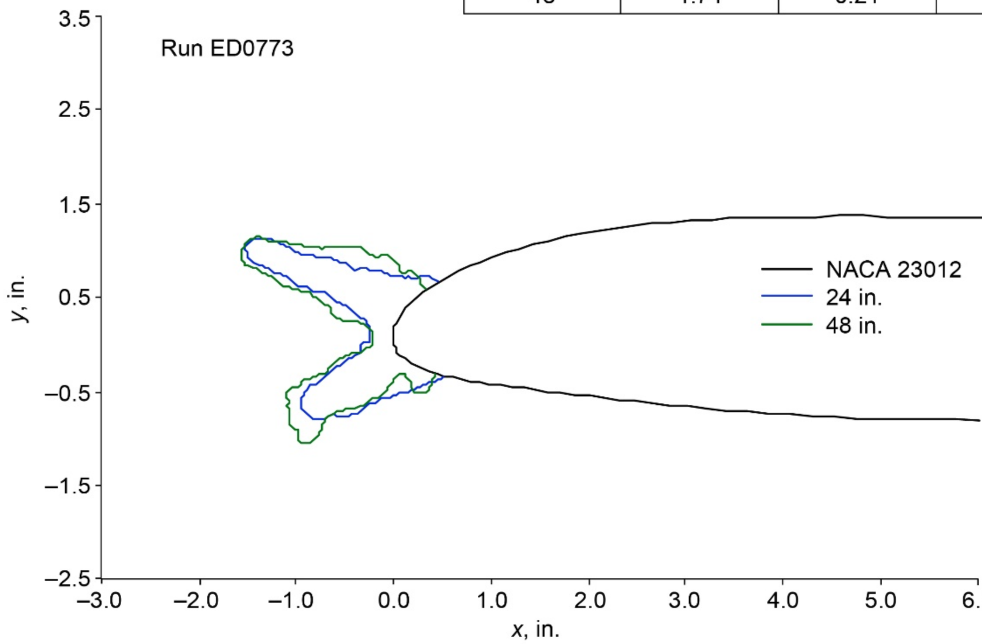

Pressure surface

Leading edge

Suction surface

Run ED0773

Appendix F.—Icing Research Tunnel NACA 23012 Full-Scale Model Test Results

Aerodynamic Test of Clean Model

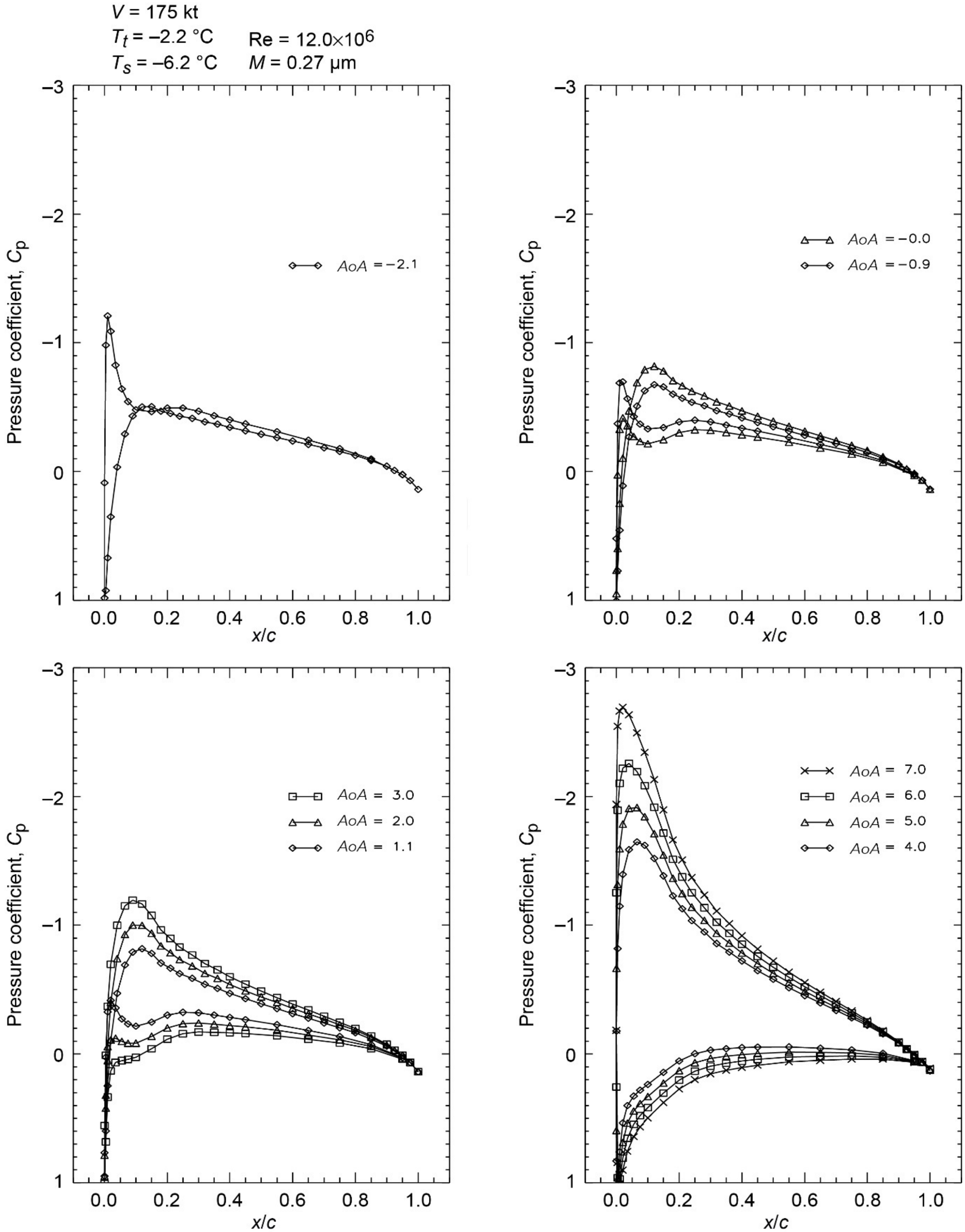

Aerodynamic Test of Clean Model

Appendix F.—IRT Full-Scale Model Tests

Run EG1109

V = 175 kt
T_t = –6.7 °C
T_s = –10.7 °C
AoA = 5.0°
LWC = 0.50 g/m^3
MVD = 20.0 µm
Exposure time = 22.5 min

Measured ice thickness

Station	Upper max, in.	Stag. line, in.	Lower max, in.
30	1.64	0.82	1.00
36	1.49	0.80	0.81
42	1.72	0.85	1.03

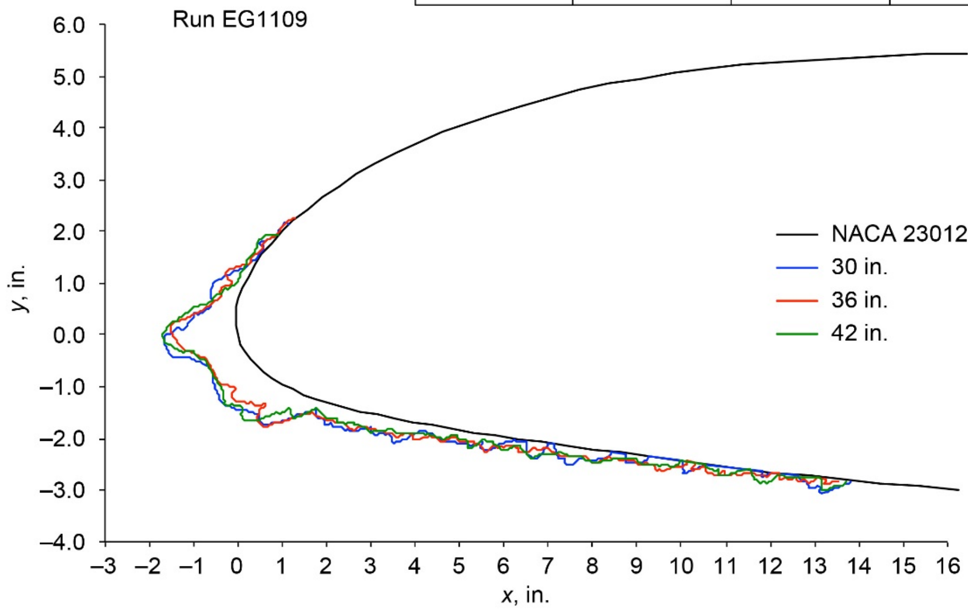

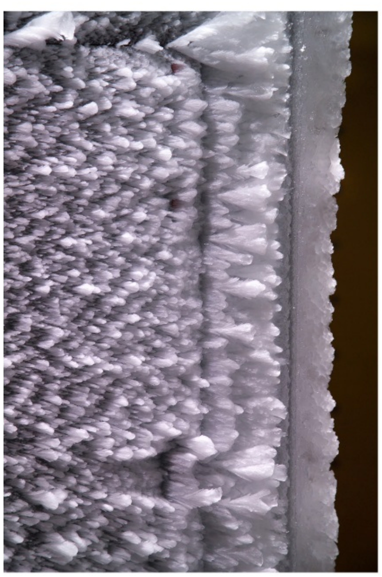

Pressure surface

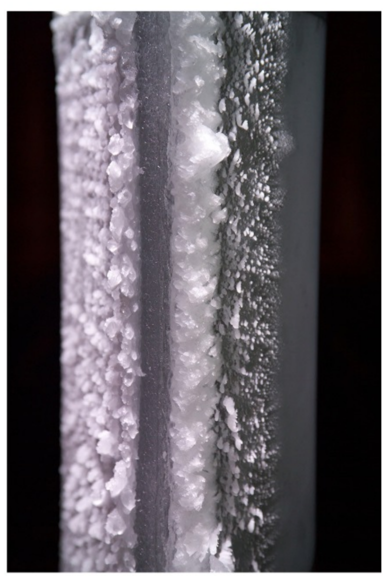

Leading edge

Suction surface

Run EG1109

Appendix F.—IRT Full-Scale Model Tests

Run EG1110

V = 175 kt
T_t = –4.4 °C
T_s = –8.4 °C
AoA = 5.0°
LWC = 0.50 g/m^3
MVD = 20.0 µm
Exposure time = 22.5 min

Measured ice thickness

Station	Upper max, in.	Stag. line, in.	Lower max, in.
30	2.24	0.62	1.30
36	1.70	0.60	1.14
42	1.93	0.62	0.97

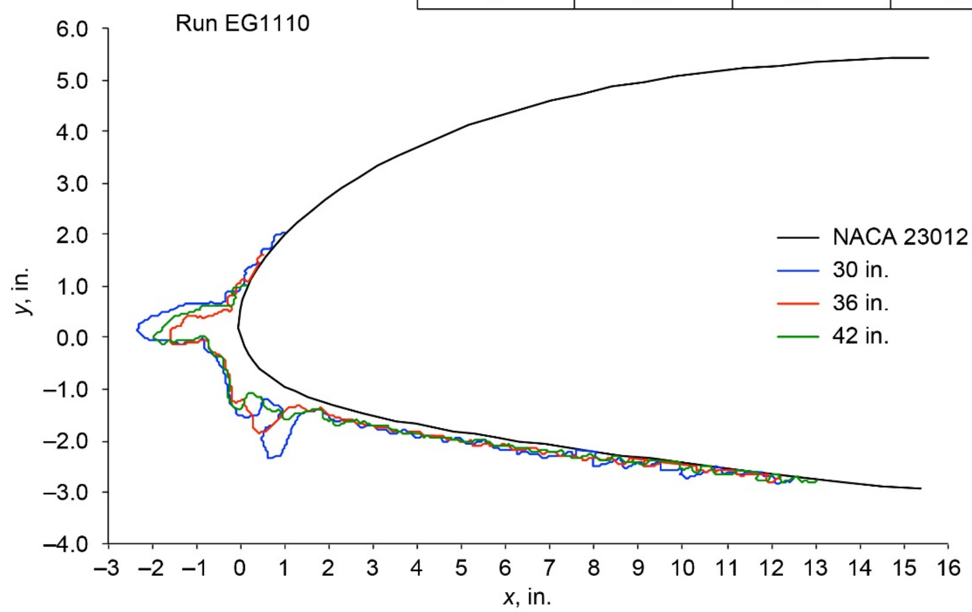

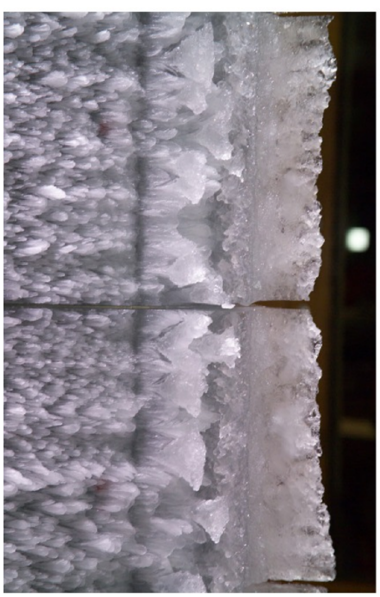

Pressure surface

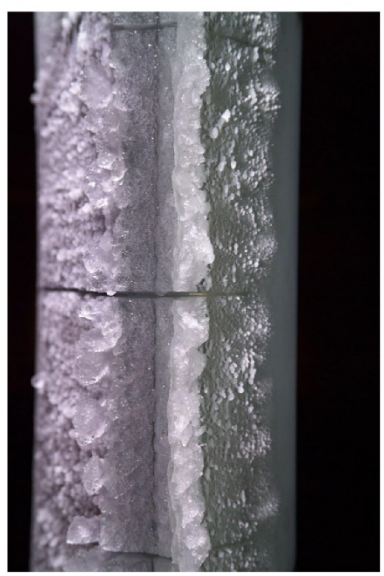

Leading edge

Suction surface

Run EG1110

Appendix F.—IRT Full-Scale Model Tests

Run EG1111

V = 175 kt
T_t = –2.2 °C
T_s = –6.2 °C
AoA = 5.0°
LWC = 0.50 g/m^3
MVD = 20.0 µm
Exposure time = 22.5 min

Measured ice thickness

Station	Upper max, in.	Stag. line, in.	Lower max, in.
30	2.36	0.43	0.86
36	2.15	0.39	1.09
42	2.11	0.46	1.00

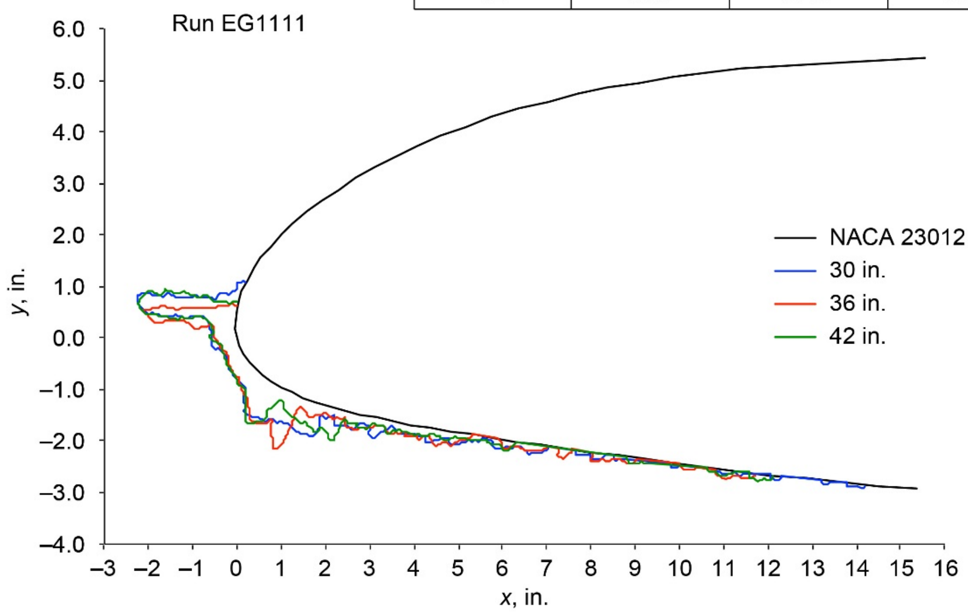

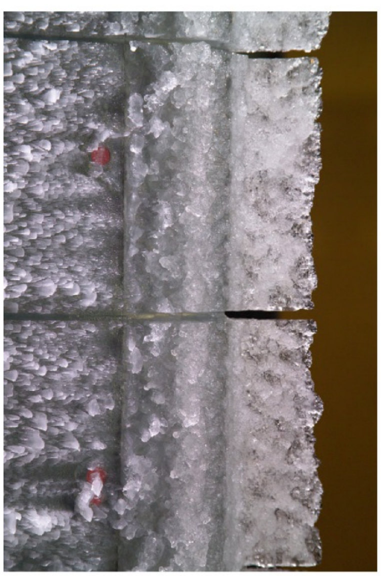

Pressure surface

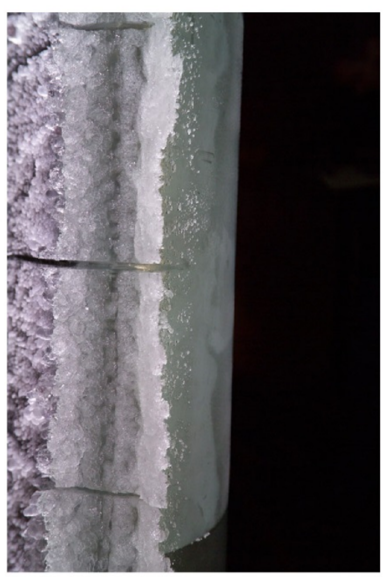

Leading edge

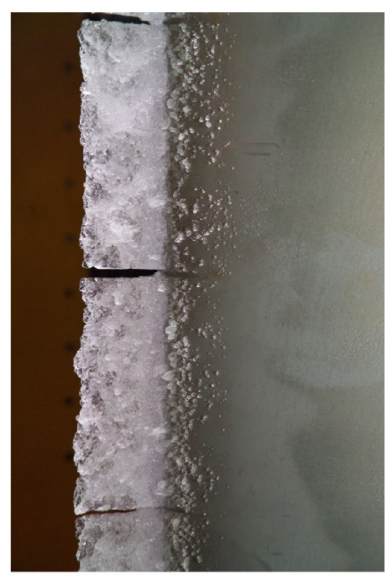

Suction surface

Run EG1111

Appendix F.—IRT Full-Scale Model Tests

Run EG1112

V = 200 kt
T_t = –2.2 °C
T_s = –7.4 °C
AoA = 2.0°
LWC = 0.50 g/m^3
MVD = 20.0 µm
Exposure time = 22.5 min

Measured ice thickness

Station	Upper max, in.	Stag. line, in.	Lower max, in.
30	2.36	0.38	1.75
36	2.09	0.39	1.75
42	2.52	0.37	1.70

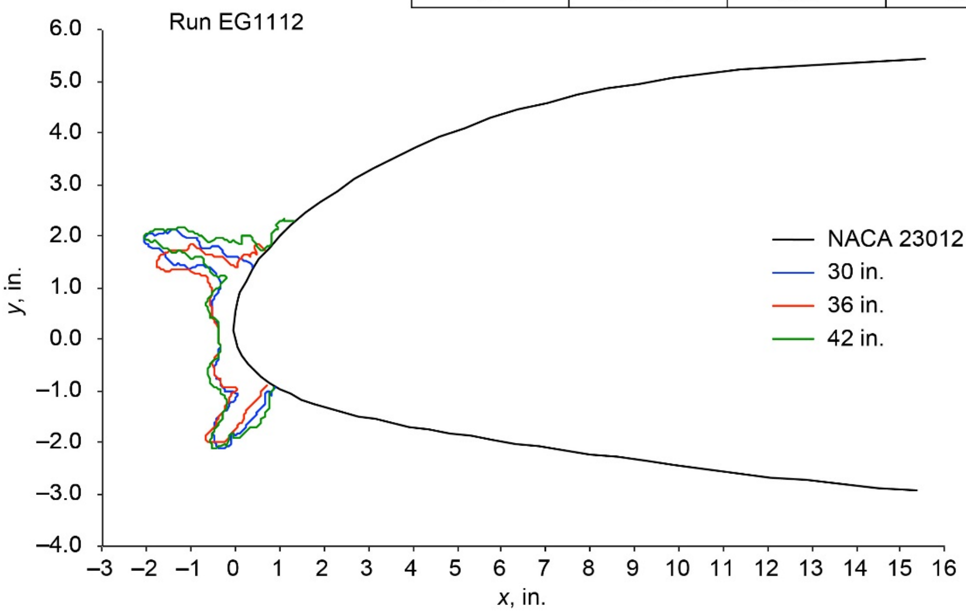

Pressure surface

Leading edge

Suction surface

Run EG1112

Appendix F.—IRT Full-Scale Model Tests

Run EG1113

V = 200 kt
T_t = –2.2 °C
T_s = –7.4 °C

AoA = 2.0°
LWC = 0.50 g/m^3
MVD = 20.0 µm
Exposure time = 22.5 min

Measured ice thickness

Station	Upper max, in.	Stag. line, in.	Lower max, in.
30	2.37	0.33	1.85
36	2.03	0.37	1.69
42	2.30	0.39	1.55

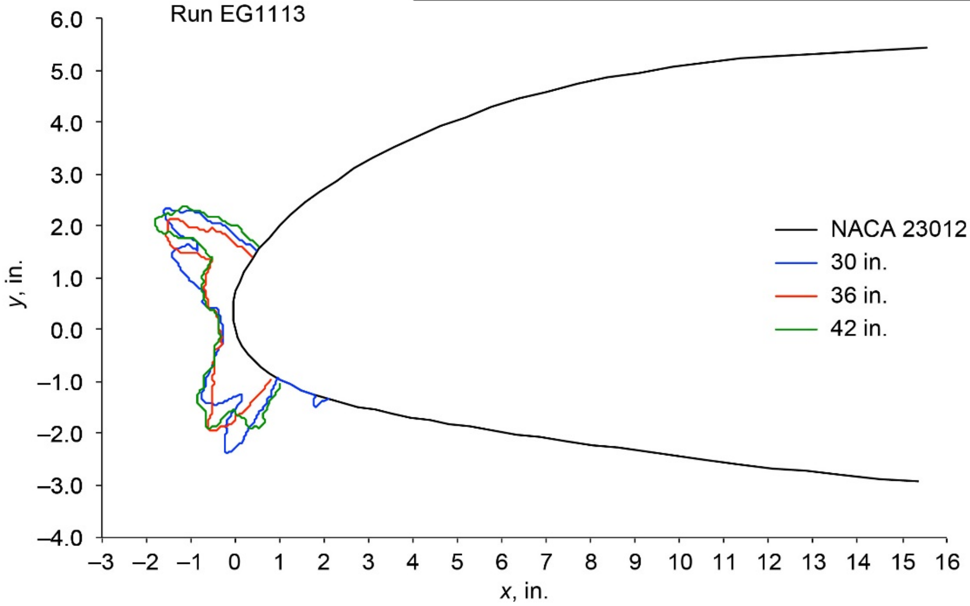

Pressure surface

Leading edge

Suction surface

Run EG1113

Appendix F.—IRT Full-Scale Model Tests

Run EG1114

V = 200 kt
T_t = –2.2 °C
T_s = –7.4 °C

AoA = 2.0°
LWC = 0.50 g/m^3
MVD = 20.0 µm
Exposure time = 22.5 min

Measured ice thickness

Station	Upper max, in.	Stag. line, in.	Lower max, in.
28.5	2.05	0.36	1.76
-	-	-	-
43.5	2.65	0.35	1.98

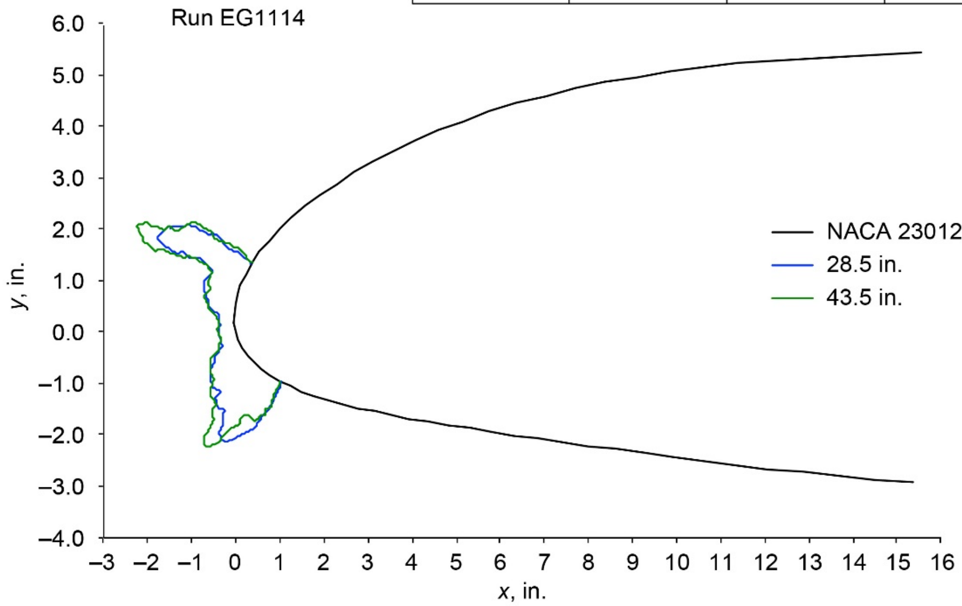

Pressure surface

Leading edge

Suction surface

Run EG1114

Appendix F.—IRT Full-Scale Model Tests

Run EG1115

V = 175 kt
T_t = –2.2 °C
T_s = –6.2 °C

AoA = 5.0°
LWC = 0.60 g/m^3
MVD = 20.0 µm
Exposure time = 22.5 min

Measured ice thickness

Station	Upper max, in.	Stag. line, in.	Lower max, in.
30	2.37	0.33	1.01
36	2.38	0.44	0.91
42	2.55	0.36	1.02

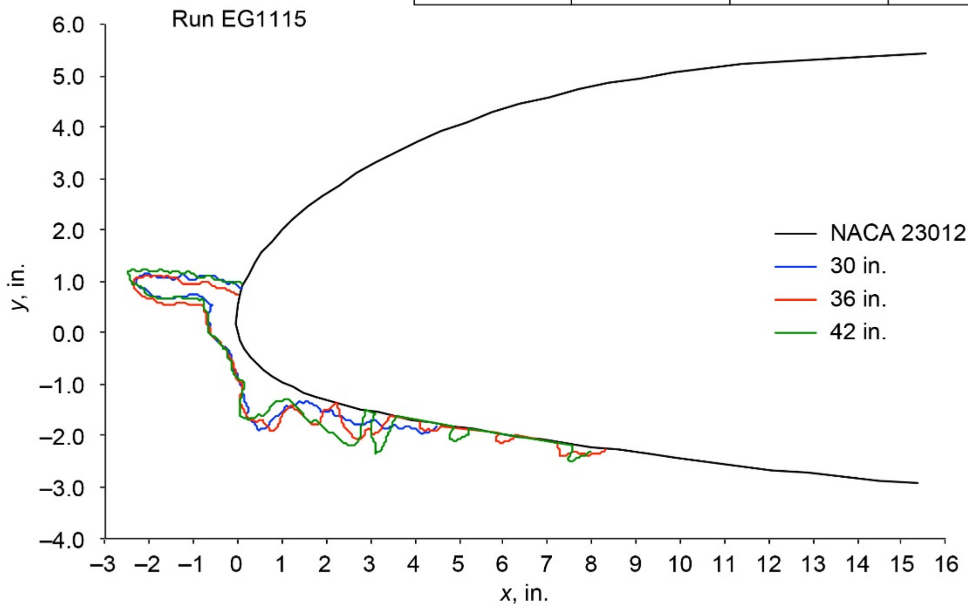

Pressure surface

Leading edge

Suction surface

Run EG1115

Appendix F.—IRT Full-Scale Model Tests

Run EG1116

V = 175 kt
T_t = –1.1 °C
T_s = –5.1 °C

AoA = 5.0°
LWC = 0.60 g/m^3
MVD = 20.0 µm
Exposure time = 22.5 min

Measured ice thickness

Station	Upper max, in.	Stag. line, in.	Lower max, in.
30	2.08	0.22	1.45
36	2.00	0.22	0.93
42	2.09	0.22	1.26

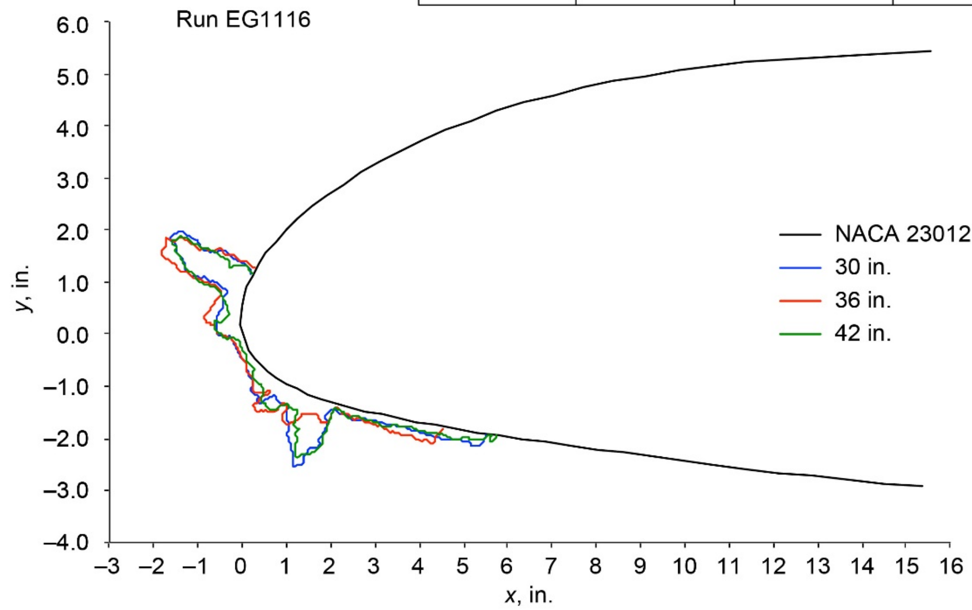

Pressure surface

Leading edge

Suction surface

Run EG1116

Appendix F.—IRT Full-Scale Model Tests

Run EG1117

V = 200 kt
T_t = –2.2 °C
T_s = –7.4 °C

AoA = 2.0°
LWC = 0.50 g/m^3
MVD = 20.0 µm
Exposure time = 2.0 min

Measured ice thickness

Station	Upper max, in.	Stag. line, in.	Lower max, in.
-	-	-	-
36	0.10	0.06	0.12
-	-	-	-

Run EG1117

No tracings

Pressure surface

Leading edge

Suction surface

Run EG1117

Appendix F.—IRT Full-Scale Model Tests

Run EG1118

V = 200 kt
T_t = –2.2 °C
T_s = –7.4 °C

AoA = 2.0°
LWC = 0.50 g/m^3
MVD = 20.0 μm
Exposure time = 1.0 min

Measured ice thickness

Station	Upper max, in.	Stag. line, in.	Lower max, in.
-	-	-	-
36	0.05	0.04	0.06
-	-	-	-

Run EG1118

No tracings

Pressure surface

Leading edge

Suction surface

Run EG1118

Appendix F.—IRT Full-Scale Model Tests

Run EG1119

V = 175 kt AoA = 5.0°
T_t = –2.2 °C LWC = 0.60 g/m^3
T_s = –6.2 °C MVD = 20.0 µm
Exposure time = 2.0 min

Measured ice thickness

Station	Upper max, in.	Stag. line, in.	Lower max, in.
-	-	-	-
36	0.13	0.07	0.08
-	-	-	-

Run EG1119

No tracings


Pressure surface


Leading edge

Suction surface

Run EG1119

Appendix F.—IRT Full-Scale Model Tests

Run EG1120

V = 200 kt
T_t = –15.6 °C
T_s = –20.7 °C
AoA = 2.0°
LWC = 0.30 g/m^3
MVD = 20.0 μm
Exposure time = 10.0 min

Measured ice thickness

Station	Upper max, in.	Stag. line, in.	Lower max, in.
30	0.21	0.32	0.21
36	0.24	0.32	0.20
42	0.40	0.50	0.34

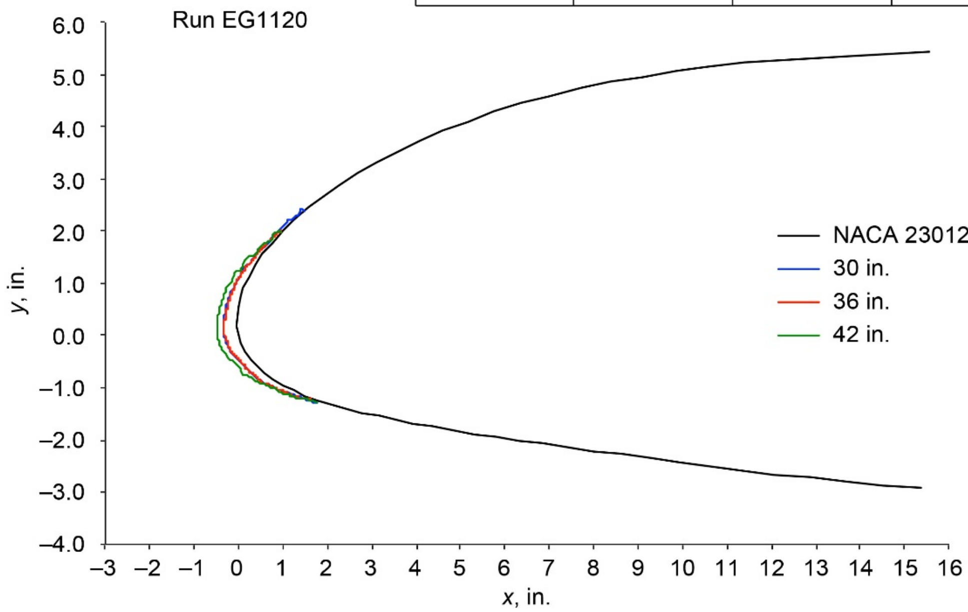

Pressure surface

Leading edge

Suction surface

Run EG1120

Appendix F.—IRT Full-Scale Model Tests

Run EG1121

V = 200 kt
T_t = –15.6 °C
T_s = –20.7 °C
AoA = 2.0°
LWC = 0.55 g/m^3
MVD = 40.0 µm
Exposure time = 10.0 min

Measured ice thickness

Station	Upper max, in.	Stag. line, in.	Lower max, in.
30	0.98	0.83	0.91
36	0.97	0.84	0.95
42	1.26	0.88	1.25

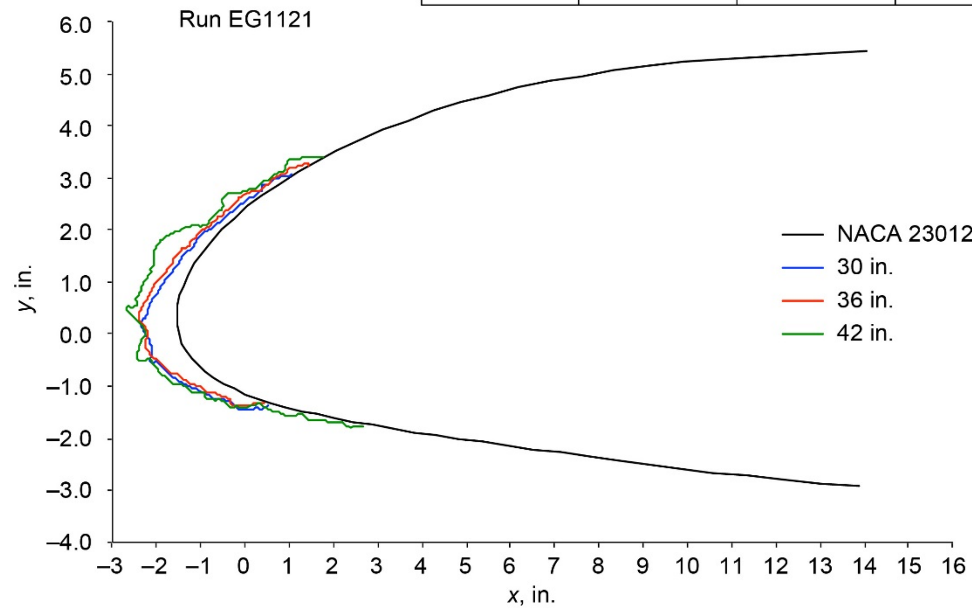

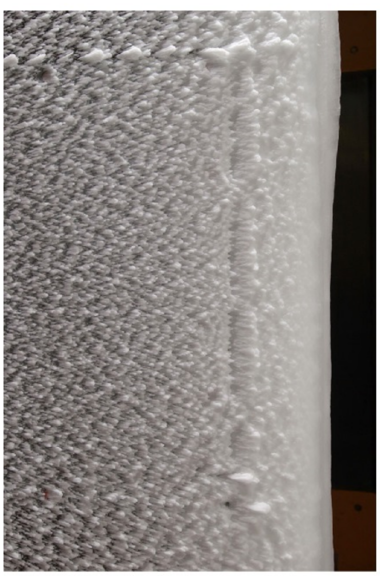

Pressure surface

Leading edge

Suction surface

Run EG1121

Appendix F.—IRT Full-Scale Model Tests

Run EG1122

Measured ice thickness

Station	Upper max, in.	Stag. line, in.	Lower max, in.
30	0.28	0.33	0.24
36	0.24	0.30	0.22
42	0.30	0.36	0.25

V = 200 kt AoA = 2.0°
T_t = –15.6 °C LWC = 0.30 g/m^3
T_s = –20.7 °C MVD = 15.0 µm
Exposure time = 10.0 min

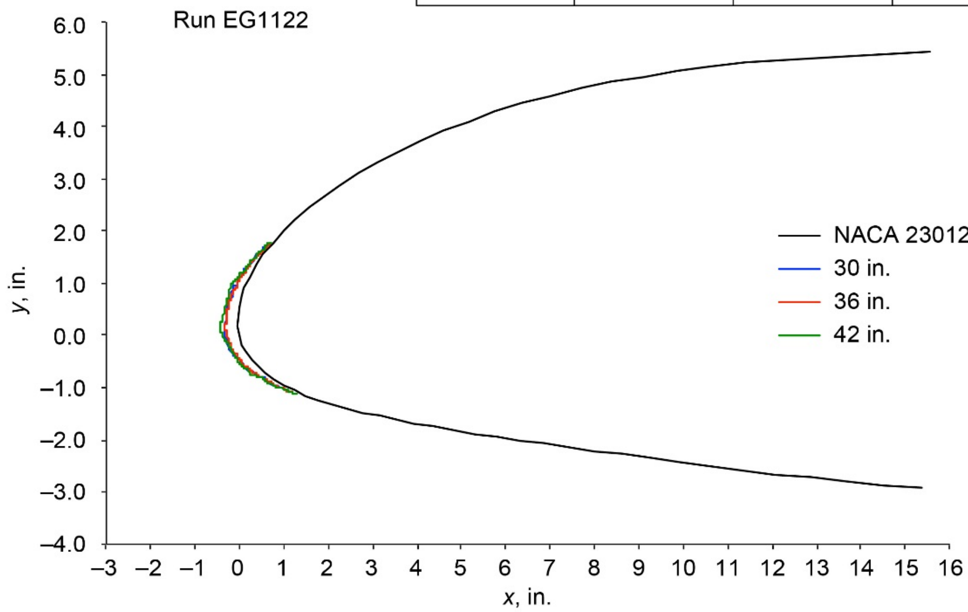

Pressure surface

Leading edge

Suction surface

Run EG1122

Appendix F.—IRT Full-Scale Model Tests

Run EG1123

V = 200 kt
T_t = –15.6 °C
T_s = –20.7 °C
AoA = 2.0°
LWC = 0.30 g/m^3
MVD = 15.0 µm
Exposure time = 20.0 min

Measured ice thickness

Station	Upper max, in.	Stag. line, in.	Lower max, in.
30	0.57	0.67	0.48
36	0.51	0.60	0.44
42	0.62	0.69	0.56

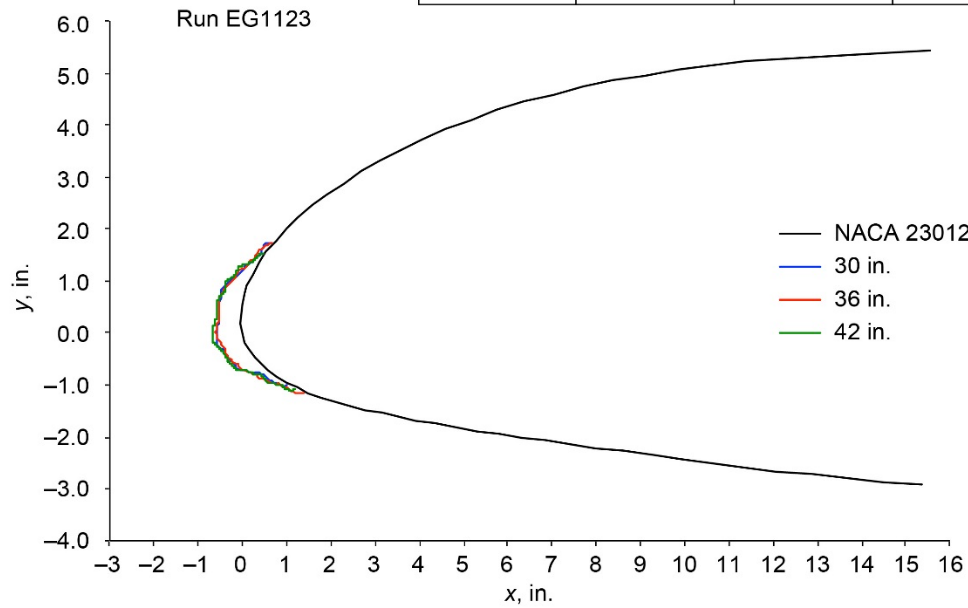

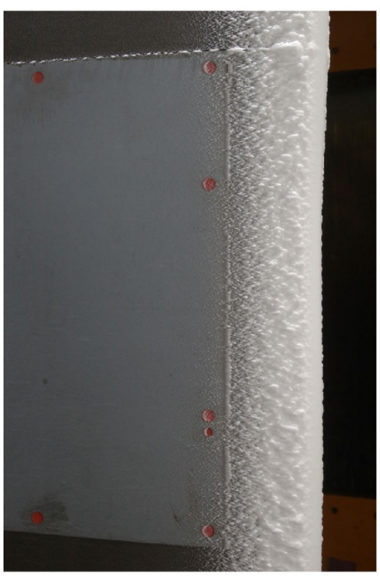

Pressure surface

Leading edge

Suction surface

Run EG1123

Appendix F.—IRT Full-Scale Model Tests

Run EG1124

V = 200 kt
T_t = –15.6 °C
T_s = –20.7 °C
AoA = 5.0°
LWC = 0.30 g/m^3
MVD = 15.0 µm
Exposure time = 20.0 min

Measured ice thickness

Station	Upper max, in.	Stag. line, in.	Lower max, in.
30	0.70	0.61	0.40
36	0.58	0.48	0.32
42	0.55	0.41	0.31

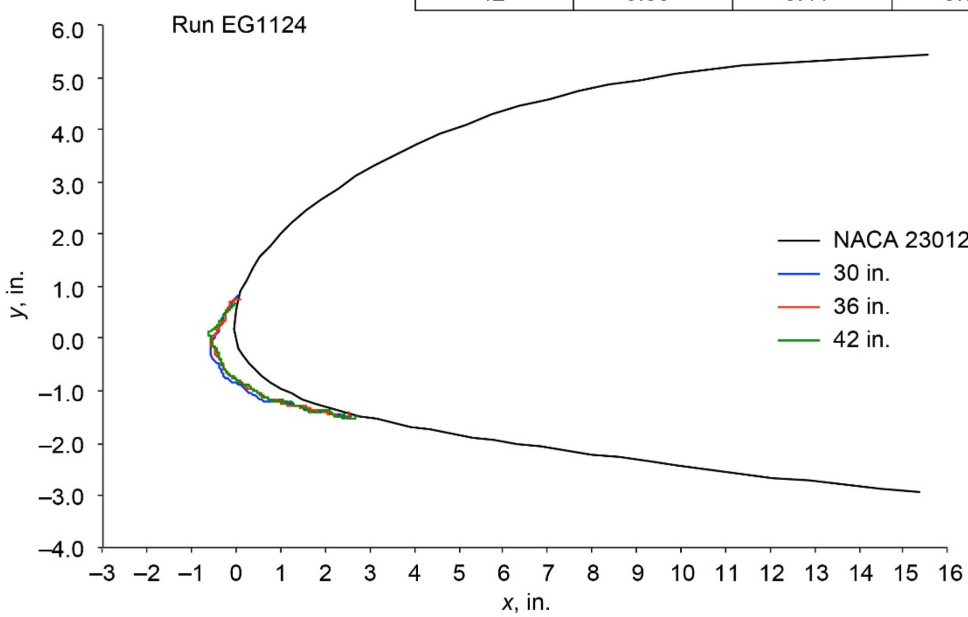

Pressure surface

Leading edge

Suction surface

Run EG1124

Appendix F.—IRT Full-Scale Model Tests

Run EG1125

V = 200 kt
T_t = –15.6 °C
T_s = –20.7 °C
AoA = 2.0°
LWC = 0.30 g/m^3
MVD = 15.0 μm
Exposure time = 20.0 min

Measured ice thickness

Station	Upper max, in.	Stag. line, in.	Lower max, in.
28.5	0.52	0.61	0.47
-	-	-	-
43.5	0.71	0.75	0.65

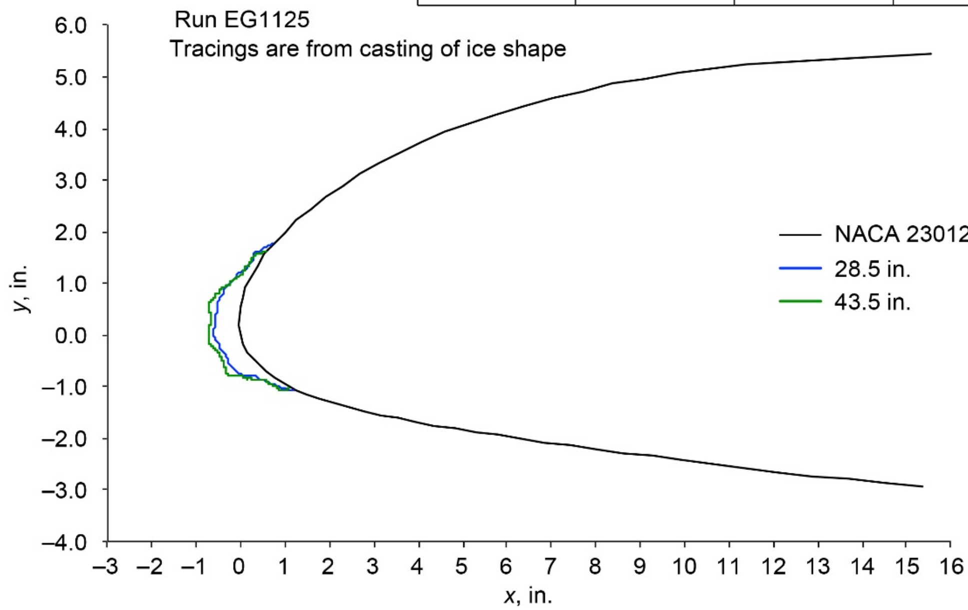

Pressure surface

Leading edge

Suction surface

Run EG1125

Appendix F.—IRT Full-Scale Model Tests

Run EG1126

V = 200 kt
T_t = –2.2 °C
T_s = –7.4 °C
AoA = 2.0°
LWC = 0.50 g/m^3
MVD = 20.0 µm
Exposure time = 2.0 min

Measured ice thickness

Station	Upper max, in.	Stag. line, in.	Lower max, in.
28.5	0.16	0.06	0.13
-	-	-	-
43.5	0.20	0.06	0.13

Run EG1126

No tracings

Pressure surface

Leading edge

Suction surface

Run EG1126

Appendix F.—IRT Full-Scale Model Tests

Run EG1127

V = 200 kt
T_t = –2.2 °C
T_s = –6.2 °C

AoA = 5.0°
LWC = 0.70 g/m^3
MVD = 20.0 µm
Exposure time = 22.5 min

Measured ice thickness

Station	Upper max, in.	Stag. line, in.	Lower max, in.
30	2.40	0.41	1.03
36	2.34	0.40	1.05
42	2.50	0.40	1.06

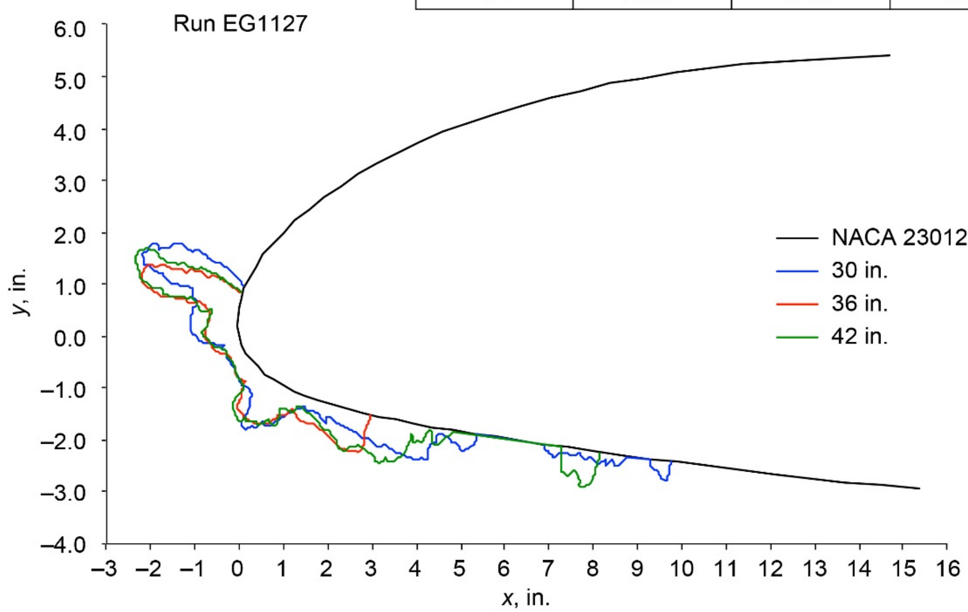

Pressure surface

Leading edge

Suction surface

Run EG1127

Appendix F.—IRT Full-Scale Model Tests

Run EG1128

V = 175 kt
T_t = –2.2 °C
T_s = –6.2 °C

AoA = 5.0°
LWC = 0.85 g/m^3
MVD = 20.0 µm
Exposure time = 22.5 min

Measured ice thickness

Station	Upper max, in.	Stag. line, in.	Lower max, in.
30	2.79	0.51	1.32
36	2.68	0.48	1.25
42	3.31	0.47	1.22

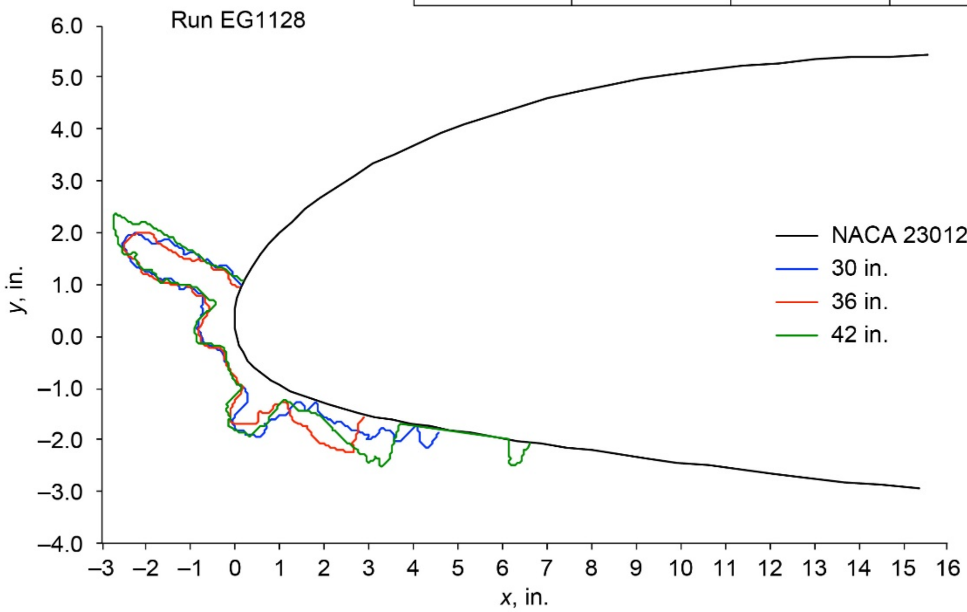


Pressure surface


Leading edge


Suction surface

Run EG1128

Run EG1129

V = 200 kt
T_t = –2.2 °C
T_s = –7.4 °C

AoA = 2.0°
LWC = 0.50 g/m^3
MVD = 20.0 µm
Exposure time = 22.5 min

Measured ice thickness

Station	Upper max, in.	Stag. line, in.	Lower max, in.
30	2.23	0.38	1.74
36	2.19	0.38	1.68
42	2.47	0.38	1.75

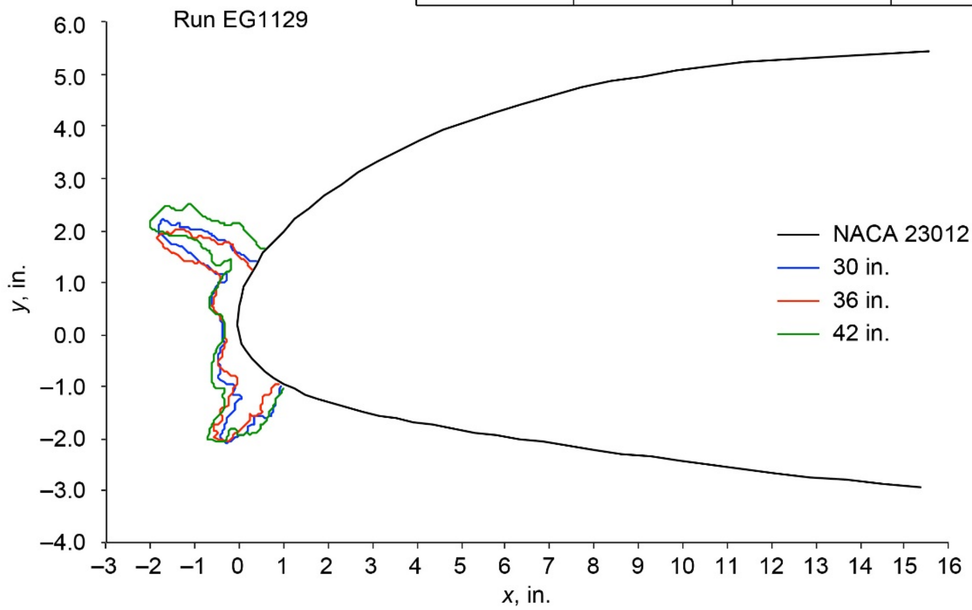

Pressure surface

Leading edge

Suction surface

Run EG1130

V = 175 kt
T_t = –2.2 °C
T_s = –6.2 °C
AoA = 5.0°
LWC = 0.85 g/m^3
MVD = 20.0 µm
Exposure time = 22.5 min

Measured ice thickness

Station	Upper max, in.	Stag. line, in.	Lower max, in.
28.5	2.92	0.38	1.31
-	-	-	-
43.5	3.04	0.39	1.26

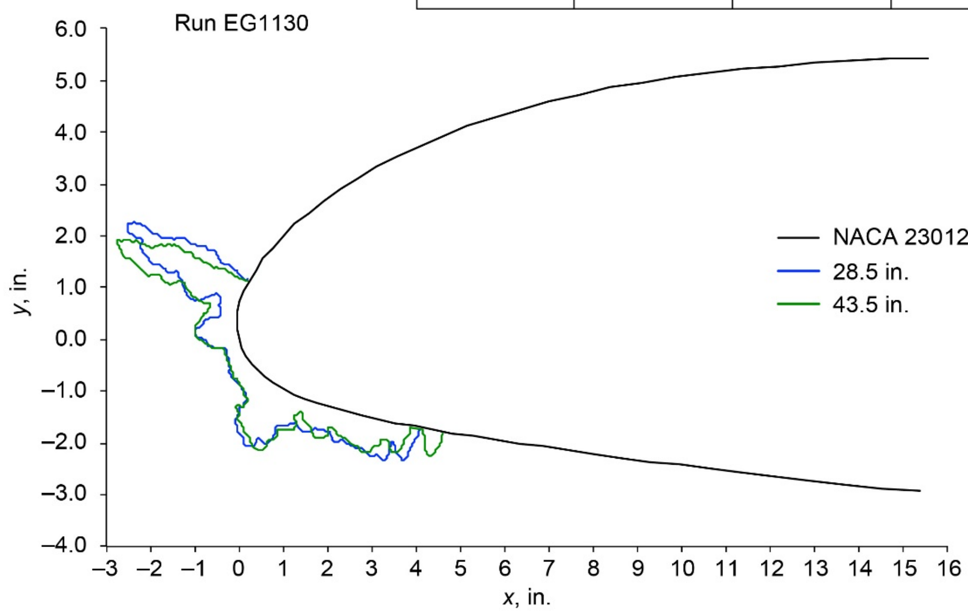

Pressure surface

Leading edge

Suction surface

App. F23—Run EG1130.

Run EG1130

Appendix F.—IRT Full-Scale Model Tests

Run EG1131

V = 200 kt
T_t = –15.6 °C
T_s = –20.7 °C

AoA = 2.0°
LWC = 0.30 g/m^3
MVD = 15.0 µm
Exposure time = 2.0 min

Measured ice thickness

Station	Upper max, in.	Stag. line, in.	Lower max, in.
-	-	-	-
36	-	0.05	-
-	-	-	-

Run EG1131

No tracings

Pressure surface

Leading edge

Suction surface

Run EG1131

Appendix F.—IRT Full-Scale Model Tests

Run EG1132

V = 200 kt AoA = 2.0°
T_t = –15.6 °C LWC = 0.30 g/m^3
T_s = –20.7 °C MVD = 15.0 µm
Exposure time = 4.0 min

Measured ice thickness

Station	Upper max, in.	Stag. line, in.	Lower max, in.
-	-	-	-
36	-	0.09	-
-	-	-	-

Run EG1132

No tracings

Pressure surface

Leading edge

Suction surface

Run EG1132

Appendix F.—IRT Full-Scale Model Tests

Run EG1133

V = 200 kt
T_t = –15.6 °C
T_s = –20.7 °C

AoA = 2.0°
LWC = 0.55 g/m^3
MVD = 40.0 µm
Exposure time = 2.0 min

Measured ice thickness

Station	Upper max, in.	Stag. line, in.	Lower max, in.
-	-	-	-
36	0.08	0.17	0.05
-	-	-	-

Run EG1133

No tracings

Pressure surface

Leading edge

Suction surface

Run EG1133

Appendix F.—IRT Full-Scale Model Tests

Run EG1134

V = 200 kt
T_t = –15.6 °C
T_s = –20.7 °C
AoA = 2.0°
LWC = 0.55 g/m^3
MVD = 40.0 µm
Exposure time = 2.0 min

Measured ice thickness

Station	Upper max, in.	Stag. line, in.	Lower max, in.
28.5	-	0.23	-
-	-	-	-
43.5	-	0.25	-

Run EG1134

No tracings

Pressure surface

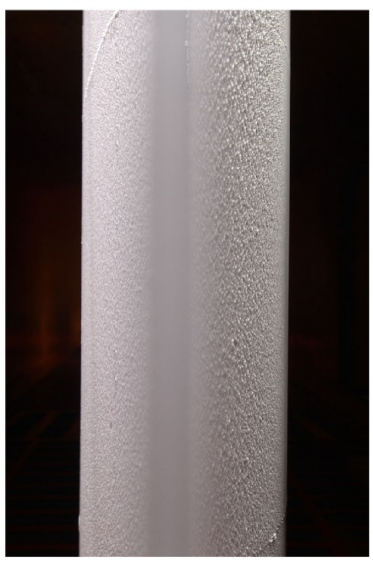

Leading edge

Suction surface

Run EG1134

Appendix F.—IRT Full-Scale Model Tests

Run EG1135

V = 200 kt
T_t = –15.6 °C
T_s = –20.7 °C

AoA = 2.0°
LWC = 0.30 g/m^3
MVD = 15.0 µm
Exposure time = 20.0 min

Measured ice thickness

Station	Upper max, in.	Stag. line, in.	Lower max, in.
30	0.58	0.67	0.53
36	0.50	0.60	0.42
42	0.62	0.70	0.51

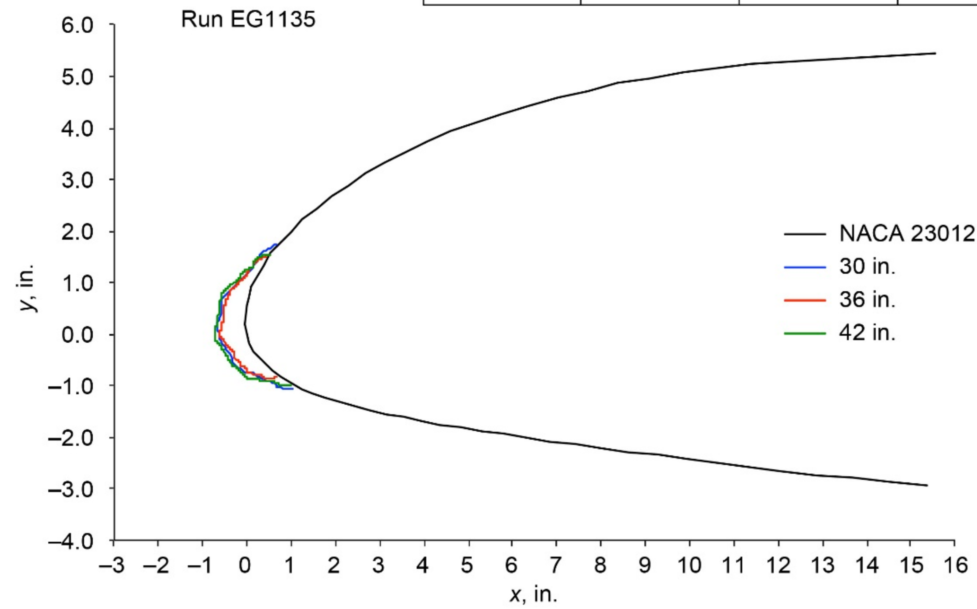

Pressure surface

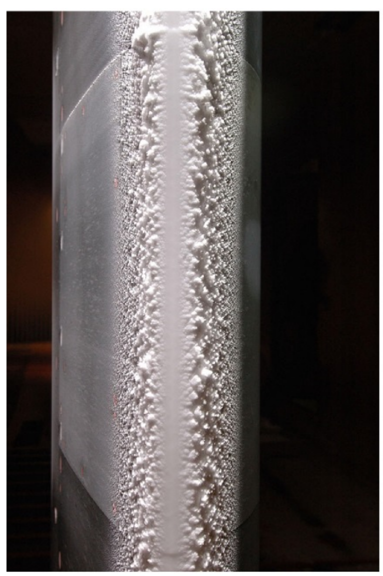

Leading edge

Suction surface

Run EG1135

Appendix F.—IRT Full-Scale Model Tests

Run EG1136

V = 200 kt AoA = 2.0°
T_t = –15.6 °C LWC = 0.55 g/m^3
T_s = –20.7 °C MVD = 40.0 μm
Exposure time = 2.0 min

Run EG1136

Measured ice thickness*

Station	Upper max, in.	Stag. line, in.	Lower max, in.
-	-	-	-
-	-	-	-
-	-	-	-

*No tracings or thickness measurements made: ice not suitable.

Pressure surface   Leading edge   Suction surface

Run EG1136

Appendix F.—IRT Full-Scale Model Tests

Run EG1137

V = 200 kt
T_t = –15.6 °C
T_s = –20.7 °C
AoA = 5.0°
LWC = 0.30 g/m^3
MVD = 15.0 μm
Exposure time = 20.0 min

Measured ice thickness

Station	Upper max, in.	Stag. line, in.	Lower max, in.
28.5	0.54	0.60	0.37
-	-	-	-
43.5	0.59	0.53	0.35

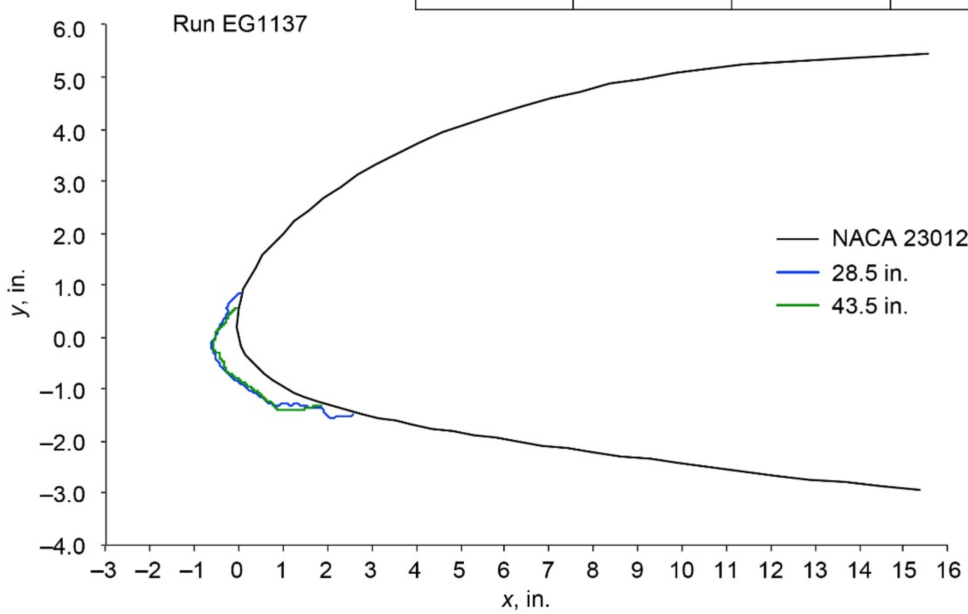

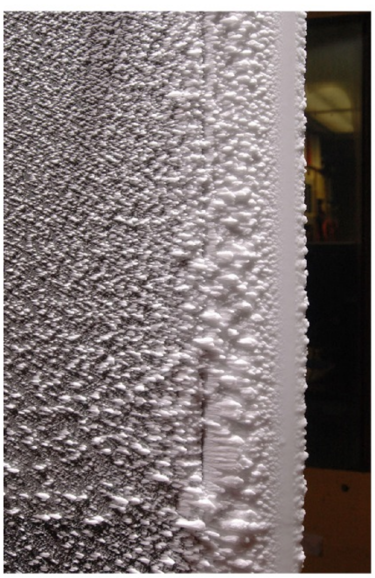

Pressure surface

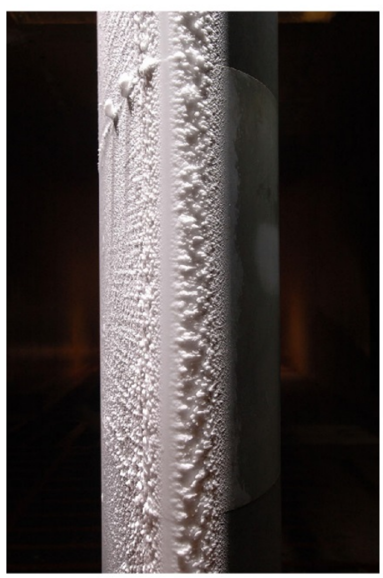

Leading edge

Suction surface

Run EG1137

Appendix F.—IRT Full-Scale Model Tests

Run EG1138

V = 175 kt
T_t = –2.2 °C
T_s = –6.2 °C

AoA = 5.0°
LWC = 0.85 g/m^3
MVD = 20.0 μm
Exposure time = 22.5 min

Measured ice thickness

Station	Upper max, in.	Stag. line, in.	Lower max, in.
30	2.92	0.45	1.23
36	2.92	0.46	1.19
42	3.10	0.44	1.16

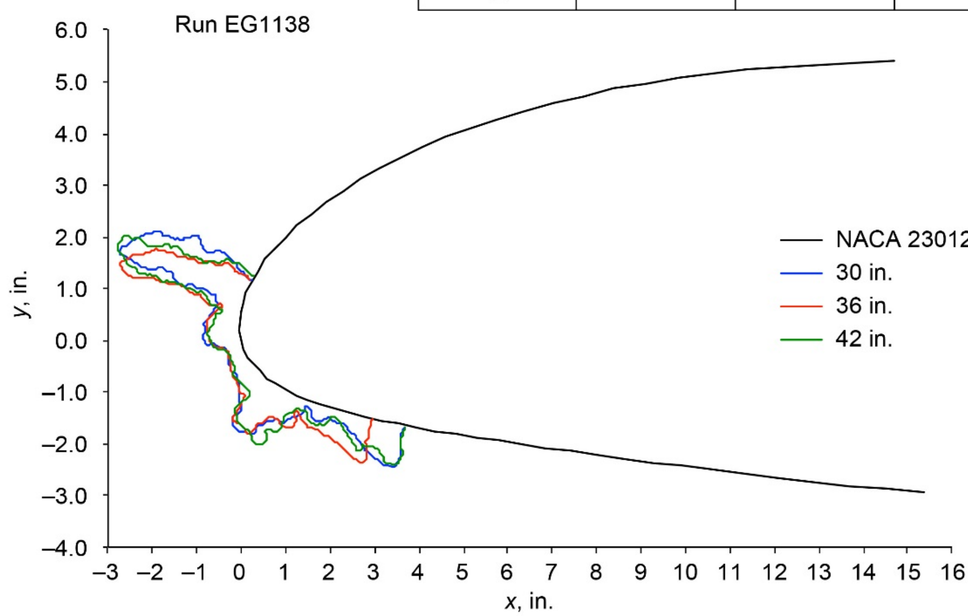

Pressure surface

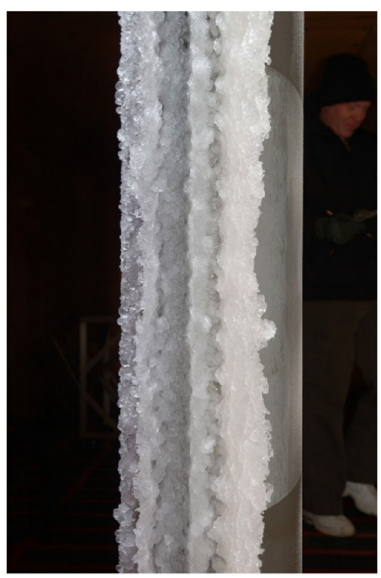

Leading edge

Suction surface

Run EG1138

Appendix F.—IRT Full-Scale Model Tests

Run EG1139

V = 175 kt
T_t = –2.2 °C
T_s = –6.2 °C

AoA = 5.0°
LWC = 0.85 g/m^3
MVD = 20.0 µm
Exposure time = 11.25 min

Measured ice thickness

Station	Upper max, in.	Stag. line, in.	Lower max, in.
30	1.60	0.19	0.74
36	1.53	0.21	0.70
42	1.60	0.20	0.65

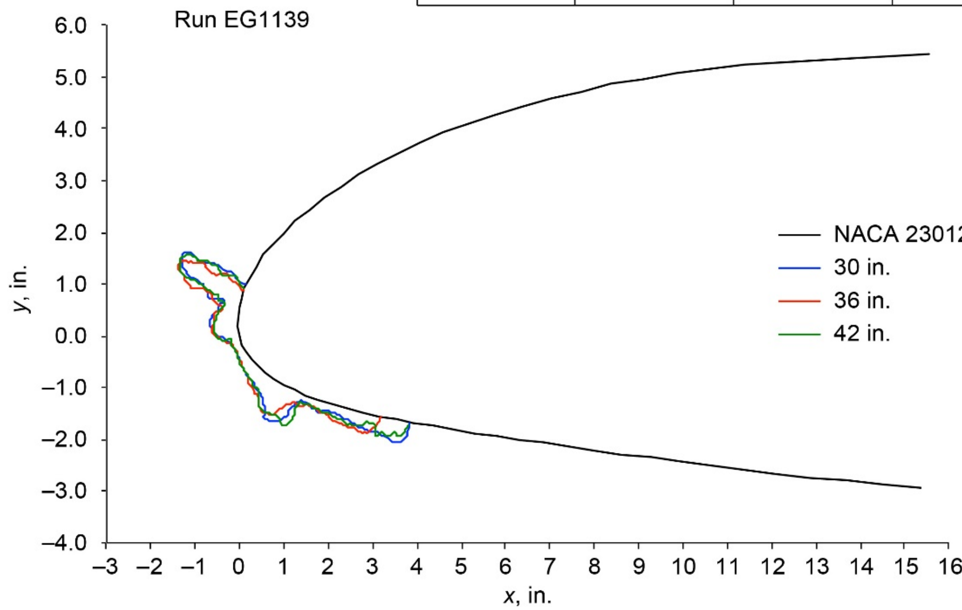

Pressure surface

Leading edge

Suction surface

Run EG1139

Appendix F.—IRT Full-Scale Model Tests

Run EG1140

V = 200 kt
T_t = –2.2 °C
T_s = –7.4 °C

AoA = 2.0°
LWC = 0.50 g/m^3
MVD = 20.0 μm
Exposure time = 2.0 min

Measured ice thickness

Station	Upper max, in.	Stag. line, in.	Lower max, in.
-	-	-	-
36	0.13	0.06	0.08
-	-	-	-

Run EG1140

No tracings

Pressure surface

Leading edge

Suction surface

Run EG1140

Appendix F.—IRT Full-Scale Model Tests

Run EG1141

V = 200 kt
T_t = –15.6 °C
T_s = –20.7 °C
AoA = 2.0°
LWC = 0.45 g/m^3
MVD = 30.0 µm
Exposure time = 10.0 min

Measured ice thickness

Station	Upper max, in.	Stag. line, in.	Lower max, in.
30	0.53	0.67	0.38
36	0.66	0.72	0.50
42	0.64	0.81	0.49

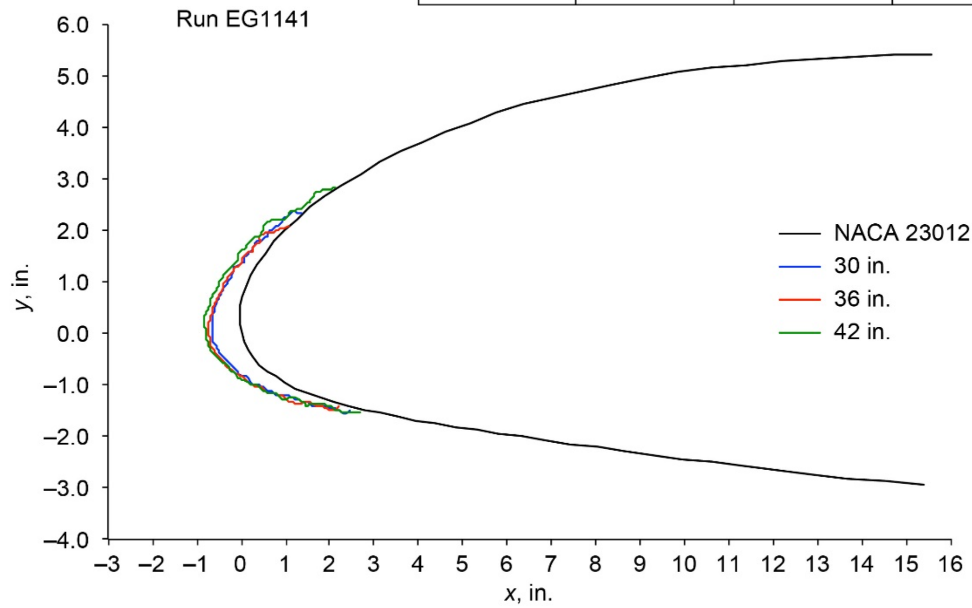

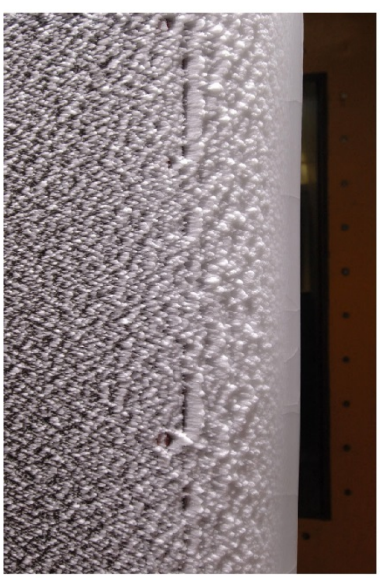

Pressure surface

Leading edge

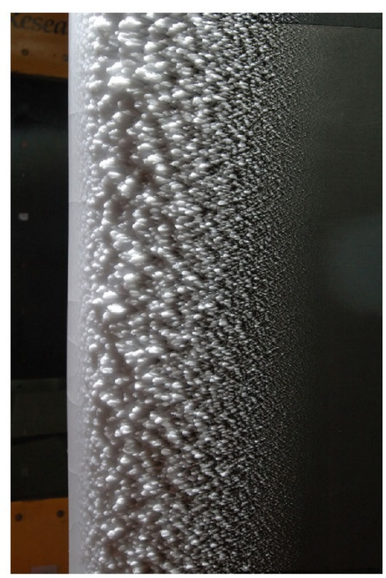

Suction surface

Run EG1141

Appendix F.—IRT Full-Scale Model Tests

Run EG1142

V = 200 kt
T_t = –6.7 °C
T_s = –11.8 °C
AoA = 2.0°
LWC = 0.50 g/m^3
MVD = 20.0 µm
Exposure time = 15.0 min

Measured ice thickness

Station	Upper max, in.	Stag. line, in.	Lower max, in.
30	0.29	-	0.92
36	0.21	-	0.63
42	0.96	-	0.89

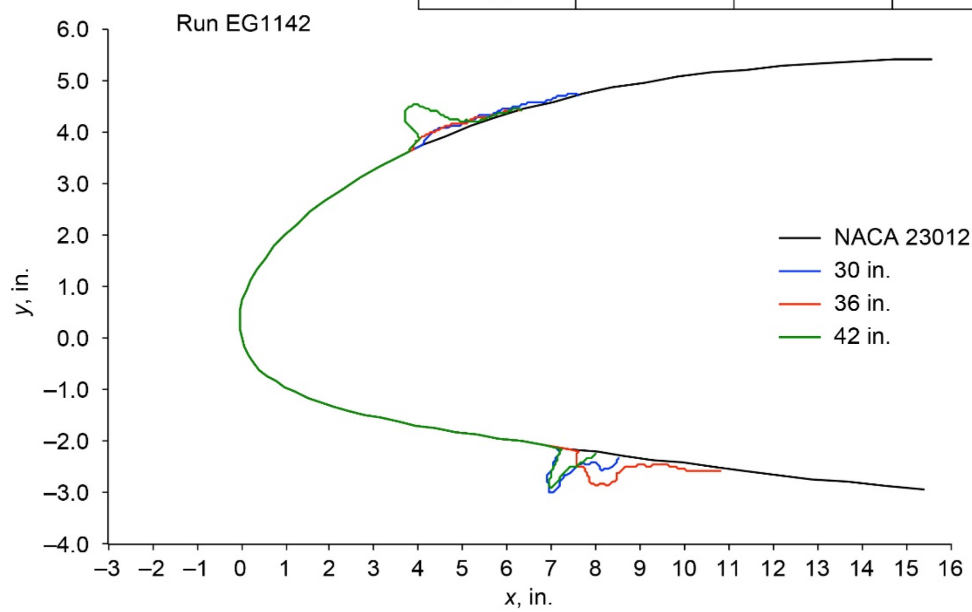

Pressure surface

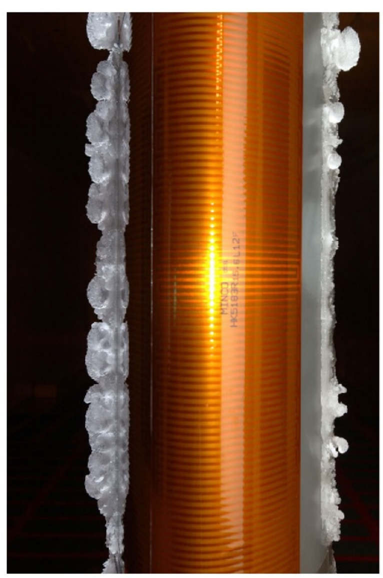

Leading edge

Suction surface

Run EG1142

Appendix F.—IRT Full-Scale Model Tests

Run EG1143

V = 200 kt
T_t = –6.7 °C
T_s = –11.8 °C
AoA = 0.0°
LWC = 0.50 g/m3
MVD = 20.0 µm
Exposure time = 15.0 min

Measured ice thickness

Station	Upper max, in.	Stag. line, in.	Lower max, in.
30	0.96	-	0.19
36	0.48	-	0.21
42	0.86	-	0.11

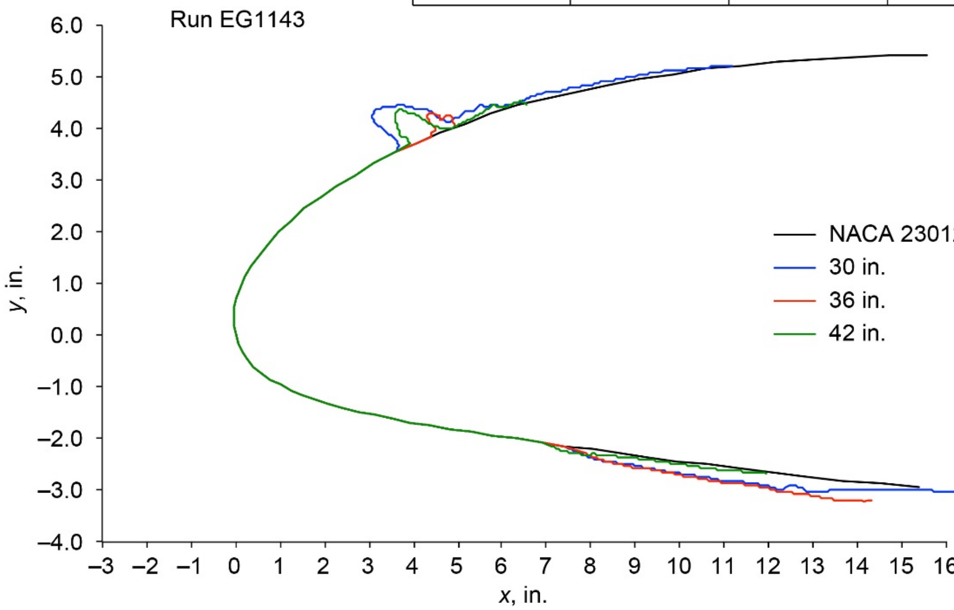

Pressure surface

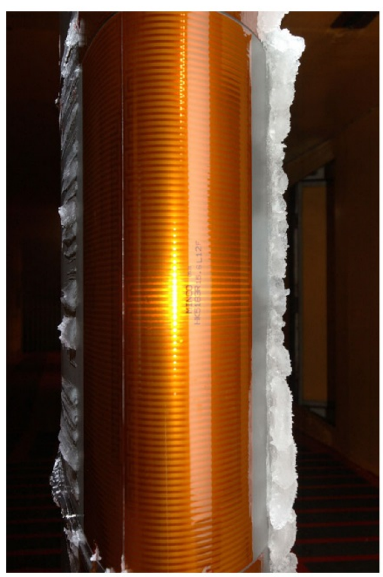

Leading edge

Suction surface

Run EG1143

Appendix F.—IRT Full-Scale Model Tests

Run EG1144

V = 200 kt
T_t = –6.7 °C
T_s = –11.8 °C
AoA = 1.0°
LWC = 0.50 g/m^3
MVD = 20.0 µm
Exposure time = 15.0 min

Measured ice thickness

Station	Upper max, in.	Stag. line, in.	Lower max, in.
30	0.90	-	0.24
36	0.37	-	0.11
42	0.20	-	0.30

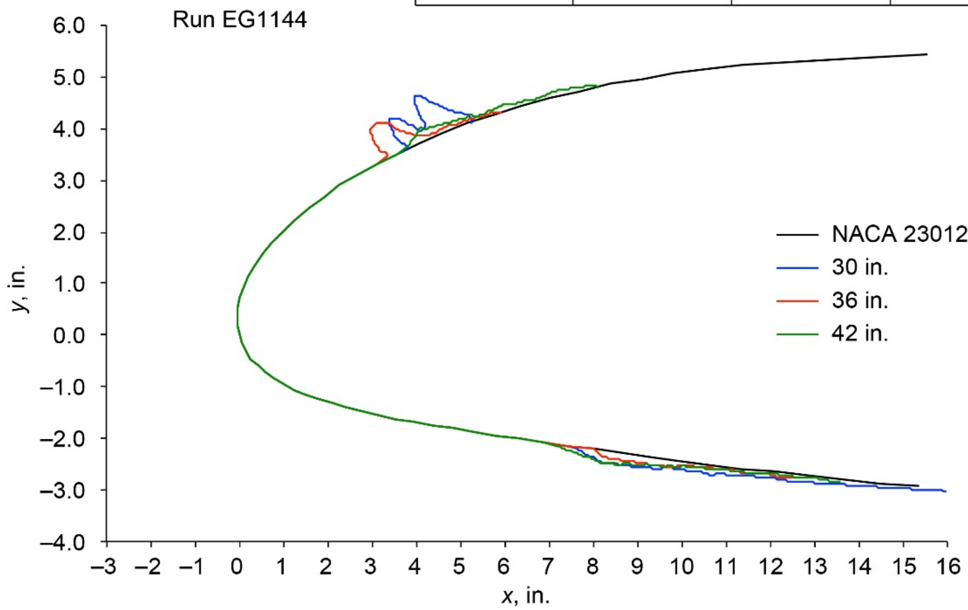

Pressure surface

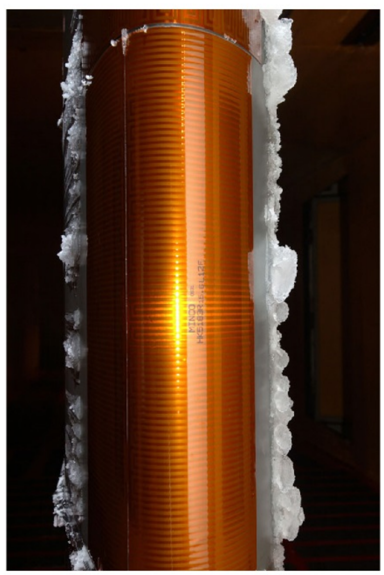

Leading edge

Suction surface

Run EG1144

Appendix F.—IRT Full-Scale Model Tests

Run EG1145

V = 200 kt
T_t = –6.7 °C
T_s = –11.8 °C
AoA = 1.5°
LWC = 0.50 g/m^3
MVD = 20.0 µm
Exposure time = 15.0 min

Measured ice thickness

Station	Upper max, in.	Stag. line, in.	Lower max, in.
30	0.20	-	0.71
36	0.10	-	0.00
42	0.18	-	0.58

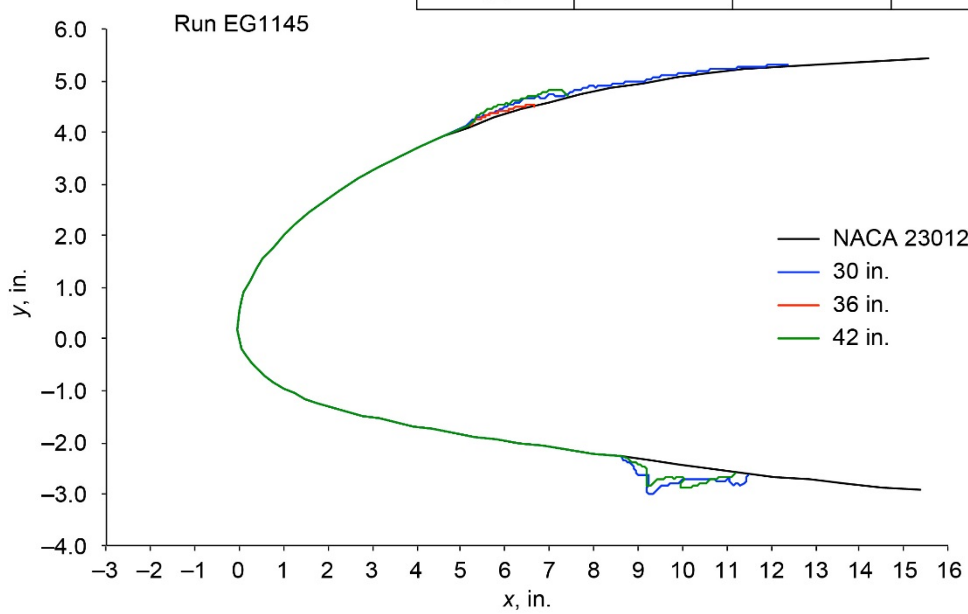

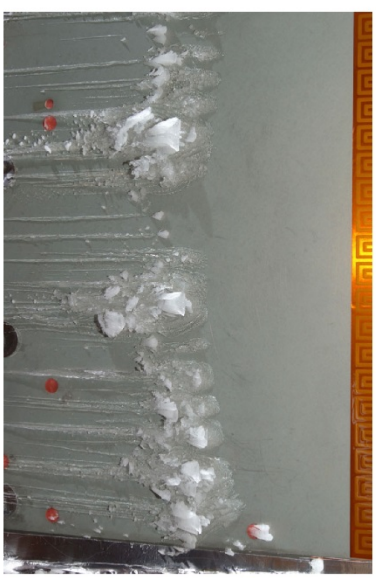

Pressure surface

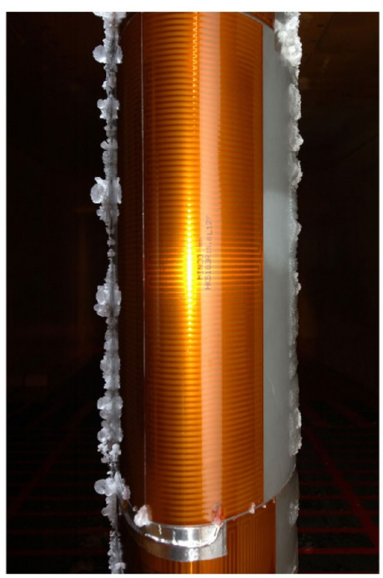

Leading edge

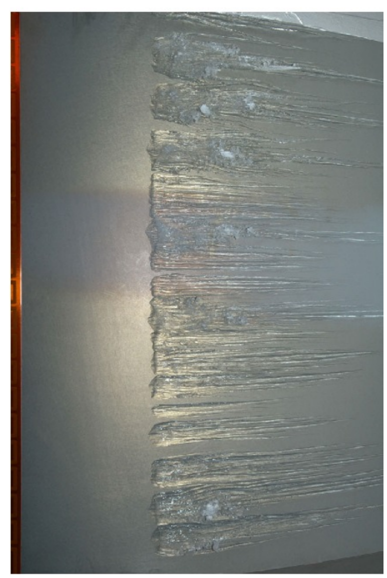

Suction surface

Run EG1145

Appendix F.—IRT Full-Scale Model Tests

Run EG1146

V = 200 kt
T_t = –6.7 °C
T_s = –11.8 °C

AoA = 1.5°
LWC = 0.50 g/m^3
MVD = 20.0 μm
Exposure time = 15.0 min

Measured ice thickness

Station	Upper max, in.	Stag. line, in.	Lower max, in.
30	0.24	-	0.26
36	0.29	-	0.24
42	0.26	-	0.29

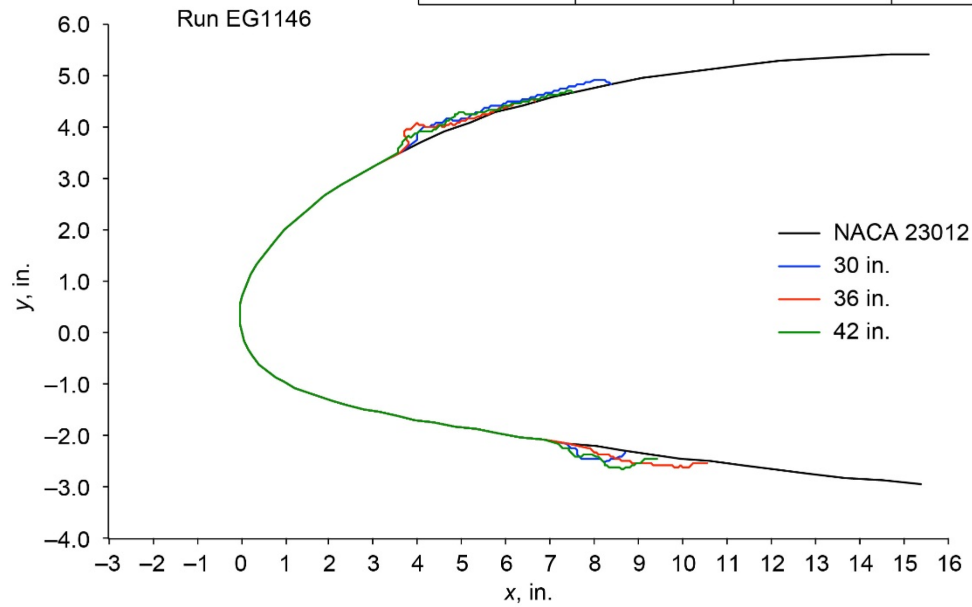

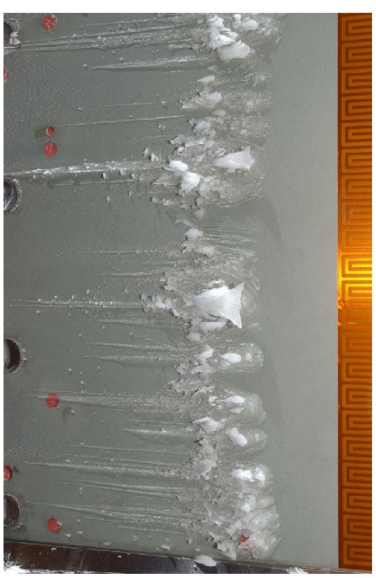

Pressure surface

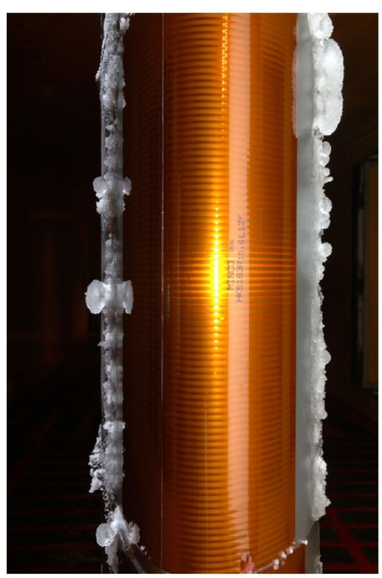

Leading edge

Suction surface

Run EG1146

Appendix F.—IRT Full-Scale Model Tests

Run EG1147

V = 200 kt
T_t = –6.7 °C
T_s = –11.8 °C

AoA^* = 0°, 2°, 1.5°
LWC = 0.50 g/m^3
MVD = 20.0 µm
Exposure time = 15.0 min

*Five minutes at each AoA.

Measured ice thickness

Station	Upper max, in.	Stag. line, in.	Lower max, in.
30	0.43	-	0.30
36	0.34	-	0.11
42	0.42	-	0.44

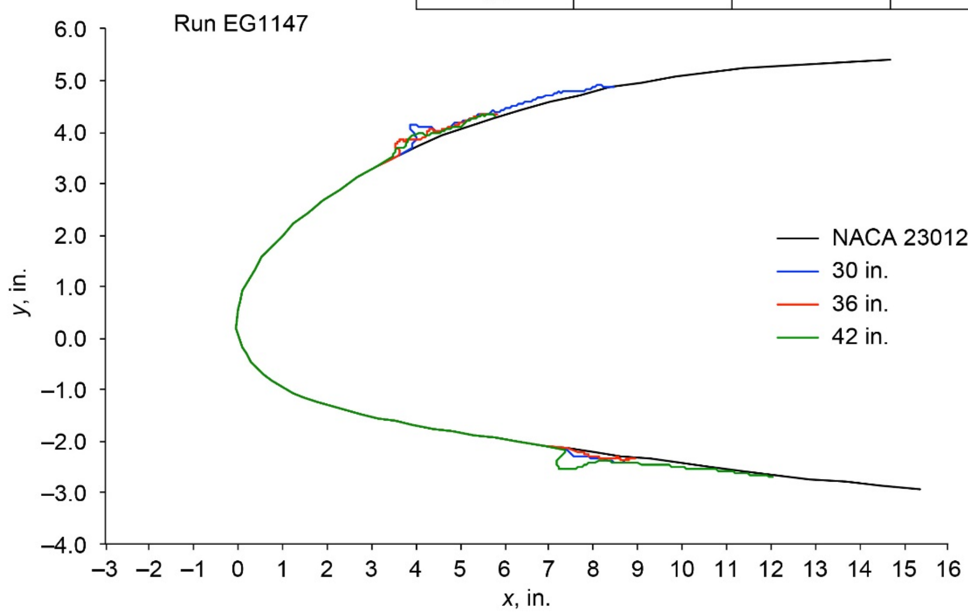

Pressure surface

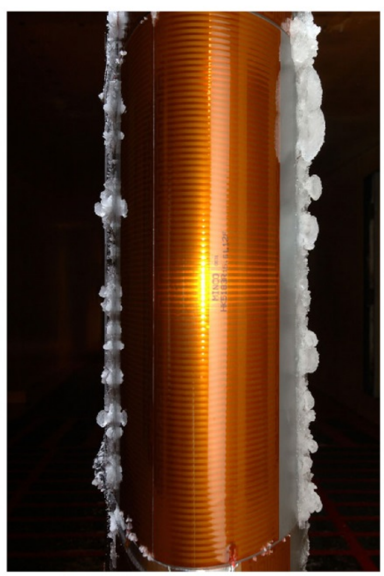

Leading edge

Suction surface

Run EG1147

Appendix F.—IRT Full-Scale Model Tests

Run EG1148

V = 200 kt
T_t = –6.7 °C
T_s = –11.8 °C
AoA = 1.5°
LWC = 0.50 g/m^3
MVD = 20.0 μm
Exposure time = 15.0 min

Measured ice thickness

Station	Upper max, in.	Stag. line, in.	Lower max, in.
30	0.24	-	0.27
36	0.23	-	0.22
42	0.34	-	0.38

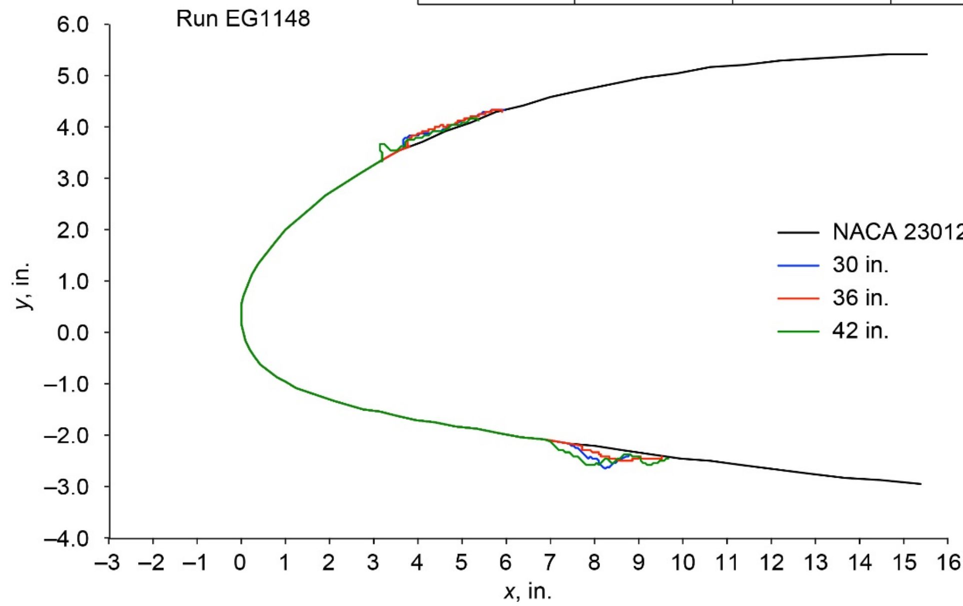

Pressure surface

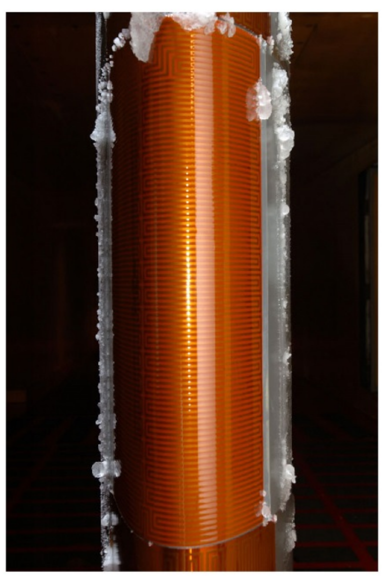

Leading edge

Suction surface

Run EG1148

Appendix F.—IRT Full-Scale Model Tests

Run EG1149

V = 150 kt
T_t = –6.7 °C
T_s = –9.6 °C

AoA = 1.5°
LWC = 0.62 g/m^3
MVD = 20.0 μm
Exposure time = 15.0 min

Measured ice thickness

Station	Upper max, in.	Stag. line, in.	Lower max, in.
30	0.13	-	0.19
36	0.13	-	0.16
42	0.13	-	0.19

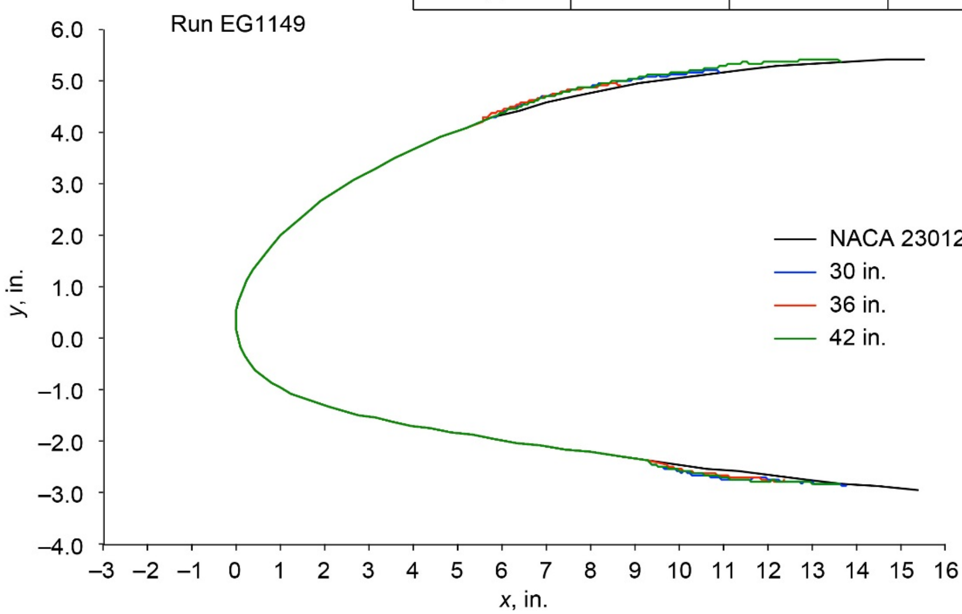

Pressure surface

Leading edge

Suction surface

Run EG1149

Appendix F.—IRT Full-Scale Model Tests

Run EG1150

V = 150 kt
T_t = –6.7 °C
T_s = –9.6 °C
AoA = 1.5°
LWC = 0.81 g/m^3
MVD = 20.0 µm
Exposure time = 15.0 min

Measured ice thickness

Station	Upper max, in.	Stag. line, in.	Lower max, in.
30	0.13	-	0.65
36	0.13	-	0.44
42	0.14	-	0.49

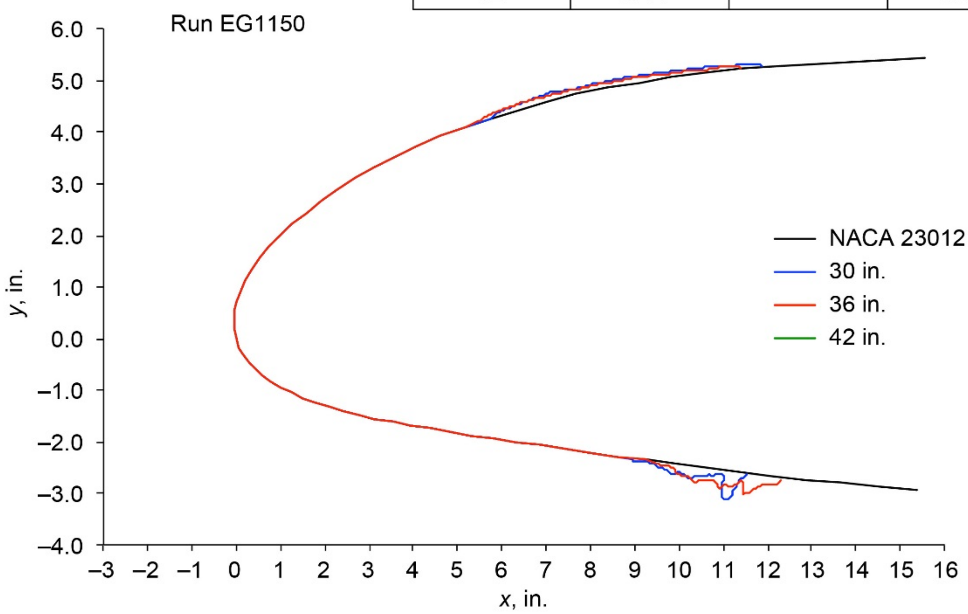

Pressure surface

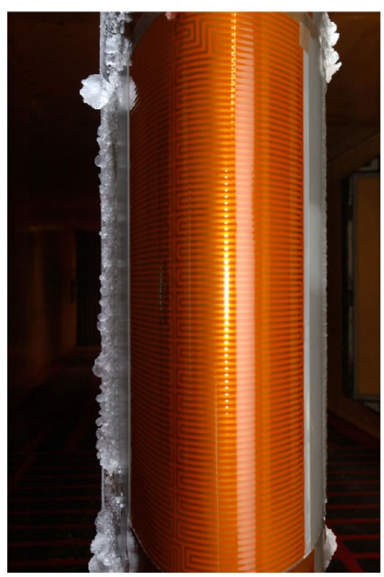

Leading edge

Suction surface

Run EG1150

Appendix F.—IRT Full-Scale Model Tests

Run EG1151

V = 150 kt
T_t = –6.7 °C
T_s = –9.6 °C

AoA = 1.5°
LWC = 0.81 g/m^3
MVD = 20.0 µm
Exposure time = 15.0 min

Measured ice thickness

Station	Upper max, in.	Stag. line, in.	Lower max, in.
30	0.41	-	0.84
36	0.68	-	0.46
42	0.71	-	0.75

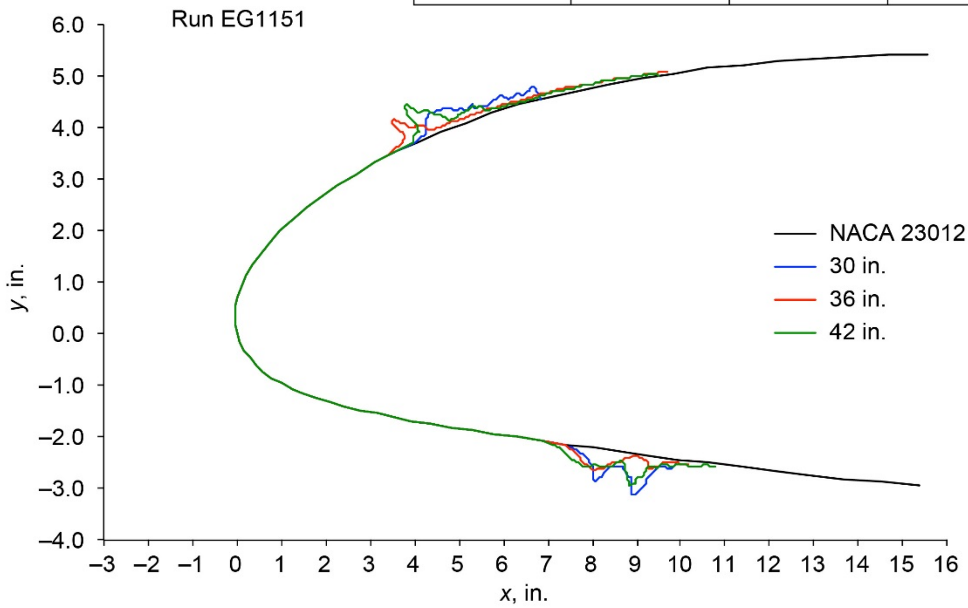

Pressure surface

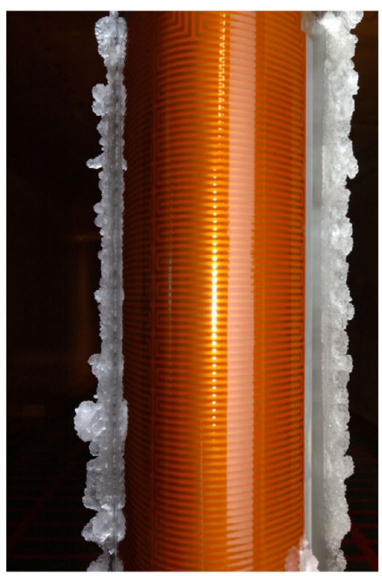

Leading edge

Suction surface

Run EG1151

Appendix F.—IRT Full-Scale Model Tests

Run EG1152

V = 150 kt
T_t = –6.7 °C
T_s = –9.6 °C

AoA = 1.5°
LWC = 0.81 g/m^3
MVD = 20.0 µm
Exposure time = 20.0 min

Measured ice thickness

Station	Upper max, in.	Stag. line, in.	Lower max, in.
30	1.20	-	1.56
36	1.26	-	0.86
42	0.85	-	0.96

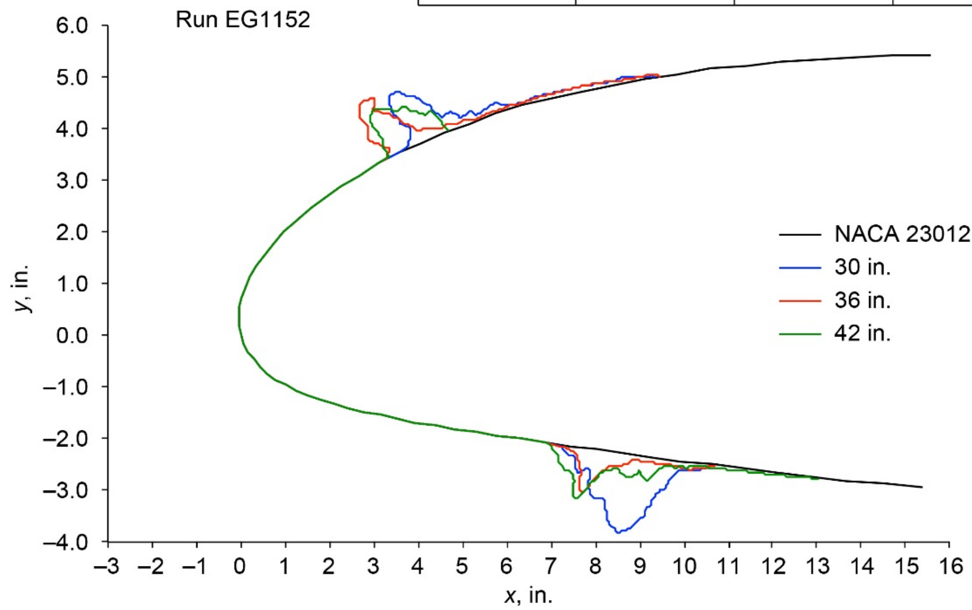

Pressure surface

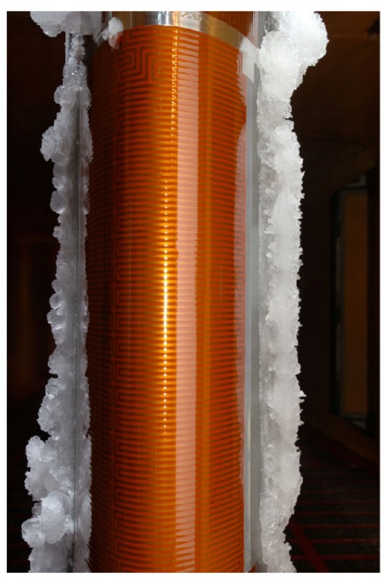

Leading edge

Suction surface

Run EG1152

Appendix F.—IRT Full-Scale Model Tests

Run EG1153

V = 150 kt
T_t = –6.7 °C
T_s = –9.6 °C

AoA = 1.5°
LWC = 0.81 g/m^3
MVD = 20.0 µm
Exposure time = 15.0 min

Run EG1153

Measured ice thickness*

Station	Upper max, in.	Stag. line, in.	Lower max, in.
-	-	-	-
-	-	-	-
-	-	-	-

*No tracings or thickness measurements made: ice not suitable.

Pressure surface

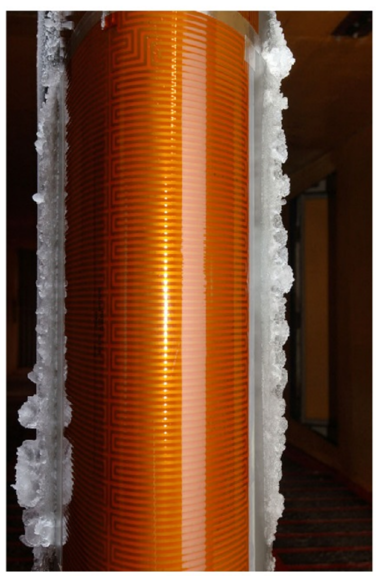

Leading edge

Suction surface

Run EG1153

Run EG1154

V = 150 kt
T_t = –4.4 °C
T_s = –7.6 °C
AoA = 1.5°
LWC = 0.81 g/m^3
MVD = 20.0 μm
Exposure time = 15.0 min

Measured ice thickness

Station	Upper max, in.	Stag. line, in.	Lower max, in.
30	0.12	-	0.49
36	0.15	-	0.39
42	0.12	-	0.46

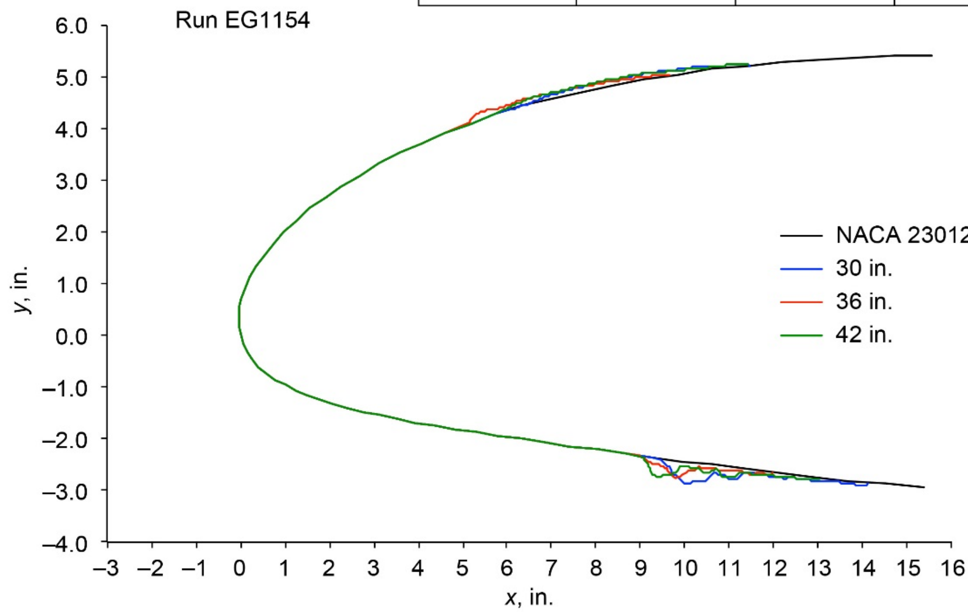

Pressure surface

Leading edge

Suction surface

Appendix F.—IRT Full-Scale Model Tests

Run EG1155

V = 150 kt
T_t = –6.7 °C
T_s = –9.6 °C

AoA = 1.5°
LWC = 0.81 g/m^3
MVD = 20.0 μm
Exposure time = 17.5 min

Measured ice thickness

Station	Upper max, in.	Stag. line, in.	Lower max, in.
30	0.54	-	0.60
36	0.82	-	0.57
42	0.82	-	0.52

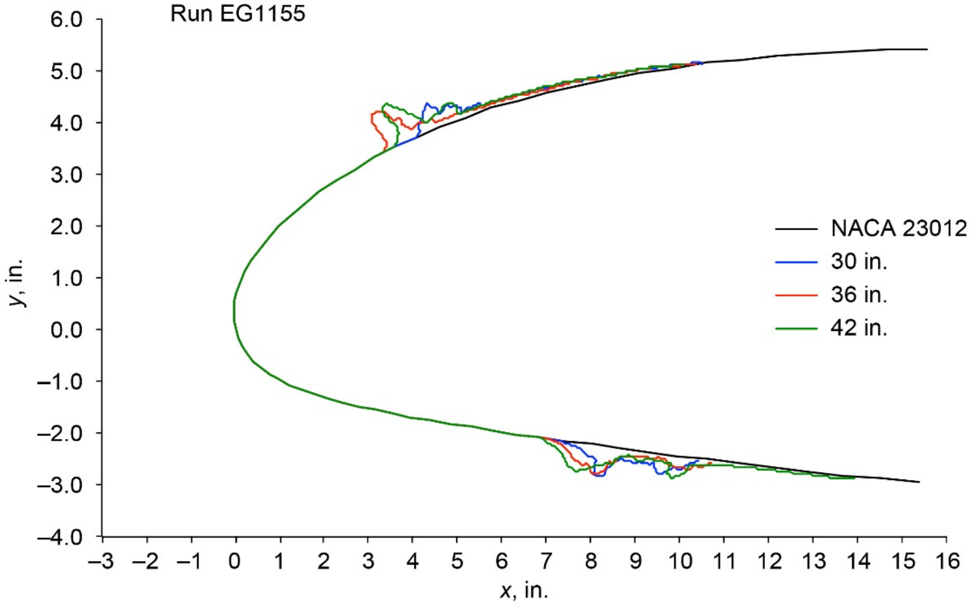

Pressure surface

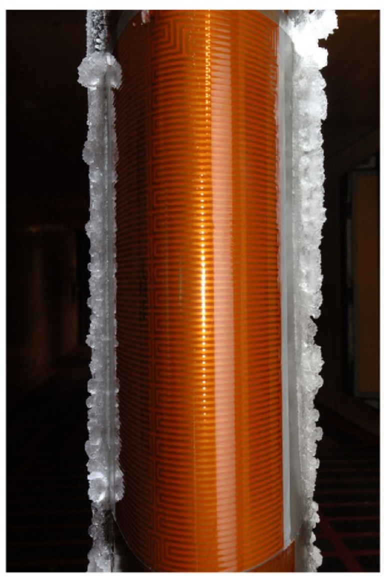

Leading edge

Suction surface

Run EG1155

Appendix F.—IRT Full-Scale Model Tests

Run EG1156

V = 150 kt
T_t = –6.7 °C
T_s = –9.6 °C
AoA = 1.5°
LWC = 0.81 g/m^3
MVD = 20.0 µm
Exposure time = 17.5 min

Measured ice thickness

Station	Upper max, in.	Stag. line, in.	Lower max, in.
30	0.77	-	1.42
36	1.05	-	0.76
42	1.16	-	1.09

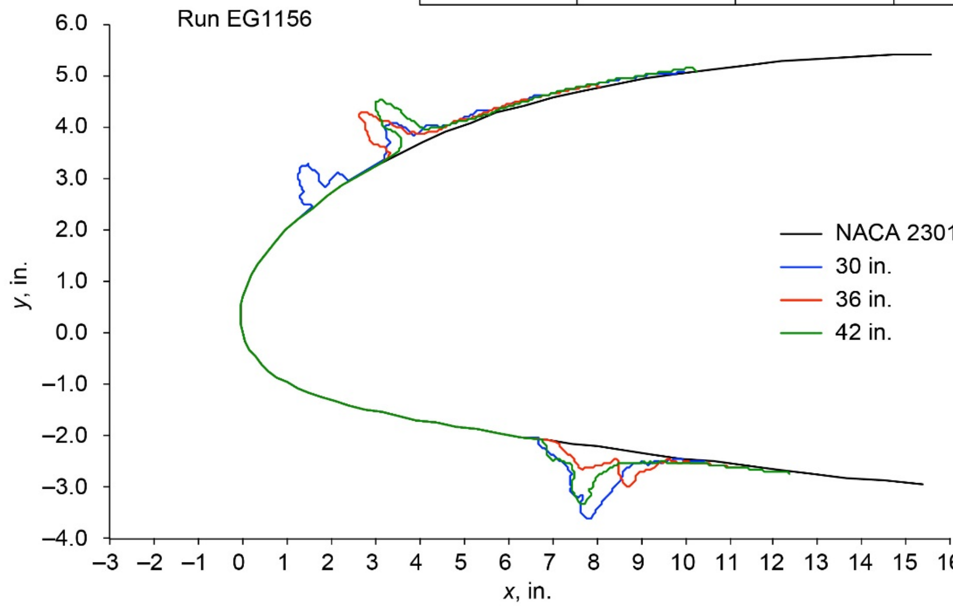

Pressure surface

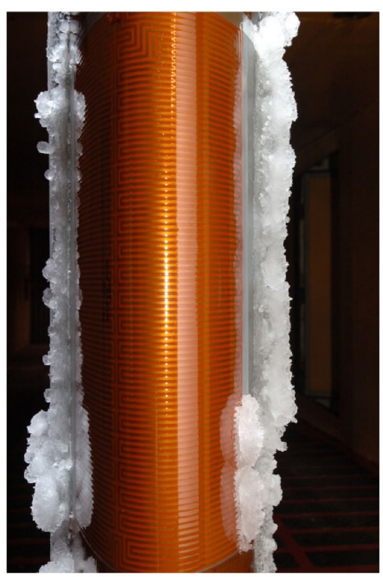

Leading edge

Suction surface

Run EG1156

Appendix F.—IRT Full-Scale Model Tests

Run EG1157

V = 150 kt
T_t = –6.7 °C
T_s = –9.6 °C

AoA = 1.5°
LWC = 0.81 g/m^3
MVD = 20.0 μm
Exposure time = 17.5 min

Measured ice thickness

Station	Upper max, in.	Stag. line, in.	Lower max, in.
30	1.02	-	1.21
36	1.00	-	0.93
42	1.40	-	1.23

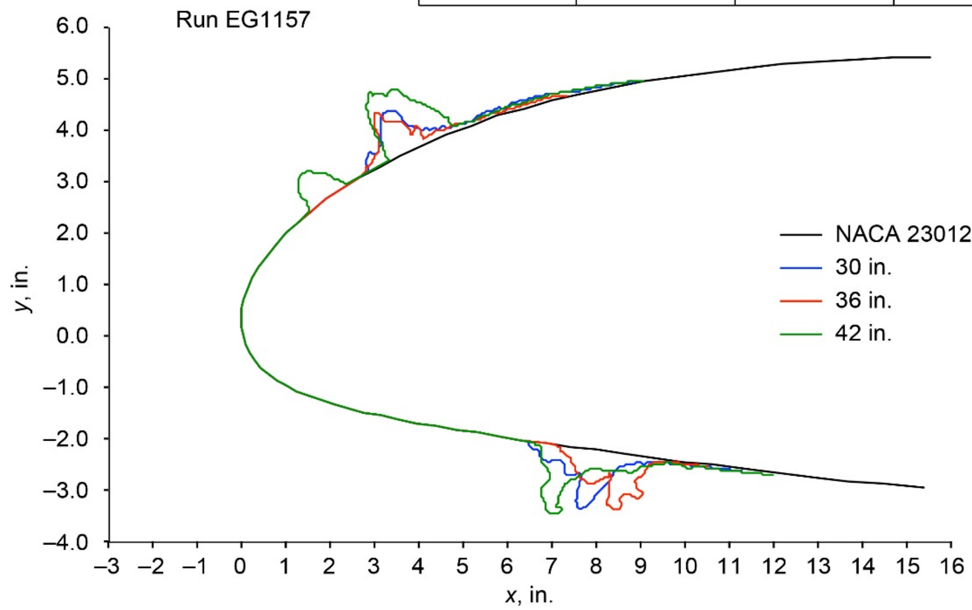

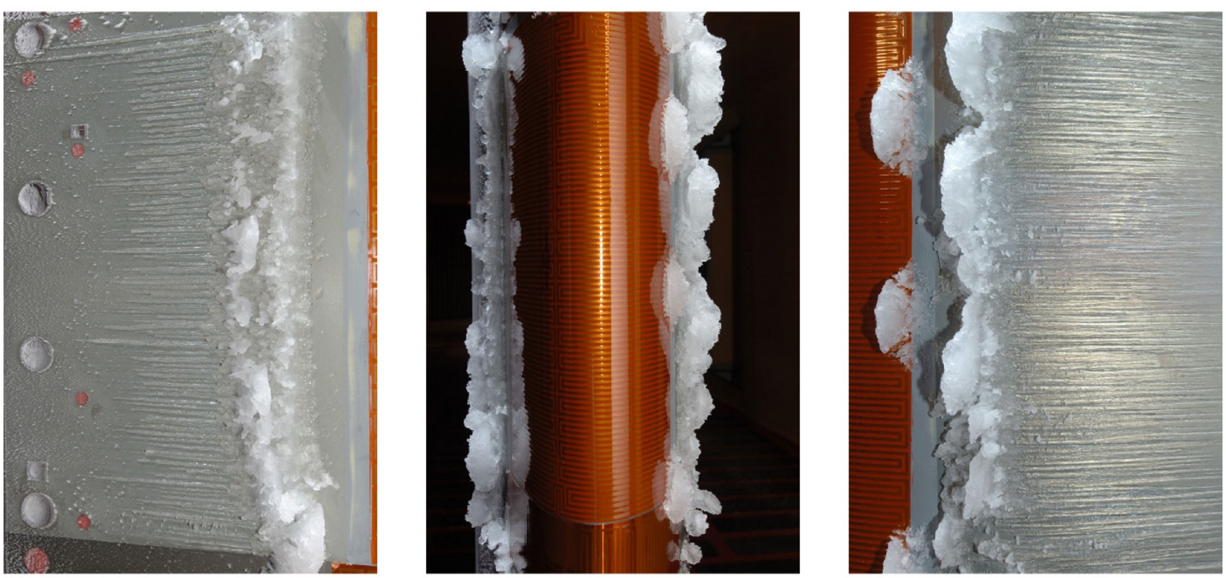

Pressure surface Leading edge Suction surface

Run EG1157

Appendix F.—IRT Full-Scale Model Tests

Run EG1158

V = 150 kt
T_t = –6.7 °C
T_s = –9.6 °C
AoA = 1.5°
LWC = 0.81 g/m^3
MVD = 20.0 μm
Exposure time = 17.5 min

Measured ice thickness

Station	Upper max, in.	Stag. line, in.	Lower max, in.
30	1.04	-	1.42
36	1.24	-	0.58
42	1.19	-	0.85

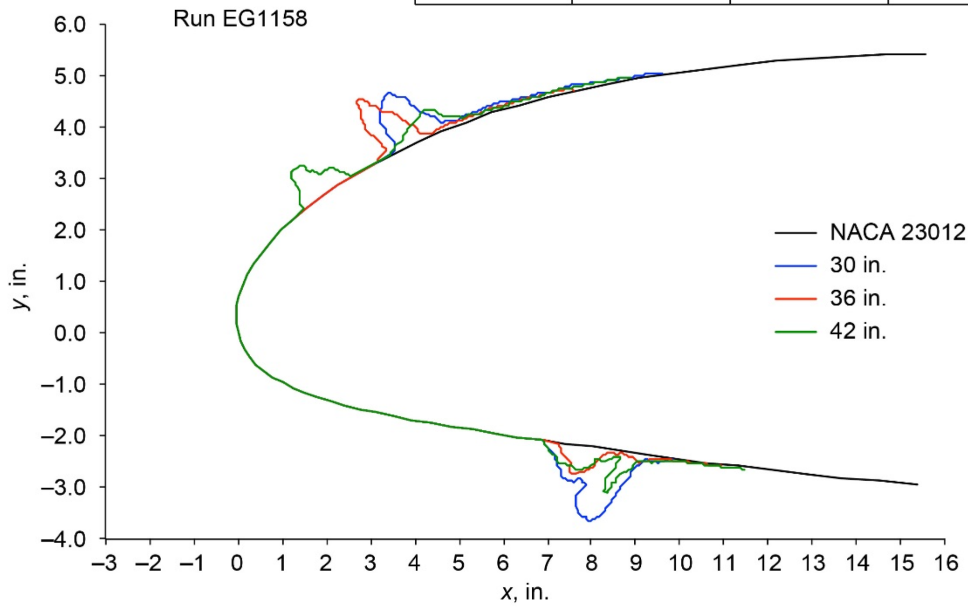

Pressure surface

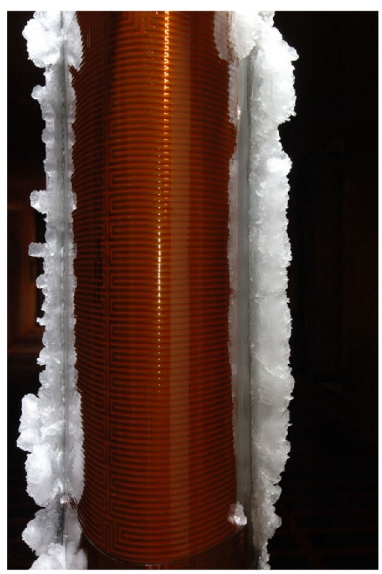

Leading edge

Suction surface

Run EG1158

Appendix F.—IRT Full-Scale Model Tests

Run EG1159

V = 150.0 kt AoA = 1.5°
T_t = –6.7 °C LWC = 0.81 g/m^3
T_s = –9.6 °C MVD = 20.0 µm
Exposure time = 15.0 min

Run EG1159

Measured ice thickness*

Station	Upper max, in.	Stag. line, in.	Lower max, in.
-	-	-	-
-	-	-	-
-	-	-	-

*No tracings or thickness measurements made: ice not suitable.


Pressure surface

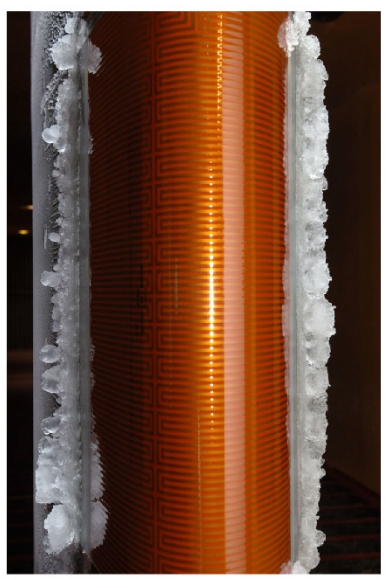
Leading edge


Suction surface

Run EG1159

Appendix F.—IRT Full-Scale Model Tests

Run EG1160

V = 175 kt
T_t = –20.6 °C
T_s = –24.6 °C
AoA = 2.0°
LWC = 0.50 g/m^3
MVD = 30.0 µm
Exposure time = 10.0 min

Measured ice thickness

Station	Upper max, in.	Stag. line, in.	Lower max, in.
30	0.53	0.81	0.43
36	0.49	0.64	0.41
42	0.62	0.72	0.43

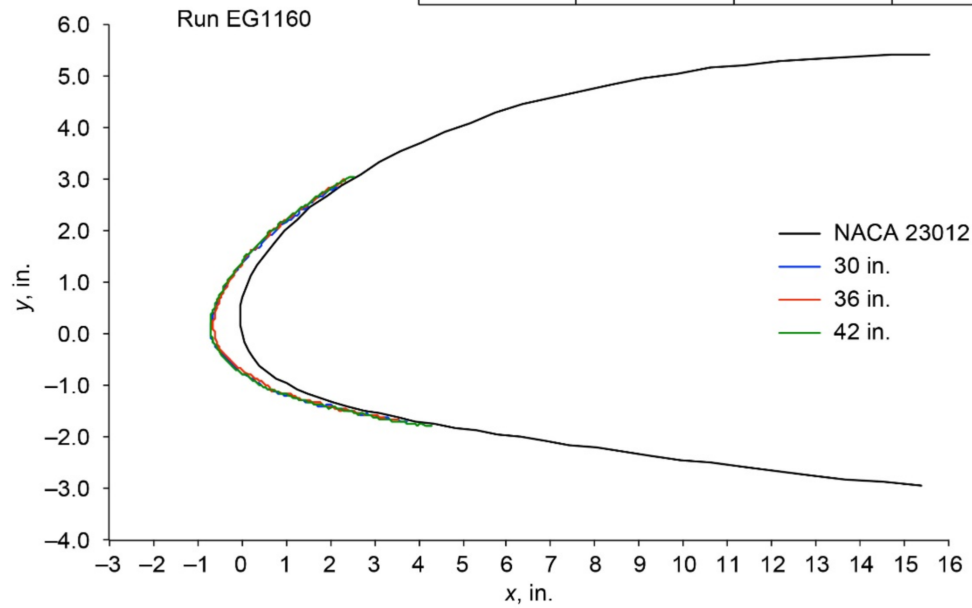

Pressure surface

Leading edge

Suction surface

Run EG1160

Appendix F.—IRT Full-Scale Model Tests

Run EG1161

V = 150 kt
T_t = –22.2 °C
T_s = –25.2 °C
AoA = 2.0°
LWC = 0.55 g/m^3
MVD = 30.0 μm
Exposure time = 10.0 min

Measured ice thickness

Station	Upper max, in.	Stag. line, in.	Lower max, in.
30	0.60	0.75	0.38
36	0.59	0.74	0.39
42	0.66	0.83	0.48

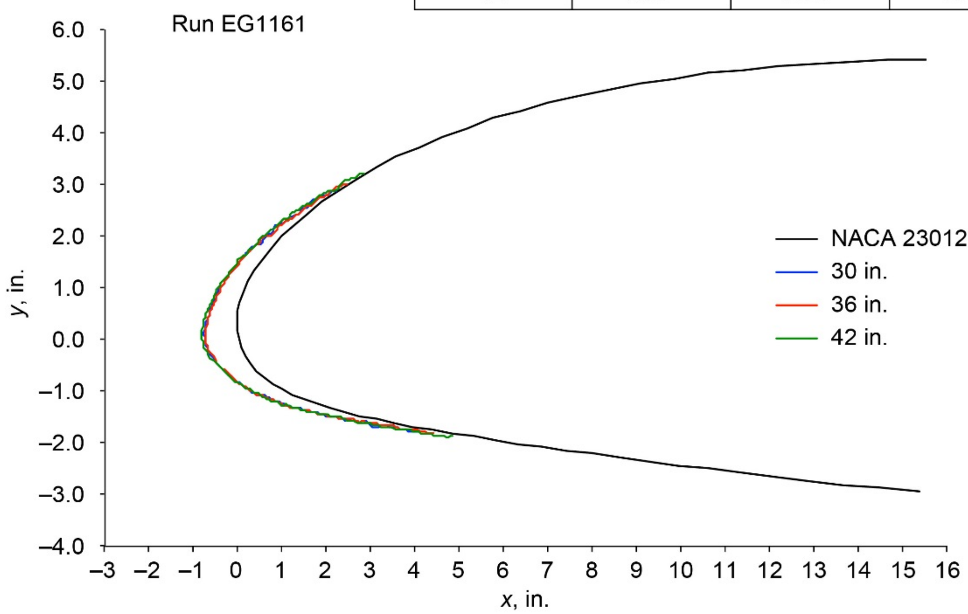

Pressure surface

Leading edge

Suction surface

Run EG1161

Appendix F.—IRT Full-Scale Model Tests

Run EG1162

V = 150 kt
T_t = –22.2 °C
T_s = –25.2 °C

AoA = 2.0°
LWC = 0.55 g/m^3
MVD = 30.0 µm
Exposure time = 10.0 min

Measured ice thickness

Station	Upper max, in.	Stag. line, in.	Lower max, in.
28.5	0.52	0.75	0.39
-	-	-	-
43.5	0.64	0.89	0.45

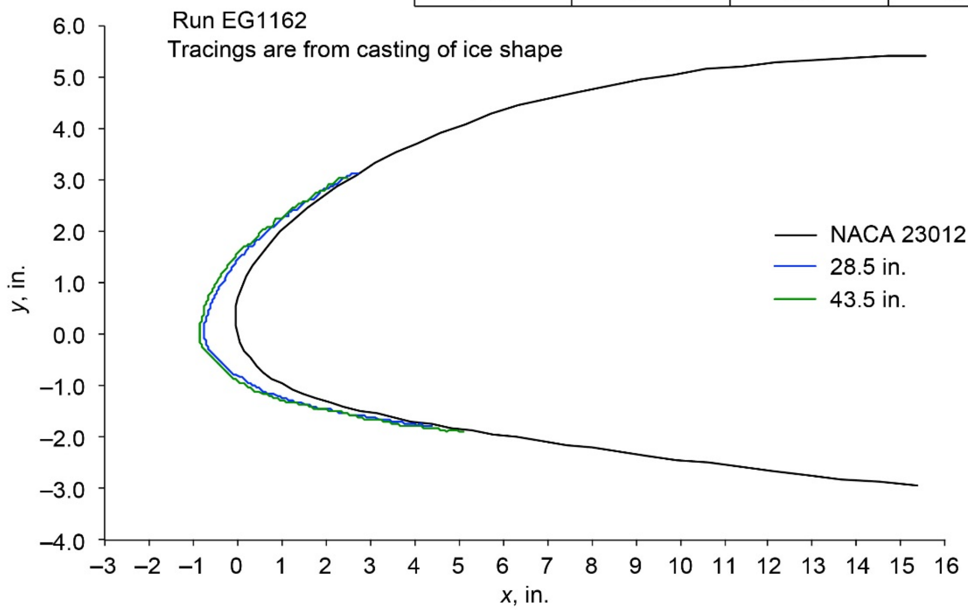

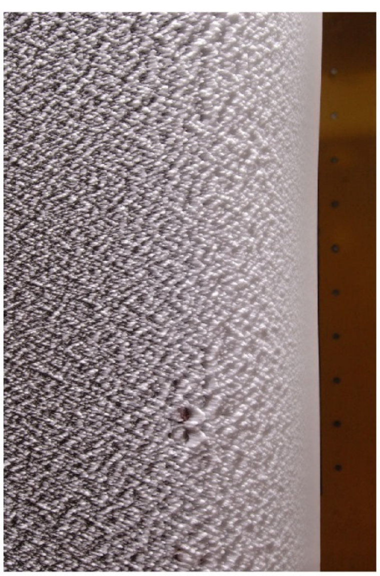

Pressure surface

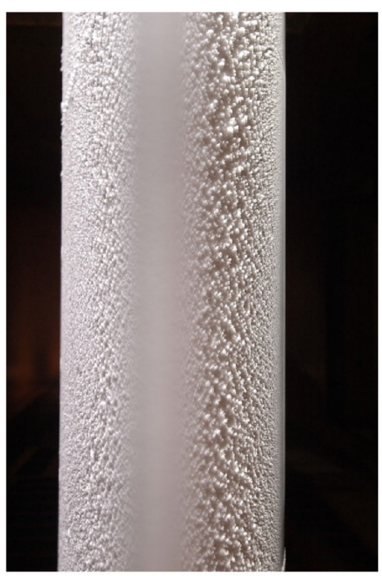

Leading edge

Suction surface

Run EG1162

Appendix F.—IRT Full-Scale Model Tests

Run EG1163

V = 175 kt
T_t = –2.2 °C
T_s = –6.2 °C

AoA = 5.0°
LWC = 0.64 g/m^3
MVD = 15.0 μm
Exposure time = 10.0 min

Measured ice thickness

Station	Upper max, in.	Stag. line, in.	Lower max, in.
-	-	-	-
36	0.89	0.17	0.30
-	-	-	-

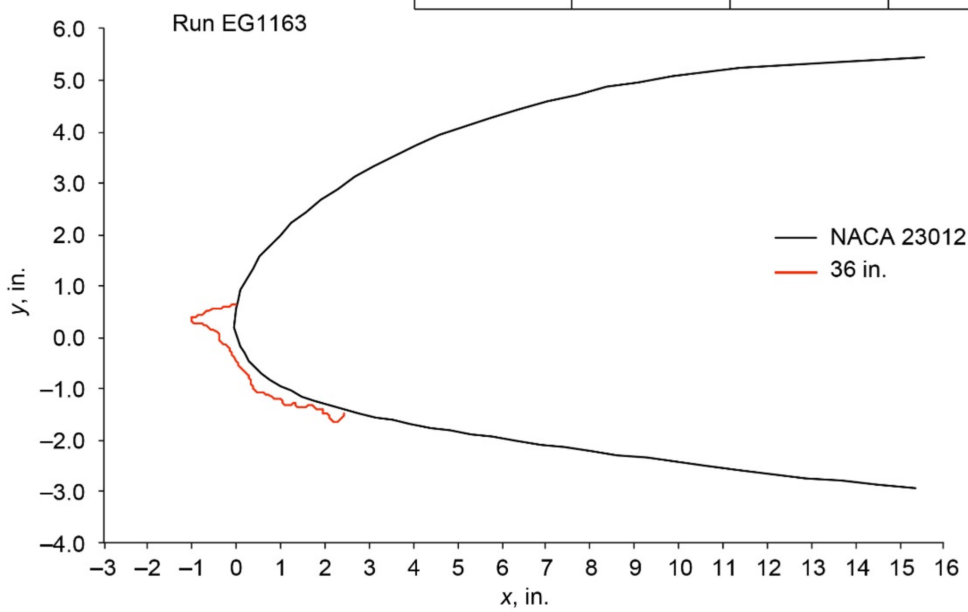

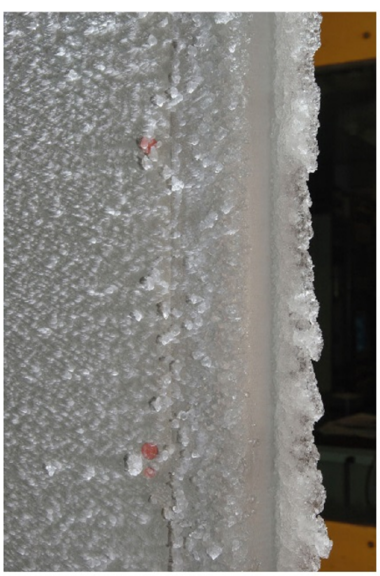

Pressure surface

Leading edge

Suction surface

Run EG1163

Appendix F.—IRT Full-Scale Model Tests

Run EG1164

V = 175 kt
T_t = –2.2 °C
T_s = –6.2 °C

AoA = 5.0°
LWC = 0.85 g/m^3
MVD = 20.0 µm
Exposure time = 11.25 min

Measured ice thickness

Station	Upper max, in.	Stag. line, in.	Lower max, in.
28.5	1.59	0.21	0.57
-	-	-	-
43.5	1.55	0.20	0.80

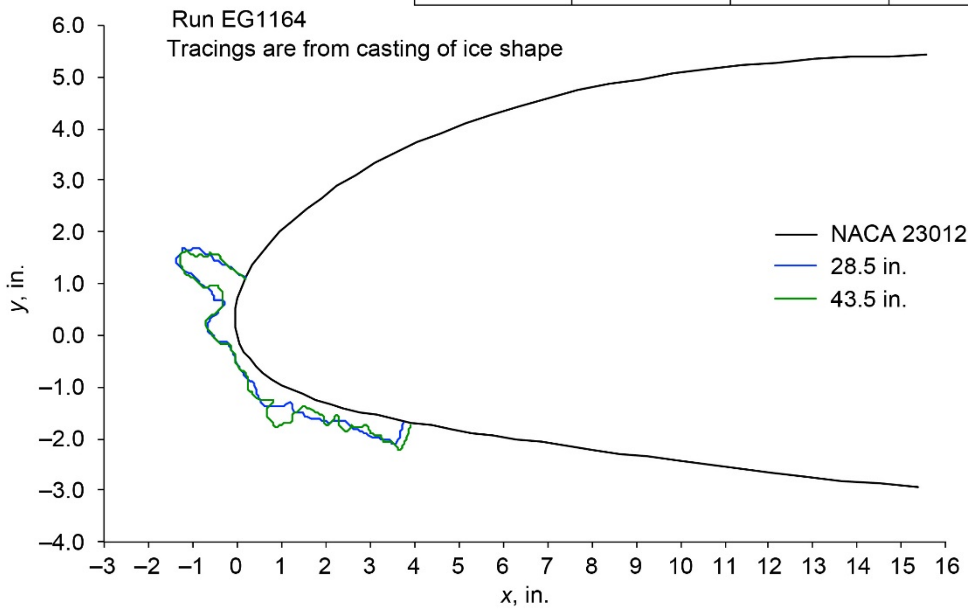

Pressure surface

Leading edge

Suction surface

Run EG1164

Appendix G.—F1 Subsonic Pressurized Wind Tunnel NACA 23012 Full-Scale Model Test Results

Clean Airfoil: M = 0.10 and Re = 4.6–4.7×10^6

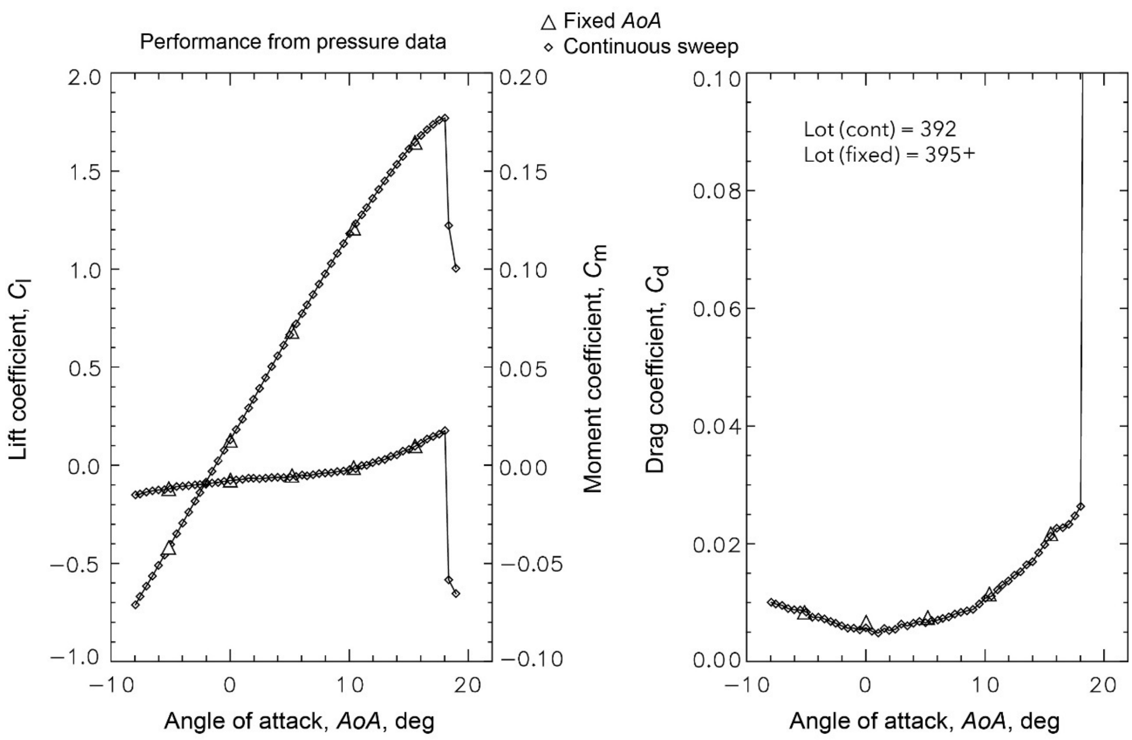

Clean Airfoil: M = 0.10 and Re = 4.6–4.7×10^6

Appendix G.—F1 Full-Scale Model Tests

Clean Airfoil: M = 0.10 and Re = 4.6–4.7×10^6

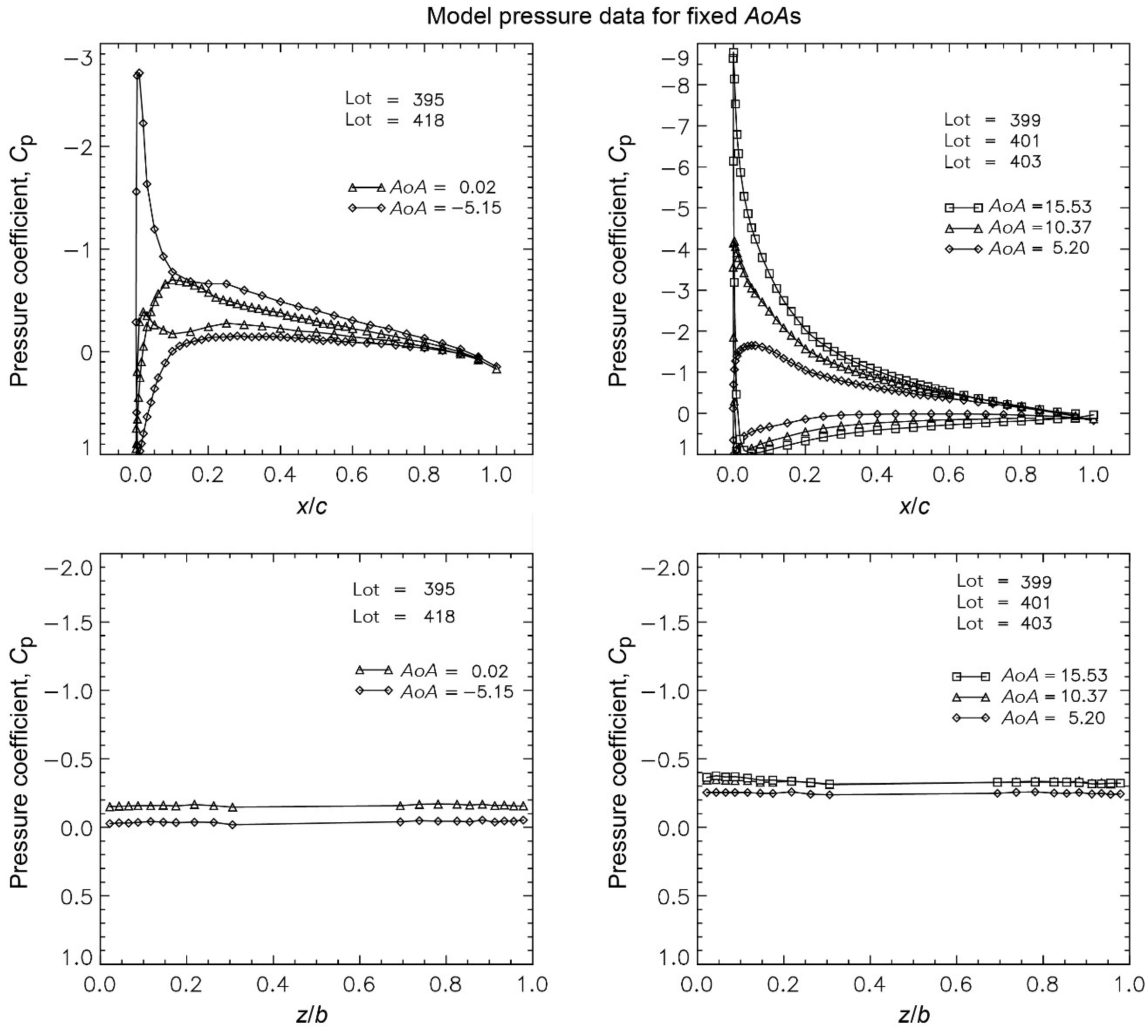

Clean Airfoil: M = 0.10 and Re = 4.6–4.7×10^6

Appendix G.—F1 Full-Scale Model Tests

Clean Airfoil: M = 0.10 and Re = 4.6–4.7×10^6

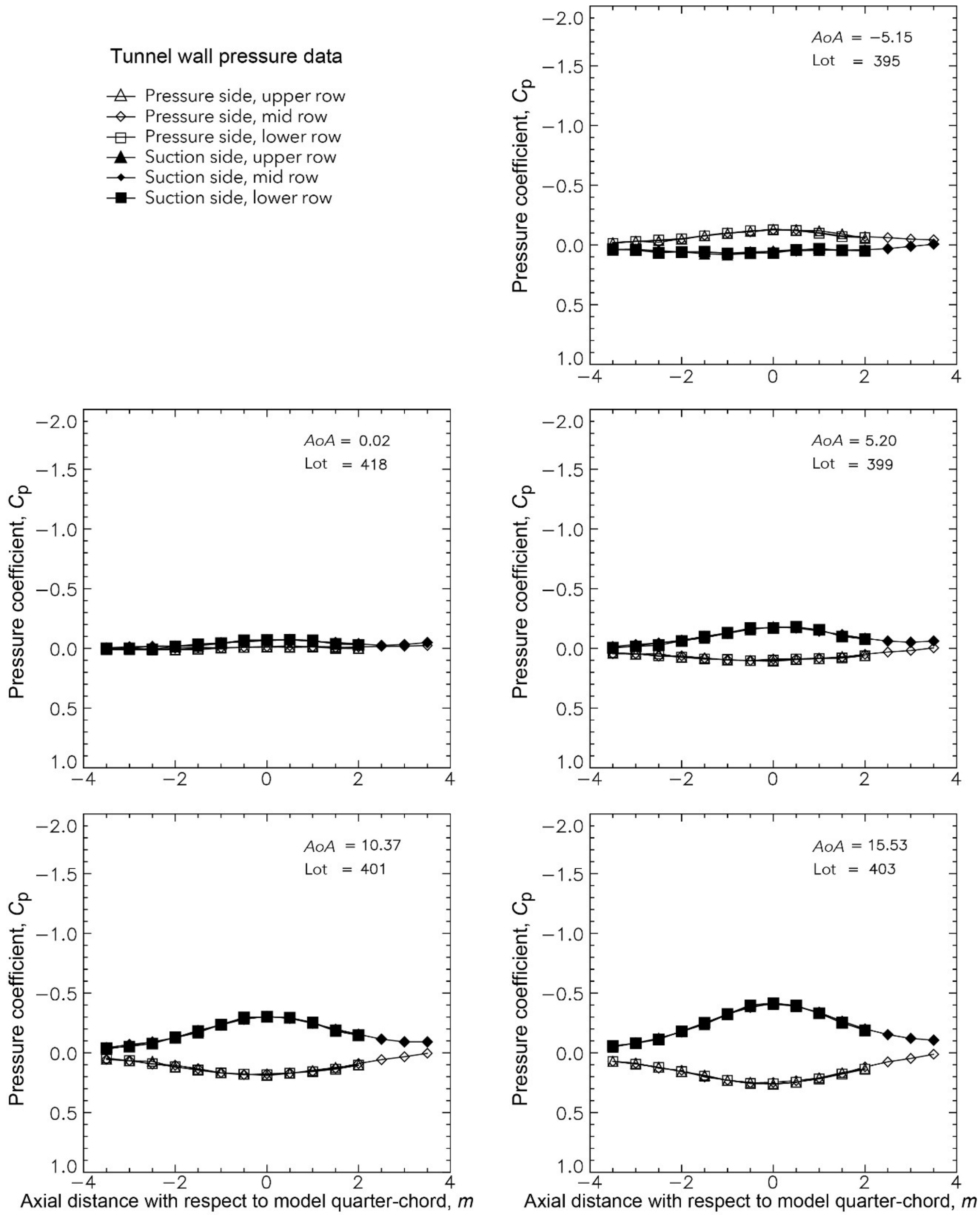

Clean Airfoil: M = 0.10 and Re = 4.6–4.7×10^6

Appendix G.—F1 Full-Scale Model Tests

Clean Airfoil: M = 0.10 and Re = 4.6–4.7×10^6

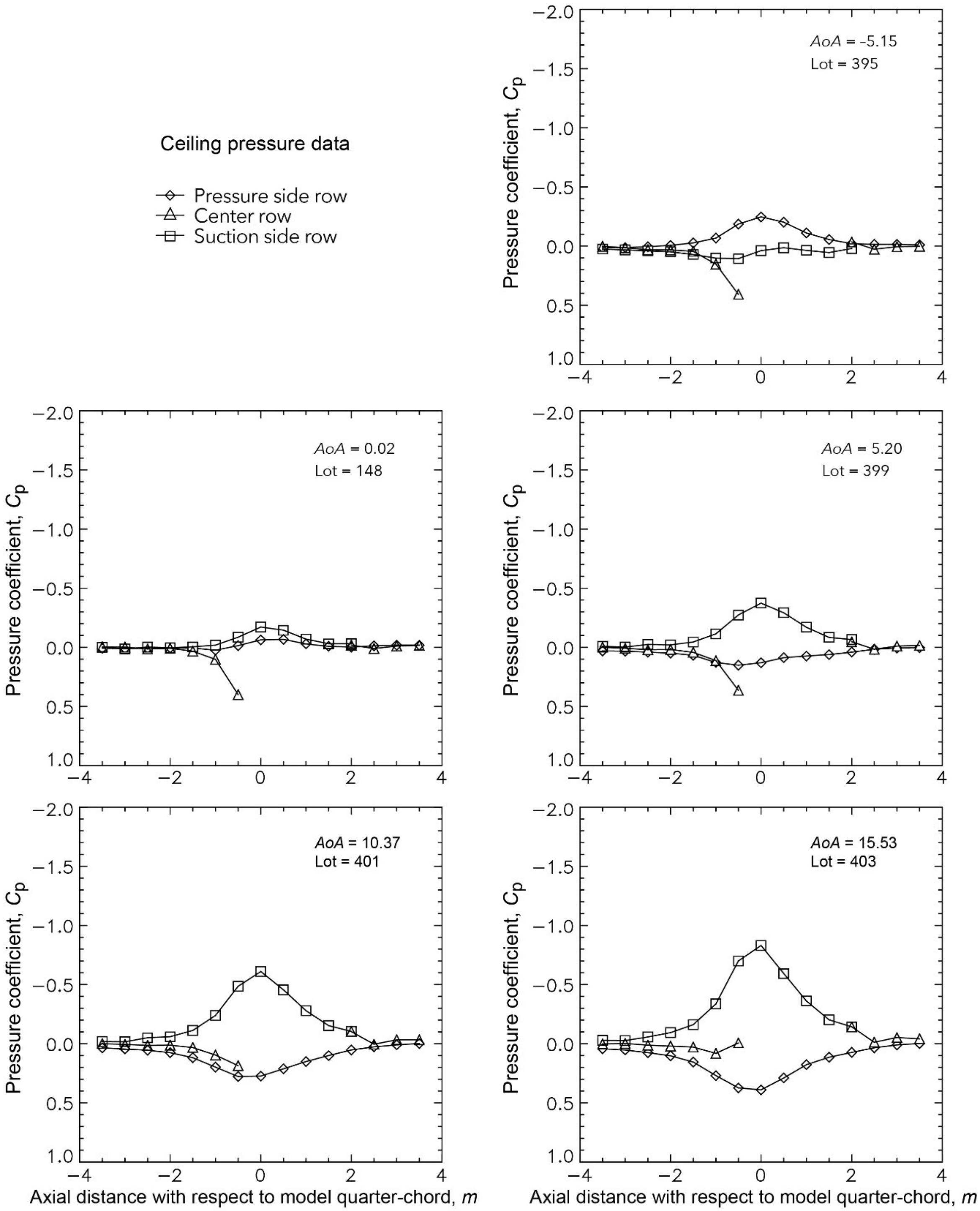

Clean Airfoil: M = 0.10 and Re = 4.6–4.7×10^6

Appendix G.—F1 Full-Scale Model Tests

Clean Airfoil: M = 0.10 and Re = 4.6–4.7×10^6

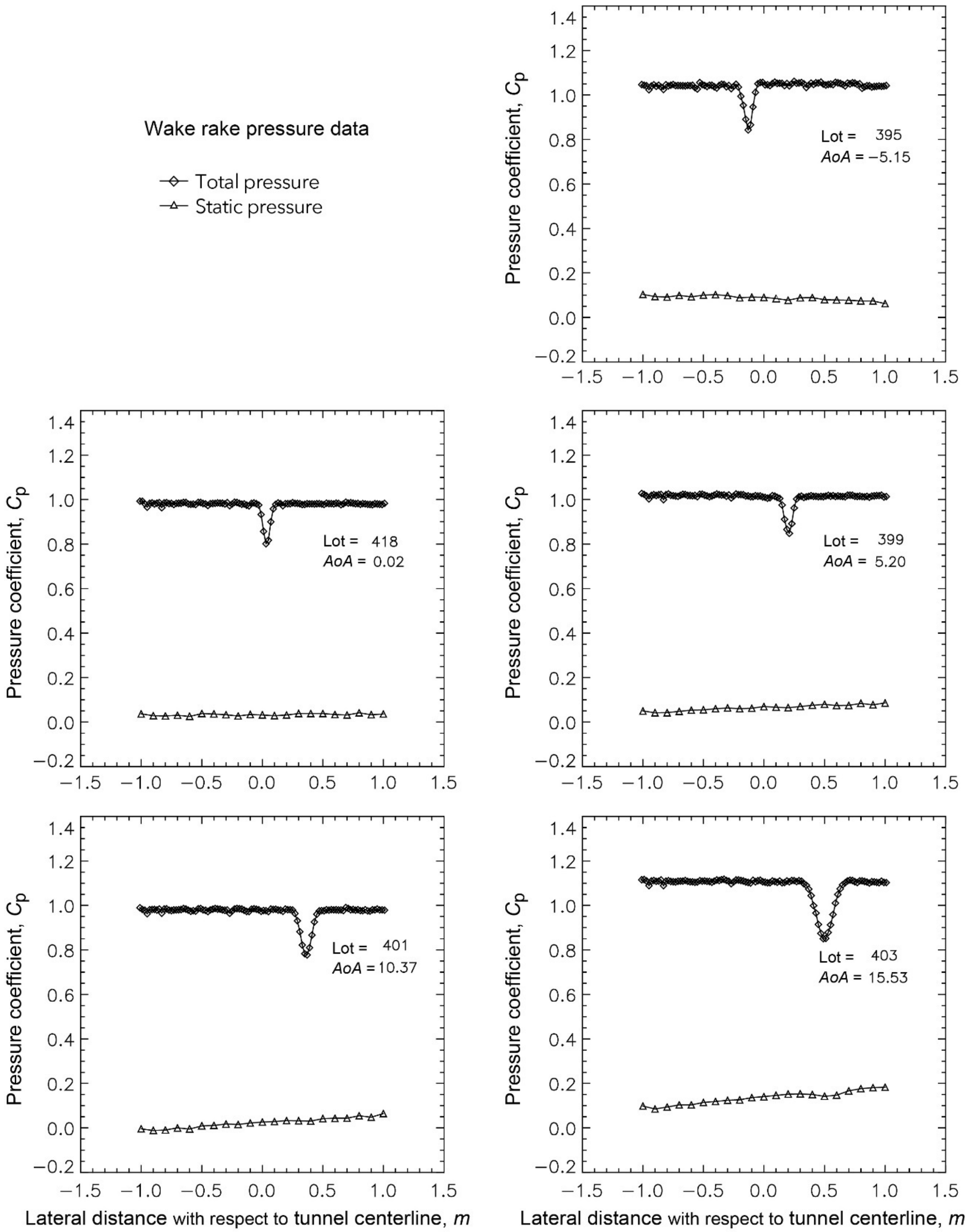

Clean Airfoil: M = 0.10 and Re = 4.6–4.7×10^6

Appendix G.—F1 Full-Scale Model Tests

Clean Airfoil: M = 0.10 and Re = 8.1×10^6

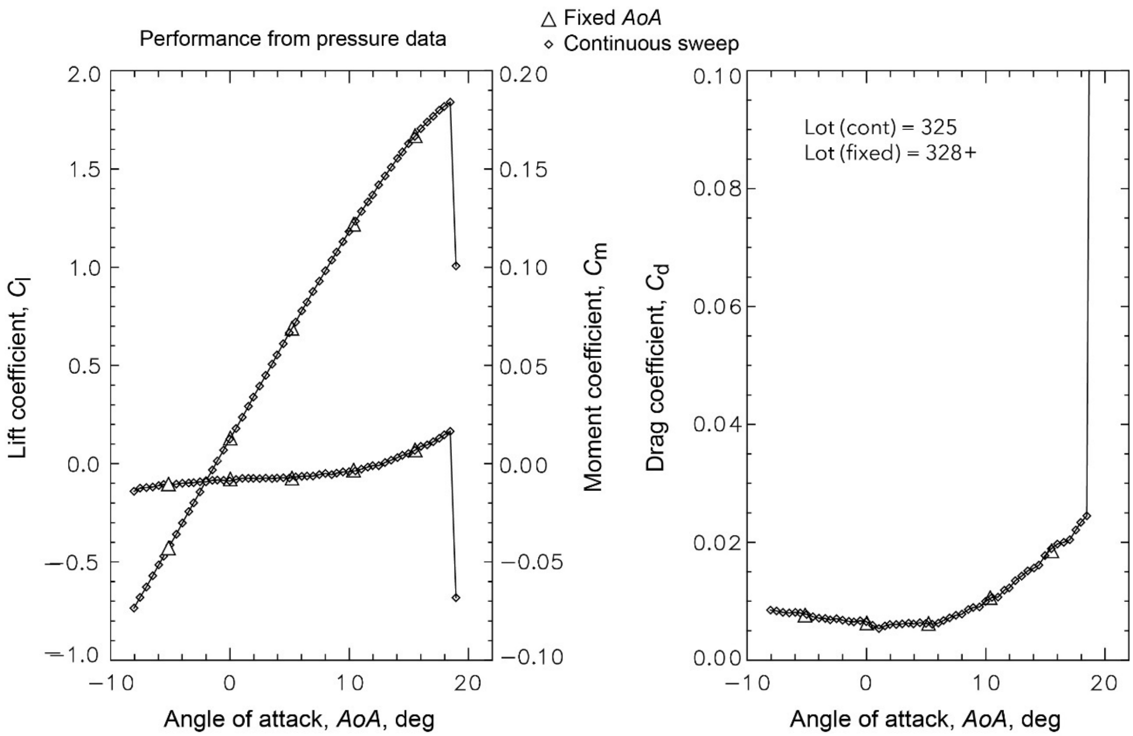

Clean Airfoil: M = 0.10 and Re = 8.1×10^6

Appendix G.—F1 Full-Scale Model Tests

Clean Airfoil: M = 0.10 and Re = 8.1×10^6

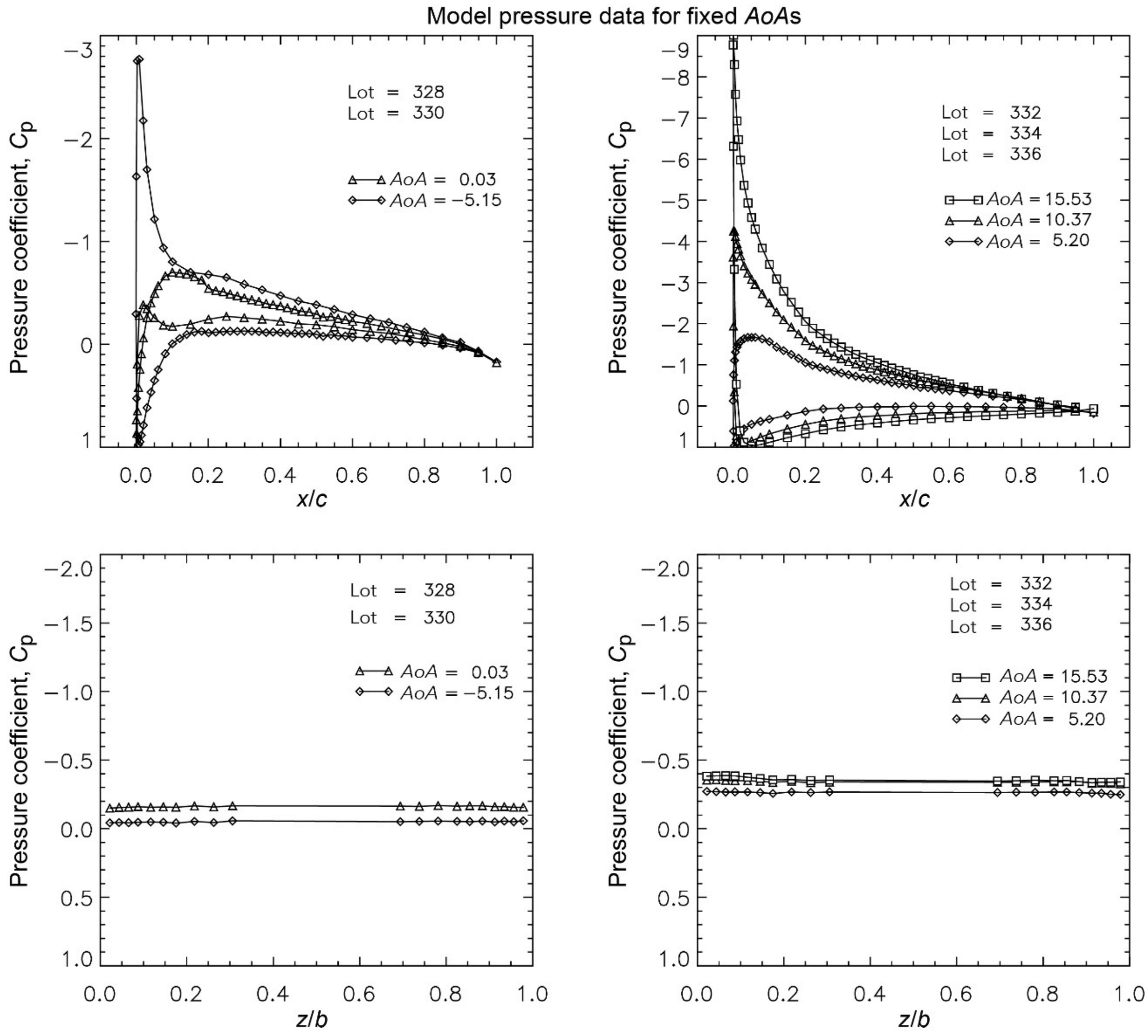

Clean Airfoil: M = 0.10 and Re = 8.1×10^6

Appendix G.—F1 Full-Scale Model Tests

Clean Airfoil: M = 0.10 and Re = 8.1×10^6

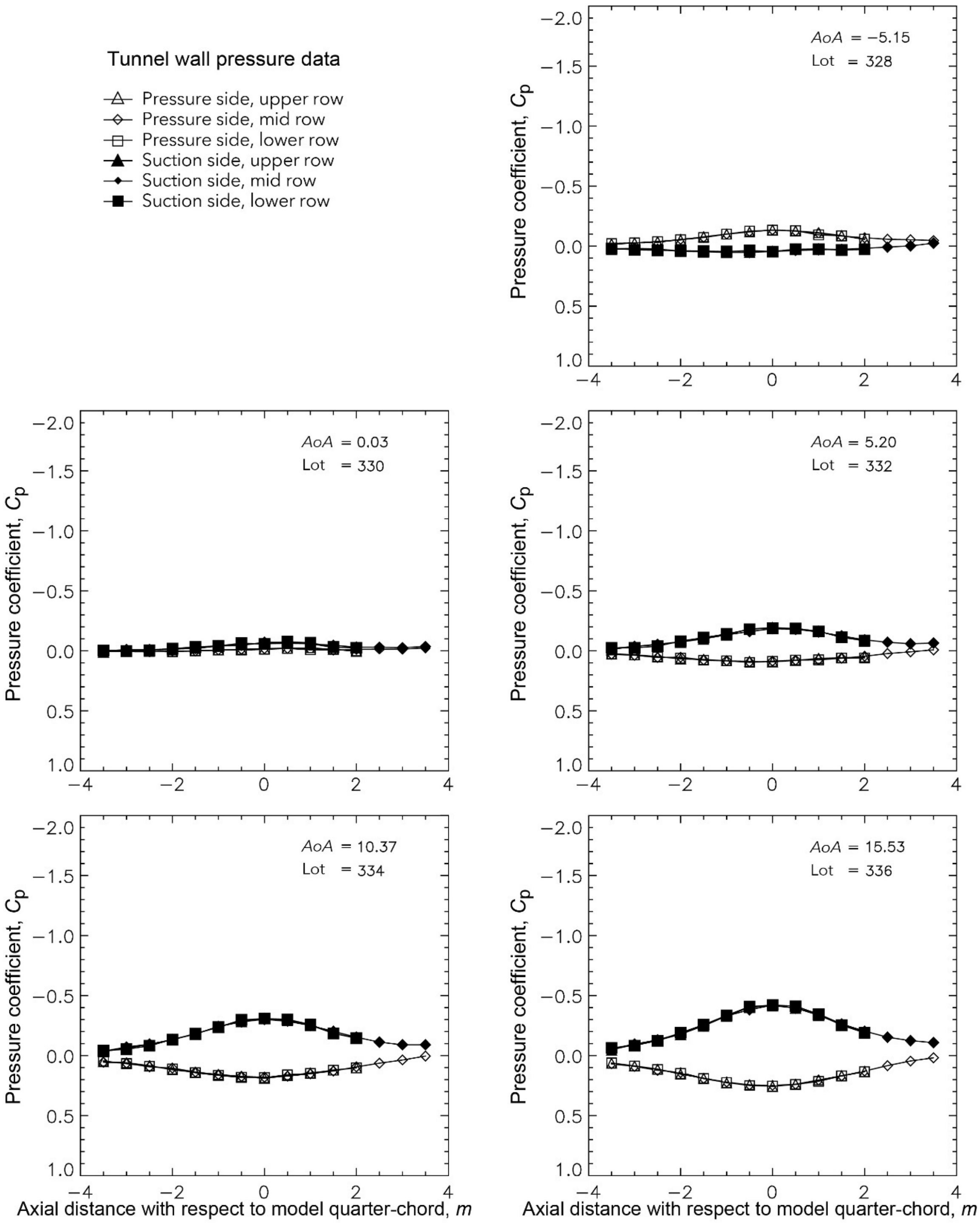

Clean Airfoil: M = 0.10 and Re = 8.1×10^6

Appendix G.—F1 Full-Scale Model Tests

Clean Airfoil: M = 0.10 and Re = 8.1×10^6

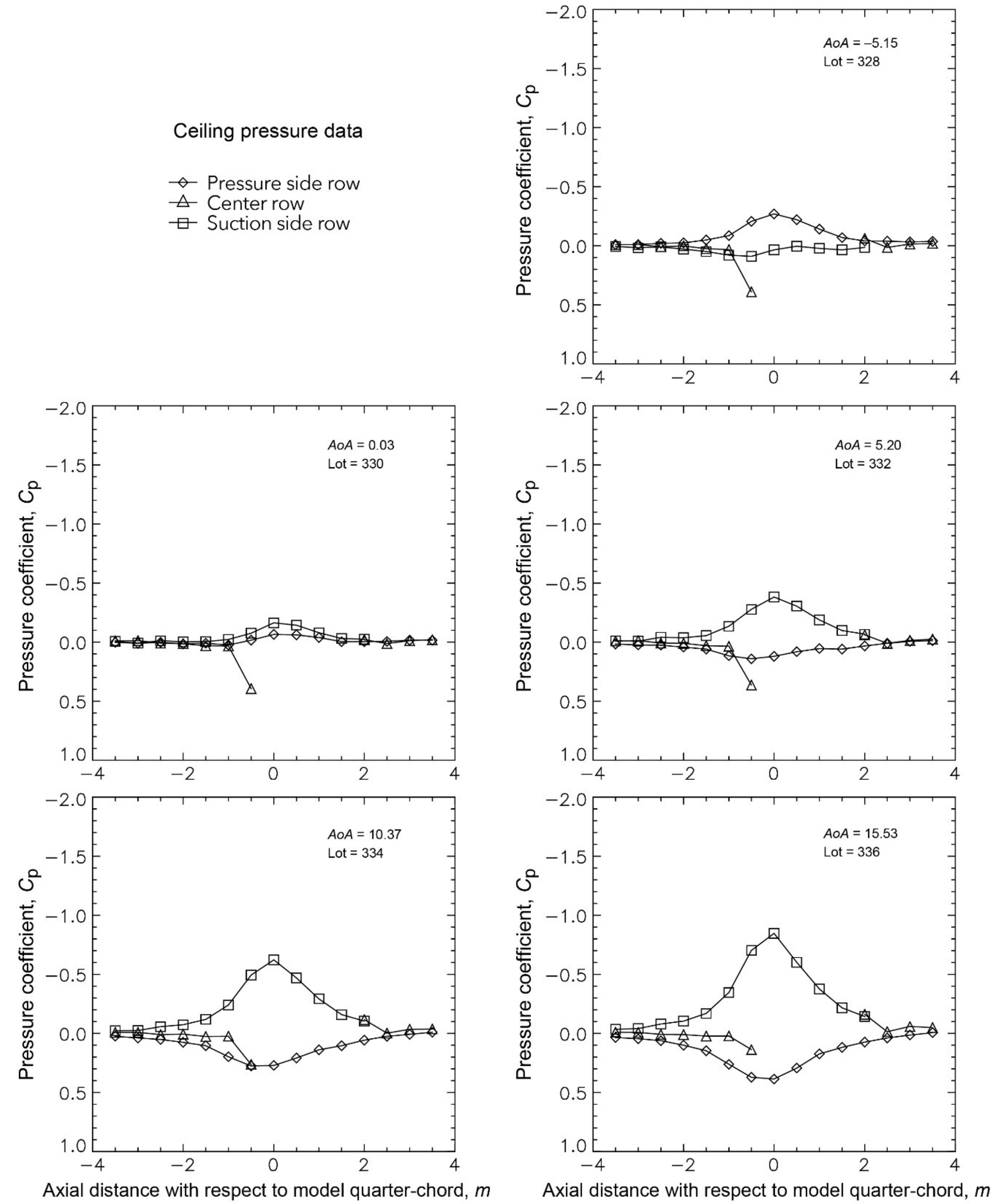

Clean Airfoil: M = 0.10 and Re = 8.1×10^6

Appendix G.—F1 Full-Scale Model Tests

Clean Airfoil: M = 0.10 and Re = 8.1×10^6

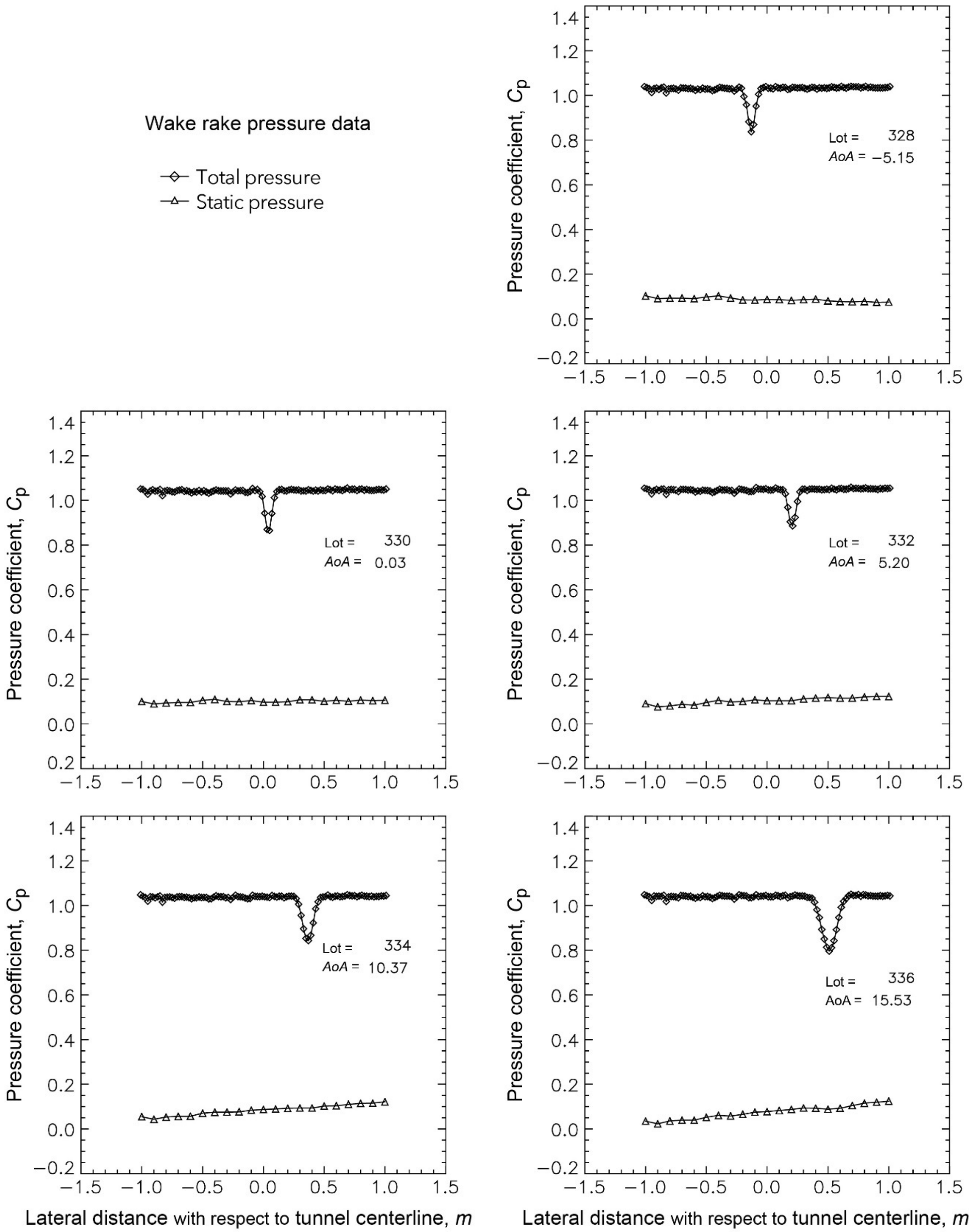

Clean Airfoil: M = 0.10 and Re = 8.1×10^6

Appendix G.—F1 Full-Scale Model Tests

Clean Airfoil: M = 0.10 and Re = 12.2–12.3×10^6

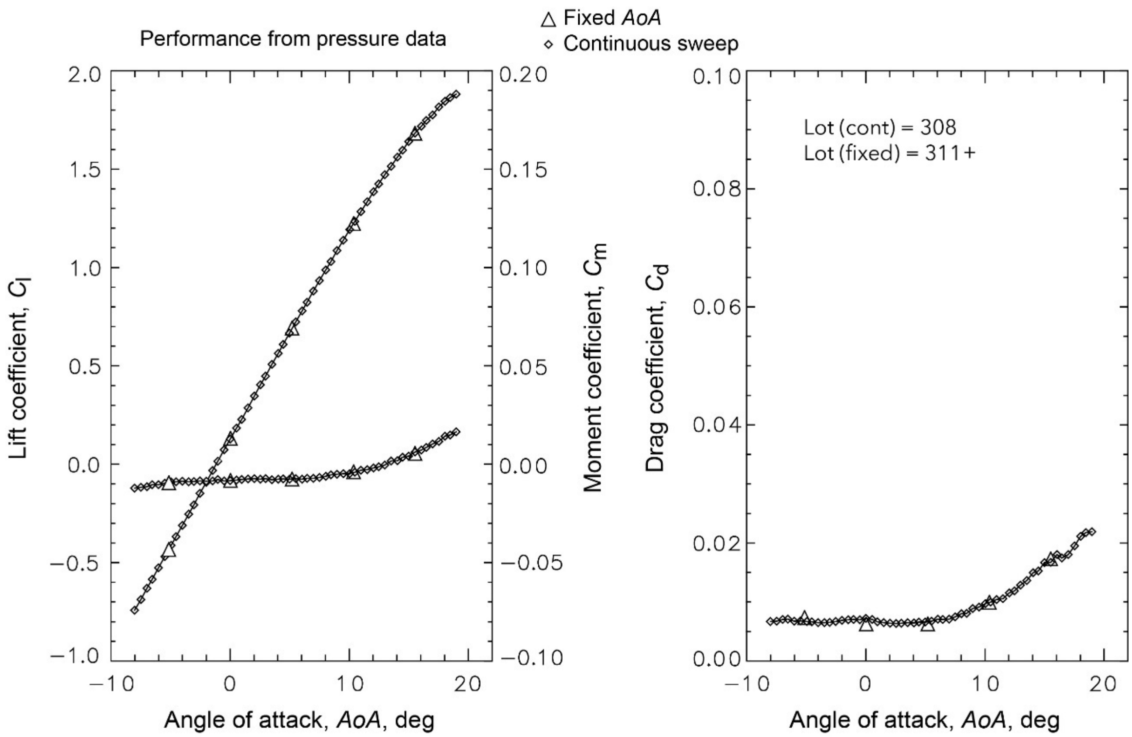

Clean Airfoil: M = 0.10 and Re = 12.2–12.3×10^6

Appendix G.—F1 Full-Scale Model Tests

Clean Airfoil: M = 0.10 and Re = 12.2–12.3×10^6

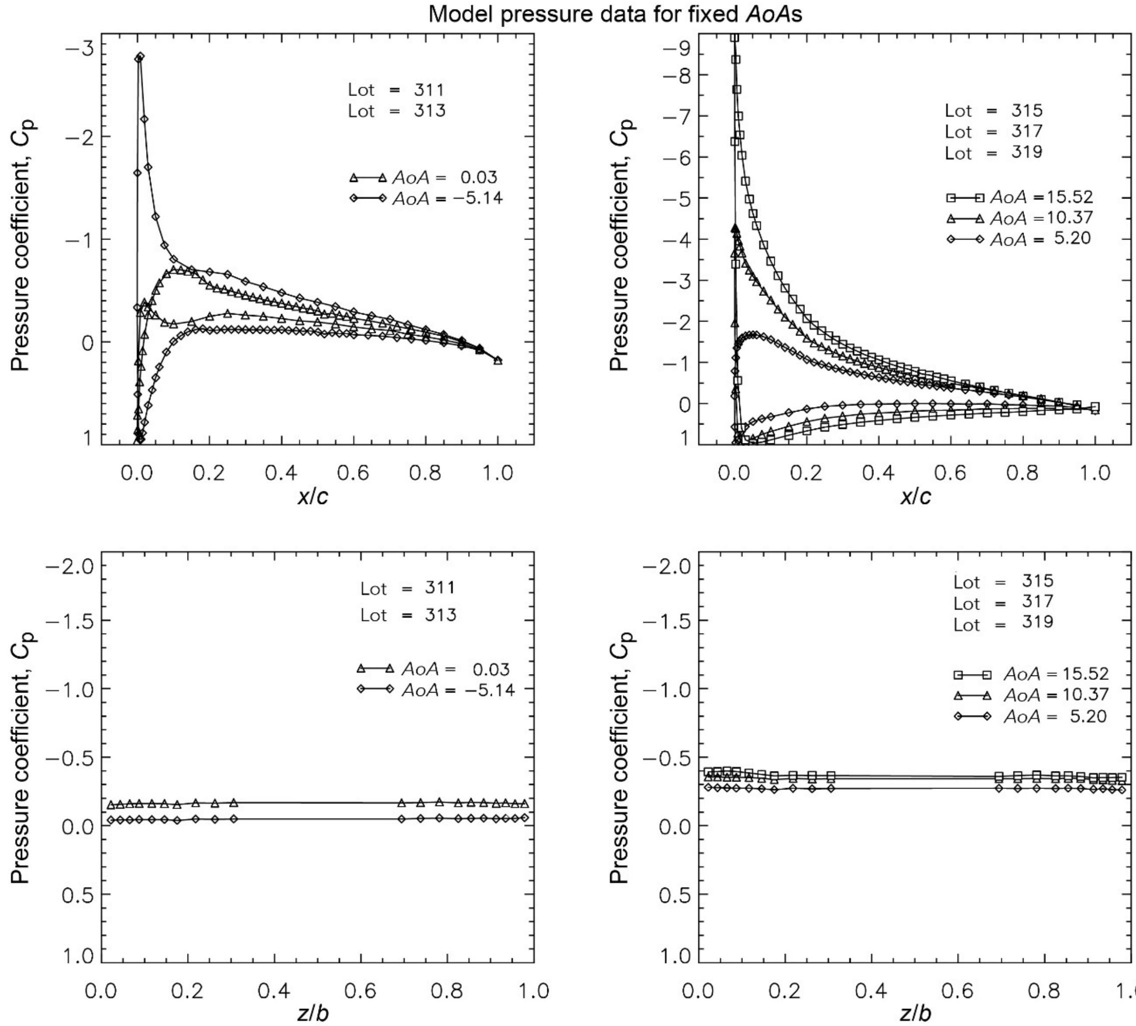

Clean Airfoil: M = 0.10 and Re = 12.2–12.3×10^6

Appendix G.—F1 Full-Scale Model Tests

Clean Airfoil: M = 0.10 and Re = 12.2–12.3×10^6

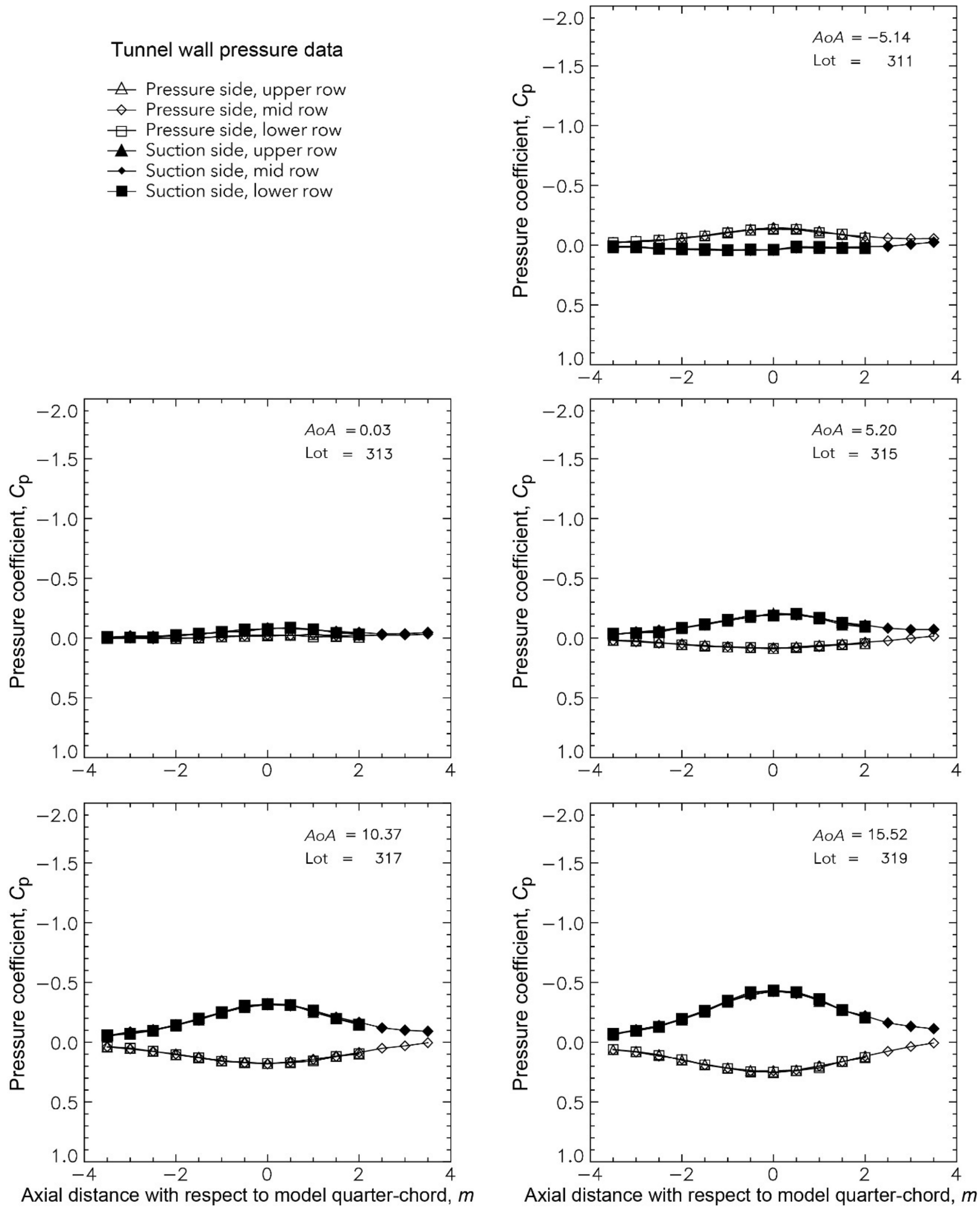

Clean Airfoil: M = 0.10 and Re = 12.2–12.3×10^6

Appendix G.—F1 Full-Scale Model Tests

Clean Airfoil: M = 0.10 and Re = 12.2–12.3×10^6

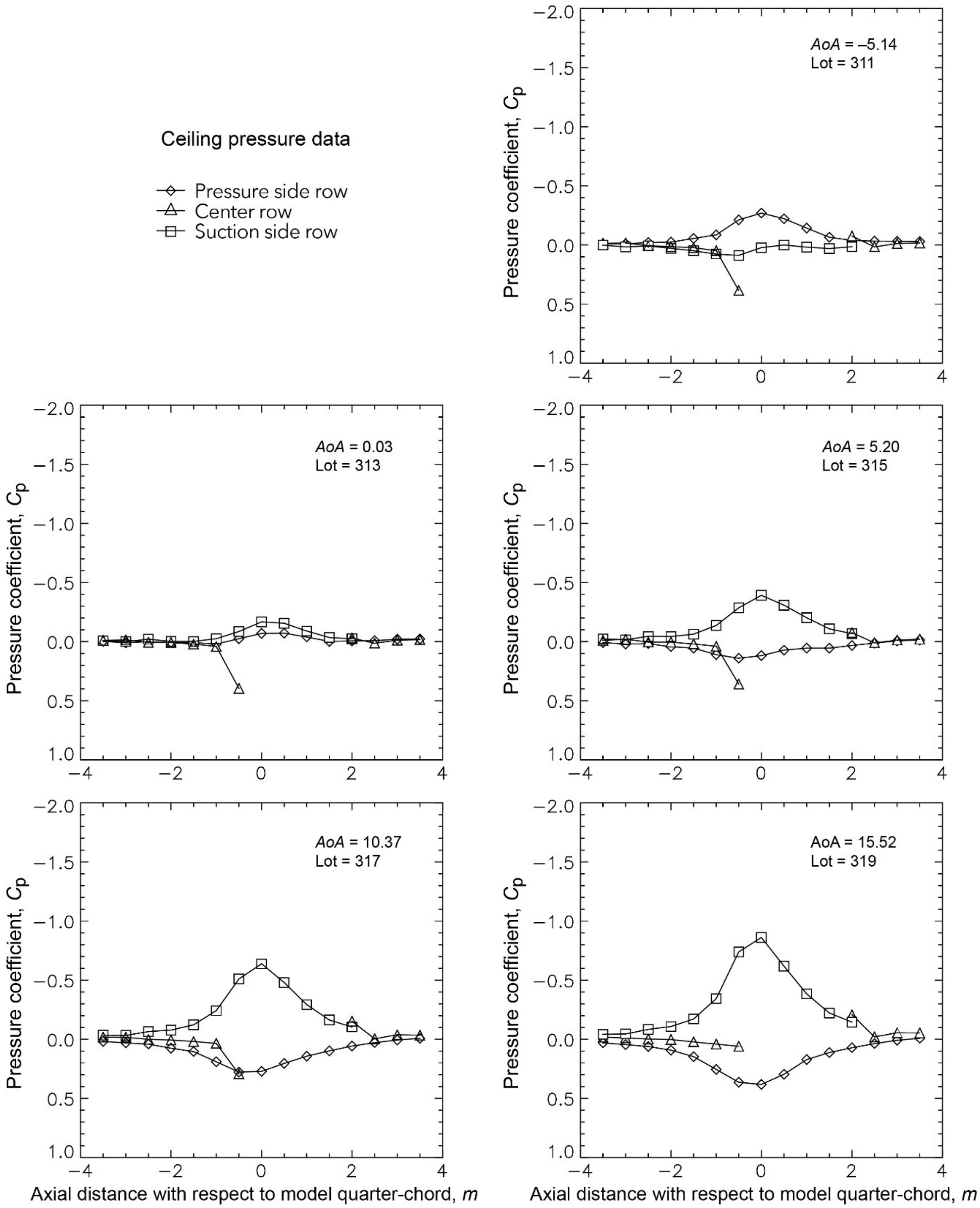

Clean Airfoil: M = 0.10 and Re = 12.2–12.3×10^6

Appendix G.—F1 Full-Scale Model Tests

Clean Airfoil: M = 0.10 and Re = 12.2–12.3×10^6

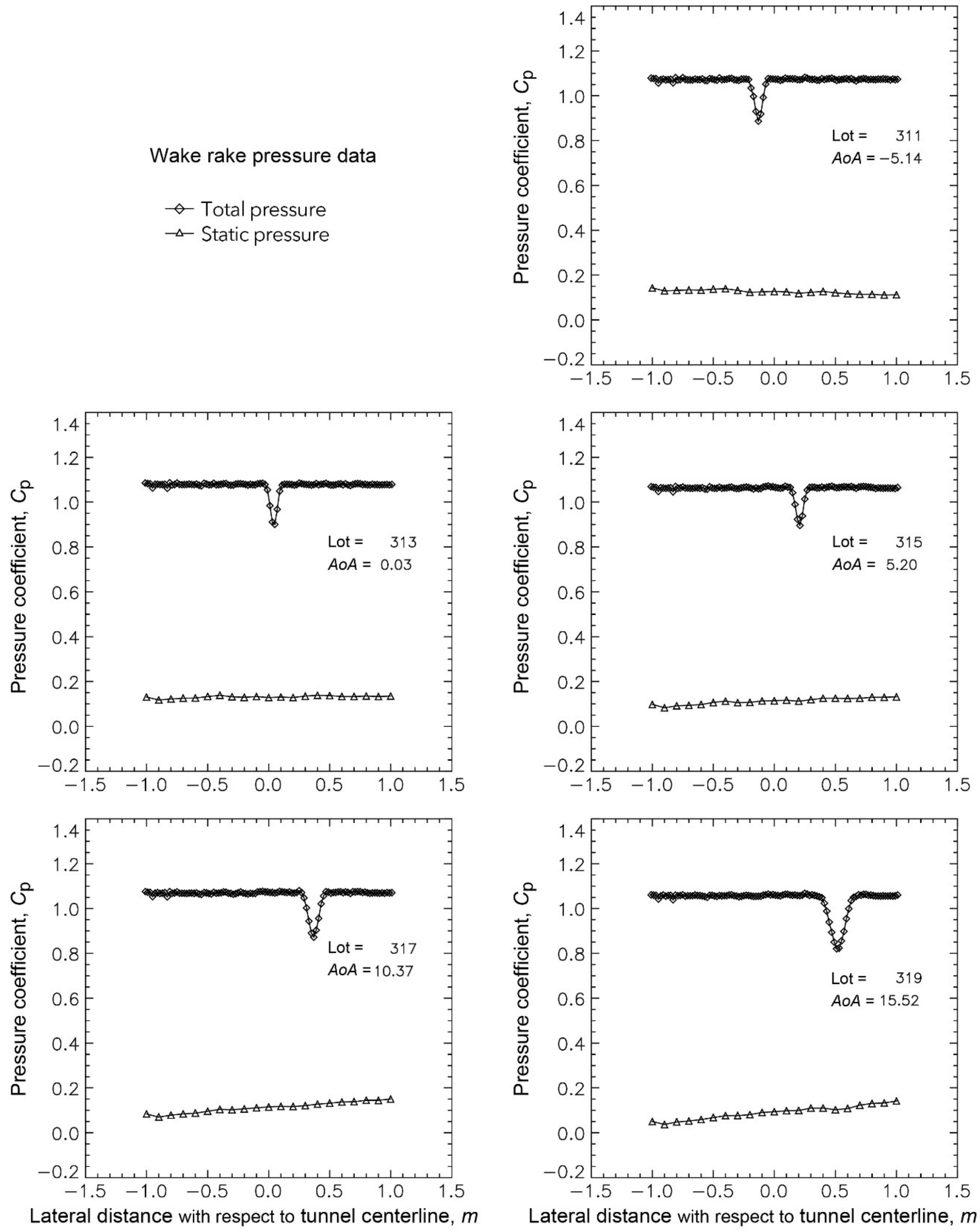

Clean Airfoil: M = 0.10 and Re = 12.2–12.3×10^6

Appendix G.—F1 Full-Scale Model Tests

Clean Airfoil: M = 0.20 to 0.21 and Re = 9.1×10^6

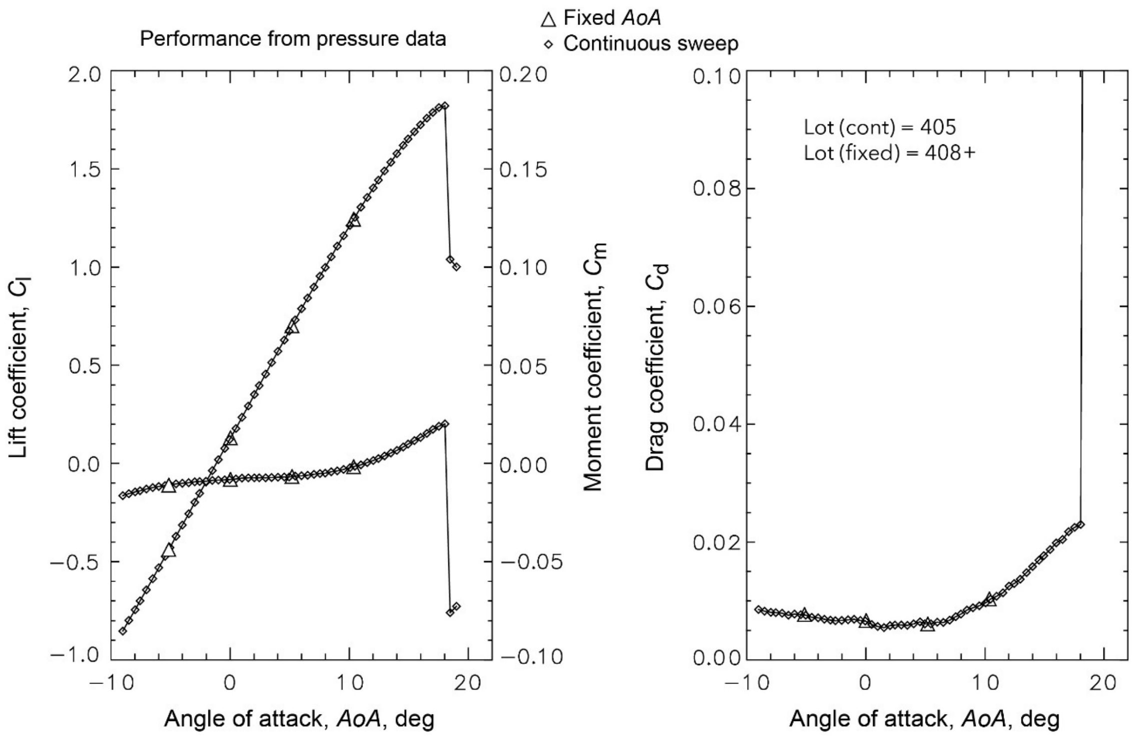

Clean Airfoil: M = 0.20 to 0.21 and Re = 9.1×10^6

Appendix G.—F1 Full-Scale Model Tests

Clean Airfoil: M = 0.20 to 0.21 and Re = 9.1×10^6

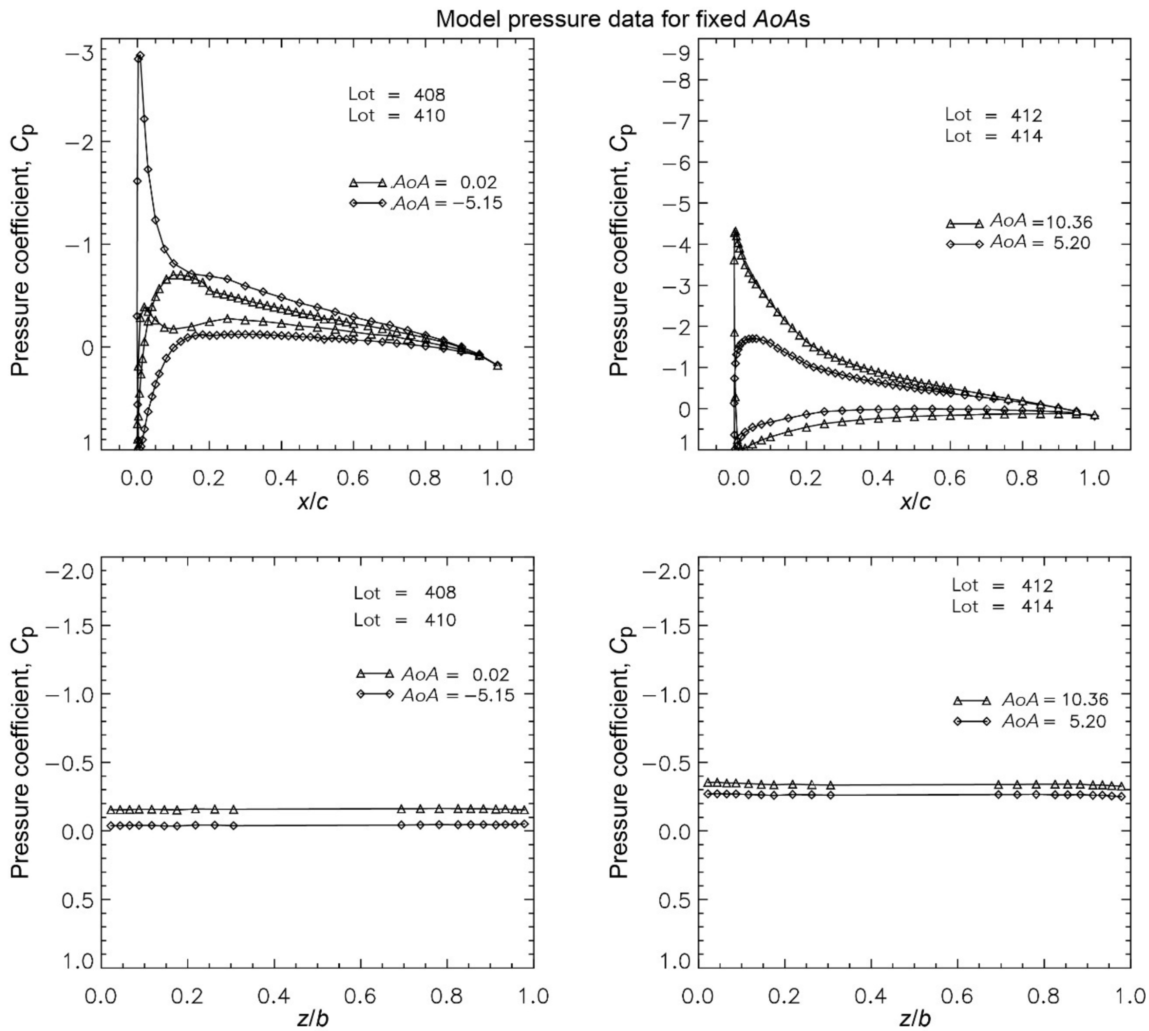

Clean Airfoil: M = 0.20 to 0.21 and Re = 9.1×10^6

Appendix G.—F1 Full-Scale Model Tests

Clean Airfoil: M = 0.20 to 0.21 and Re = 9.1×10^6

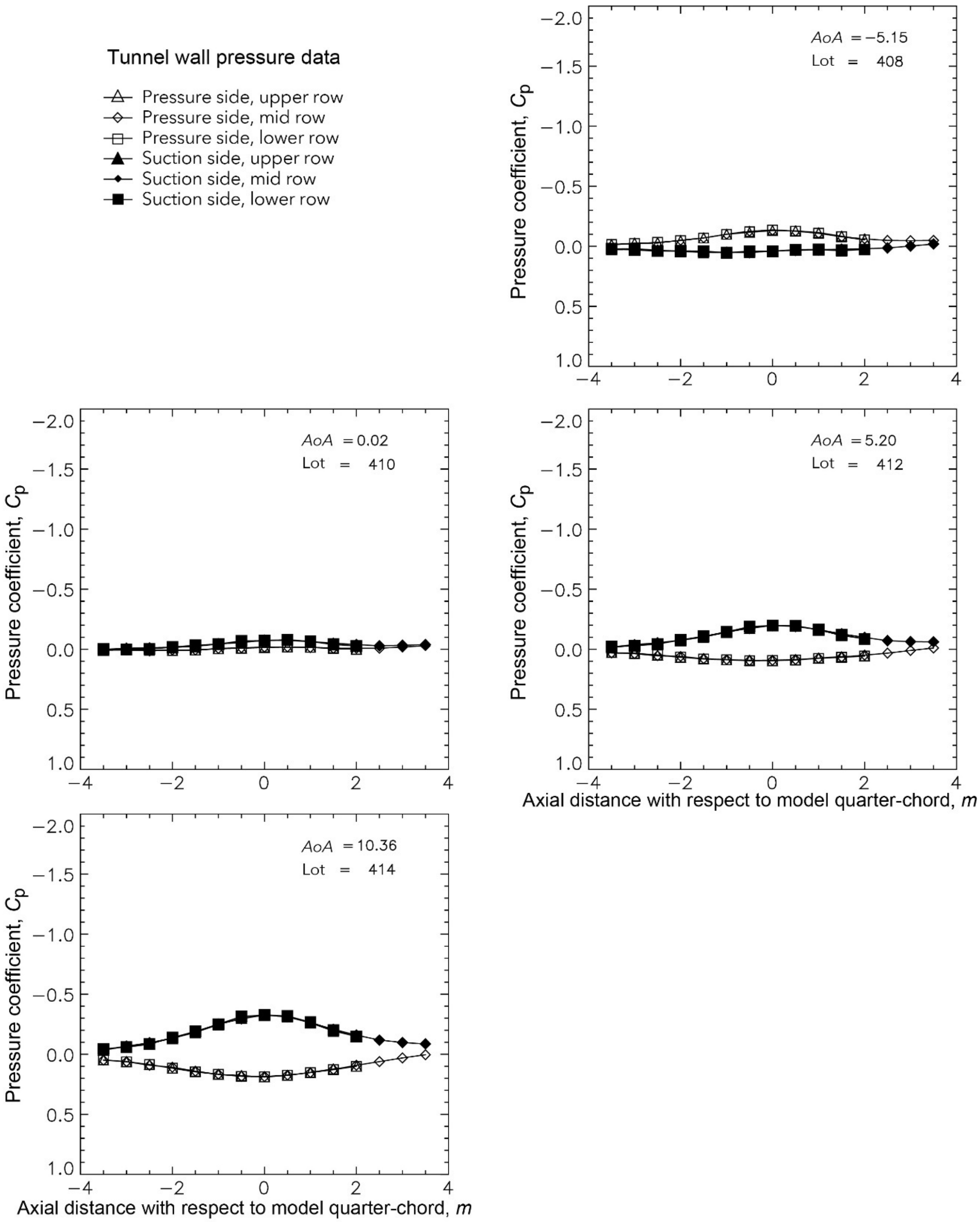

Clean Airfoil: M = 0.20 to 0.21 and Re = 9.1×10^6

Appendix G.—F1 Full-Scale Model Tests

Clean Airfoil: M = 0.20 to 0.21 and Re = 9.1×10^6

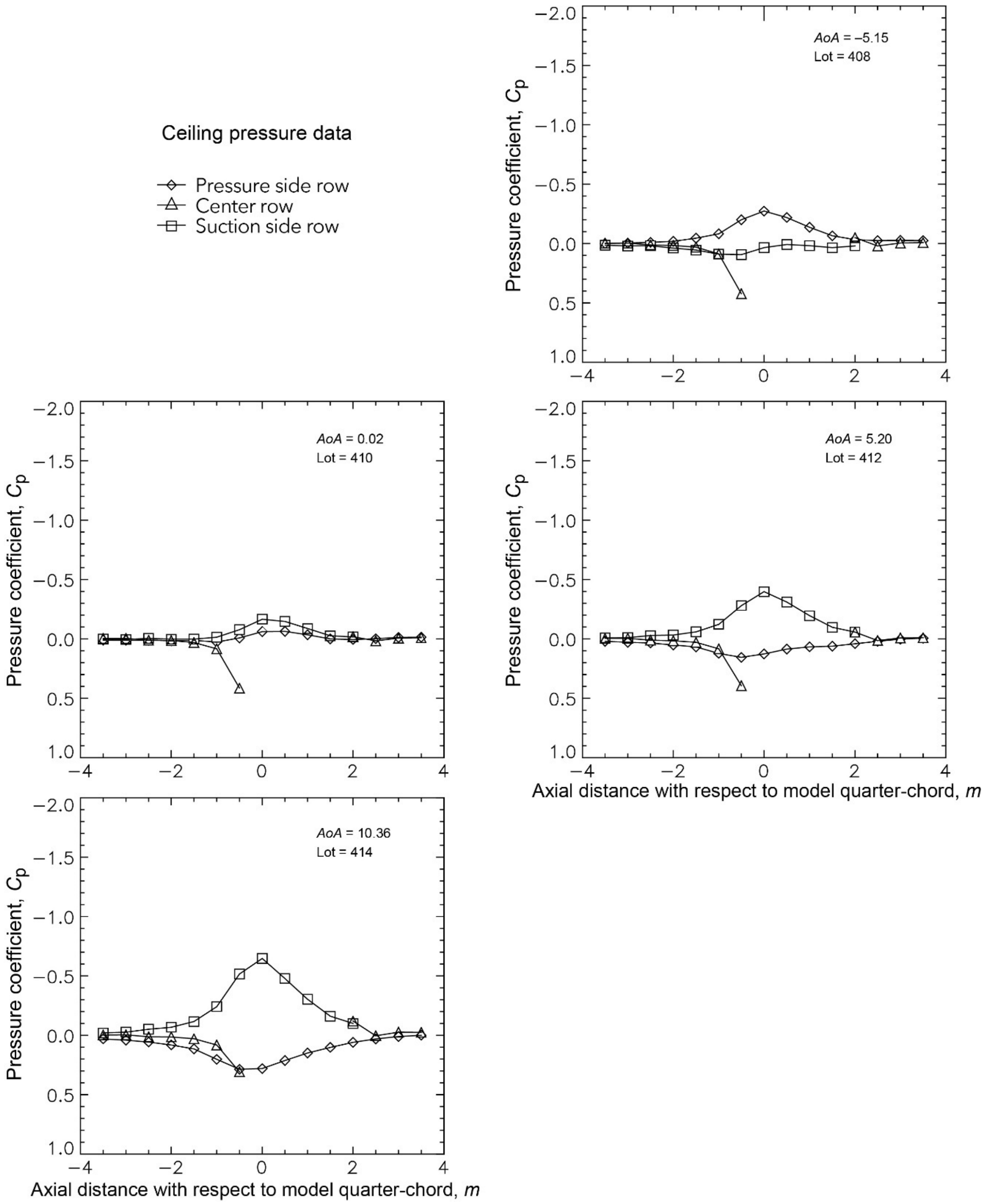

Clean Airfoil: M = 0.20 to 0.21 and Re = 9.1×10^6

Appendix G.—F1 Full-Scale Model Tests

Clean Airfoil: M = 0.20 to 0.21 and Re = 9.1×10^6

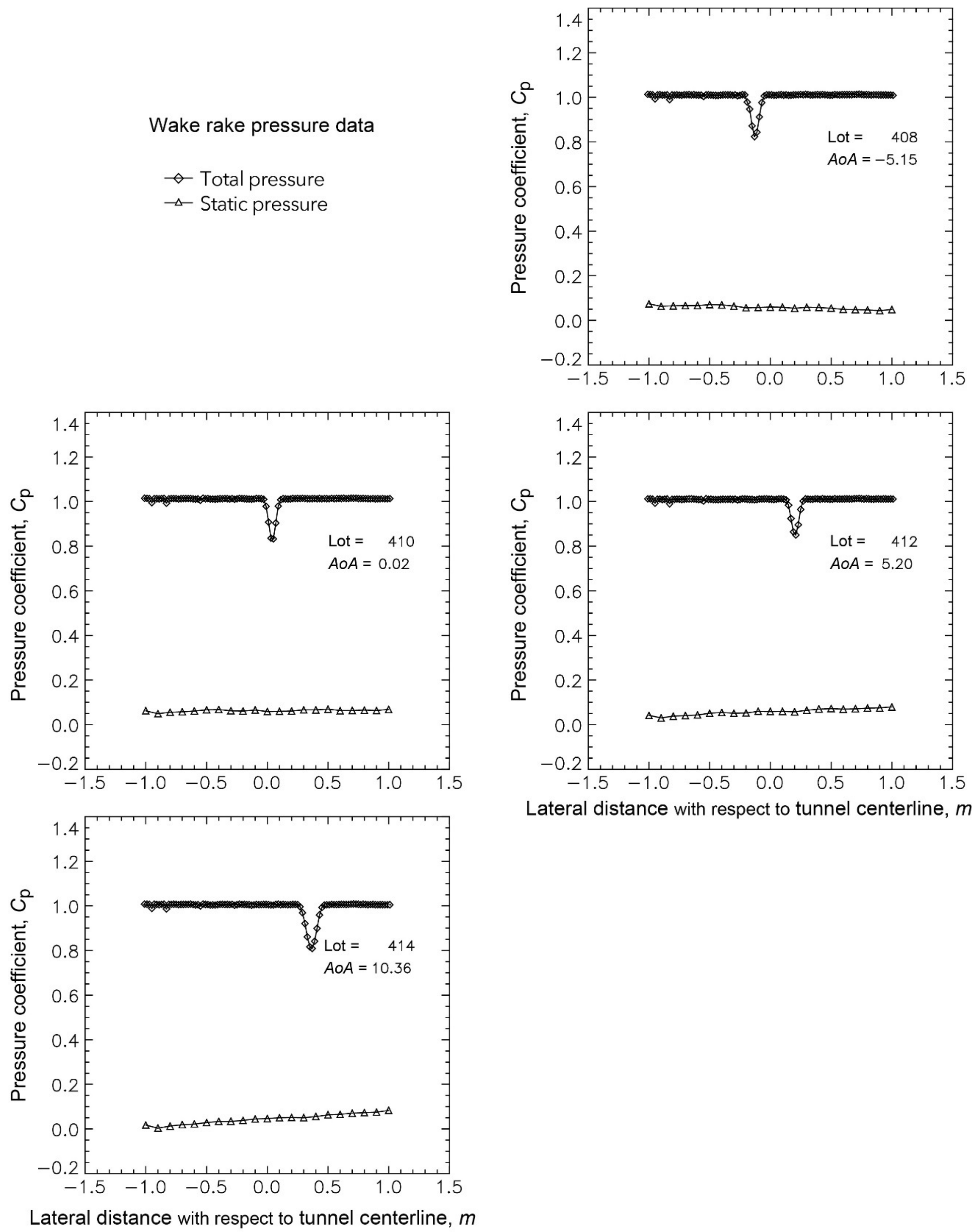

Clean Airfoil: M = 0.20 to 0.21 and Re = 9.1×10^6

Appendix G.—F1 Full-Scale Model Tests

Clean Airfoil: M = 0.20 to 0.21 and Re = 11.9–12.0×10^6

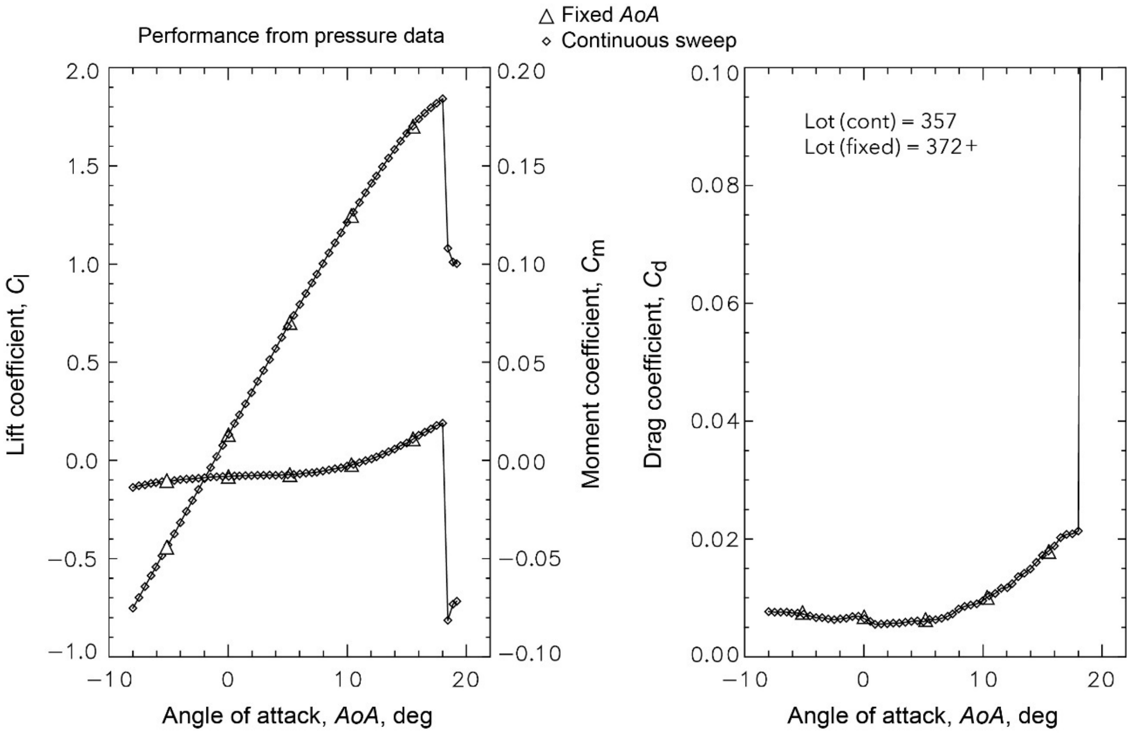

Clean Airfoil: M = 0.20 to 0.21 and Re = 11.9–12.0×10^6

Appendix G.—F1 Full-Scale Model Tests

Clean Airfoil: M = 0.20 to 0.21 and Re = 11.9–12.0×10^{6}

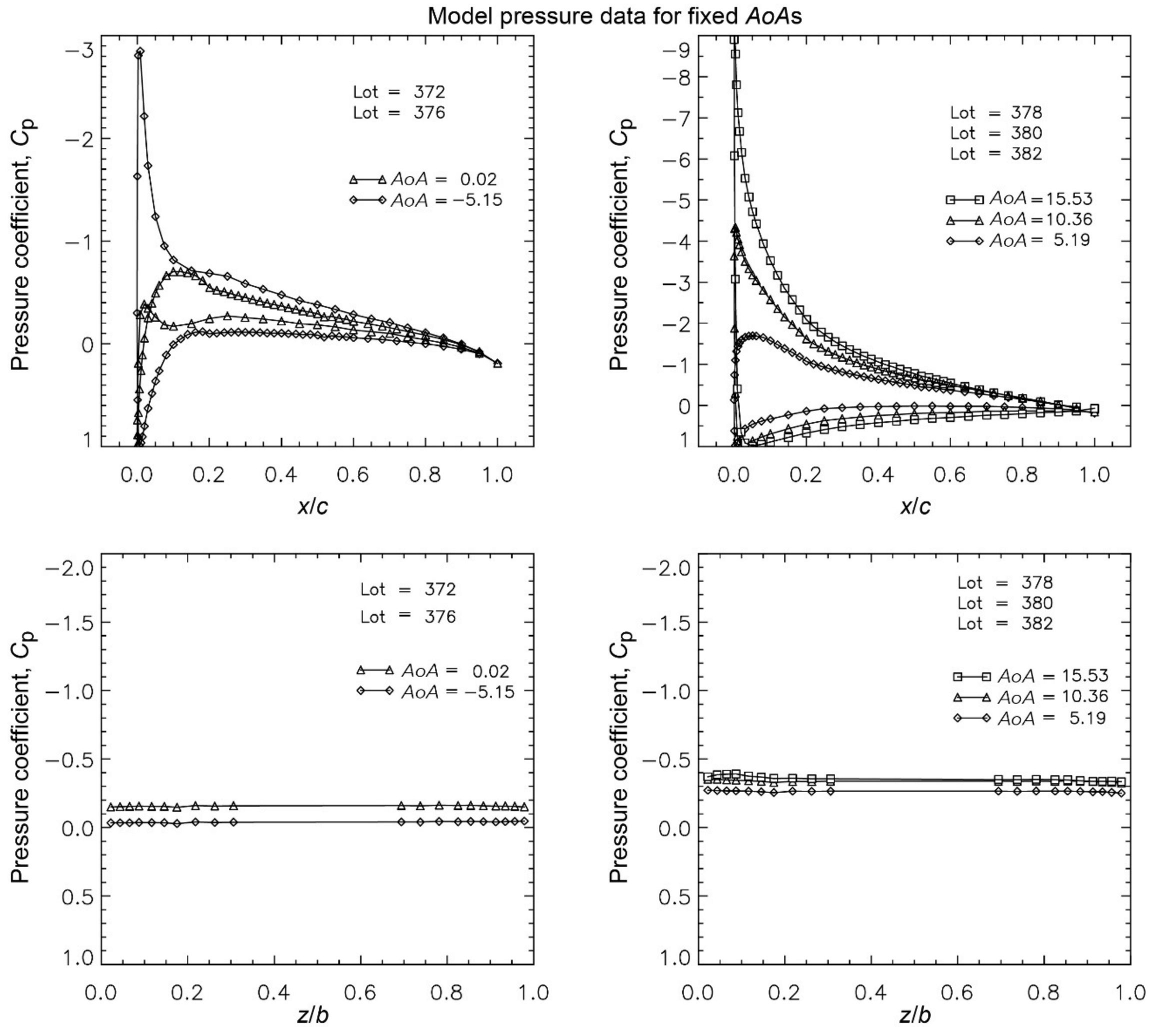

Clean Airfoil: M = 0.20 to 0.21 and Re = 11.9–12.0×10^{6}

Appendix G.—F1 Full-Scale Model Tests

Clean Airfoil: M = 0.20 to 0.21 and Re = 11.9–12.0×10^6

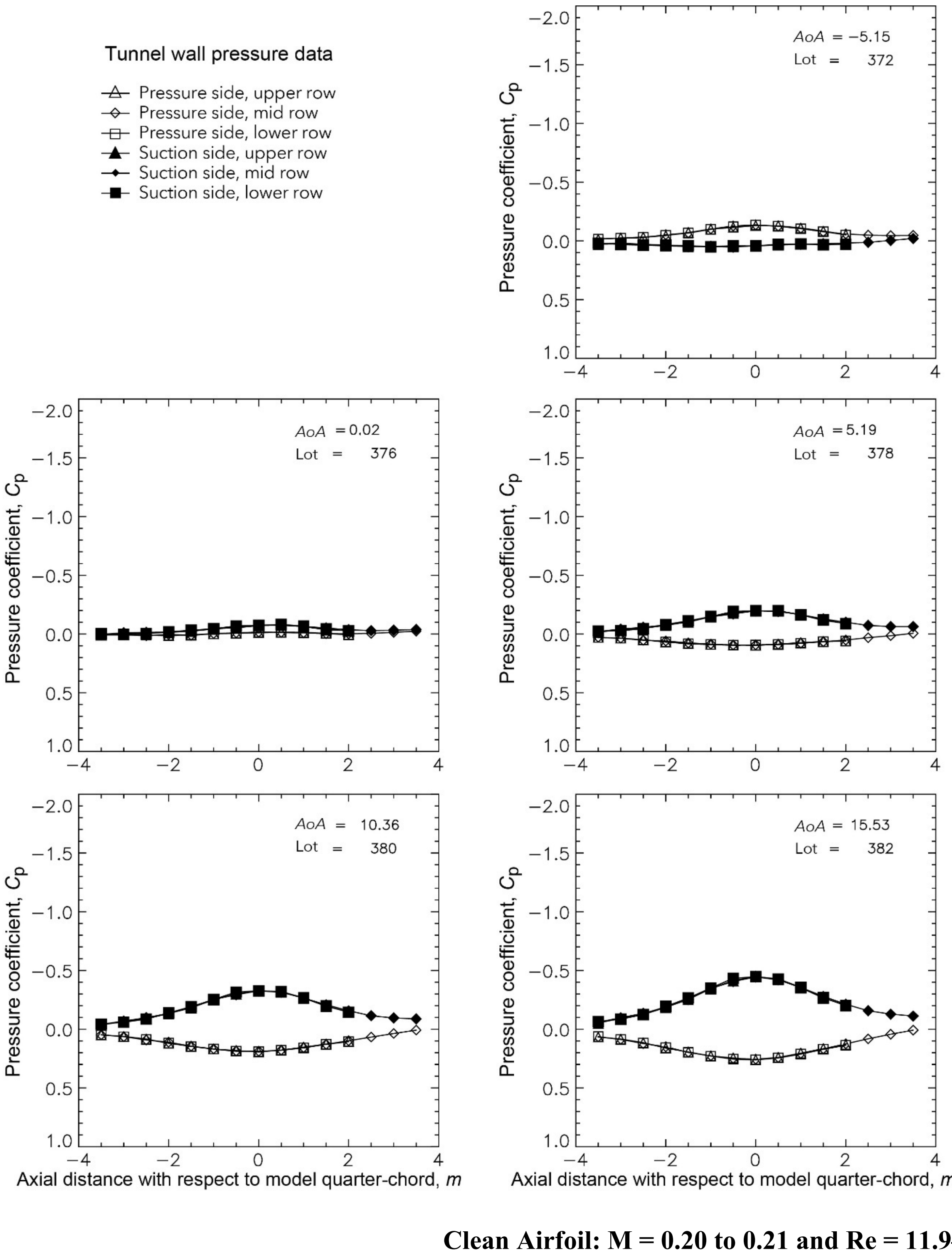

Clean Airfoil: M = 0.20 to 0.21 and Re = 11.9–12.0×10^6

Appendix G.—F1 Full-Scale Model Tests

Clean Airfoil: M = 0.20 to 0.21 and Re = 11.9–12.0×10^6

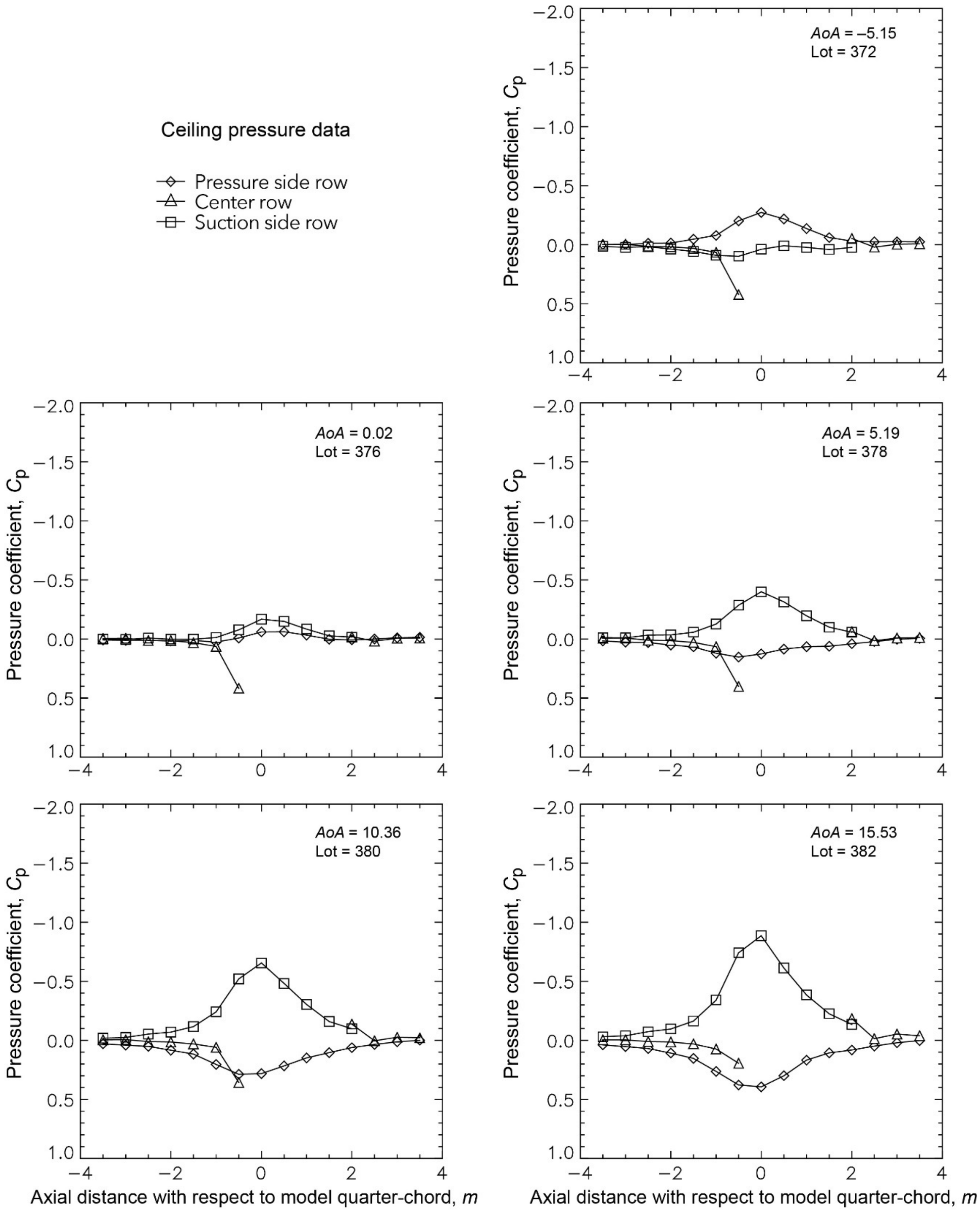

Clean Airfoil: M = 0.20 to 0.21 and Re = 11.9–12.0×10^6

Appendix G.—F1 Full-Scale Model Tests

Clean Airfoil: M = 0.20 to 0.21 and Re = 11.9–12.0×10^6

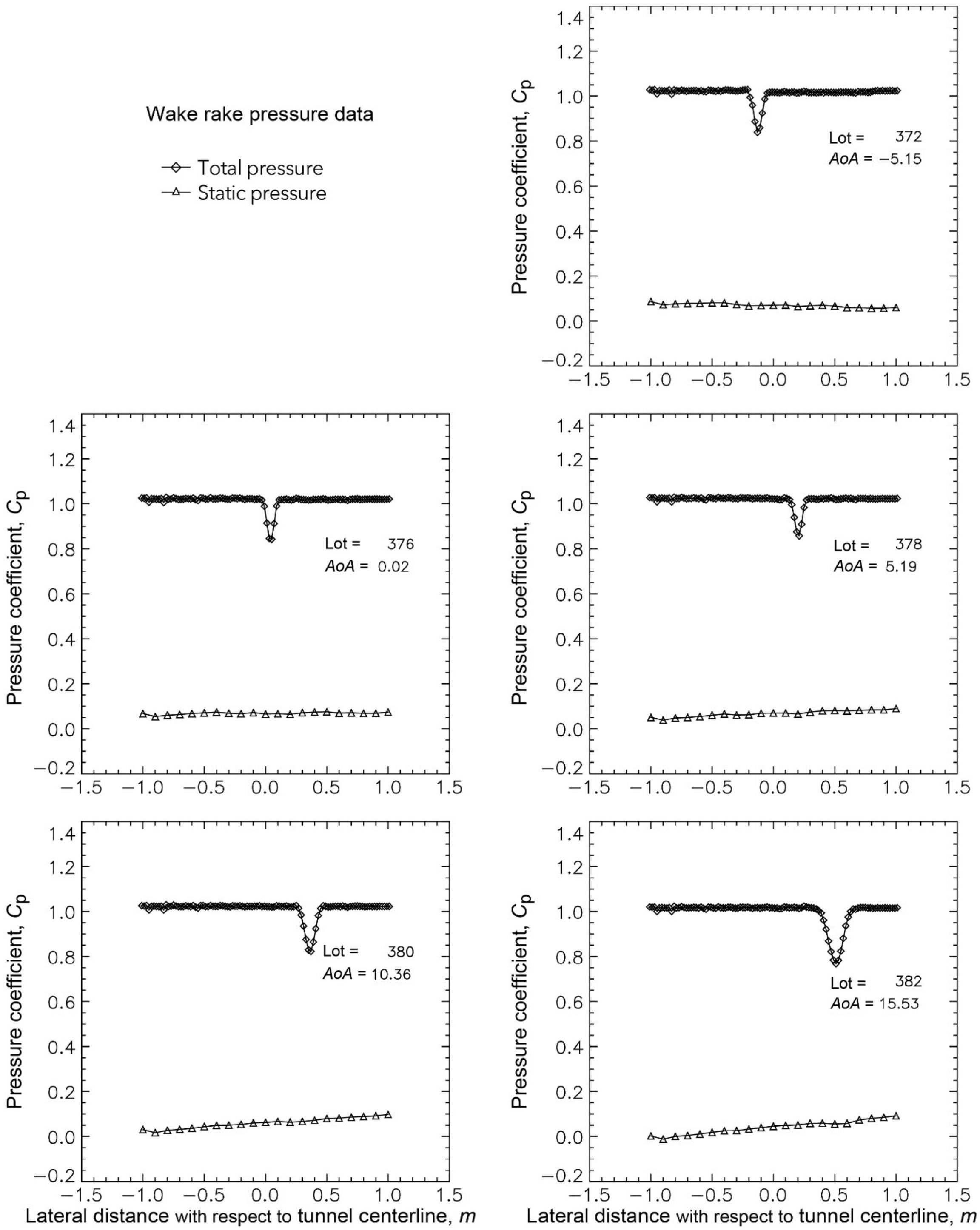

Clean Airfoil: M = 0.20 to 0.21 and Re = 11.9–12.0×10^6

Appendix G.—F1 Full-Scale Model Tests

Clean Airfoil: M = 0.20 and Re = 15.9×10^6

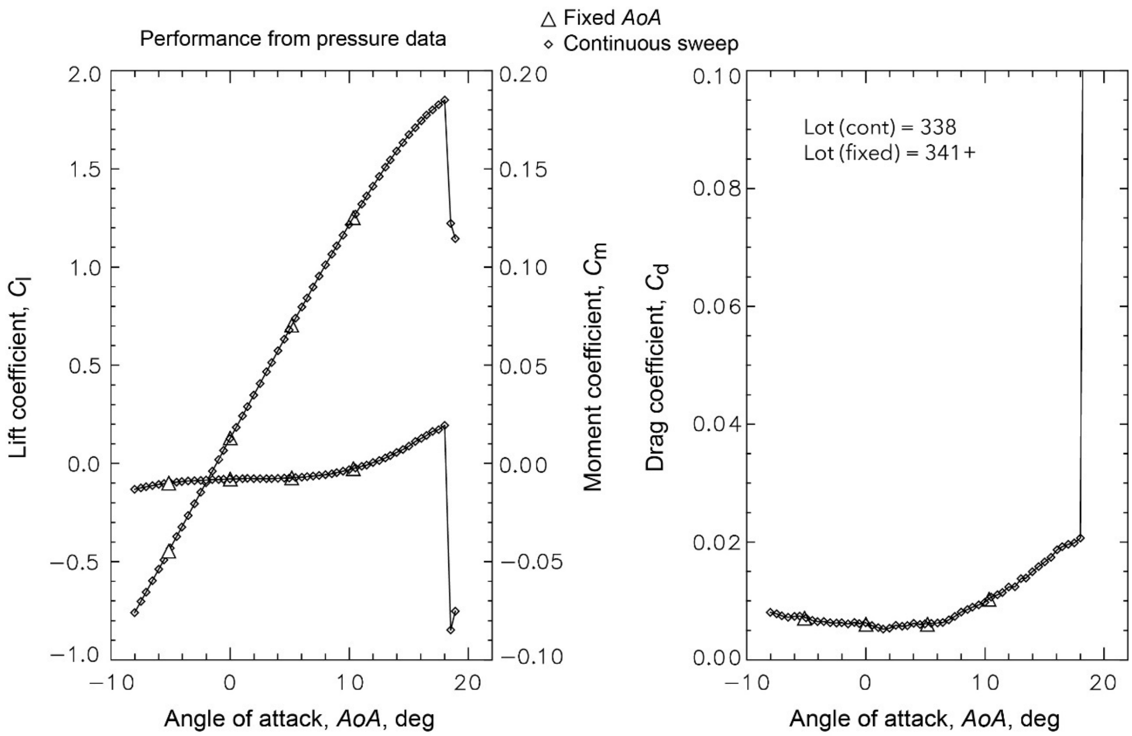

Clean Airfoil: M = 0.20 and Re = 15.9×10^6

Appendix G.—F1 Full-Scale Model Tests

Clean Airfoil: M = 0.20 and Re = 15.9×10^6

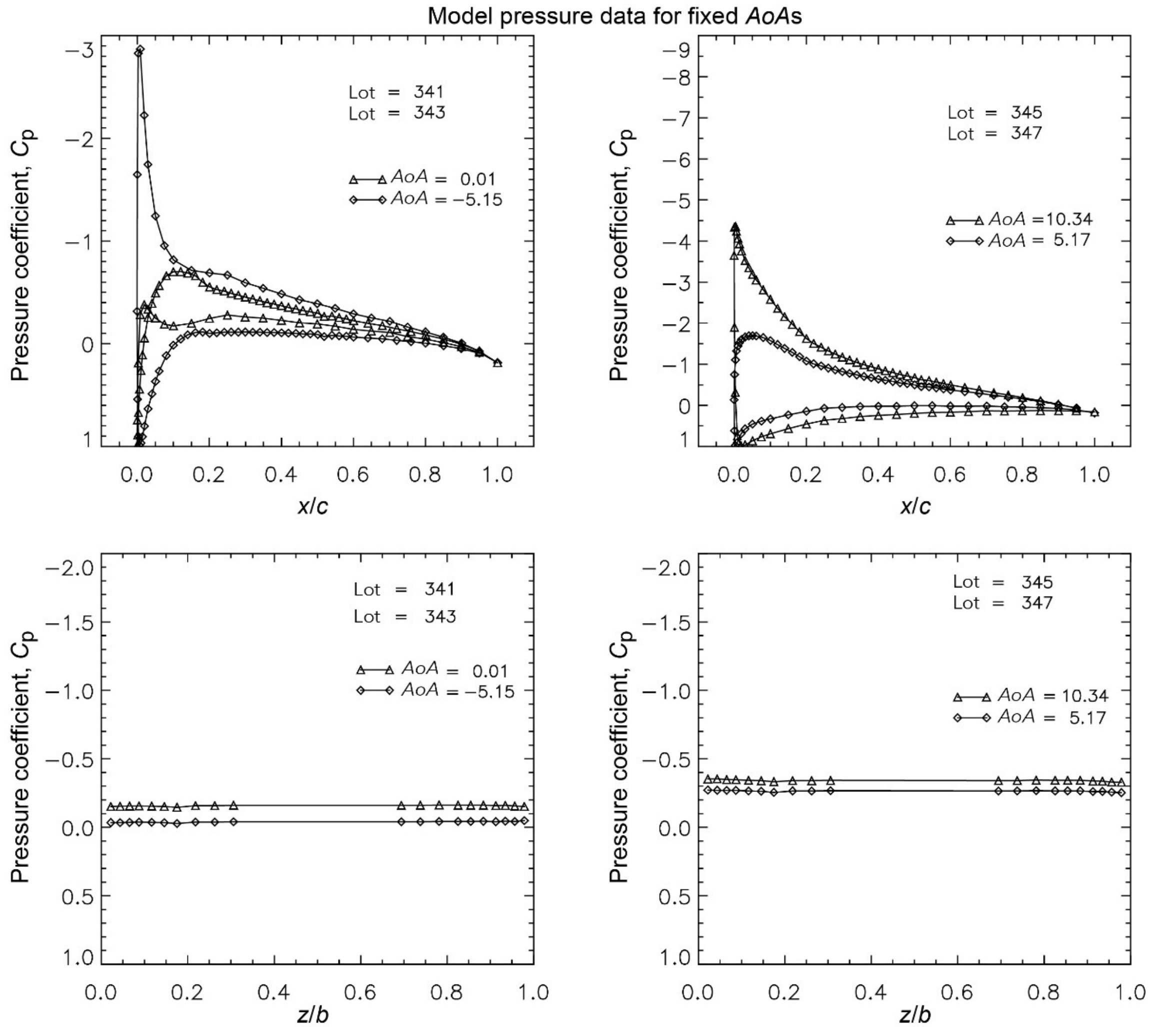

Clean Airfoil: M = 0.20 and Re = 15.9×10^6

Appendix G.—F1 Full-Scale Model Tests

Clean Airfoil: M = 0.20 and Re = 15.9×10^6

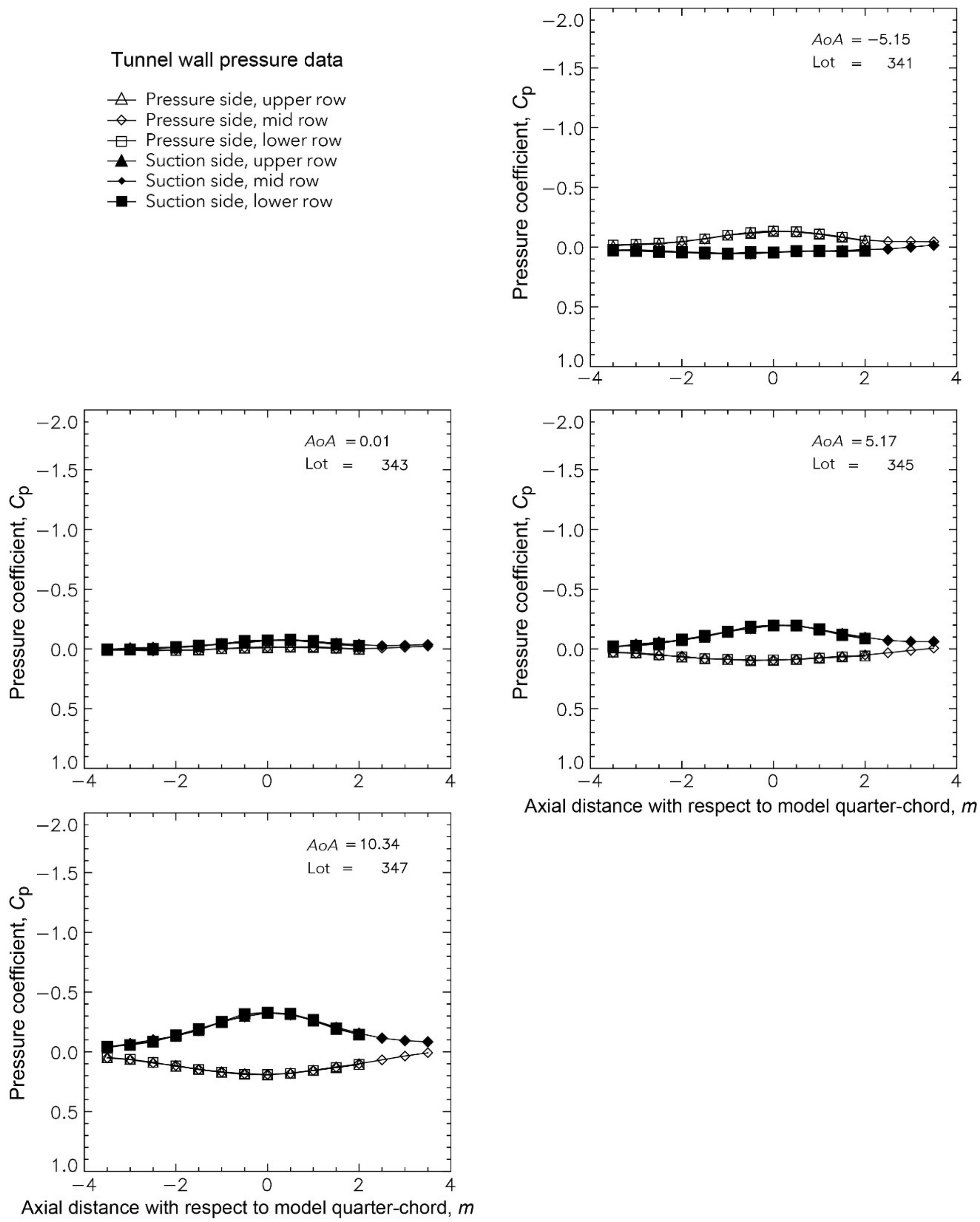

Clean Airfoil: M = 0.20 and Re = 15.9×10^6

Appendix G.—F1 Full-Scale Model Tests

Clean Airfoil: M = 0.20 and Re = 15.9×10^6

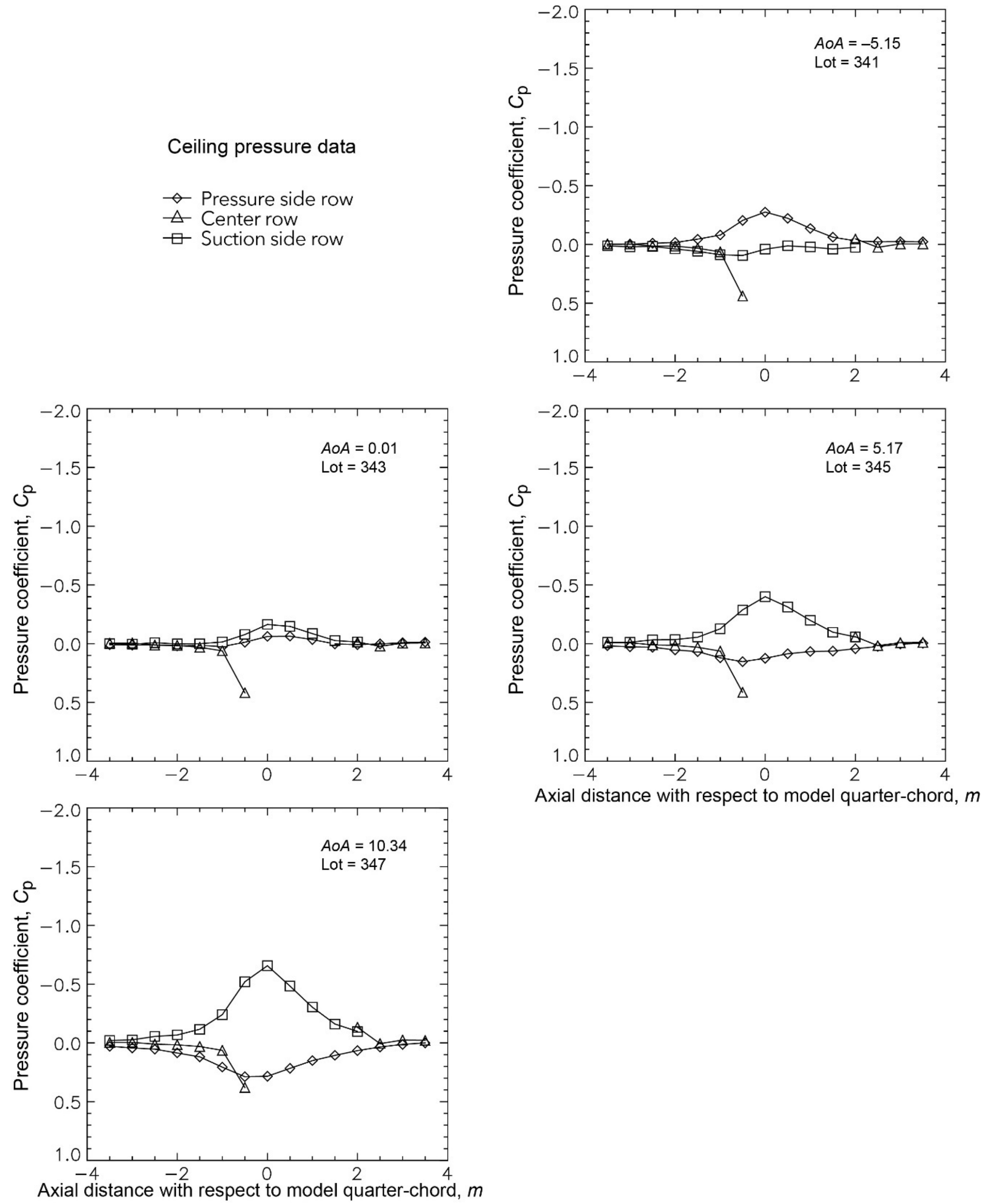

Clean Airfoil: M = 0.20 and Re = 15.9×10^6

Appendix G.—F1 Full-Scale Model Tests

Clean Airfoil: M = 0.20 and Re = 15.9×10^6

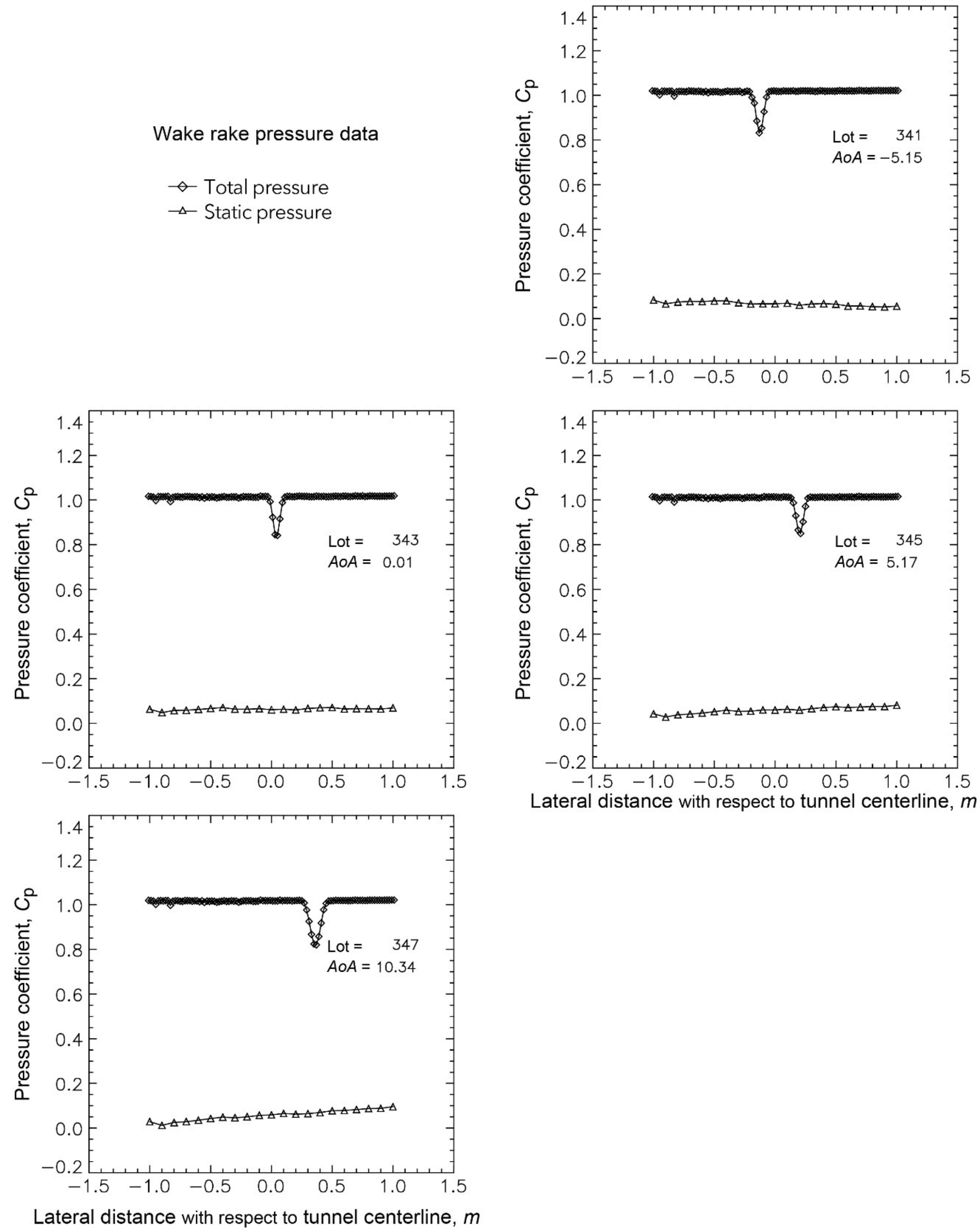

Clean Airfoil: M = 0.20 and Re = 15.9×10^6

Appendix G.—F1 Full-Scale Model Tests

Clean Airfoil: M = 0.28 to 0.29 and Re = 12.1–12.2×10^6

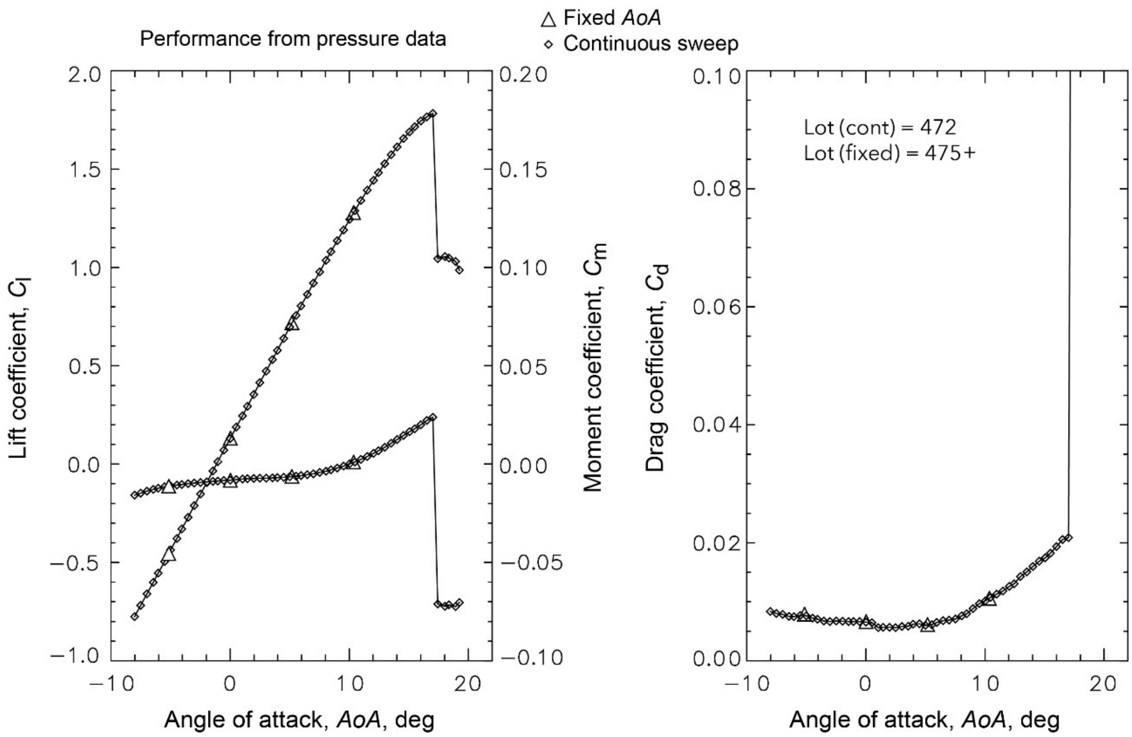

Clean Airfoil: M = 0.28 to 0.29 and Re = 12.1–12.2×10^6

Appendix G.—F1 Full-Scale Model Tests

Clean Airfoil: M = 0.28 to 0.29 and Re = 12.1–12.2×10⁶

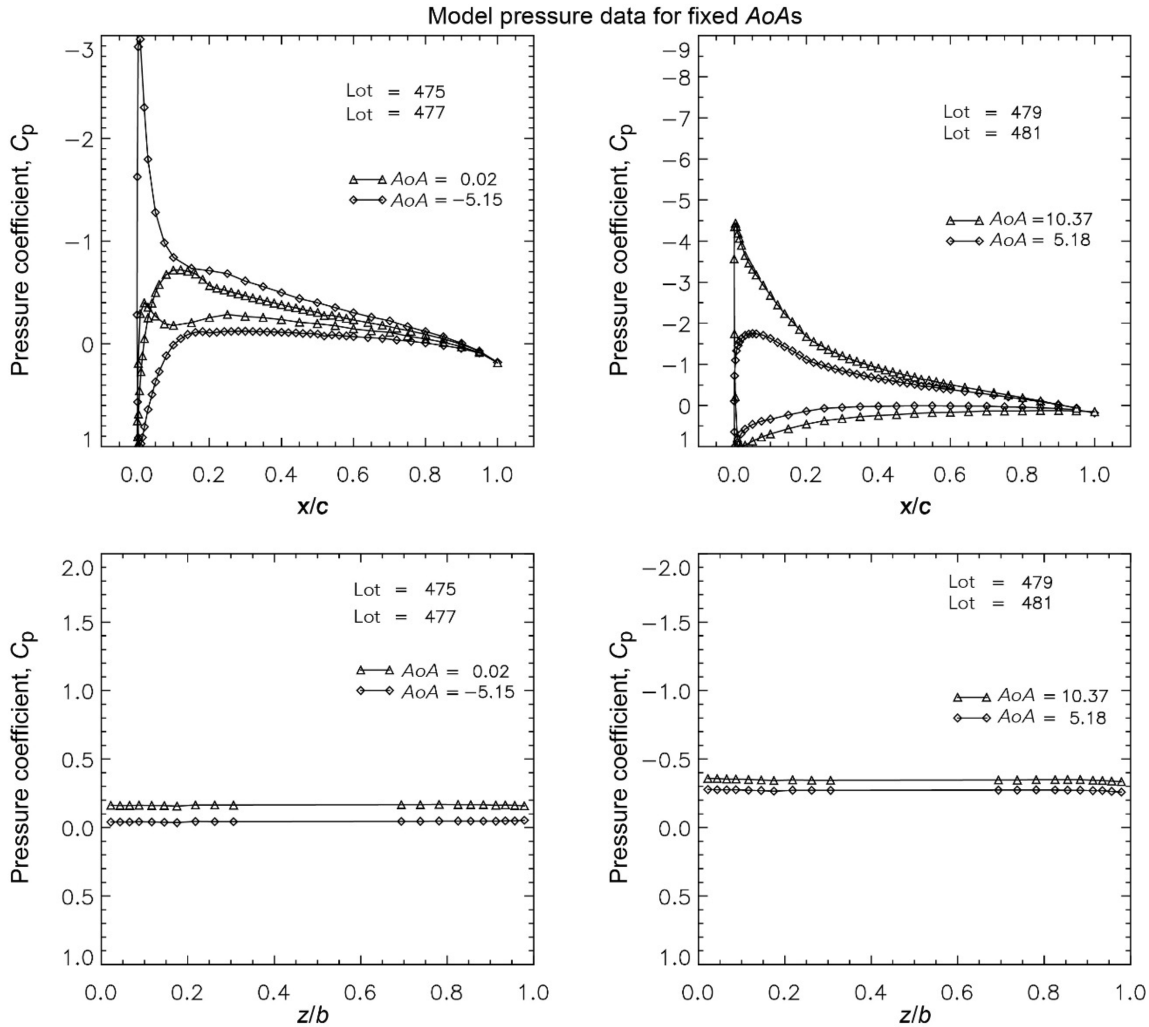

Clean Airfoil: M = 0.28 to 0.29 and Re = 12.1–12.2×10⁶

Appendix G.—F1 Full-Scale Model Tests

Clean Airfoil: M = 0.28 to 0.29 and Re = 12.1–12.2×10^6

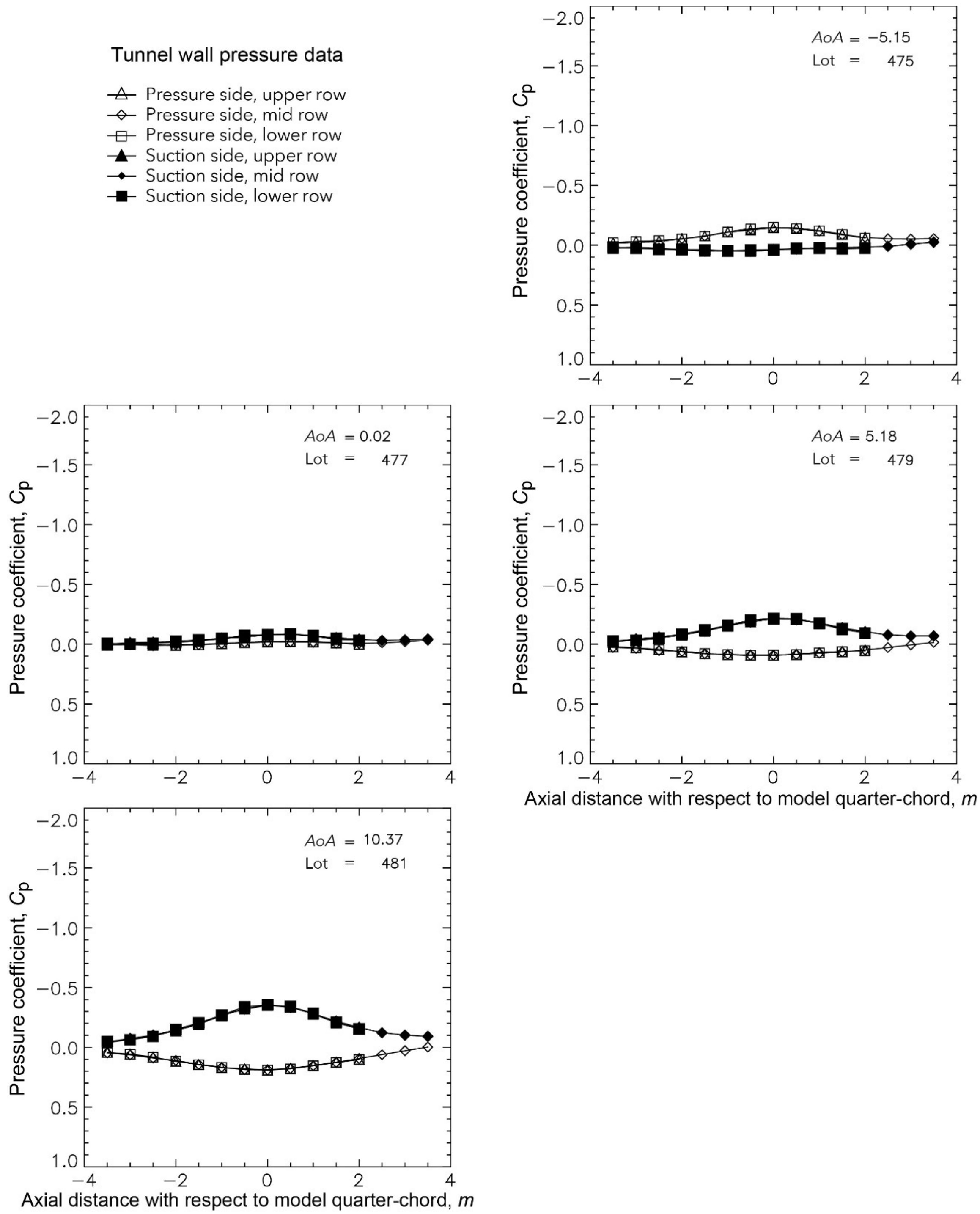

Clean Airfoil: M = 0.28 to 0.29 and Re = 12.1–12.2×10^6

Appendix G.—F1 Full-Scale Model Tests

Clean Airfoil: M = 0.28 to 0.29 and Re = 12.1–12.2×10^6

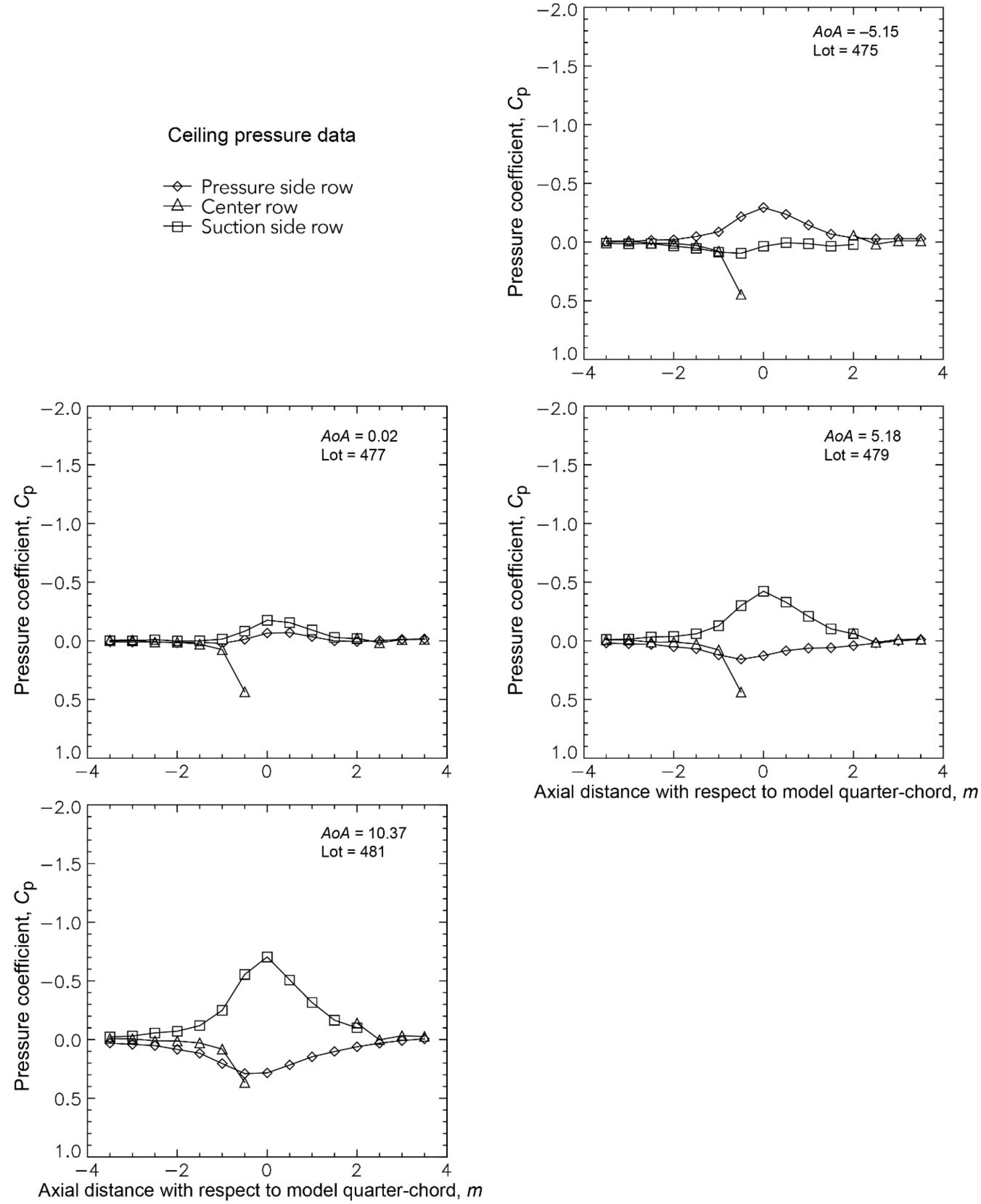

Clean Airfoil: M = 0.28 to 0.29 and Re = 12.1–12.2×10^6

Appendix G.—F1 Full-Scale Model Tests

Clean Airfoil: M = 0.28 to 0.29 and Re = 12.1–12.2×10^6

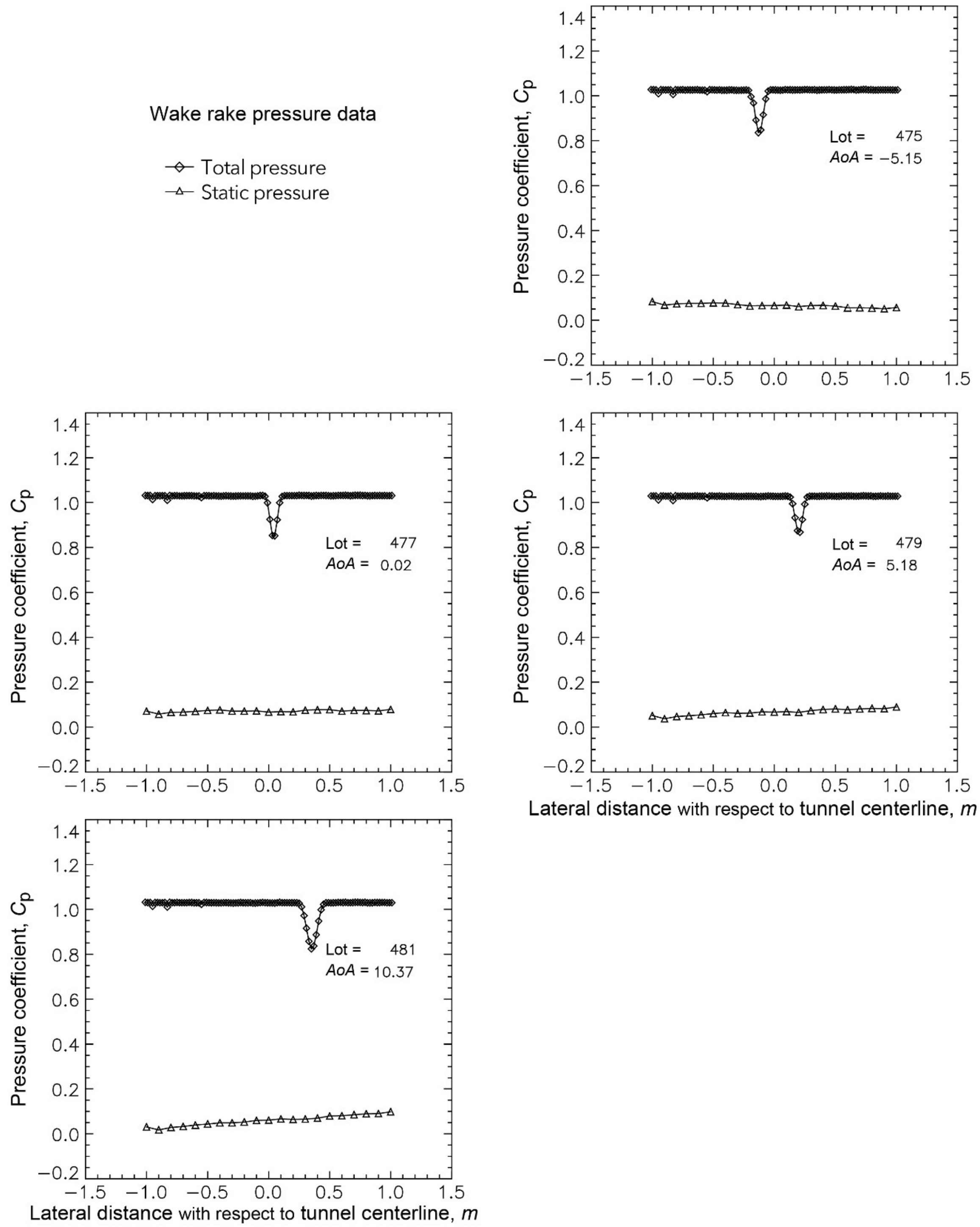

Clean Airfoil: M = 0.28 to 0.29 and Re = 12.1–12.2×10^6

Appendix G.—F1 Full-Scale Model Tests

Clean Airfoil With Trip Tape: M = 0.10 and Re = 4.5×10^6

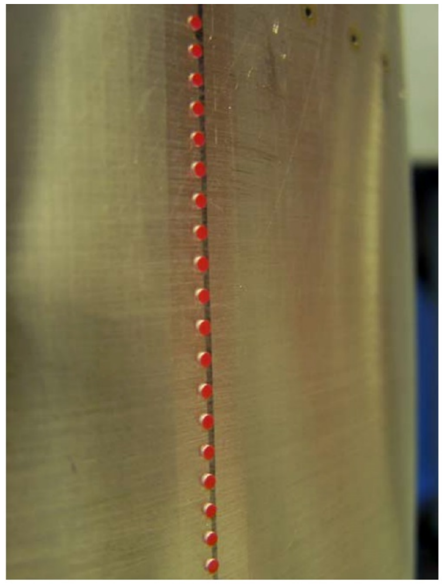

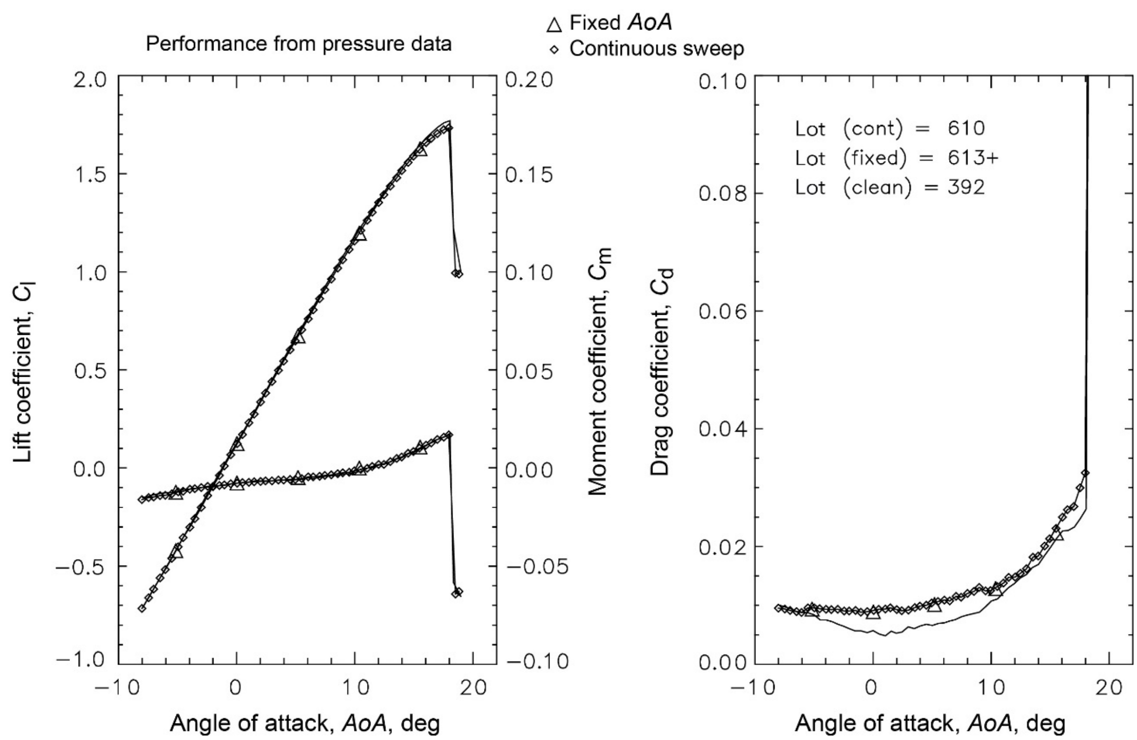

Clean Airfoil With Trip Tape: M = 0.10 and Re = 4.5×10^6

Appendix G.—F1 Full-Scale Model Tests

Clean Airfoil With Trip Tape: M = 0.10 and Re = 4.5×10^6

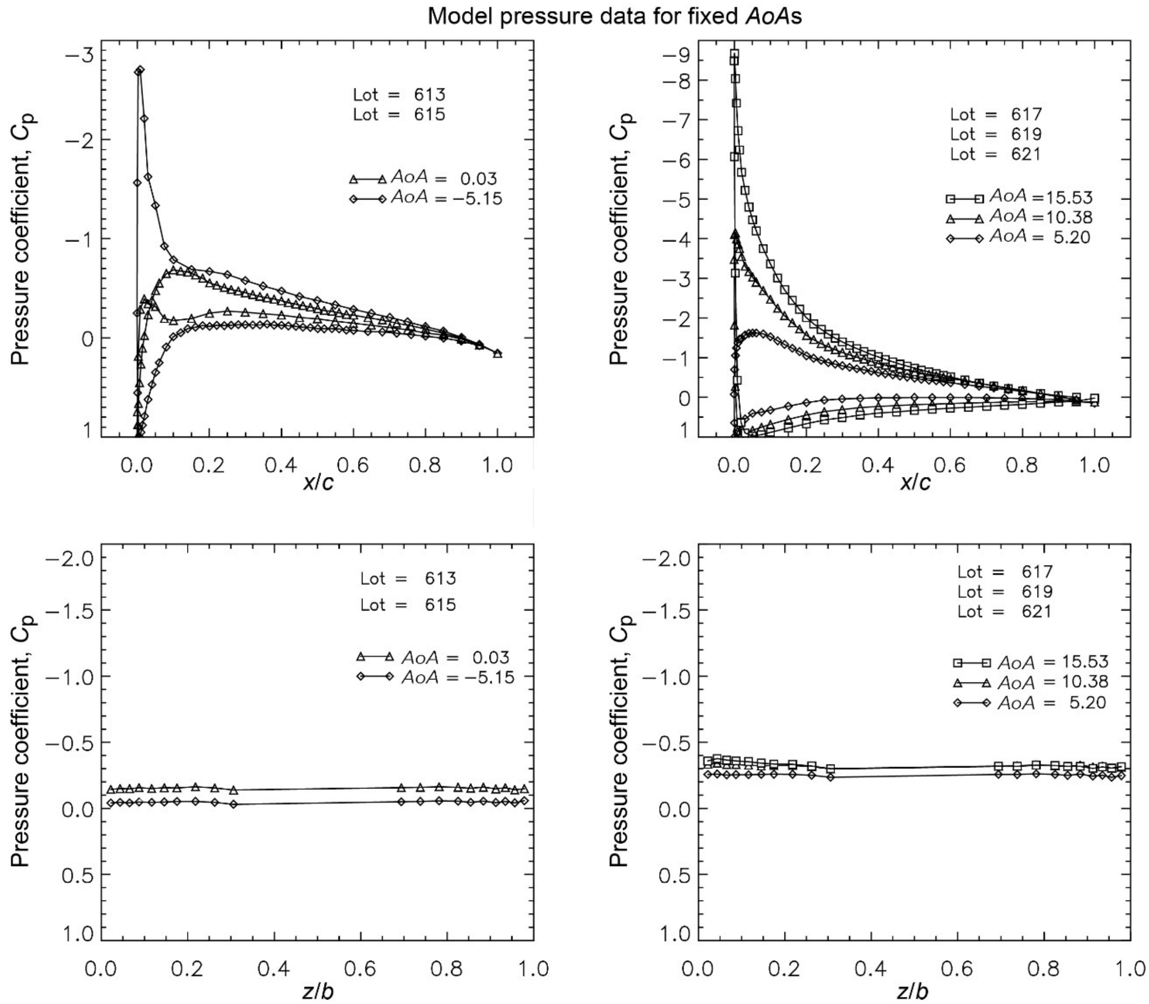

Clean Airfoil With Trip Tape: M = 0.10 and Re = 4.5×10^6

Appendix G.—F1 Full-Scale Model Tests

Clean Airfoil With Trip Tape: M = 0.10 and Re = 4.5×10^6

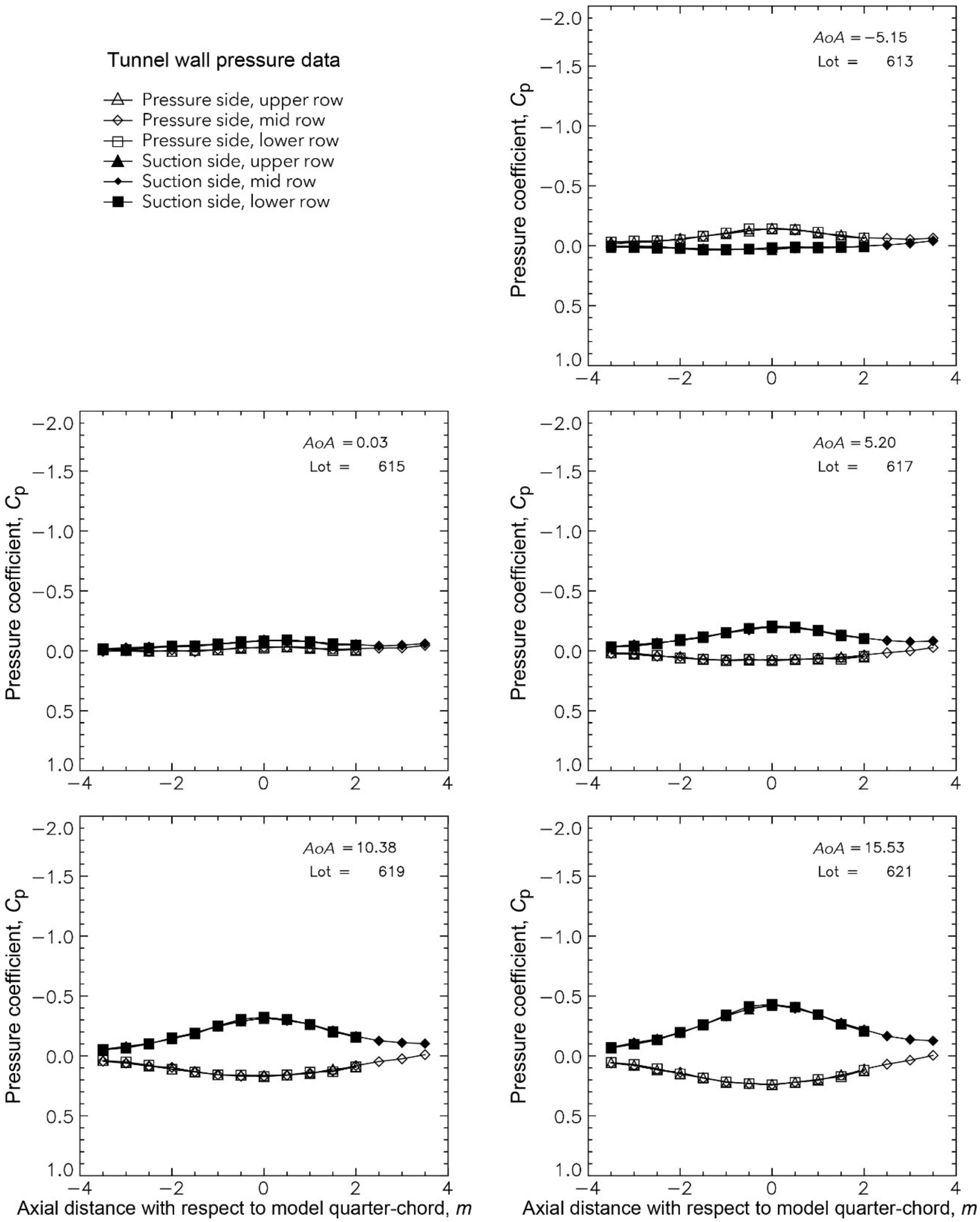

Clean Airfoil With Trip Tape: M = 0.10 and Re = 4.5×10^6

Appendix G.—F1 Full-Scale Model Tests

Clean Airfoil With Trip Tape: M = 0.10 and Re = 4.5×10⁶

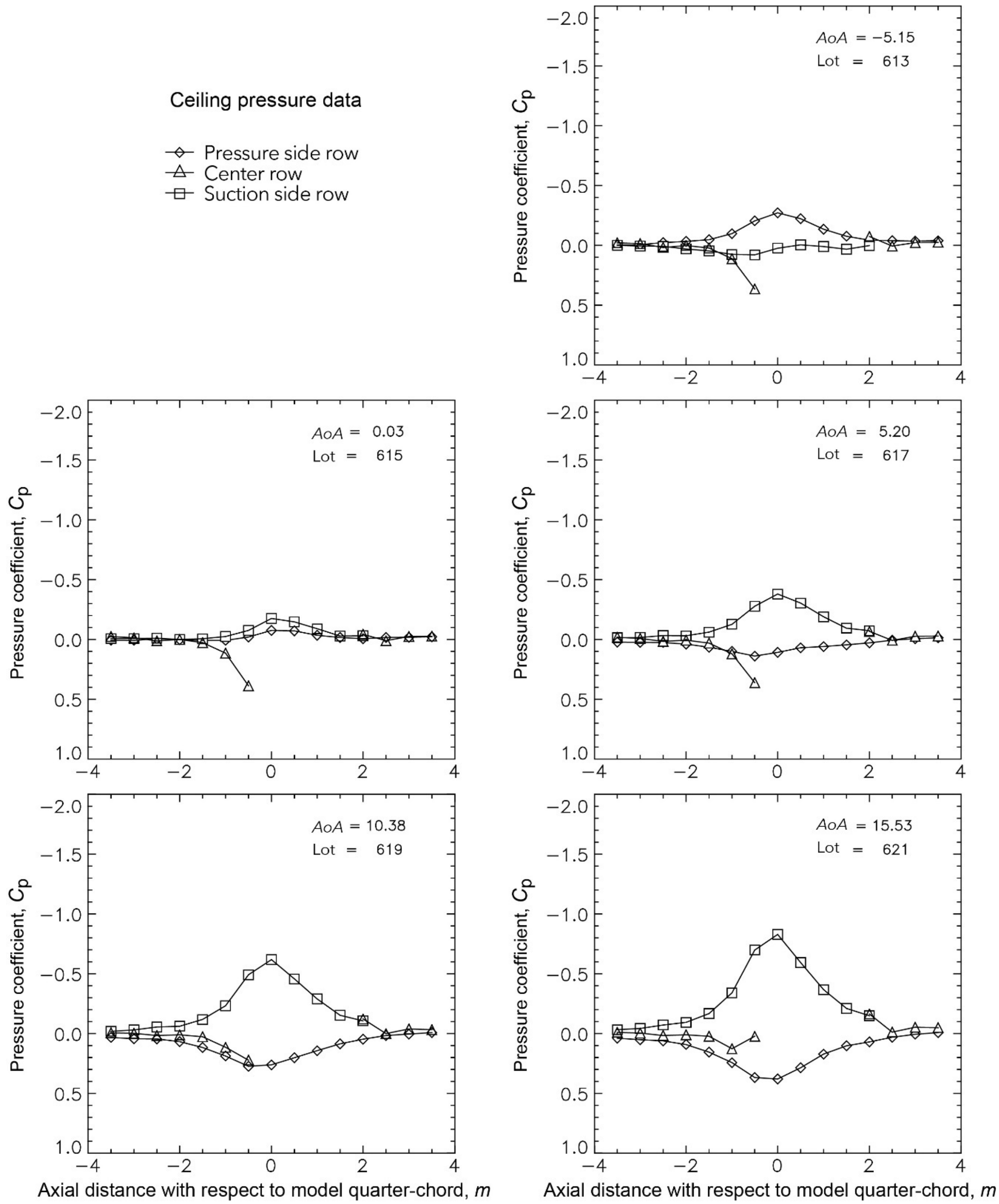

Clean Airfoil With Trip Tape: M = 0.10 and Re = 4.5×10⁶

Appendix G.—F1 Full-Scale Model Tests

Clean Airfoil With Trip Tape: M = 0.10 and Re = 4.5×10⁶

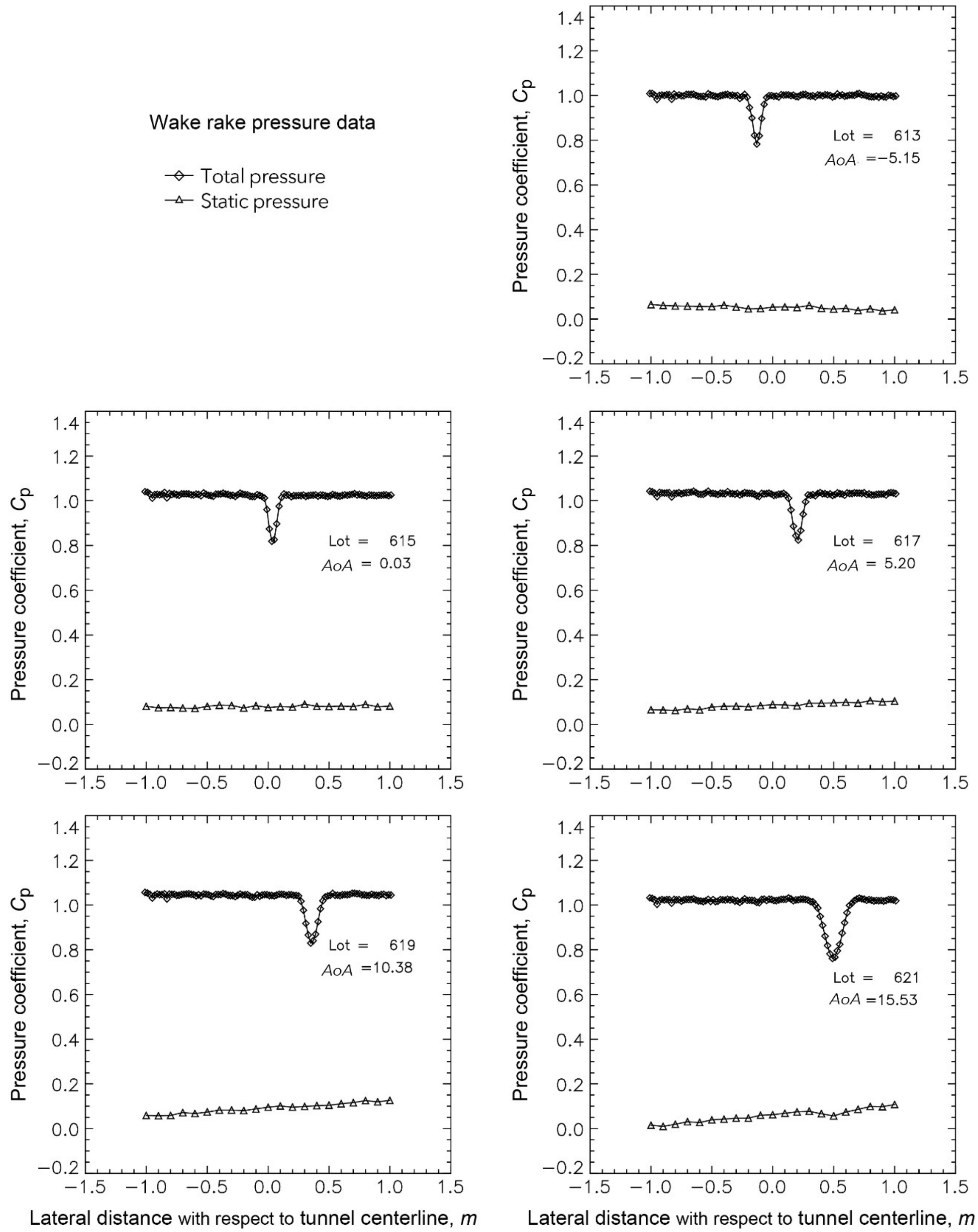

Clean Airfoil With Trip Tape: M = 0.10 and Re = 4.5×10⁶

Appendix G.—F1 Full-Scale Model Tests

Clean Airfoil With Trip Tape: M = 0.10 and Re = 8.0×10^6

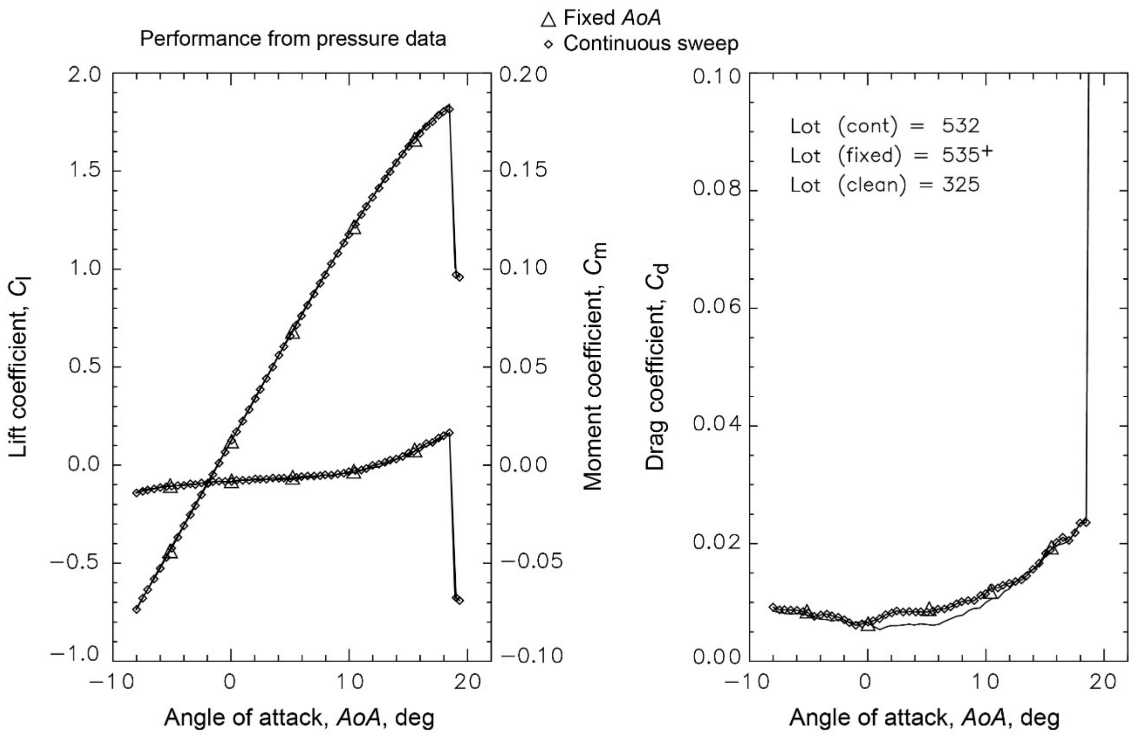

Clean Airfoil With Trip Tape: M = 0.10 and Re = 8.0×10^6

Appendix G.—F1 Full-Scale Model Tests

Clean Airfoil With Trip Tape: M = 0.10 and Re = 8.0×10⁶

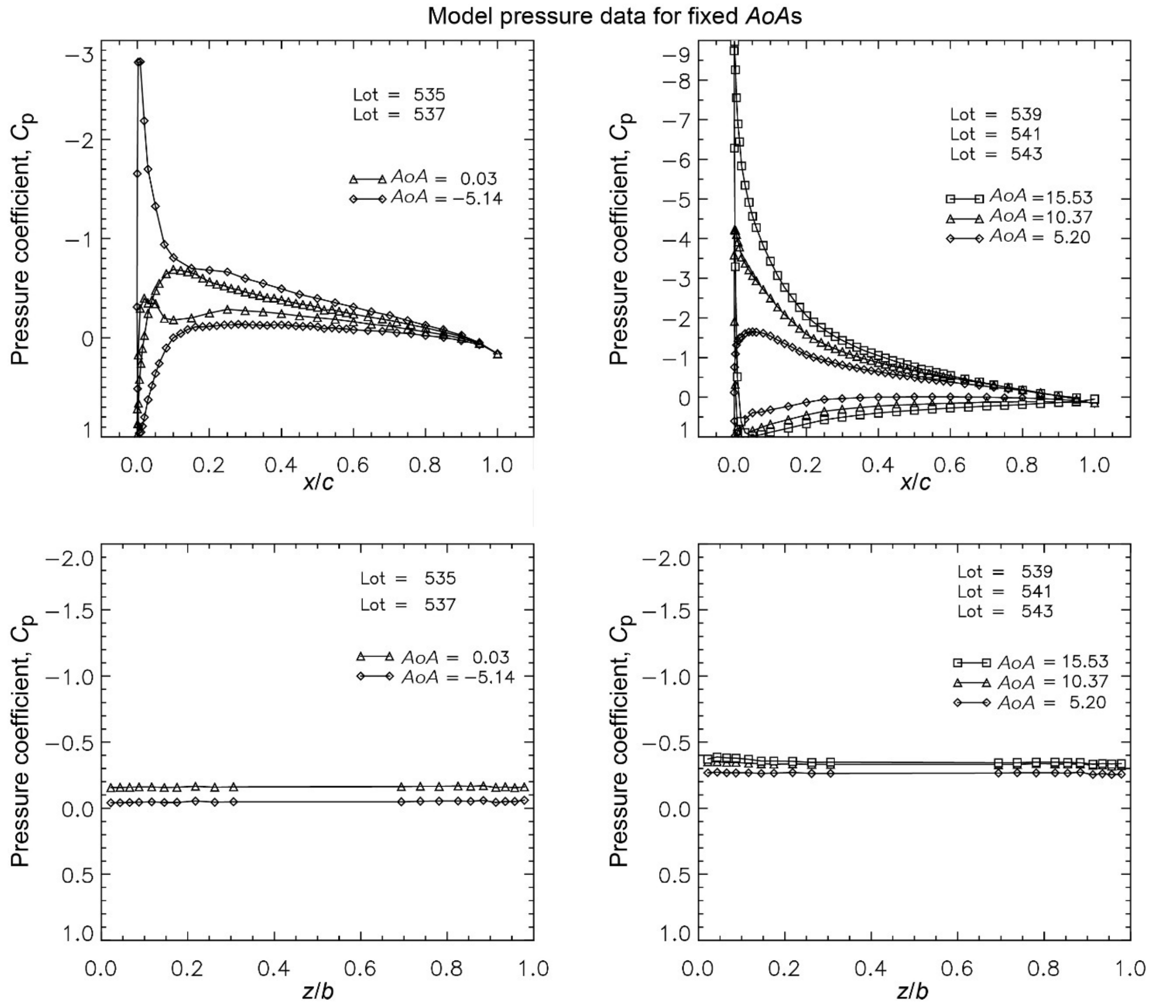

Clean Airfoil With Trip Tape: M = 0.10 and Re = 8.0×10⁶

Appendix G.—F1 Full-Scale Model Tests

Clean Airfoil With Trip Tape: M = 0.10 and Re = 8×10^6

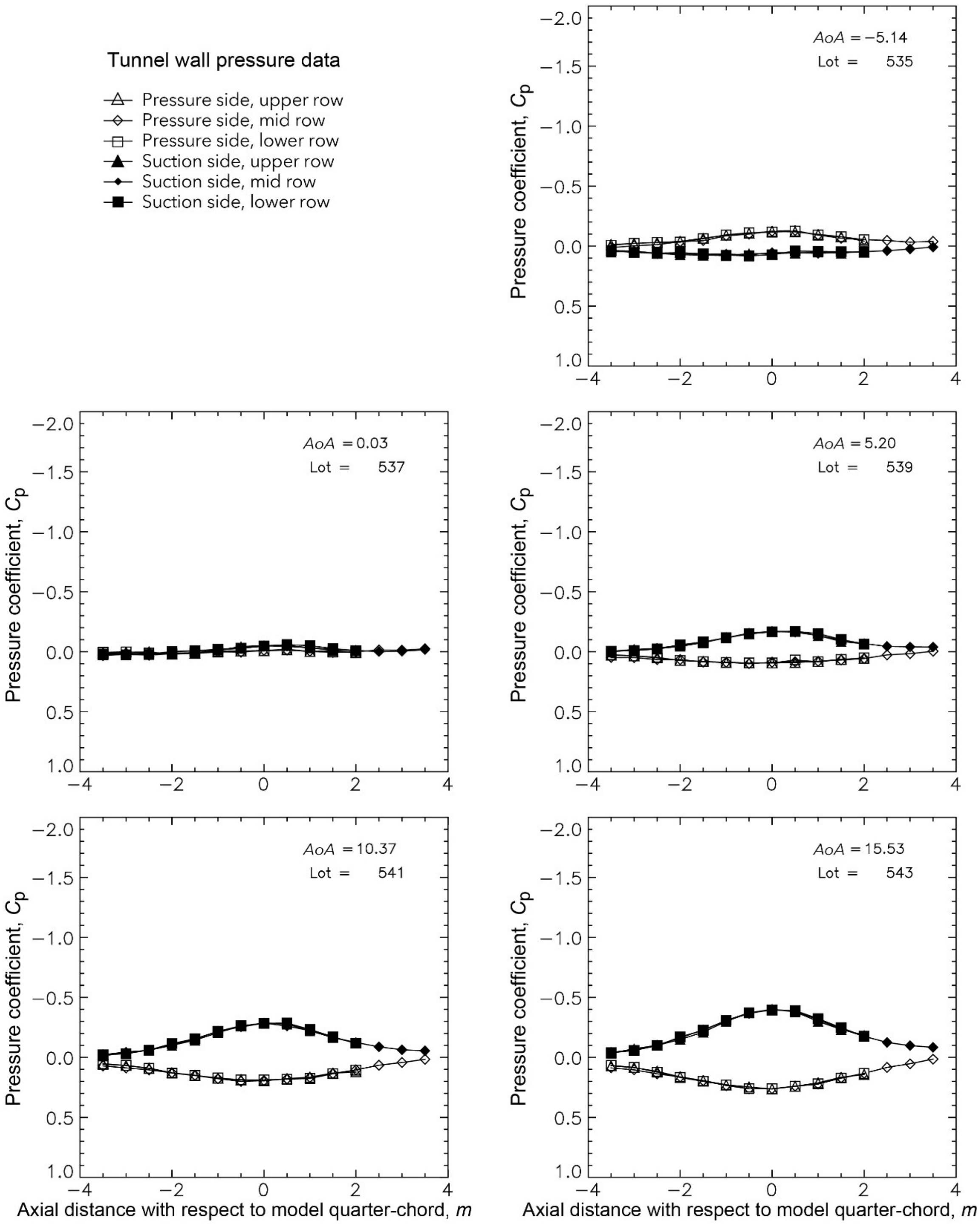

Clean Airfoil With Trip Tape: M = 0.10 and Re = 8.0×10^6

Appendix G.—F1 Full-Scale Model Tests

Clean Airfoil With Trip Tape: M = 0.10 and Re = 8.0×10^6

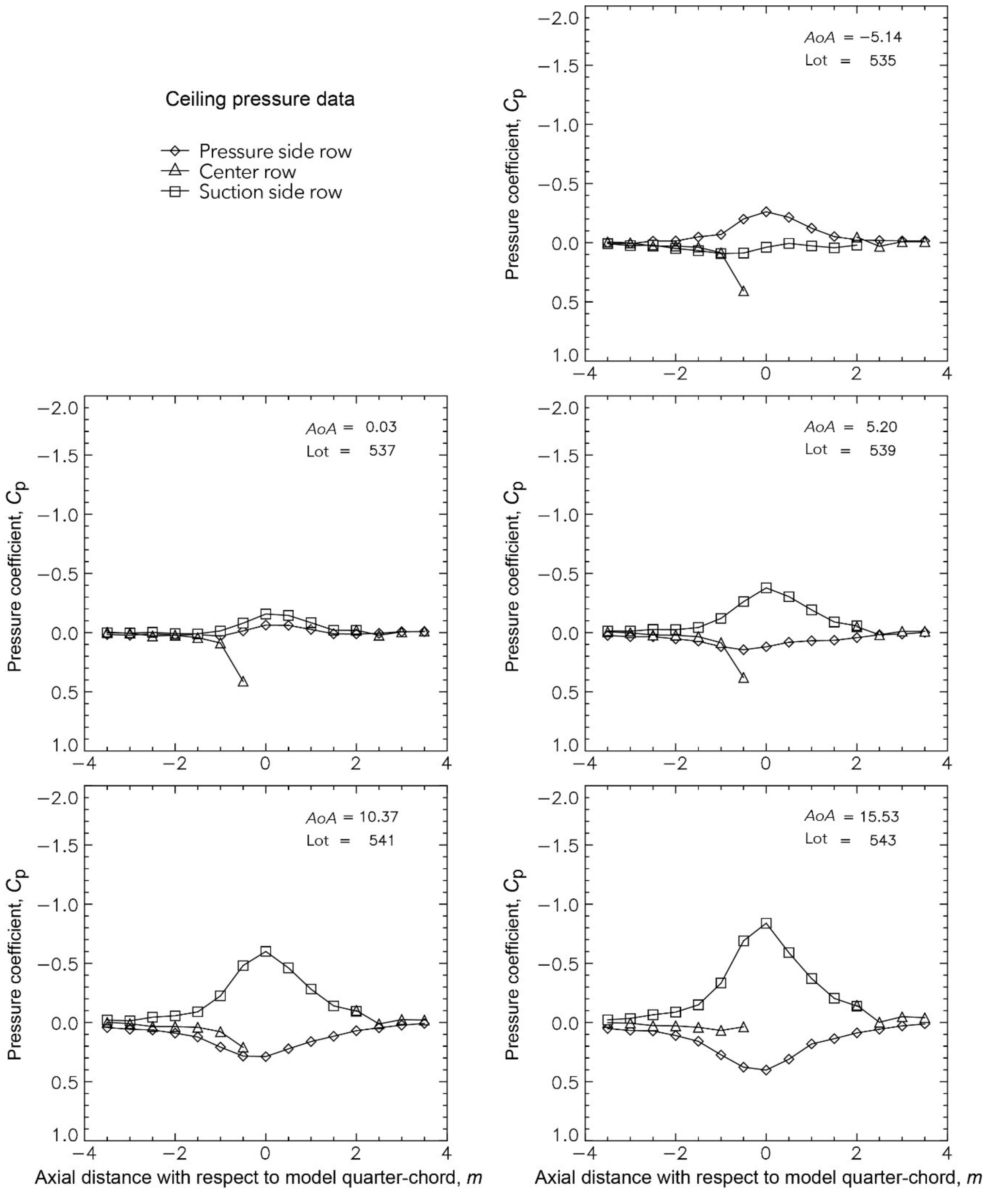

Clean Airfoil With Trip Tape: M = 0.10 and Re = 8.0×10^6

Appendix G.—F1 Full-Scale Model Tests

Clean Airfoil With Trip Tape: M = 0.10 and Re = 8.0×10^6

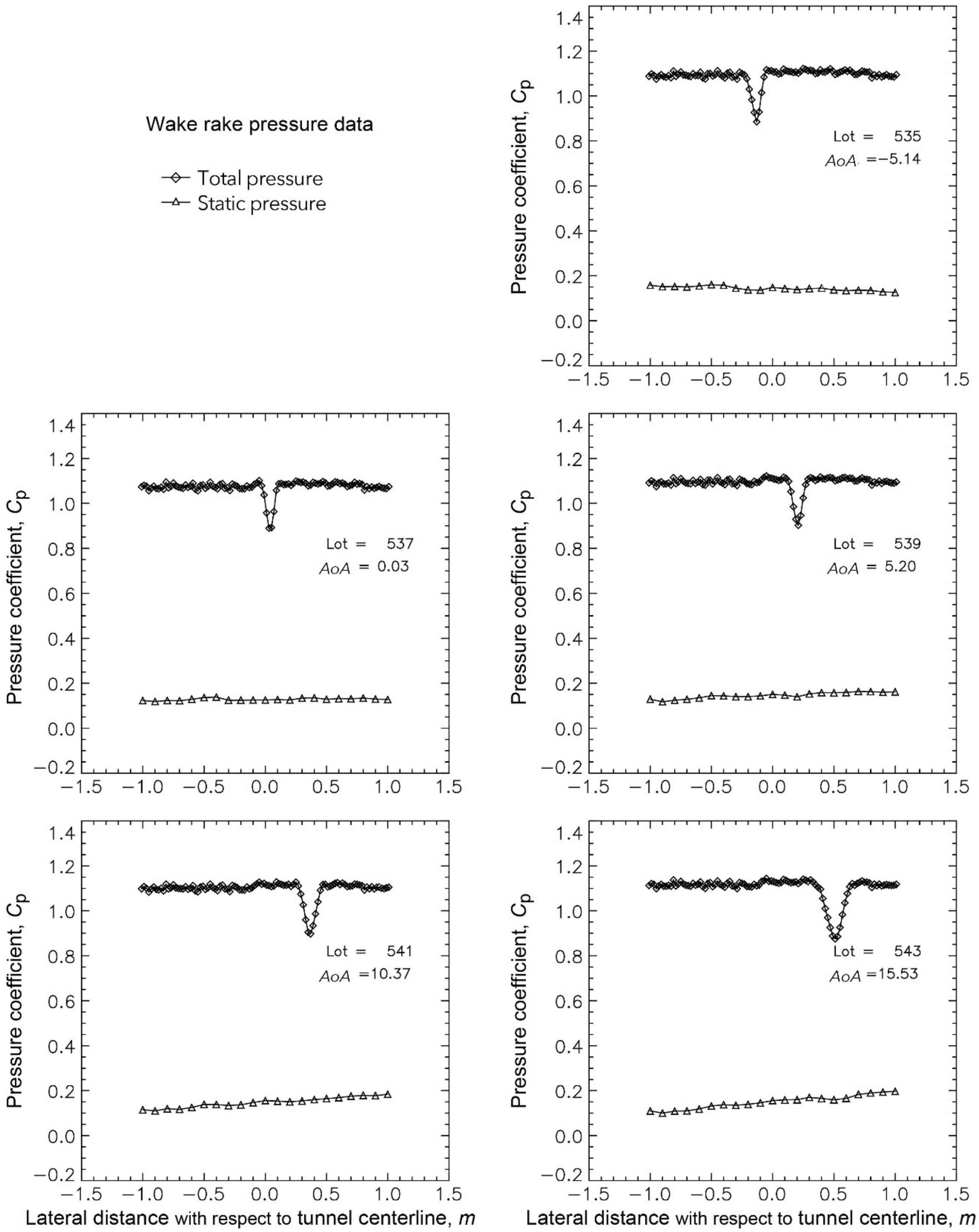

Clean Airfoil With Trip Tape: M = 0.10 and Re = 8.0×10^6

Appendix G.—F1 Full-Scale Model Tests

Clean Airfoil With Trip Tape: M = 0.10 and Re = 12.0–12.2×10^6

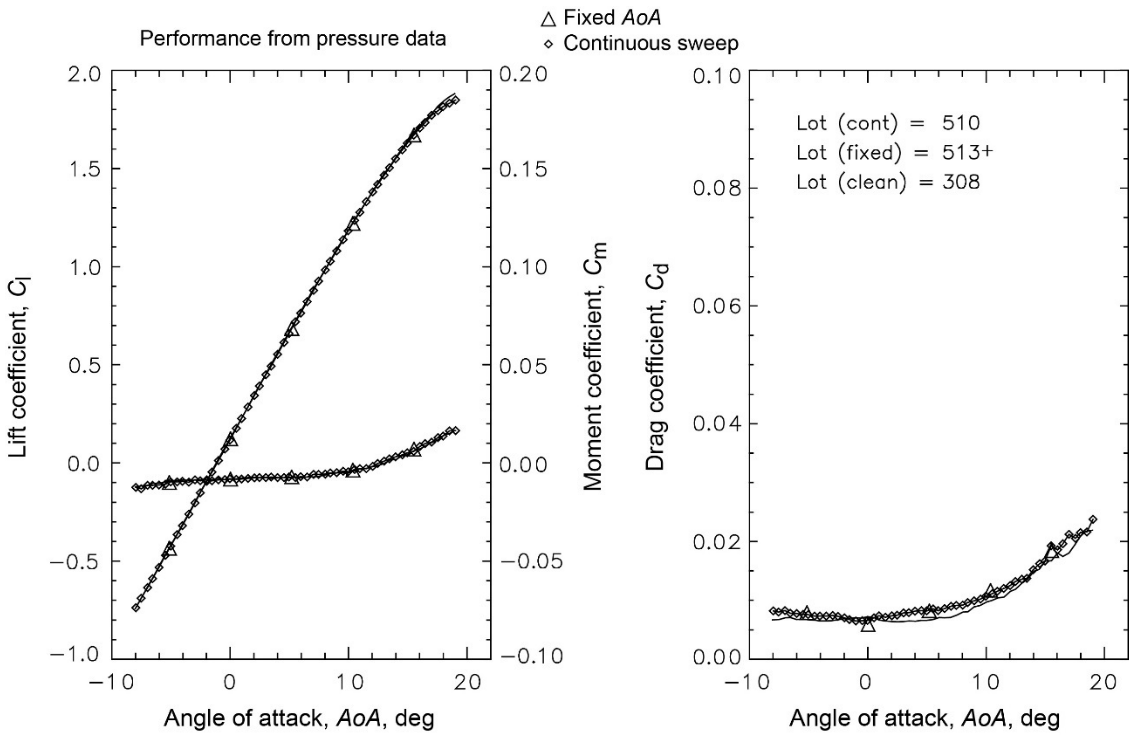

Clean Airfoil With Trip Tape: M = 0.10 and Re = 12.0–12.2×10^6

Appendix G.—F1 Full-Scale Model Tests

Clean Airfoil With Trip Tape: M = 0.10 and Re = 12.0–12.2×10^6

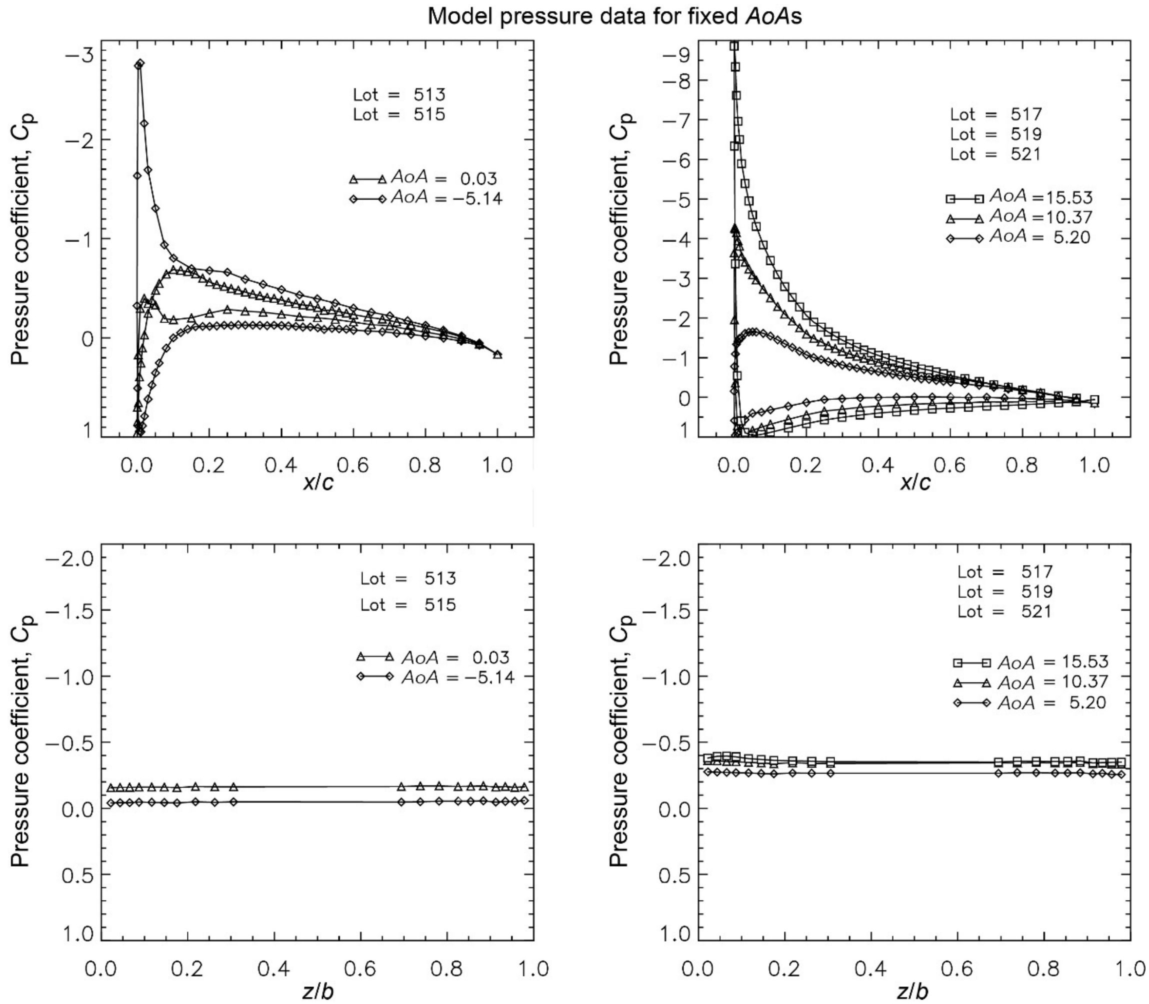

Clean Airfoil With Trip Tape: M = 0.10 and Re = 12.0–12.2×10^6

Clean Airfoil With Trip Tape: M = 0.10 and Re = 12.0–12.2×10^6

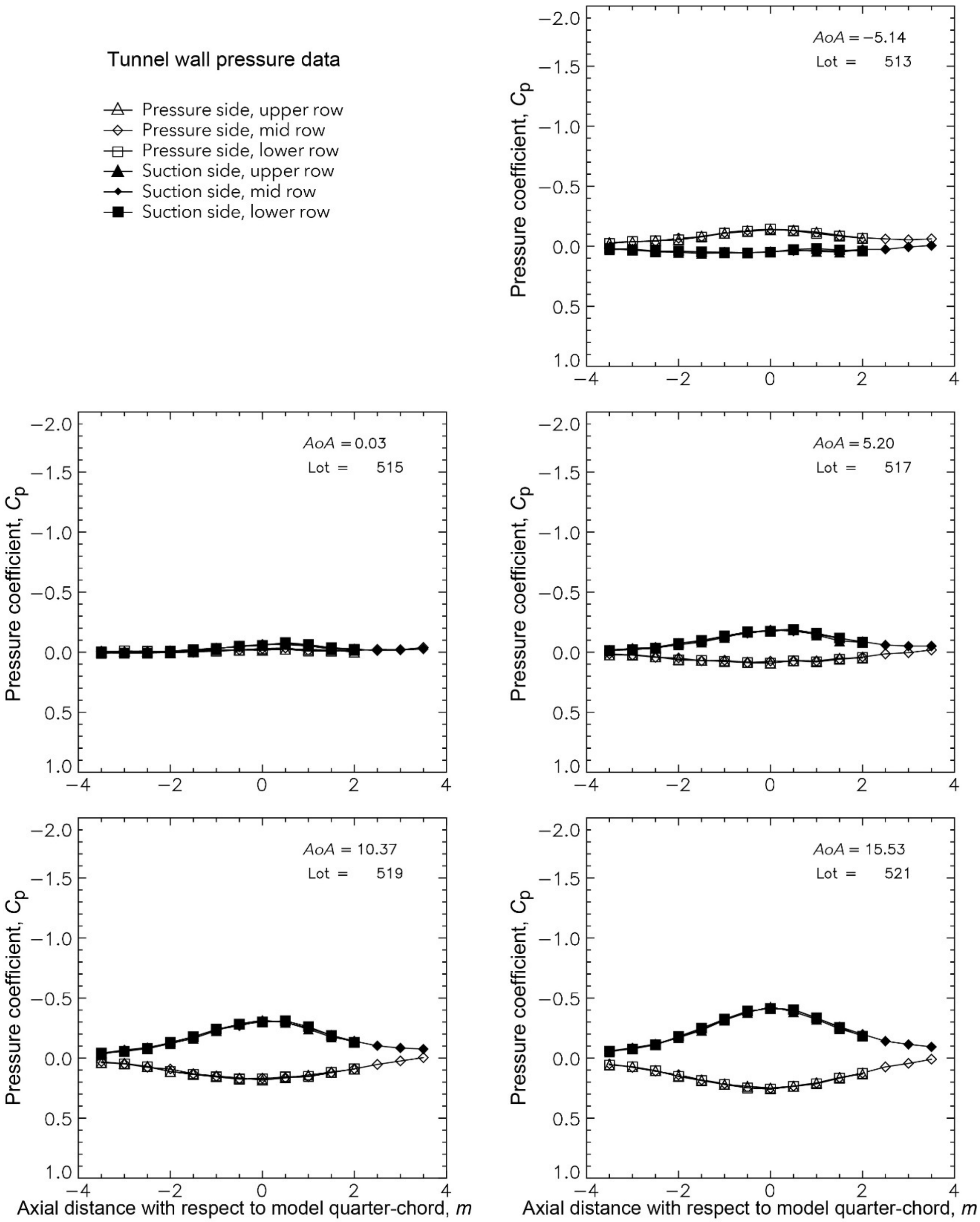

Clean Airfoil With Trip Tape: M = 0.10 and Re = 12.0–12.2×10^6

Appendix G.—F1 Full-Scale Model Tests

Clean Airfoil With Trip Tape: M = 0.10 and Re = 12.0–12.2×10^6

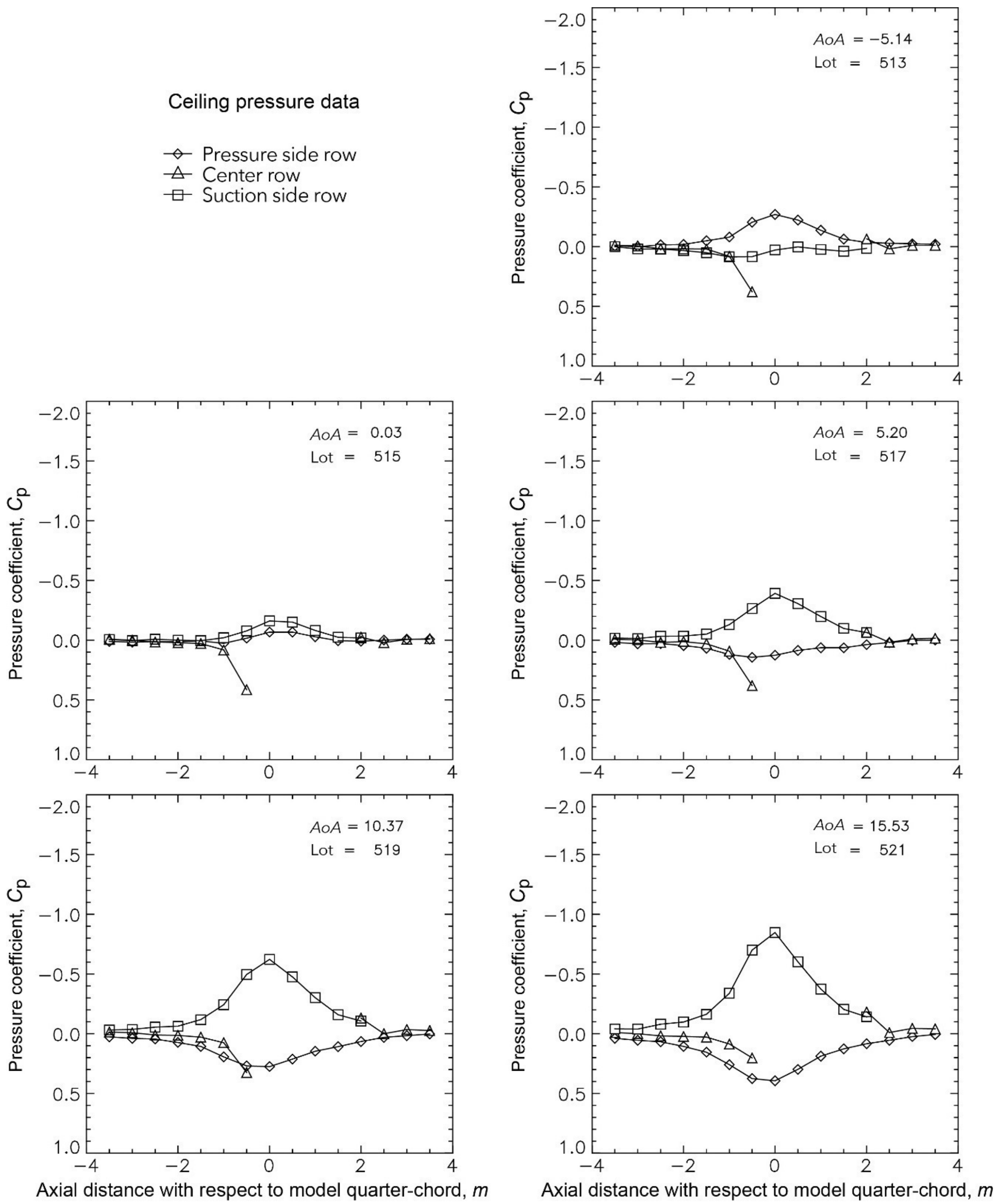

Clean Airfoil With Trip Tape: M = 0.10 and Re = 12.0–12.2×10^6

Appendix G.—F1 Full-Scale Model Tests

Clean Airfoil With Trip Tape: M = 0.10 and Re = 12.0–12.2×10^6

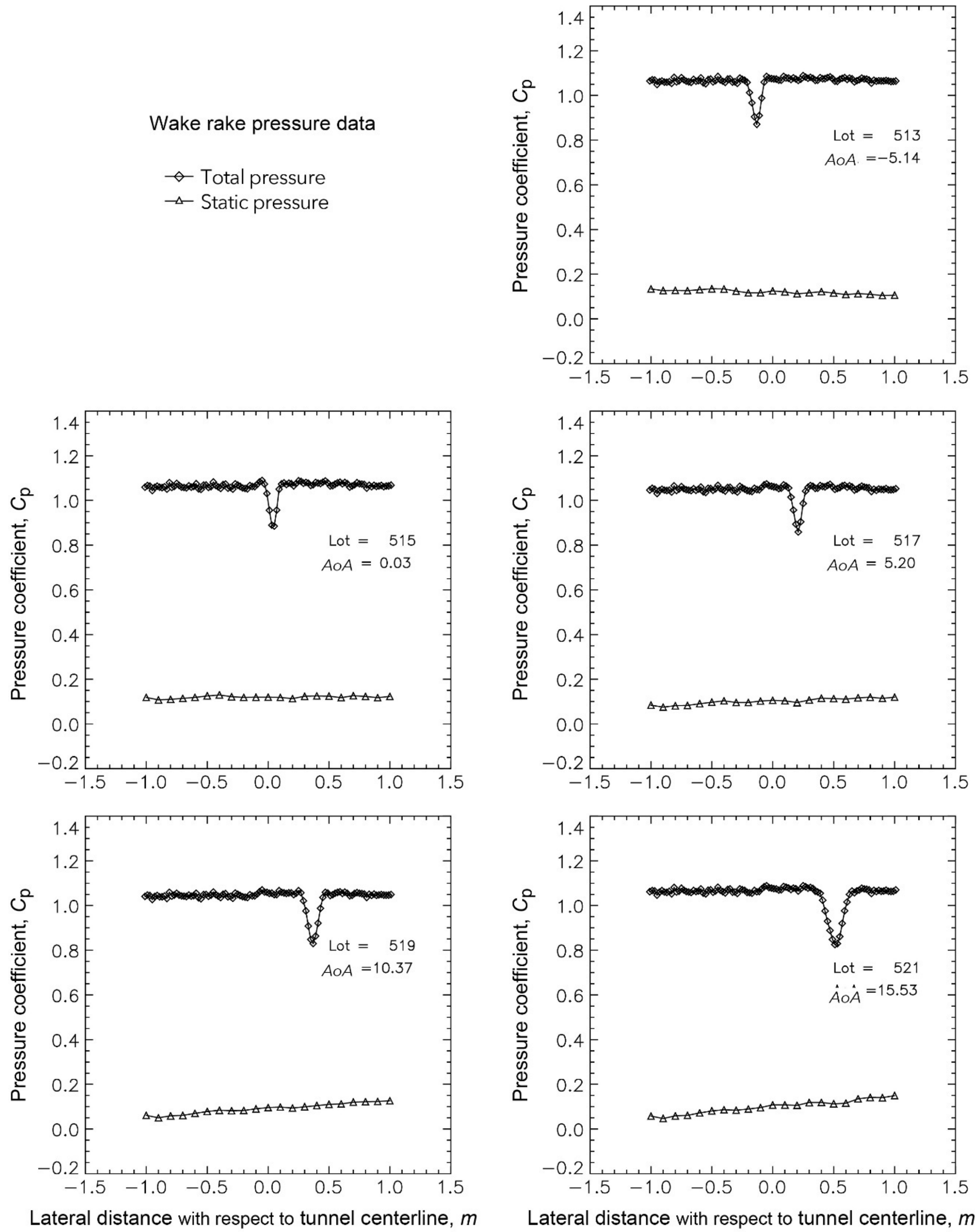

Clean Airfoil With Trip Tape: M = 0.10 and Re = 12.0–12.2×10^6

Appendix G.—F1 Full-Scale Model Tests

Clean Airfoil With Trip Tape: M = 0.20 to 0.21 and Re = 9.0–9.1×10^6

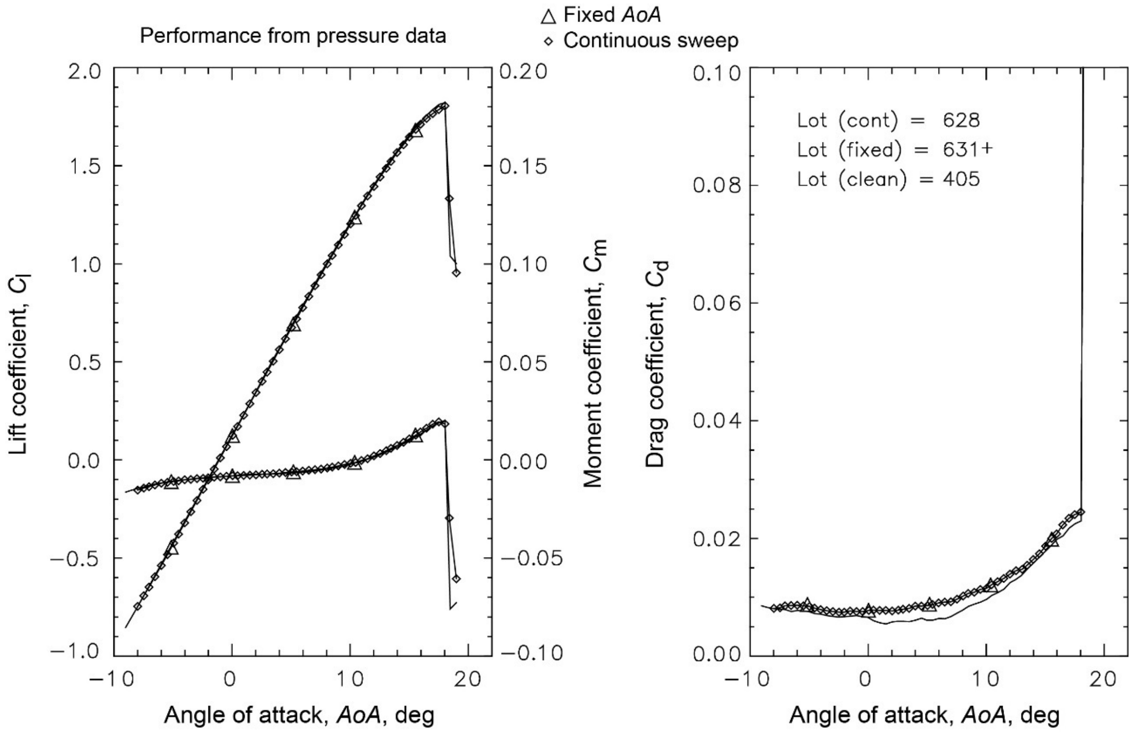

Clean Airfoil With Trip Tape: M = 0.20 to 0.21 and Re = 9.0–9.1×10^6

Appendix G.—F1 Full-Scale Model Tests

Clean Airfoil With Trip Tape: M = 0.20 to 0.21 and Re = 9.0–9.1×10^6

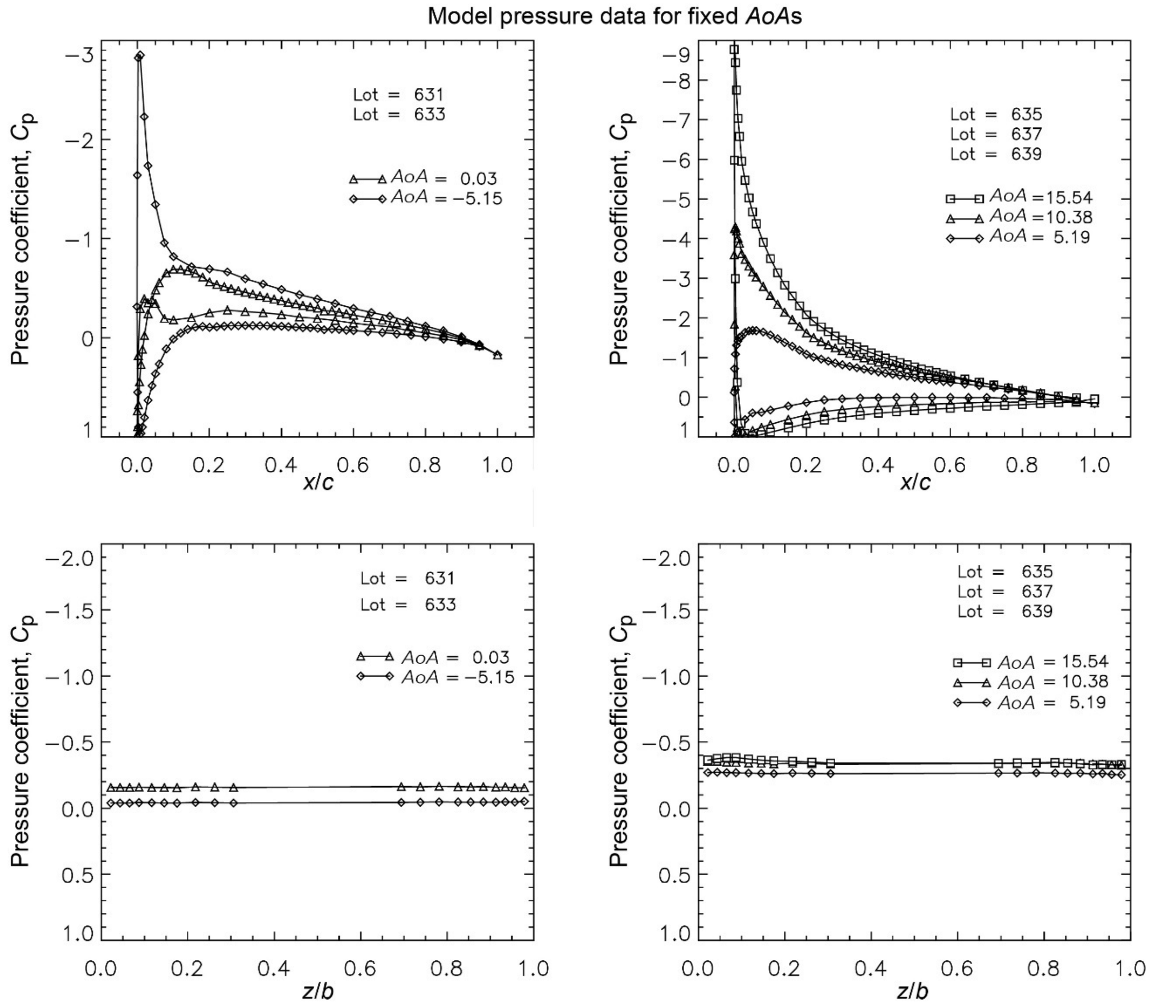

Clean Airfoil With Trip Tape: M = 0.20 to 0.21 and Re = 9.0–9.1×10^6

Appendix G.—F1 Full-Scale Model Tests

Clean Airfoil With Trip Tape: M = 0.20 to 0.21 and Re = 9.0–9.1×10^6

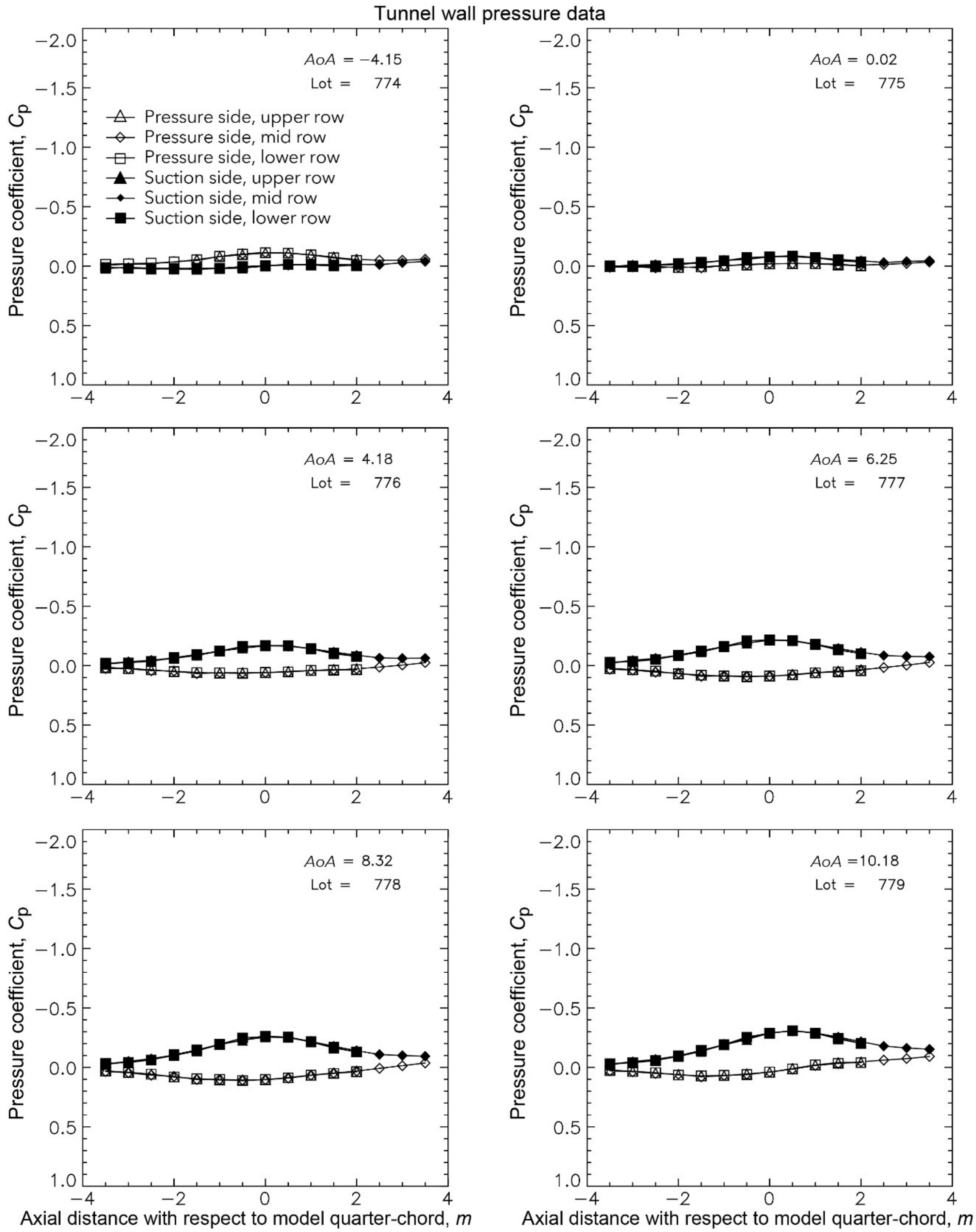

Clean Airfoil With Trip Tape: M = 0.20 to 0.21 and Re = 9.0–9.1×10^6

Appendix G.—F1 Full-Scale Model Tests

Clean Airfoil With Trip Tape: M = 0.20 to 0.21 and Re = 9.0–9.1×10^6

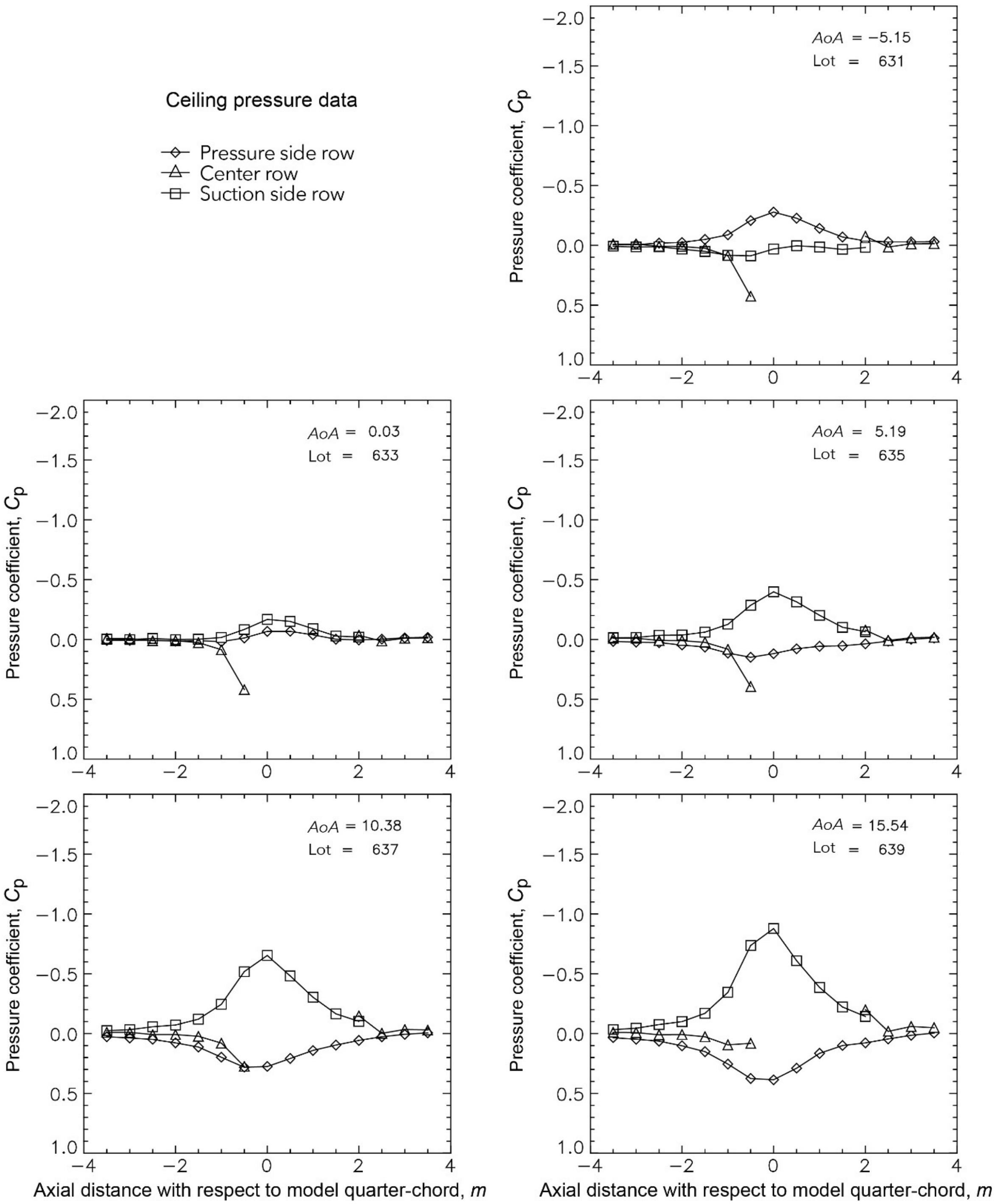

Clean Airfoil With Trip Tape: M = 0.20 to 0.21 and Re = 9.0–9.1×10^6

Appendix G.—F1 Full-Scale Model Tests

Clean Airfoil With Trip Tape: M = 0.20 to 0.21 and Re = 9.0–9.1×10^6

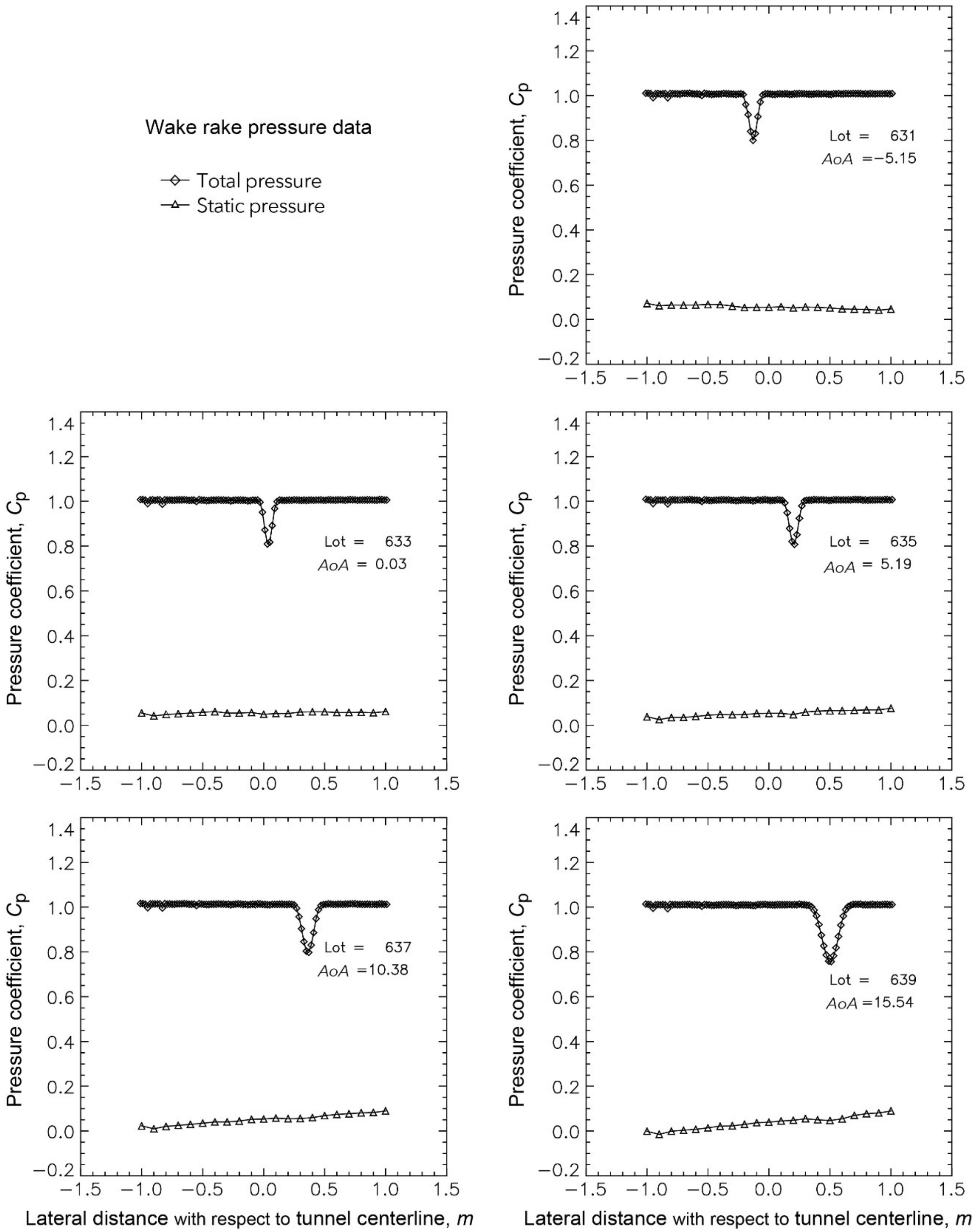

Clean Airfoil With Trip Tape: M = 0.20 to 0.21 and Re = 9.0–9.1×10^6

Appendix G.—F1 Full-Scale Model Tests

Clean Airfoil With Trip Tape: M = 0.20 to 0.21 and Re = 11.9–12.0×10^6

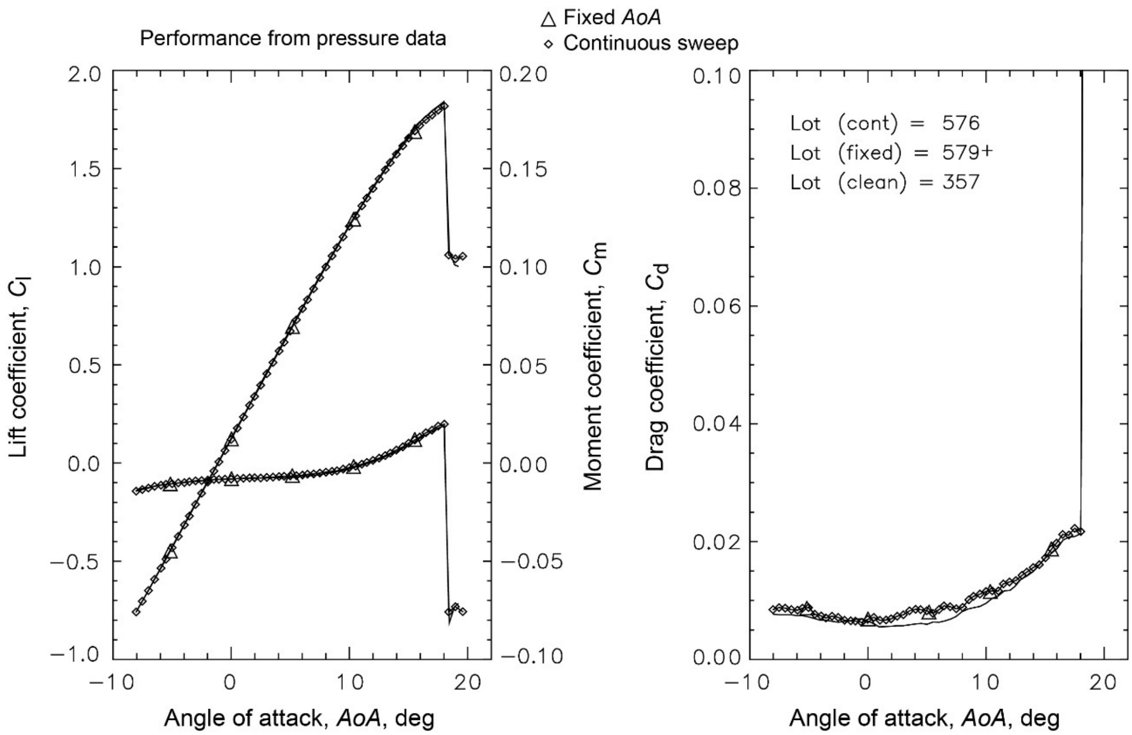

Clean Airfoil With Trip Tape: M = 0.20 to 0.21 and Re = 11.9–12.0×10^6

Appendix G.—F1 Full-Scale Model Tests

Clean Airfoil With Trip Tape: M = 0.20 to 0.21 and Re = 11.9–12.0×10^6

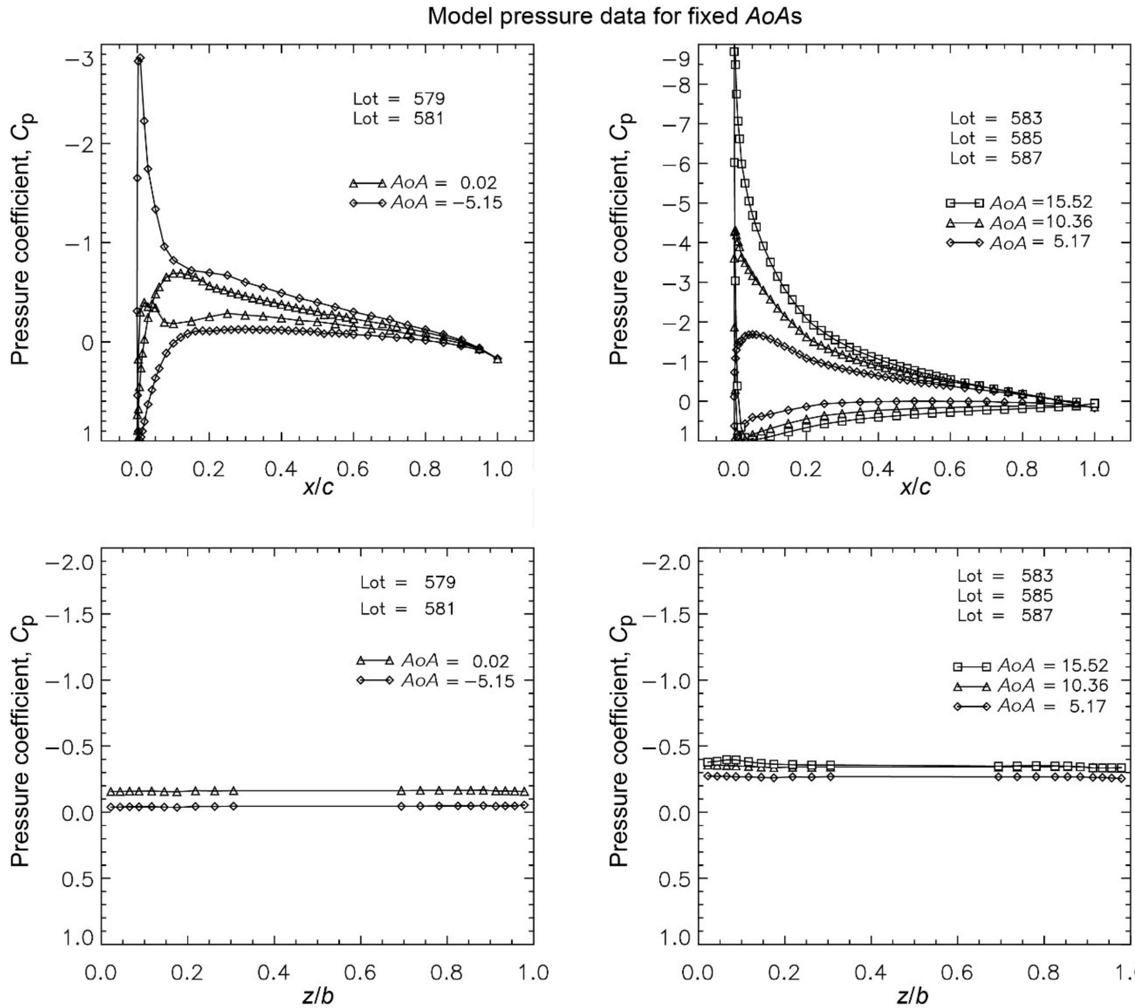

Clean Airfoil With Trip Tape: M = 0.20 to 0.21 and Re = 11.9–12.0×10^6

Appendix G.—F1 Full-Scale Model Tests

Clean Airfoil With Trip Tape: M = 0.20 to 0.21 and Re = 11.9–12.0×10^6

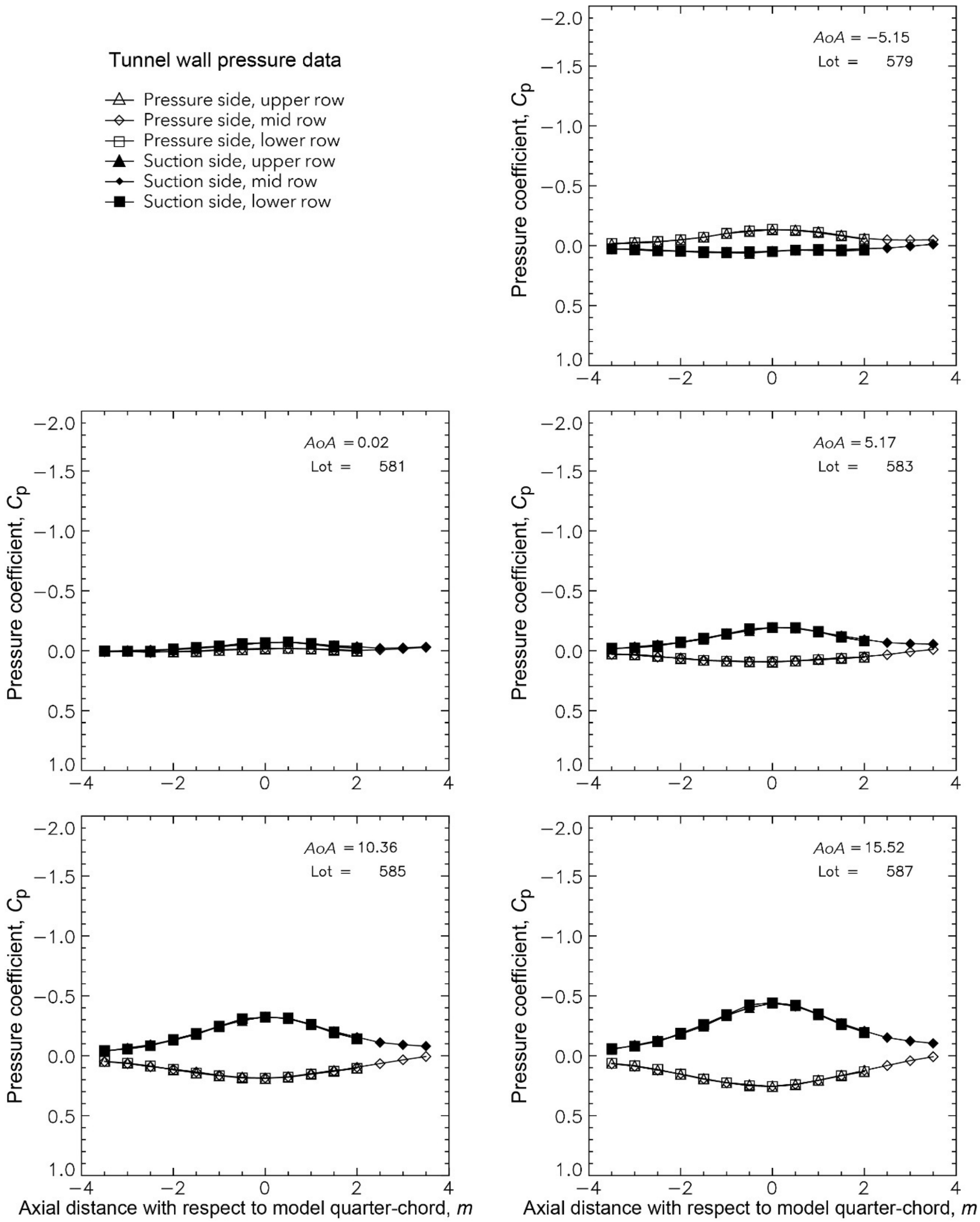

Clean Airfoil With Trip Tape: M = 0.20 to 0.21 and Re = 11.9–12.0×10^6

Appendix G.—F1 Full-Scale Model Tests

Clean Airfoil With Trip Tape: M = 0.20 to 0.21 and Re = 11.9–12.0×10^6

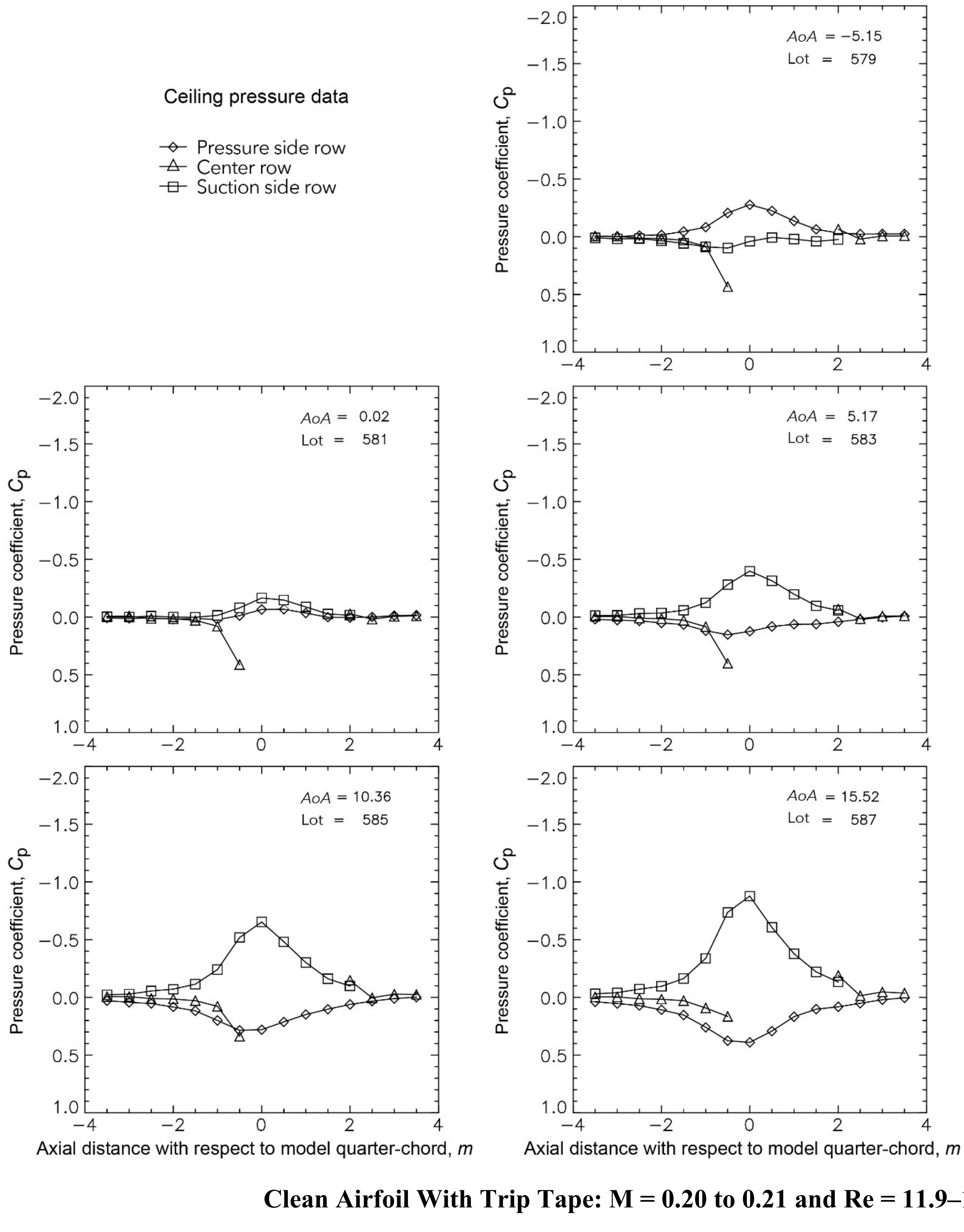

Clean Airfoil With Trip Tape: M = 0.20 to 0.21 and Re = 11.9–12.0×10^6

Appendix G.—F1 Full-Scale Model Tests

Clean Airfoil With Trip Tape: M = 0.20 to 0.21 and Re = 11.9–12.0×10^6

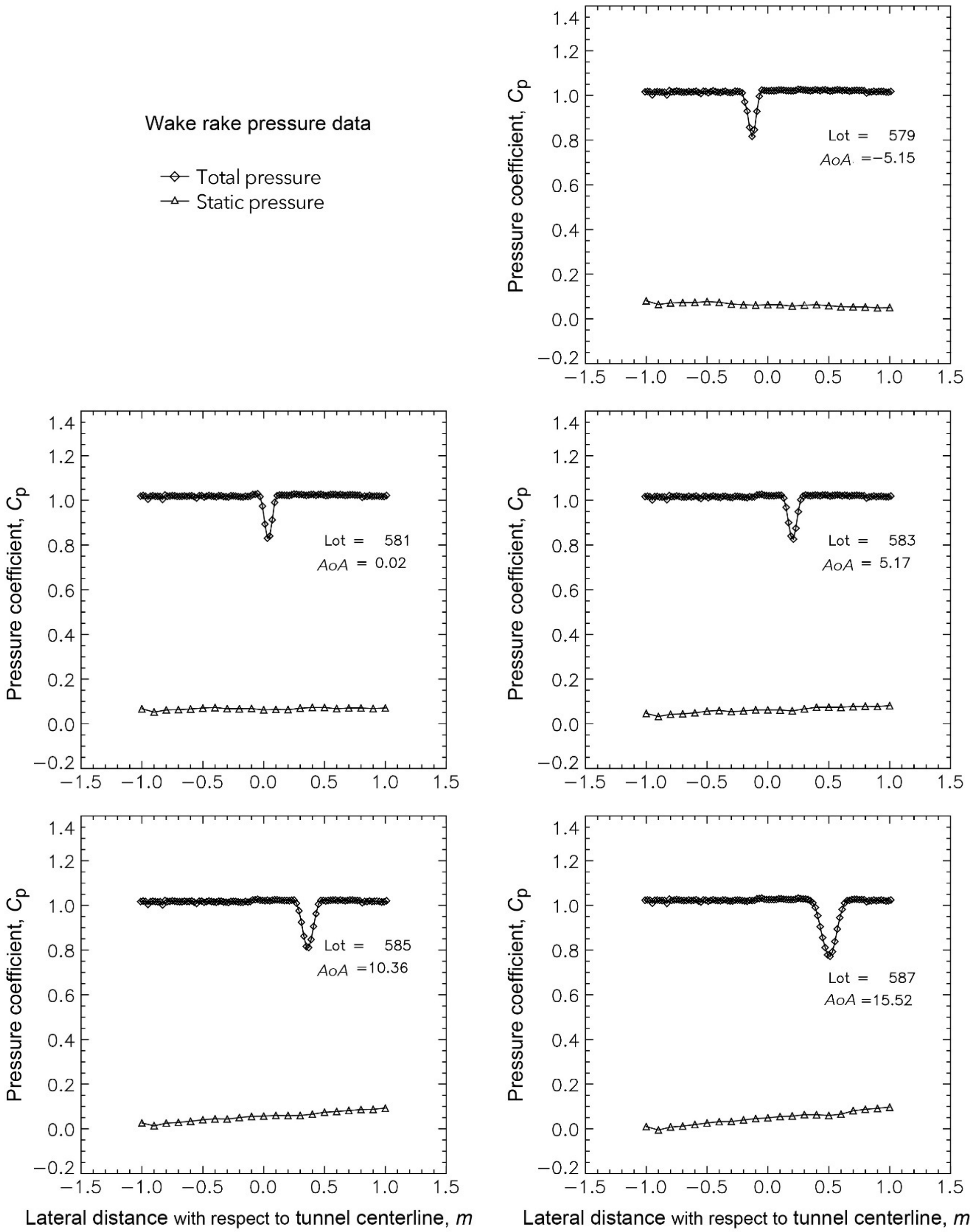

Clean Airfoil With Trip Tape: M = 0.20 to 0.21 and Re = 11.9–12.0×10^6

Appendix G.—F1 Full-Scale Model Tests

Clean Airfoil With Trip Tape: M = 0.20 to 0.21 and Re = 15.9–16.0×10^6

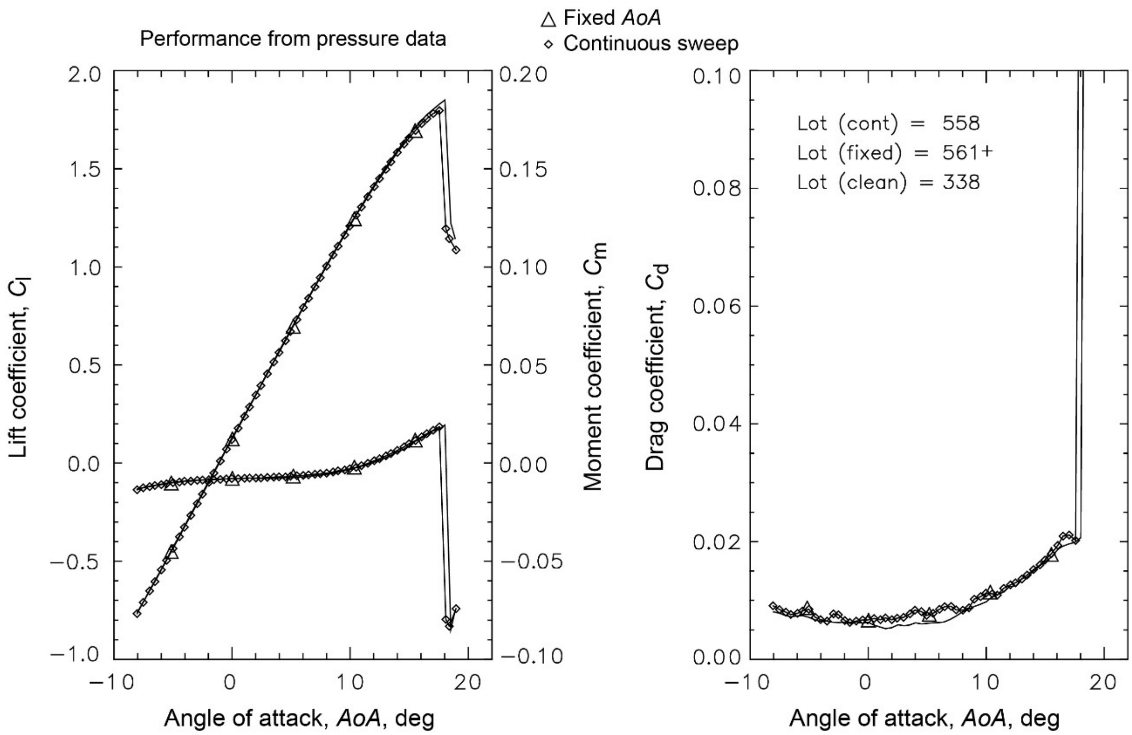

Clean Airfoil With Trip Tape: M = 0.20 to 0.21 and Re = 15.9–16.0×10^6

Appendix G.—F1 Full-Scale Model Tests

Clean Airfoil With Trip Tape: M = 0.20 to 0.21 and Re = 15.9–16.0×10⁶

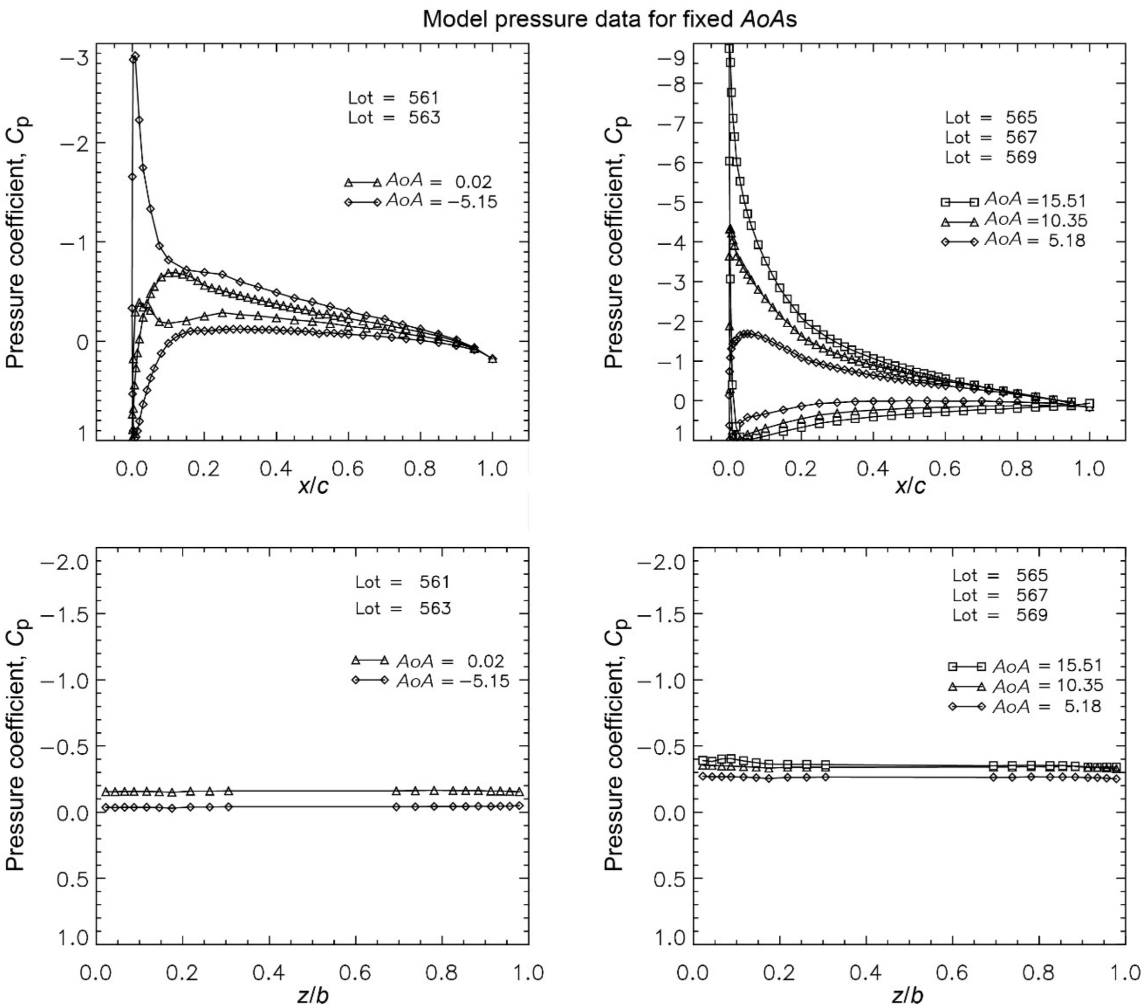

Clean Airfoil With Trip Tape: M = 0.20 to 0.21 and Re = 15.9–16.0×10⁶

Appendix G.—F1 Full-Scale Model Tests

Clean Airfoil With Trip Tape: M = 0.20 to 0.21 and Re = 15.9–16.0×10^6

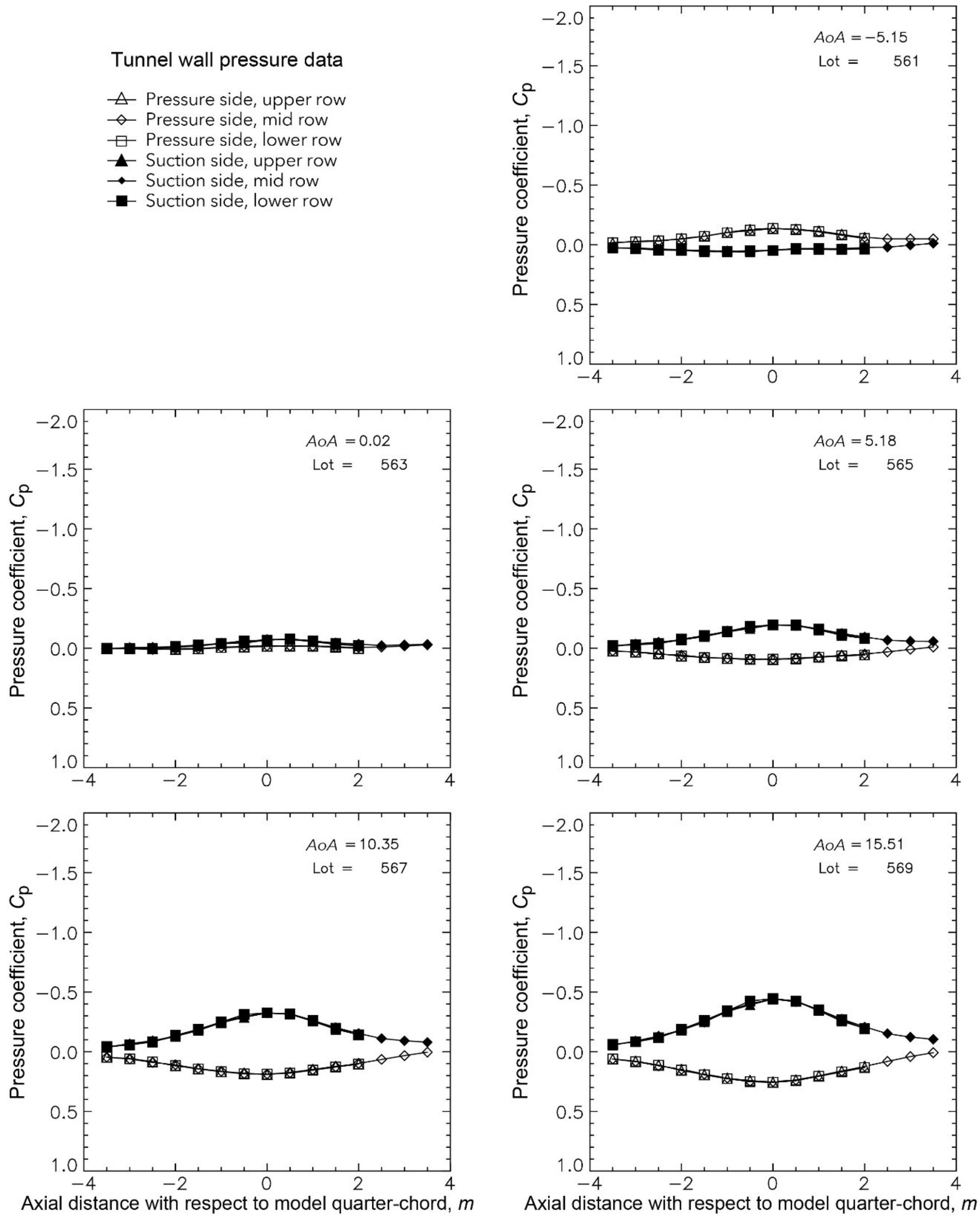

Clean Airfoil With Trip Tape: M = 0.20 to 0.21 and Re = 15.9–16.0×10^6

Appendix G.—F1 Full-Scale Model Tests

Clean Airfoil With Trip Tape: M = 0.20 to 0.21 and Re = 15.9–16.0×10^6

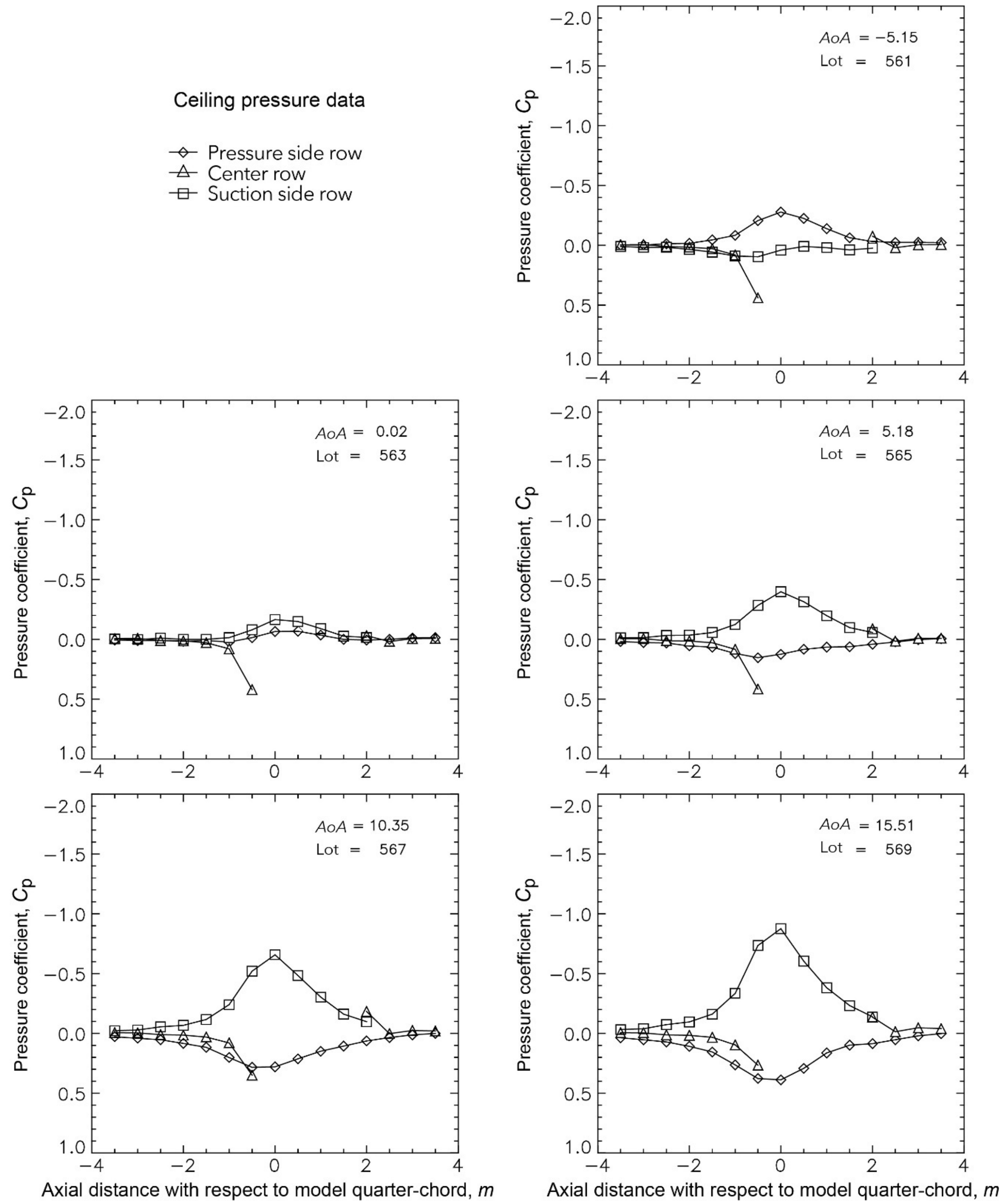

Clean Airfoil With Trip Tape: M = 0.20 to 0.21 and Re = 15.9–16.0×10^6

Appendix G.—F1 Full-Scale Model Tests

Clean Airfoil With Trip Tape: M = 0.20 to 0.21 and Re = 15.9–16.0×10^6

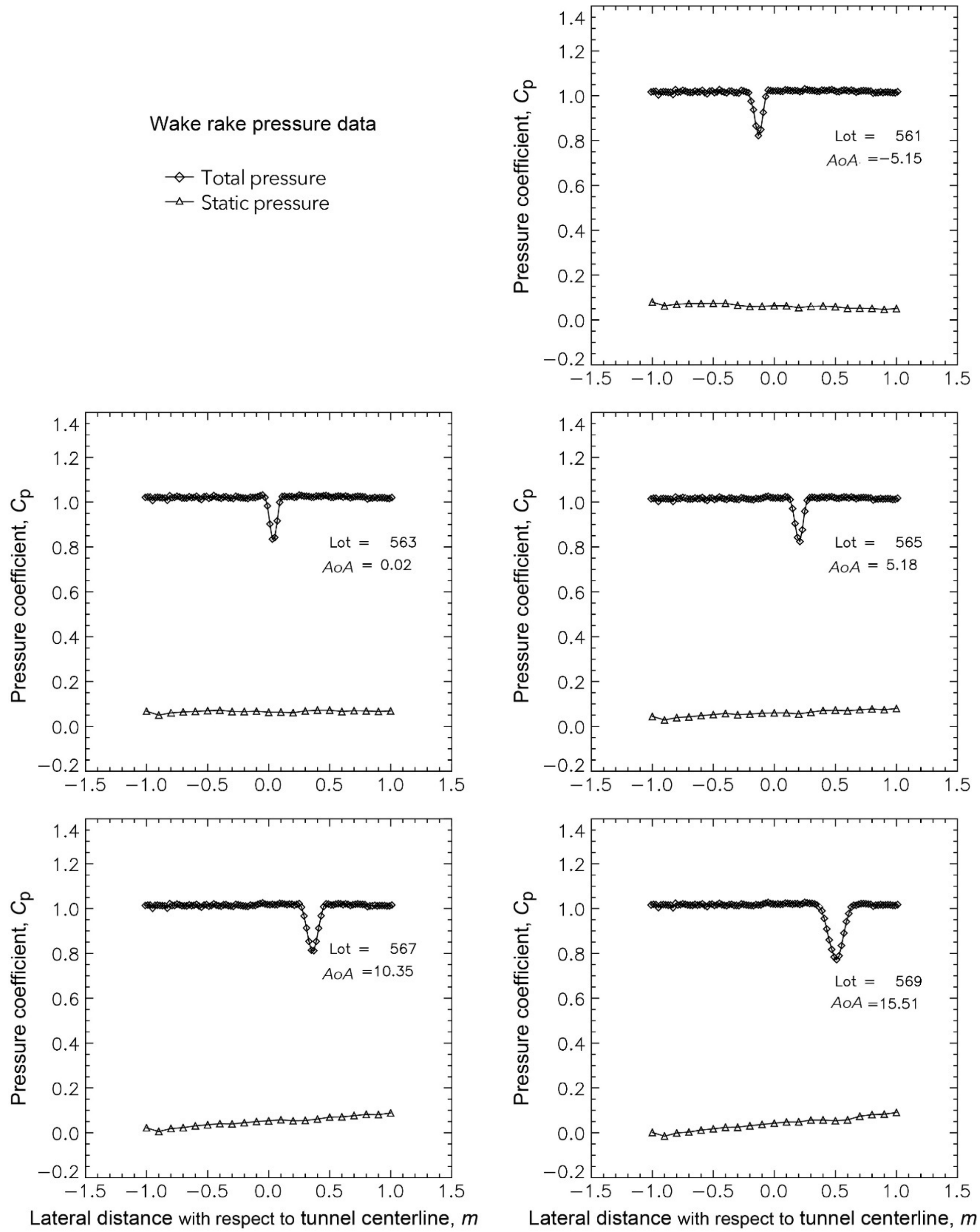

Clean Airfoil With Trip Tape: M = 0.20 to 0.21 and Re = 15.9–16.0×10^6

Appendix G.—F1 Full-Scale Model Tests

Clean Airfoil With Trip Tape: M = 0.29 and Re = 12.2 to 12.3×10^6

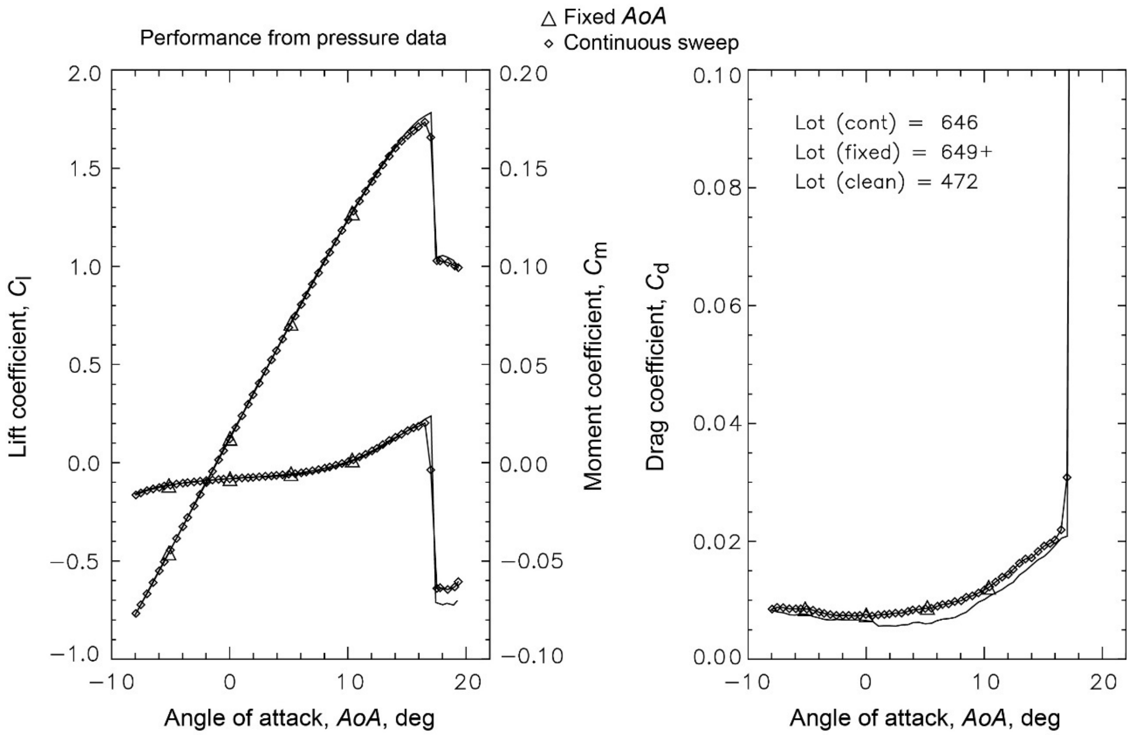

Clean Airfoil With Trip Tape: M = 0.29 and Re = 12.2–12.3×10^6

Appendix G.—F1 Full-Scale Model Tests

Clean Airfoil With Trip Tape: M = 0.29 and Re = 12.2–12.3×10⁶

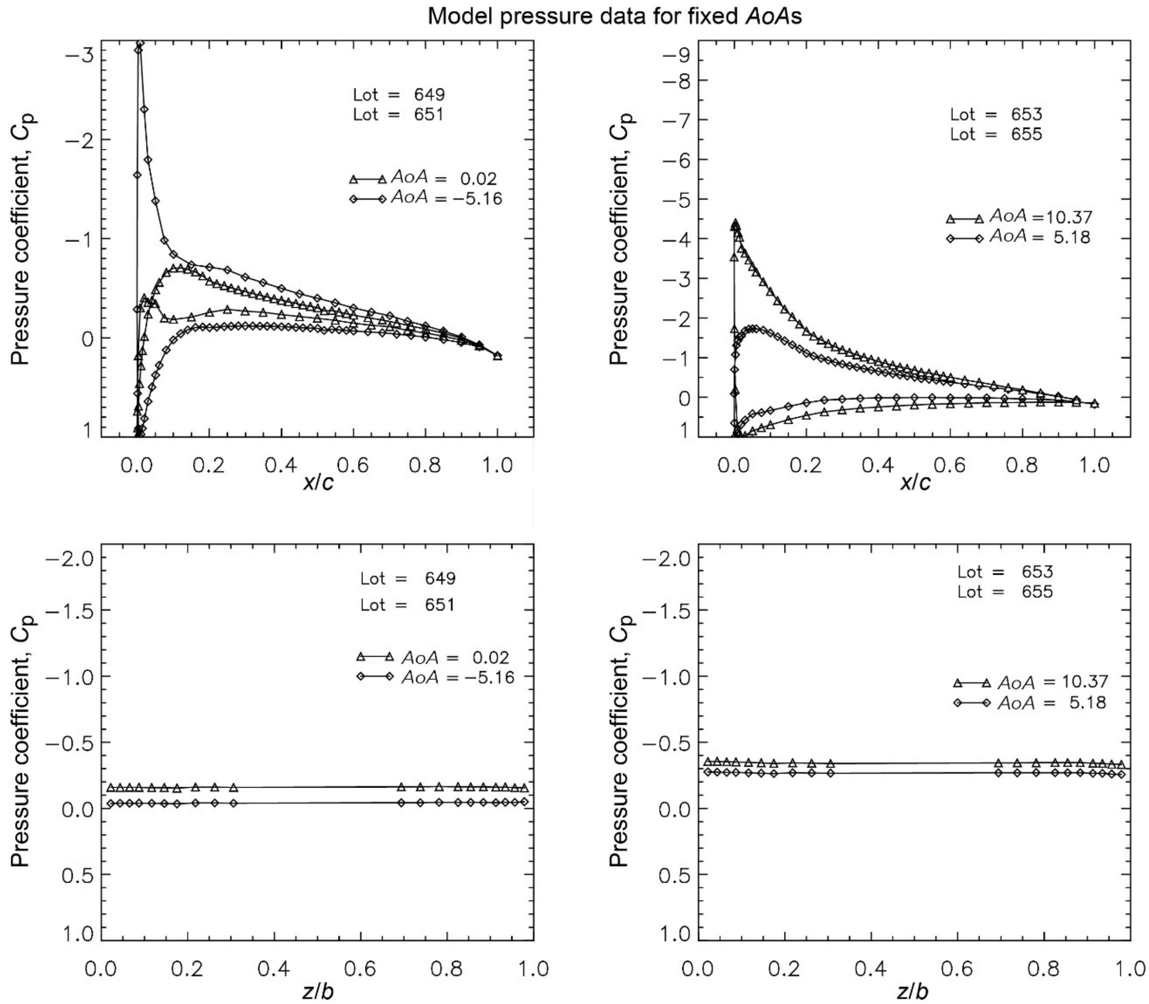

Clean Airfoil With Trip Tape: M = 0.29 and Re = 12.2–12.3×10⁶

Appendix G.—F1 Full-Scale Model Tests

Clean Airfoil With Trip Tape: M = 0.29 and Re = 12.2–12.3×10^6

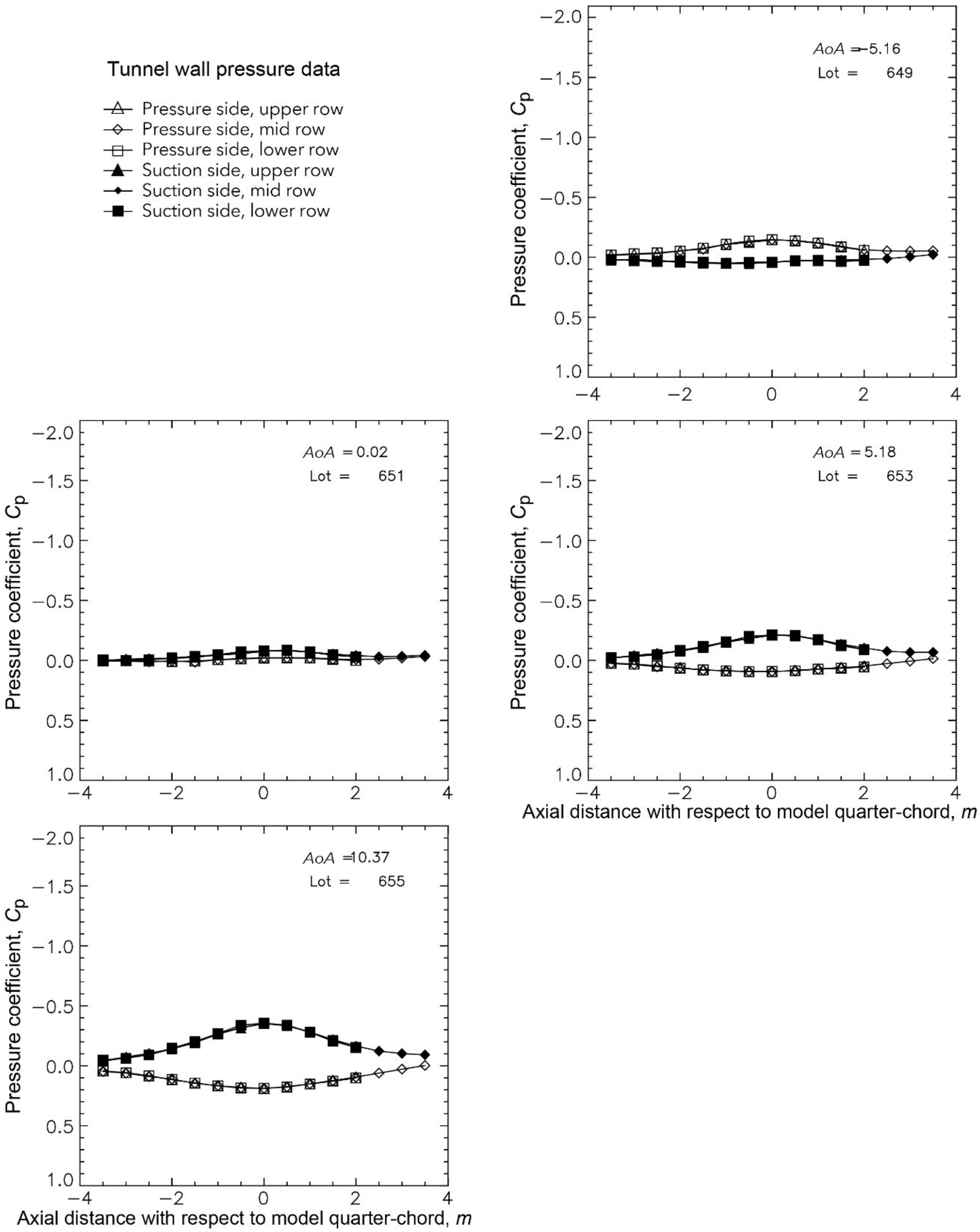

Clean Airfoil With Trip Tape: M = 0.29 and Re = 12.2–12.3×10^6

Appendix G.—F1 Full-Scale Model Tests

Clean Airfoil With Trip Tape: M = 0.29 and Re = 12.2–12.3×10^6

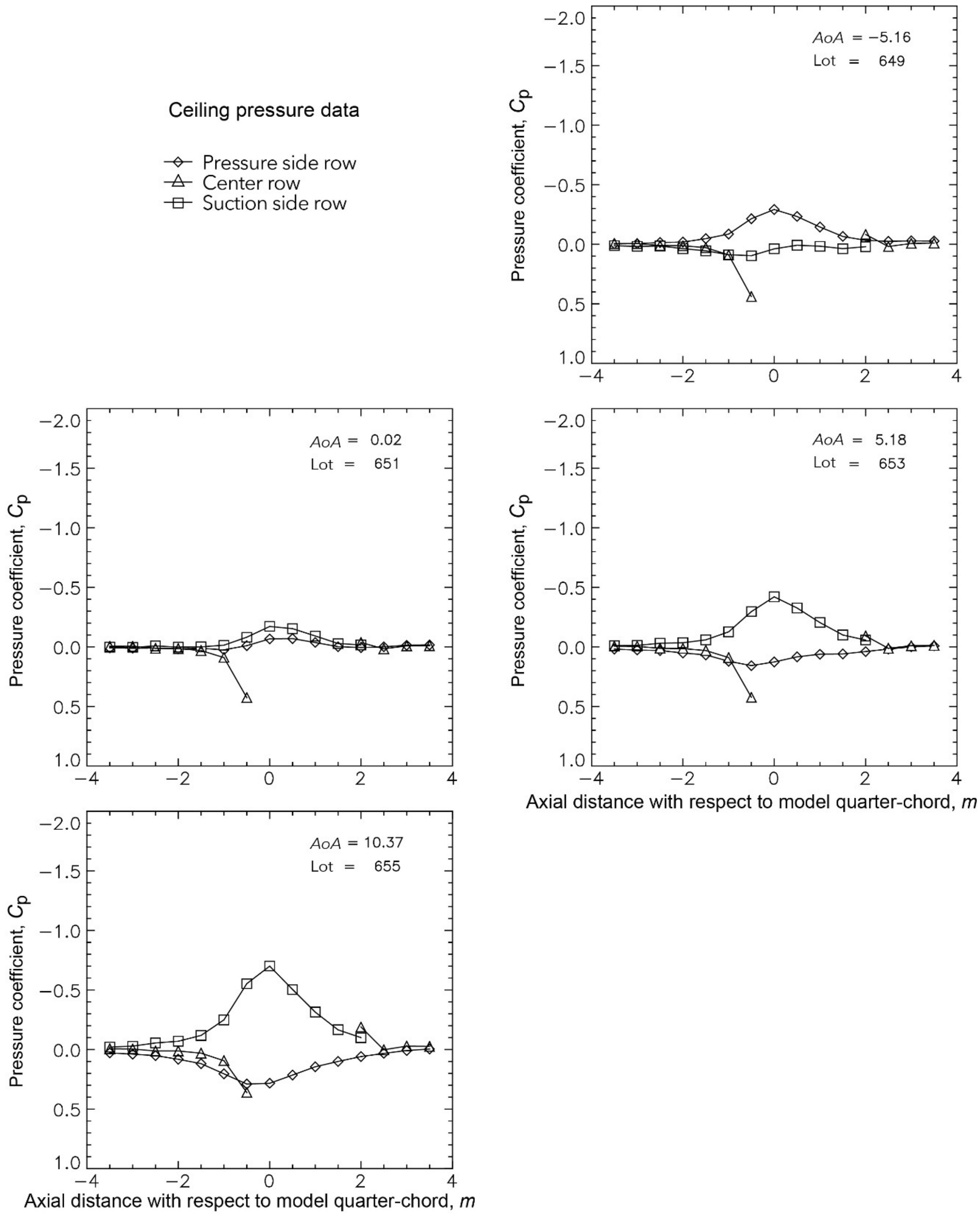

Clean Airfoil With Trip Tape: M = 0.29 and Re = 12.2–12.3×10^6

Appendix G.—F1 Full-Scale Model Tests

Clean Airfoil With Trip Tape: M = 0.29 and Re = 12.2–12.3×10^6

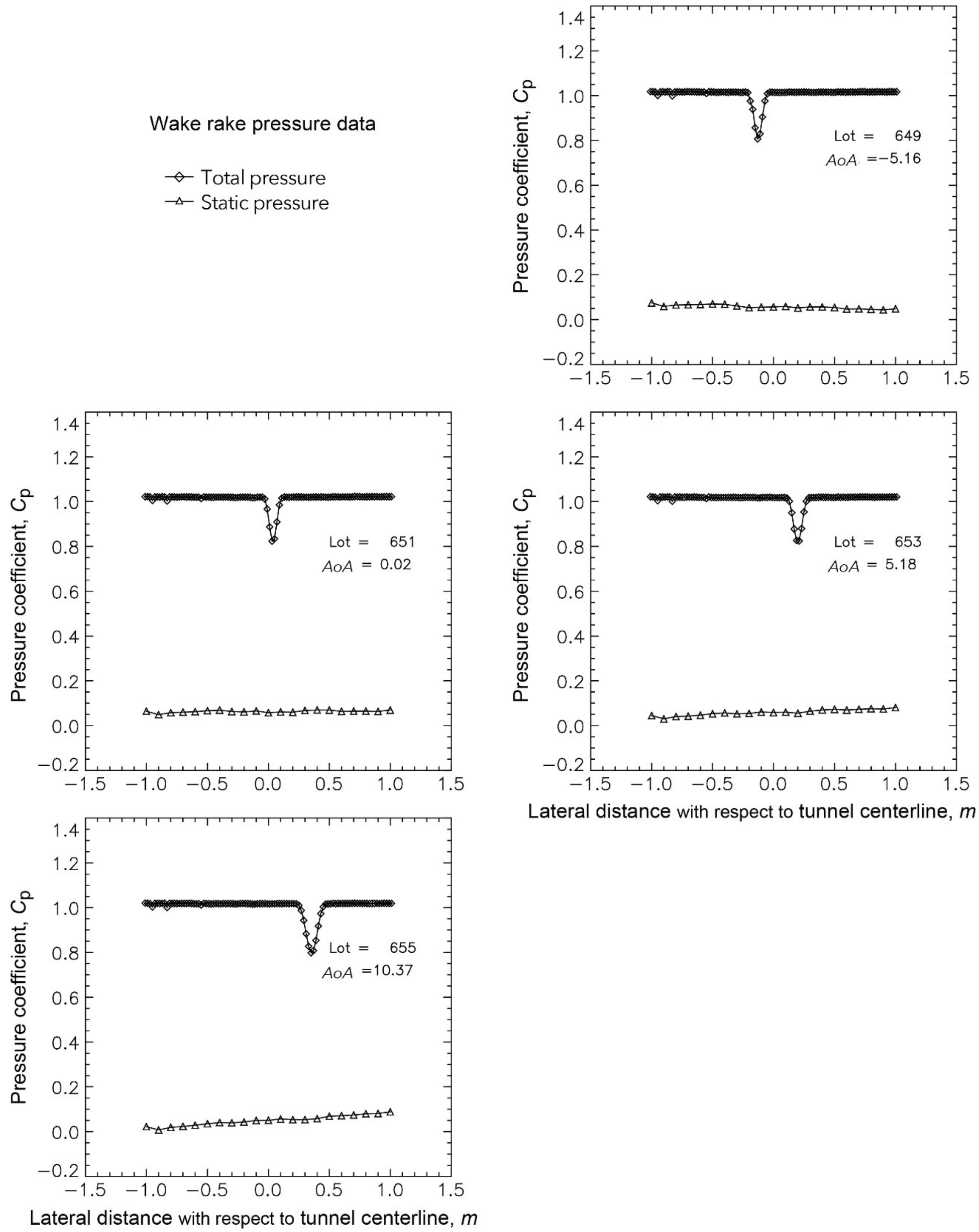

Clean Airfoil With Trip Tape: M = 0.29 and Re = 12.2–12.3×10^6

Appendix G.—F1 Full-Scale Model Tests

Horn Ice—Lot EG1164: M = 0.10 and Re = 4.5×10^6

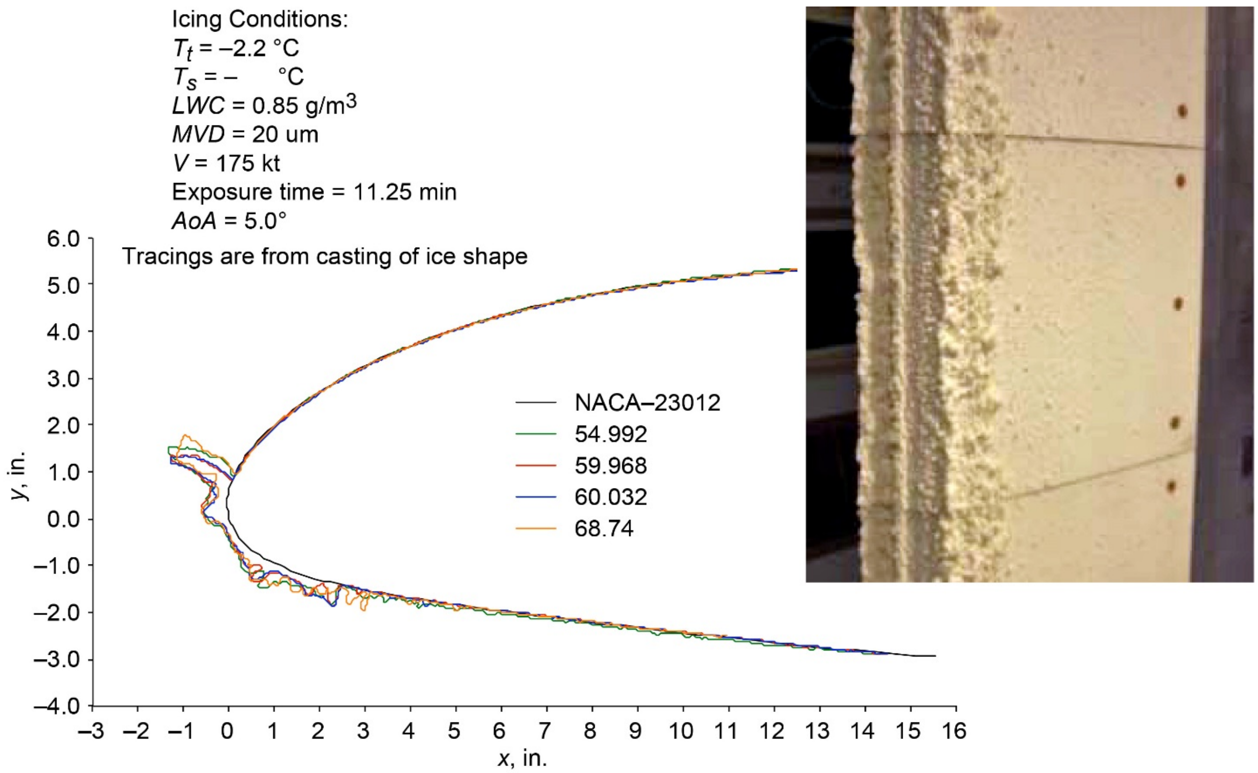

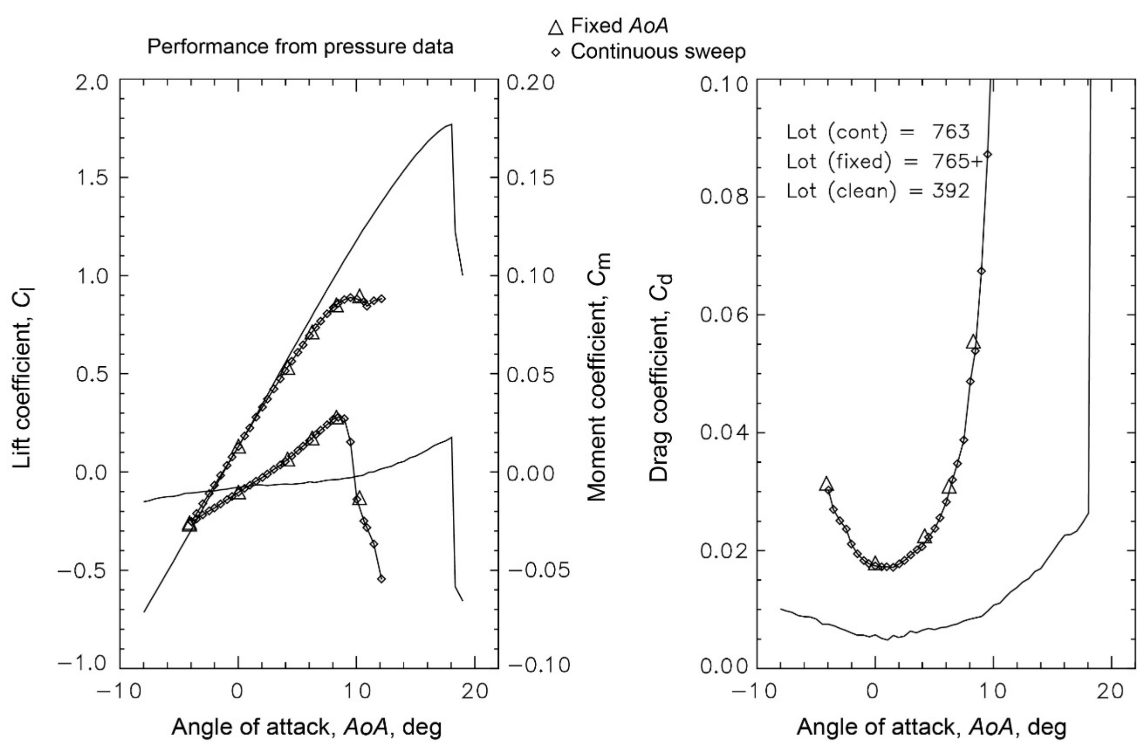

Horn Ice—Lot EG1164: M = 0.10 and Re = 4.5×10^6

Appendix G.—F1 Full-Scale Model Tests

Horn Ice—Lot EG1164: M = 0.10 and Re = 4.5×10^6

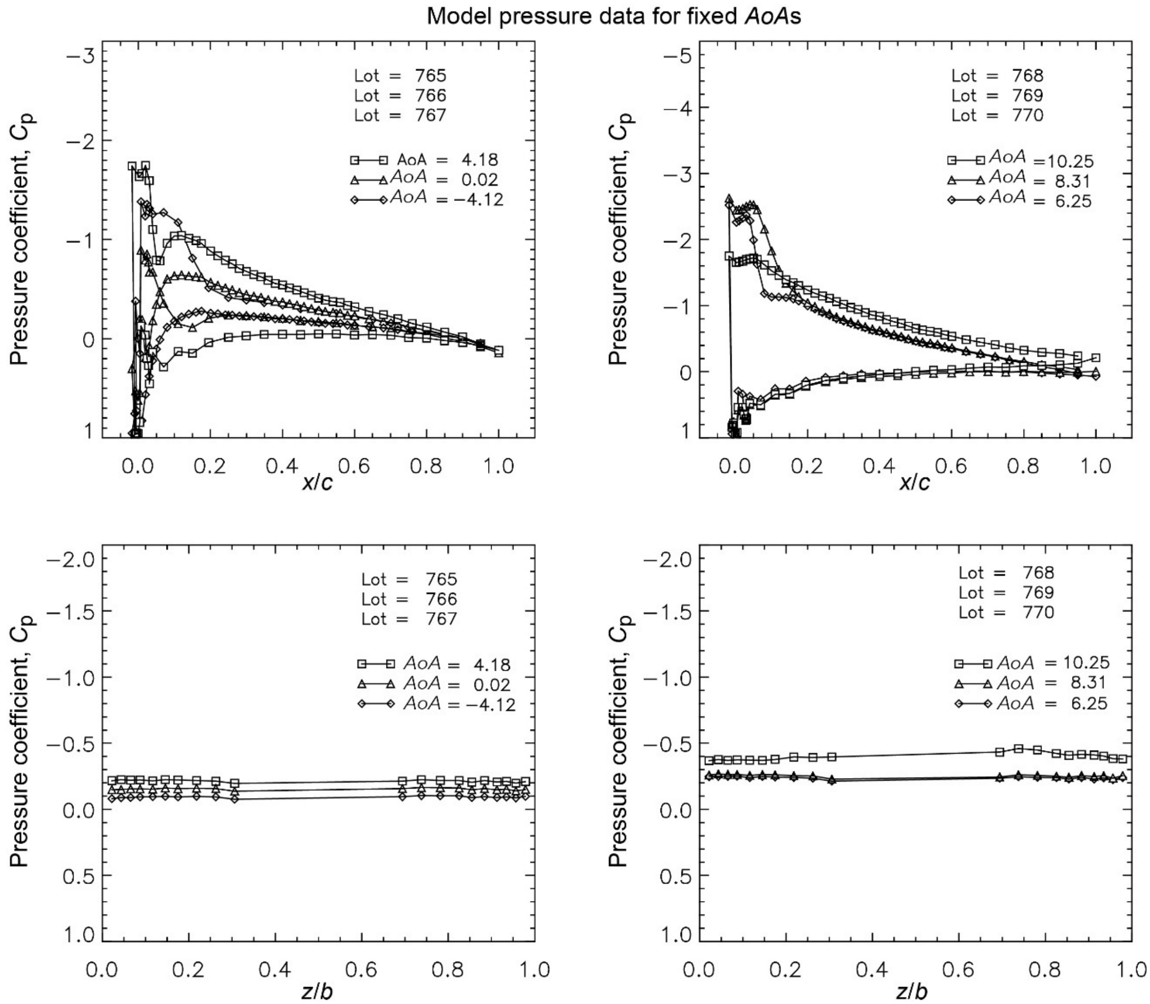

Horn Ice—Lot EG1164: M = 0.10 and Re = 4.5×10^6

Appendix G.—F1 Full-Scale Model Tests

Horn Ice—Lot EG1164: M = 0.10 and Re = 4.5×10^6

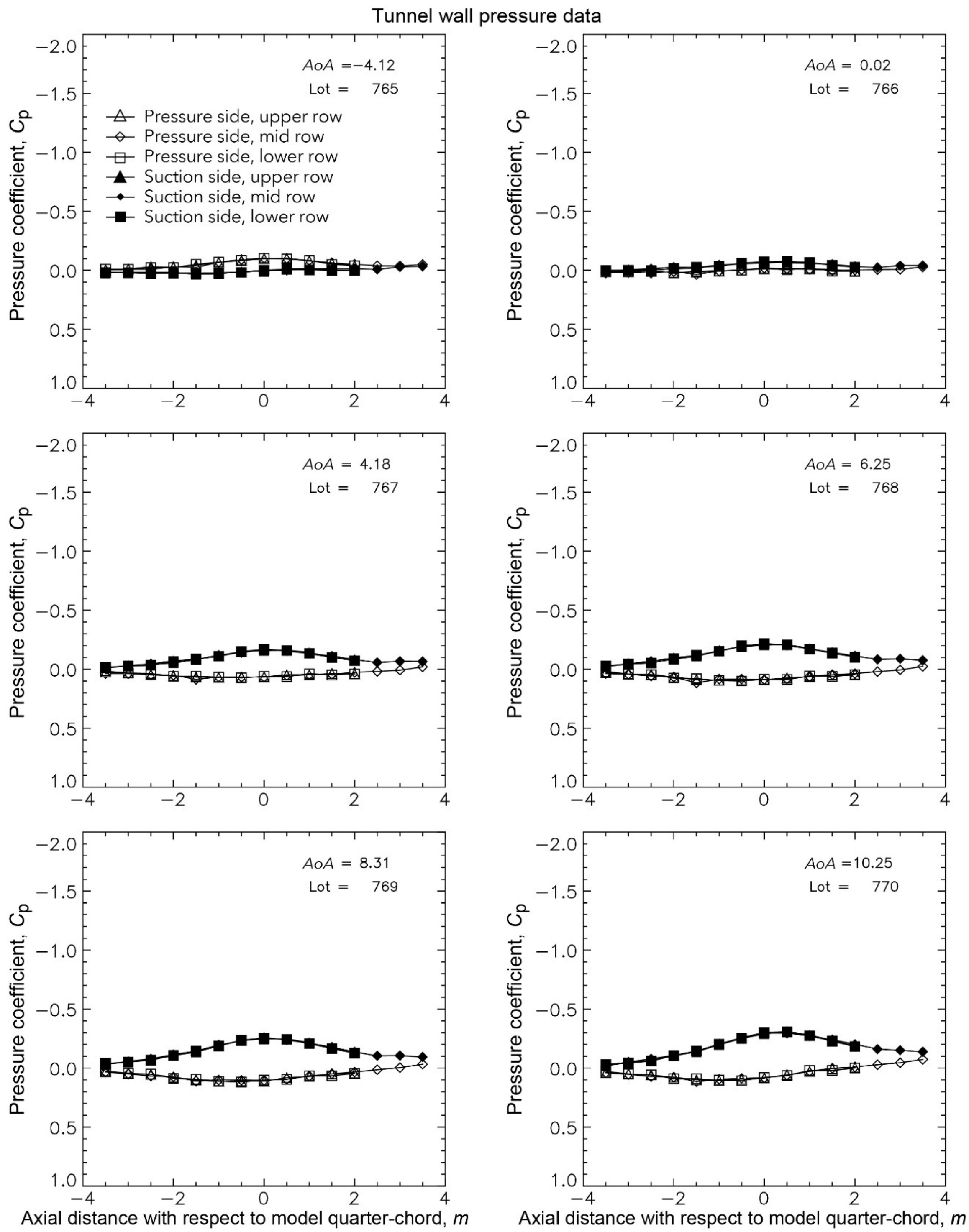

Horn Ice—Lot EG1164: M = 0.10 and Re = 4.5×10^6

Appendix G.—F1 Full-Scale Model Tests

Horn Ice—Lot EG1164: M = 0.10 and Re = 4.5×10[6]

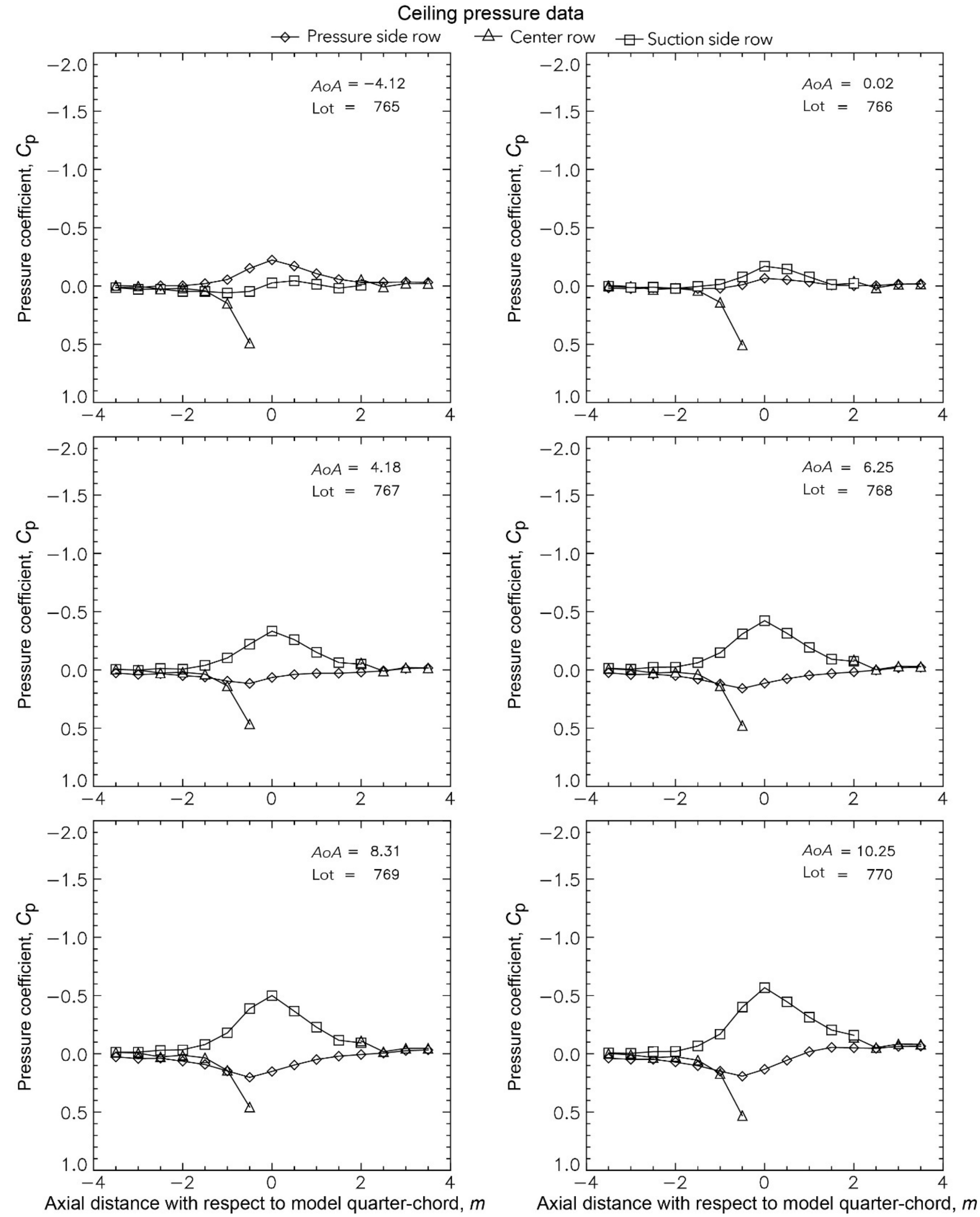

Horn Ice—Lot EG1164: M = 0.10 and Re = 4.5×10[6]

Appendix G.—F1 Full-Scale Model Tests

Horn Ice—Lot EG1164: M = 0.10 and Re = 4.5×10^6

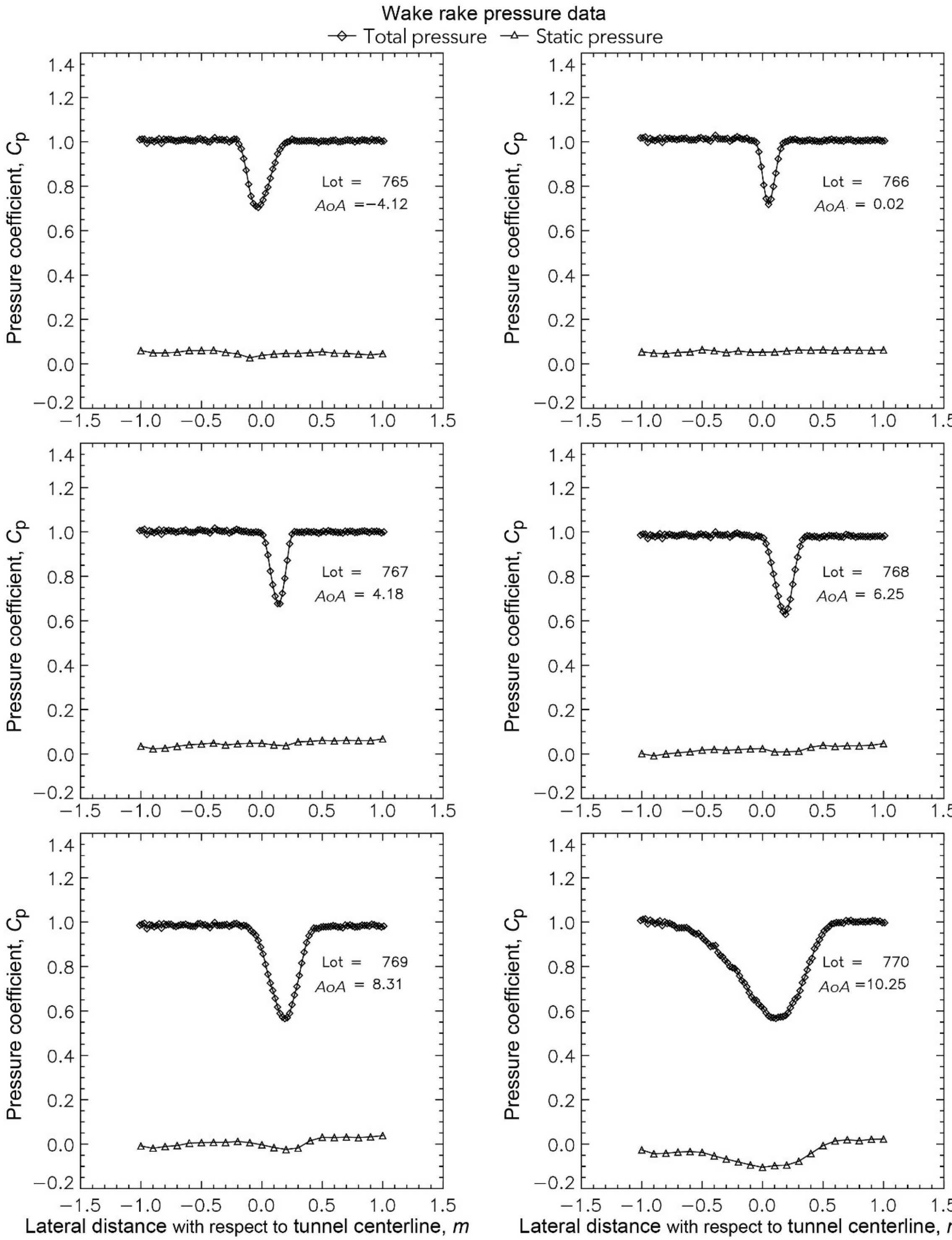

Horn Ice—Lot EG1164: M = 0.10 and Re = 4.5×10^6

Appendix G.—F1 Full-Scale Model Tests

Horn Ice—Lot EG1164: M = 0.10 and Re = 8.2–8.3×10^6

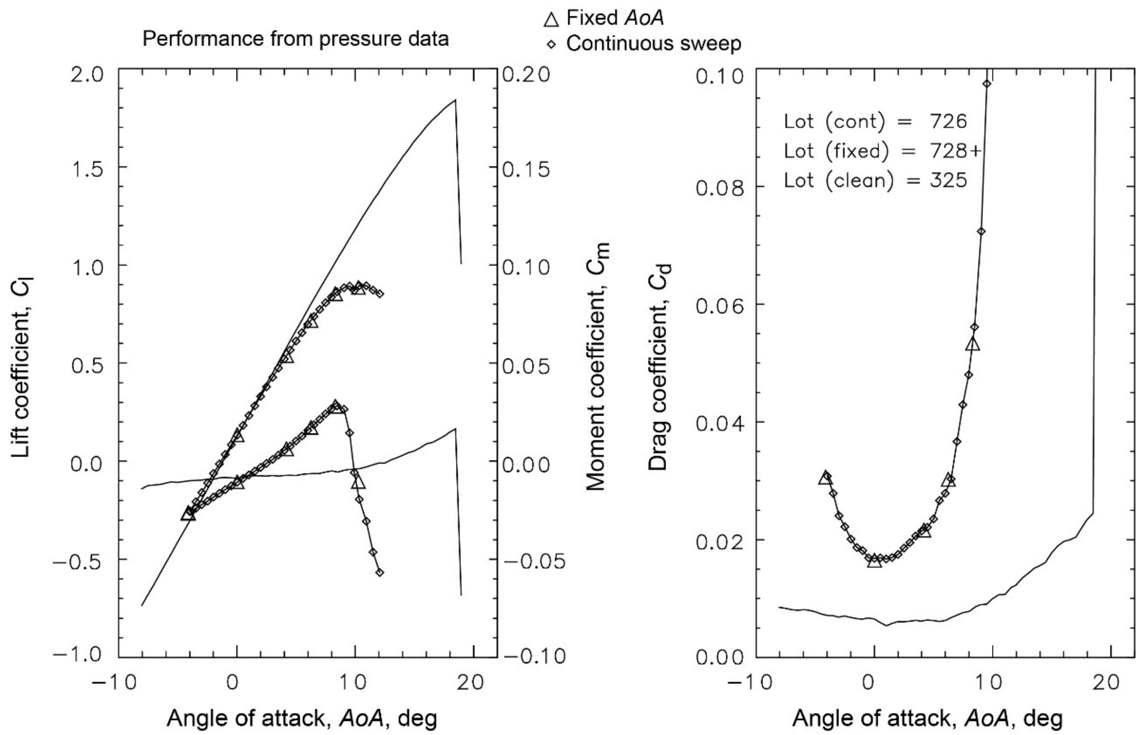

Horn Ice—Lot EG1164: M = 0.10 and Re = 8.2–8.3×10^6

Appendix G.—F1 Full-Scale Model Tests

Horn Ice—Lot EG1164: M = 0.10 and Re = 8.2–8.3×10^6

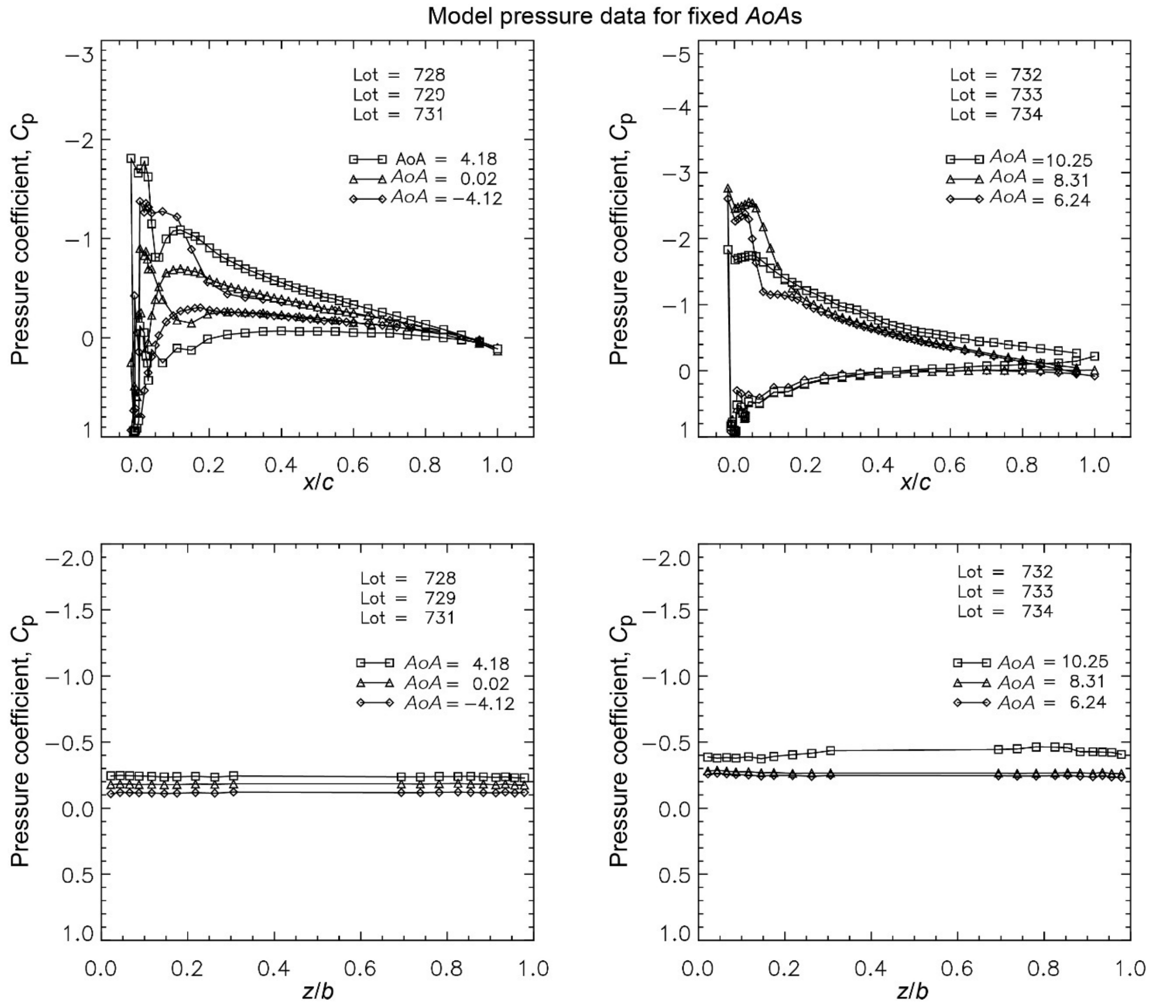

Horn Ice—Lot EG1164: M = 0.10 and Re = 8.2–8.3×10^6

Appendix G.—F1 Full-Scale Model Tests

Horn Ice—Lot EG1164: M = 0.10 and Re = 8.2–8.3×10^6

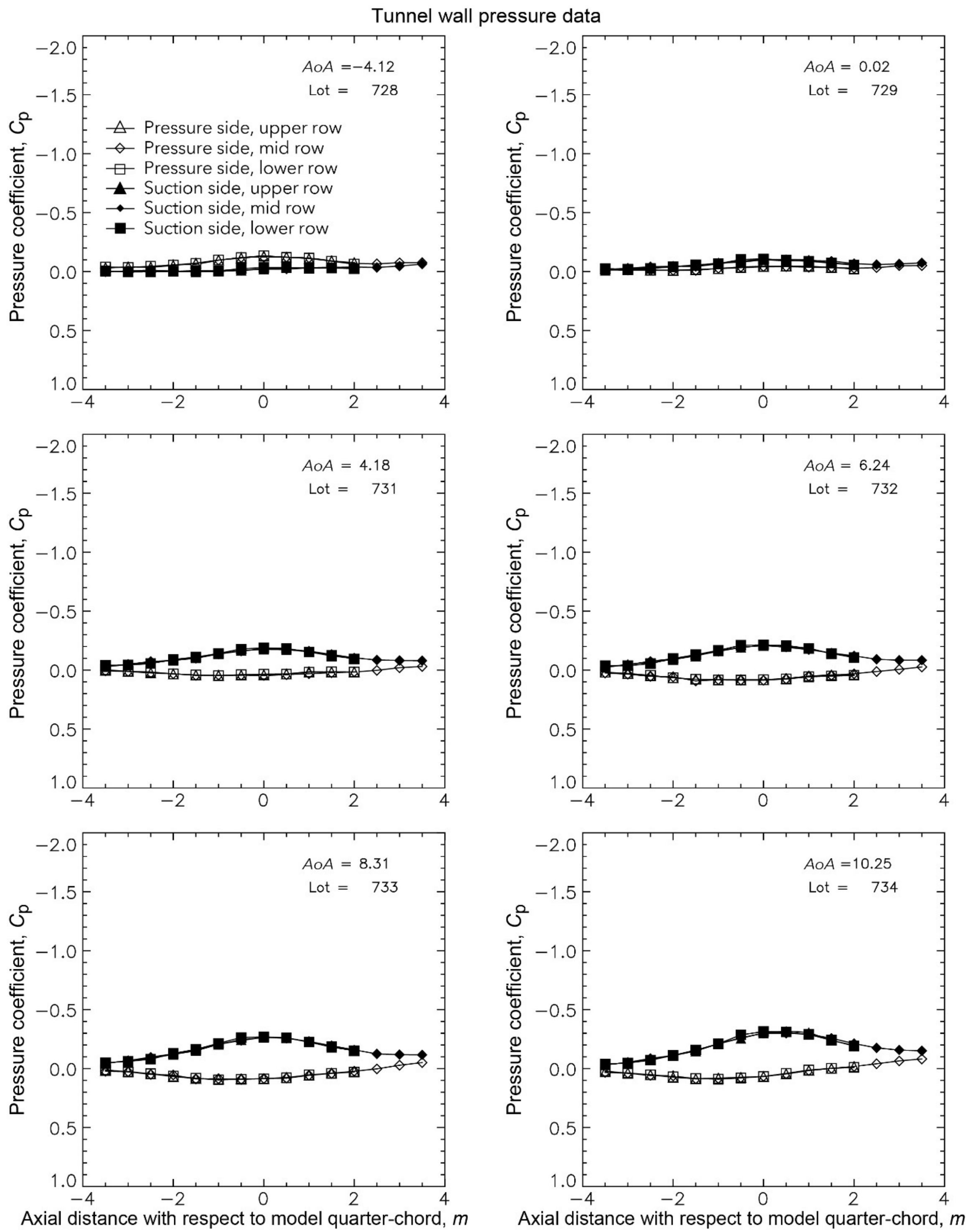

Horn Ice—Lot EG1164: M = 0.10 and Re = 8.2–8.3×10^6

Appendix G.—F1 Full-Scale Model Tests

Horn Ice—Lot EG1164: M = 0.10 and Re = 8.2–8.3×10^6

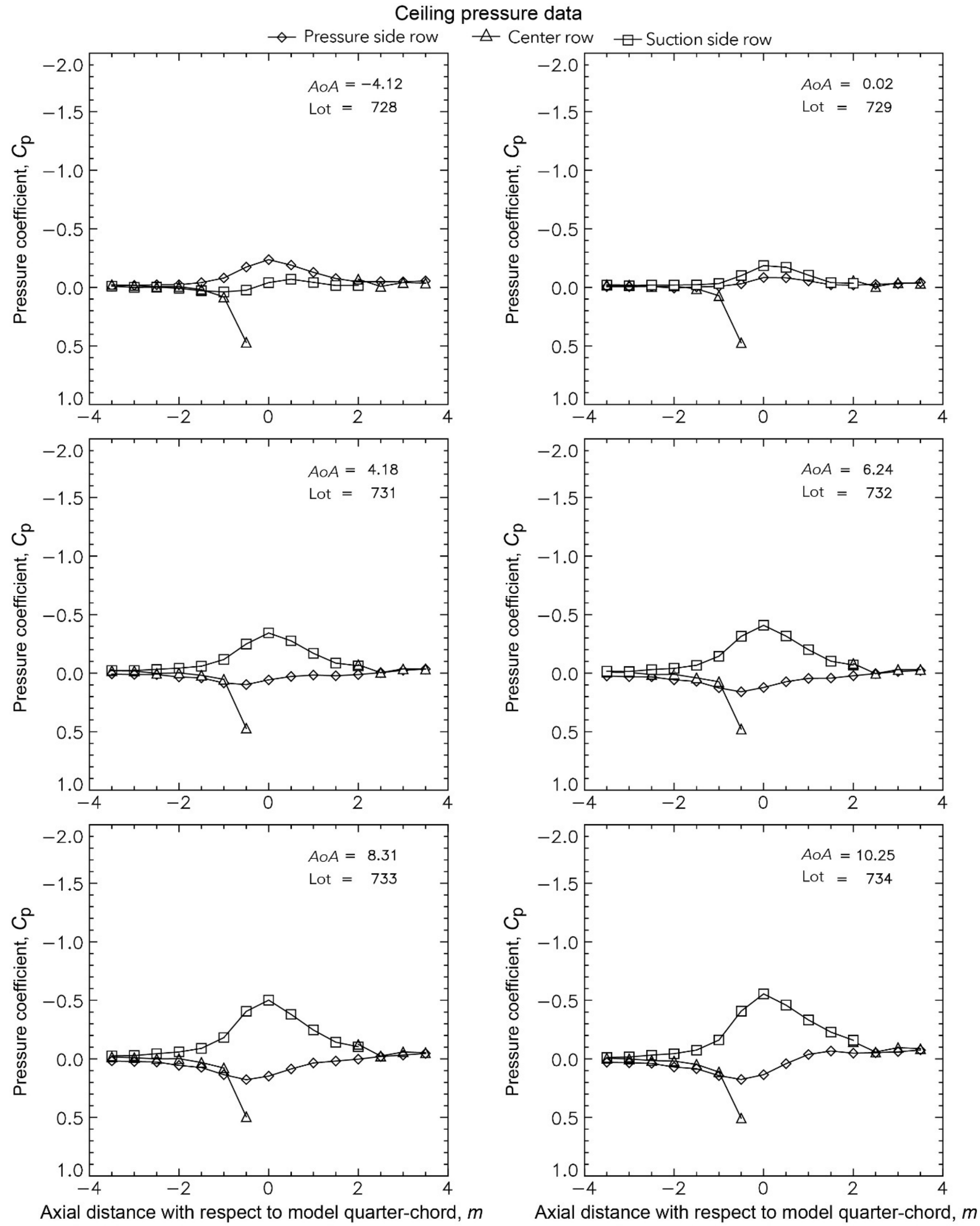

Horn Ice—Lot EG1164: M = 0.10 and Re = 8.2–8.3×10^6

Appendix G.—F1 Full-Scale Model Tests

Horn Ice—Lot EG1164: M = 0.10 and Re = 8.2–8.3×10[6]

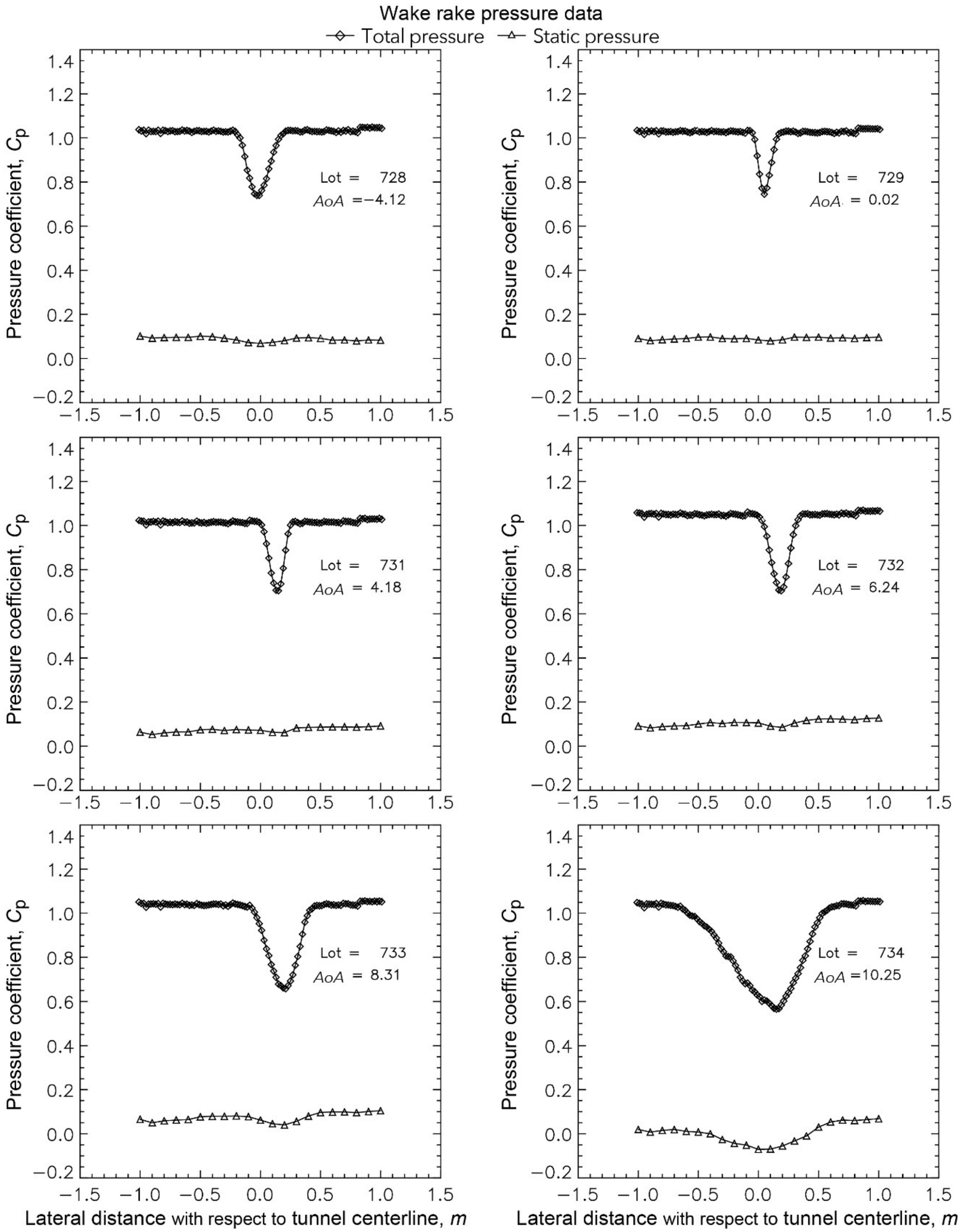

Horn Ice—Lot EG1164: M = 0.10 and Re = 8.2–8.3×10[6]

Appendix G.—F1 Full-Scale Model Tests

Horn Ice—Lot EG1164: M = 0.10 and Re = 11.9–12.2×10^6

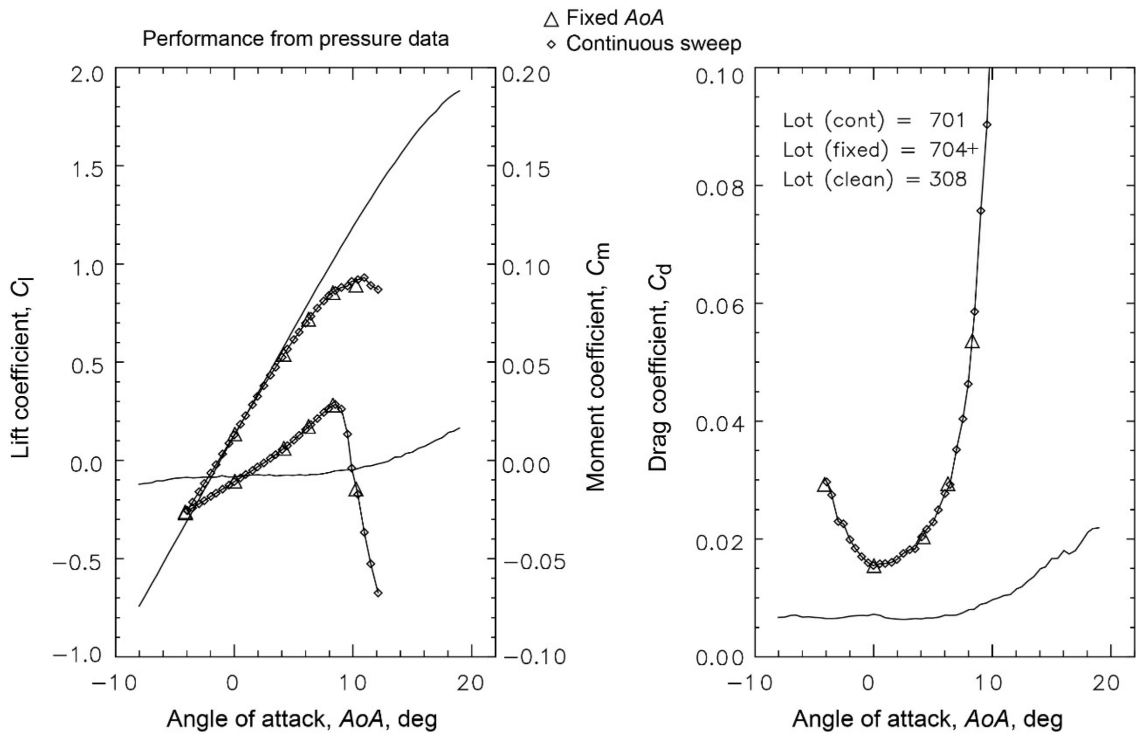

Horn Ice—Lot EG1164: M = 0.10 and Re = 11.9–12.2×10^6

Appendix G.—F1 Full-Scale Model Tests

Horn Ice—Lot EG1164: M = 0.10 and Re = 11.9–12.2×10^6

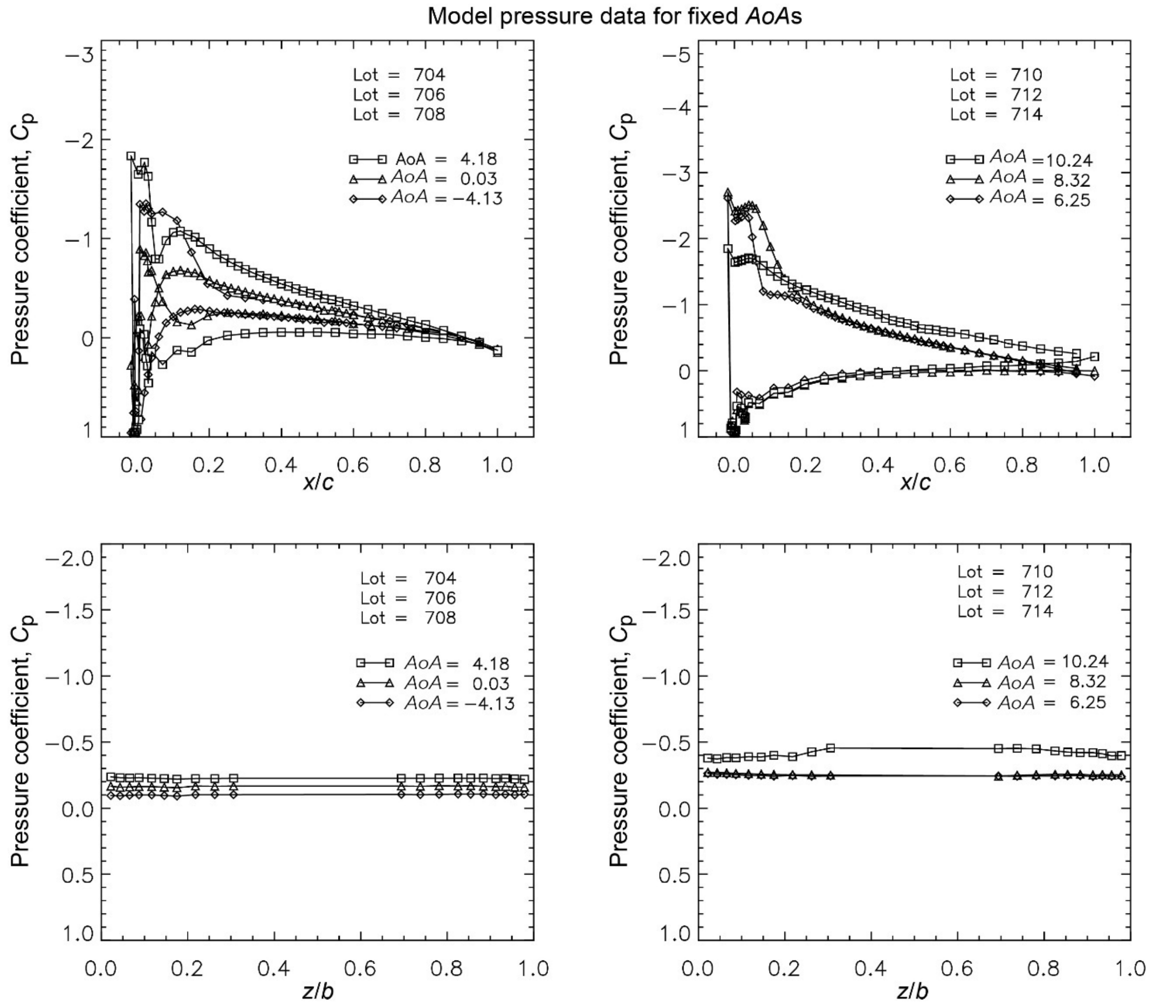

Horn Ice—Lot EG1164: M = 0.10 and Re = 11.9–12.2×10^6

Appendix G.—F1 Full-Scale Model Tests

Horn Ice—Lot EG1164: M = 0.10 and Re = 11.9–12.2×10^6

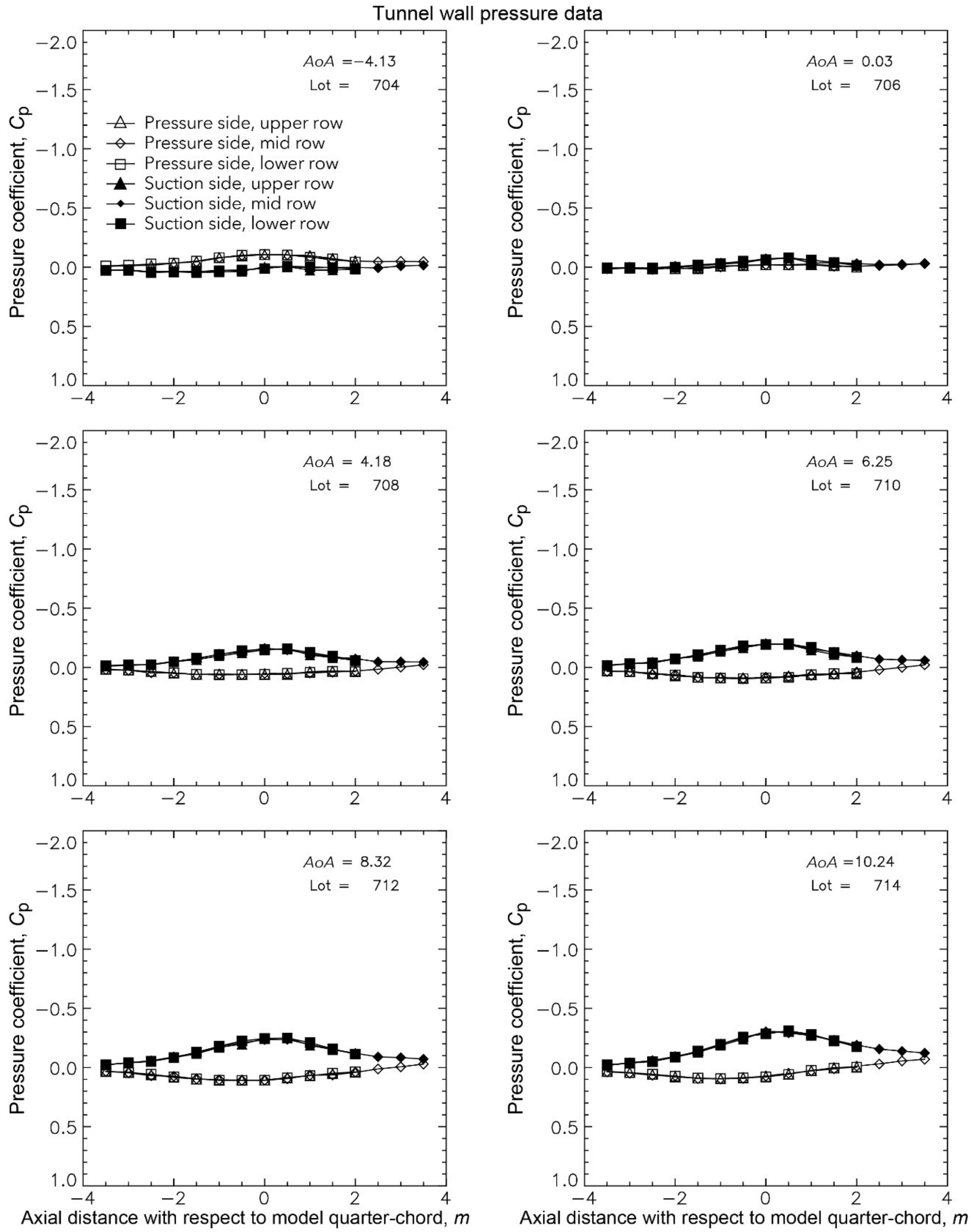

Horn Ice—Lot EG1164: M = 0.10 and Re = 11.9–12.2×10^6

Appendix G.—F1 Full-Scale Model Tests

Horn Ice—Lot EG1164: M = 0.10 and Re = 11.9–12.2×10^6

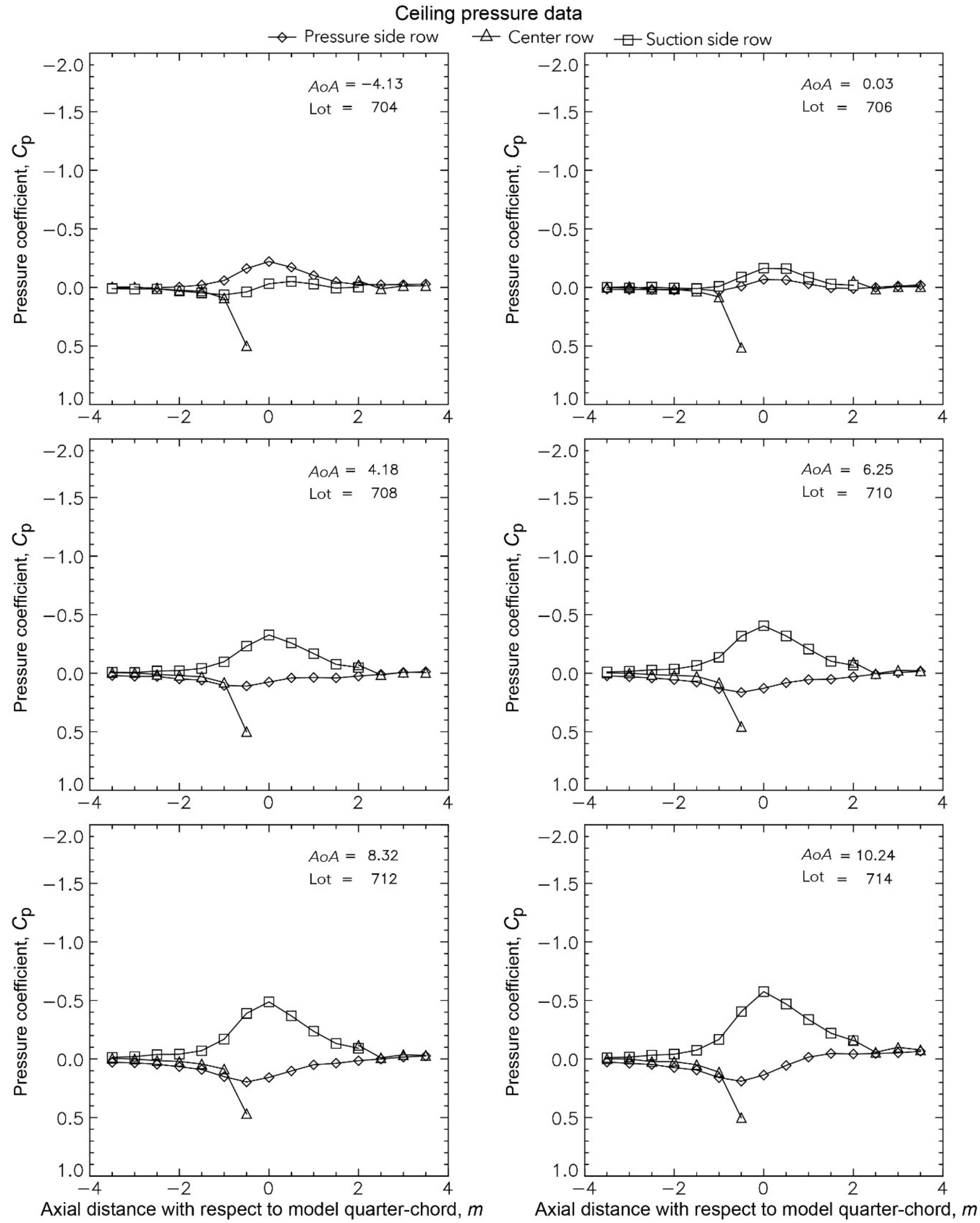

Horn Ice—Lot EG1164: M = 0.10 and Re = 11.9–12.2×10^6

Appendix G.—F1 Full-Scale Model Tests

Horn Ice—Lot EG1164: M = 0.10 and Re = 11.9–12.2×10^6

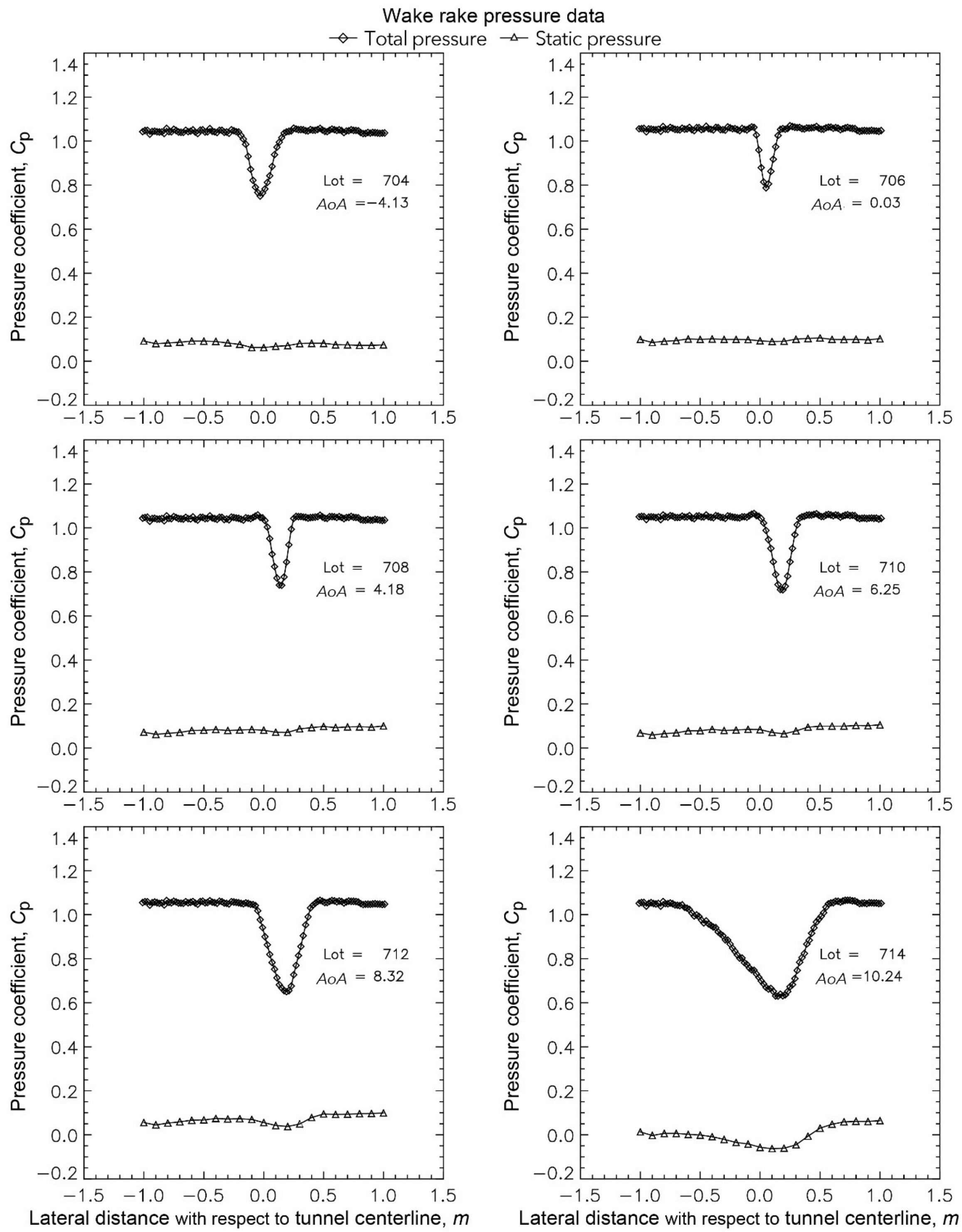

Horn Ice—Lot EG1164: M = 0.10 and Re = 11.9–12.2×10^6

Appendix G.—F1 Full-Scale Model Tests

Horn Ice—Lot EG1164: M = 0.20 to 0.21 and Re = 8.8–9.0×10^6

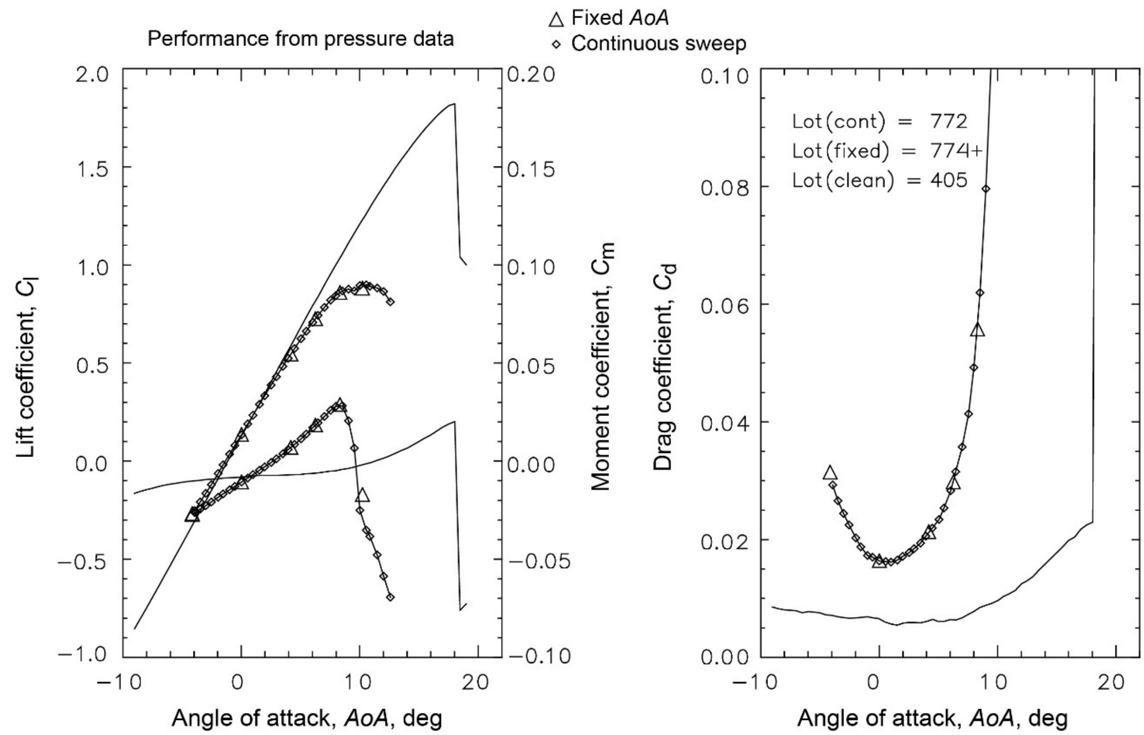

Horn Ice—Lot EG1164: M = 0.20 to 0.21 and Re = 8.8–9.0×10^6

Appendix G.—F1 Full-Scale Model Tests

Horn Ice—Lot EG1164: M = 0.20 to 0.21 and Re = 8.8–9.0×10^6

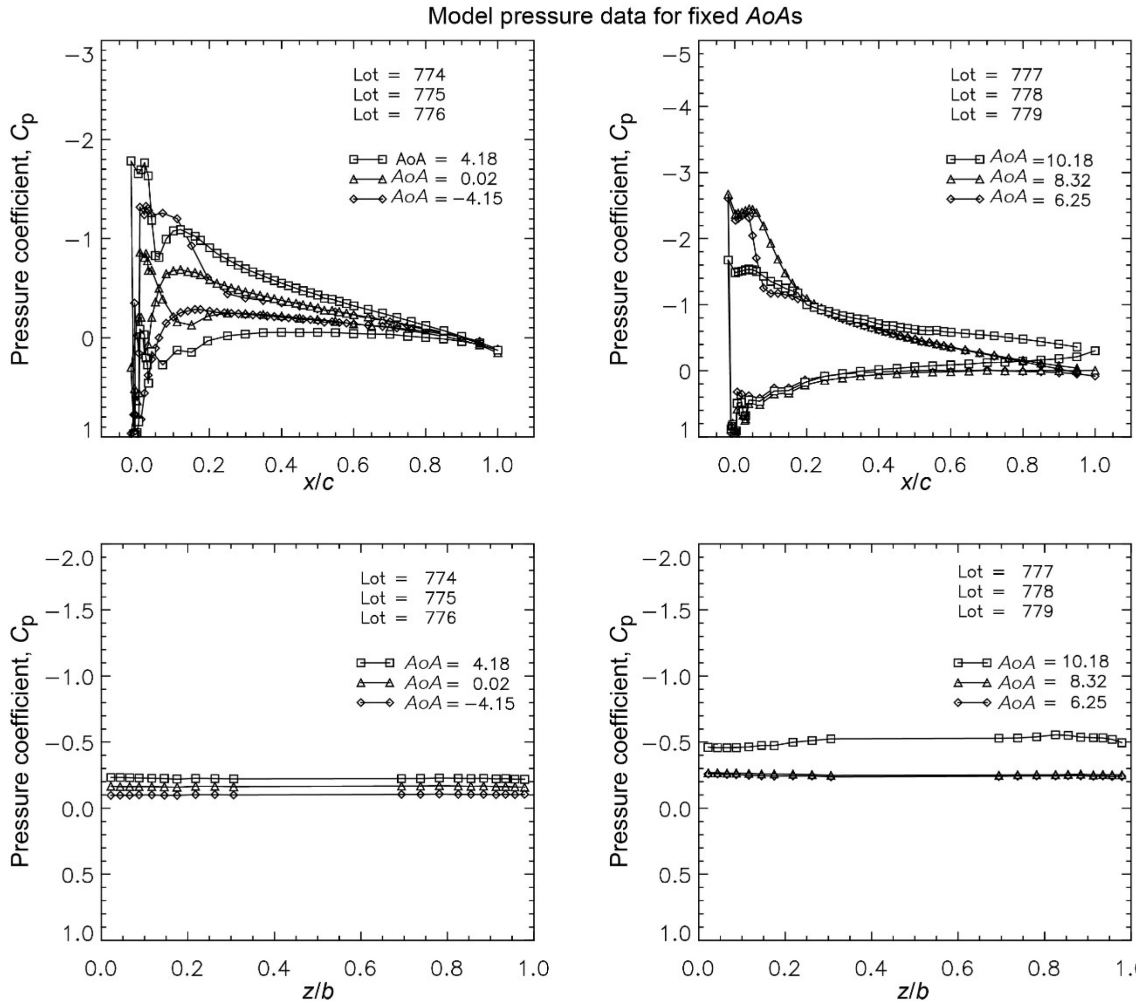

Horn Ice—Lot EG1164: M = 0.20 to 0.21 and Re = 8.8–9.0×10^6

Appendix G.—F1 Full-Scale Model Tests

Horn Ice—Lot EG1164: M = 0.20 to 0.21 and Re = 8.8–9.0×10^6

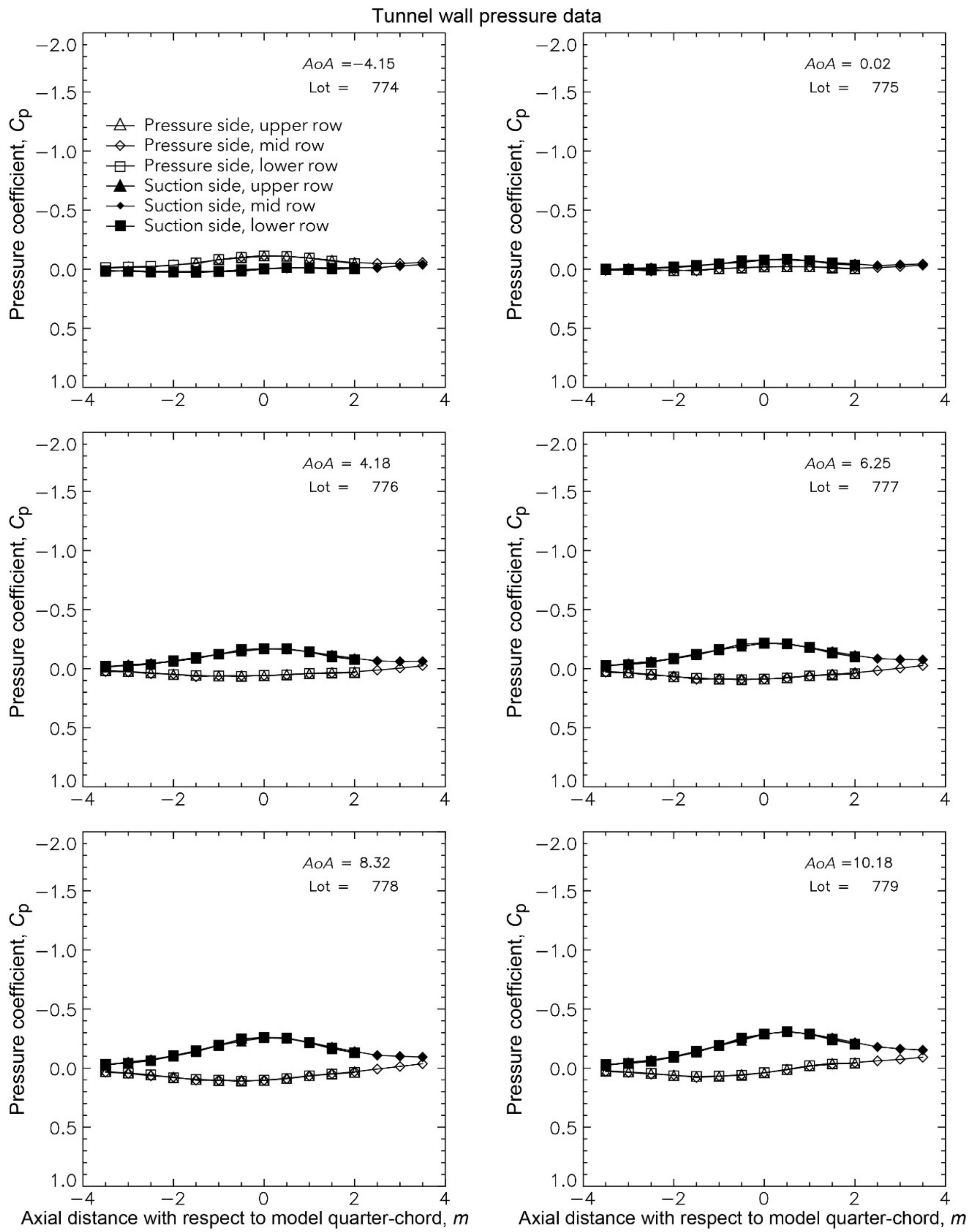

Horn Ice—Lot EG1164: M = 0.20 to 0.21 and Re = 8.8–9.0×10^6

Appendix G.—F1 Full-Scale Model Tests

Horn Ice—Lot EG1164: M = 0.20 to 0.21 and Re = 8.8–9.0×10[6]

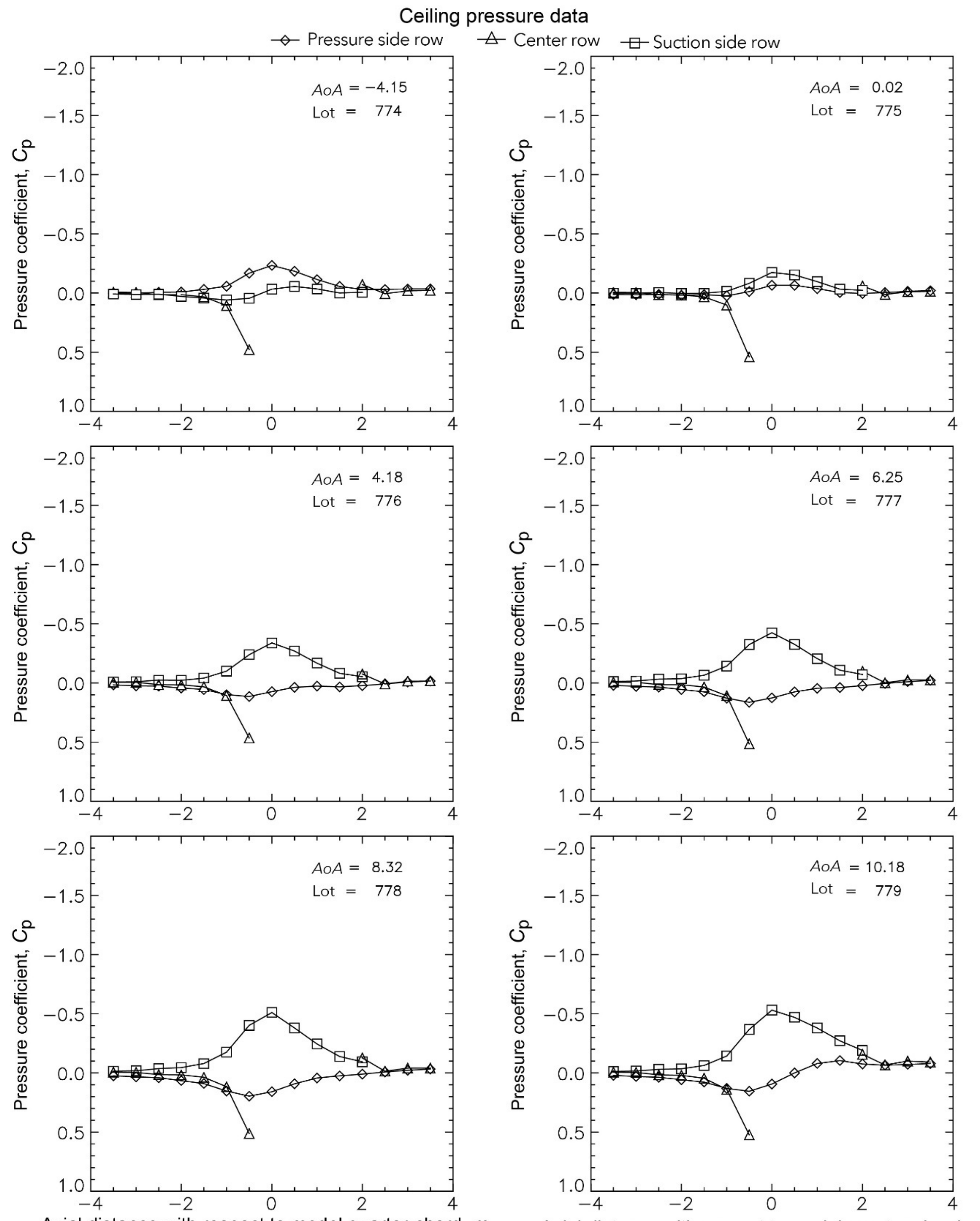

Horn Ice—Lot EG1164: M = 0.20 to 0.21 and Re = 8.8–9.0×10[6]

Appendix G.—F1 Full-Scale Model Tests

Horn Ice—Lot EG1164: M = 0.20 to 0.21 and Re = 8.8–9.0×10[6]

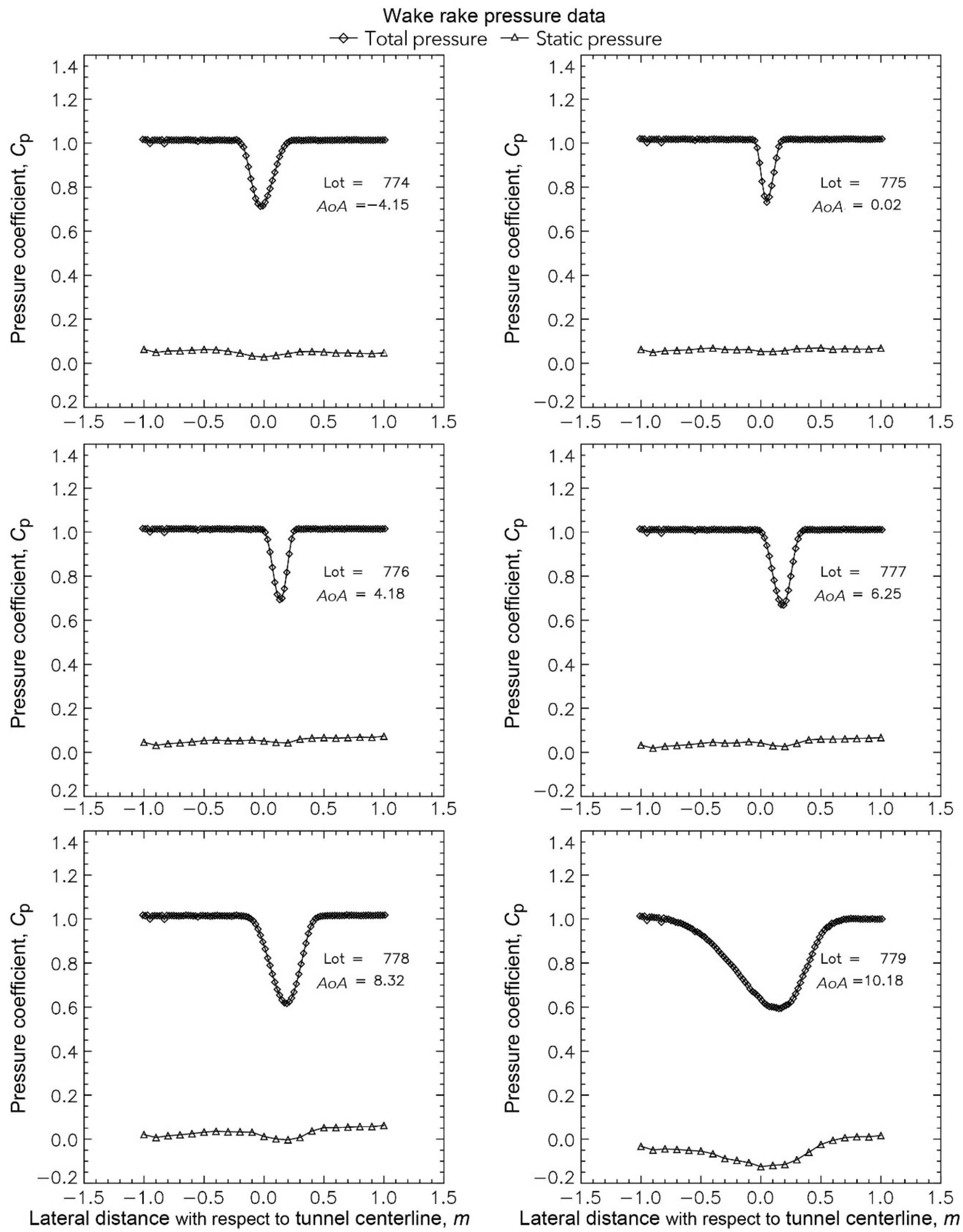

Horn Ice—Lot EG1164: M = 0.20 to 0.21 and Re = 8.8–9.0×10[6]

Appendix G.—F1 Full-Scale Model Tests

Horn Ice—Lot EG1164: M = 0.20 to 0.21 and Re = 12.0–12.2×10^6

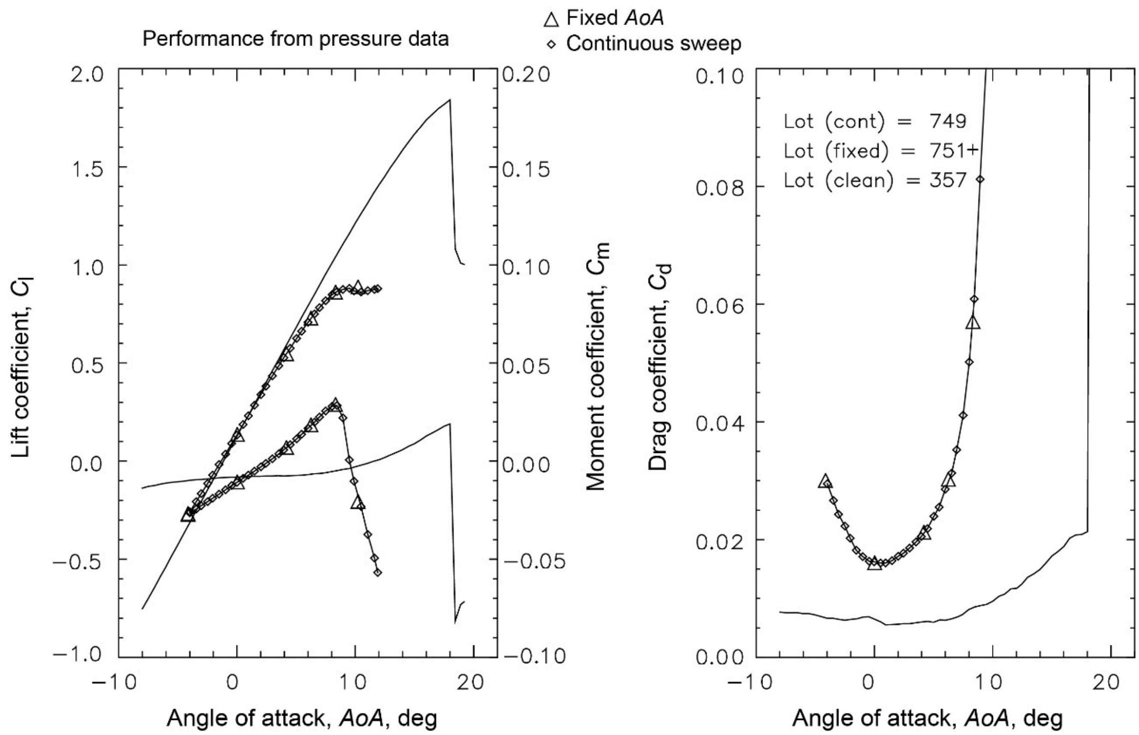

Horn Ice—Lot EG1164: M = 0.20 to 0.21 and Re = 12.0–12.2×10^6

Appendix G.—F1 Full-Scale Model Tests

Horn Ice—Lot EG1164: M = 0.20 to 0.21 and Re = 12.0–12.2×10^6

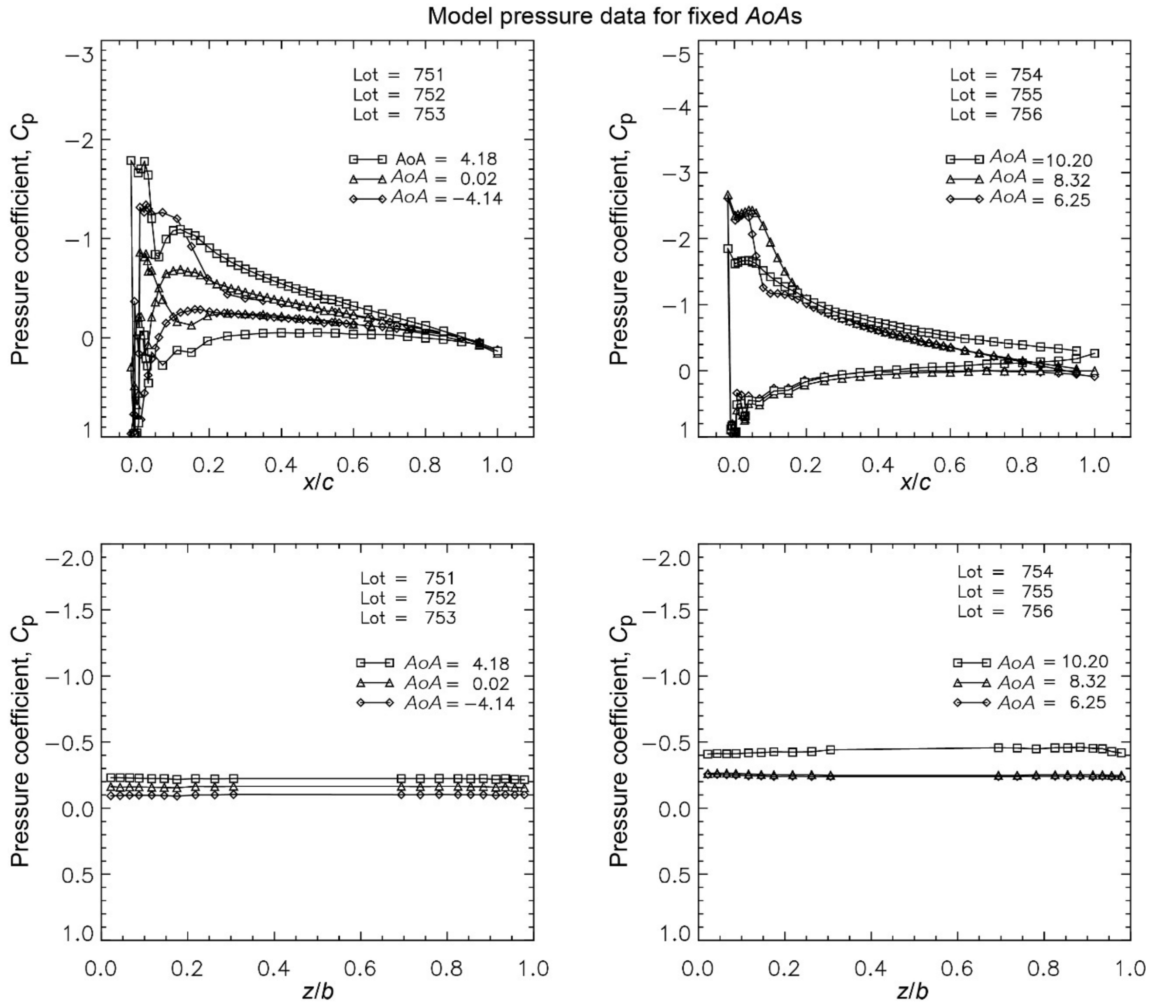

Horn Ice—Lot EG1164: M = 0.20 to 0.21 and Re = 12.0–12.2×10^6

Appendix G.—F1 Full-Scale Model Tests

Horn Ice—Lot EG1164: M = 0.20 to 0.21 and Re = 12.0–12.2×10^6

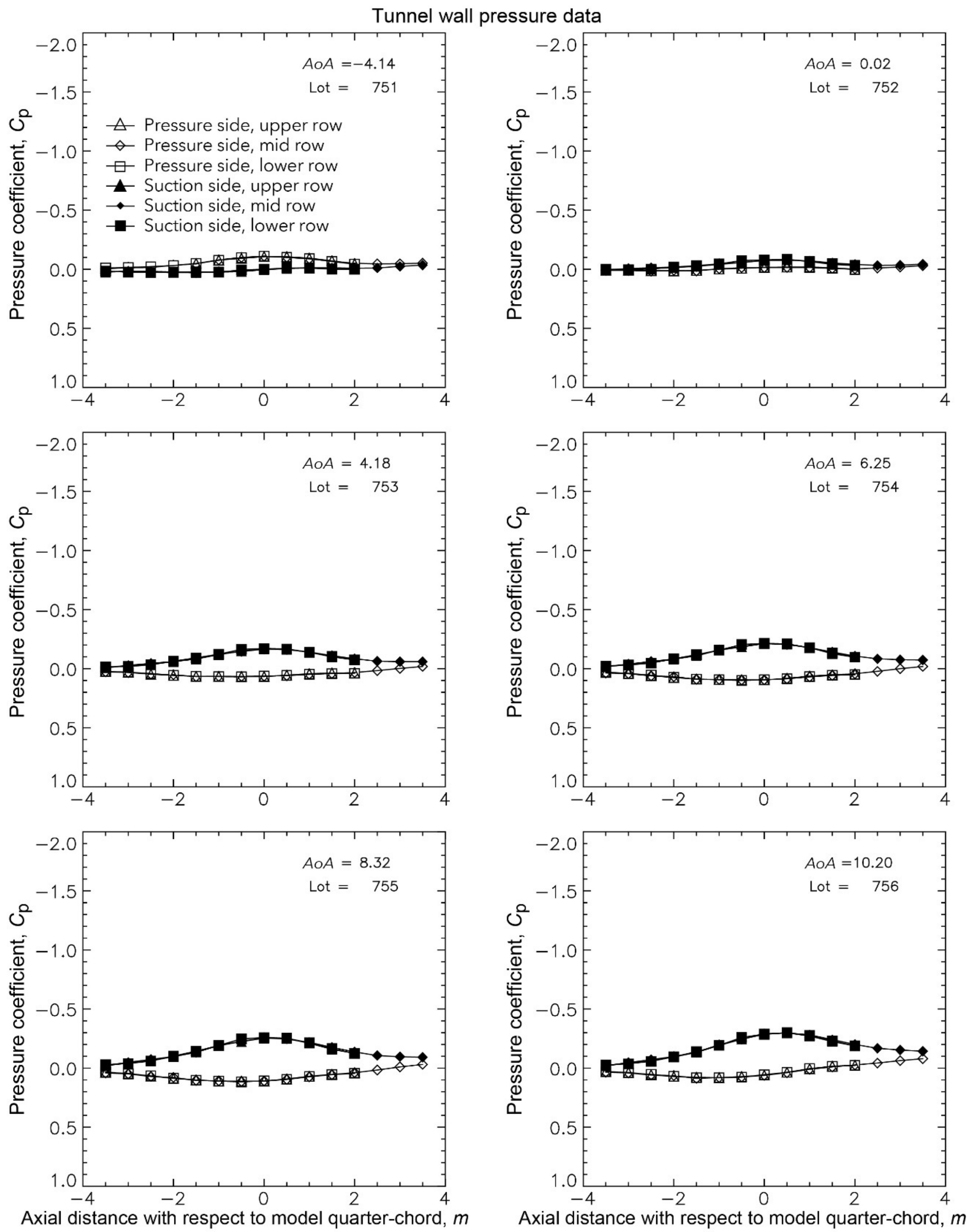

Horn Ice—Lot EG1164: M = 0.20 to 0.21 and Re = 12.0–12.2×10^6

Appendix G.—F1 Full-Scale Model Tests

Horn Ice—Lot EG1164: M = 0.20 to 0.21 and Re = 12.0–12.2×10⁶

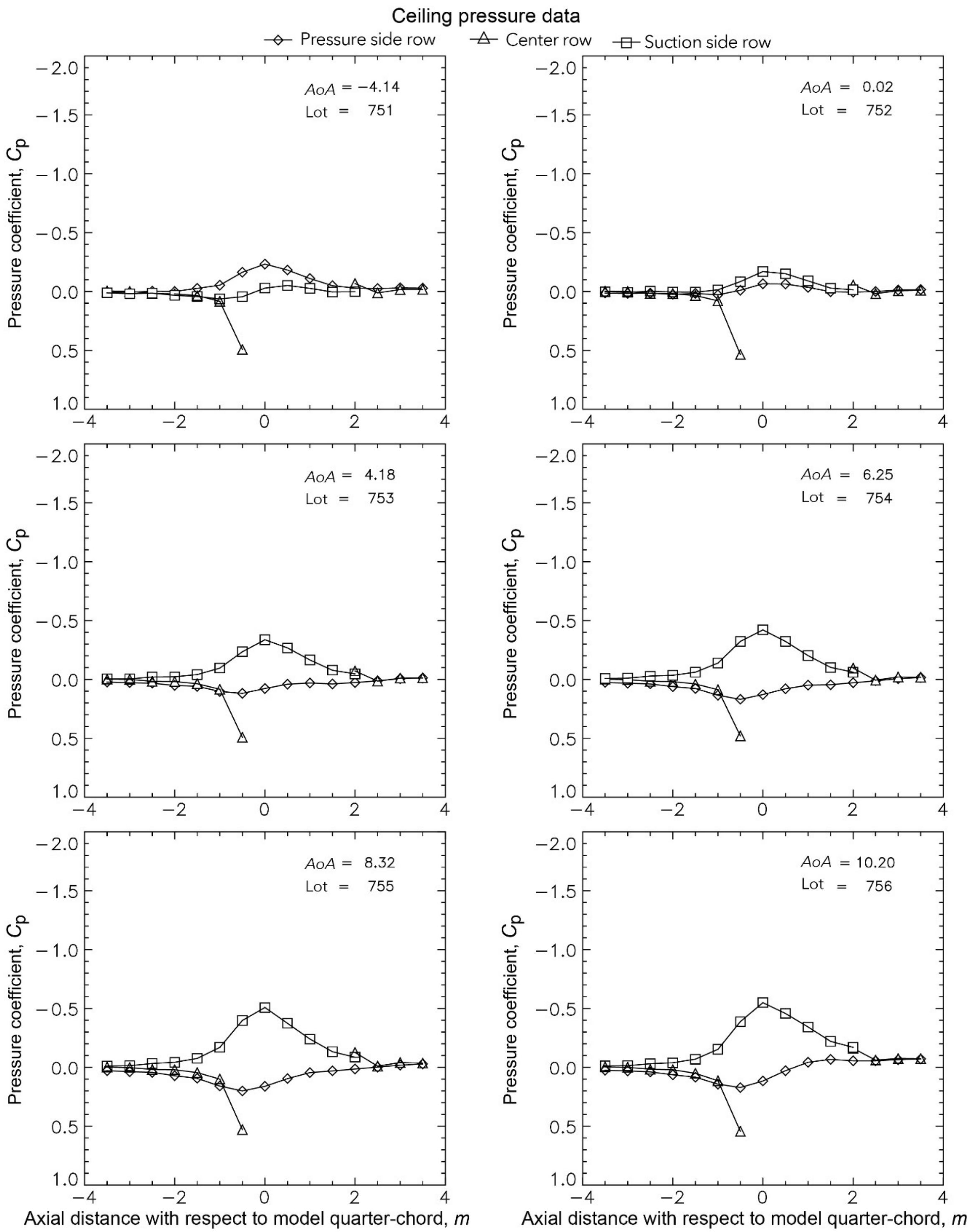

Horn Ice—Lot EG1164: M = 0.20 to 0.21 and Re = 12.0–12.2×10⁶

Appendix G.—F1 Full-Scale Model Tests

Horn Ice—Lot EG1164: M = 0.20 to 0.21 and Re = 12.0–12.2×10^6

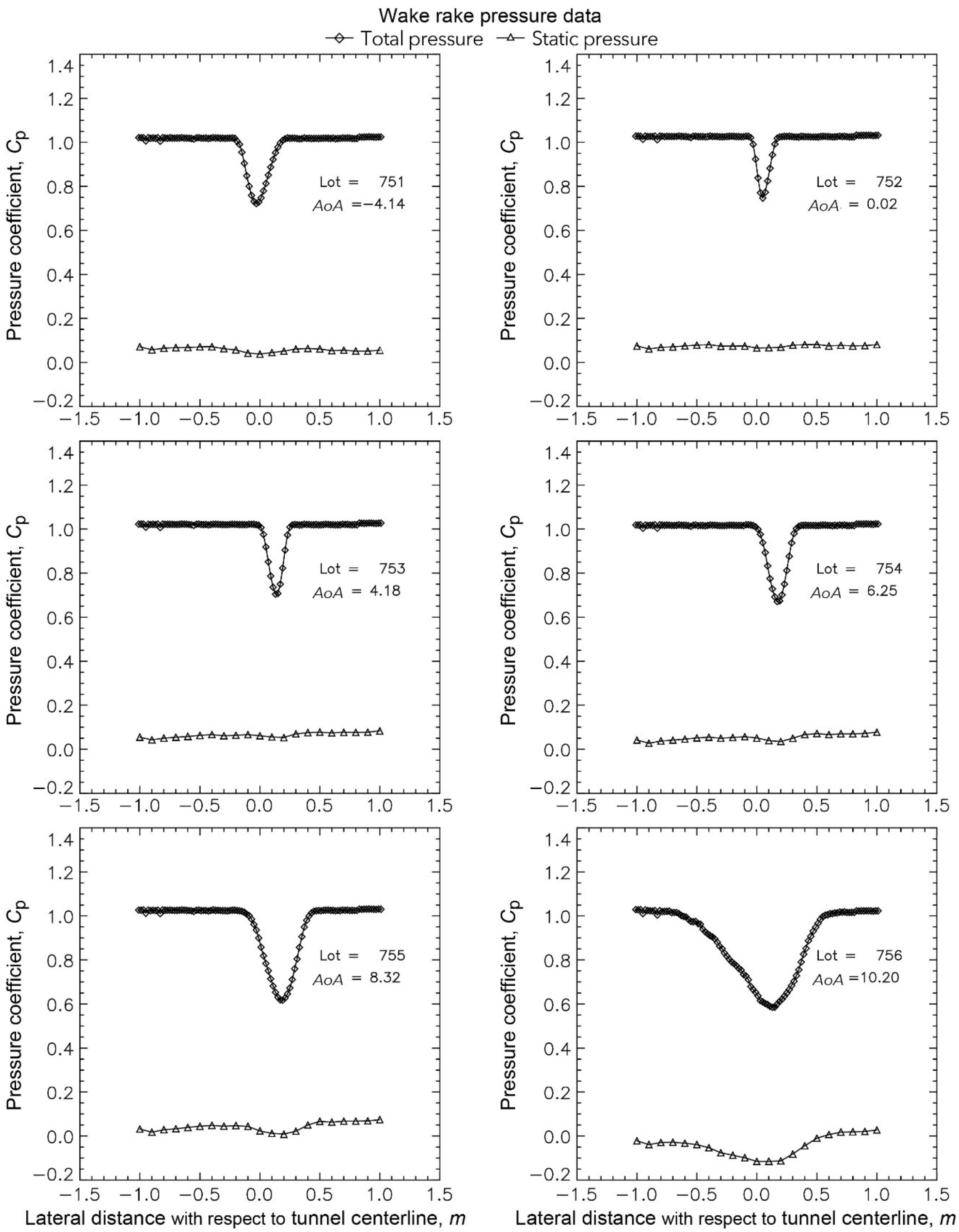

Horn Ice—Lot EG1164: M = 0.20 to 0.21 and Re = 12.0–12.2×10^6

Appendix G.—F1 Full-Scale Model Tests

Horn Ice—Lot EG1164: M = 0.20 to 0.21 and Re = 15.6–16.0×10^6

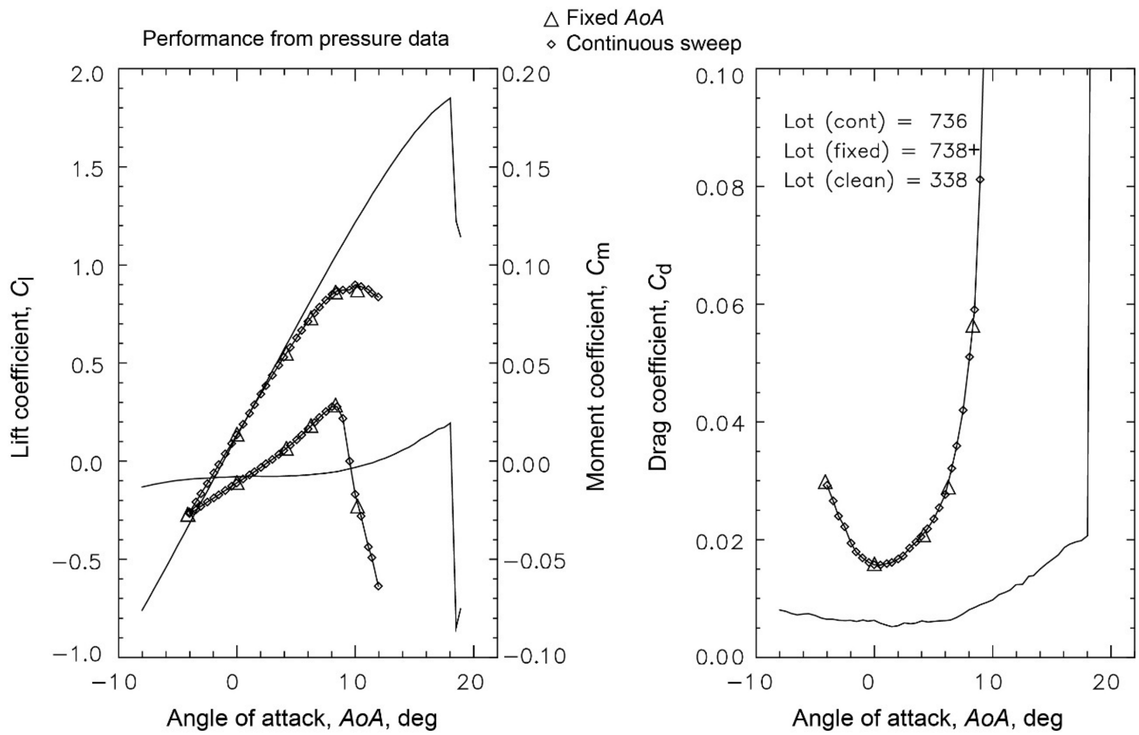

Horn Ice—Lot EG1164: M = 0.20 to 0.21 and Re = 15.6–16.0×10^6

Appendix G.—F1 Full-Scale Model Tests

Horn Ice—Lot EG1164: M = 0.20 to 0.21 and Re = 15.6–16.0×10^6

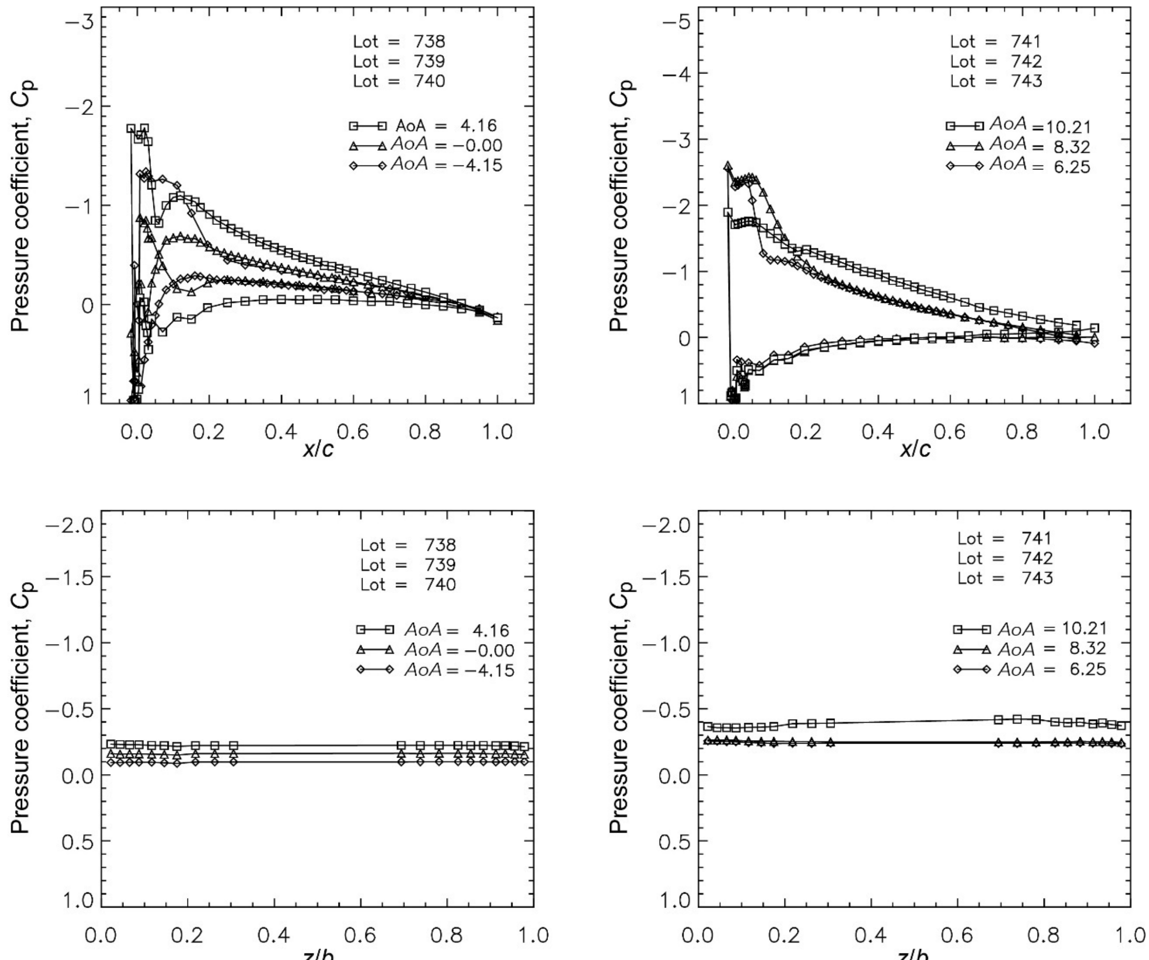

Model pressure data for fixed *AoA*s

Horn Ice—Lot EG1164: M = 0.20 to 0.21 and Re = 15.6–16.0×10^6

Appendix G.—F1 Full-Scale Model Tests

Horn Ice—Lot EG1164: M = 0.20 to 0.21 and Re = 15.6–16.0×10^6

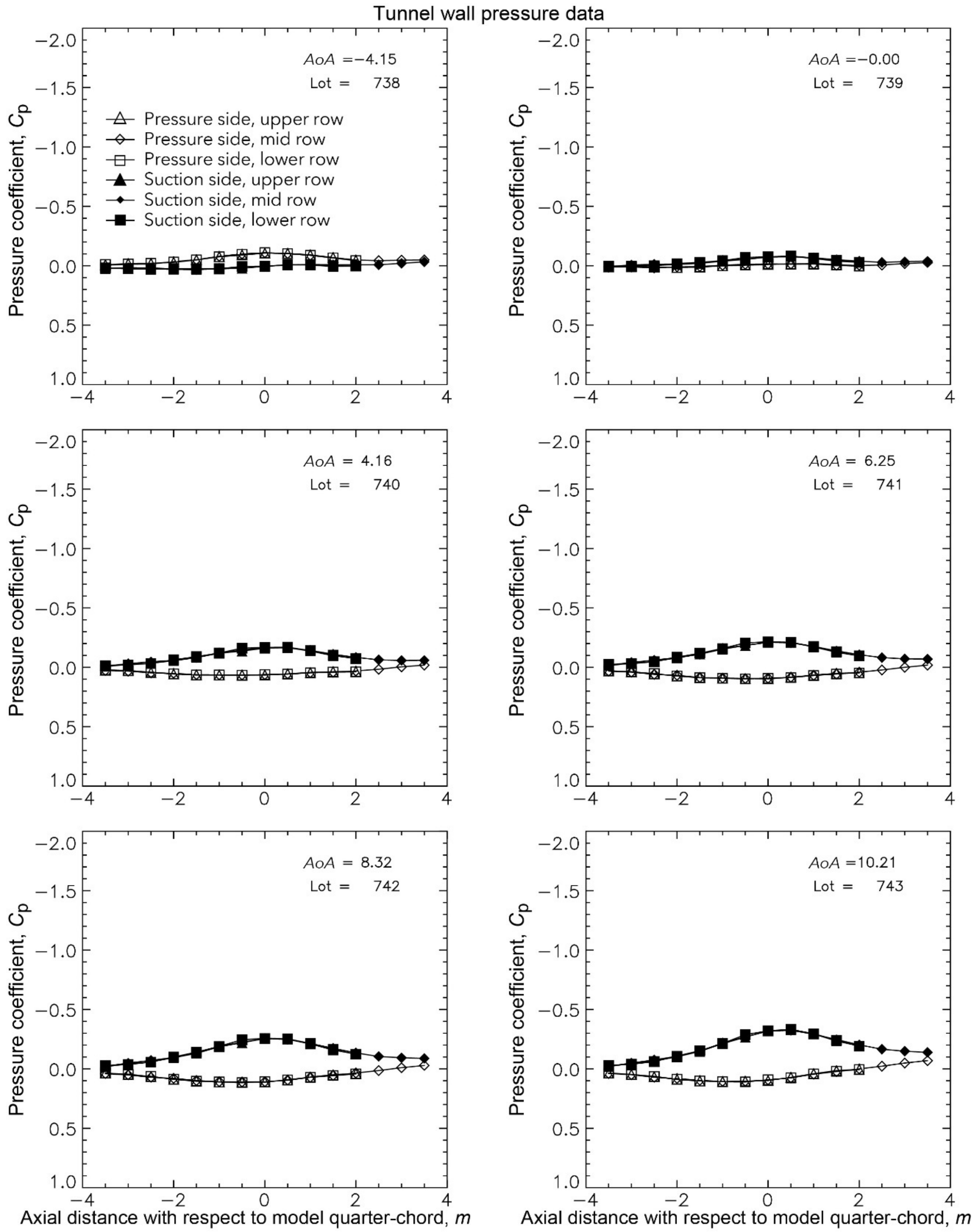

Horn Ice—Lot EG1164: M = 0.20 to 0.21 and Re = 15.6–16.0×10^6

Appendix G.—F1 Full-Scale Model Tests

Horn Ice—Lot EG1164: M = 0.20 to 0.21 and Re = 15.6–16.0×10⁶

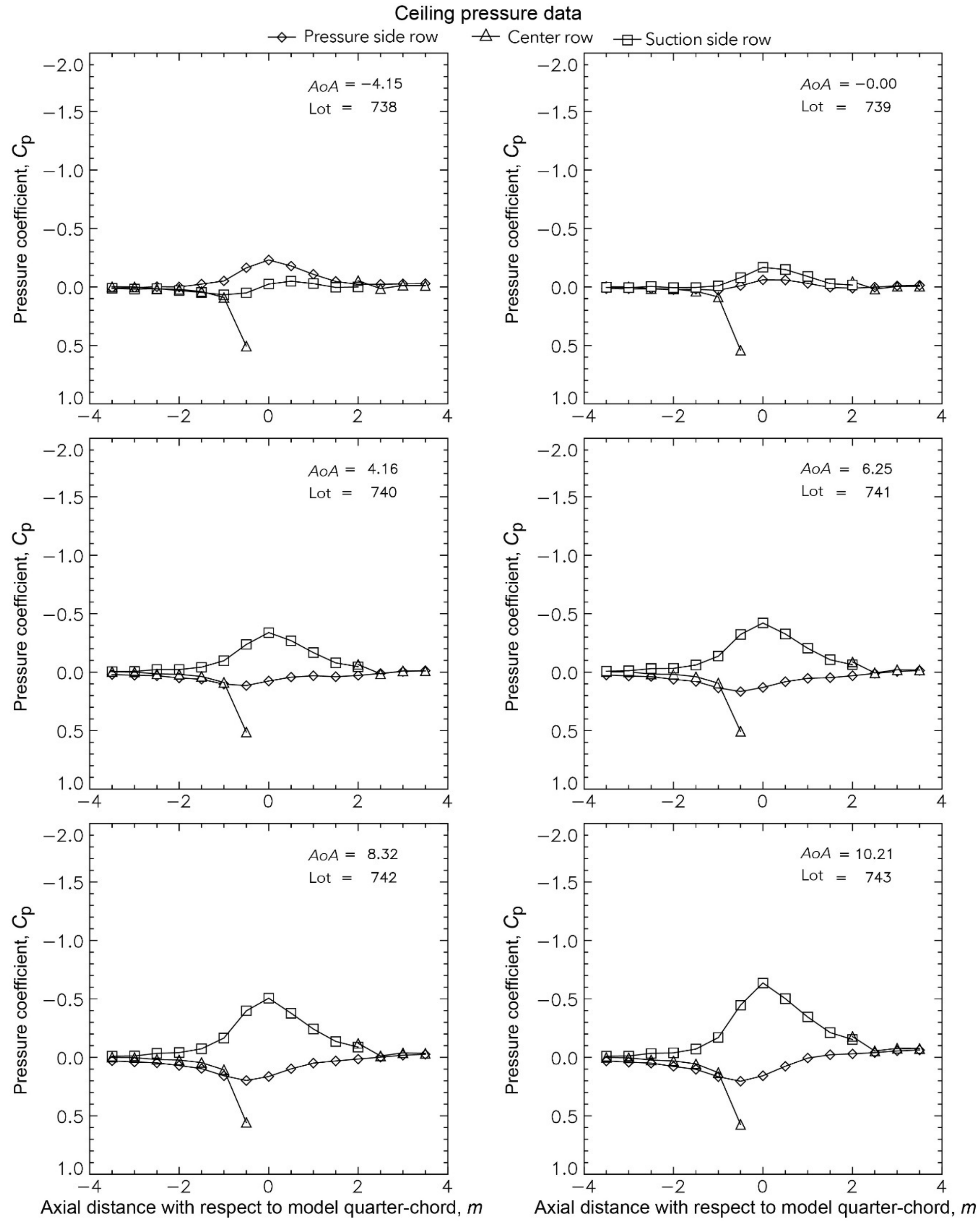

Horn Ice—Lot EG1164: M = 0.20 to 0.21 and Re = 15.6–16.0×10⁶

Appendix G.—F1 Full-Scale Model Tests

Horn Ice—Lot EG1164: M = 0.20 to 0.21 and Re = 15.6–16.0×10[6]

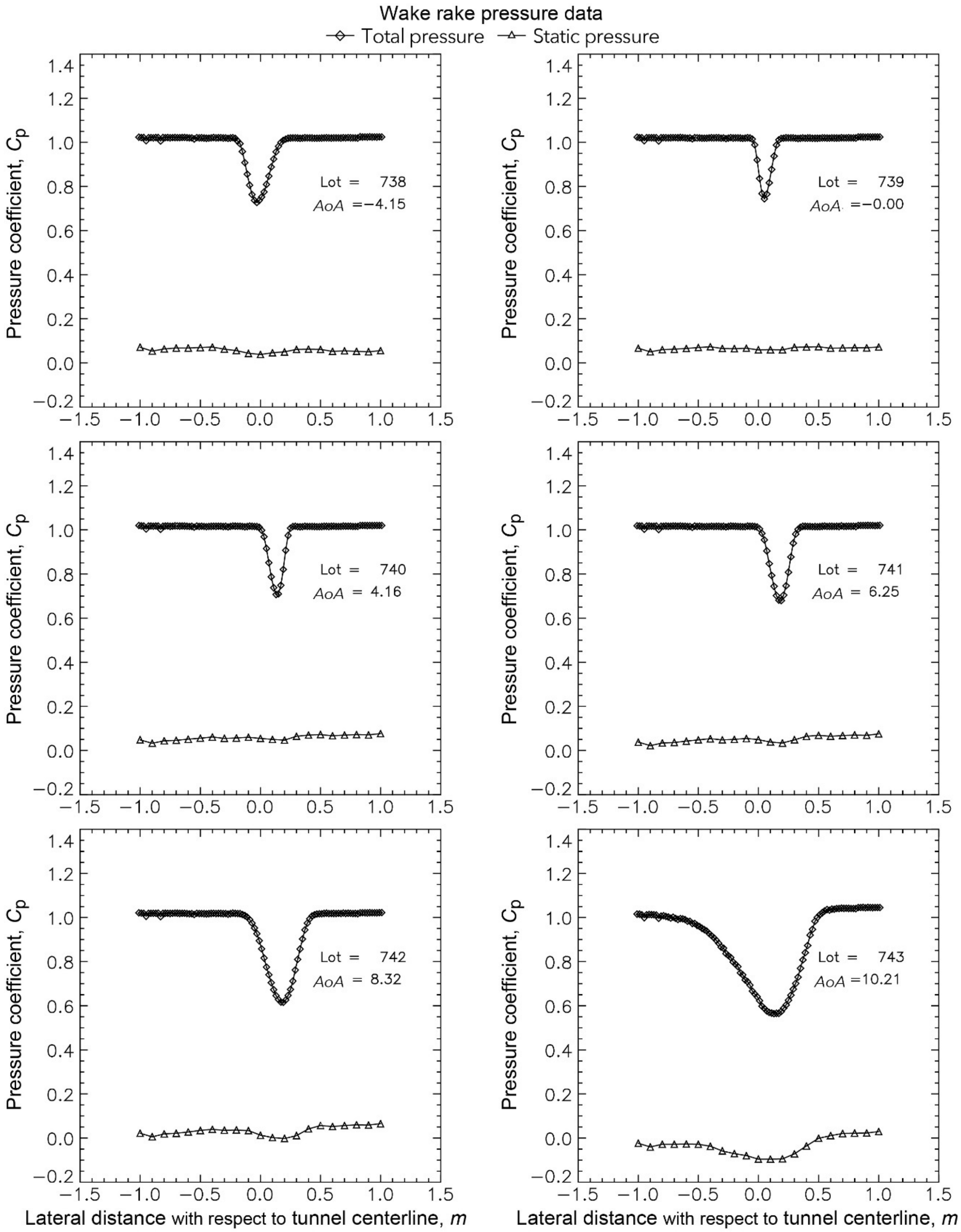

Horn Ice—Lot EG1164: M = 0.20 to 0.21 and Re = 15.6–16.0×10[6]

Appendix G.—F1 Full-Scale Model Tests

Horn Ice—Lot EG1164: M = 0.29 and Re = 12.1–12.2×10[6]

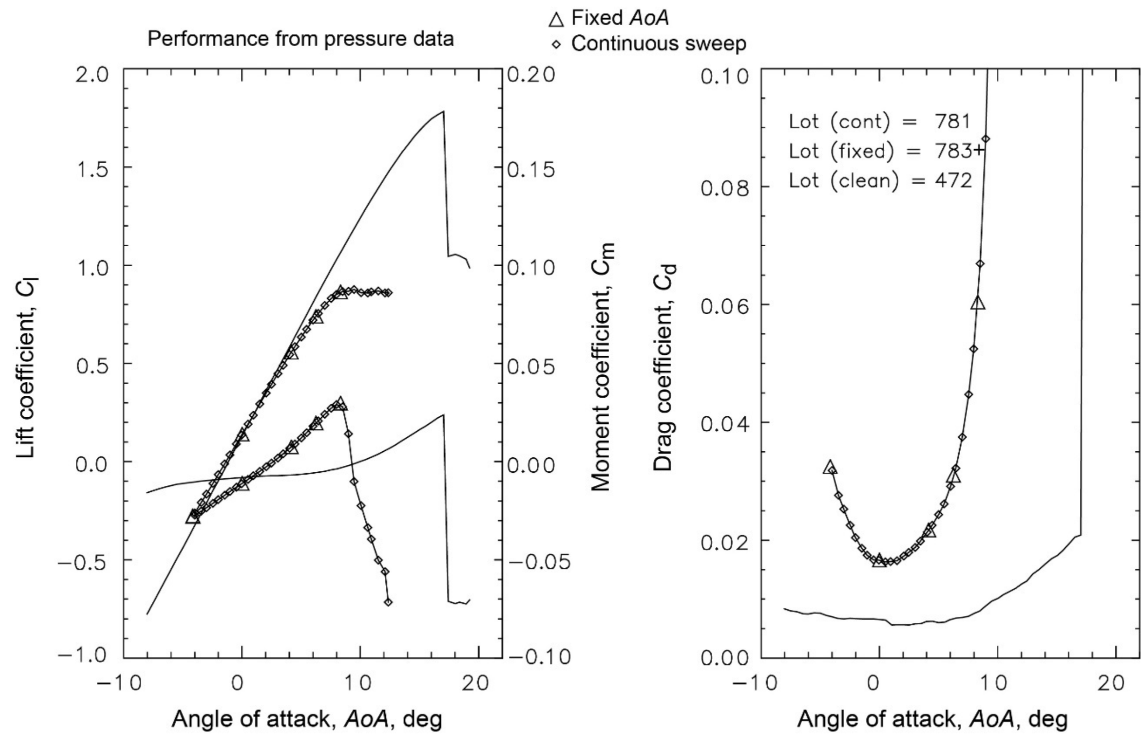

Horn Ice—Lot EG1164: M = 0.29 and Re = 12.1–12.2×10[6]

Appendix G.—F1 Full-Scale Model Tests

Horn Ice—Lot EG1164: M = 0.29 and Re = 12.1–12.2×10^6

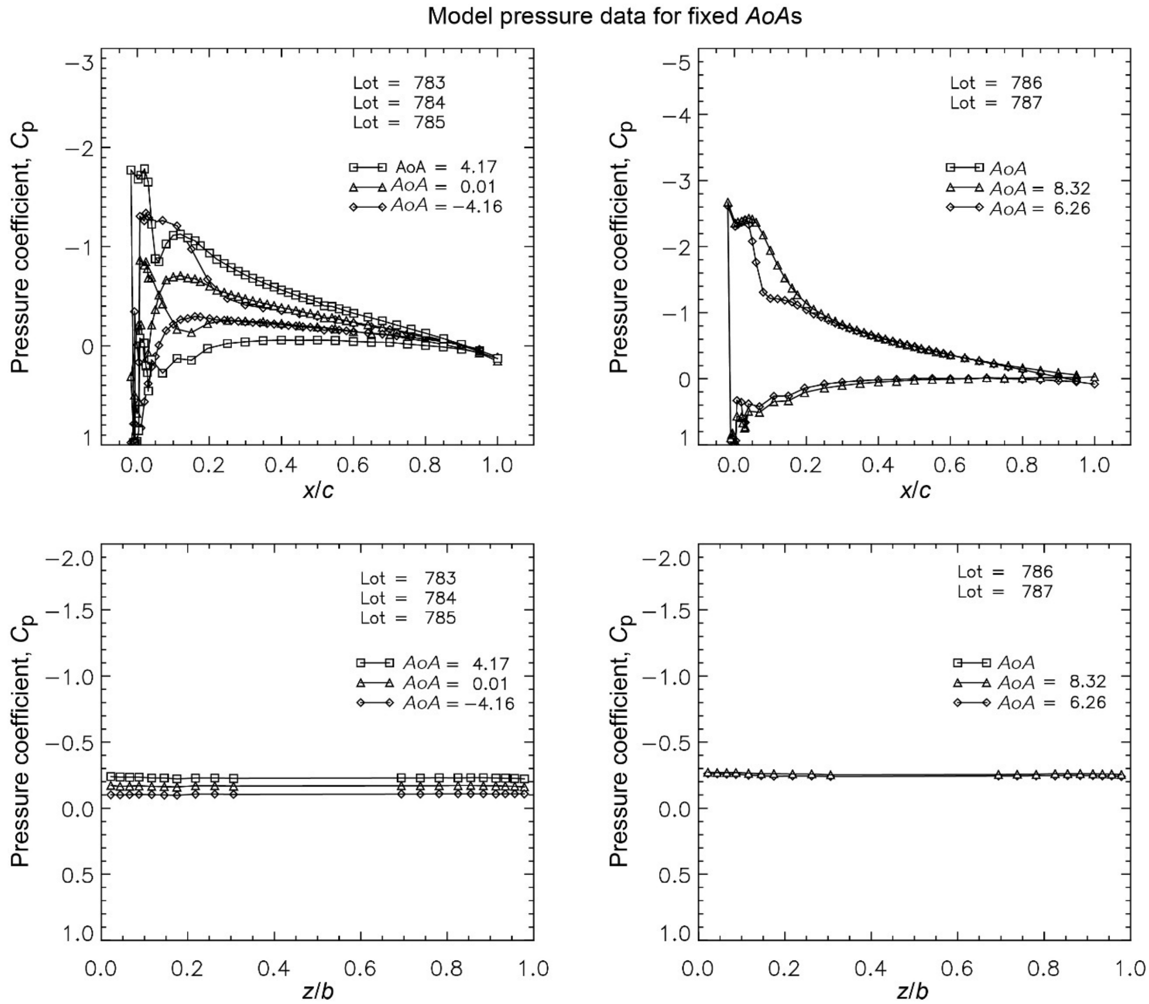

Horn Ice—Lot EG1164: M = 0.29 and Re = 12.1–12.2×10^6

Appendix G.—F1 Full-Scale Model Tests

Horn Ice—Lot EG1164: M = 0.29 and Re = 12.1–12.2×10^6

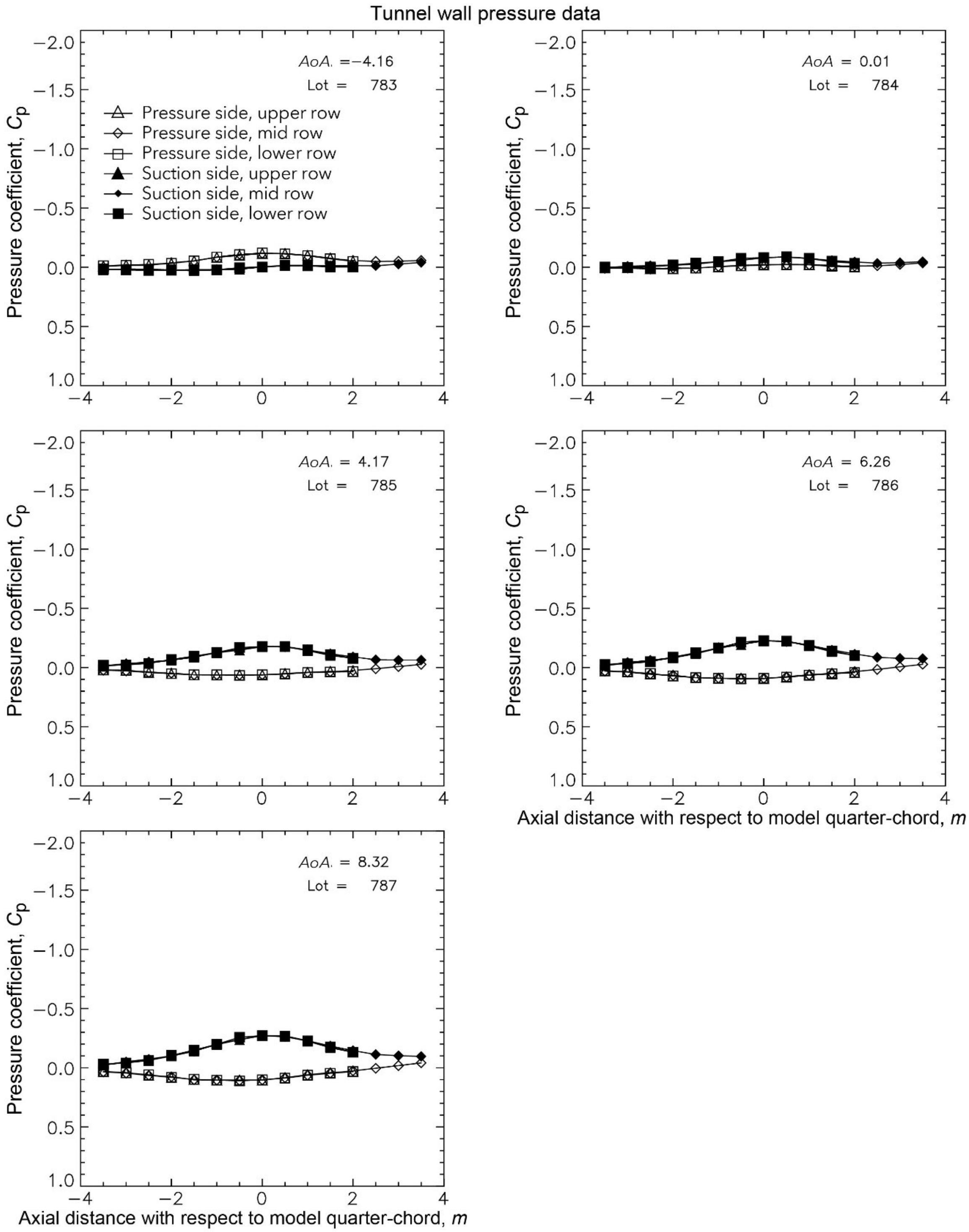

Horn Ice—Lot EG1164: M = 0.29 and Re = 12.1–12.2×10^6

Appendix G.—F1 Full-Scale Model Tests

Horn Ice—Lot EG1164: M = 0.29 and Re = 12.1–12.2×10^6

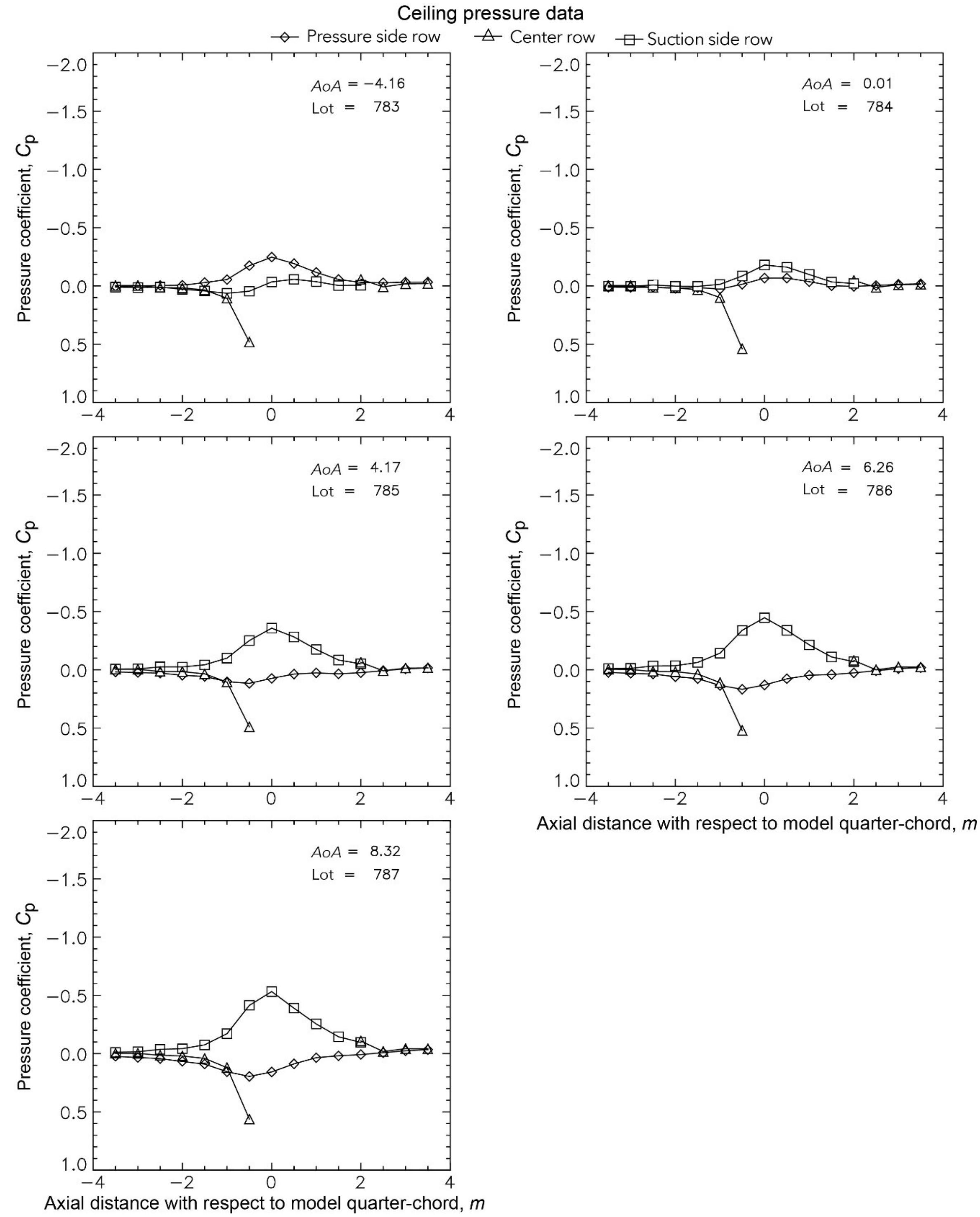

Horn Ice—Lot EG1164: M = 0.29 and Re = 12.1–12.2×10^6

Appendix G.—F1 Full-Scale Model Tests

Horn Ice—Lot EG1164: M = 0.29 and Re = 12.1–12.2×10^6

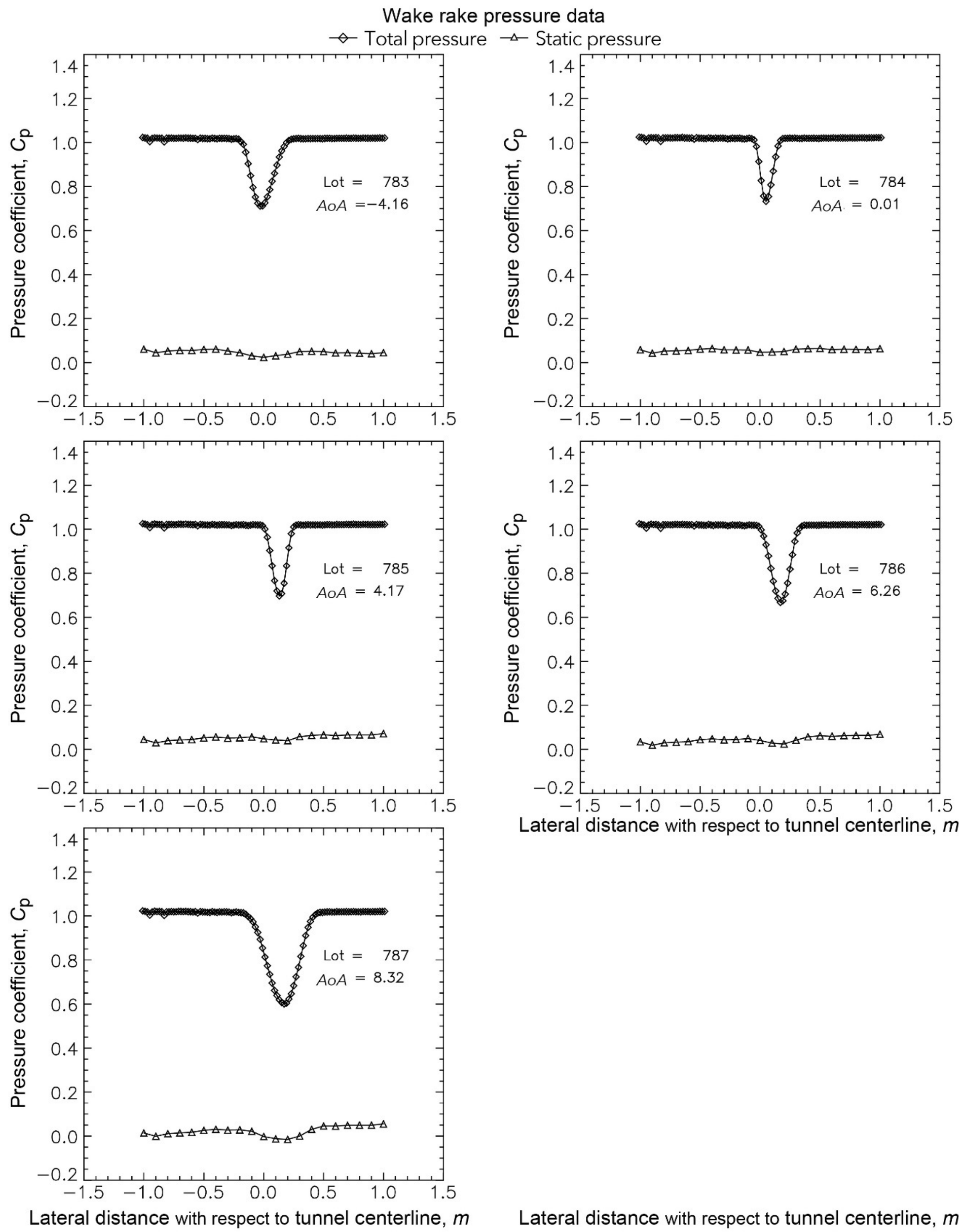

Horn Ice—Lot EG1164: M = 0.29 and Re = 12.1–12.2×10^6

Appendix G.—F1 Full-Scale Model Tests

Streamwise Ice 1—Lot EG1162: M = 0.10 and Re = 4.5×10^6

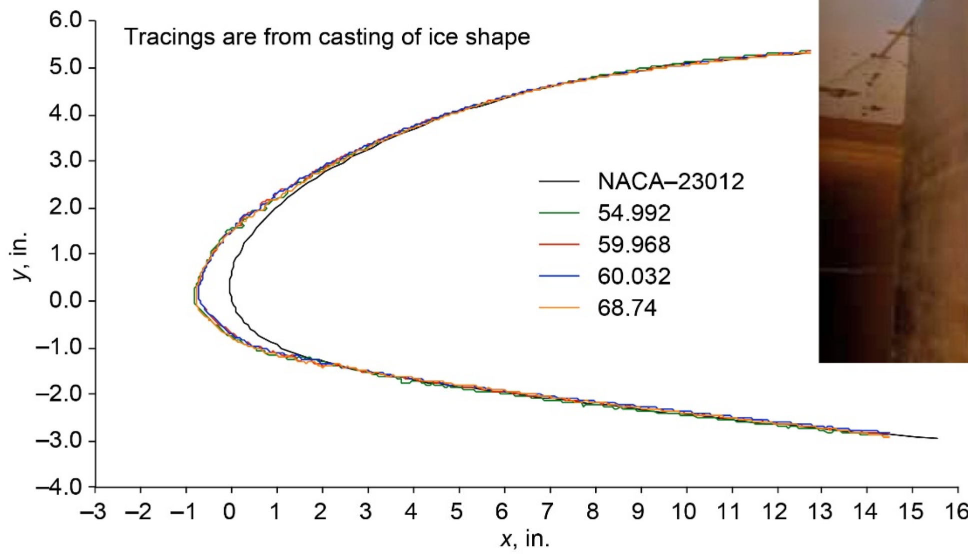

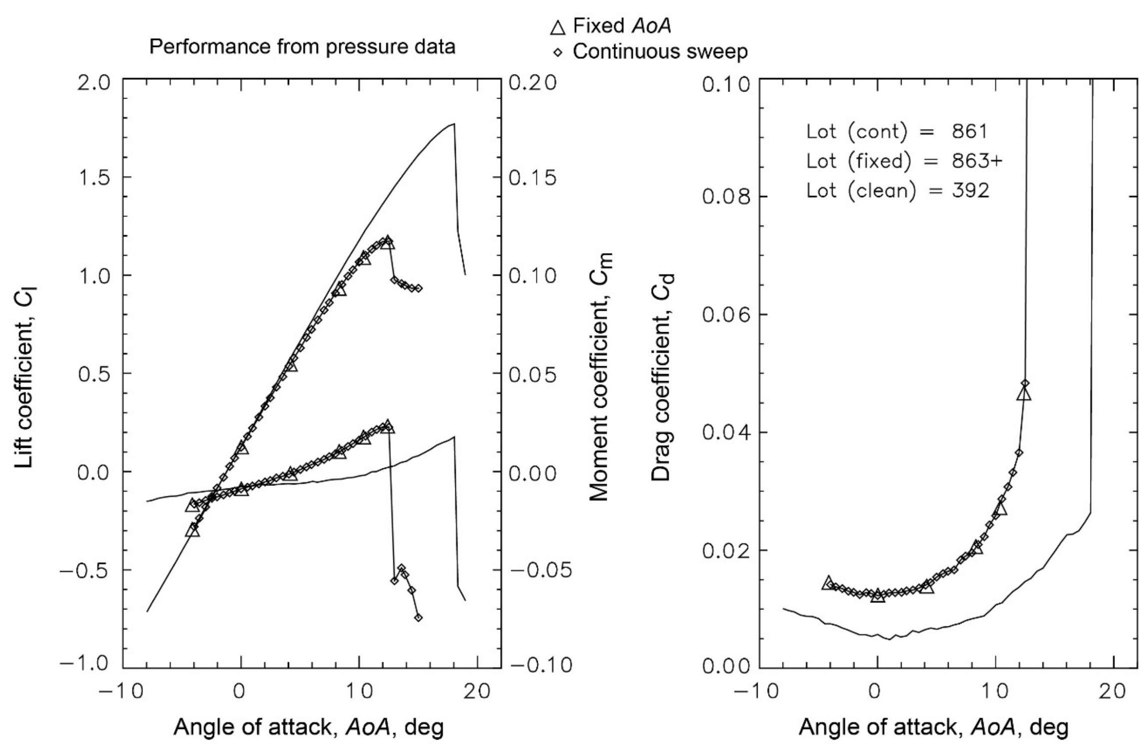

Streamwise Ice 1—Lot EG1162: M = 0.10 and Re = 4.5×10^6

Appendix G.—F1 Full-Scale Model Tests

Streamwise Ice 1—Lot EG1162: M = 0.10 and Re = 4.5×10[6]

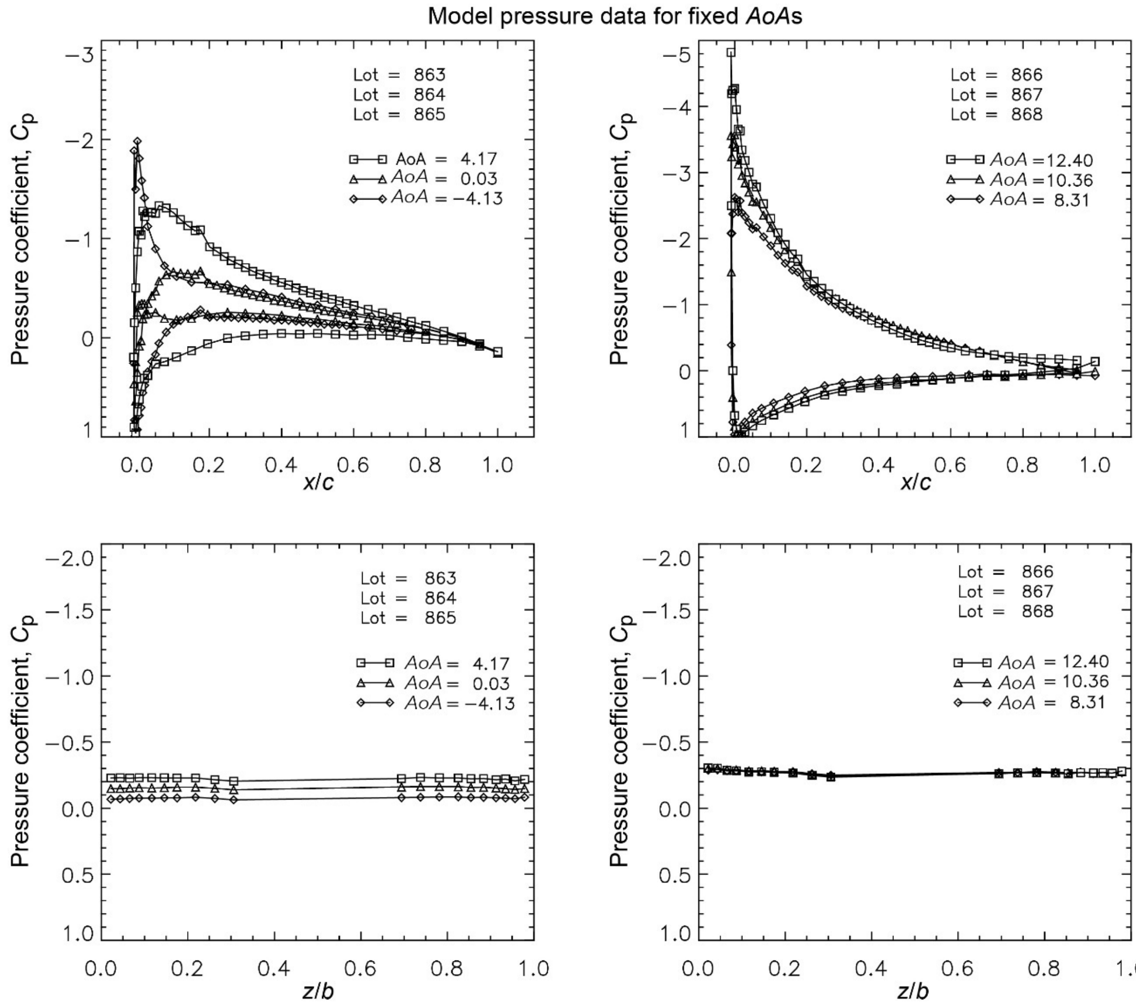

Streamwise Ice 1—Lot EG1162: M = 0.10 and Re = 4.5×10[6]

Appendix G.—F1 Full-Scale Model Tests

Streamwise Ice 1—Lot EG1162: M = 0.10 and Re = 4.5×10⁶

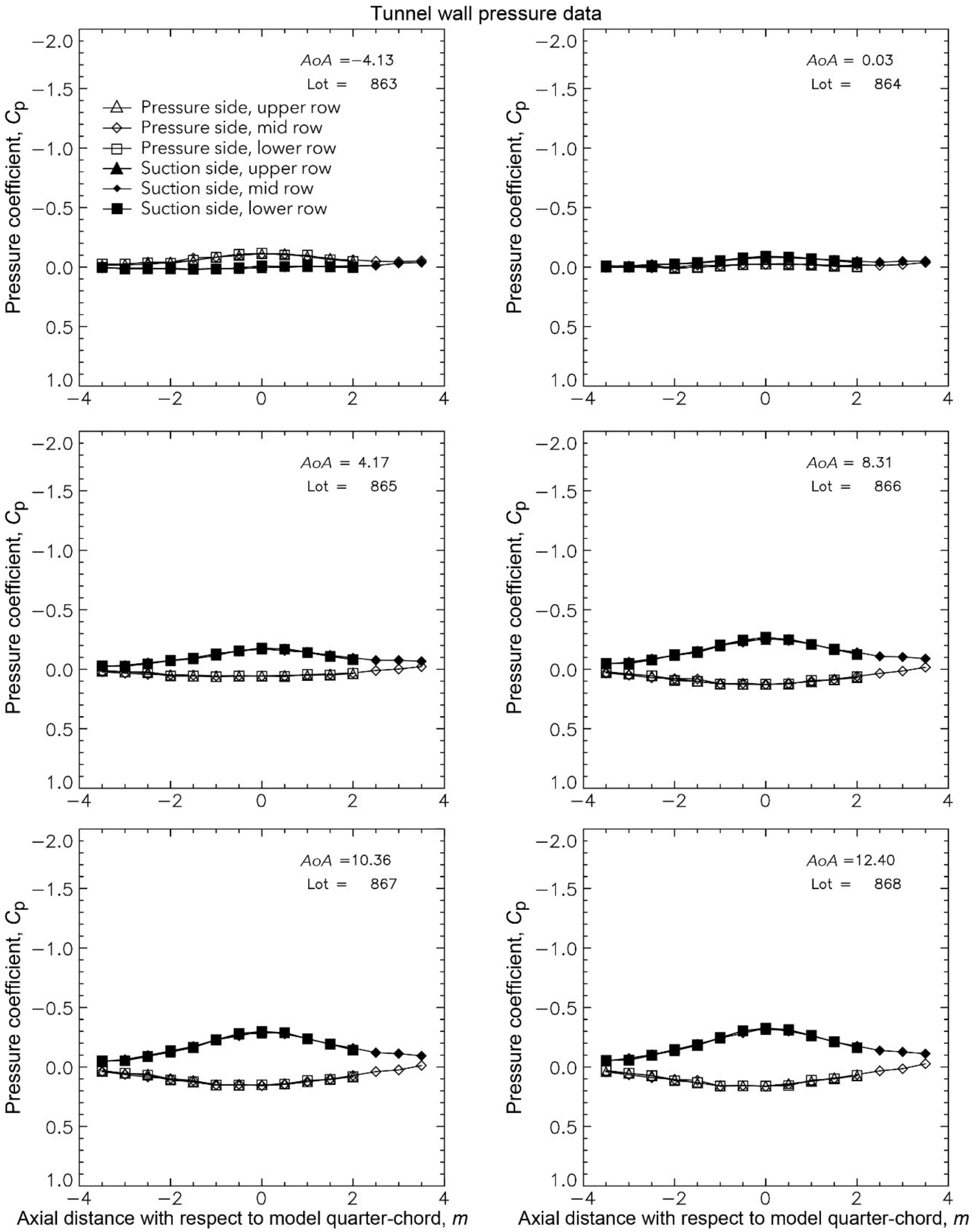

Streamwise Ice 1—Lot EG1162: M = 0.10 and Re = 4.5×10⁶

Appendix G.—F1 Full-Scale Model Tests

Streamwise Ice 1—Lot EG1162: M = 0.10 and Re = 4.5×10^6

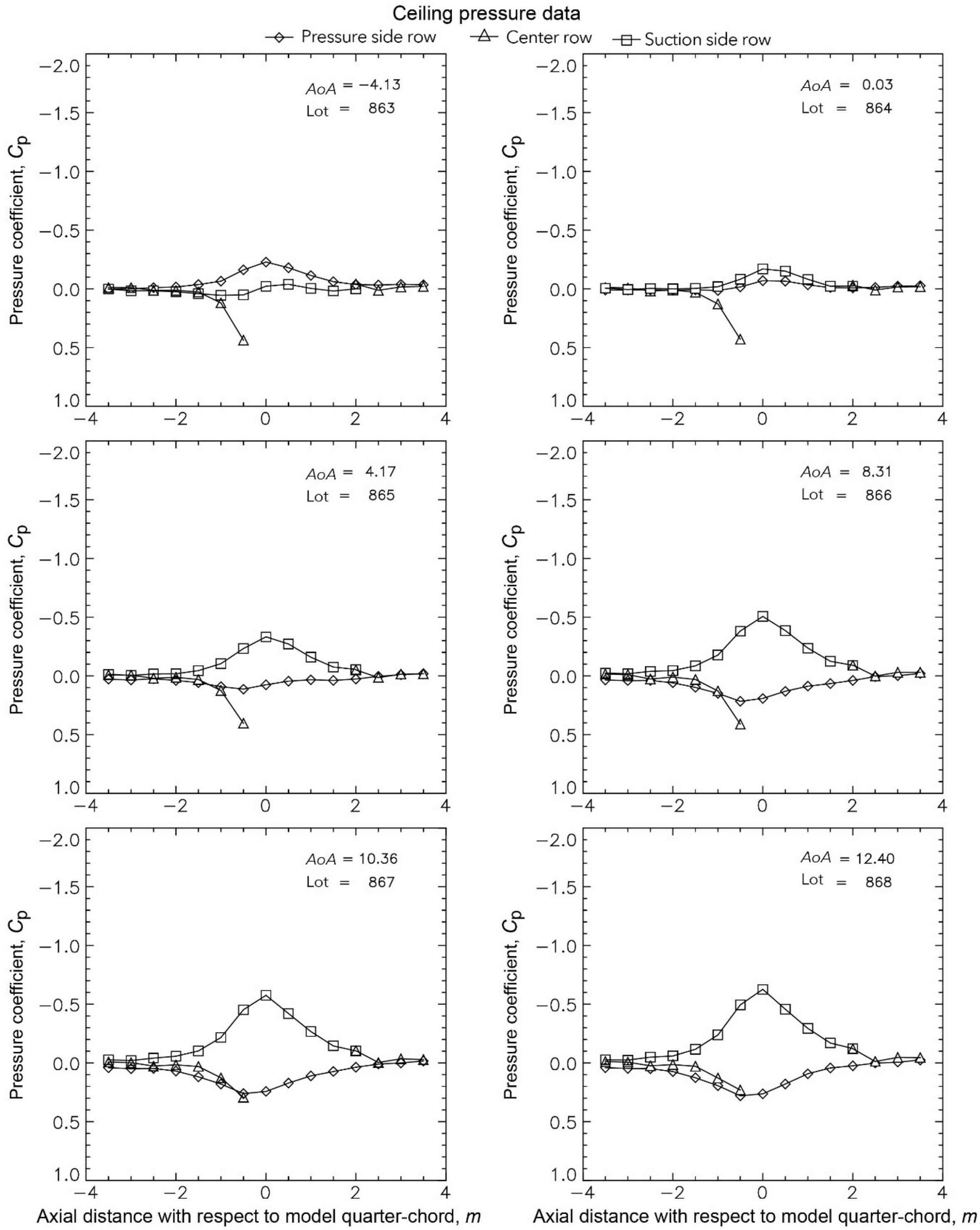

Streamwise Ice 1—Lot EG1162: M = 0.10 and Re = 4.5×10^6

Appendix G.—F1 Full-Scale Model Tests

Streamwise Ice 1—Lot EG1162: M = 0.10 and Re = 4.5×10^6

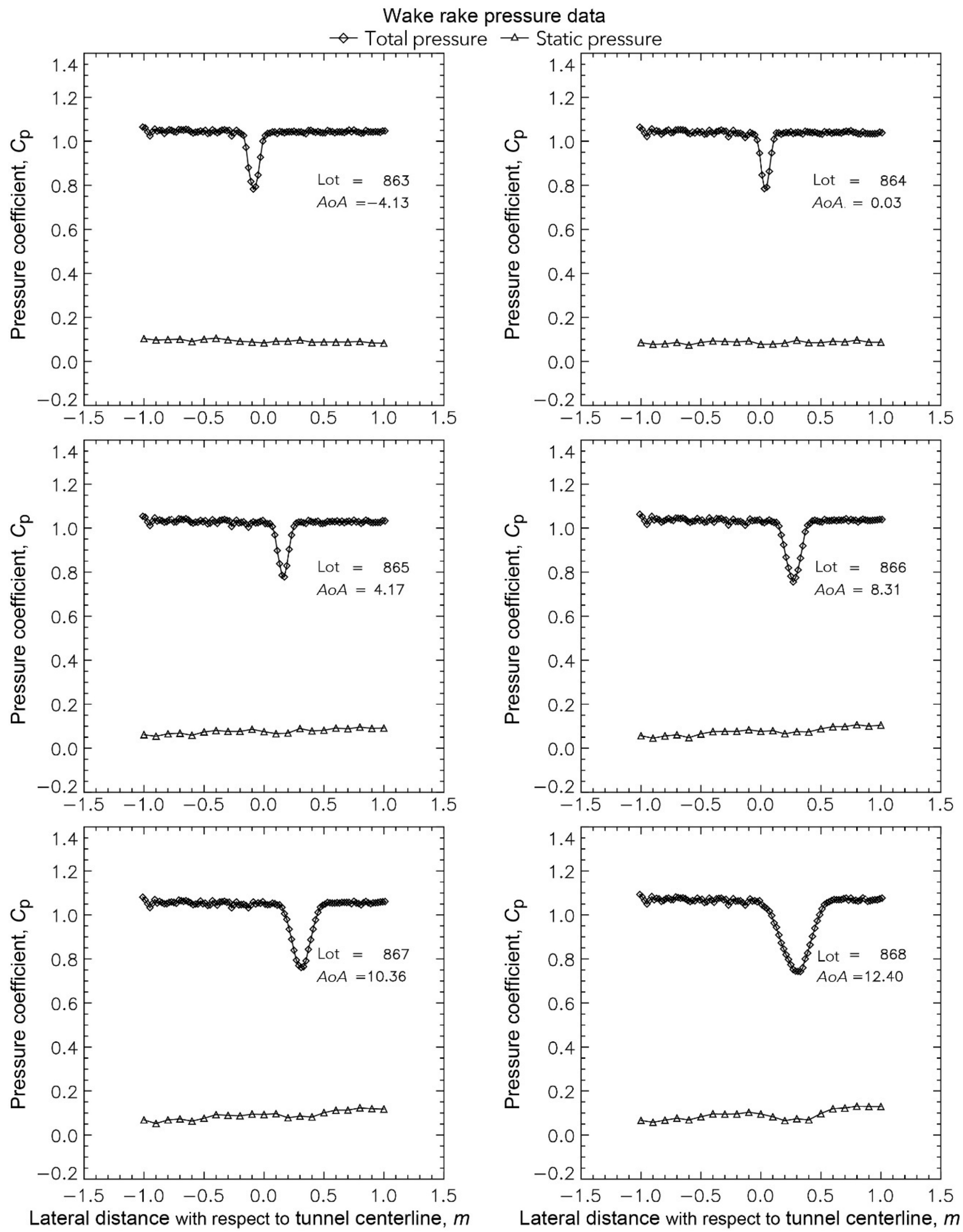

Streamwise Ice 1—Lot EG1162: M = 0.10 and Re = 4.5×10^6

Appendix G.—F1 Full-Scale Model Tests

Streamwise Ice 1—Lot EG1162: M = 0.10 and Re = 8.4–8.5×10^6

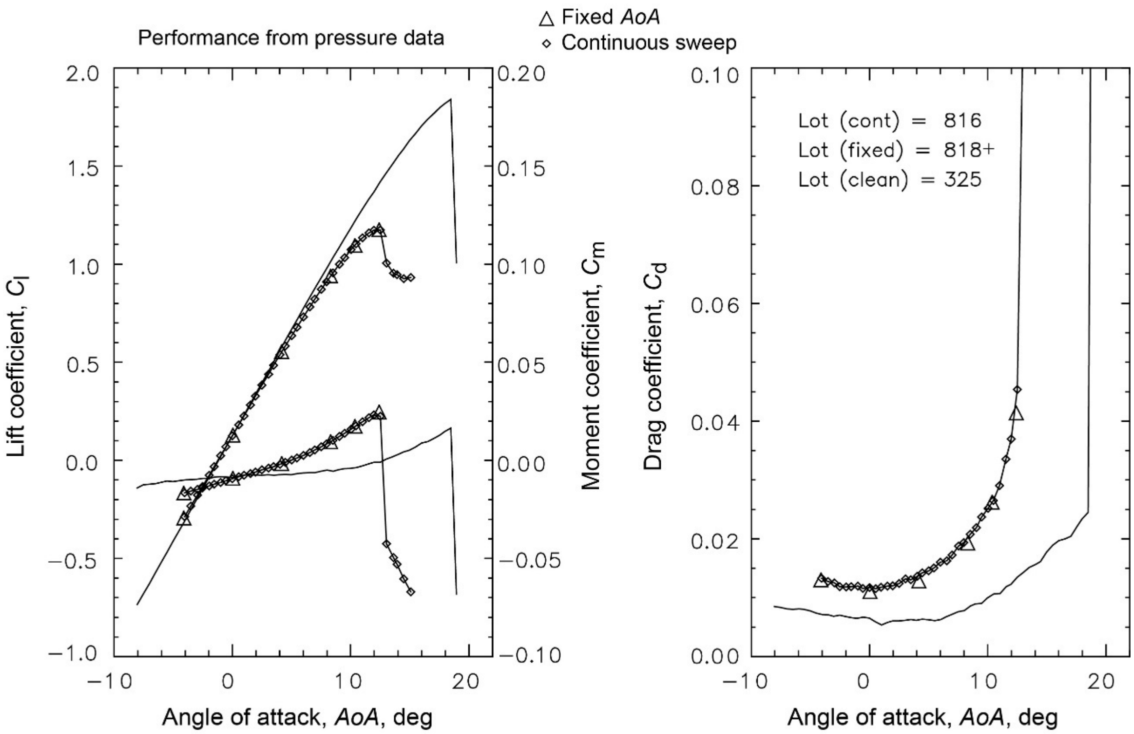

Streamwise Ice 1—Lot EG1162: M = 0.10 and Re = 8.4–8.5×10^6

Appendix G.—F1 Full-Scale Model Tests

Streamwise Ice 1—Lot EG1162: M = 0.10 and Re = 8.4–8.5×10^6

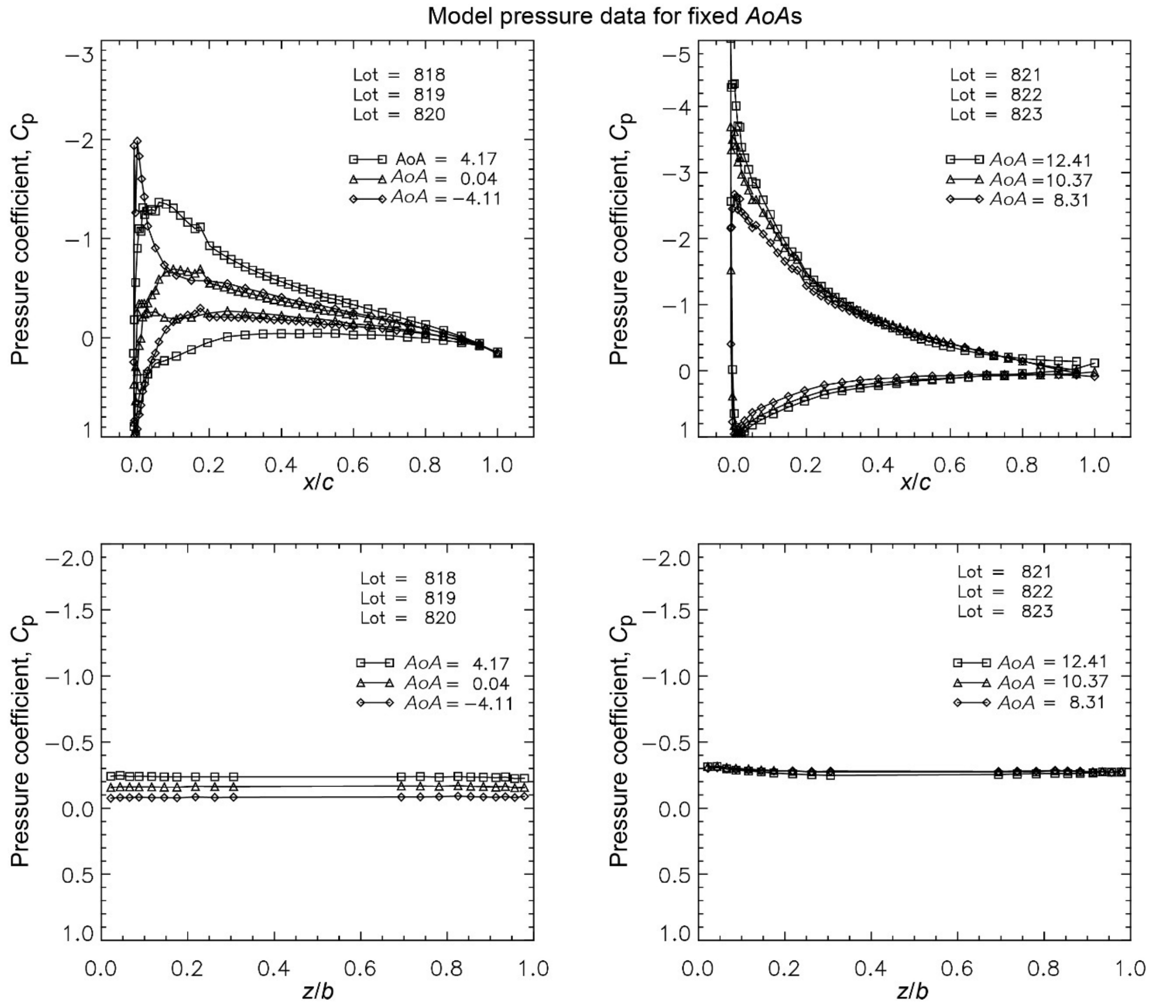

Streamwise Ice 1—Lot EG1162: M = 0.10 and Re = 8.4–8.5×10^6

Appendix G.—F1 Full-Scale Model Tests

Streamwise Ice 1—Lot EG1162: M = 0.10 and Re = 8.4–8.5×10^6

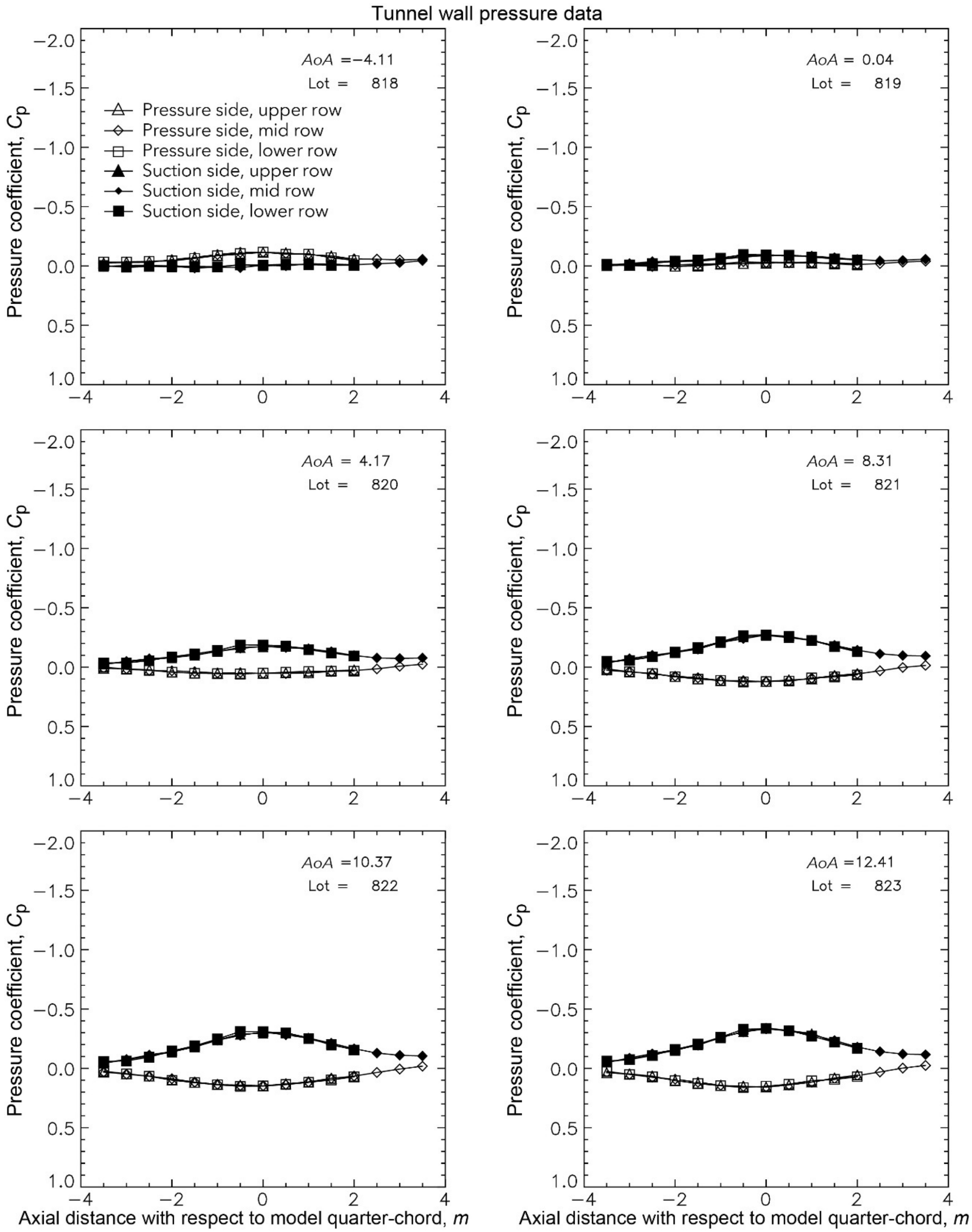

Streamwise Ice 1—Lot EG1162: M = 0.10 and Re = 8.4–8.5×10^6

Streamwise Ice 1—Lot EG1162: M = 0.10 and Re = 8.4–8.5×10^6

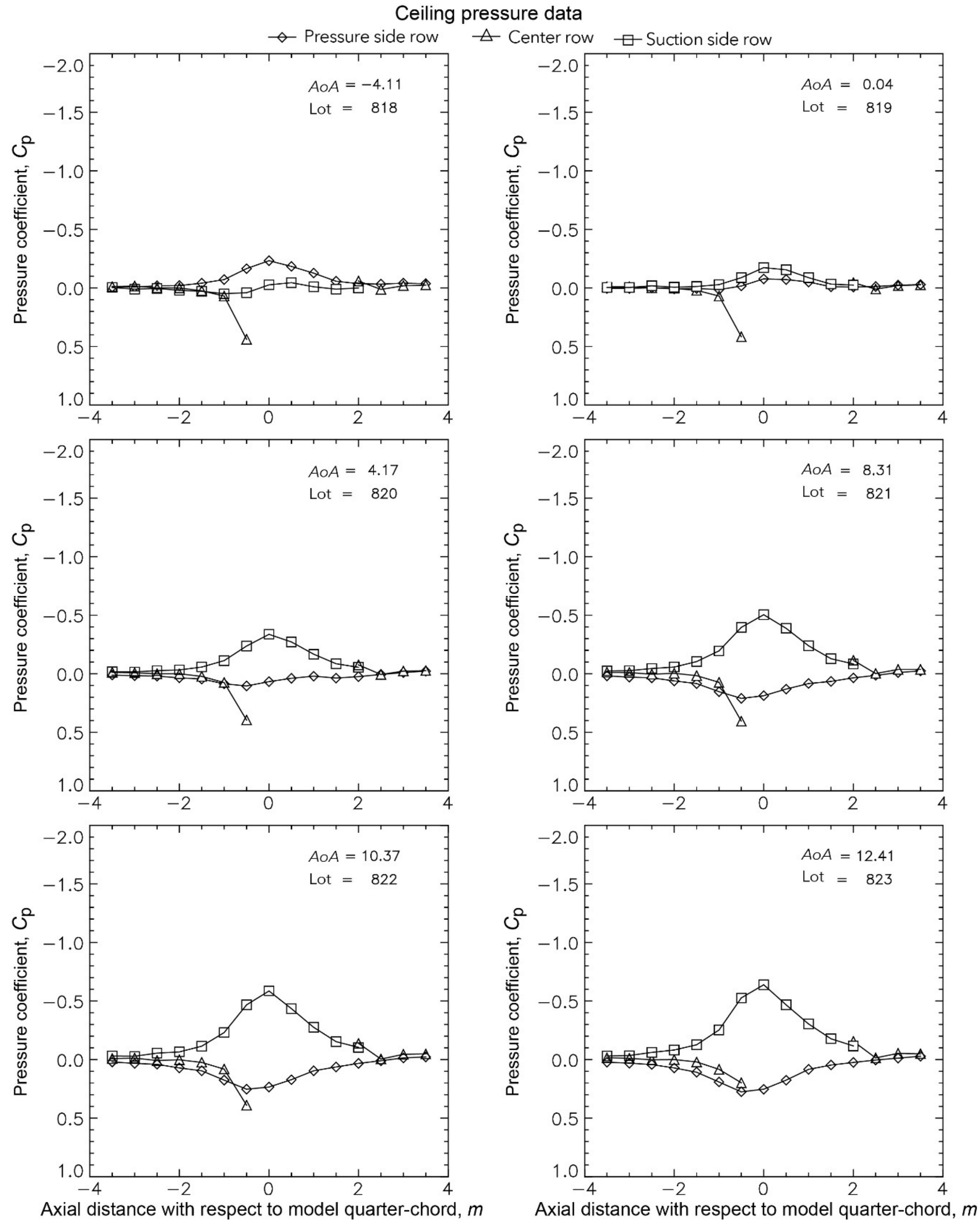

Streamwise Ice 1—Lot EG1162: M = 0.10 and Re = 8.4–8.5×10^6

Appendix G.—F1 Full-Scale Model Tests

Streamwise Ice 1—Lot EG1162: M = 0.10 and Re = 8.4–8.5×10^6

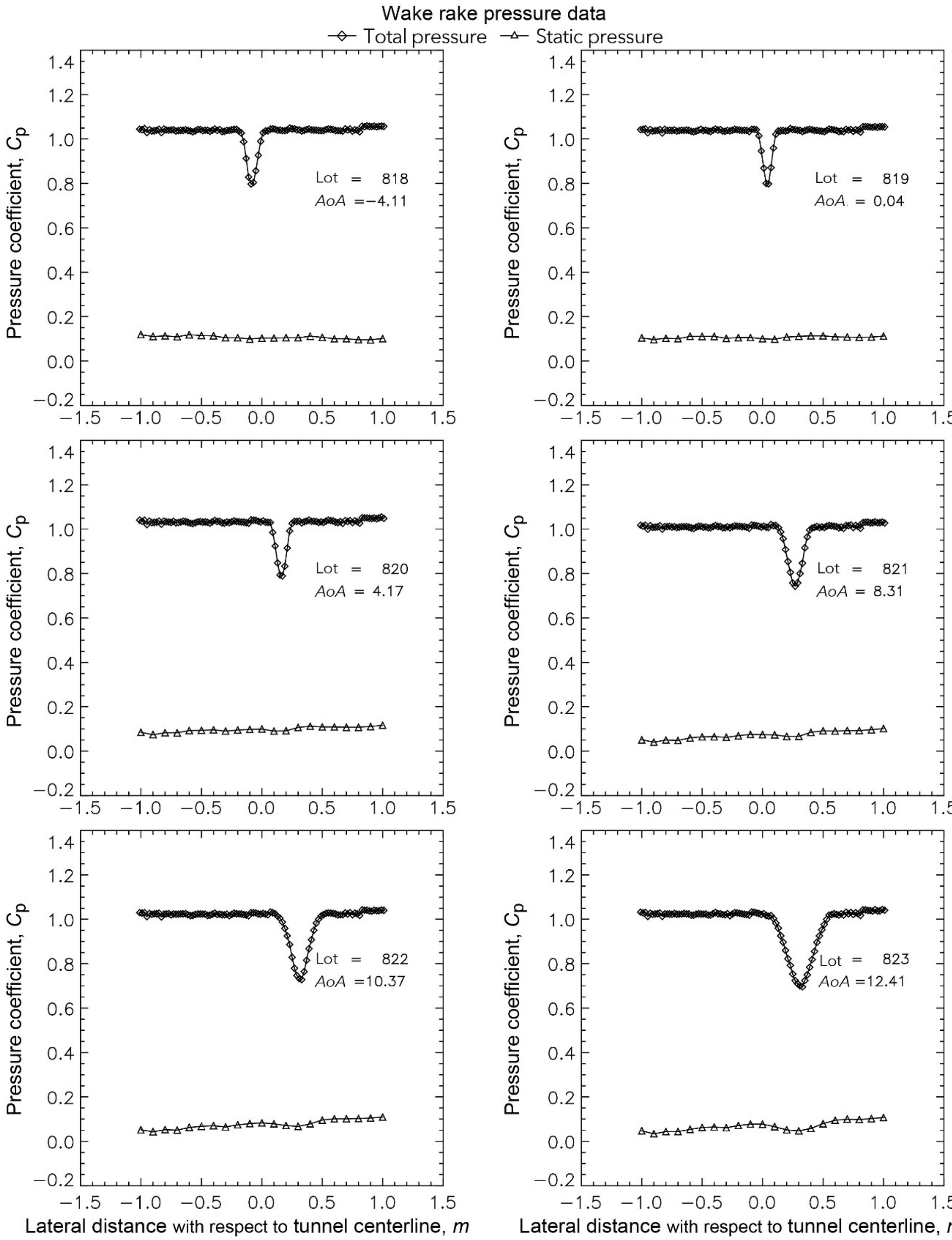

Streamwise Ice 1—Lot EG1162: M = 0.10 and Re = 8.4–8.5×10^6

Appendix G.—F1 Full-Scale Model Tests

Streamwise Ice 1—Lot EG1162: M = 0.10 and Re = 12.1–12.3×10^6

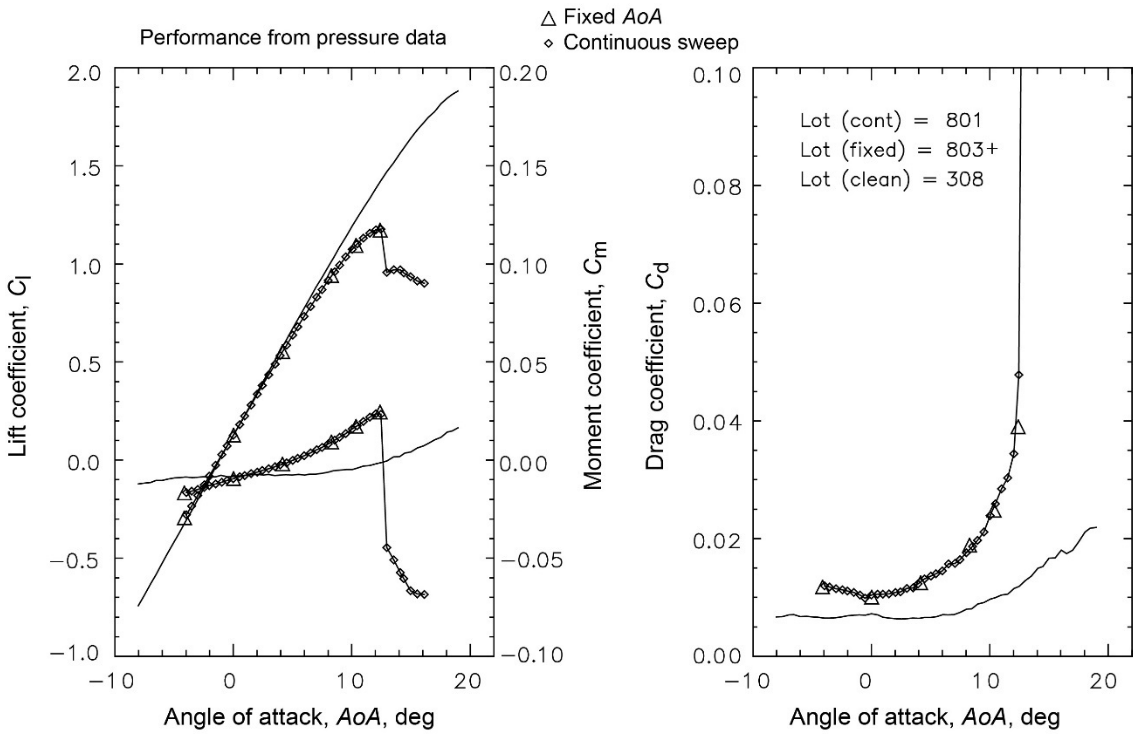

Streamwise Ice 1—Lot EG1162: M = 0.10 and Re = 12.1–12.3×10^6

Appendix G.—F1 Full-Scale Model Tests

Streamwise Ice 1—Lot EG1162: M = 0.10 and Re = 12.1–12.3×10⁶

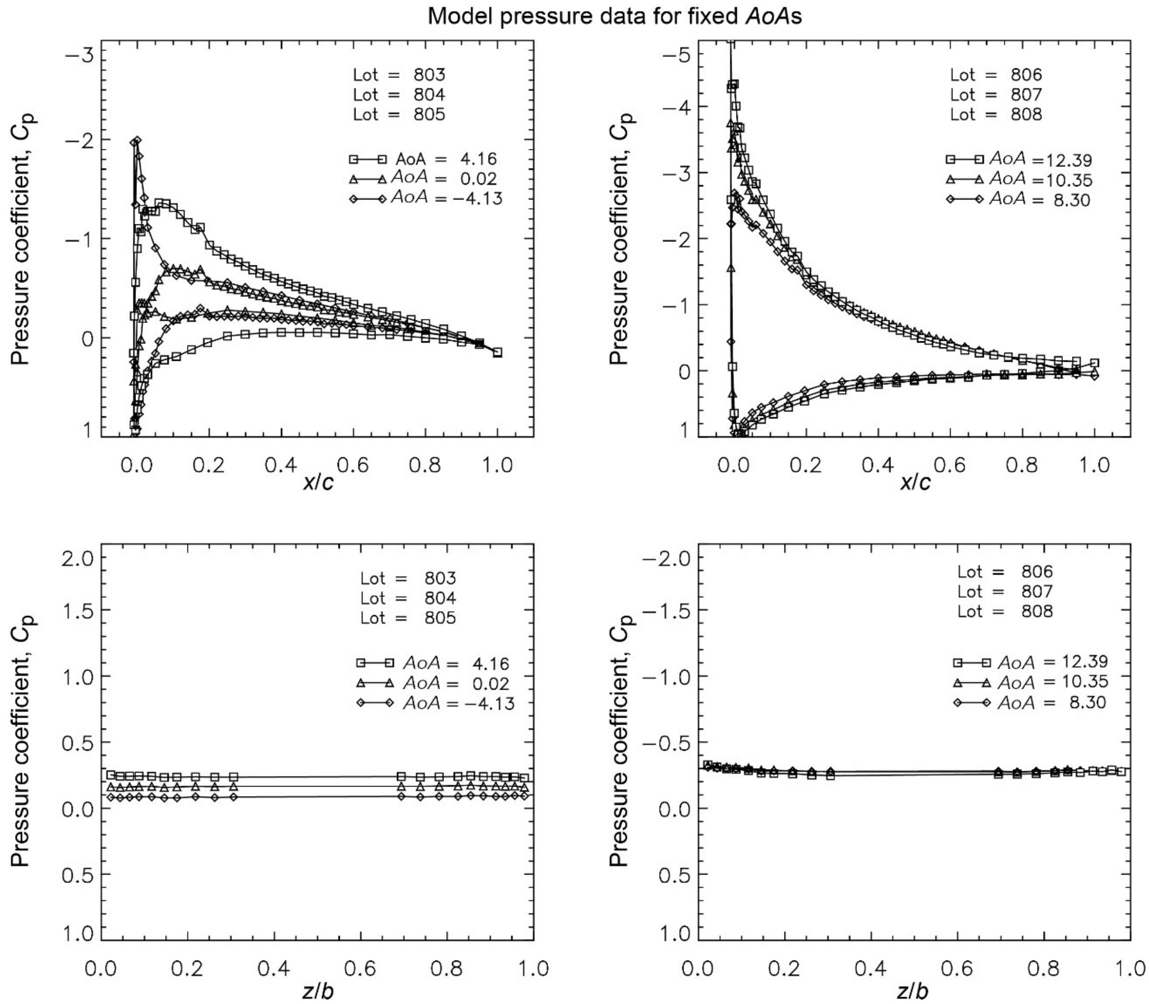

Streamwise Ice 1—Lot EG1162: M = 0.10 and Re = 12.1–12.3×10⁶

Appendix G.—F1 Full-Scale Model Tests

Streamwise Ice 1—Lot EG1162: M = 0.10 and Re = 12.1–12.3×10^6

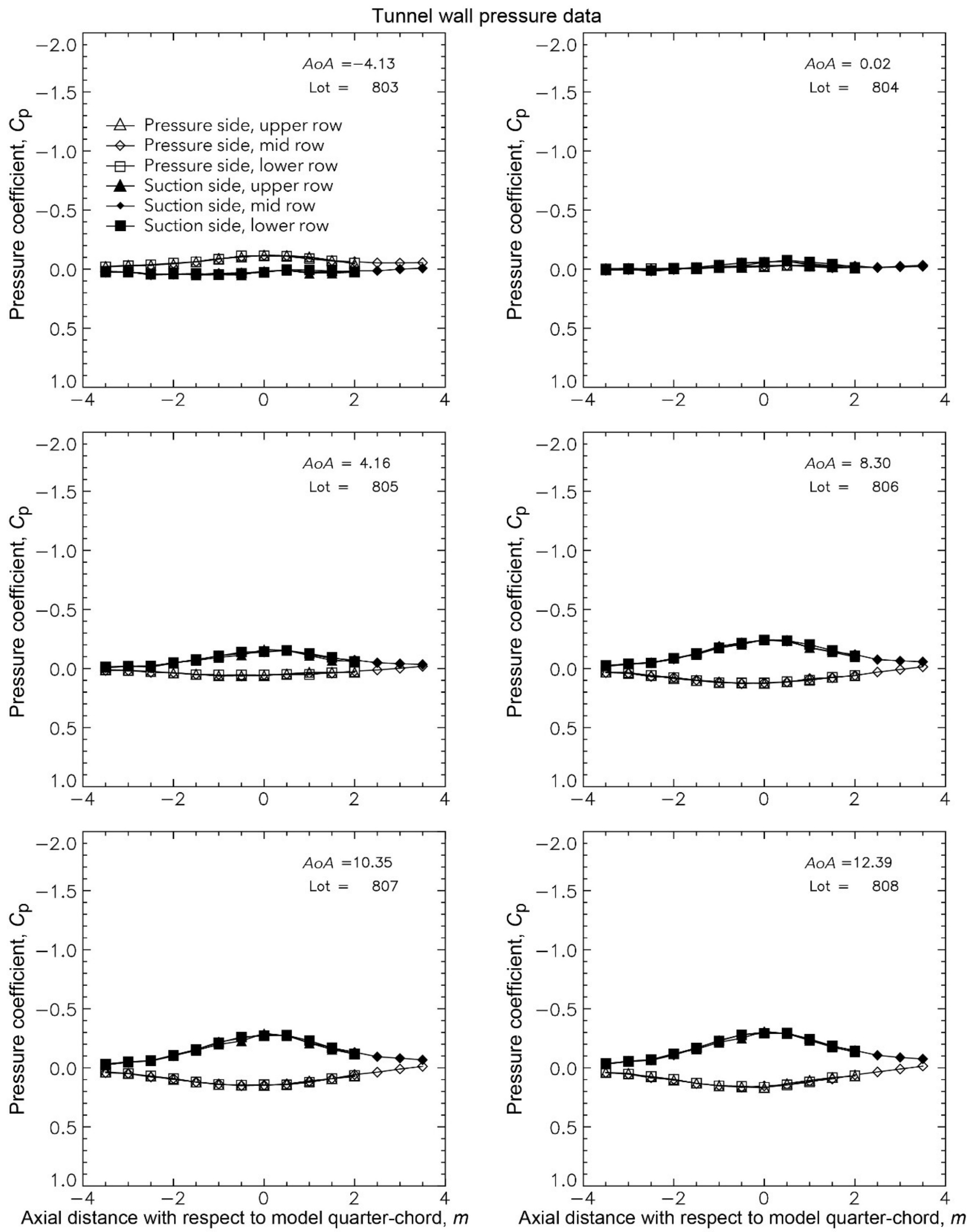

Streamwise Ice 1—Lot EG1162: M = 0.10 and Re = 12.1–12.3×10^6

Appendix G.—F1 Full-Scale Model Tests

Streamwise Ice 1—Lot EG1162: M = 0.10 and Re = 12.1–12.3×10^6

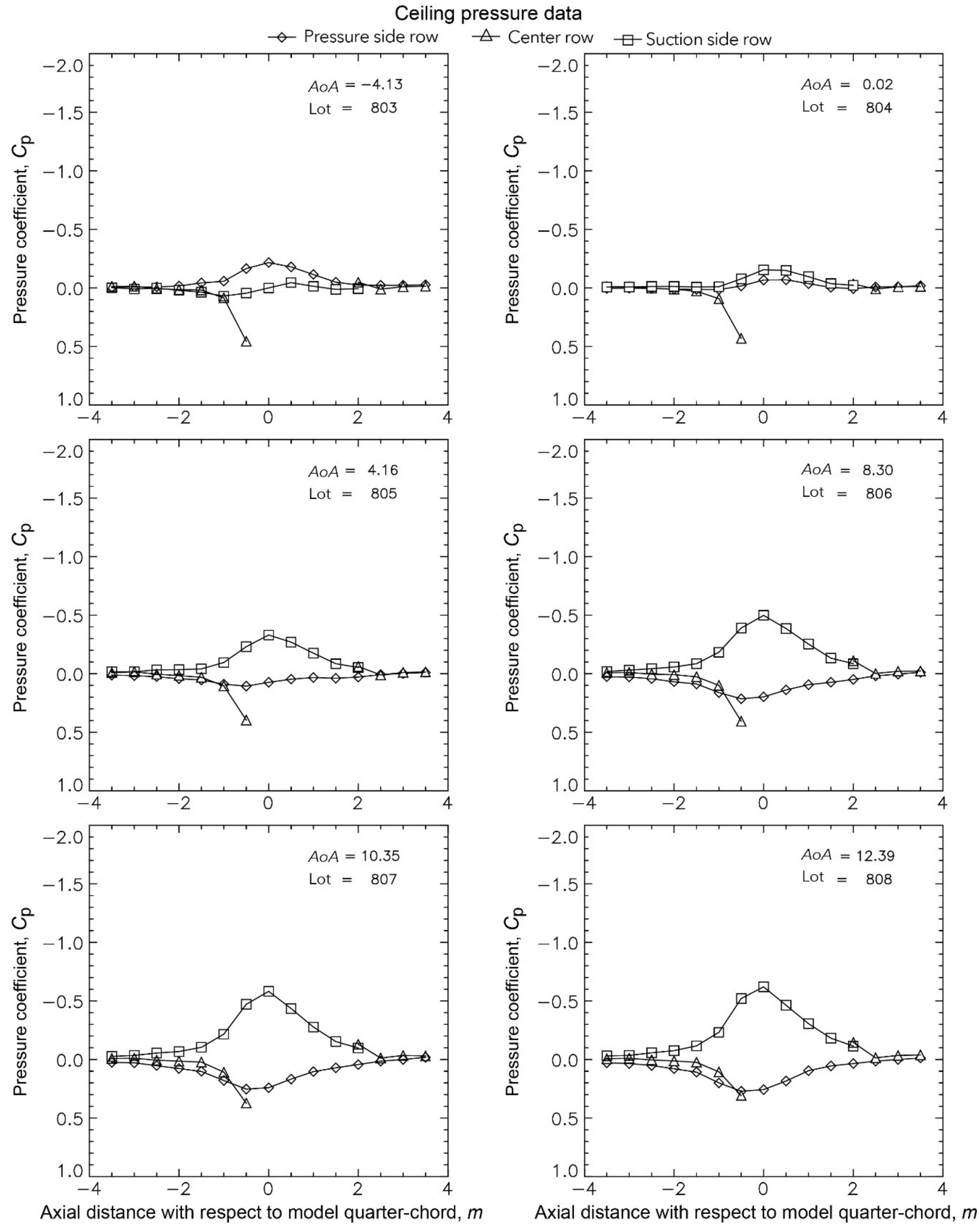

Streamwise Ice 1—Lot EG1162: M = 0.10 and Re = 12.1–12.3×10^6

Appendix G.—F1 Full-Scale Model Tests

Streamwise Ice 1—Lot EG1162: M = 0.10 and Re = 12.1–12.3×10^6

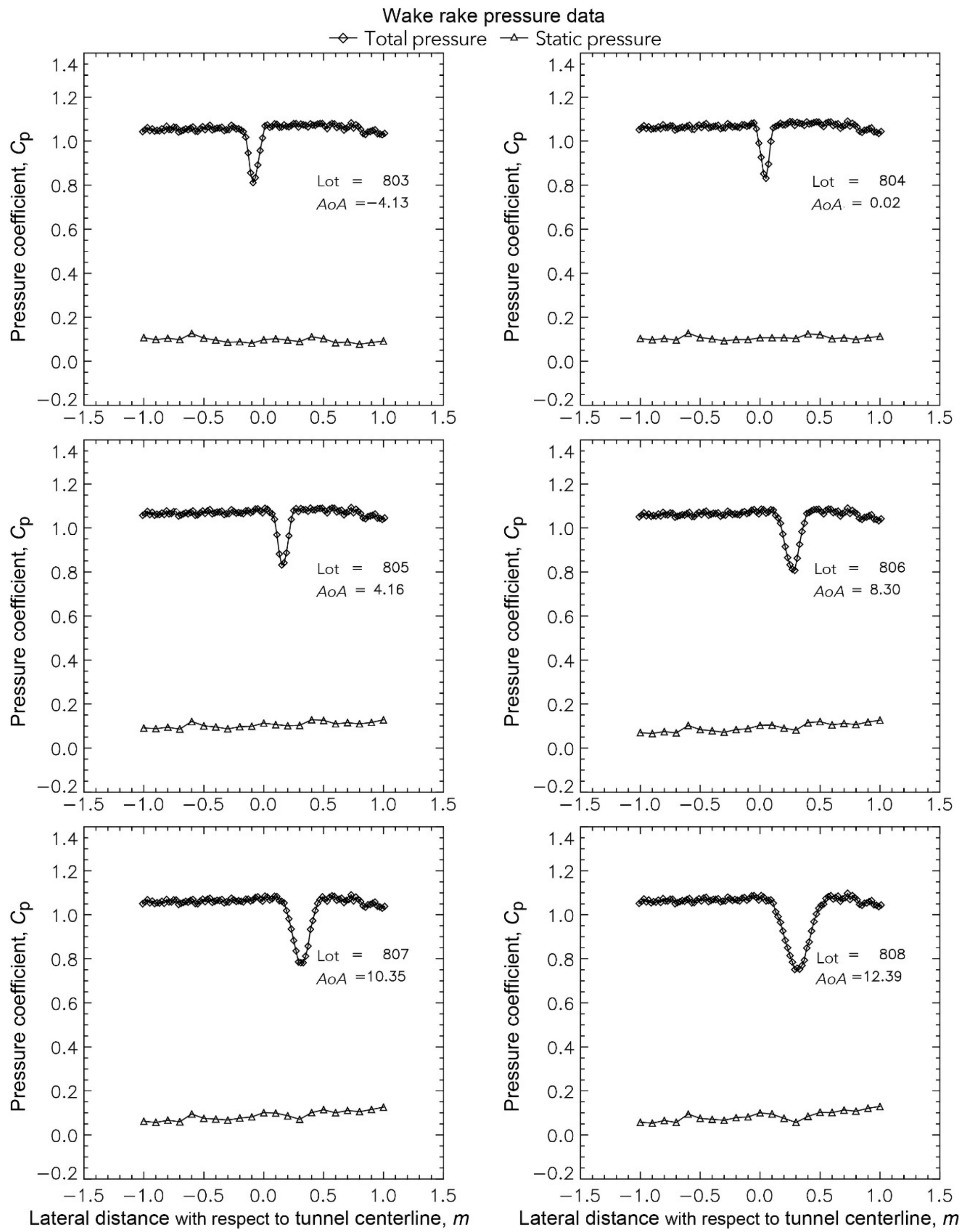

Streamwise Ice 1—Lot EG1162: M = 0.10 and Re = 12.1–12.3×10^6

Appendix G.—F1 Full-Scale Model Tests

Streamwise Ice 1—Lot EG1162: M = 0.20 to 0.21 and Re = 8.9–9.0×10^6

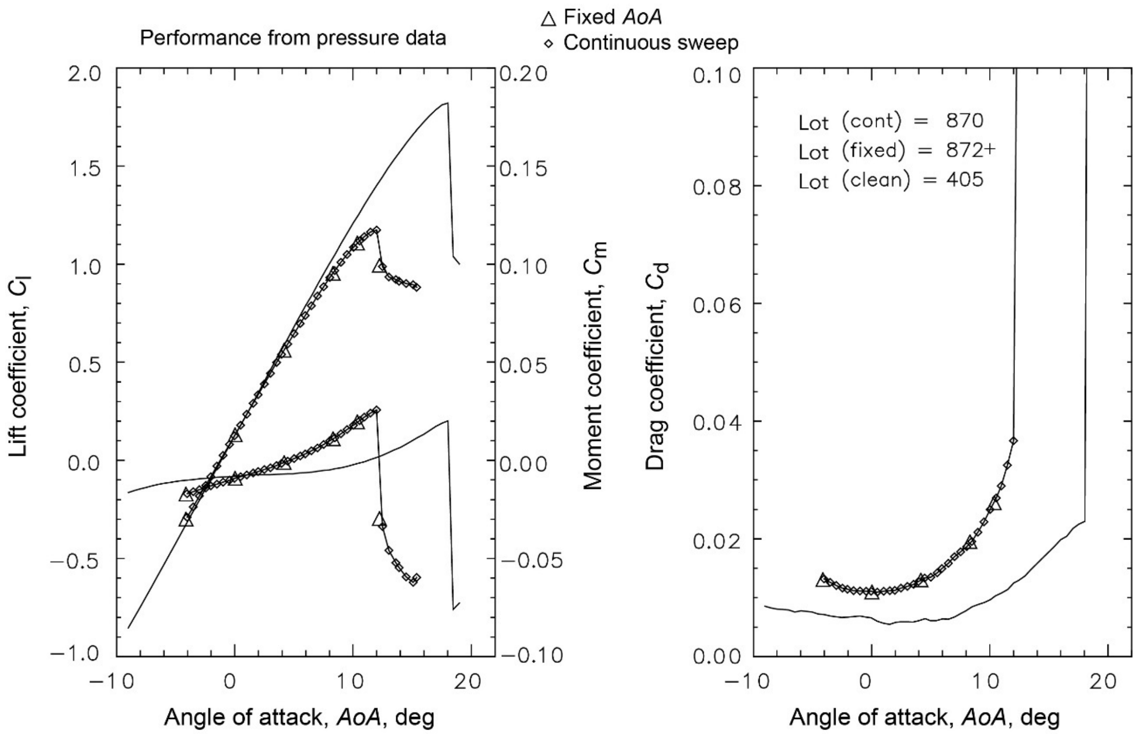

Streamwise Ice 1—Lot EG1162: M = 0.20 to 0.21 and Re = 8.9–9.0×10^6

Appendix G.—F1 Full-Scale Model Tests

Streamwise Ice 1—Lot EG1162: M = 0.20 to 0.21 and Re = 8.9–9.0×10^6

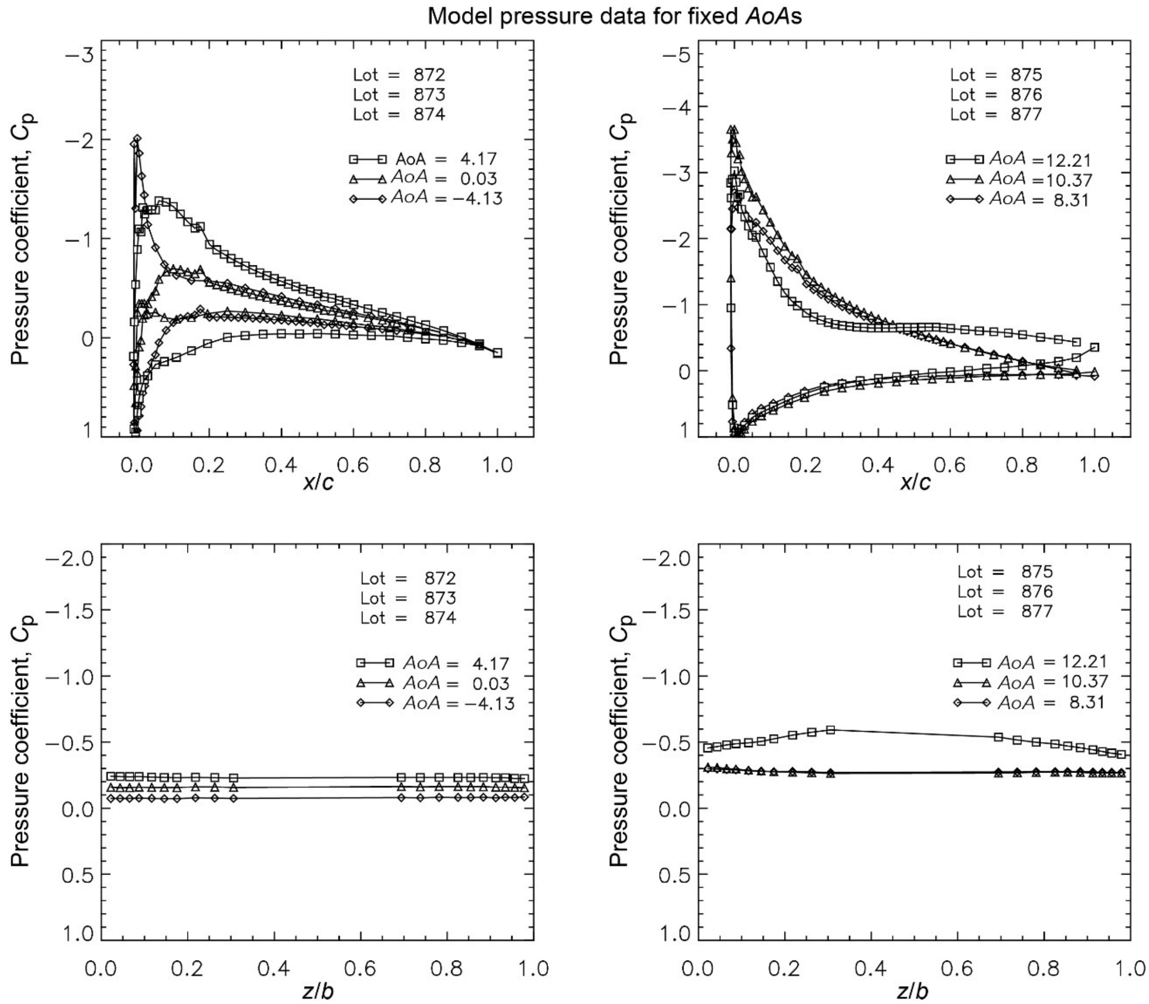

Streamwise Ice 1—Lot EG1162: M = 0.20 to 0.21 and Re = 8.9–9.0×10^6

Appendix G.—F1 Full-Scale Model Tests

Streamwise Ice 1—Lot EG1162: M = 0.20 to 0.21 and Re = 8.9–9.0×10^6

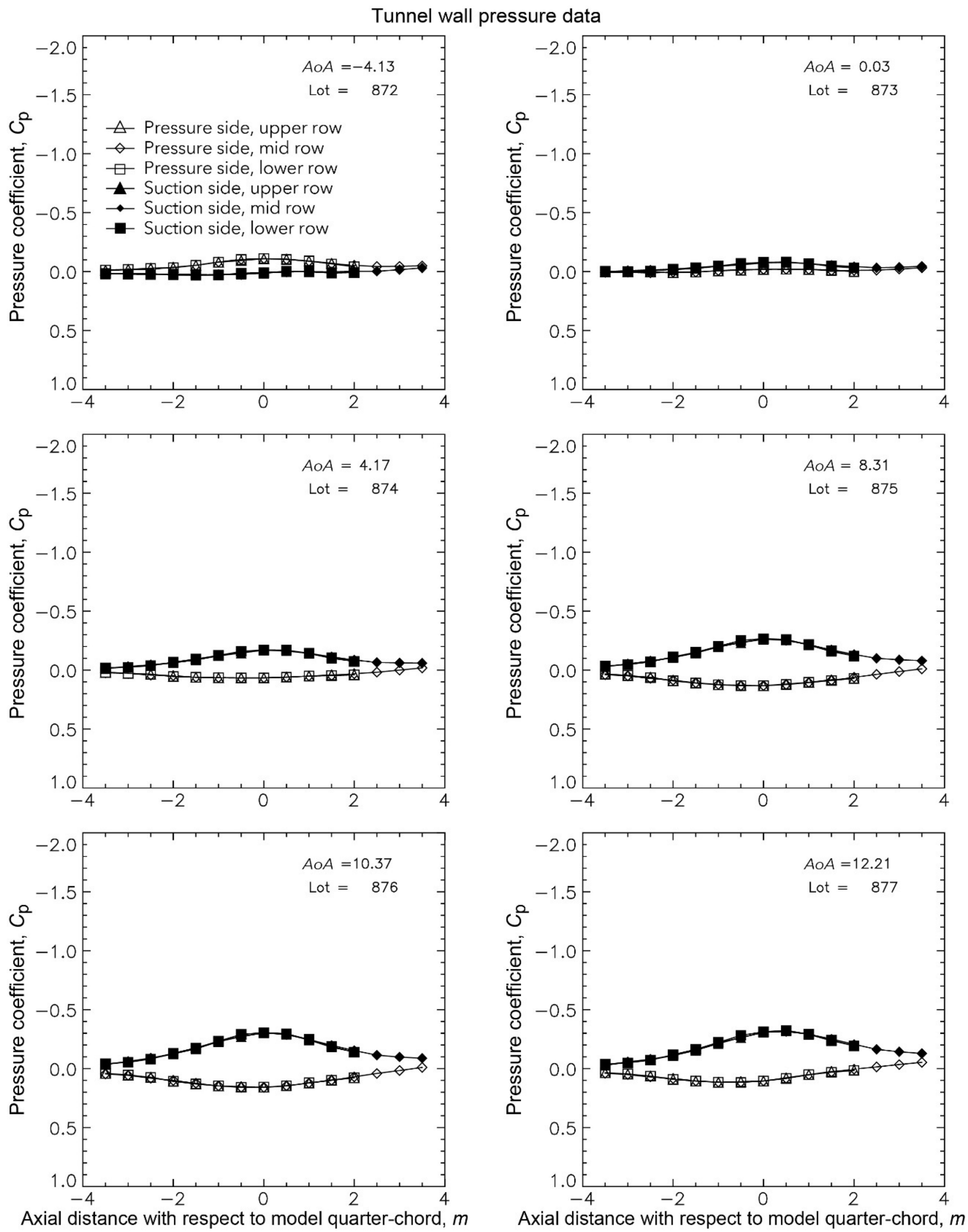

Streamwise Ice 1—Lot EG1162: M = 0.20 to 0.21 and Re = 8.9–9.0×10^6

Appendix G.—F1 Full-Scale Model Tests

Streamwise Ice 1—Lot EG1162: M = 0.20 to 0.21 and Re = 8.9–9.0×10^6

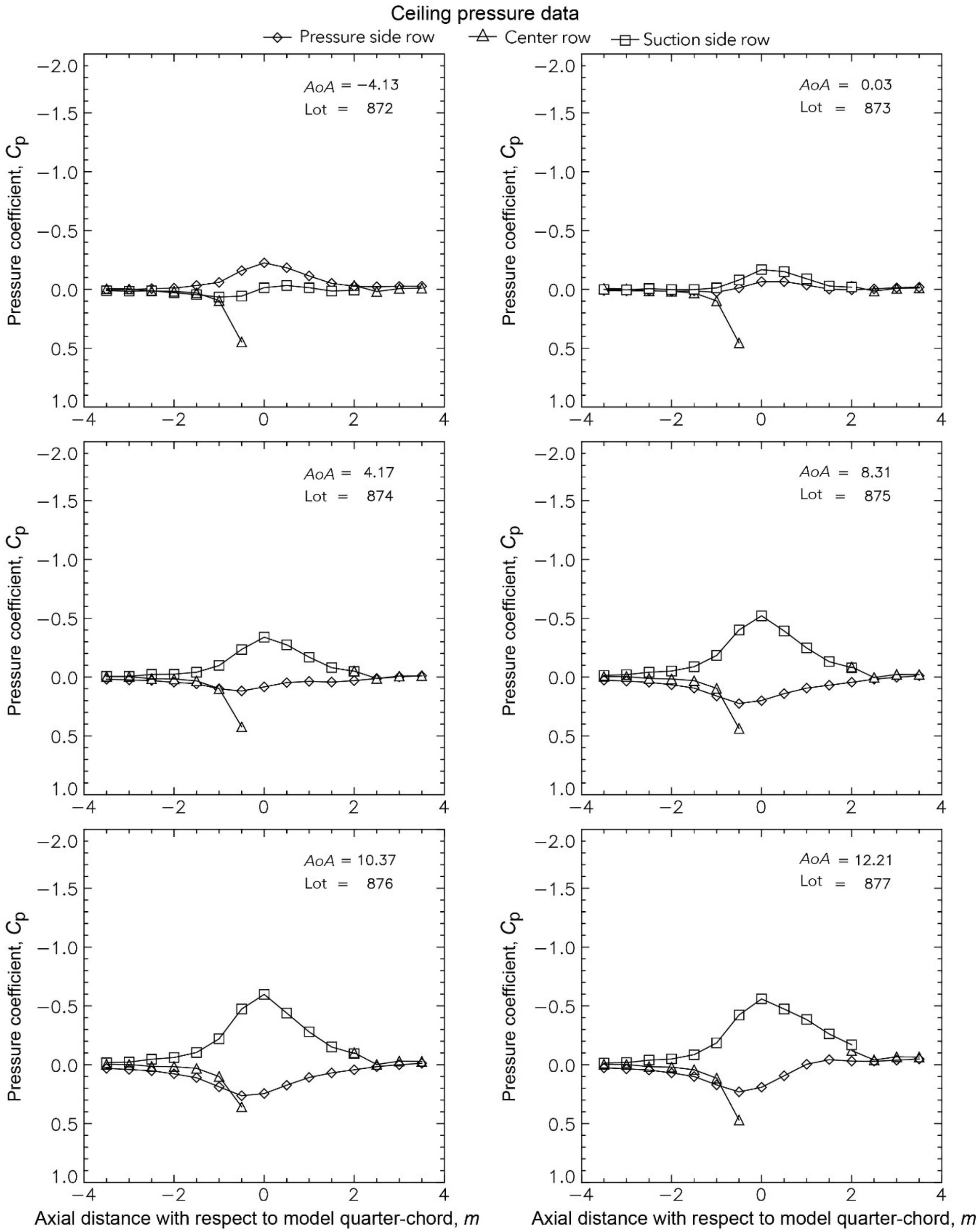

Streamwise Ice 1—Lot EG1162: M = 0.20 to 0.21 and Re = 8.9–9.0×10^6

Appendix G.—F1 Full-Scale Model Tests

Streamwise Ice 1—Lot EG1162: M = 0.20 to 0.21 and Re = 8.9–9.0×10^6

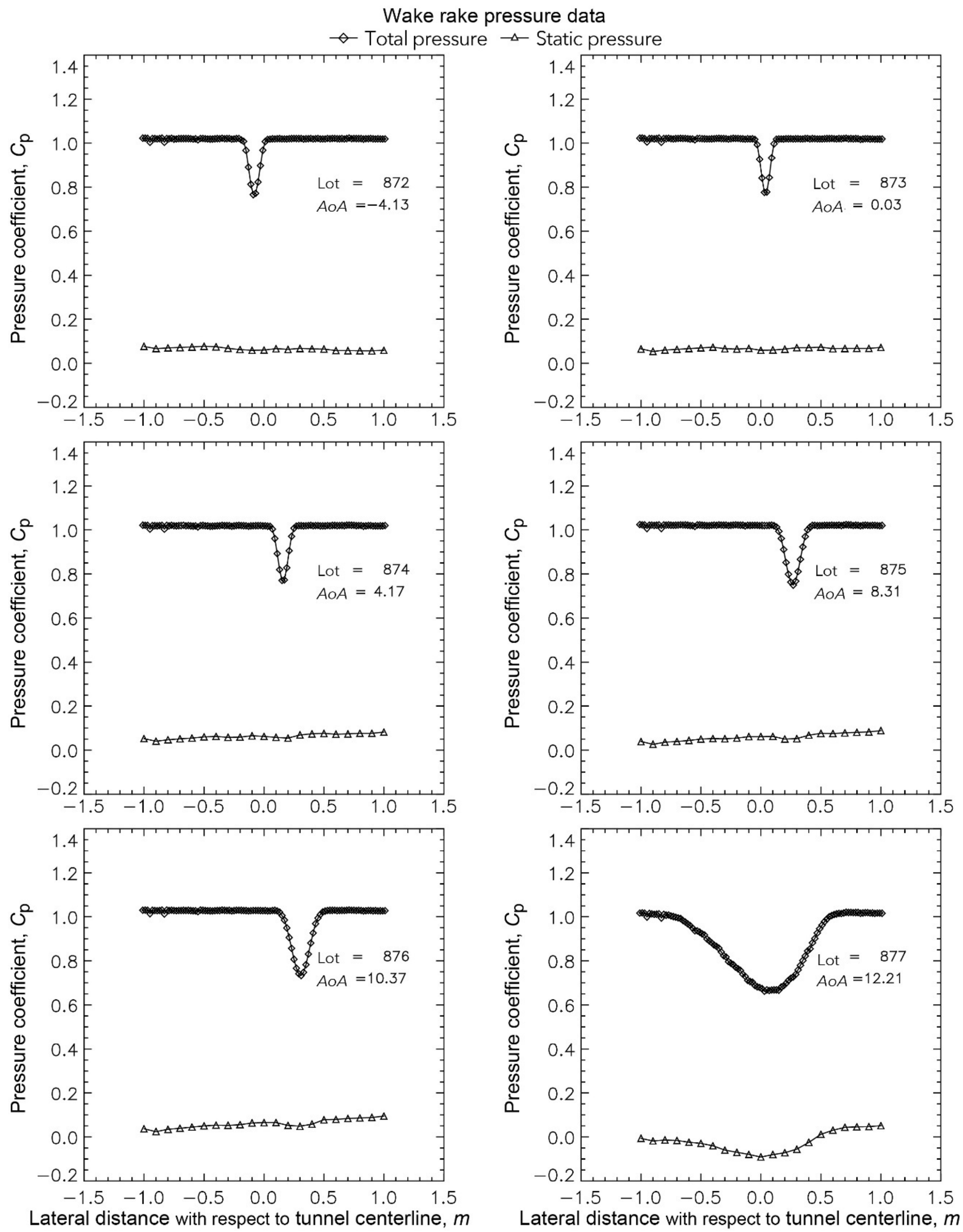

Streamwise Ice 1—Lot EG1162: M = 0.20 to 0.21 and Re = 8.9–9.0×10^6

Appendix G.—F1 Full-Scale Model Tests

Streamwise Ice 1—Lot EG1162: M = 0.20 to 0.21 and Re = 12.0–12.2×10^6

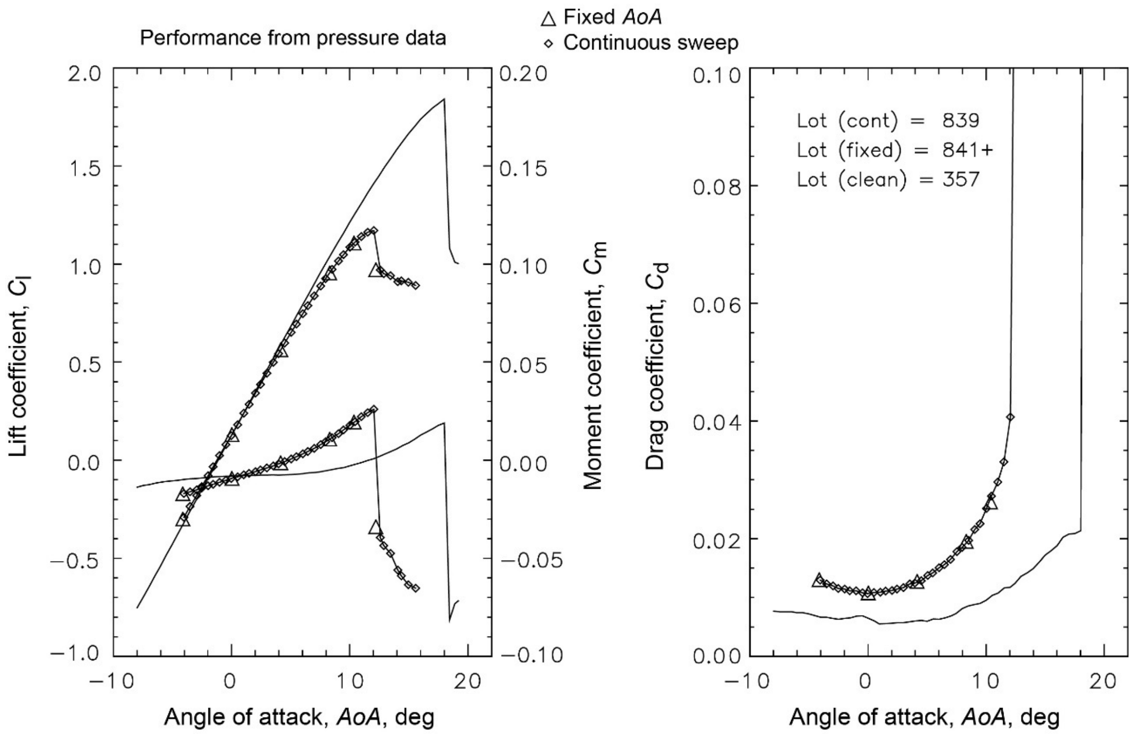

Streamwise Ice 1—Lot EG1162: M = 0.20 to 0.21 and Re = 12.0–12.2×10^6

Appendix G.—F1 Full-Scale Model Tests

Streamwise Ice 1—Lot EG1162: M = 0.20 to 0.21 and Re = 12.0–12.2×10^6

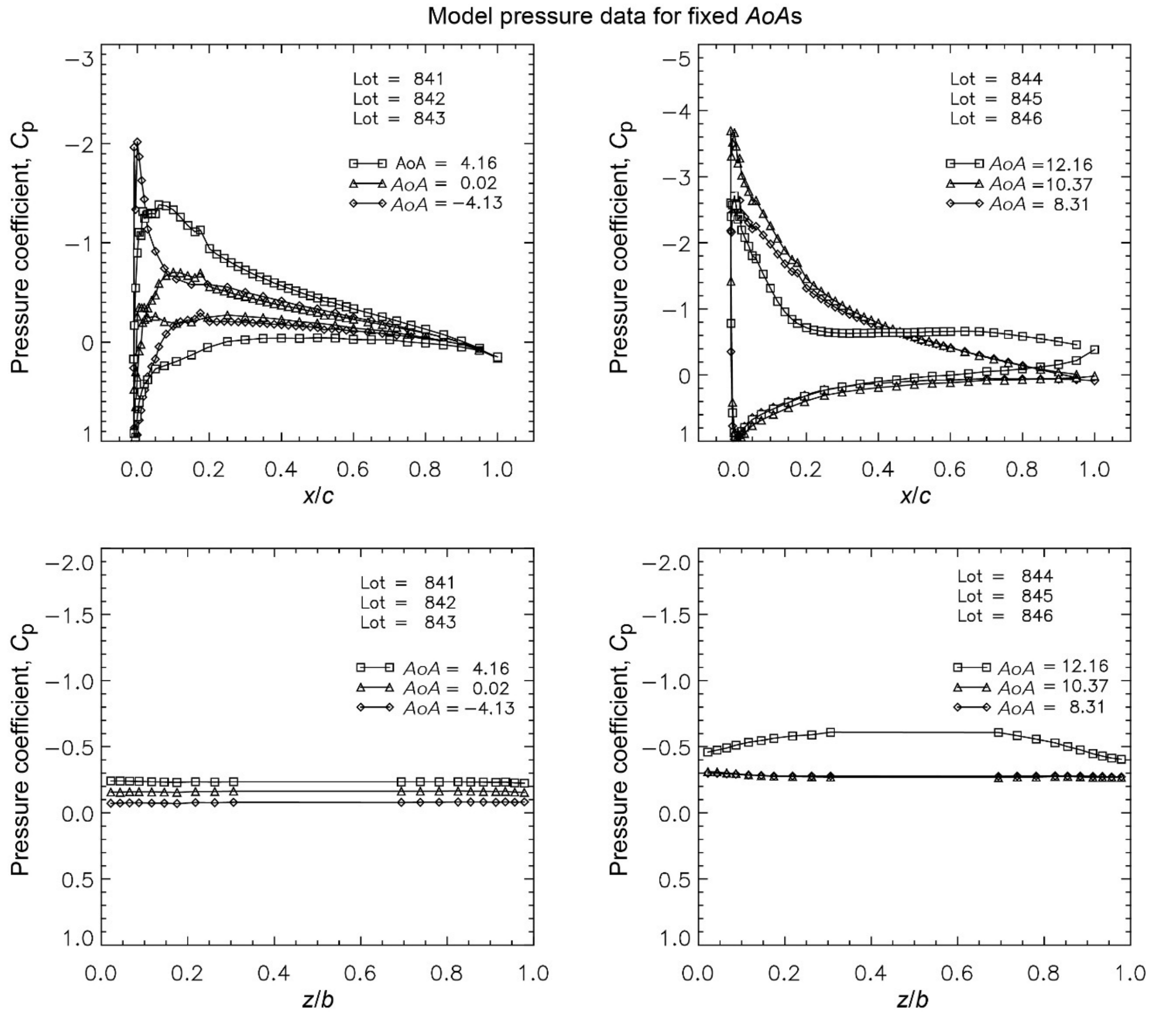

Streamwise Ice 1—Lot EG1162: M = 0.20 to 0.21 and Re = 12.0–12.2×10^6

Appendix G.—F1 Full-Scale Model Tests

Streamwise Ice 1—Lot EG1162: M = 0.20 to 0.21 and Re = 12.0–12.2×10^6

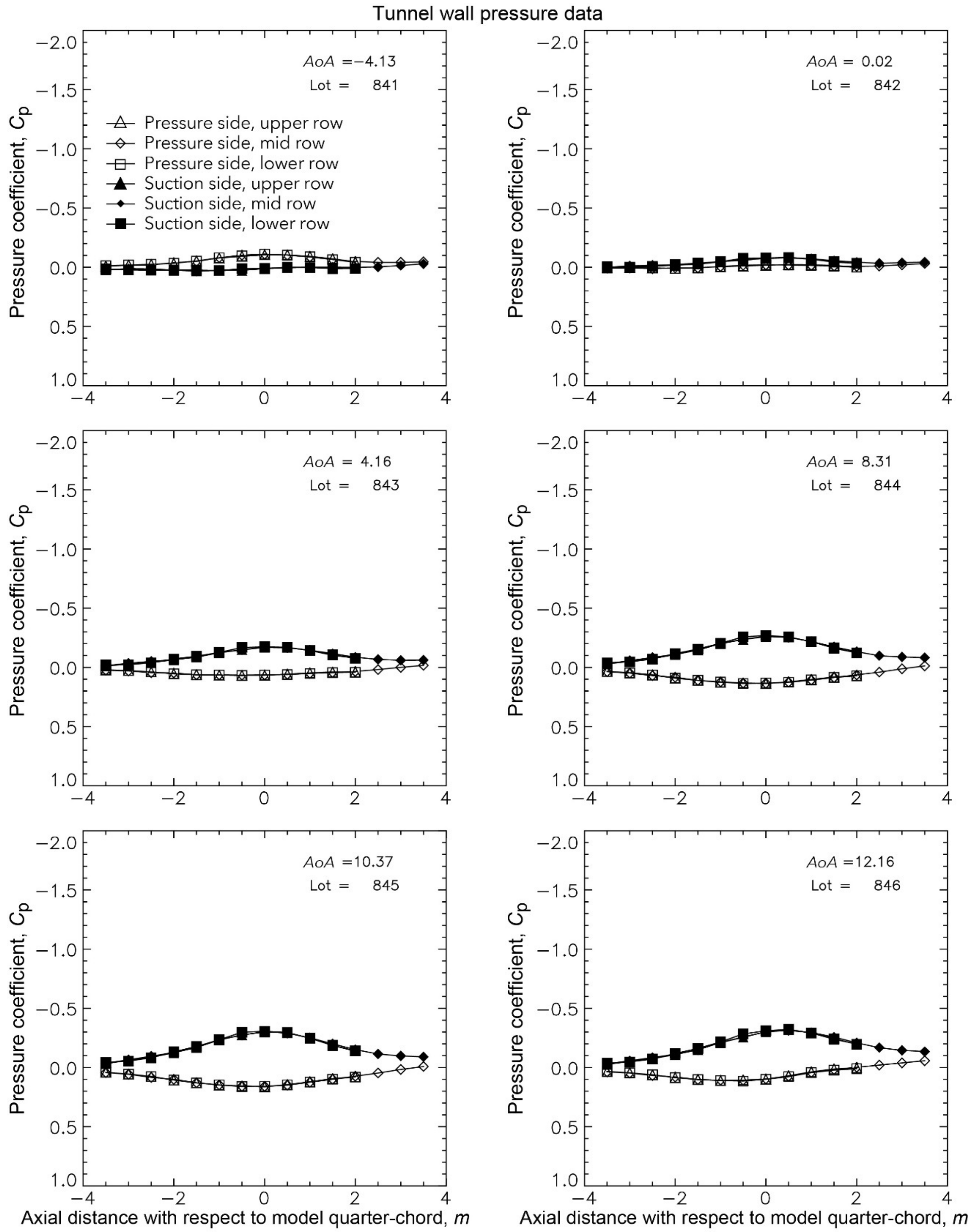

Streamwise Ice 1—Lot EG1162: M = 0.20 to 0.21 and Re = 12.0–12.2×10^6

Appendix G.—F1 Full-Scale Model Tests

Streamwise Ice 1—Lot EG1162: M = 0.20 to 0.21 and Re = 12.0–12.2×10^6

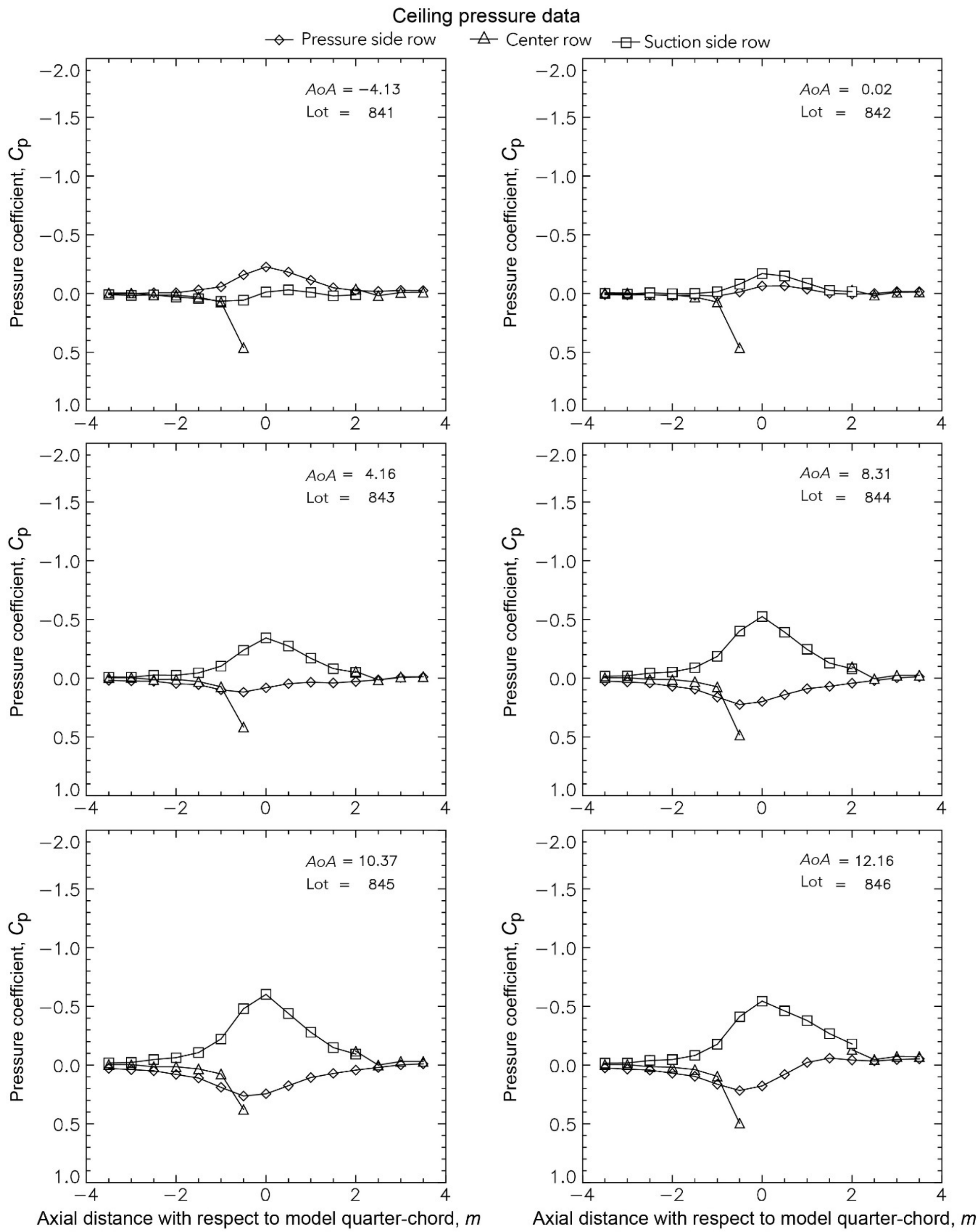

Streamwise Ice 1—Lot EG1162: M = 0.20 to 0.21 and Re = 12.0–12.2×10^6

Appendix G.—F1 Full-Scale Model Tests

Streamwise Ice 1—Lot EG1162: M = 0.20 to 0.21 and Re = 12.0–12.2×10^6

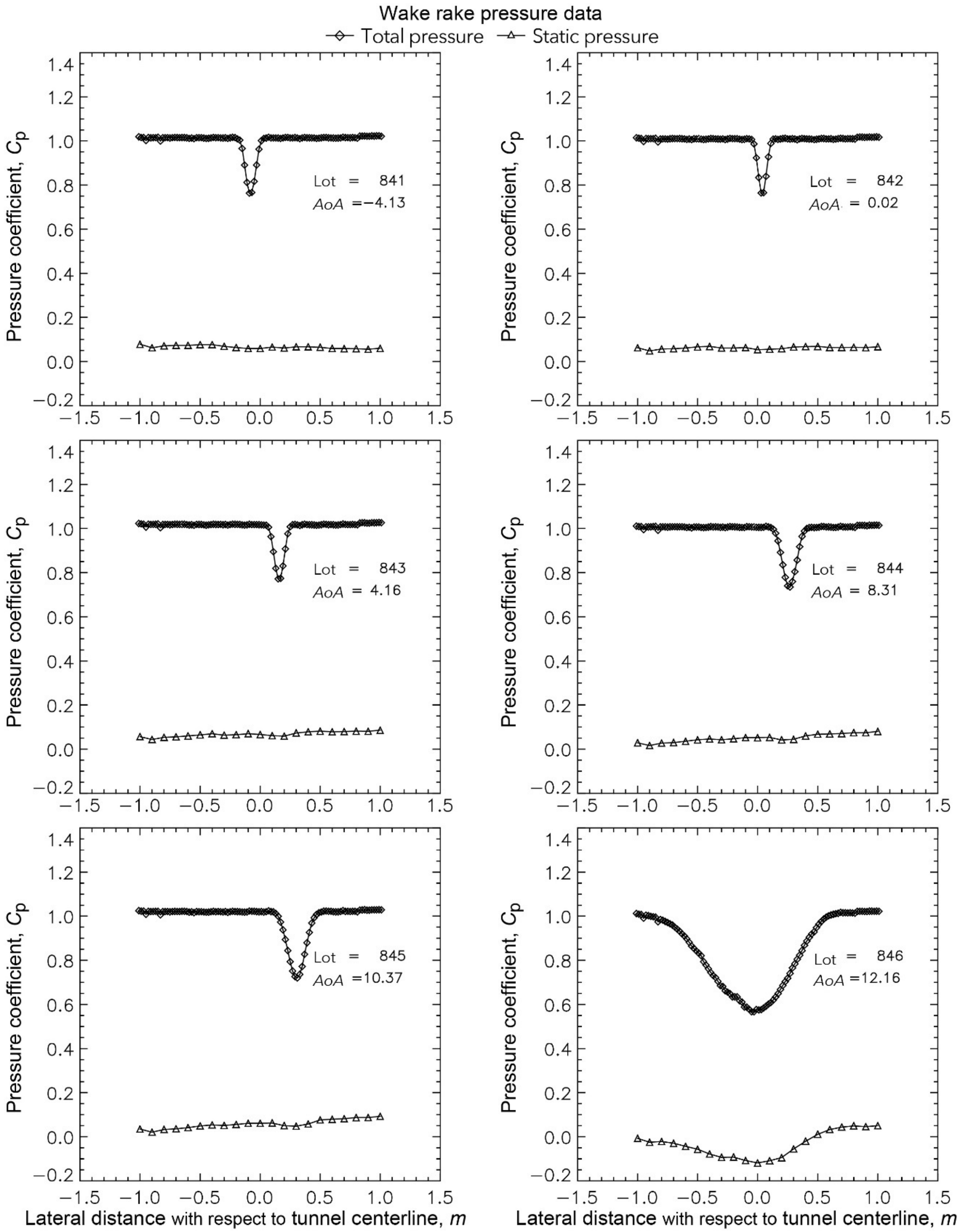

Streamwise Ice 1—Lot EG1162: M = 0.20 to 0.21 and Re = 12.0–12.2×10^6

Appendix G.—F1 Full-Scale Model Tests

Streamwise Ice 1—Lot EG1162: M = 0.20 to 0.21 and Re = 15.7–16.0×10^6

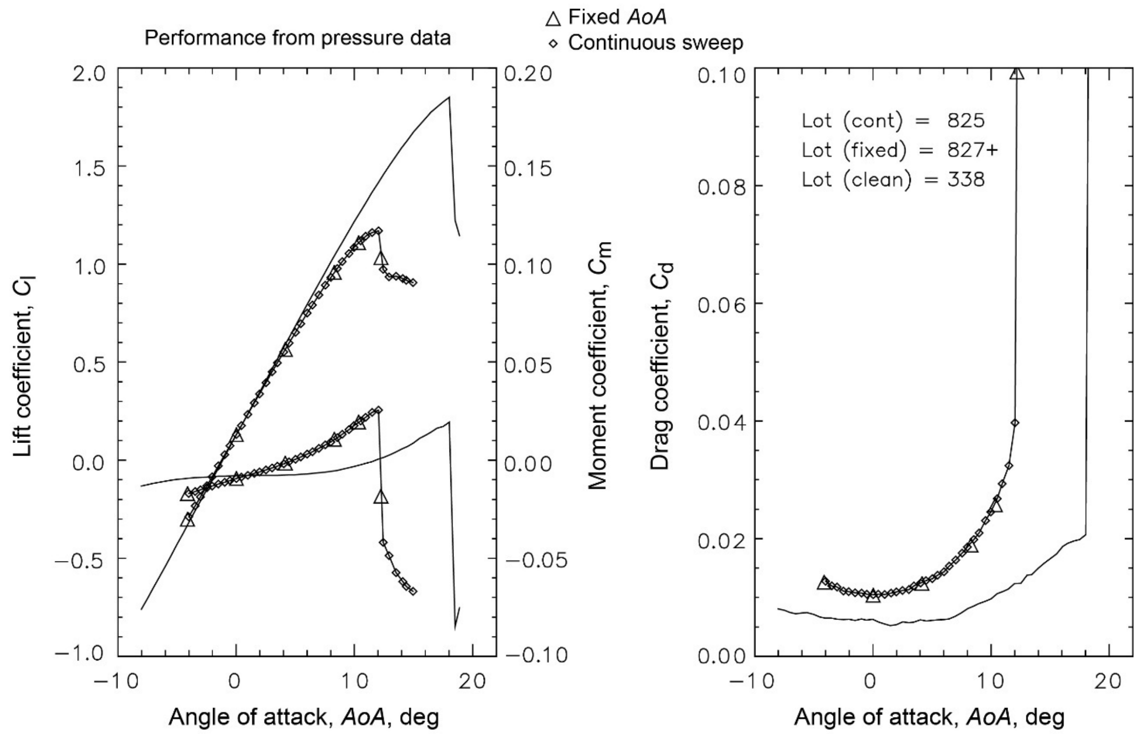

Streamwise Ice 1—Lot EG1162: M = 0.20 to 0.21 and Re = 15.7–16.0×10^6

Appendix G.—F1 Full-Scale Model Tests

Streamwise Ice 1—Lot EG1162: M = 0.20 to 0.21 and Re = 15.7–16.0×10^6

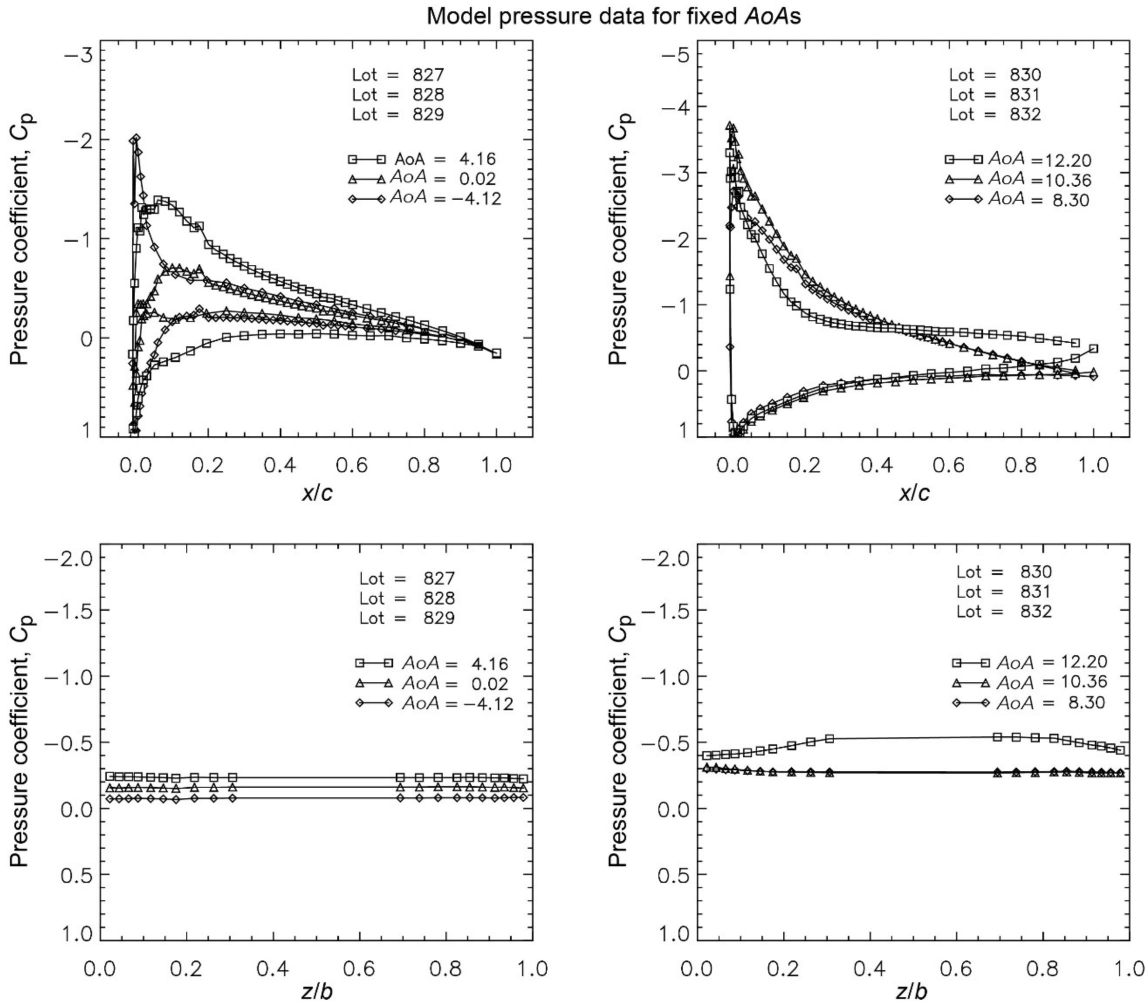

Streamwise Ice 1—Lot EG1162: M = 0.20 to 0.21 and Re = 15.7–16.0×10^6

Appendix G.—F1 Full-Scale Model Tests

Streamwise Ice 1—Lot EG1162: M = 0.20 to 0.21 and Re = 15.7–16.0×10^6

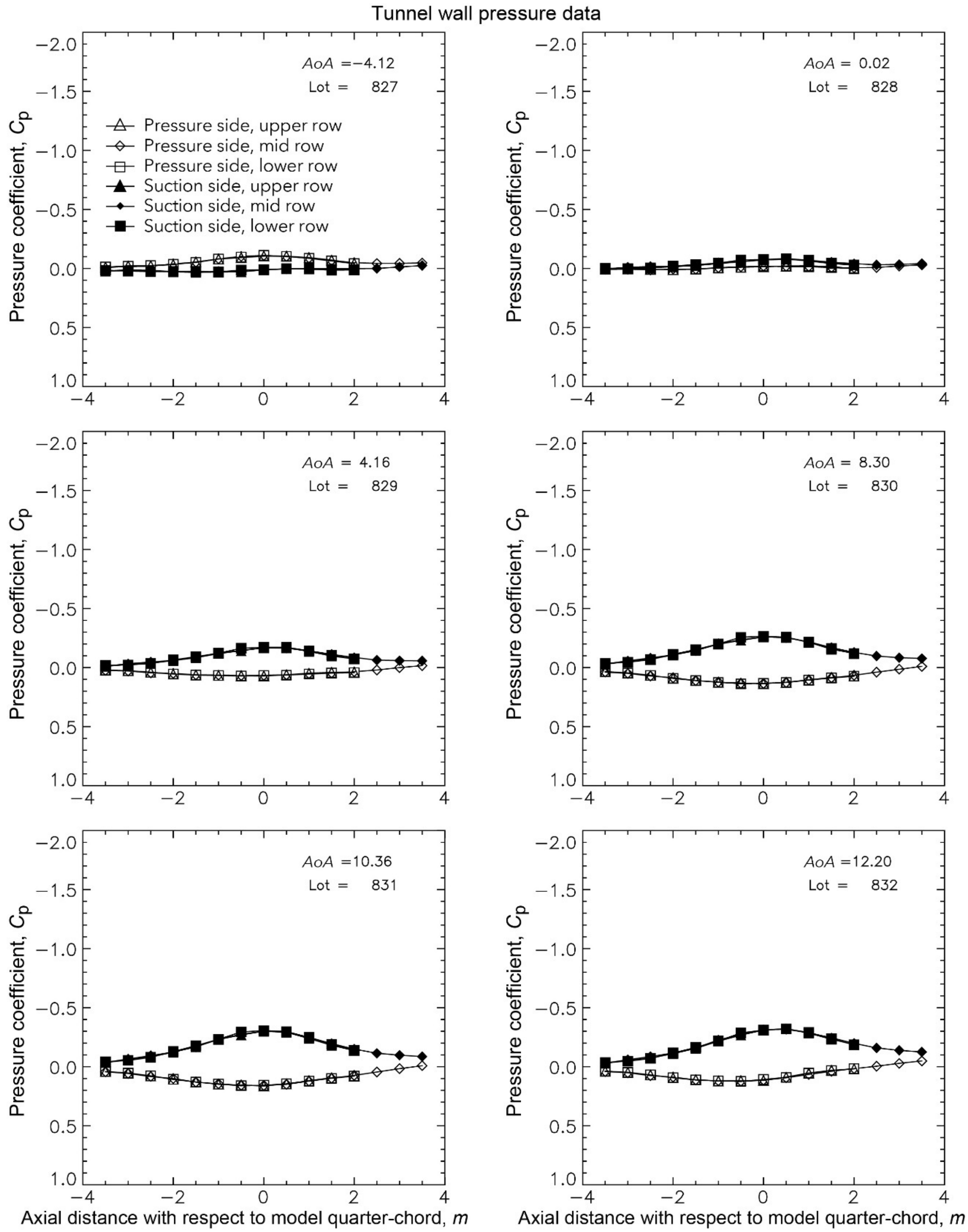

Streamwise Ice 1—Lot EG1162: M = 0.20 to 0.21 and Re = 15.7–16.0×10^6

Appendix G.—F1 Full-Scale Model Tests

Streamwise Ice 1—Lot EG1162: M = 0.20 to 0.21 and Re = 15.7–16.0×10^6

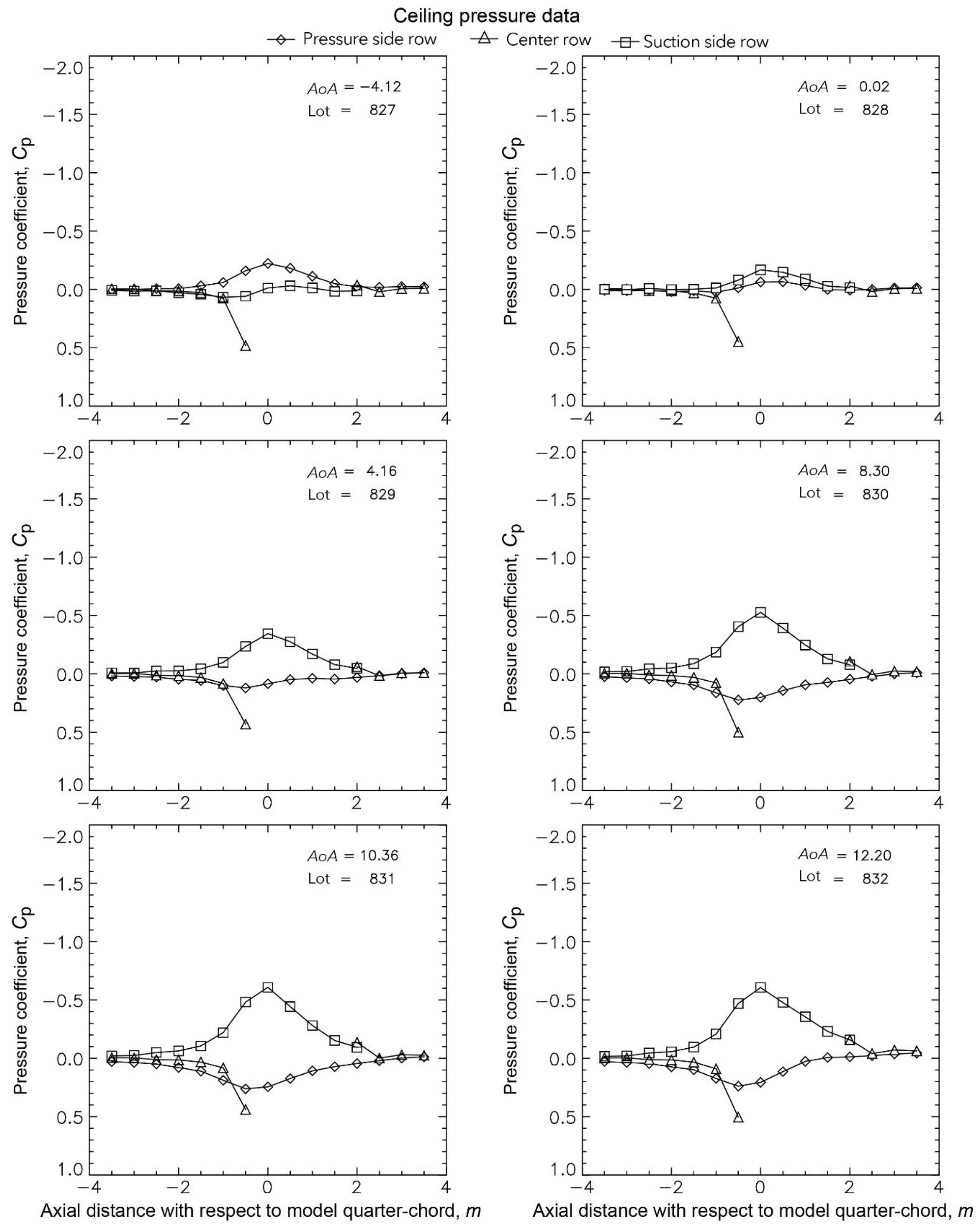

Streamwise Ice 1—Lot EG1162: M = 0.20 to 0.21 and Re = 15.7–16.0×10^6

Appendix G.—F1 Full-Scale Model Tests

Streamwise Ice 1—Lot EG1162: M = 0.20 to 0.21 and Re = 15.7–16.0×10[6]

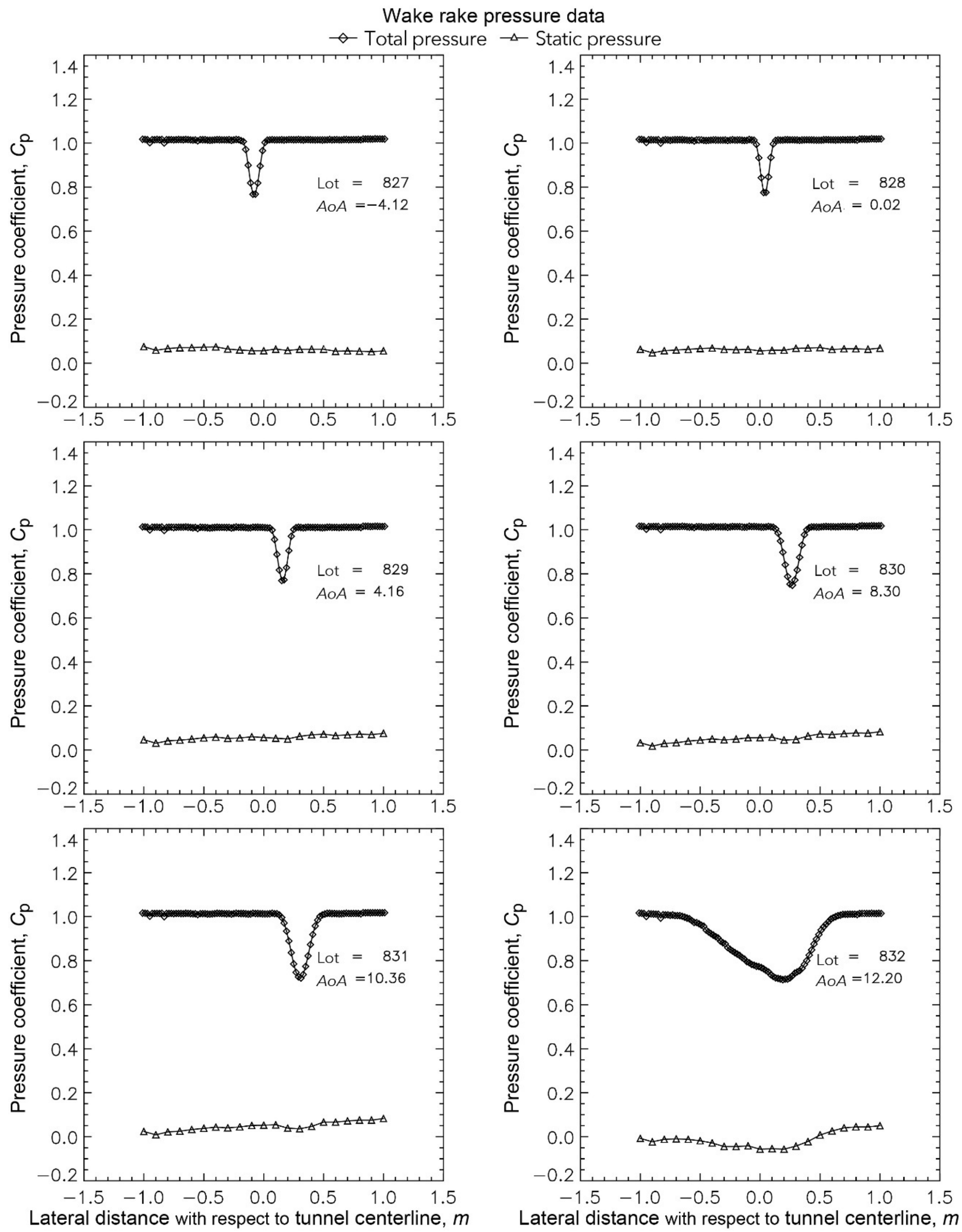

Streamwise Ice 1—Lot EG1162: M = 0.20 to 0.21 and Re = 15.7–16.0×10[6]

Appendix G.—F1 Full-Scale Model Tests

Streamwise Ice 1—Lot EG1162: M = 0.28 to 0.29 and Re = 12.1–12.2×10[6]

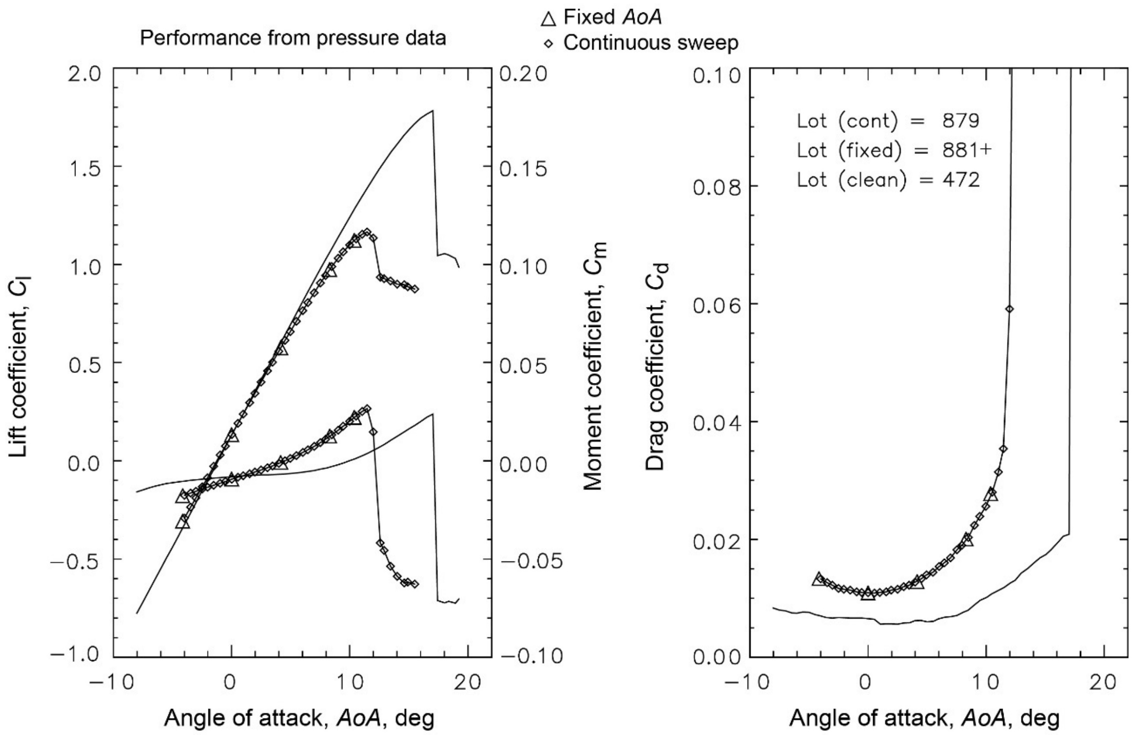

Streamwise Ice 1—Lot EG1162: M = 0.28 to 0.29 and Re = 12.1–12.2×10[6]

Appendix G.—F1 Full-Scale Model Tests

Streamwise Ice 1—Lot EG1162: M = 0.28 to 0.29 and Re = 12.1–12.2×10^6

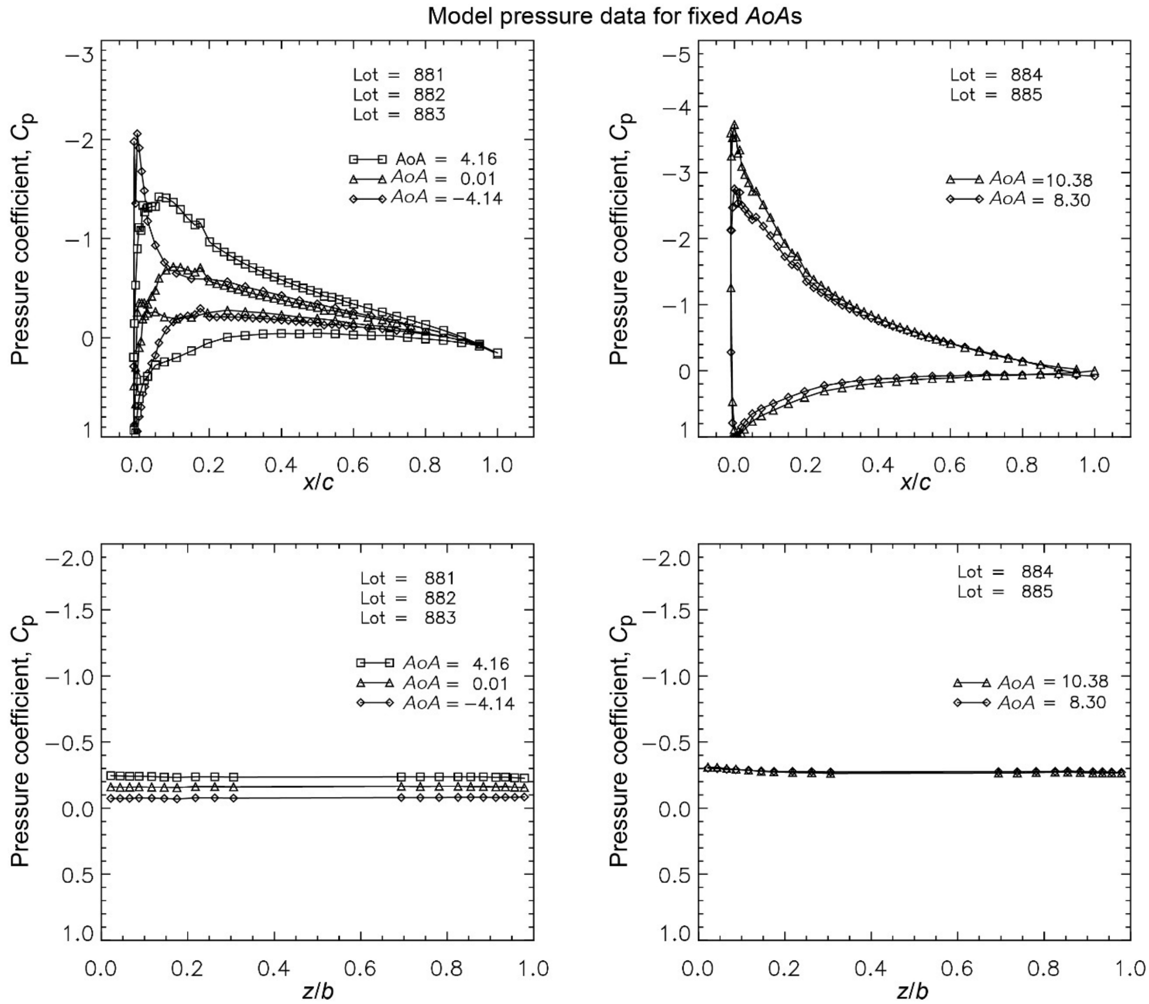

Streamwise Ice 1—Lot EG1162: M = 0.28 to 0.29 and Re = 12.1–12.2×10^6

Appendix G.—F1 Full-Scale Model Tests

Streamwise Ice 1—Lot EG1162: M = 0.28 to 0.29 and Re = 12.1–12.2×10^6

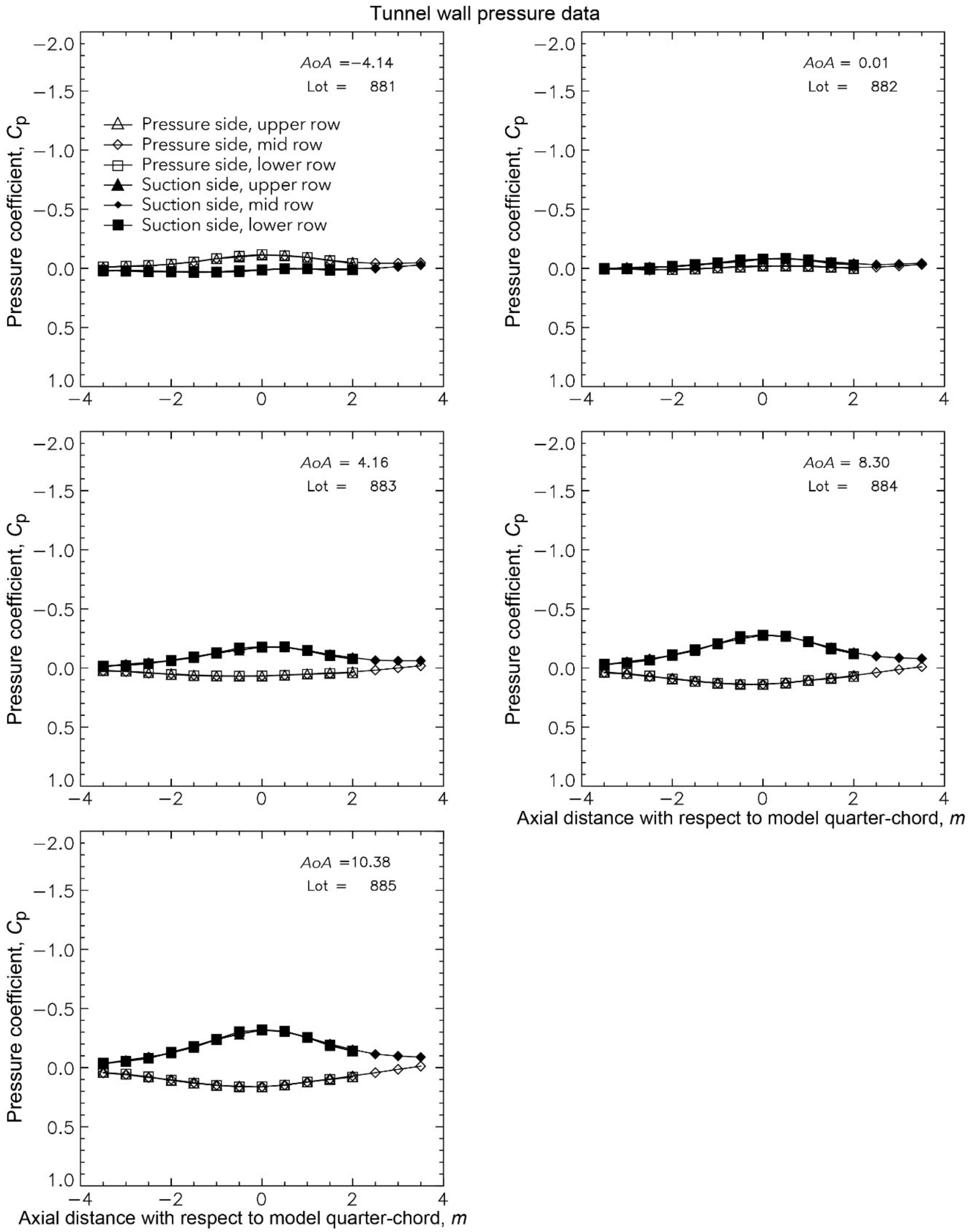

Streamwise Ice 1—Lot EG1162: M = 0.28 to 0.29 and Re = 12.1–12.2×10^6

Appendix G.—F1 Full-Scale Model Tests

Streamwise Ice 1—Lot EG1162: M = 0.28 to 0.29 and Re = 12.1–12.2×10^6

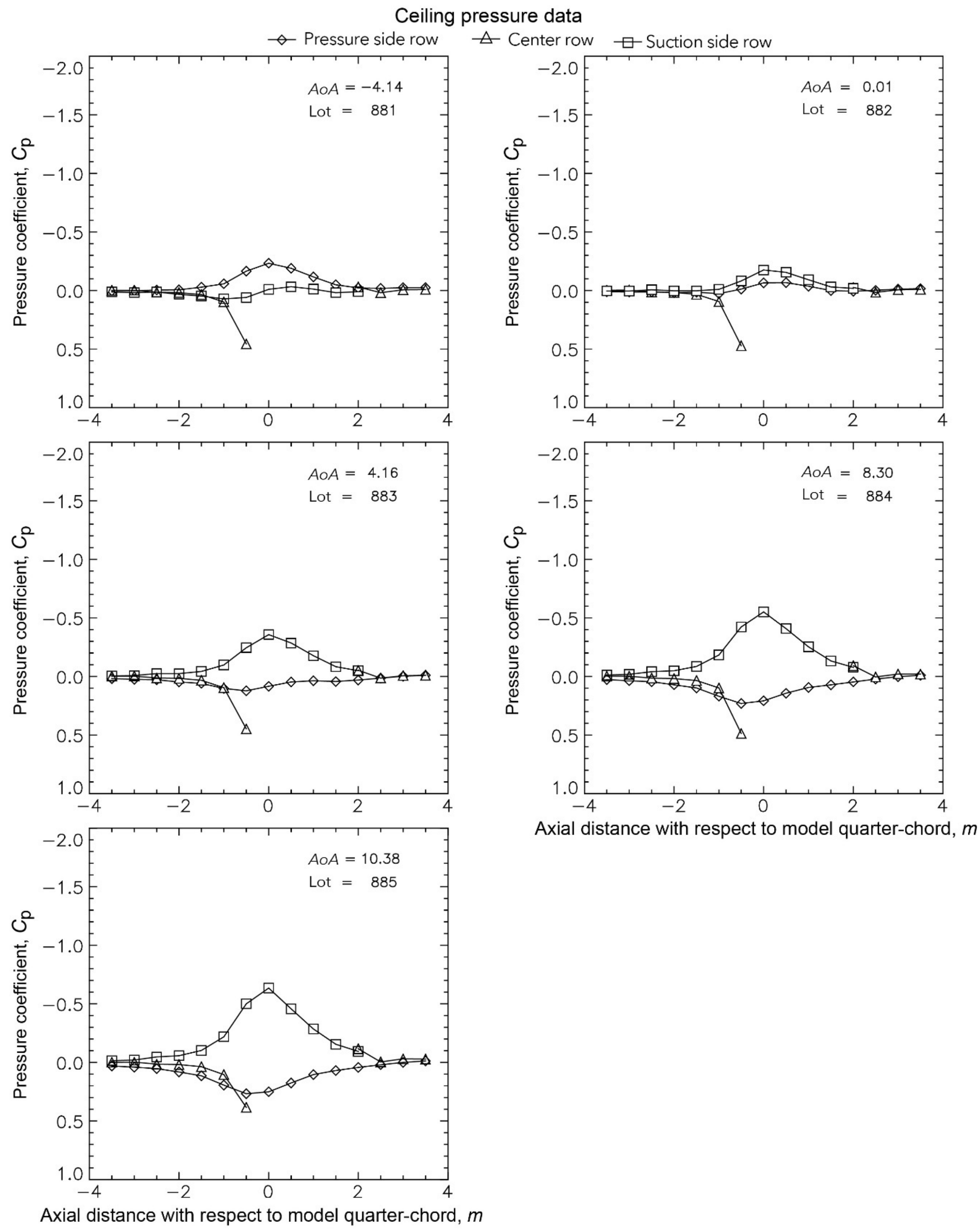

Streamwise Ice 1—Lot EG1162: M = 0.28 to 0.29 and Re = 12.1–12.2×10^6

Appendix G.—F1 Full-Scale Model Tests

Streamwise Ice 1—Lot EG1162: M = 0.28 to 0.29 and Re = 12.1–12.2×10^6

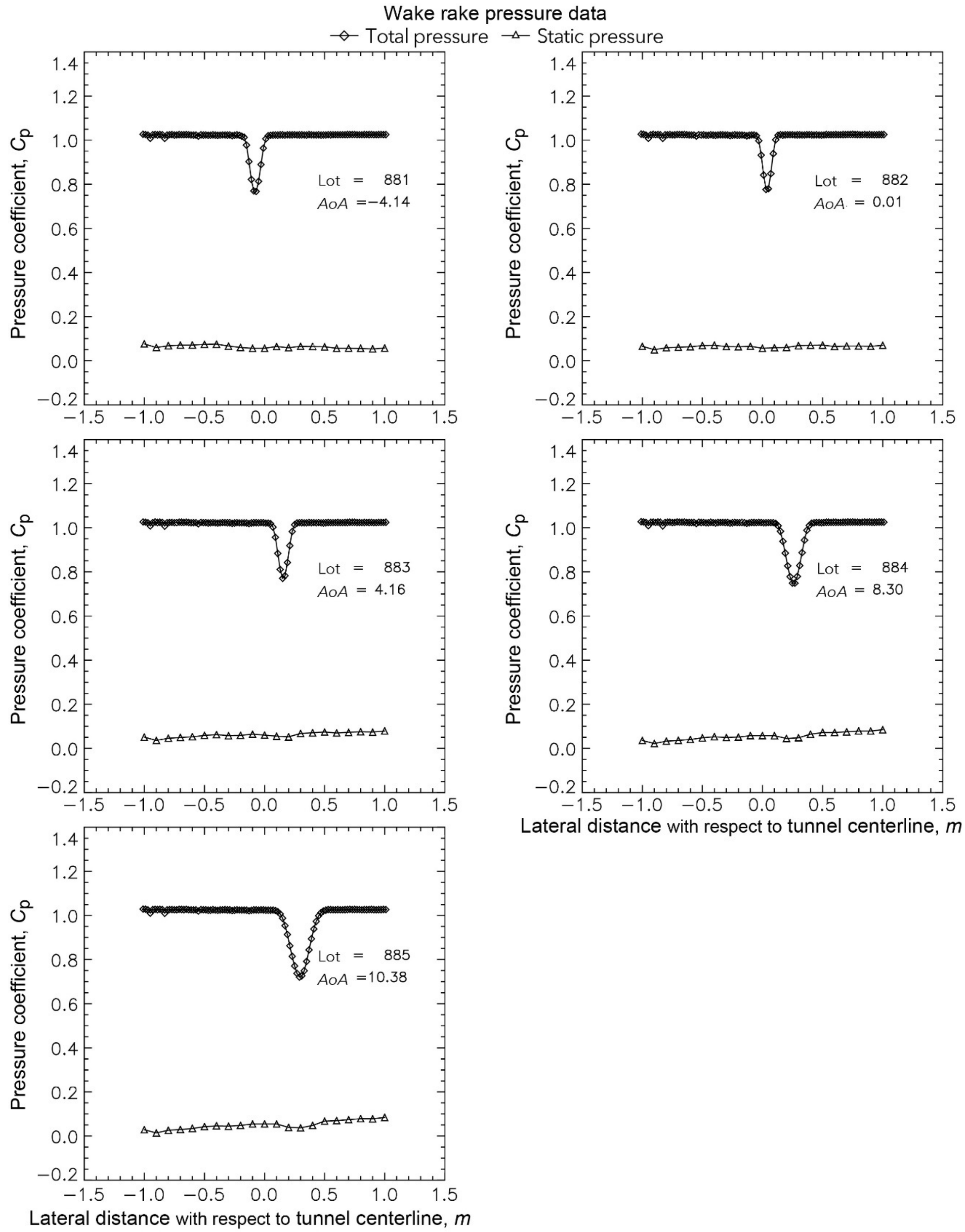

Streamwise Ice 1—Lot EG1162: M = 0.28 to 0.29 and Re = 12.1–12.2×10^6

Appendix G.—F1 Full-Scale Model Tests

Roughness Ice 1—Lot EG1126: M = 0.11 and Re = 4.6×10^{6}

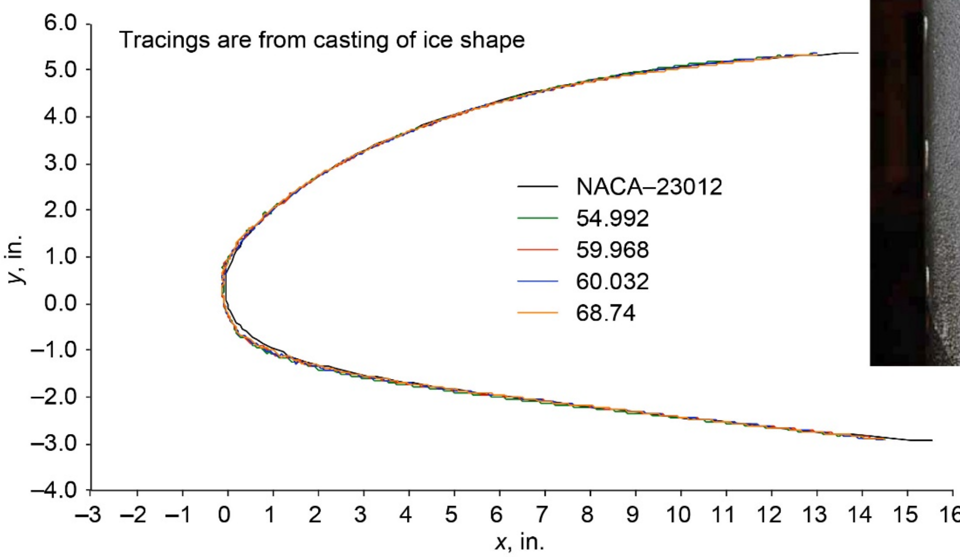

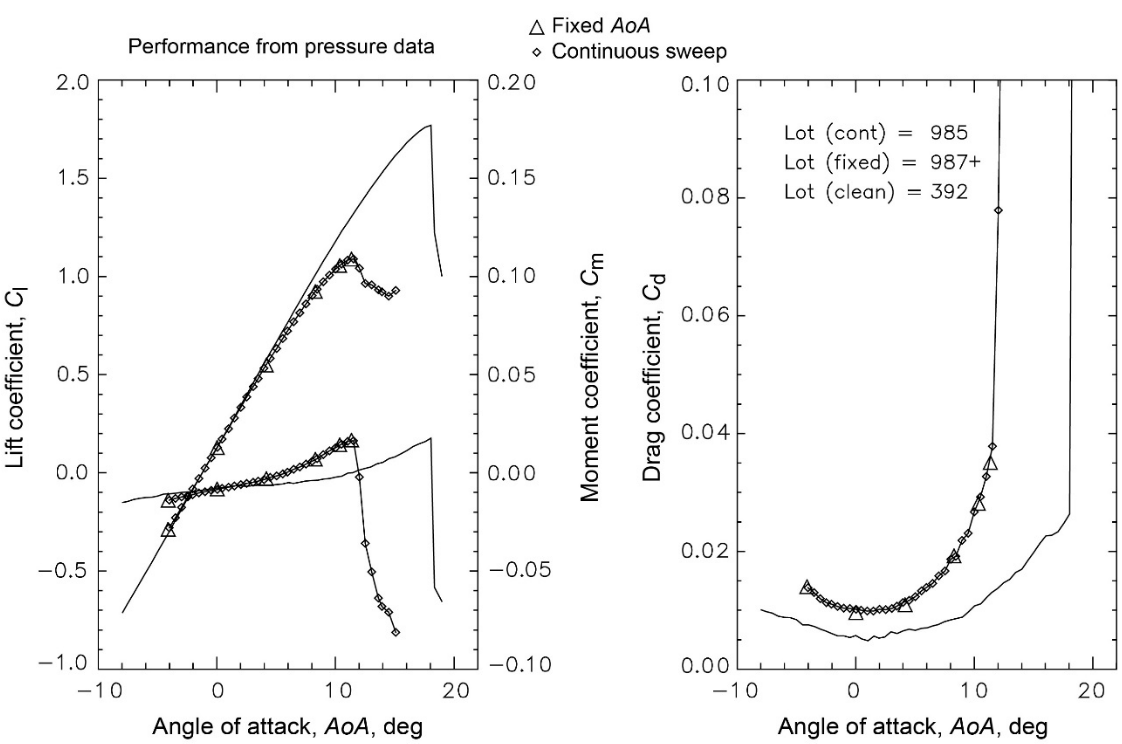

Roughness Ice 1—Lot EG1126: M = 0.11 and Re = 4.6×10^{6}

Appendix G.—F1 Full-Scale Model Tests

Roughness Ice 1—Lot EG1126: M = 0.11 and Re = 4.6×10^6

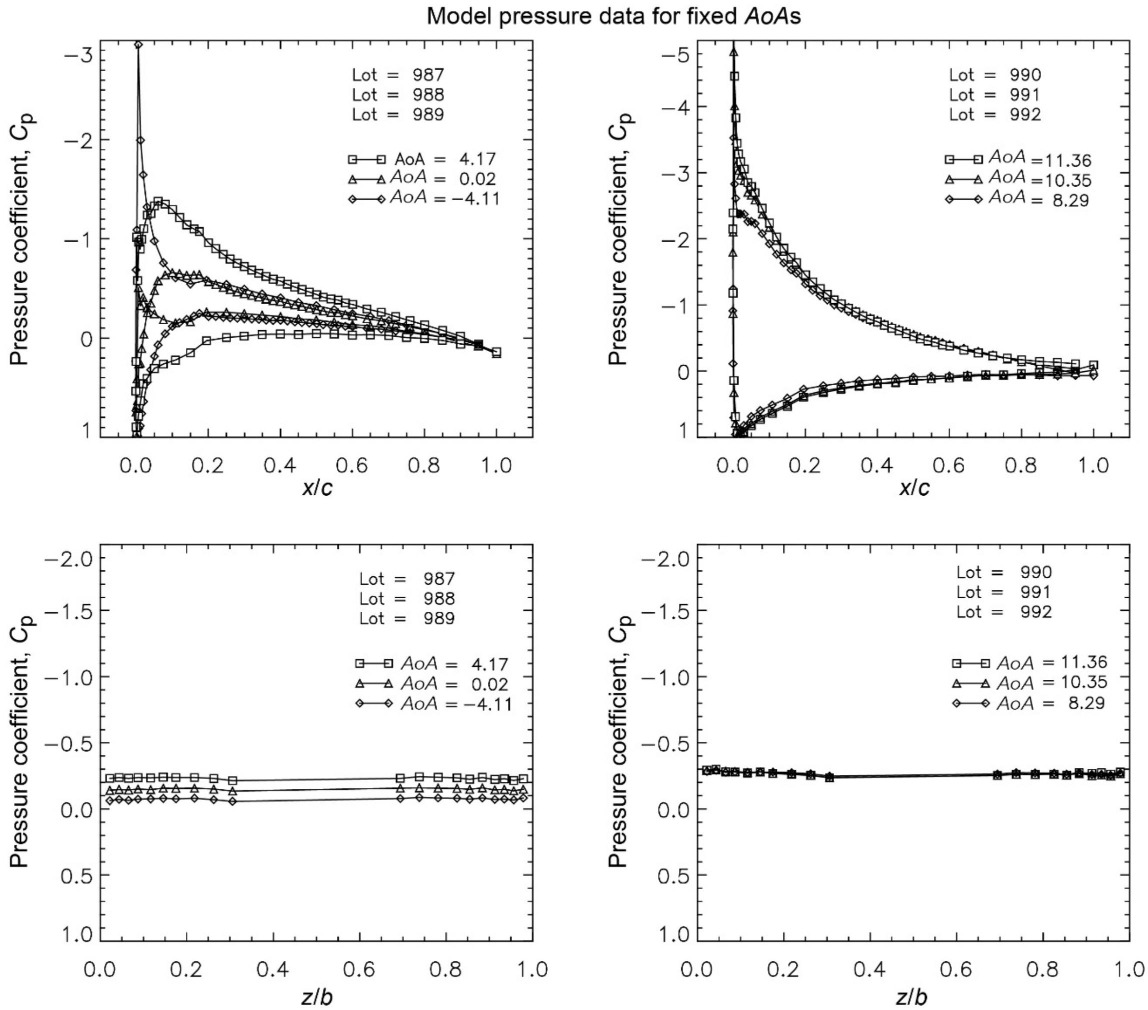

App. G143.—Mcp0

Roughness Ice 1—Lot EG1126: M = 0.11 and Re = 4.6×10^6

Appendix G.—F1 Full-Scale Model Tests

Roughness Ice 1—Lot EG1126: M = 0.11 and Re = 4.6×10^6

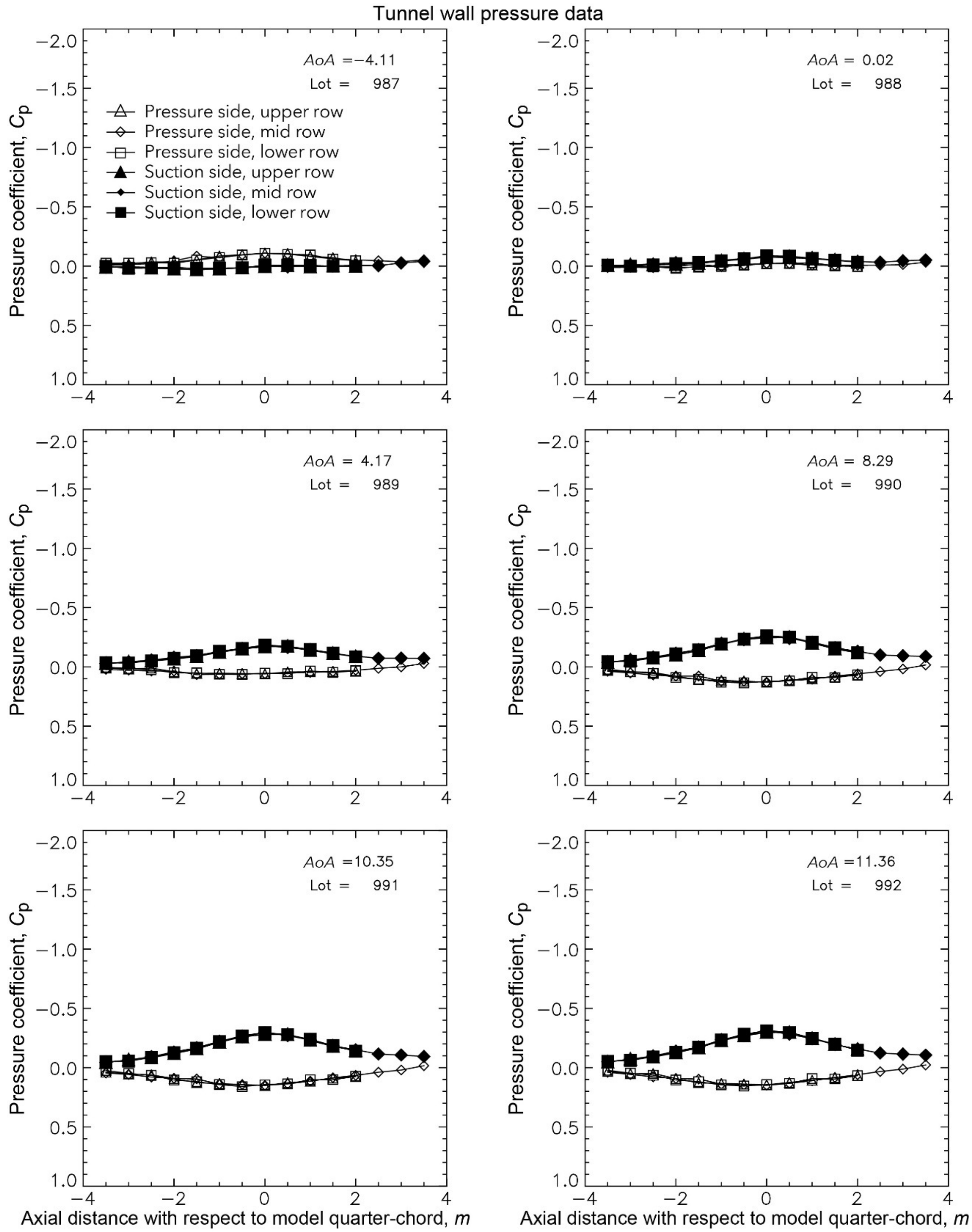

Roughness Ice 1—Lot EG1126: M = 0.11 and Re = 4.6×10^6

Appendix G.—F1 Full-Scale Model Tests

Roughness Ice 1—Lot EG1126: M = 0.11 and Re = 4.6×10^6

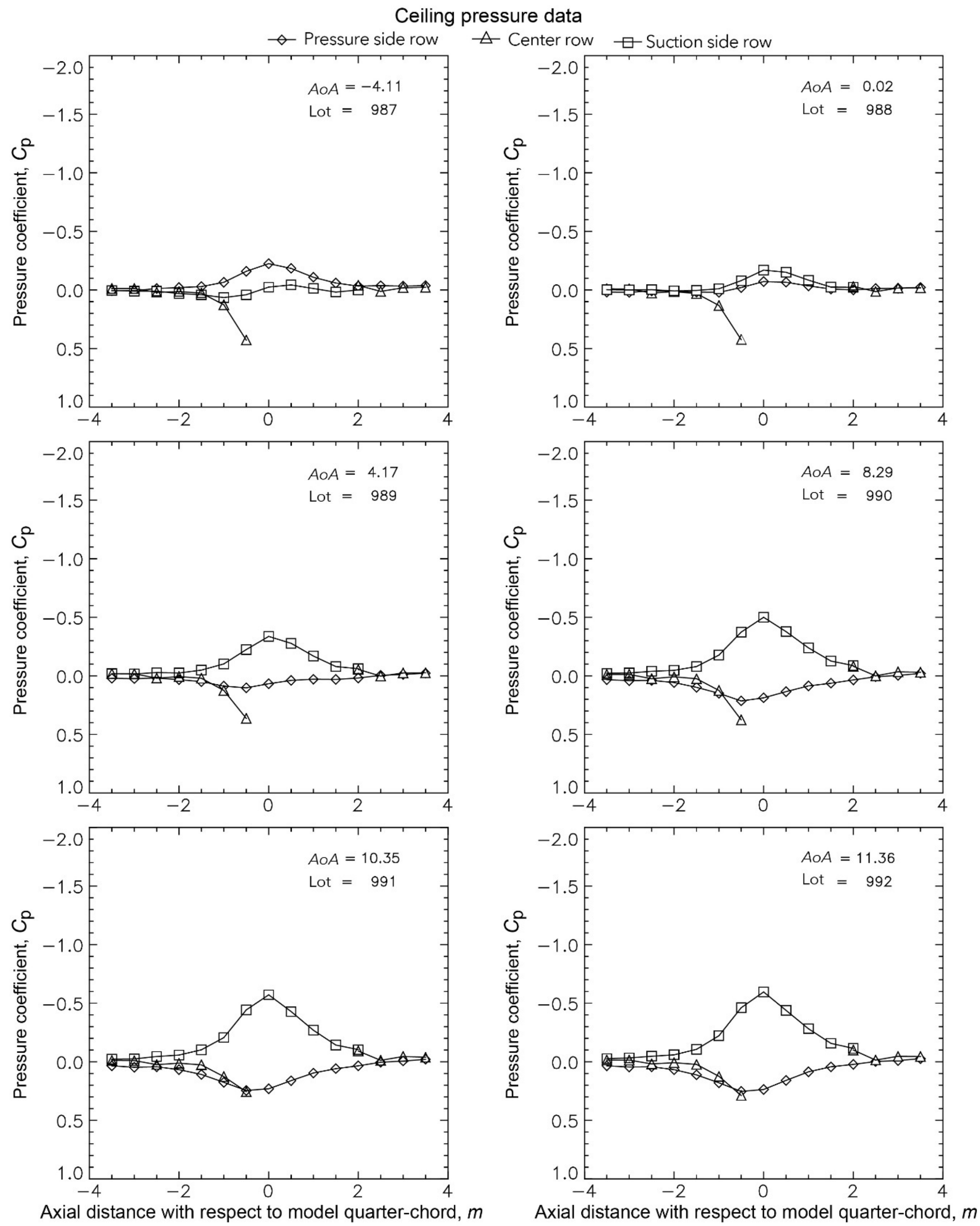

Roughness Ice 1—Lot EG1126: M = 0.11 and Re = 4.6×10^6

Appendix G.—F1 Full-Scale Model Tests

Roughness Ice 1—Lot EG1126: M = 0.11 and Re = 4.6×10^6

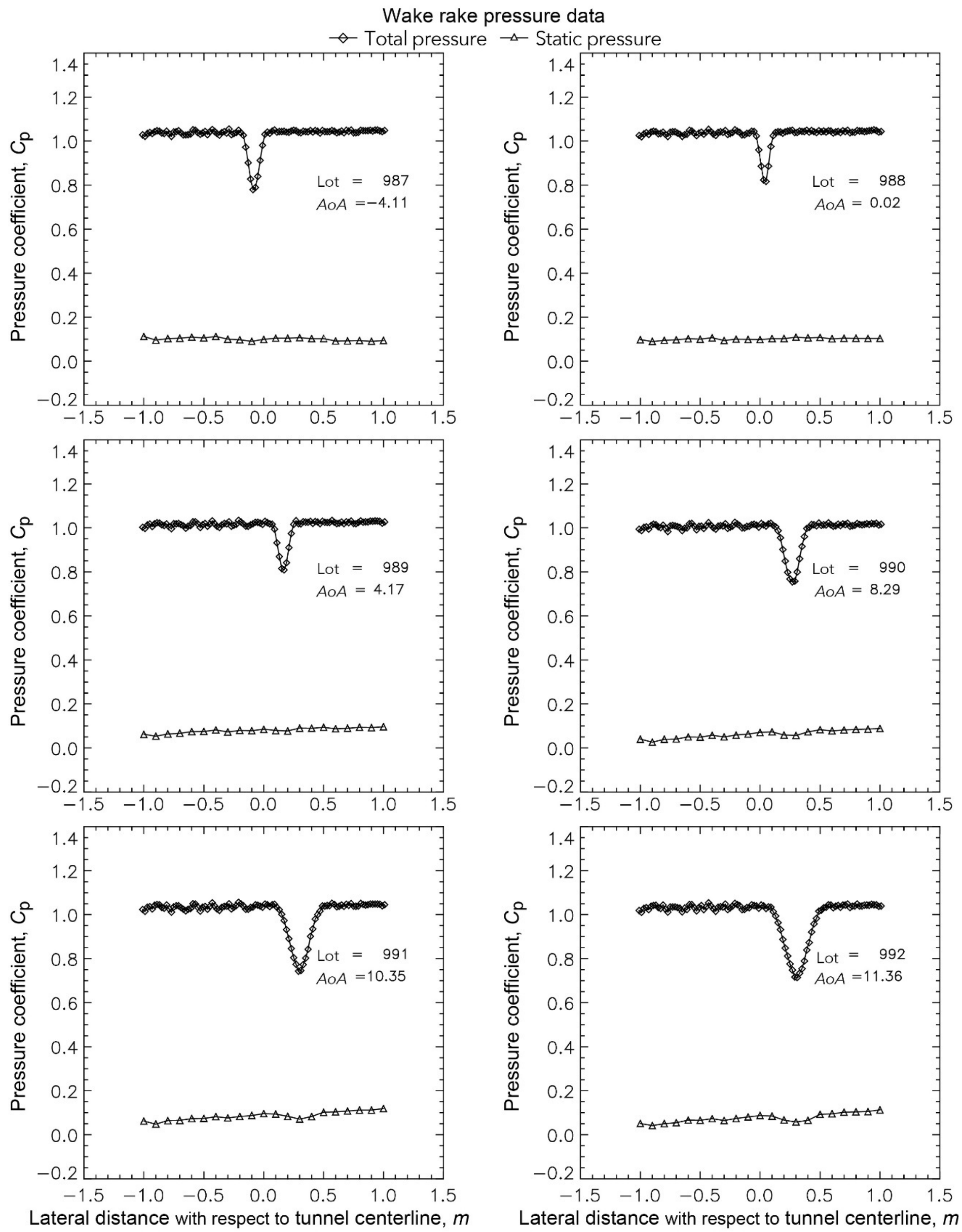

Roughness Ice 1—Lot EG1126: M = 0.11 and Re = 4.6×10^6

Appendix G.—F1 Full-Scale Model Tests

Roughness Ice 1—Lot EG1126: M = 0.10 and Re = 8.6–8.7×10^6

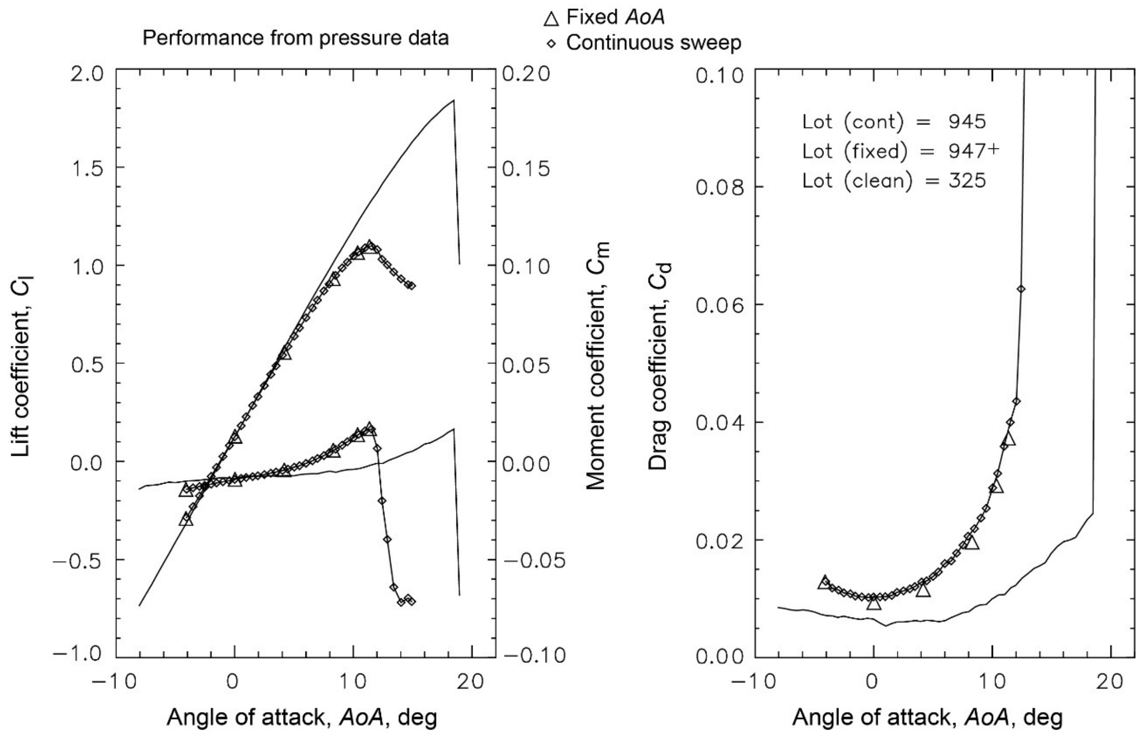

Roughness Ice 1—Lot EG1126: M = 0.10 and Re = 8.6–8.7×10^6

Appendix G.—F1 Full-Scale Model Tests

Roughness Ice 1—Lot EG1126: M = 0.10 and Re = 8.6–8.7×10^6

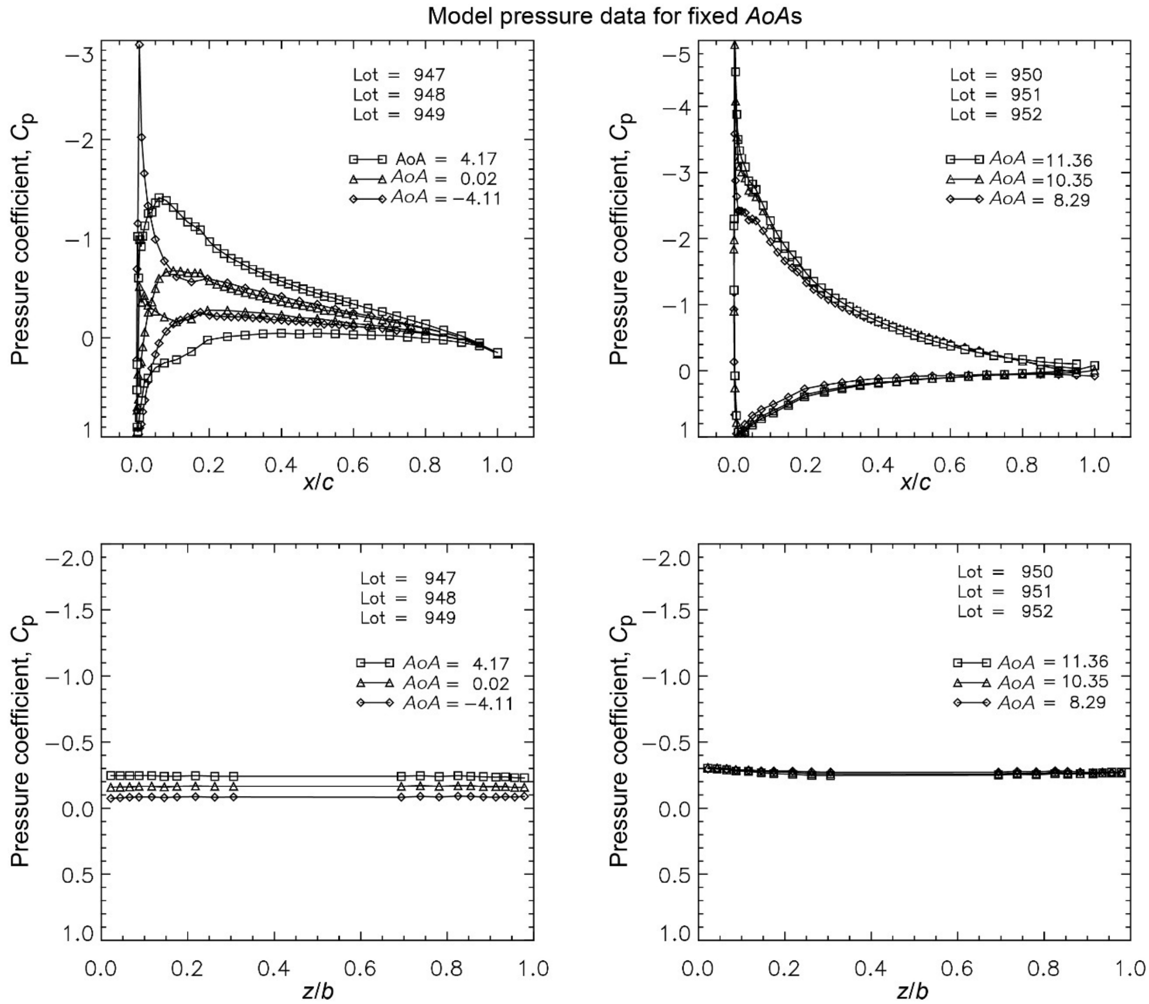

Roughness Ice 1—Lot EG1126: M = 0.10 and Re = 8.6–8.7×10^6

Appendix G.—F1 Full-Scale Model Tests

Roughness Ice 1—Lot EG1126: M = 0.10 and Re = 8.6–8.7×10⁶

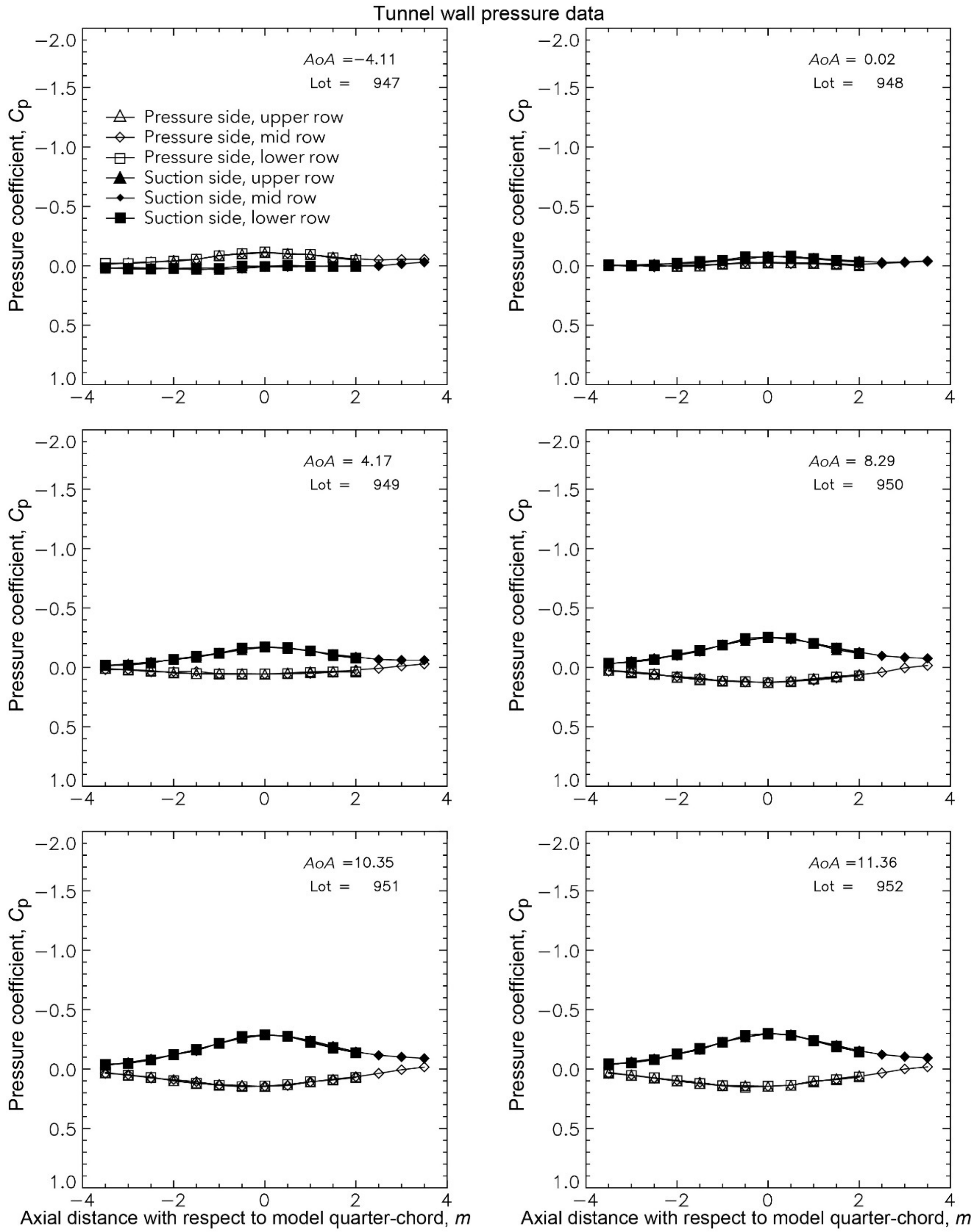

Roughness Ice 1—Lot EG1126: M = 0.10 and Re = 8.6–8.7×10⁶

Appendix G.—F1 Full-Scale Model Tests

Roughness Ice 1—Lot EG1126: M = 0.10 and Re = 8.6–8.7×10⁶

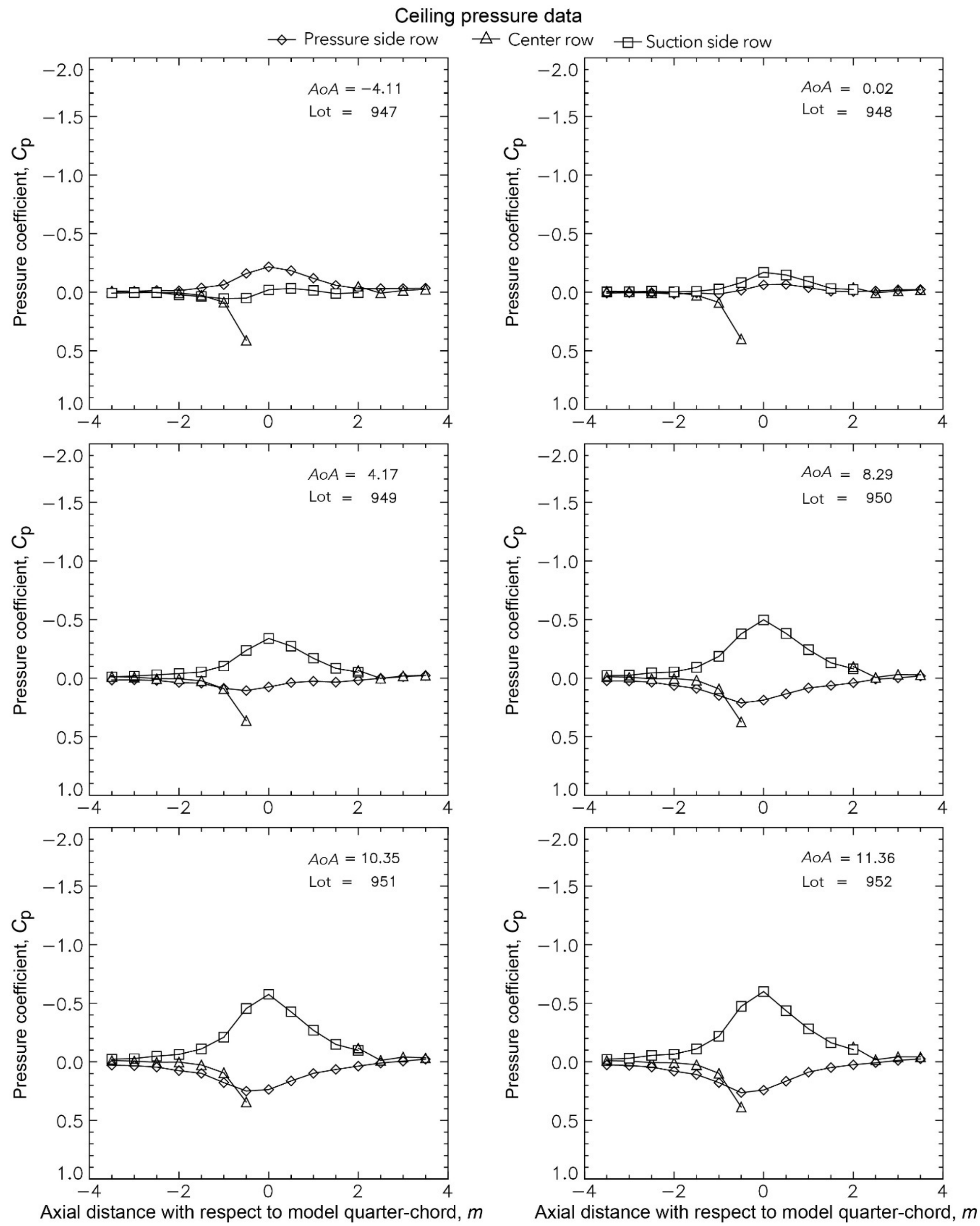

Roughness Ice 1—Lot EG1126: M = 0.10 and Re = 8.6–8.7×10⁶

Appendix G.—F1 Full-Scale Model Tests

Roughness Ice 1—Lot EG1126: M = 0.10 and Re = 8.6–8.7×10^6

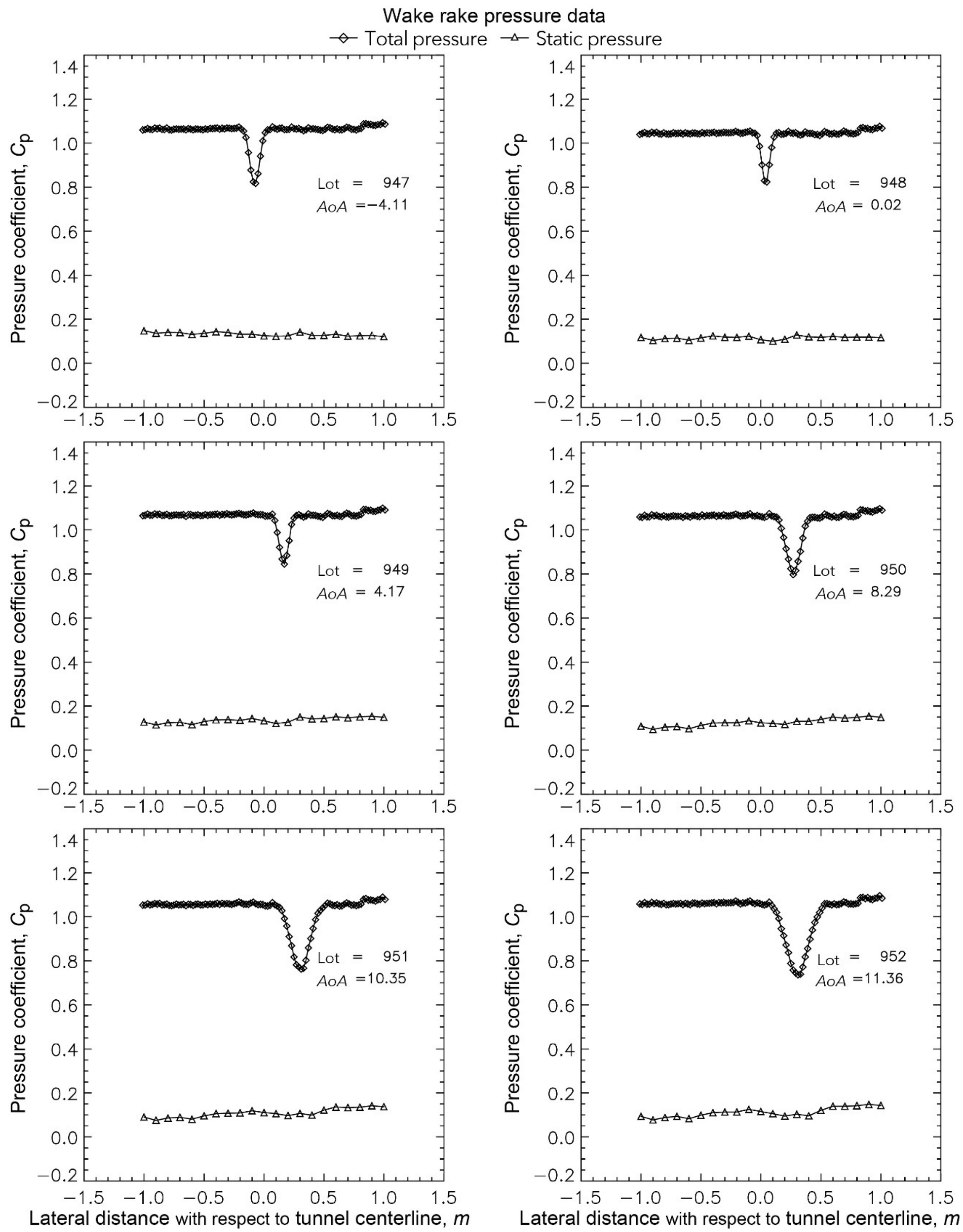

Roughness Ice 1—Lot EG1126: M = 0.10 and Re = 8.6–8.7×10^6

Appendix G.—F1 Full-Scale Model Tests

Roughness Ice 1—Lot EG1126: M = 0.10 and Re = 12.1–12.2×10^6

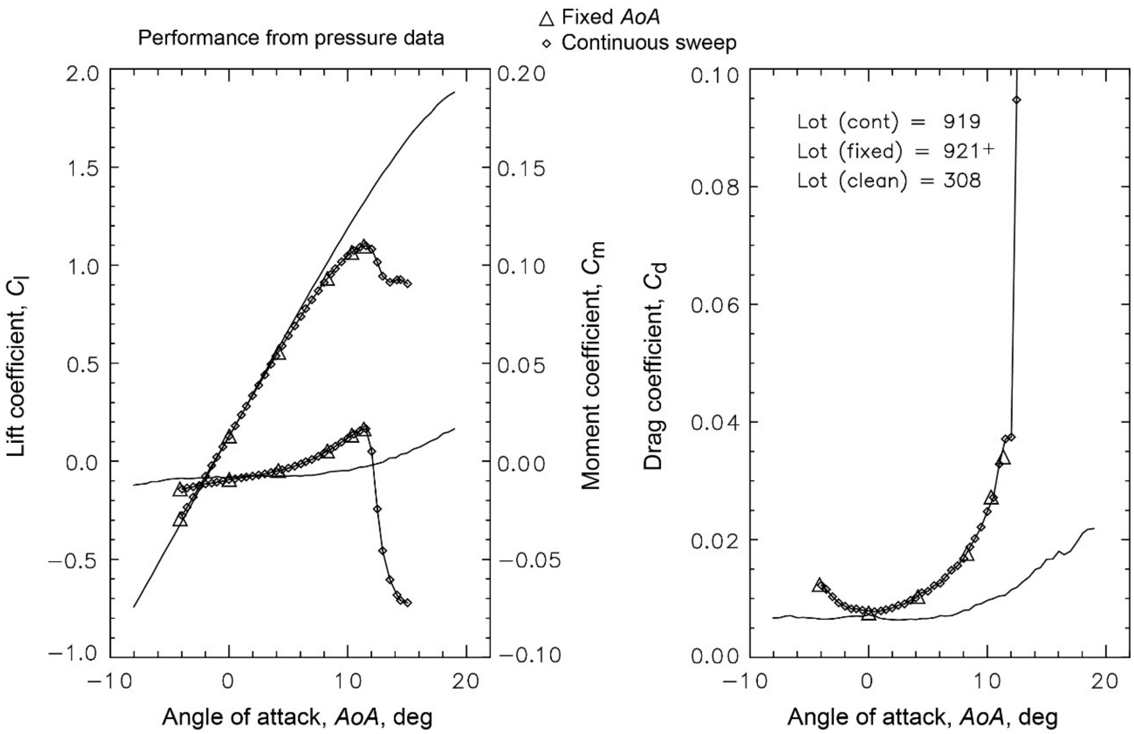

Roughness Ice 1—Lot EG1126: M = 0.10 and Re = 12.1–12.2×10^6

Appendix G.—F1 Full-Scale Model Tests

Roughness Ice 1—Lot EG1126: M = 0.10 and Re = 12.1–12.2×10^6

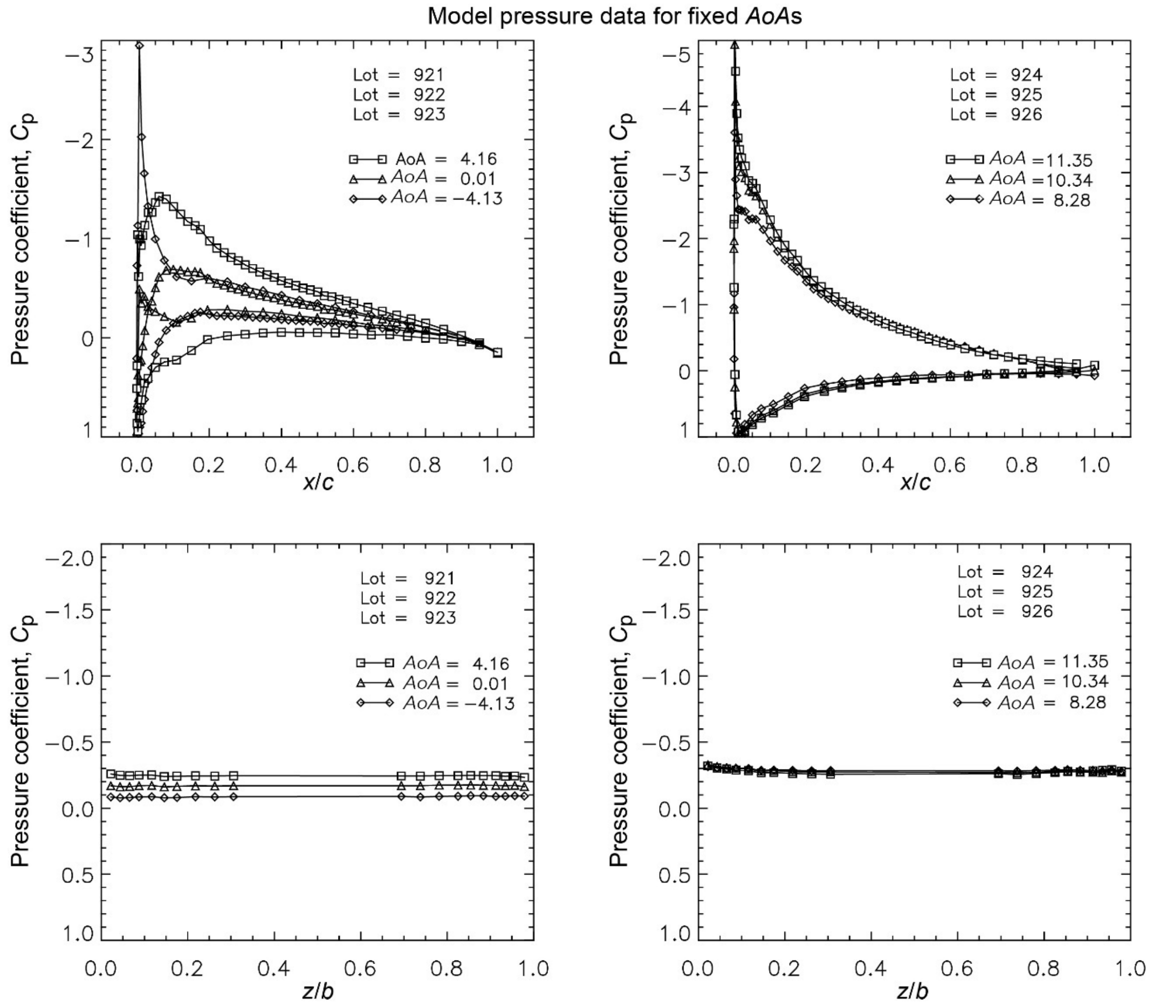

Roughness Ice 1—Lot EG1126: M = 0.10 and Re = 12.1–12.2×10^6

Appendix G.—F1 Full-Scale Model Tests

Roughness Ice 1—Lot EG1126: M = 0.10 and Re = 12.1–12.2×10^6

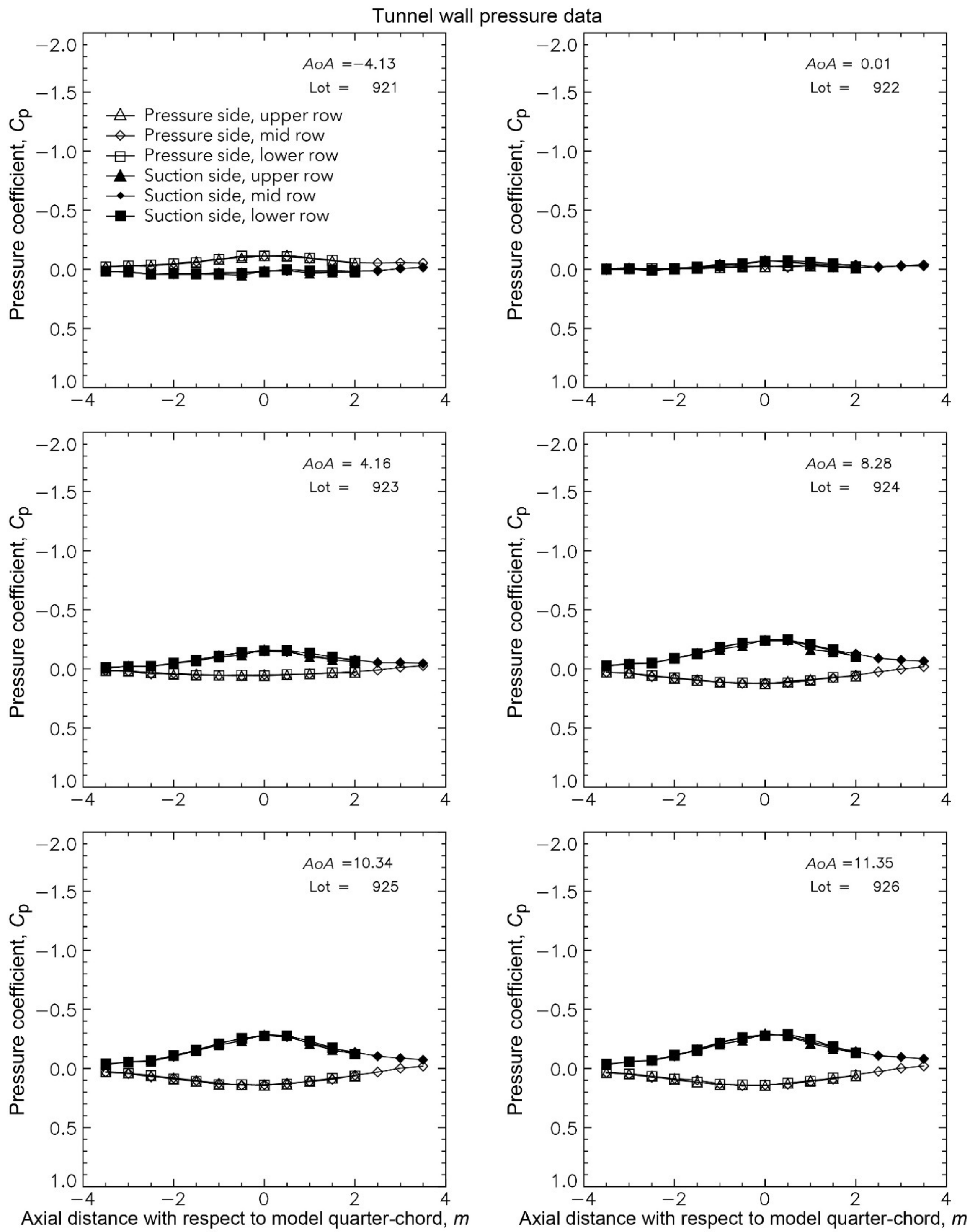

Roughness Ice 1—Lot EG1126: M = 0.10 and Re = 12.1–12.2×10^6

Appendix G.—F1 Full-Scale Model Tests

Roughness Ice 1—Lot EG1126: M = 0.10 and Re = 12.1–12.2×10^6

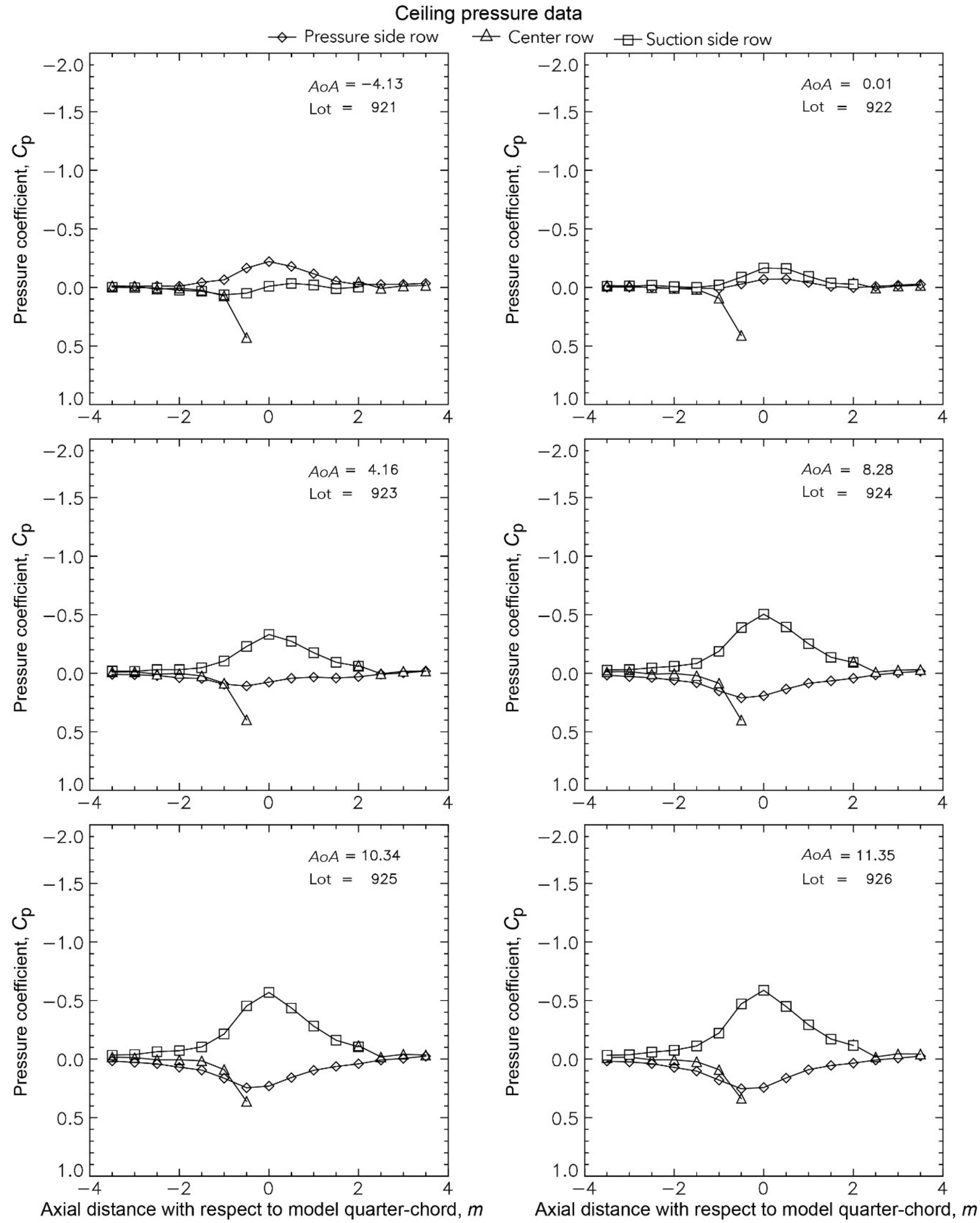

Roughness Ice 1—Lot EG1126: M = 0.10 and Re = 12.1–12.2×10^6

Appendix G.—F1 Full-Scale Model Tests

Roughness Ice 1—Lot EG1126: M = 0.10 and Re = 12.1–12.2×10^6

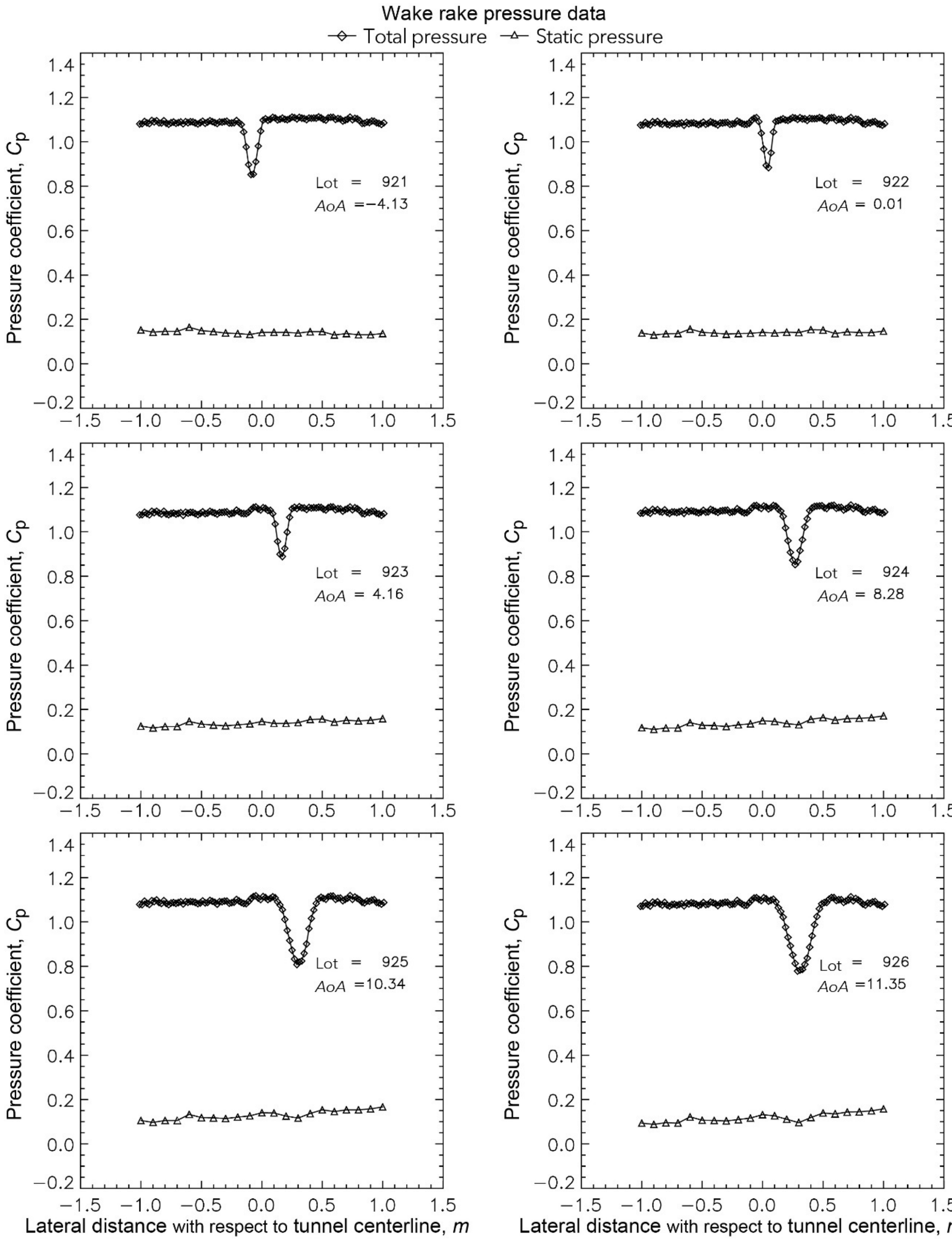

Roughness Ice 1—Lot EG1126: M = 0.10 and Re = 12.1–12.2×10^6

Appendix G.—F1 Full-Scale Model Tests

Roughness Ice 1—Lot EG1126: M = 0.20 to 0.21 and Re = 8.8×10^6

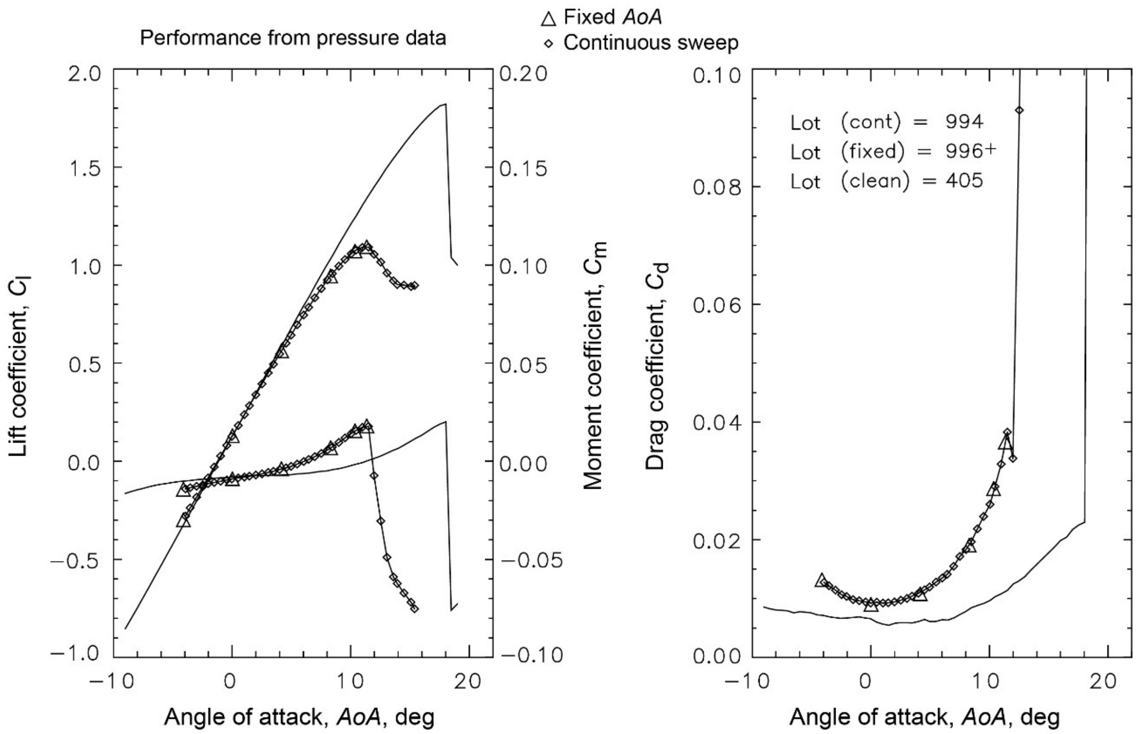

Roughness Ice 1—Lot EG1126: M = 0.20 to 0.21 and Re = 8.8×10^6

Appendix G.—F1 Full-Scale Model Tests

Roughness Ice 1—Lot EG1126: M = 0.20 to 0.21 and Re = 8.8×10^6

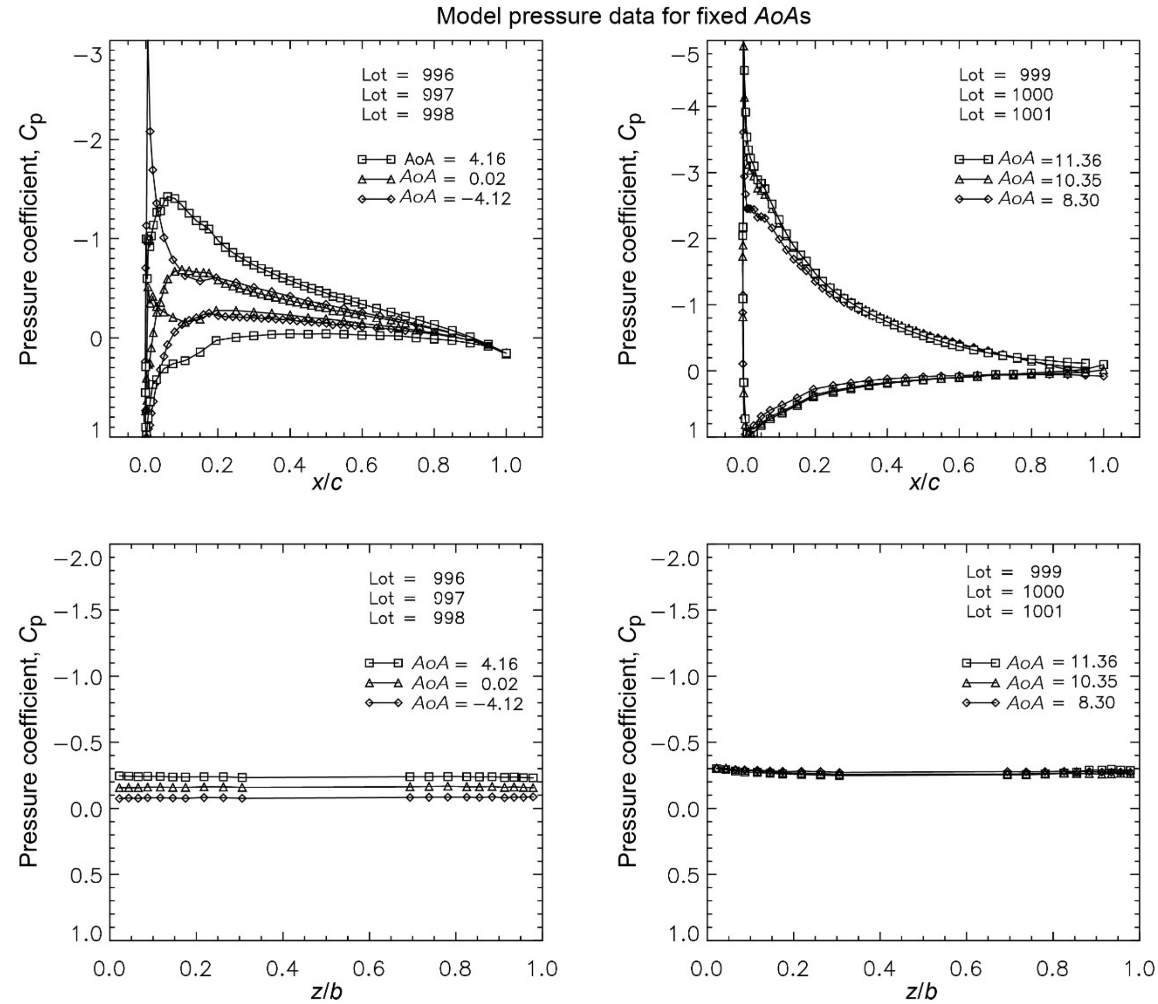

Roughness Ice 1—Lot EG1126: M = 0.20 to 0.21 and Re = 8.8×10^6

Roughness Ice 1—Lot EG1126: M = 0.20 to 0.21 and Re = 8.8×10^6

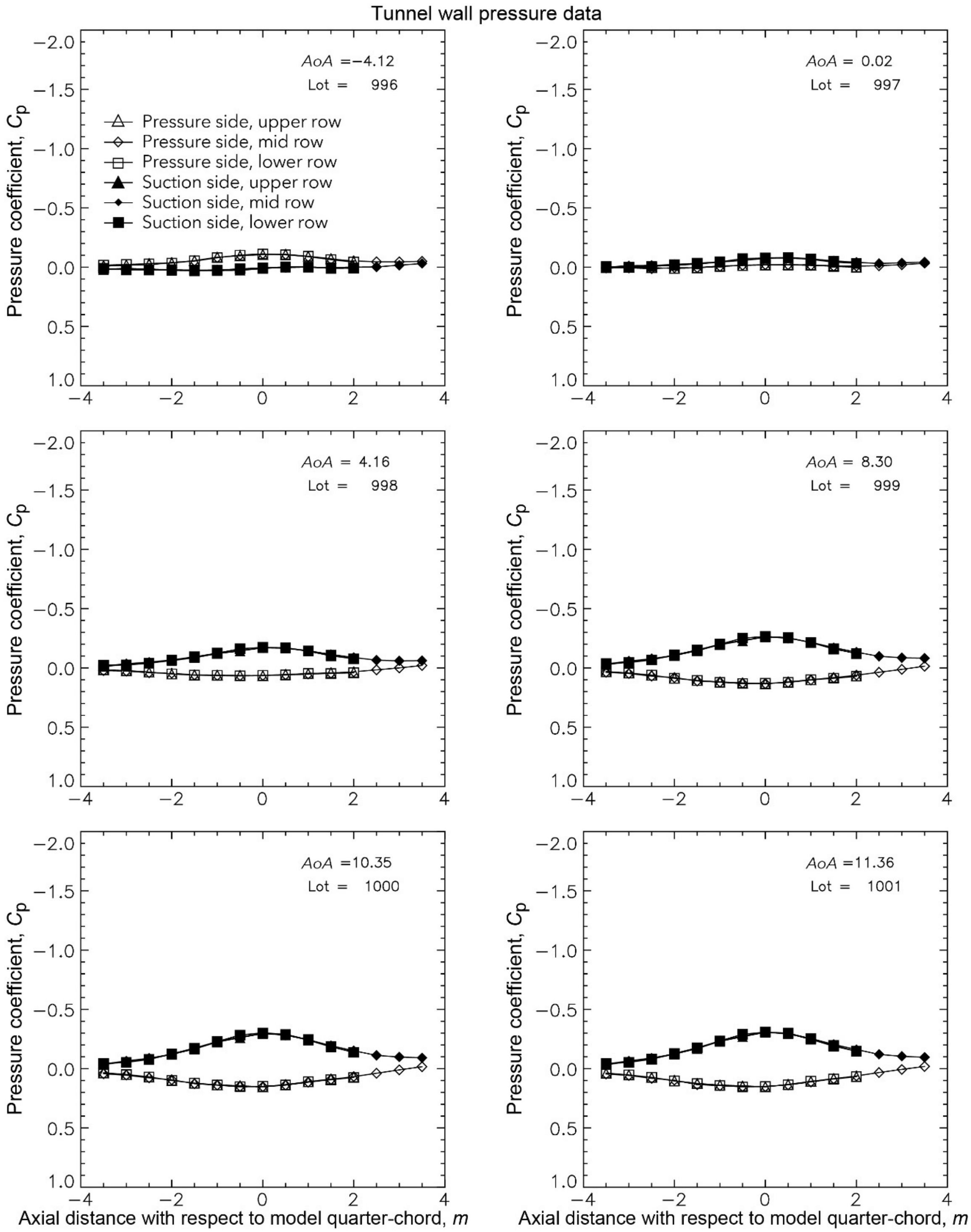

Roughness Ice 1—Lot EG1126: M = 0.20 to 0.21 and Re = 8.8×10^6

Appendix G.—F1 Full-Scale Model Tests

Roughness Ice 1—Lot EG1126: M = 0.20 to 0.21 and Re = 8.8×10^6

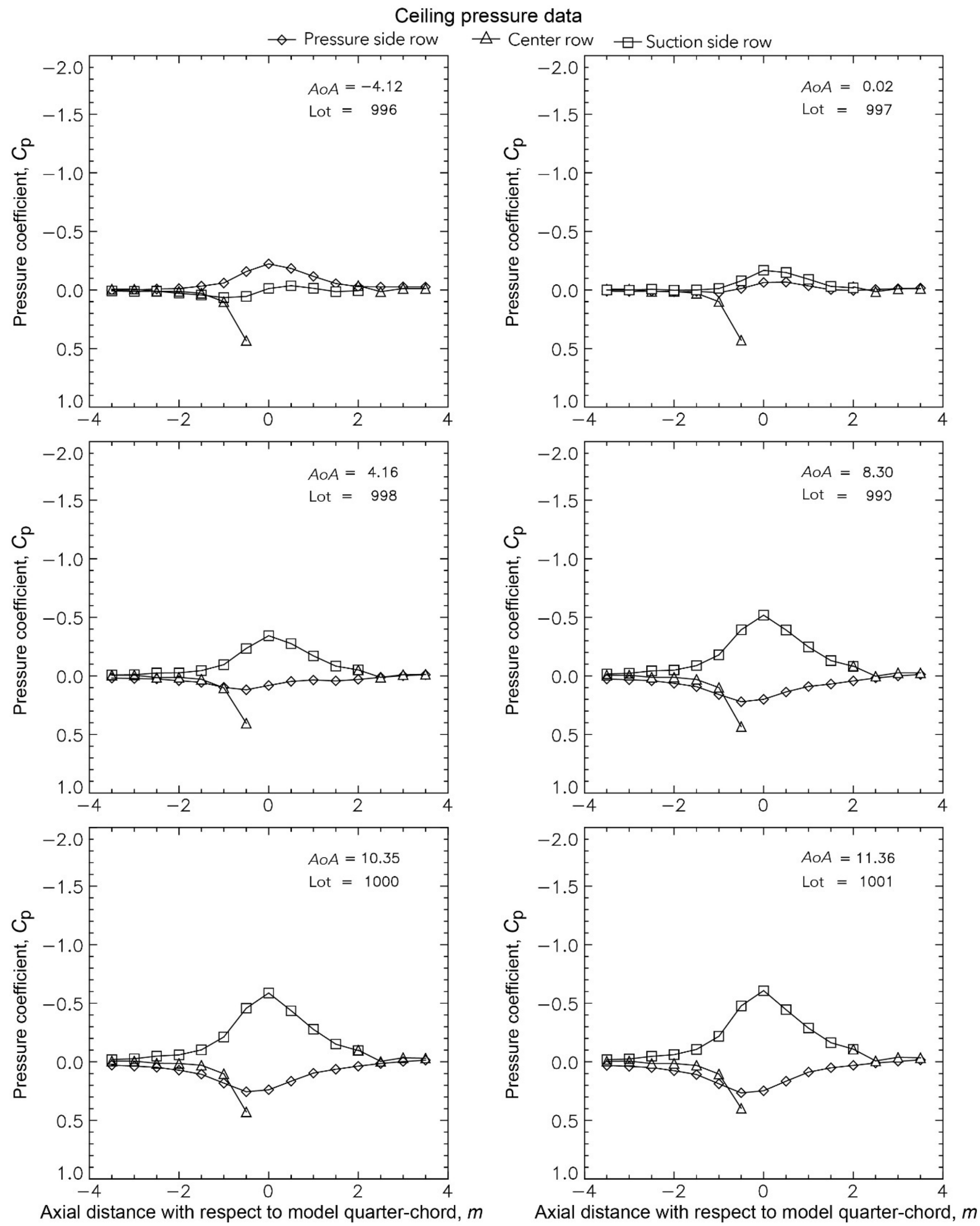

Roughness Ice 1—Lot EG1126: M = 0.20 to 0.21 and Re = 8.8×10^6

Appendix G.—F1 Full-Scale Model Tests

Roughness Ice 1—Lot EG1126: M = 0.20 to 0.21 and Re = 8.8×10^6

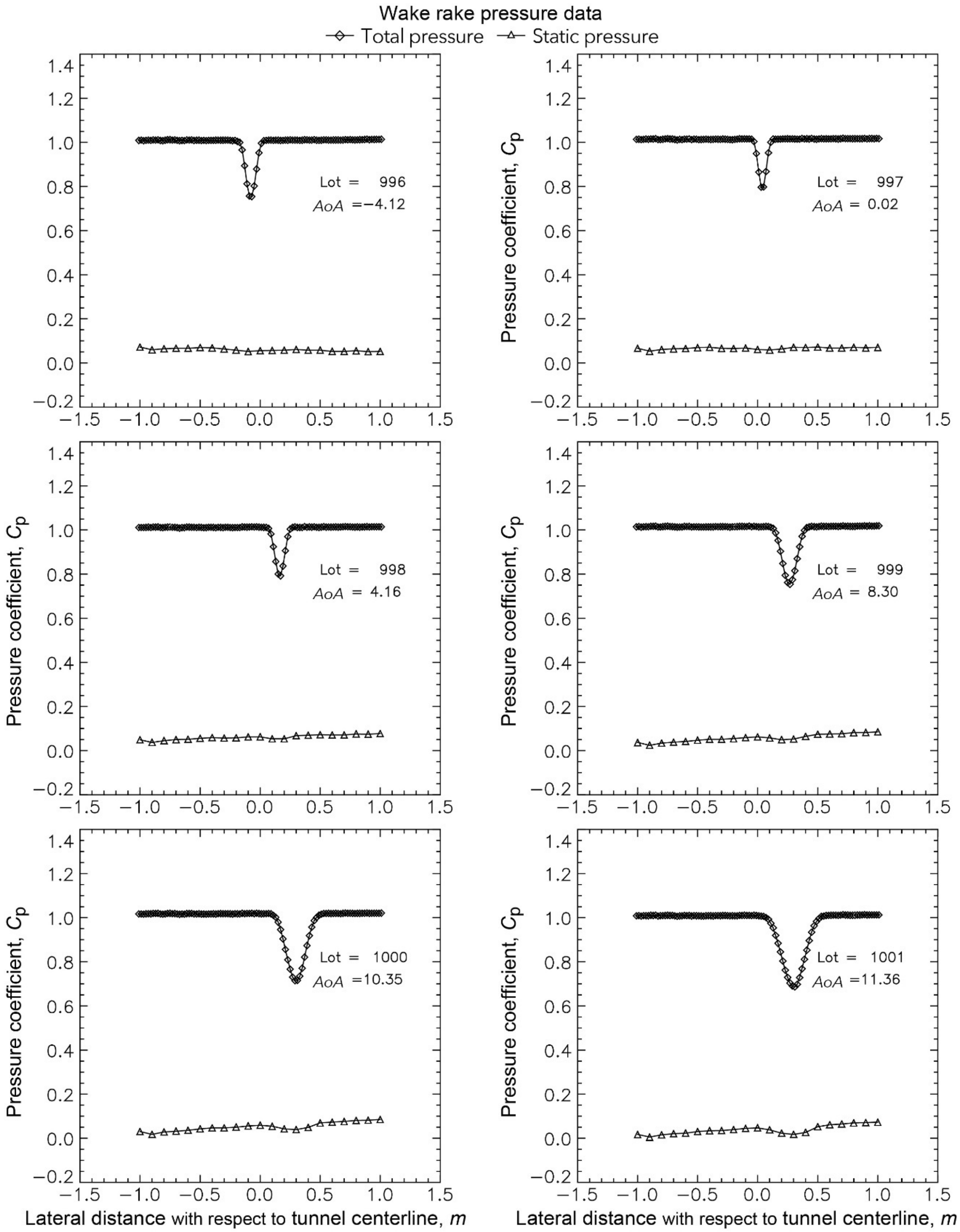

Roughness Ice 1—Lot EG1126: M = 0.20 to 0.21 and Re = 8.8×10^6

Appendix G.—F1 Full-Scale Model Tests

Roughness Ice 1—Lot EG1126: M = 0.20 to 0.21 and Re = 12.1×10^6

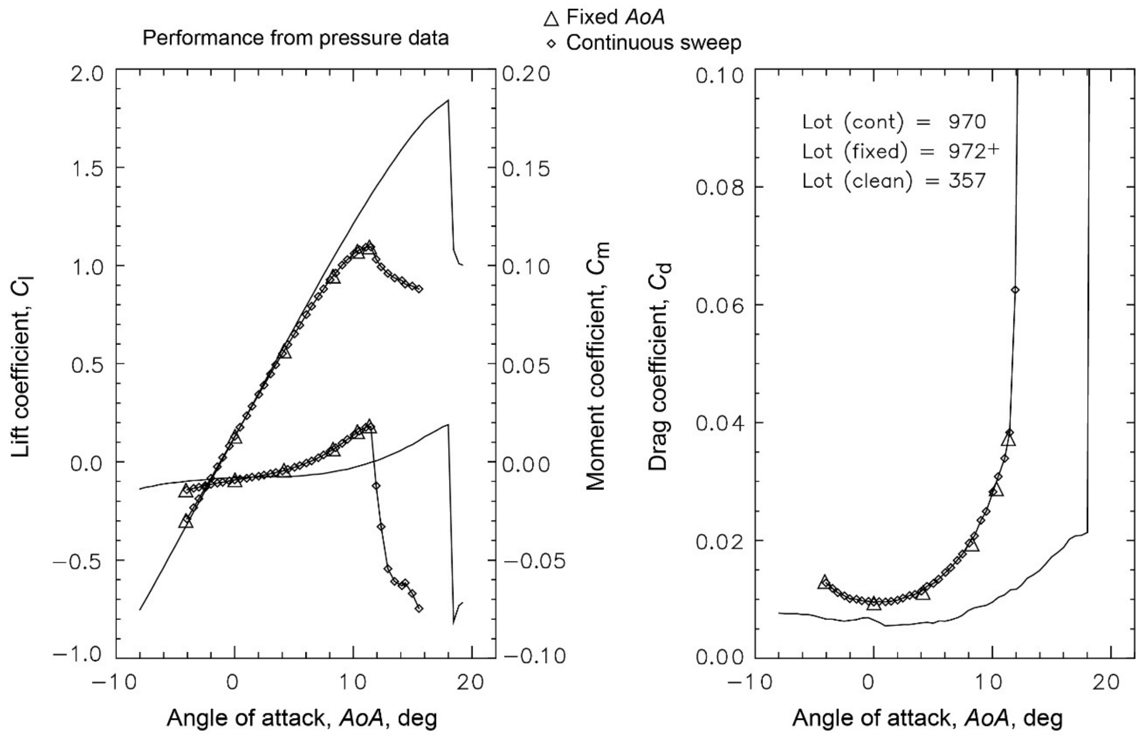

Roughness Ice 1—Lot EG1126: M = 0.20 to 0.21 and Re = 12.1×10^6

Appendix G.—F1 Full-Scale Model Tests

Roughness Ice 1—Lot EG1126: M = 0.20 to 0.21 and Re = 12.1×10^6

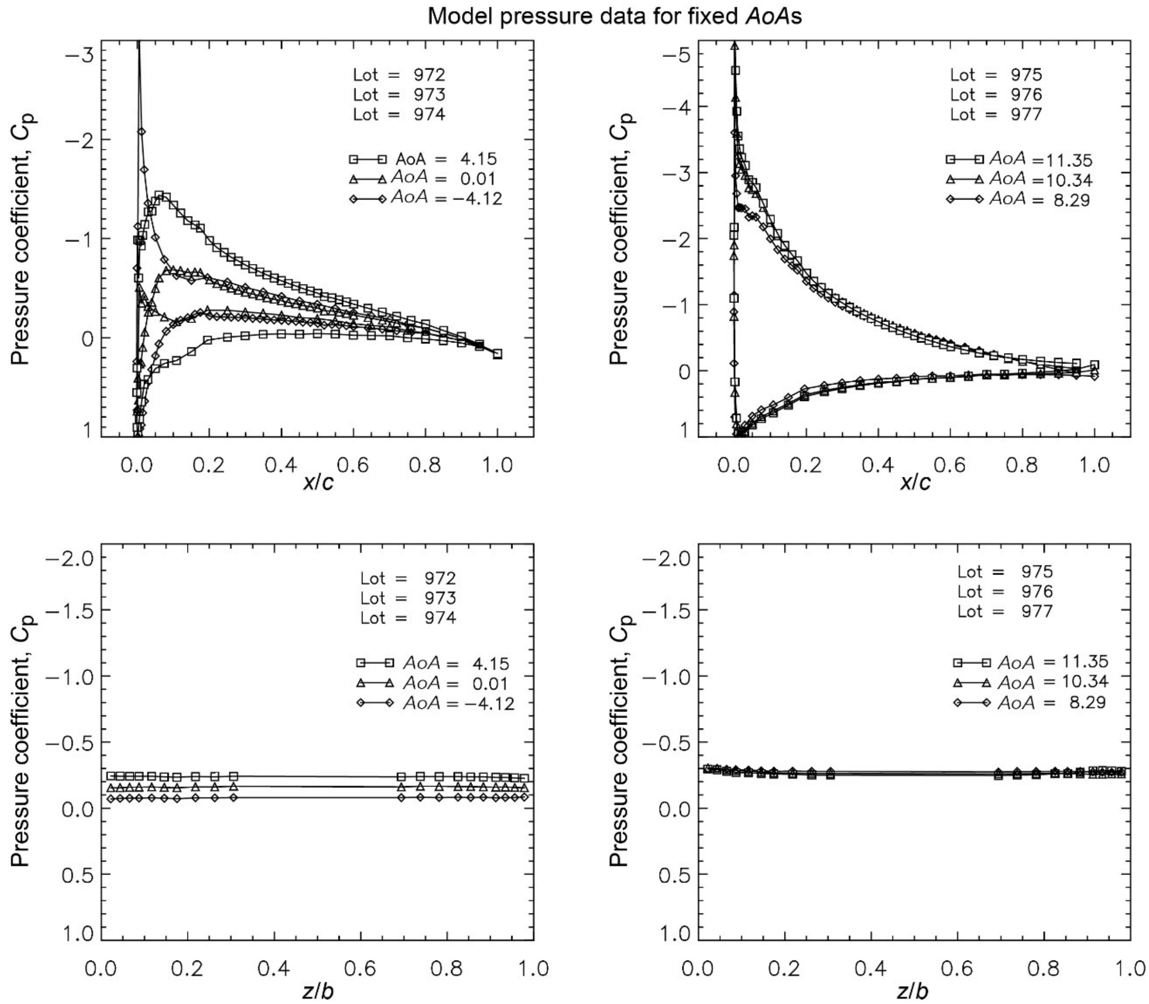

Roughness Ice 1—Lot EG1126: M = 0.20 to 0.21 and Re = 12.1×10^6

Appendix G.—F1 Full-Scale Model Tests

Roughness Ice 1—Lot EG1126: M = 0.20 to 0.21 and Re = 12.1×10^6

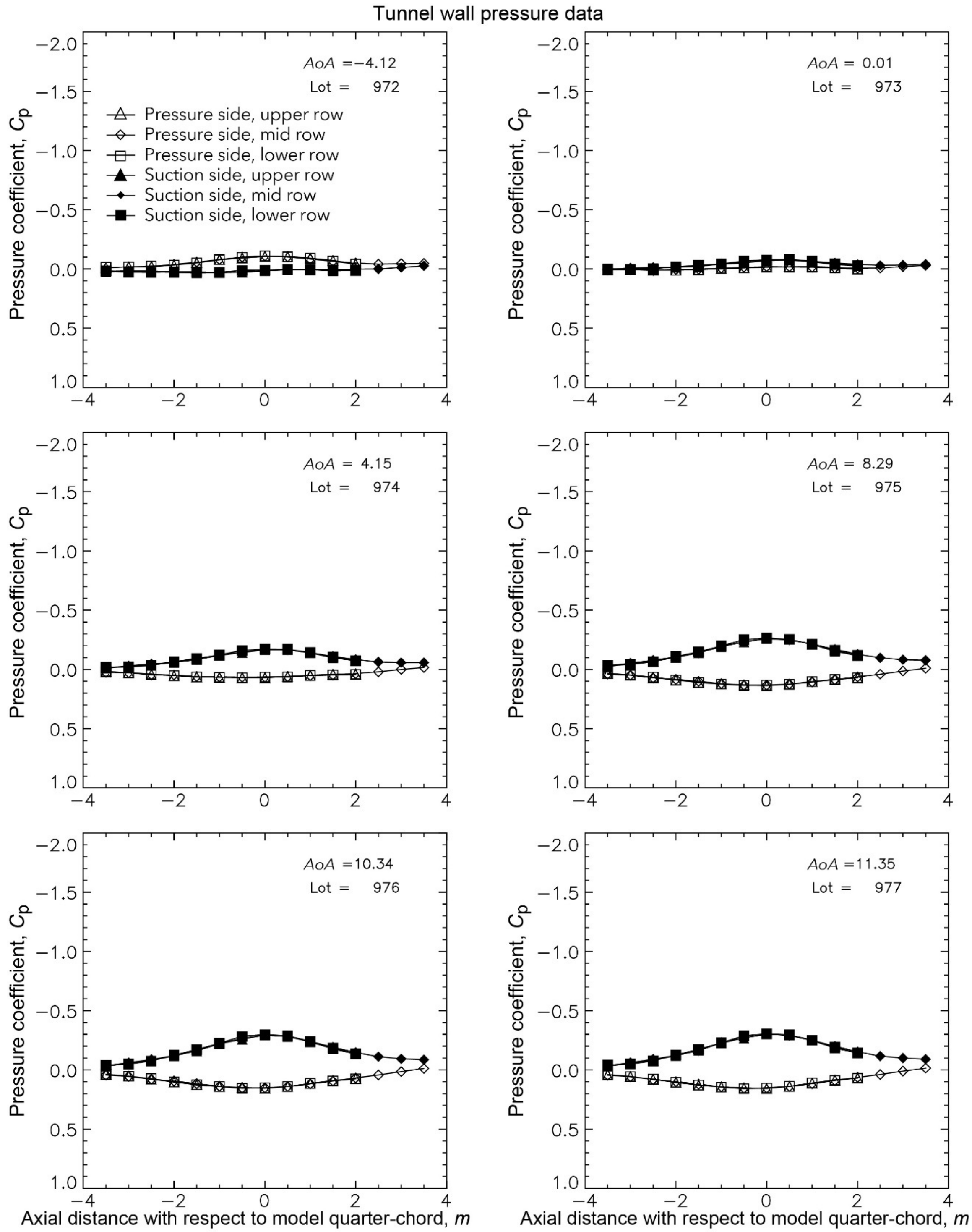

Roughness Ice 1—Lot EG1126: M = 0.20 to 0.21 and Re = 12.1×10^6

Appendix G.—F1 Full-Scale Model Tests

Roughness Ice 1—Lot EG1126: M = 0.20 to 0.21 and Re = 12.1×10^6

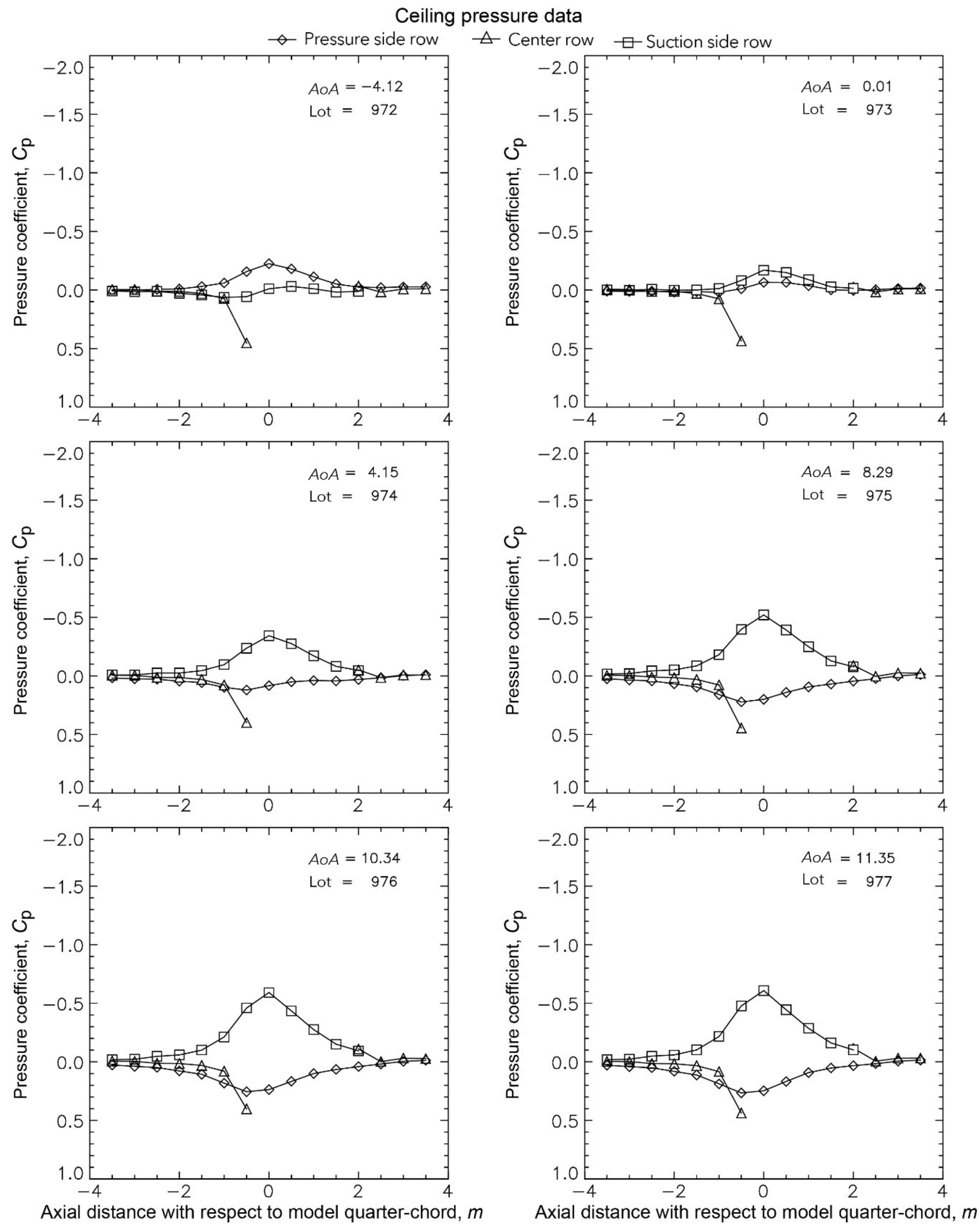

Roughness Ice 1—Lot EG1126: M = 0.20 to 0.21 and Re = 12.1×10^6

Appendix G.—F1 Full-Scale Model Tests

Roughness Ice 1—Lot EG1126: M = 0.20 to 0.21 and Re = 12.1×10^6

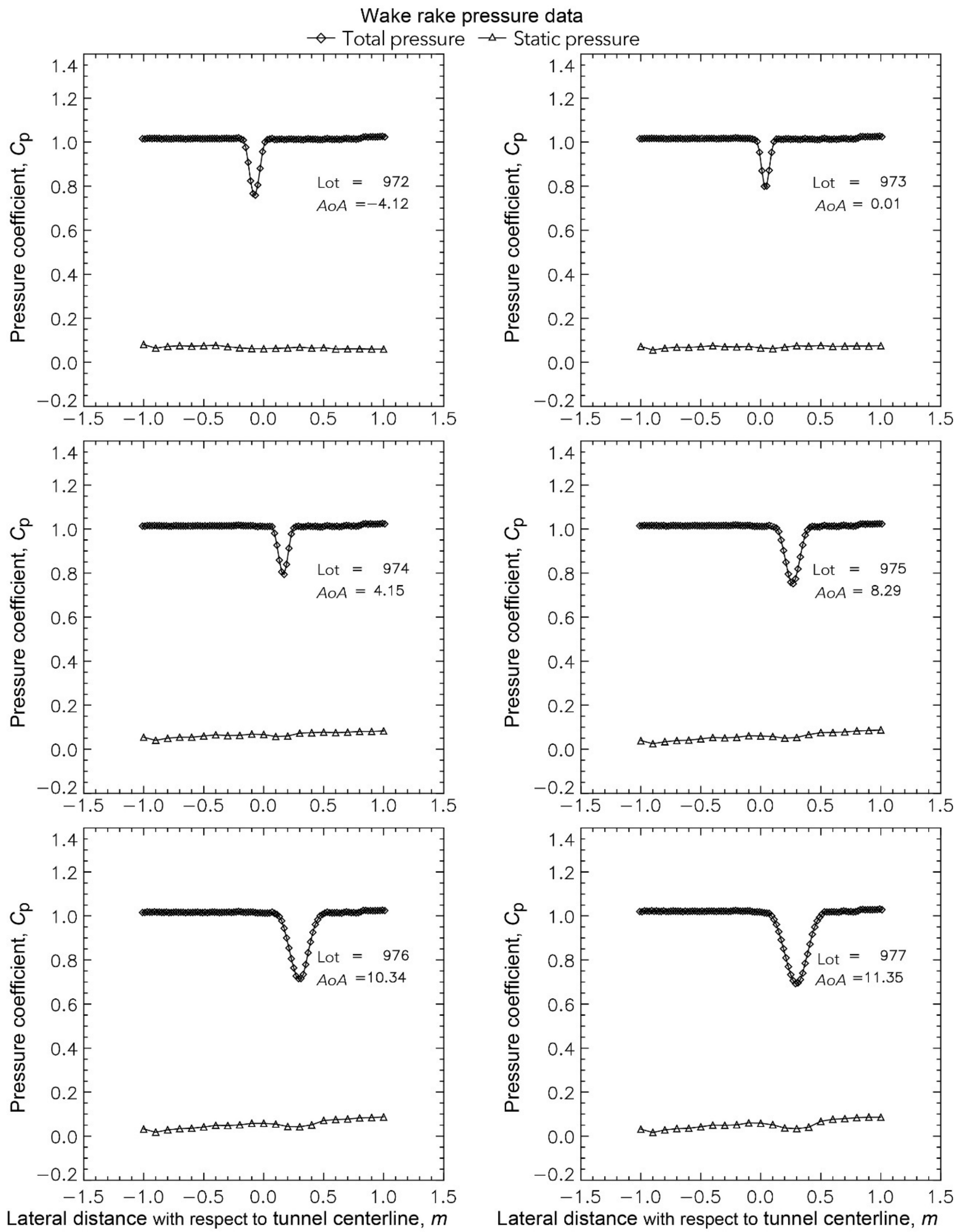

Roughness Ice 1—Lot EG1126: M = 0.20 to 0.21 and Re = 12.1×10^6

Appendix G.—F1 Full-Scale Model Tests

Roughness Ice 1—Lot EG1126: M = 0.20 to 0.21 and Re = 15.9–16.0×10^6

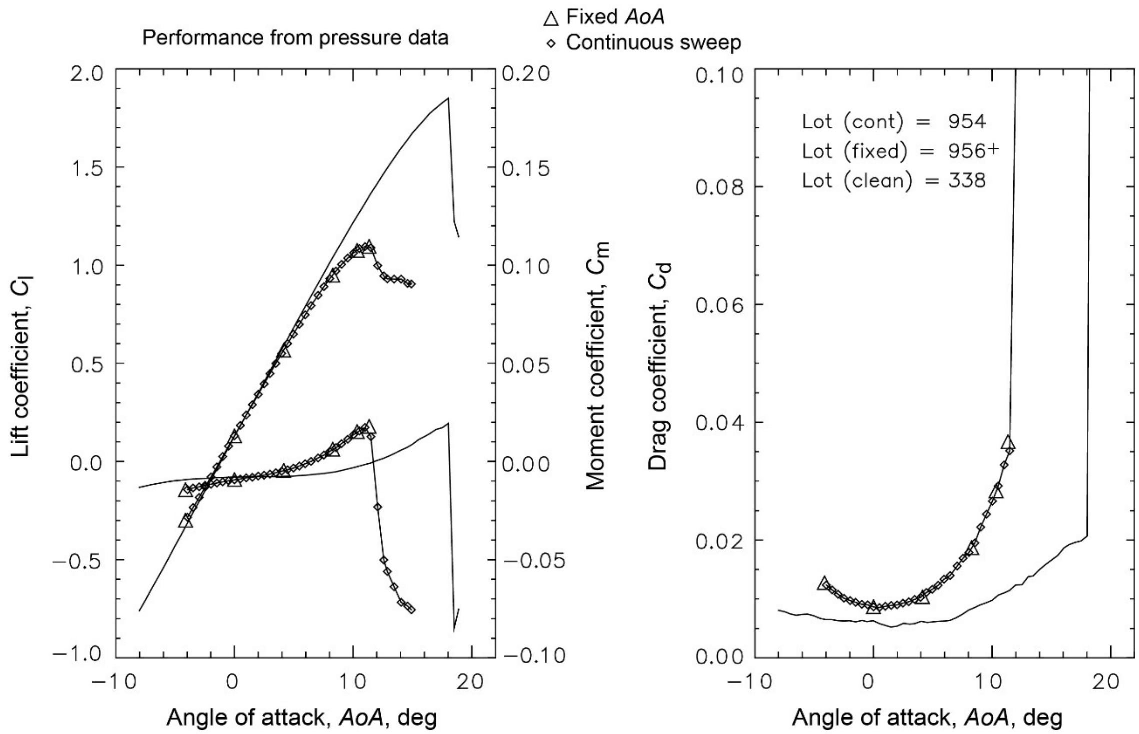

Roughness Ice 1—Lot EG1126: M = 0.20 to 0.21 and Re = 15.9–16.0×10^6

Appendix G.—F1 Full-Scale Model Tests

Roughness Ice 1—Lot EG1126: M = 0.20 to 0.21 and Re = 15.9–16.0×10[6]

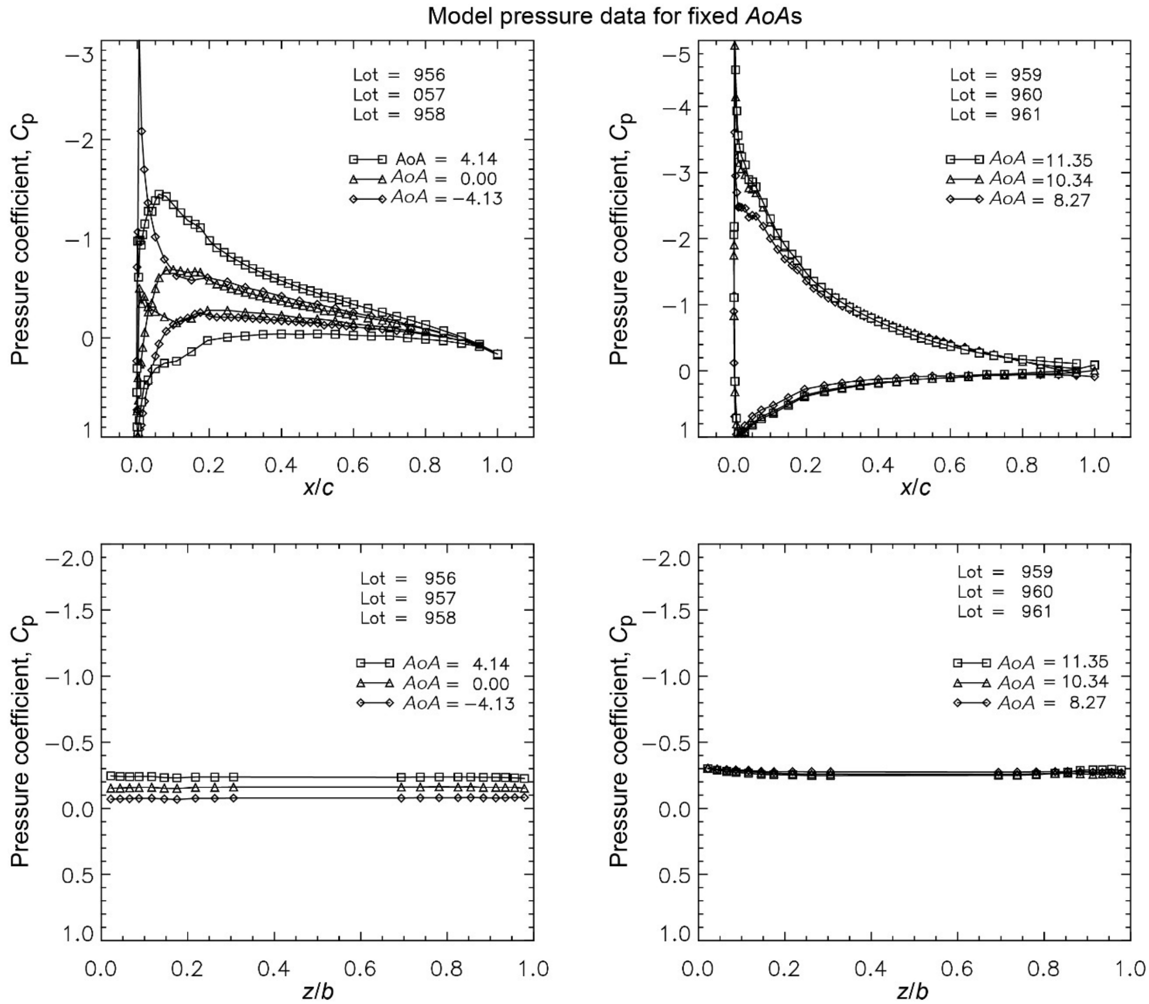

Roughness Ice 1—Lot EG1126: M = 0.20 to 0.21 and Re = 15.9–16.0×10[6]

Appendix G.—F1 Full-Scale Model Tests

Roughness Ice 1—Lot EG1126: M = 0.20 to 0.21 and Re = 15.9–16.0×10^6

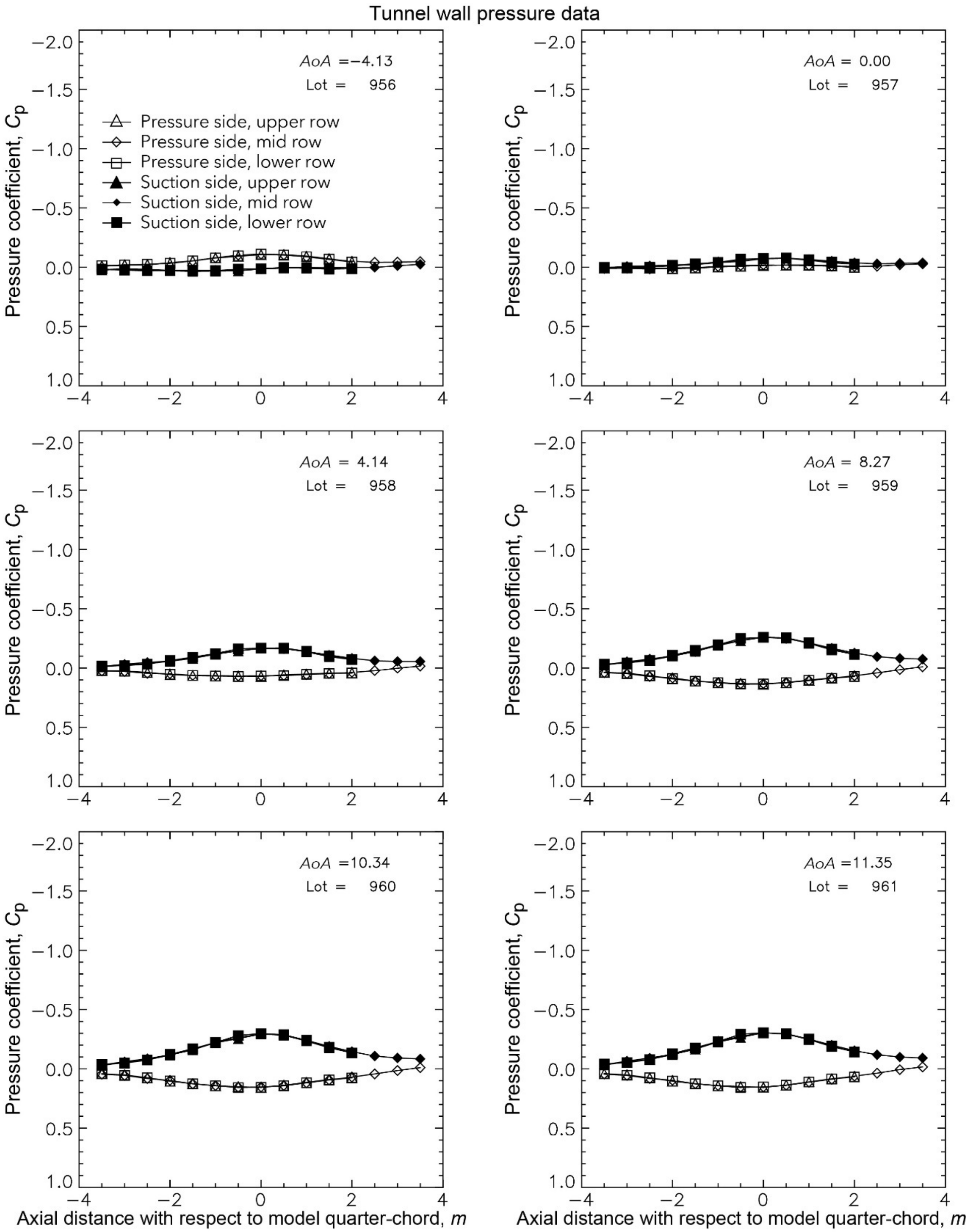

Roughness Ice 1—Lot EG1126: M = 0.20 to 0.21 and Re = 15.9–16.0×10^6

Appendix G.—F1 Full-Scale Model Tests

Roughness Ice 1—Lot EG1126: M = 0.20 to 0.21 and Re = 15.9–16.0×10^6

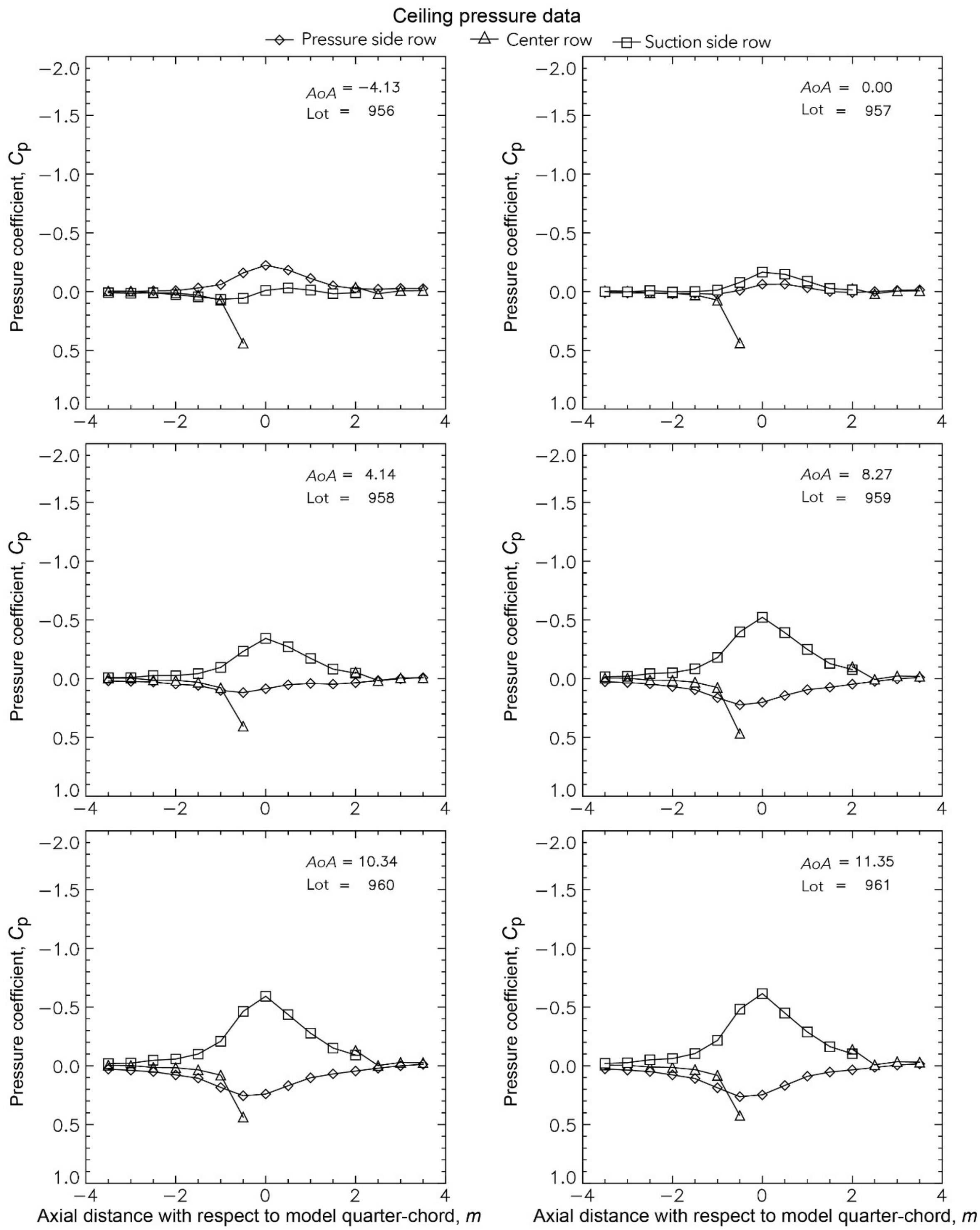

Roughness Ice 1—Lot EG1126: M = 0.20 to 0.21 and Re = 15.9–16.0×10^6

Appendix G.—F1 Full-Scale Model Tests

Roughness Ice 1—Lot EG1126: M = 0.20 to 0.21 and Re = 15.9–16.0×10^6

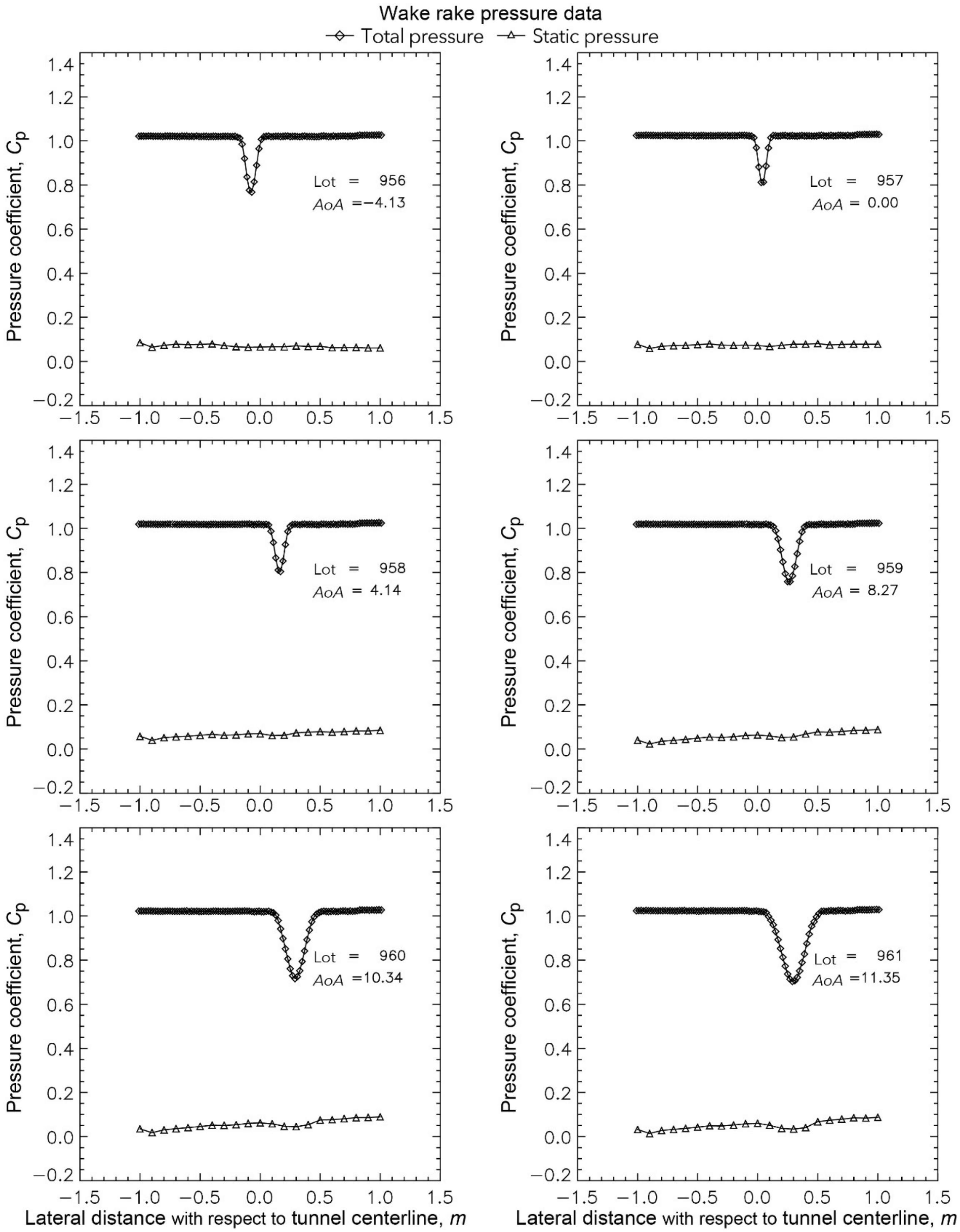

Roughness Ice 1—Lot EG1126: M = 0.20 to 0.21 and Re = 15.9–16.0×10^6

Appendix G.—F1 Full-Scale Model Tests

Roughness Ice 1—Lot EG1126: M = 0.29 and Re = 12.1–12.2×10⁶

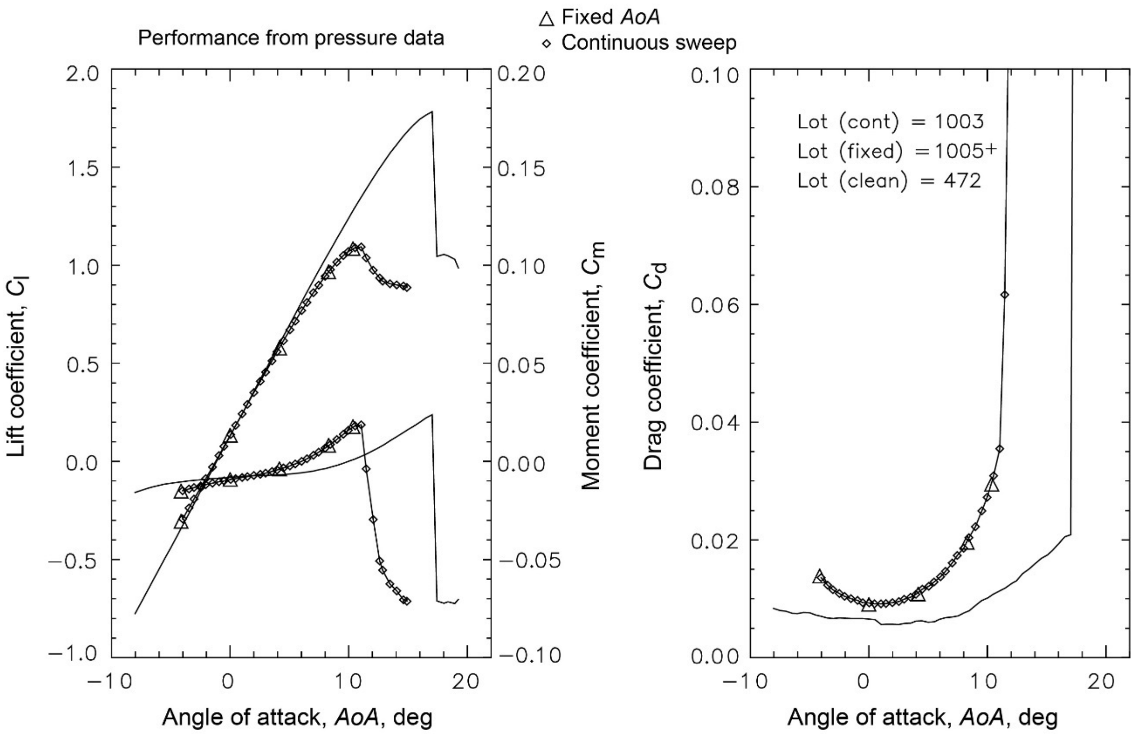

Roughness Ice 1—Lot EG1126: M = 0.29 and Re = 12.1–12.2×10^6

Appendix G.—F1 Full-Scale Model Tests

Roughness Ice 1—Lot EG1126: M = 0.29 and Re = 12.1–12.2×10^6

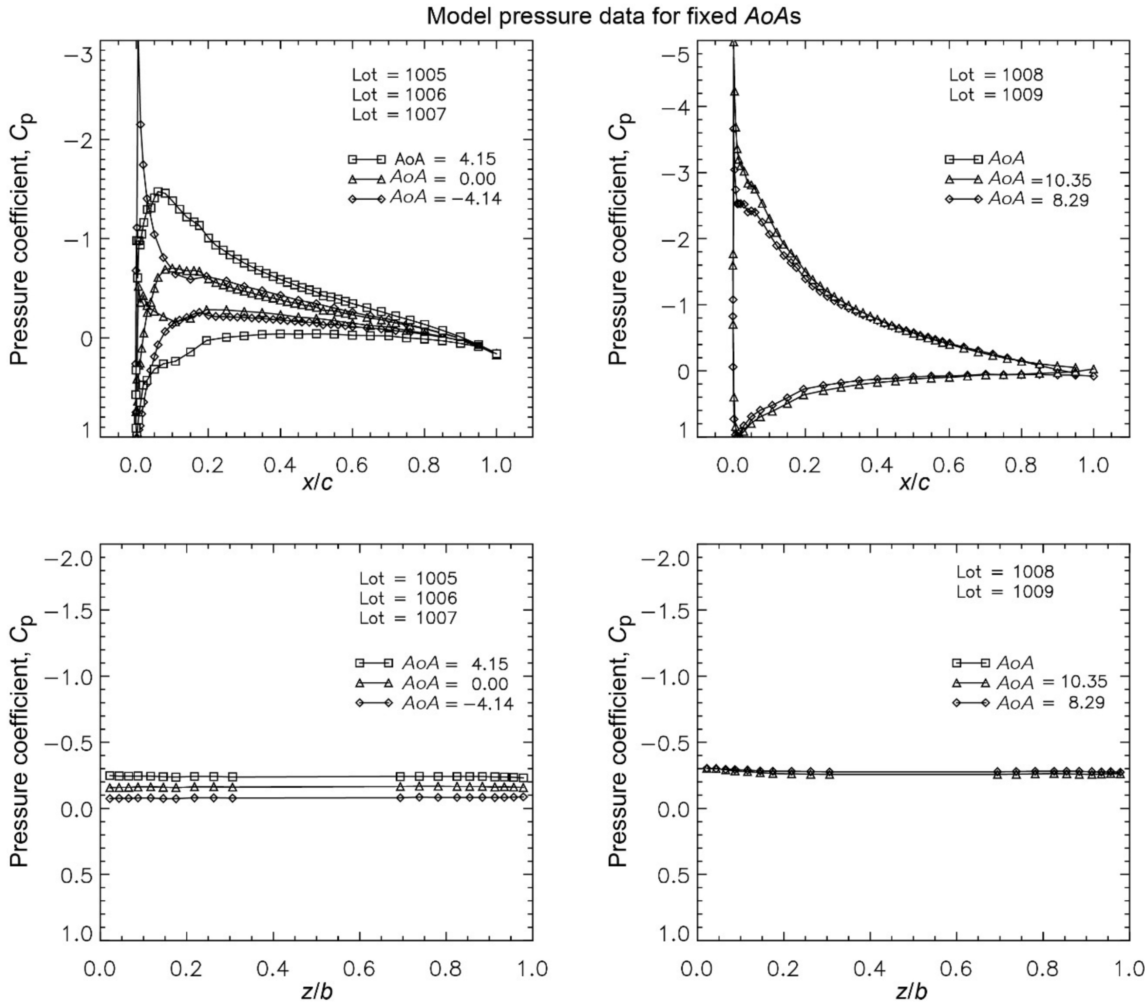

Roughness Ice 1—Lot EG1126: M = 0.29 and Re = 12.1–12.2×10^6

Appendix G.—F1 Full-Scale Model Tests

Roughness Ice 1—Lot EG1126: M = 0.29 and Re = 12.1–12.2×10^6

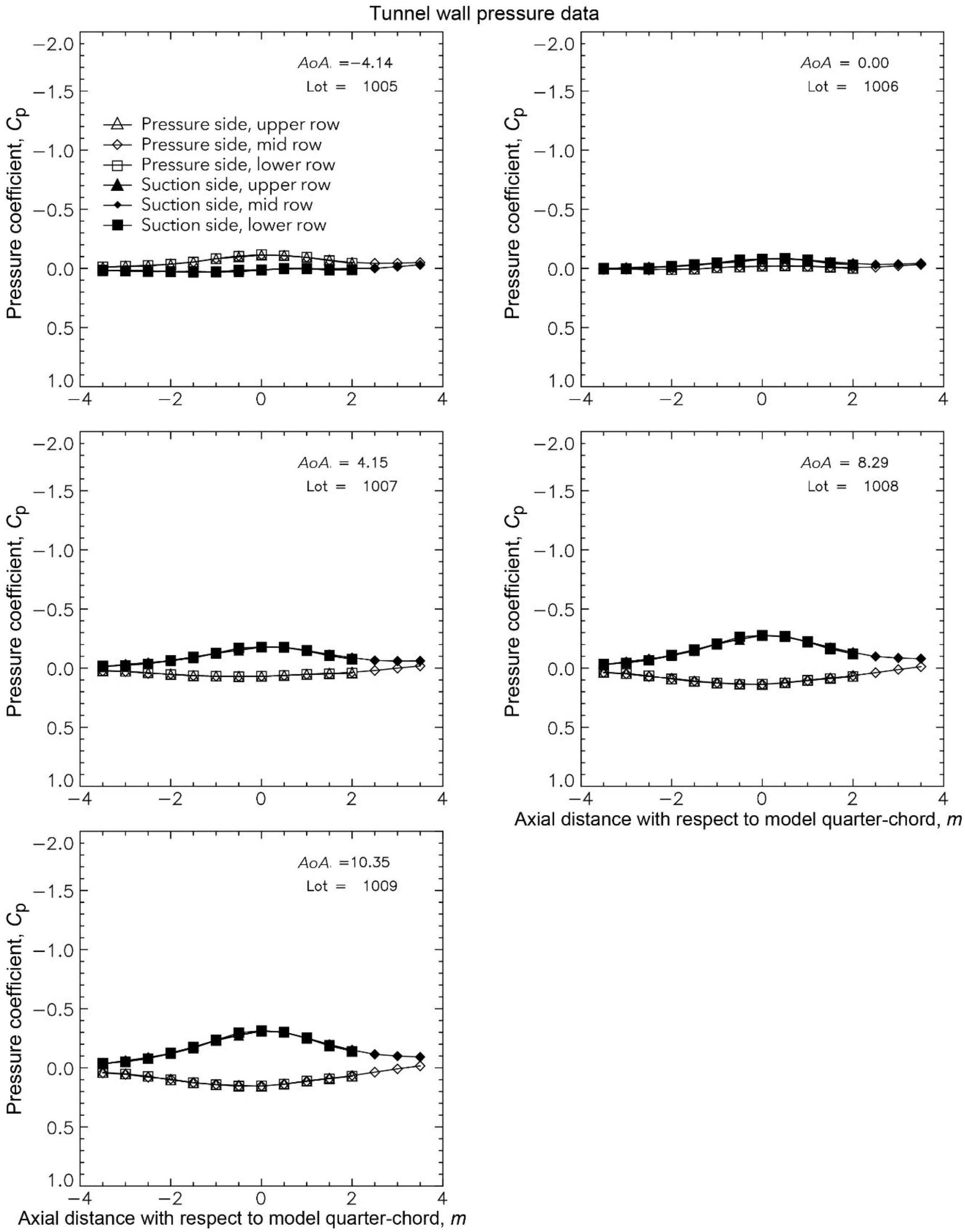

Roughness Ice 1—Lot EG1126: M = 0.29 and Re = 12.1–12.2×10^6

Appendix G.—F1 Full-Scale Model Tests

Roughness Ice 1—Lot EG1126: M = 0.29 and Re = 12.1–12.2×10^6

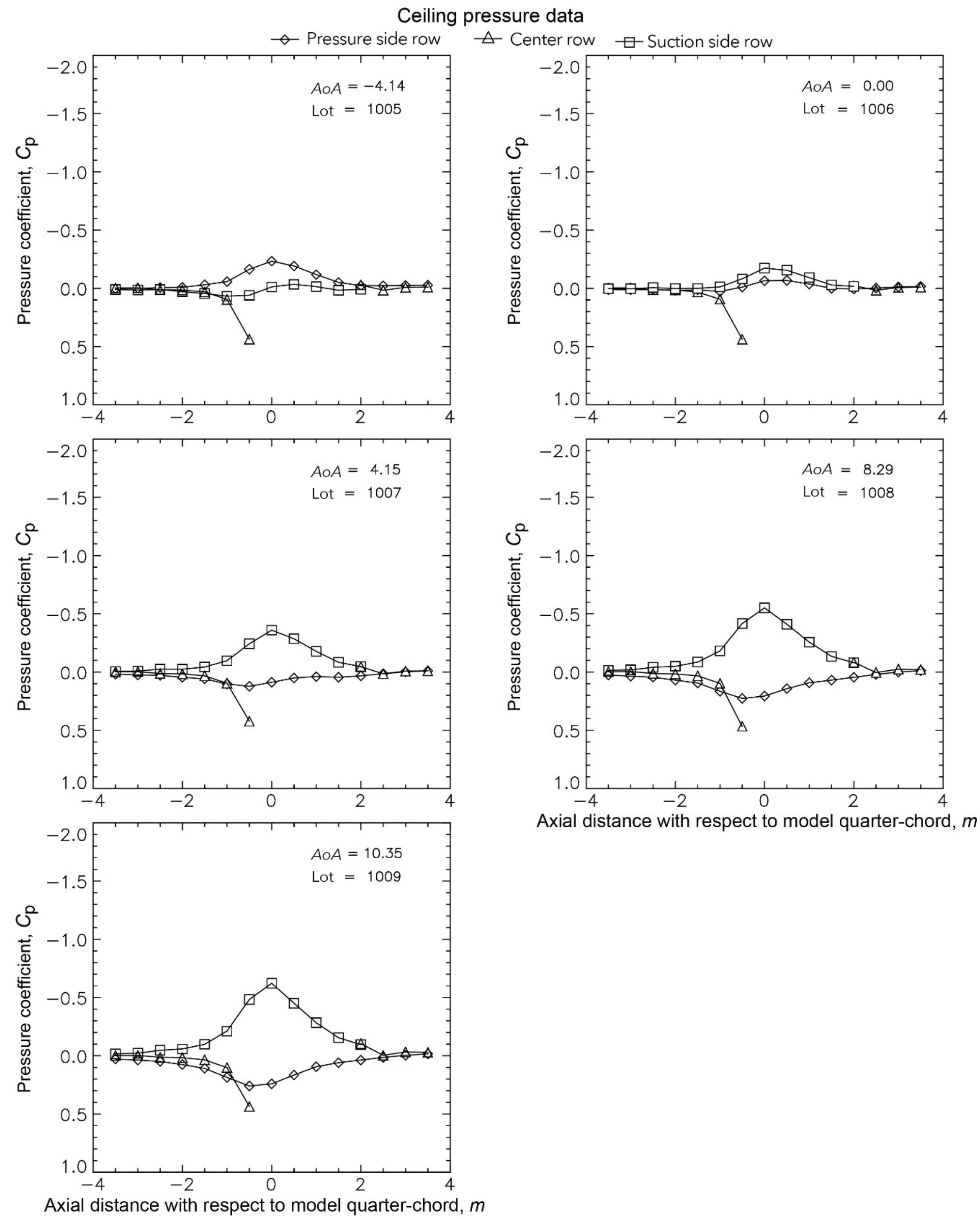

Roughness Ice 1—Lot EG1126: M = 0.29 and Re = 12.1–12.2×10^6

Appendix G.—F1 Full-Scale Model Tests

Roughness Ice 1—Lot EG1126: M = 0.29 and Re = 12.1–12.2×10^6

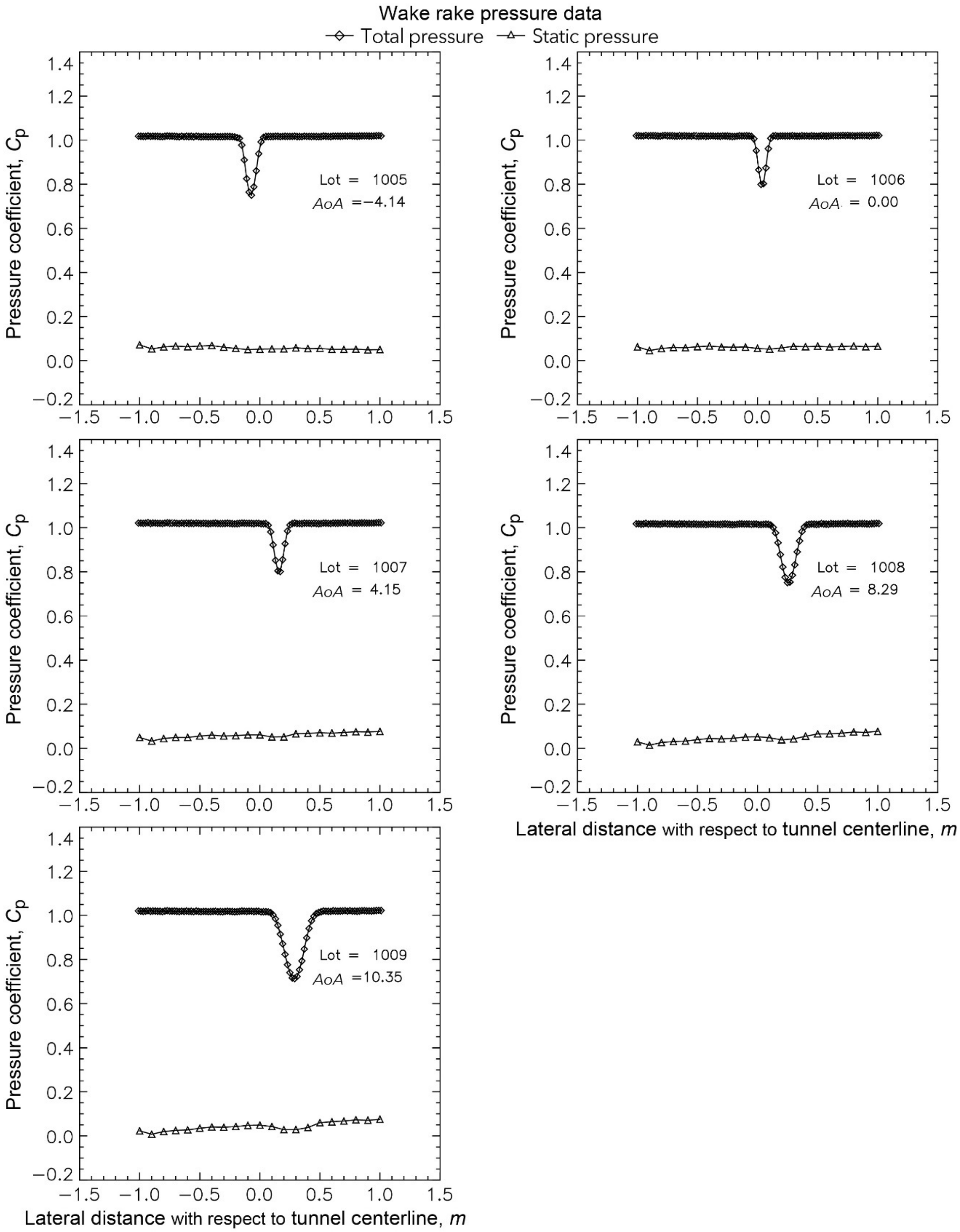

Roughness Ice 1—Lot EG1126: M = 0.29 and Re = 12.1–12.2×10^6

Appendix G.—F1 Full-Scale Model Tests

Spanwise Ridge Ice—Lot EG1159: M = 0.10 to 0.11 and Re = 4.6×10^6

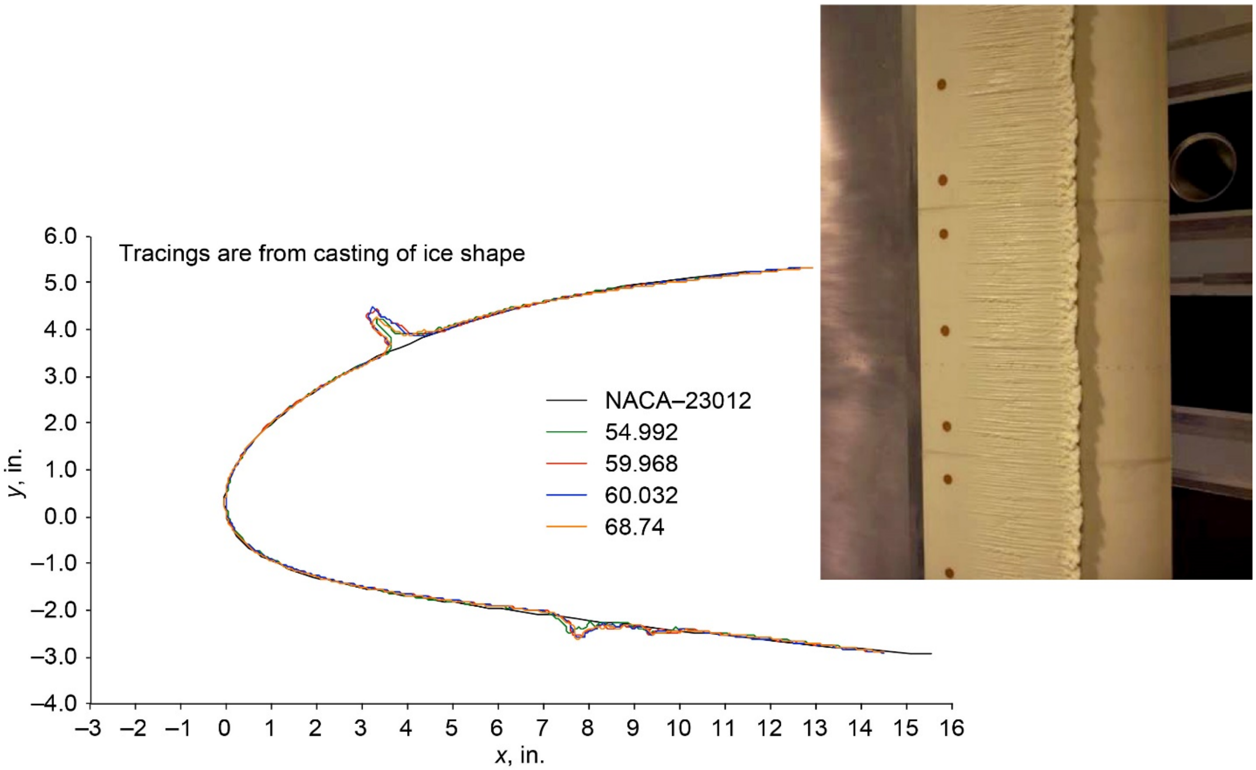

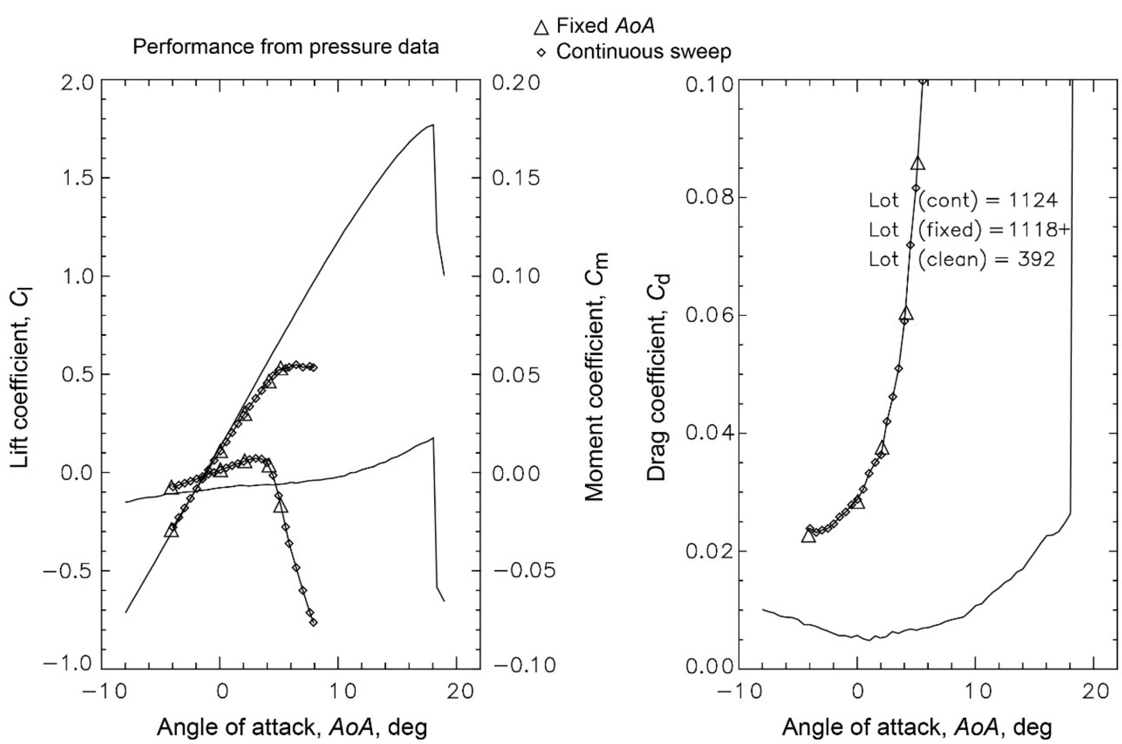

Spanwise Ridge Ice—Lot EG1159: M = 0.10 to 0.11 and Re = 4.6×10^6

Appendix G.—F1 Full-Scale Model Tests

Spanwise Ridge Ice—Lot EG1159: M = 0.10 to 0.11 and Re = 4.6×10^6

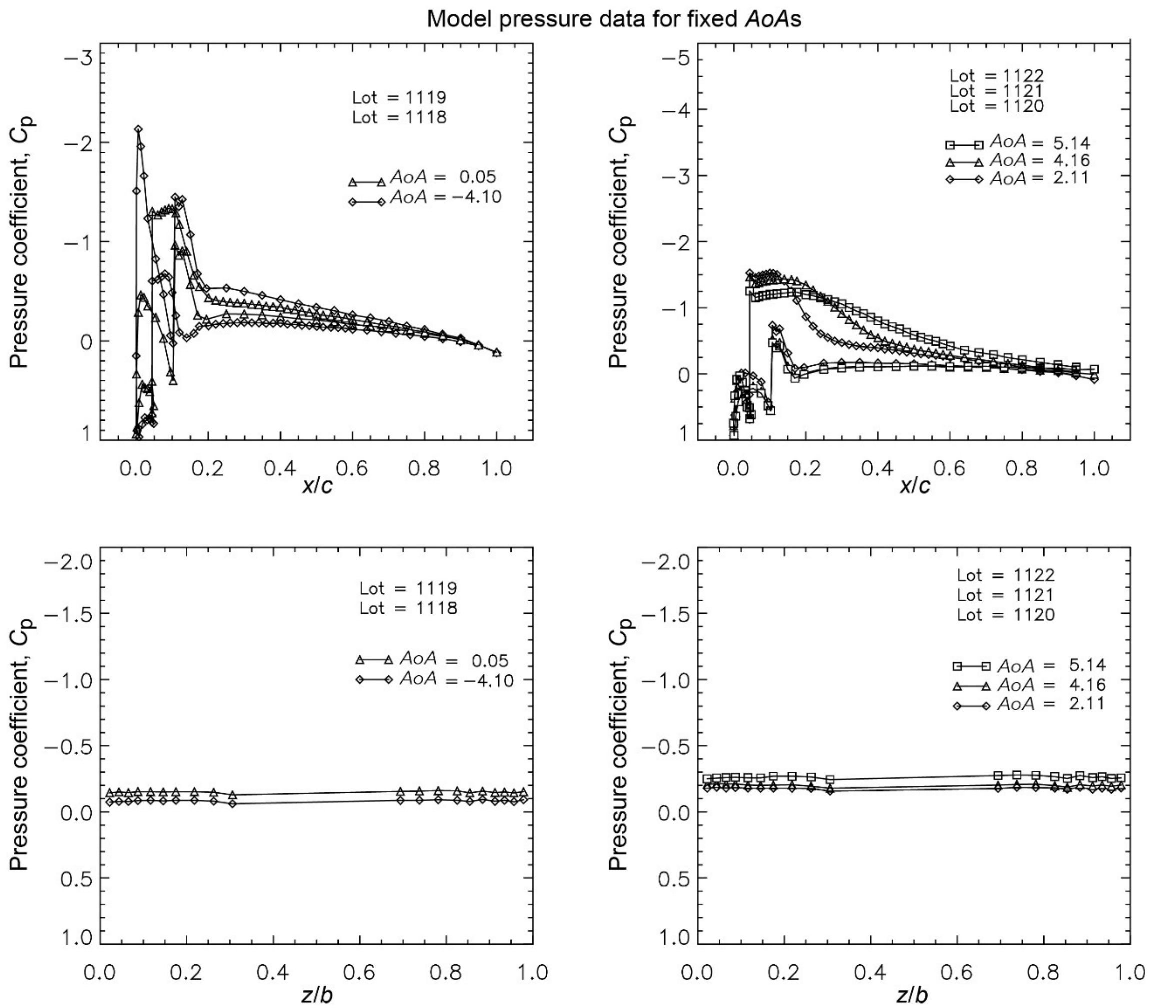

Spanwise Ridge Ice—Lot EG1159: M = 0.10 to 0.11 and Re = 4.6×10^6

Spanwise Ridge Ice—Lot EG1159: M = 0.10 to 0.11 and Re = 4.6×10^6

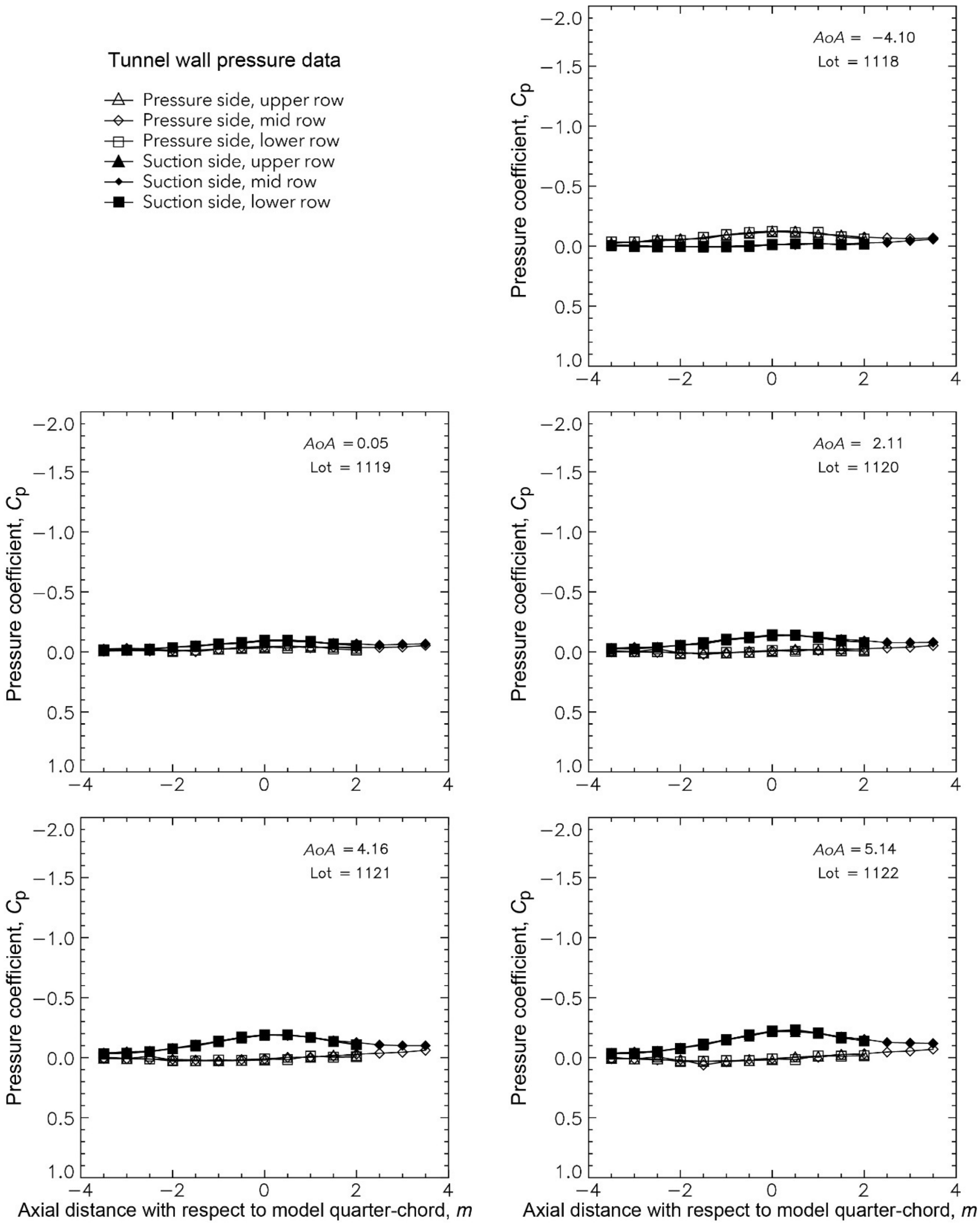

Spanwise Ridge Ice—Lot EG1159: M = 0.10 to 0.11 and Re = 4.6×10^6

Appendix G.—F1 Full-Scale Model Tests

Spanwise Ridge Ice—Lot EG1159: M = 0.10 to 0.11 and Re = 4.6×10^6

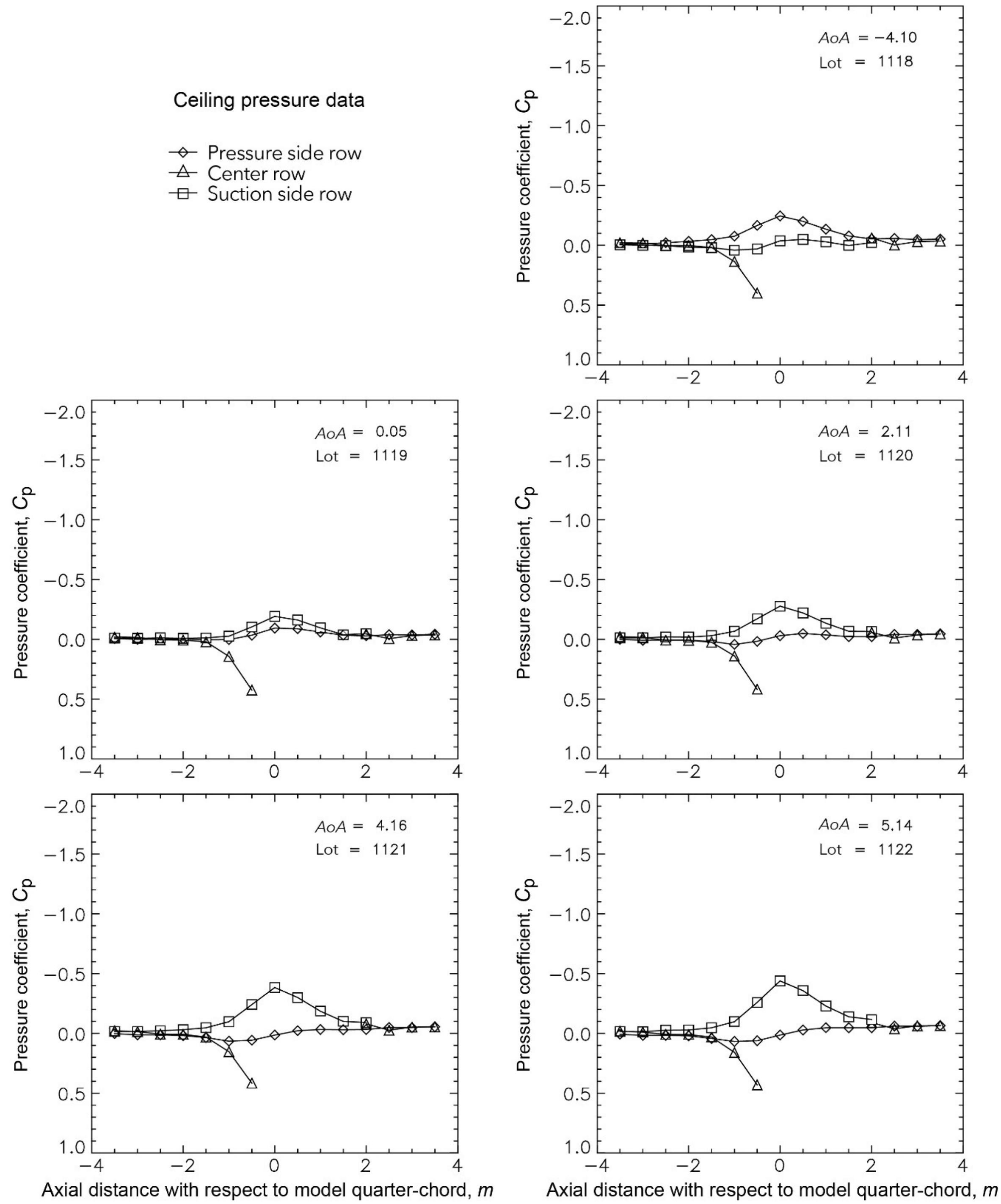

Spanwise Ridge Ice—Lot EG1159: M = 0.10 to 0.11 and Re = 4.6×10^6

Appendix G.—F1 Full-Scale Model Tests

Spanwise Ridge Ice—Lot EG1159: M = 0.10 to 0.11 and Re = 4.6×10^6

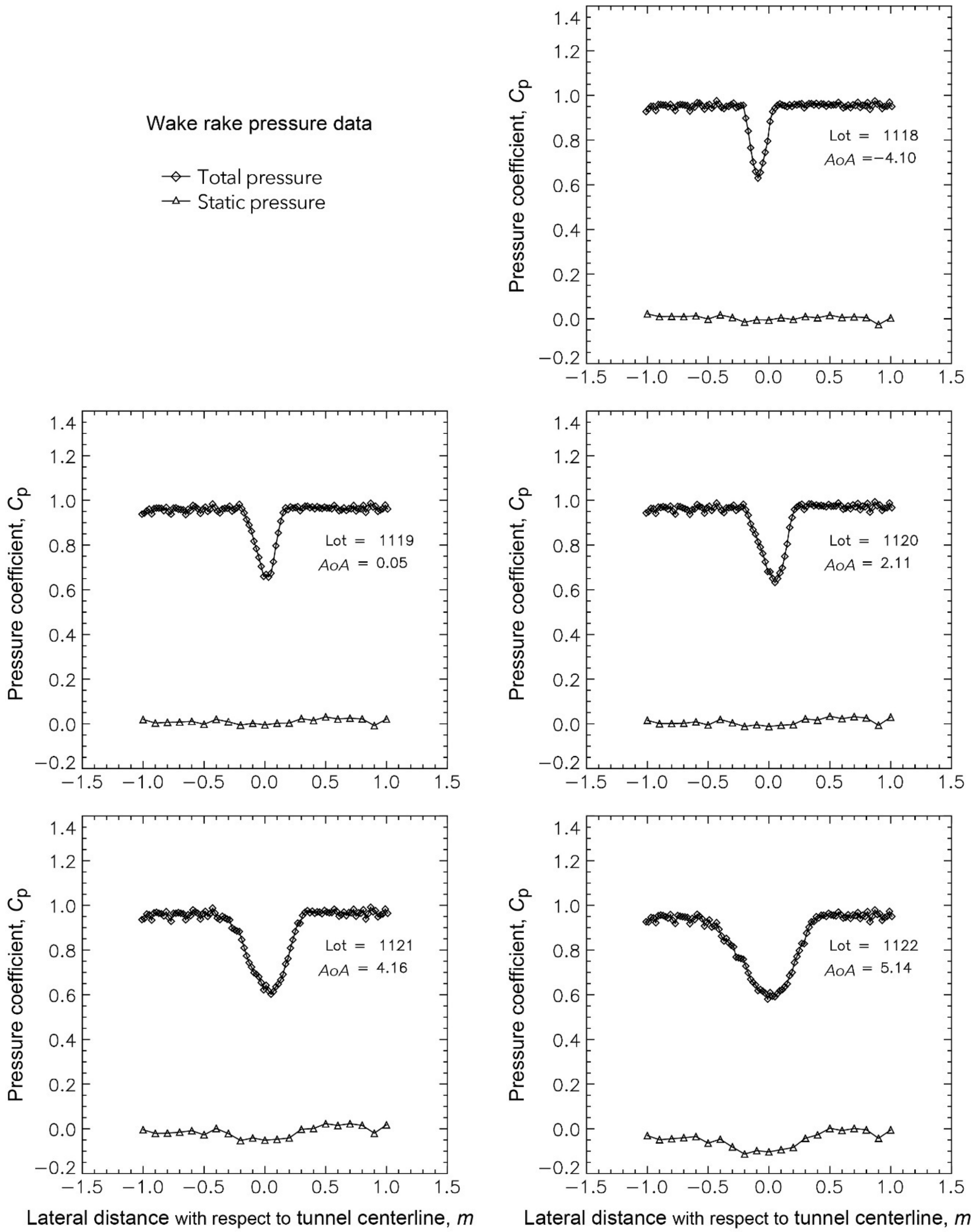

Spanwise Ridge Ice—Lot EG1159: M = 0.10 to 0.11 and Re = 4.6×10^6

Appendix G.—F1 Full-Scale Model Tests

Spanwise Ridge Ice—Lot EG1159: M = 0.10 to 0.11 and Re = 8.4–8.5×10^6

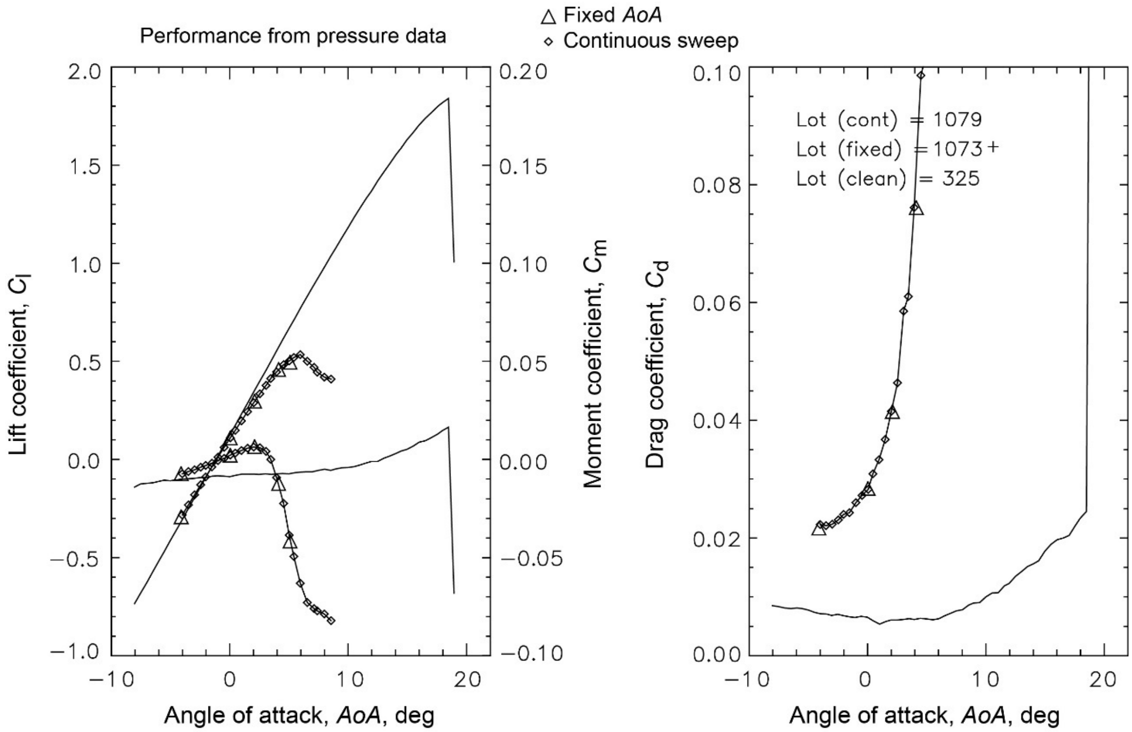

Spanwise Ridge Ice—Lot EG1159: M = 0.10 to 0.11 and Re = 8.4–8.5×10^6

Appendix G.—F1 Full-Scale Model Tests

Spanwise Ridge Ice—Lot EG1159: M = 0.10 to 0.11 and Re = 8.4–8.5×10⁶

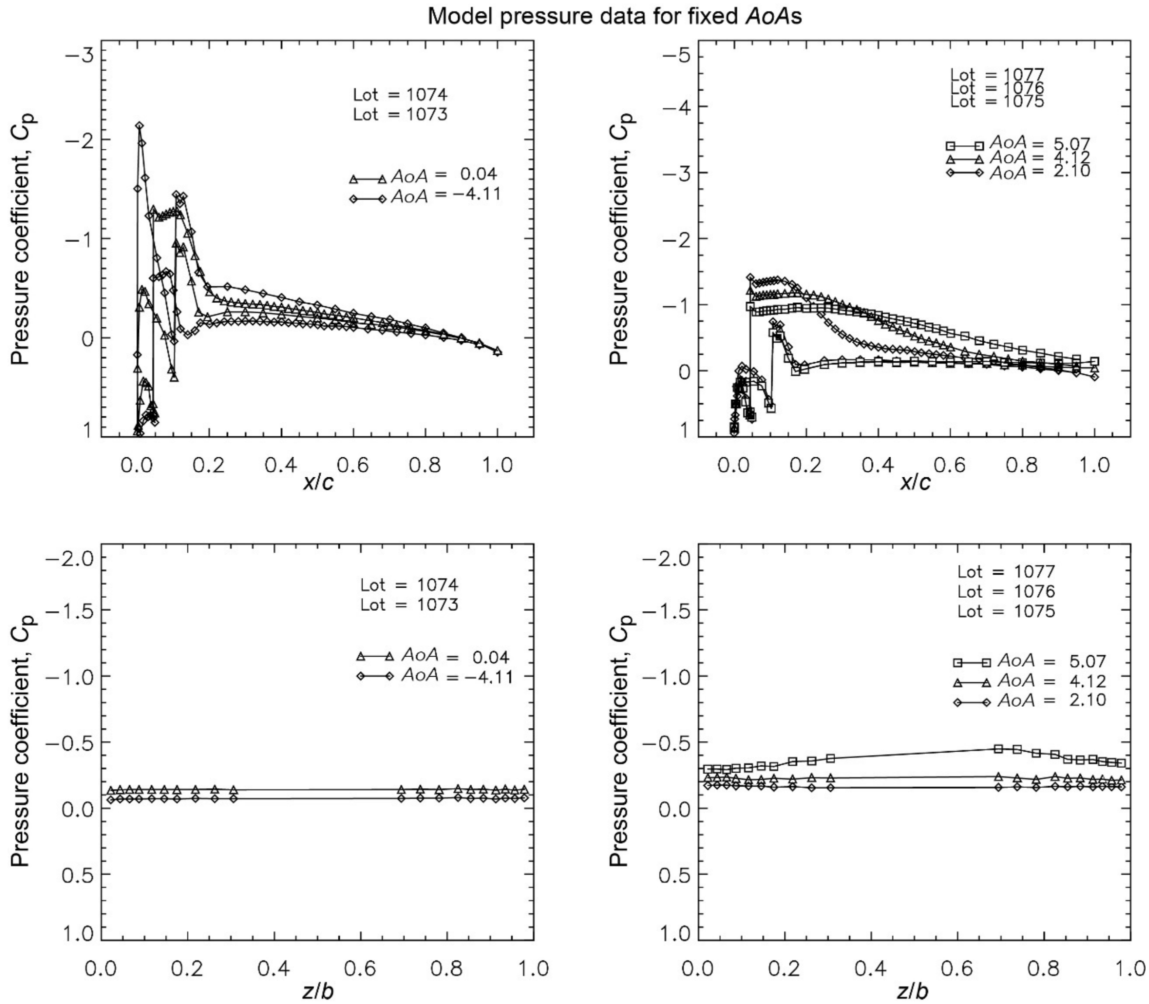

Spanwise Ridge Ice—Lot EG1159: M = 0.10 to 0.11 and Re = 8.4–8.5×10⁶

Appendix G.—F1 Full-Scale Model Tests

Spanwise Ridge Ice—Lot EG1159: M = 0.10 to 0.11 and Re = 8.4–8.5×10^6

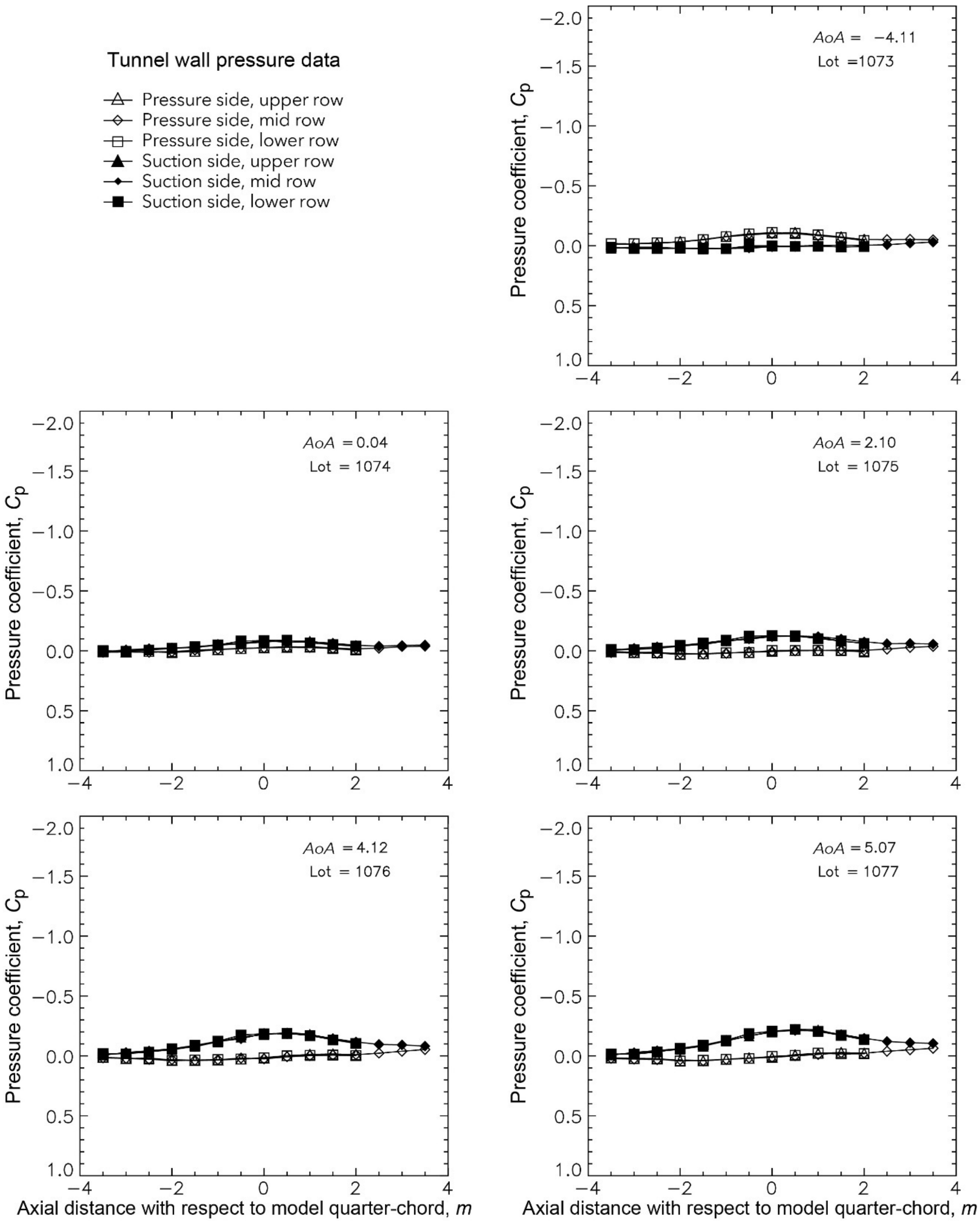

Spanwise Ridge Ice—Lot EG1159: M = 0.10 to 0.11 and Re = 8.4–8.5×10^6

Appendix G.—F1 Full-Scale Model Tests

Spanwise Ridge Ice—Lot EG1159: M = 0.10 to 0.11 and Re = 8.4–8.5×10[6]

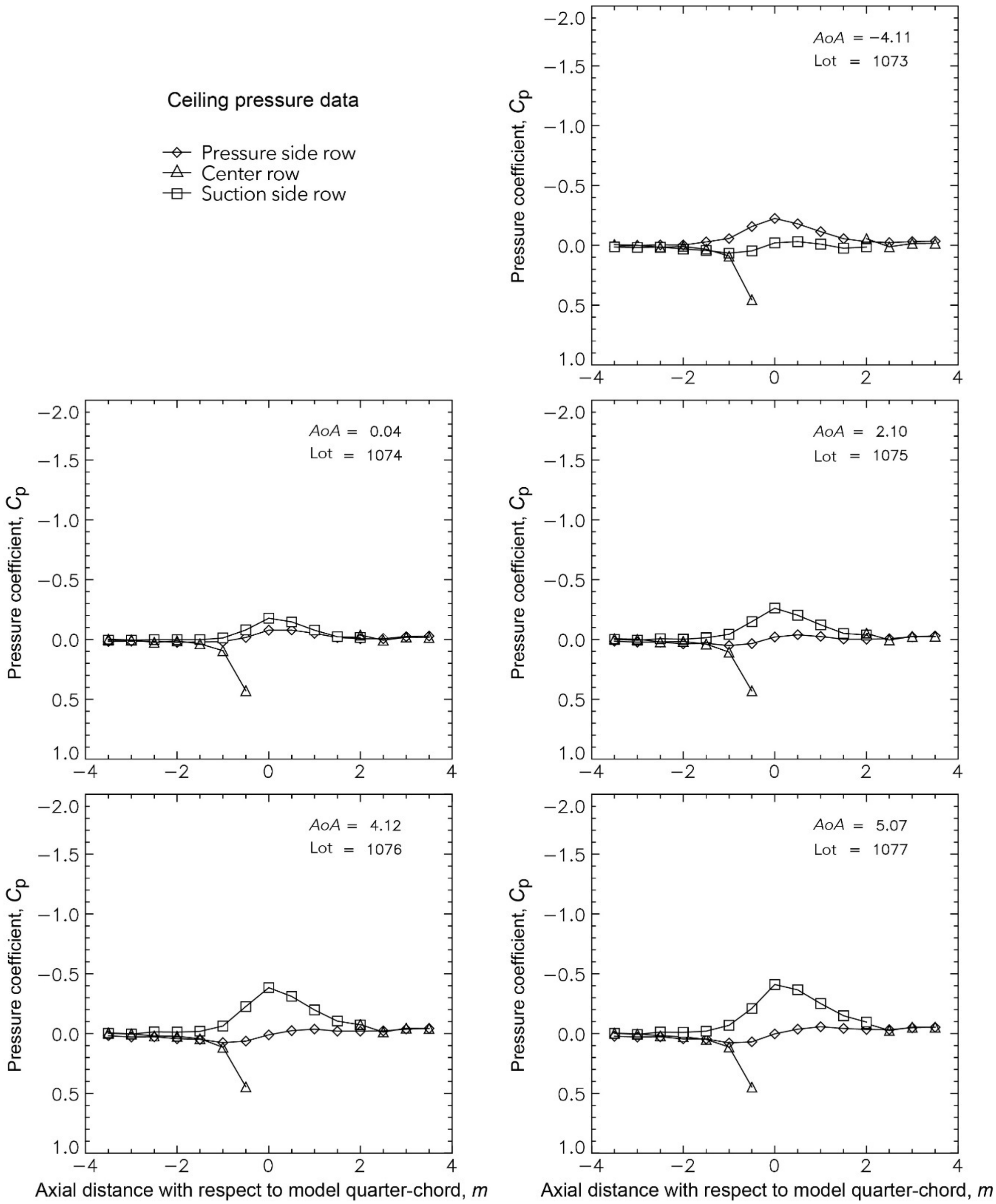

Spanwise Ridge Ice—Lot EG1159: M = 0.10 to 0.11 and Re = 8.4–8.5×10[6]

Appendix G.—F1 Full-Scale Model Tests

Spanwise Ridge Ice—Lot EG1159: M = 0.10 to 0.11 and Re = 8.4–8.5×10^6

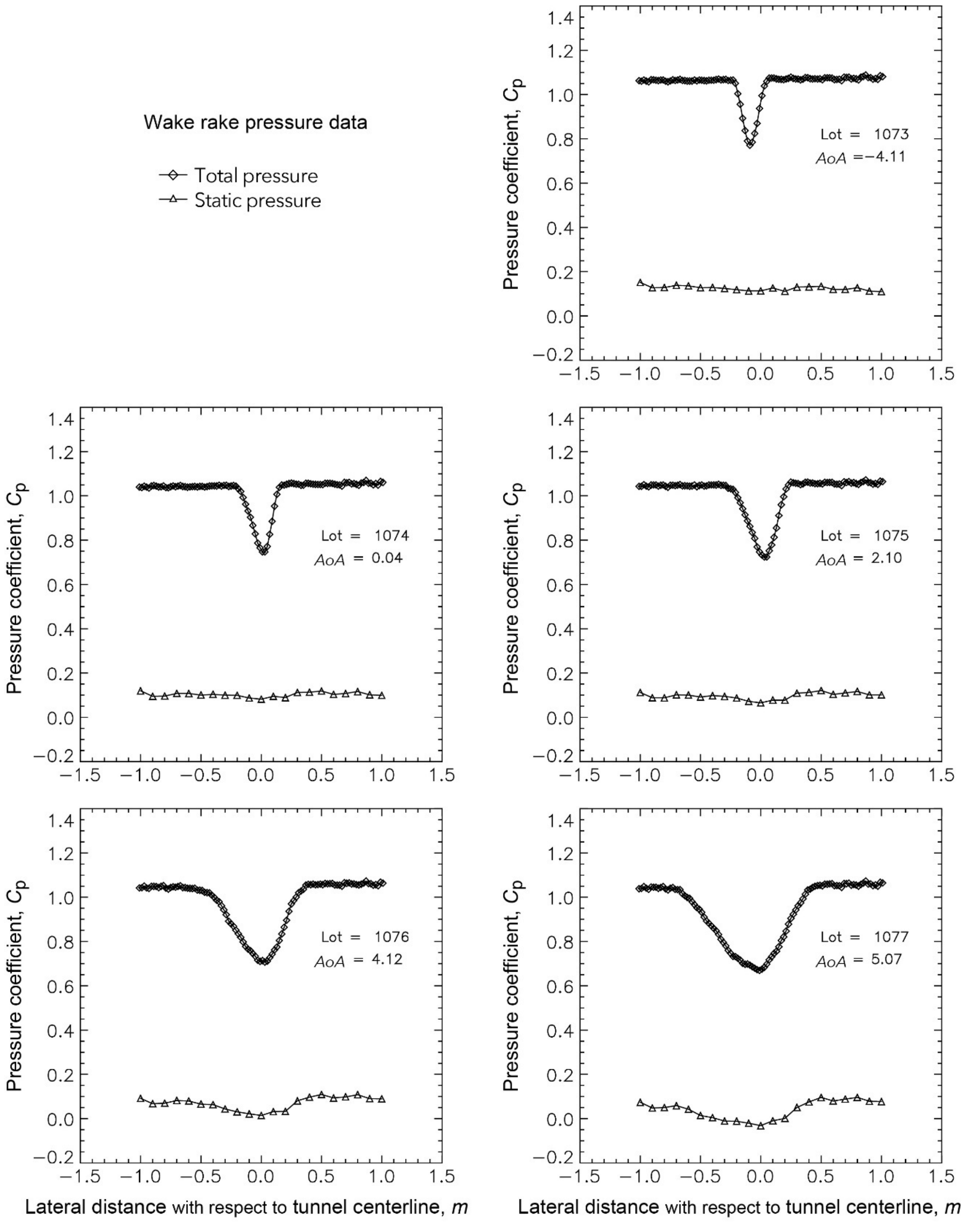

Spanwise Ridge Ice—Lot EG1159: M = 0.10 to 0.11 and Re = 8.4–8.5×10^6

Appendix G.—F1 Full-Scale Model Tests

Spanwise Ridge Ice—Lot EG1159: M = 0.10 and Re = 12.1–12.2×10^6

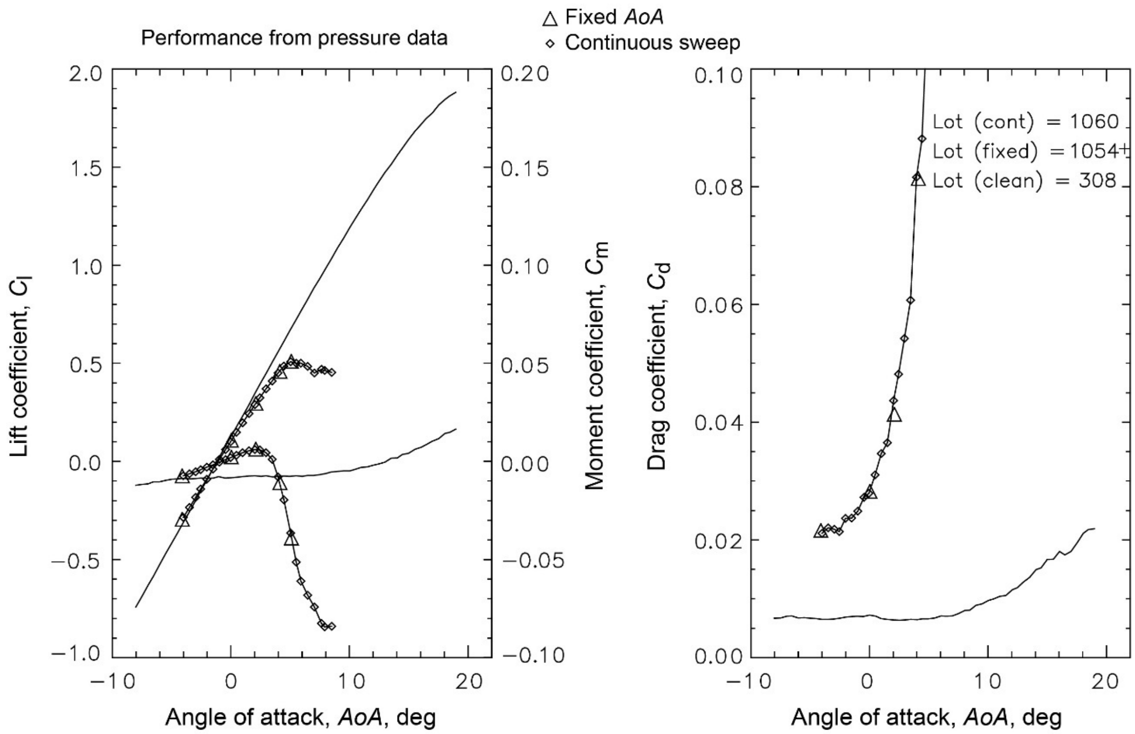

Spanwise Ridge Ice—Lot EG1159: M = 0.10 and Re = 12.1–12.2×10^6

Appendix G.—F1 Full-Scale Model Tests

Spanwise Ridge Ice—Lot EG1159: M = 0.10 and Re = 12.1–12.2×10^6

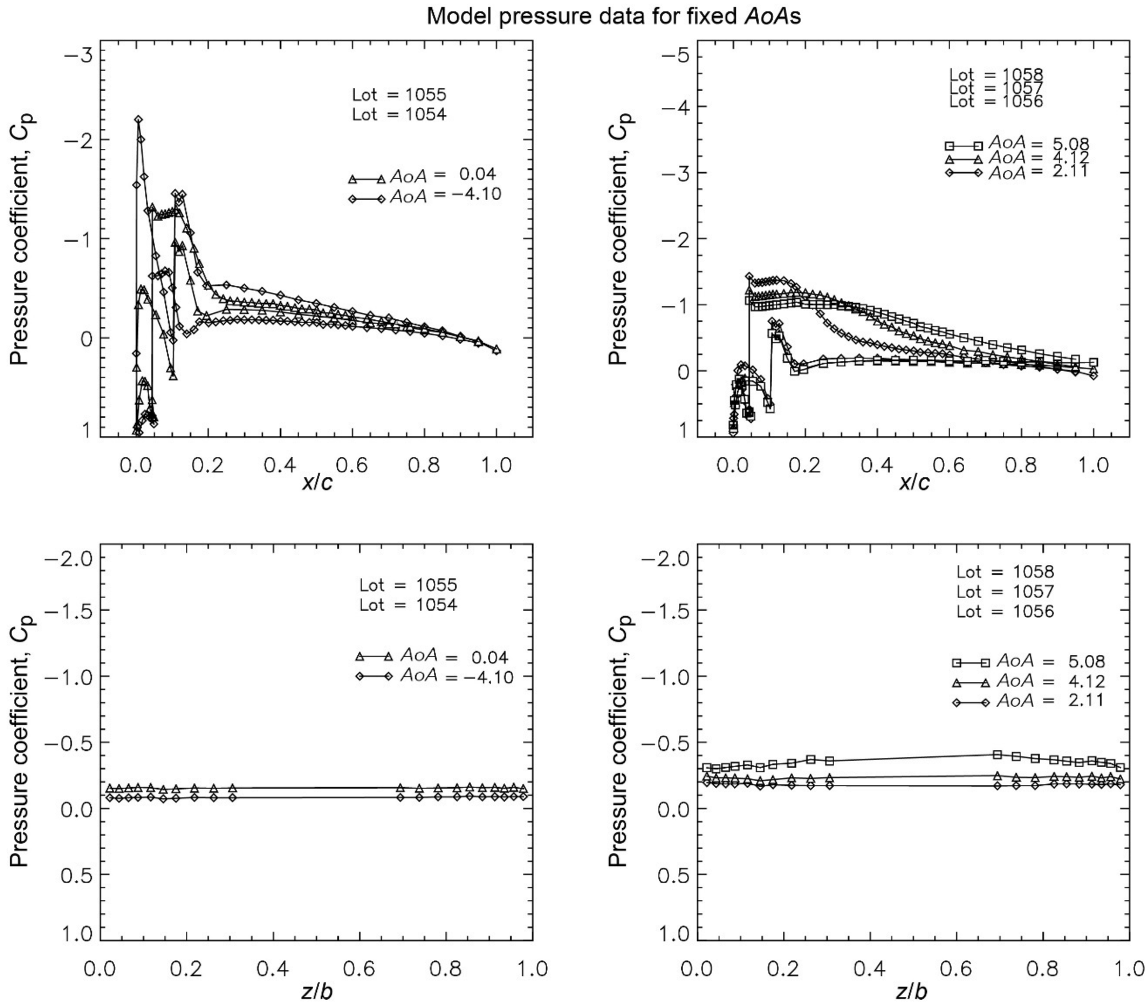

Spanwise Ridge Ice—Lot EG1159: M = 0.10 and Re = 12.1–12.2×10^6

Appendix G.—F1 Full-Scale Model Tests

Spanwise Ridge Ice—Lot EG1159: M = 0.10 and Re = 12.1–12.2×10^6

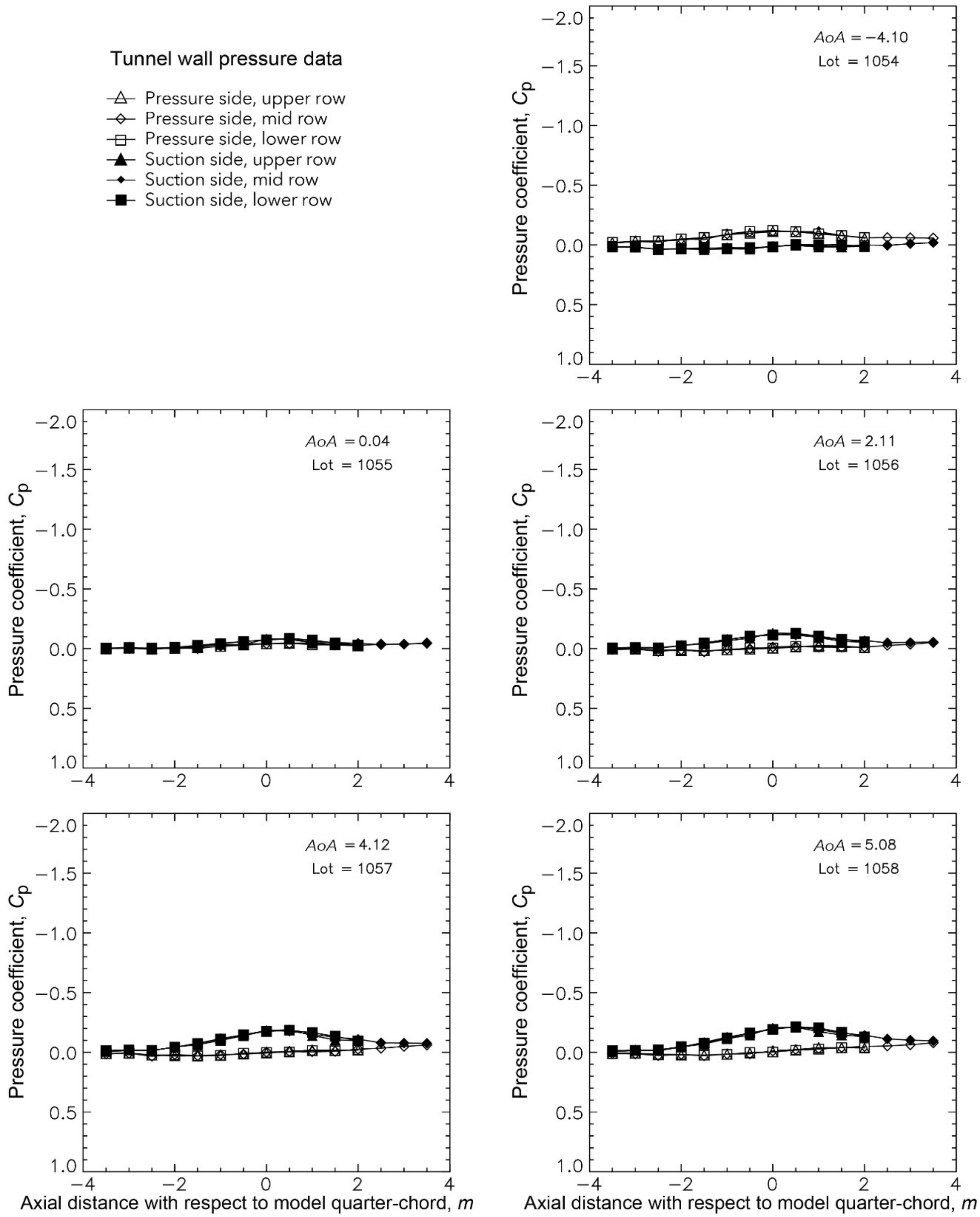

Spanwise Ridge Ice—Lot EG1159: M = 0.10 and Re = 12.1–12.2×10^6

Appendix G.—F1 Full-Scale Model Tests

Spanwise Ridge Ice—Lot EG1159: M = 0.10 and Re = 12.1–12.2×10[6]

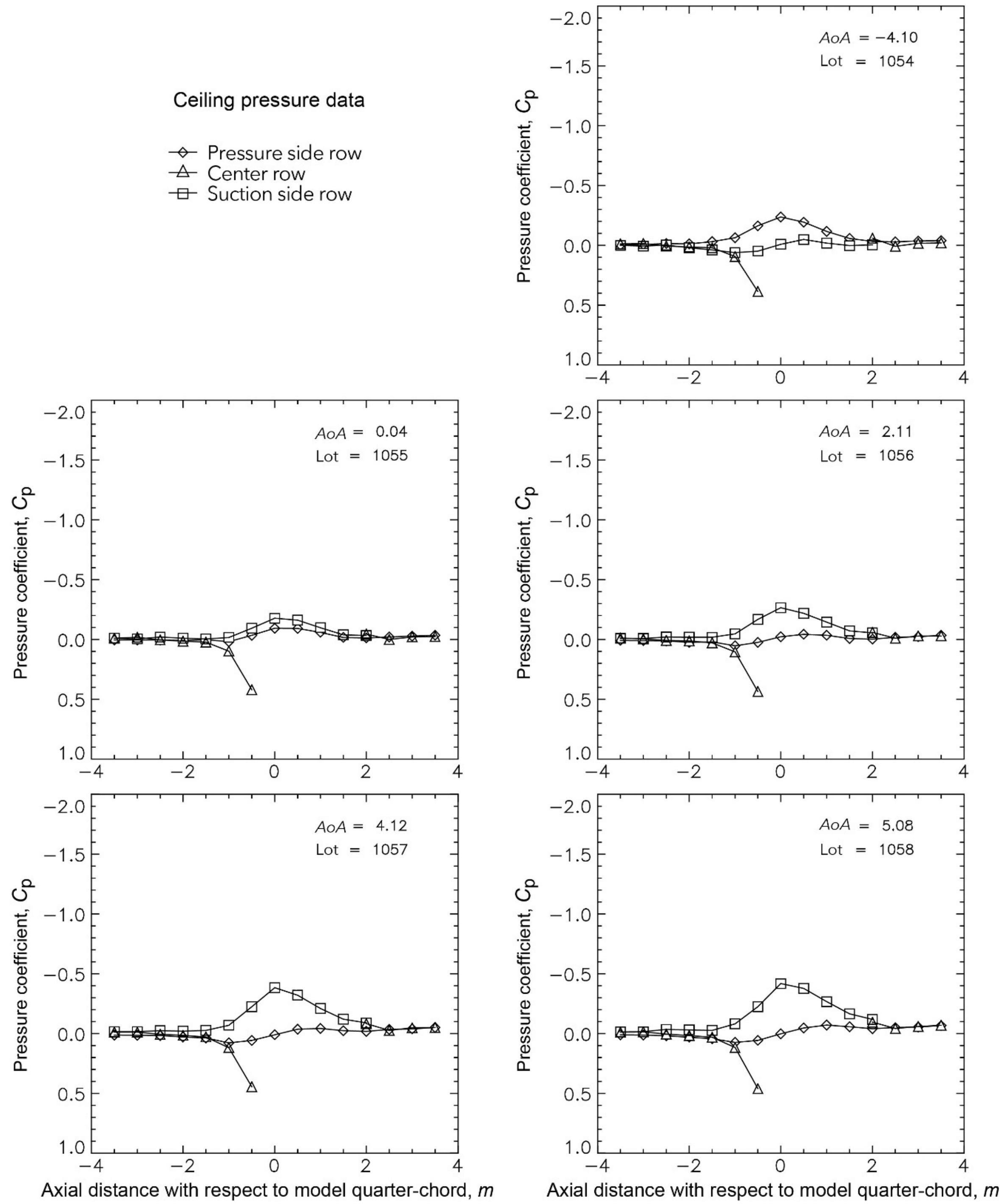

Spanwise Ridge Ice—Lot EG1159: M = 0.10 and Re = 12.1–12.2×10[6]

Appendix G.—F1 Full-Scale Model Tests

Spanwise Ridge Ice—Lot EG1159: M = 0.10 and Re = 12.1–12.2×10[6]

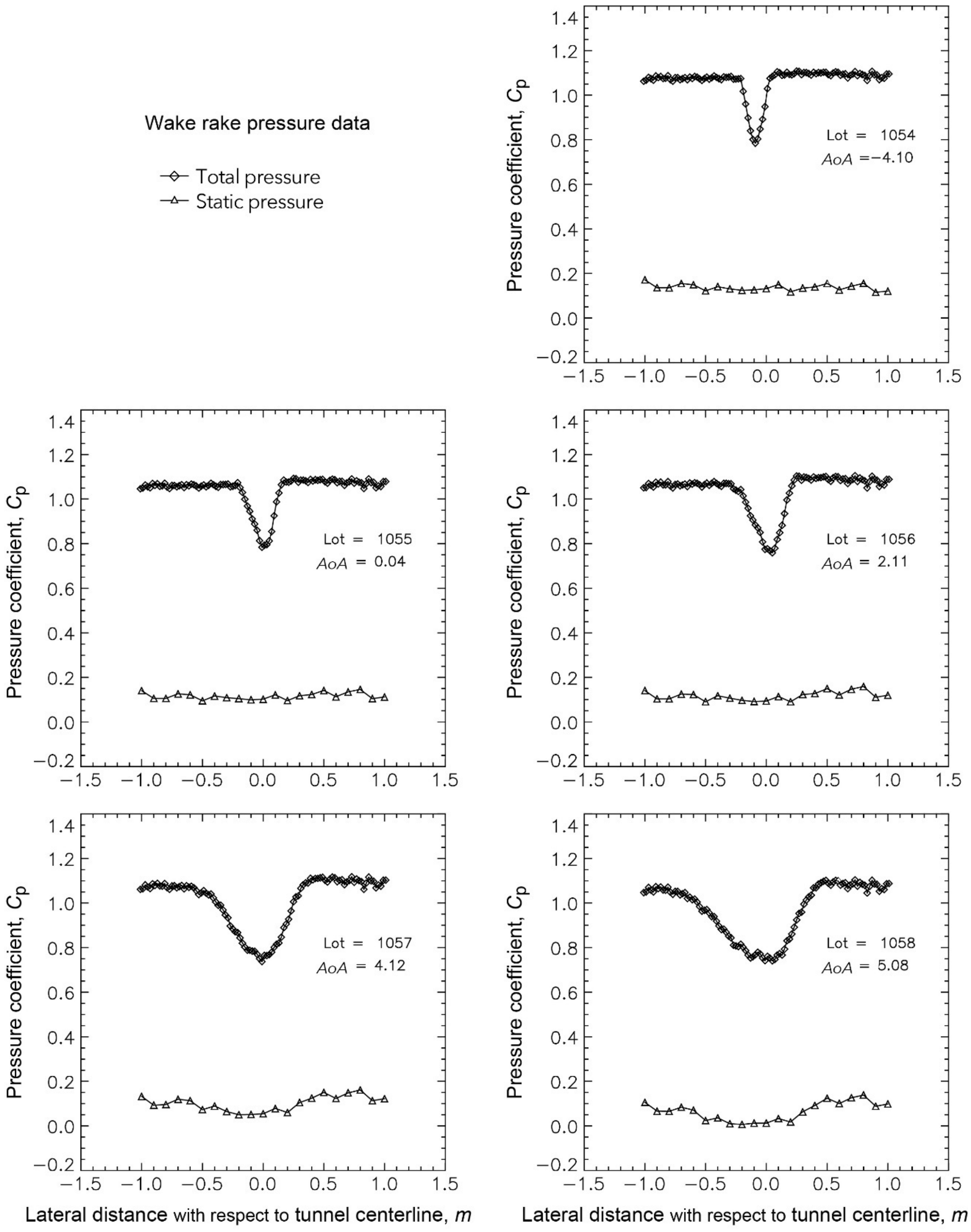

Spanwise Ridge Ice—Lot EG1159: M = 0.10 and Re = 12.1–12.2×10[6]

Appendix G.—F1 Full-Scale Model Tests

Spanwise Ridge Ice—Lot EG1159: M = 0.20 to 0.21 and Re = 8.6–8.7×10[6]

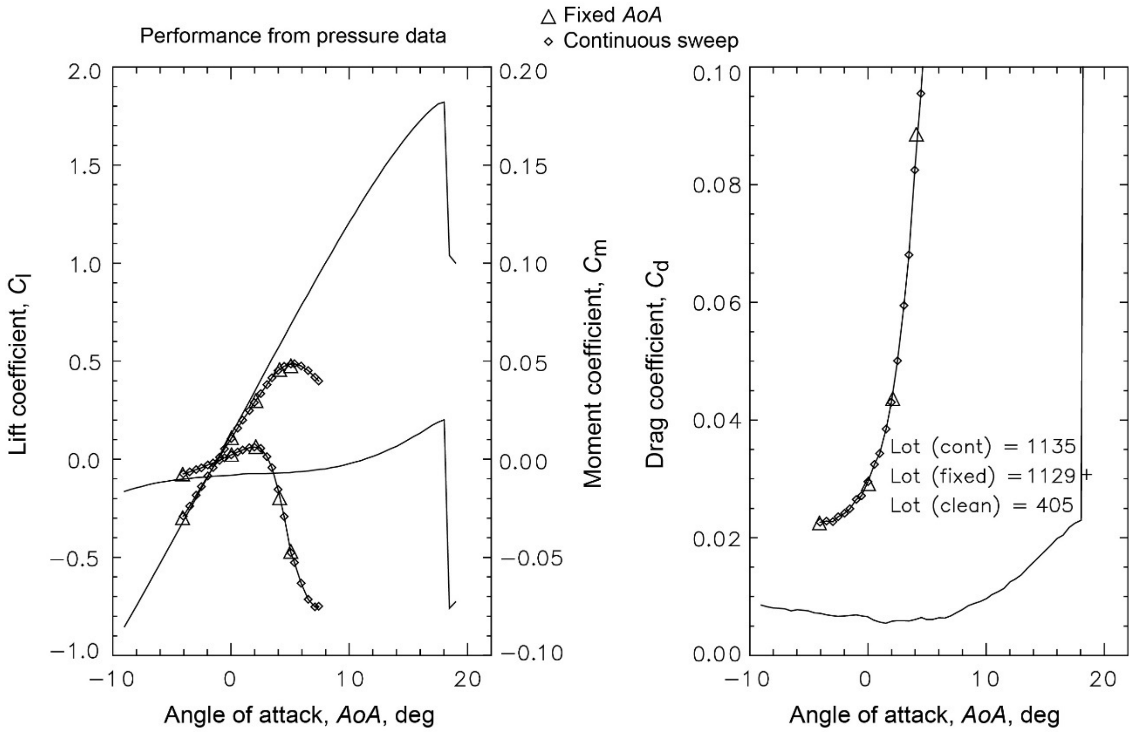

Spanwise Ridge Ice—Lot EG1159: M = 0.20 to 0.21 and Re = 8.6–8.7×10[6]

Appendix G.—F1 Full-Scale Model Tests

Spanwise Ridge Ice—Lot EG1159: M = 0.20 to 0.21 and Re = 8.6–8.7×10⁶

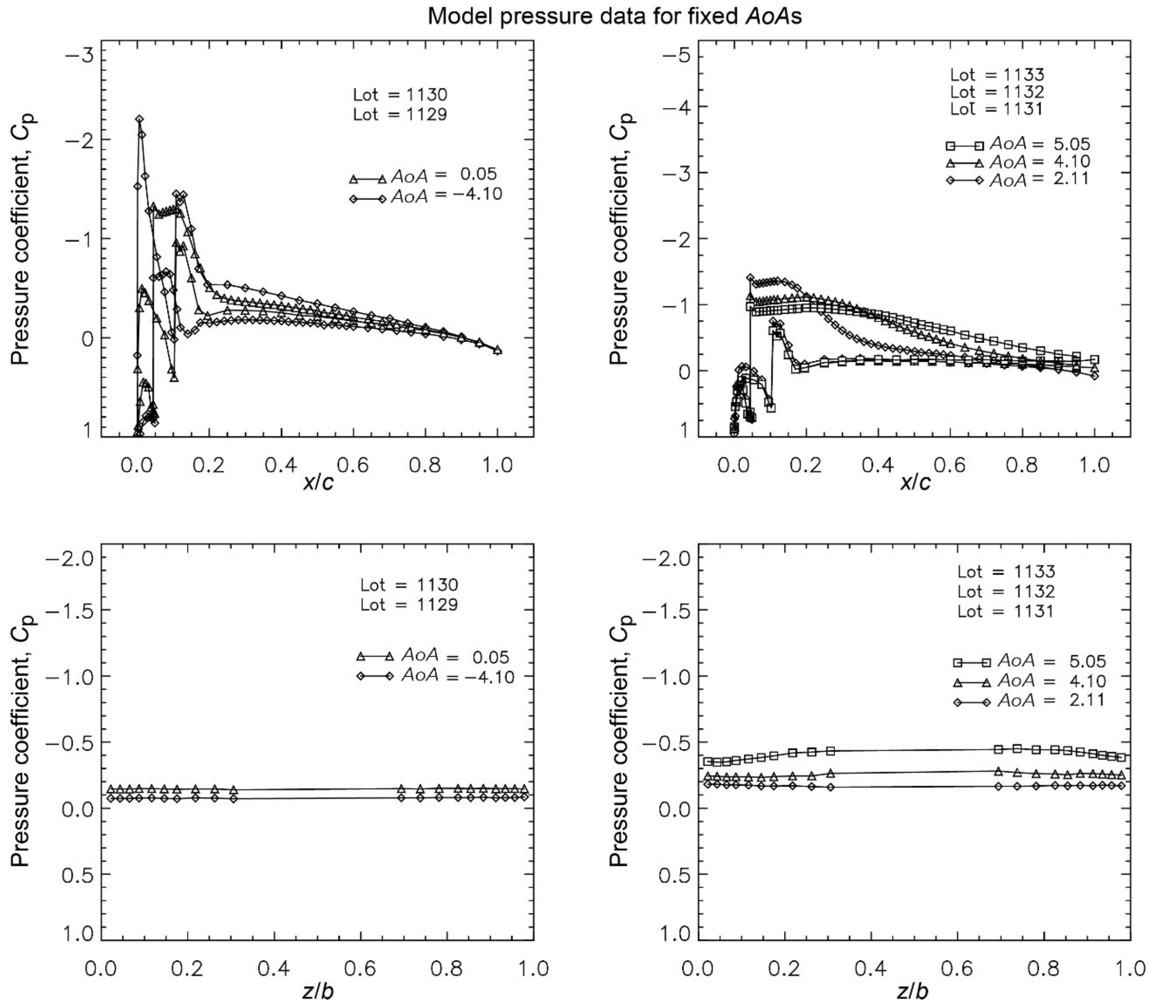

Spanwise Ridge Ice—Lot EG1159: M = 0.20 to 0.21 and Re = 8.6–8.7×10⁶

Appendix G.—F1 Full-Scale Model Tests

Spanwise Ridge Ice—Lot EG1159: M = 0.20 to 0.21 and Re = 8.6–8.7×10^6

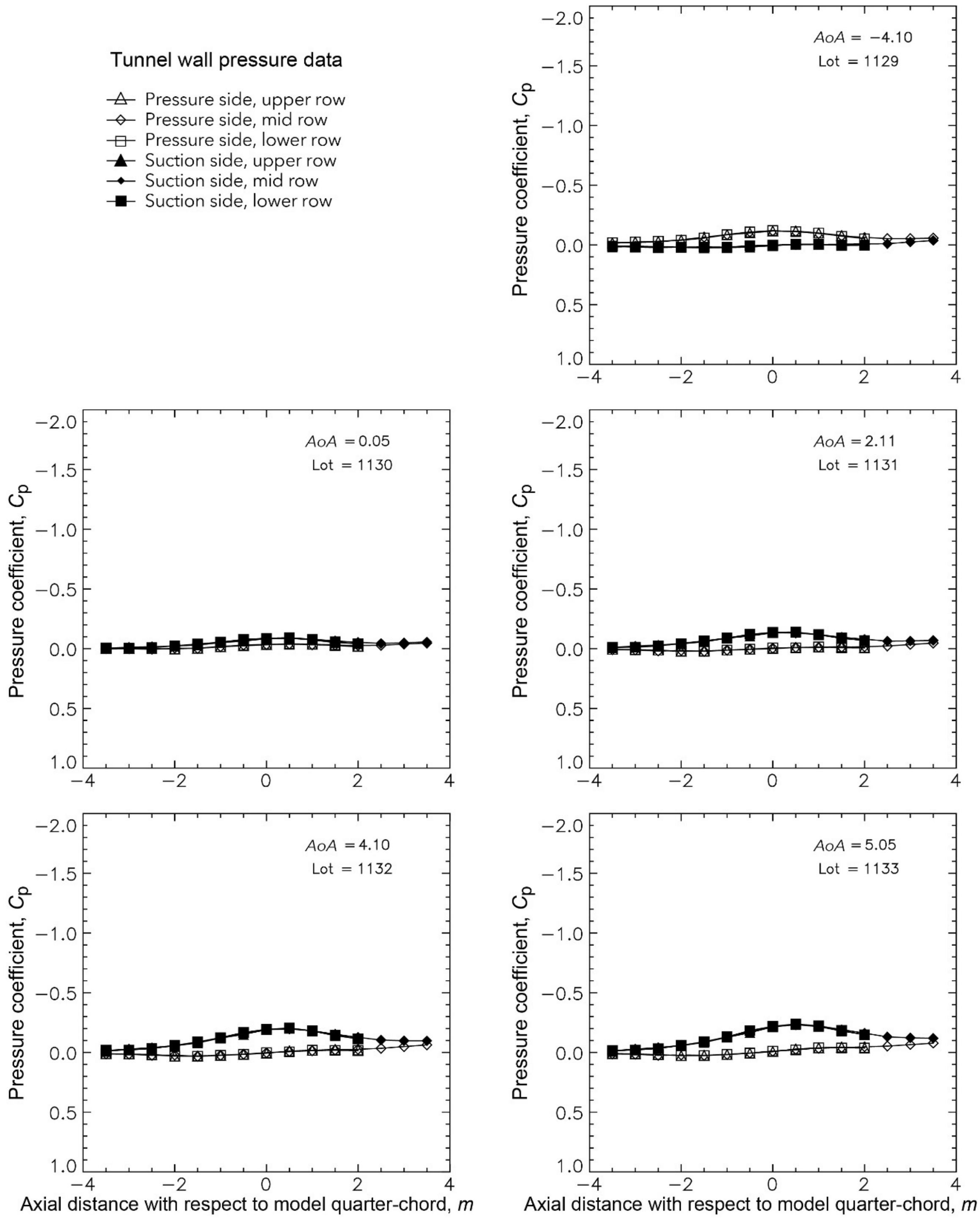

Spanwise Ridge Ice—Lot EG1159: M = 0.20 to 0.21 and Re = 8.6–8.7×10^6

Appendix G.—F1 Full-Scale Model Tests

Spanwise Ridge Ice—Lot EG1159: M = 0.20 to 0.21 and Re = 8.6–8.7×10^6

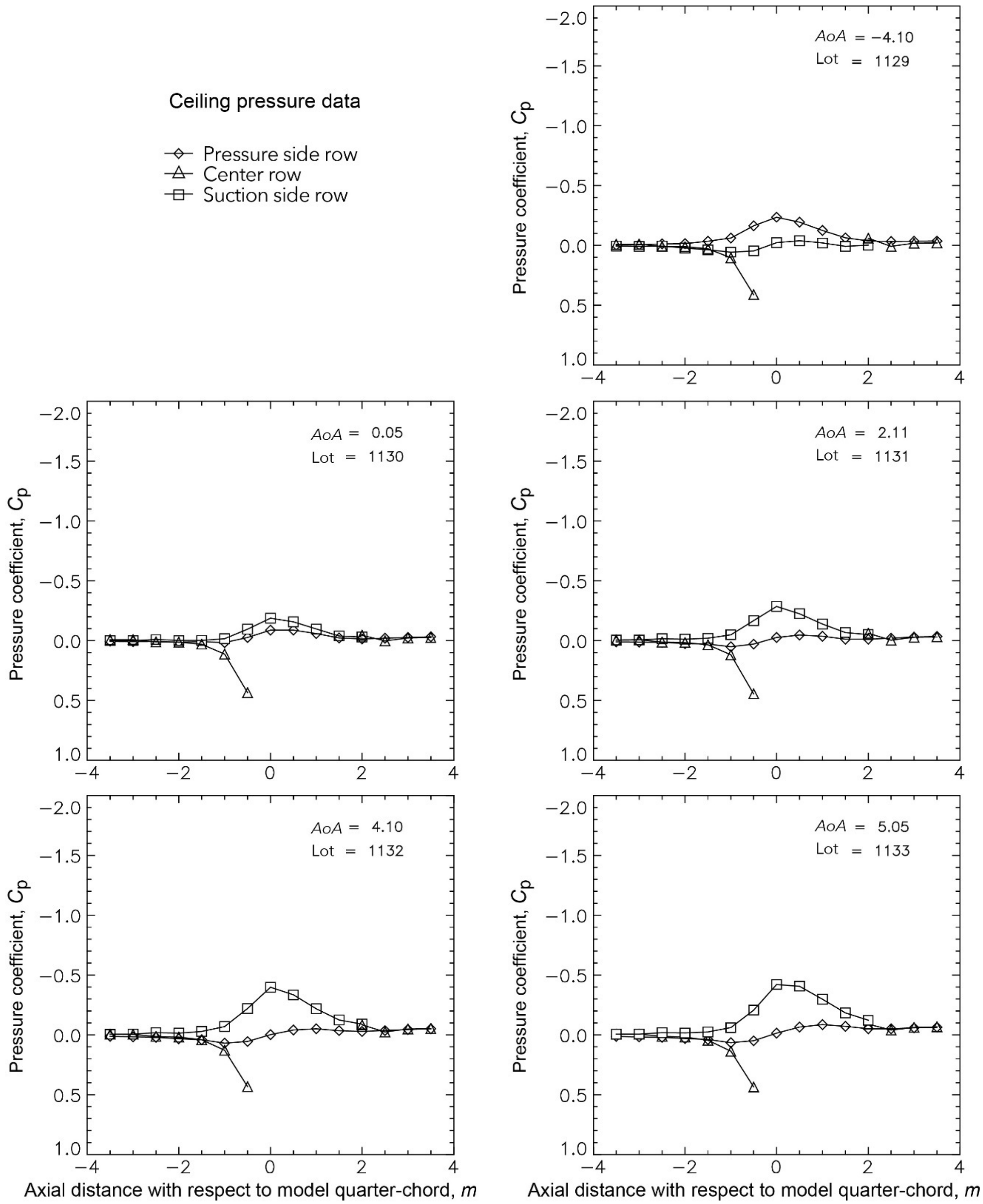

Spanwise Ridge Ice—Lot EG1159: M = 0.20 to 0.21 and Re = 8.6–8.7×10^6

Appendix G.—F1 Full-Scale Model Tests

Spanwise Ridge Ice—Lot EG1159: M = 0.20 to 0.21 and Re = 8.6–8.7×10^6

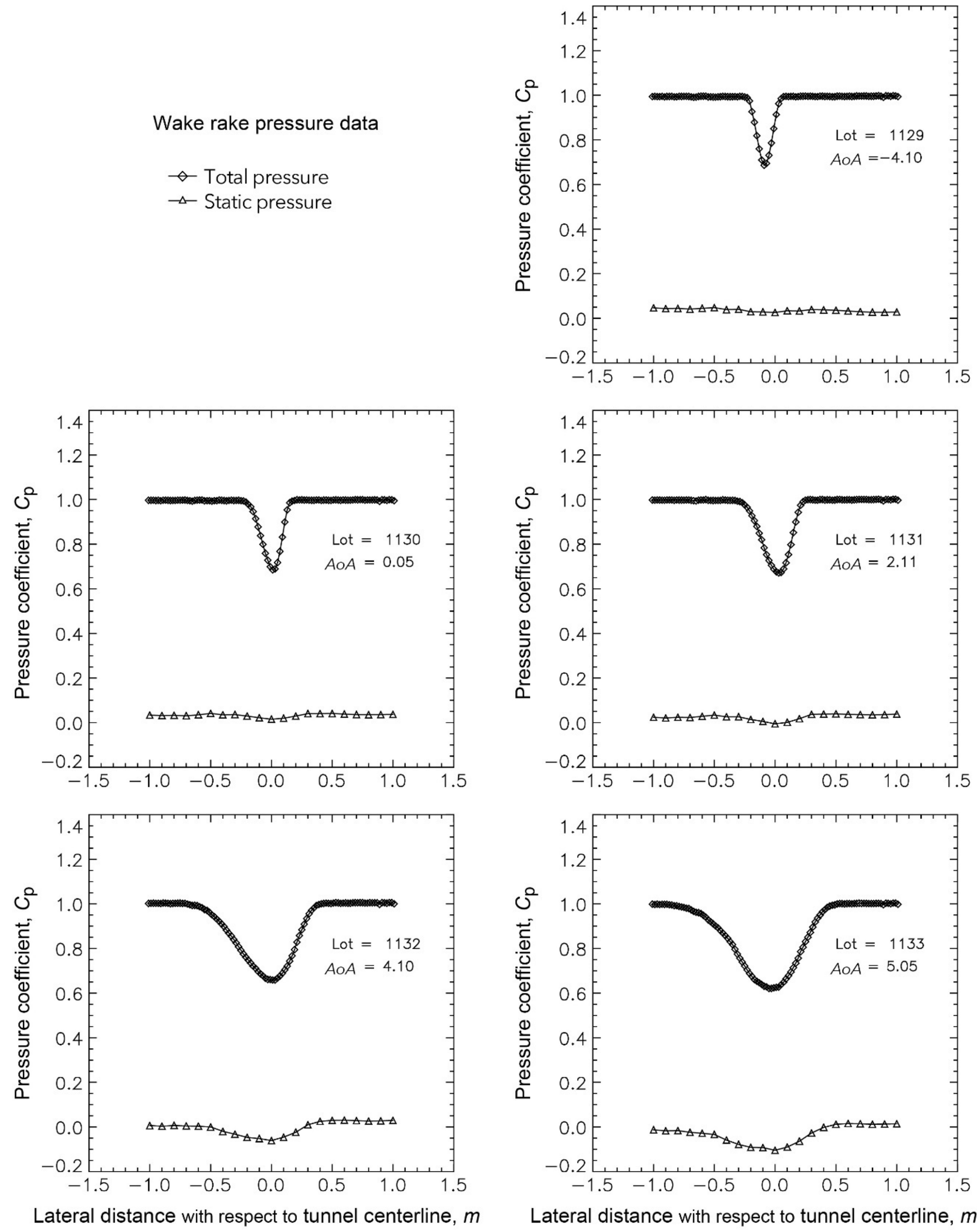

Spanwise Ridge Ice—Lot EG1159: M = 0.20 to 0.21 and Re = 8.6–8.7×10^6

Appendix G.—F1 Full-Scale Model Tests

Spanwise Ridge Ice—Lot EG1159: M = 0.20 to 0.21 and Re = 12.1–12.3×10[6]

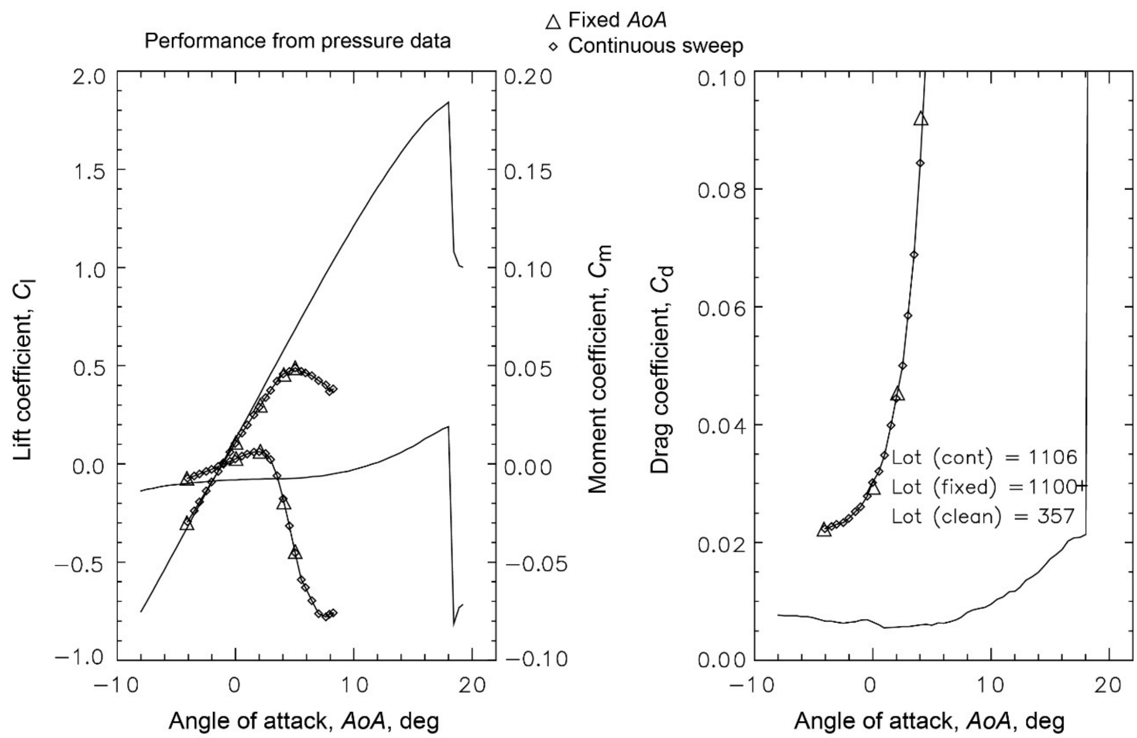

Spanwise Ridge Ice—Lot EG1159: M = 0.20 to 0.21 and Re = 12.1–12.3×10[6]

Appendix G.—F1 Full-Scale Model Tests

Spanwise Ridge Ice—Lot EG1159: M = 0.20 to 0.21 and Re = 12.1–12.3×10^6

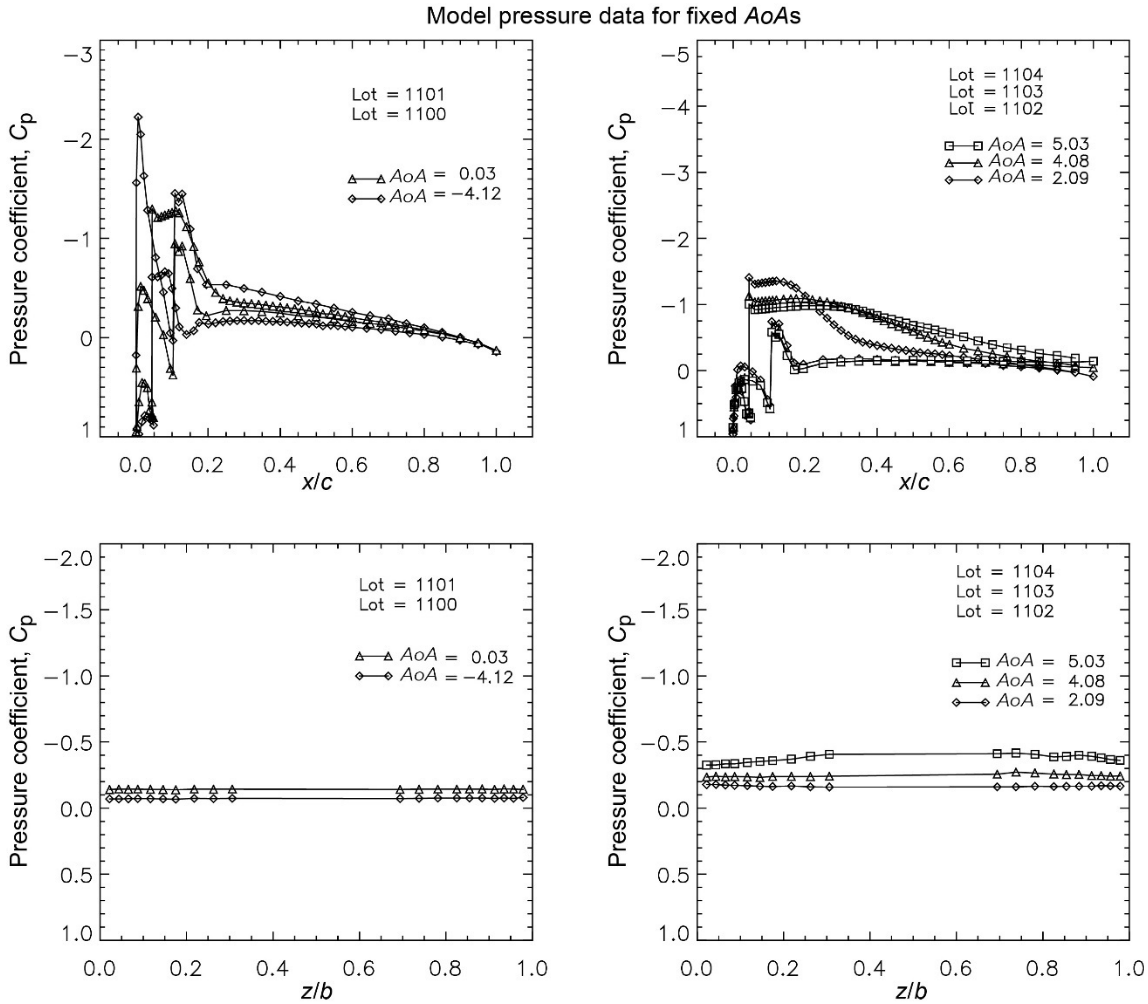

Spanwise Ridge Ice—Lot EG1159: M = 0.20 to 0.21 and Re = 12.1–12.3×10^6

Appendix G.—F1 Full-Scale Model Tests

Spanwise Ridge Ice—Lot EG1159: M = 0.20 to 0.21 and Re = 12.1–12.3×10^6

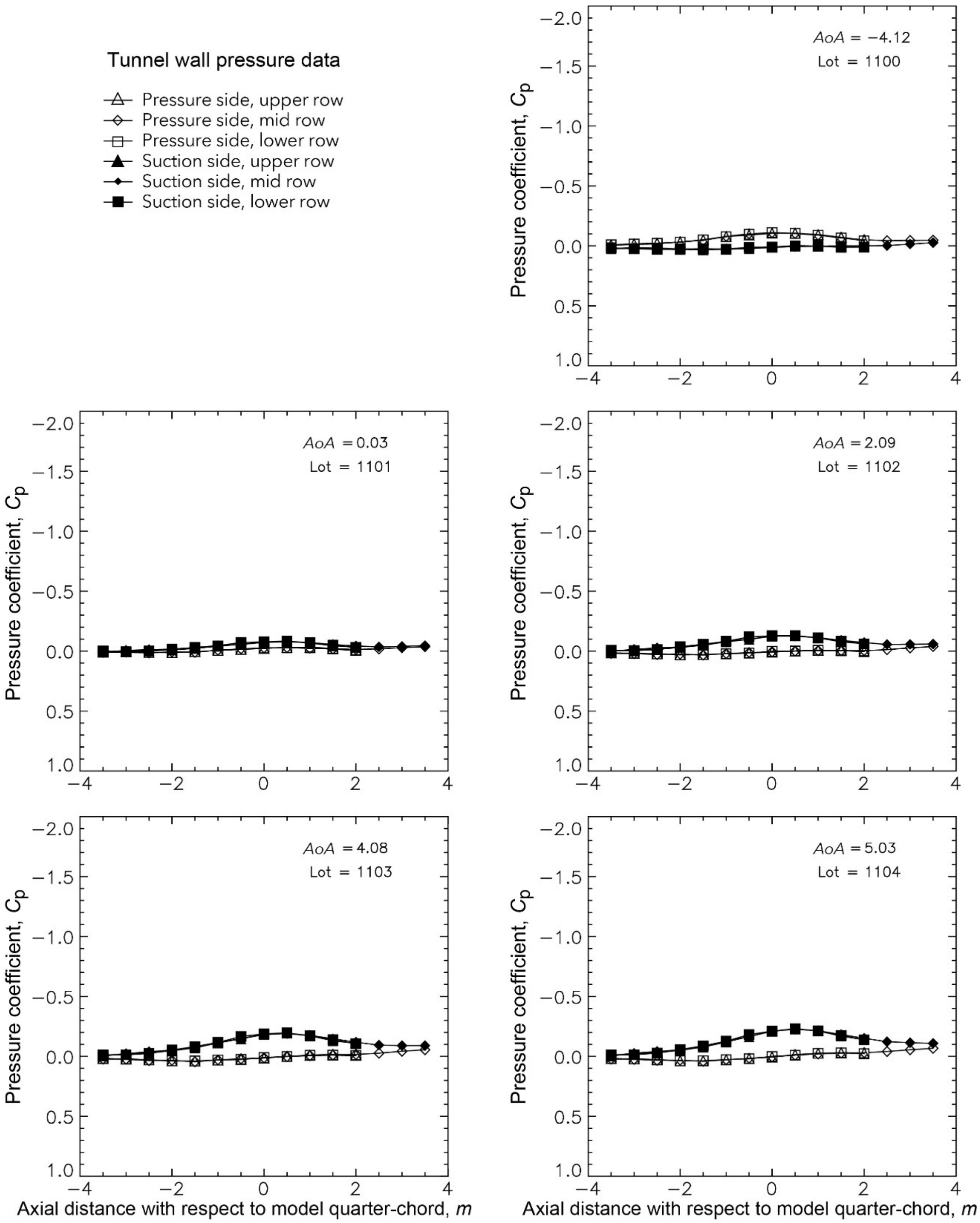

Spanwise Ridge Ice—Lot EG1159: M = 0.20 to 0.21 and Re = 12.1–12.3×10^6

Appendix G.—F1 Full-Scale Model Tests

Spanwise Ridge Ice—Lot EG1159: M = 0.20 to 0.21 and Re = 12.1–12.3×10^6

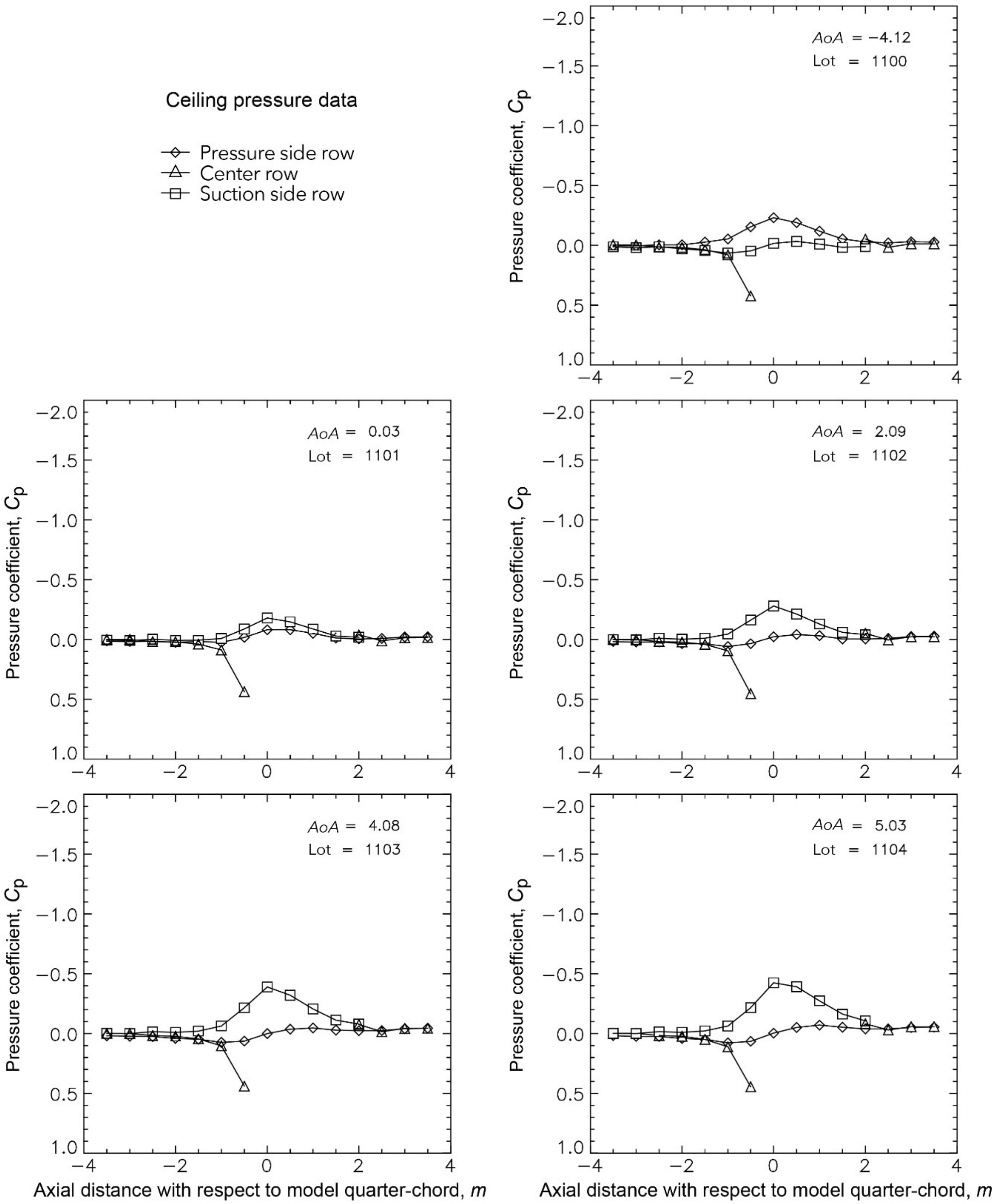

Spanwise Ridge Ice—Lot EG1159: M = 0.20 to 0.21 and Re = 12.1–12.3×10^6

Appendix G.—F1 Full-Scale Model Tests

Spanwise Ridge Ice—Lot EG1159: M = 0.20 to 0.21 and Re = 12.1–12.3×10⁶

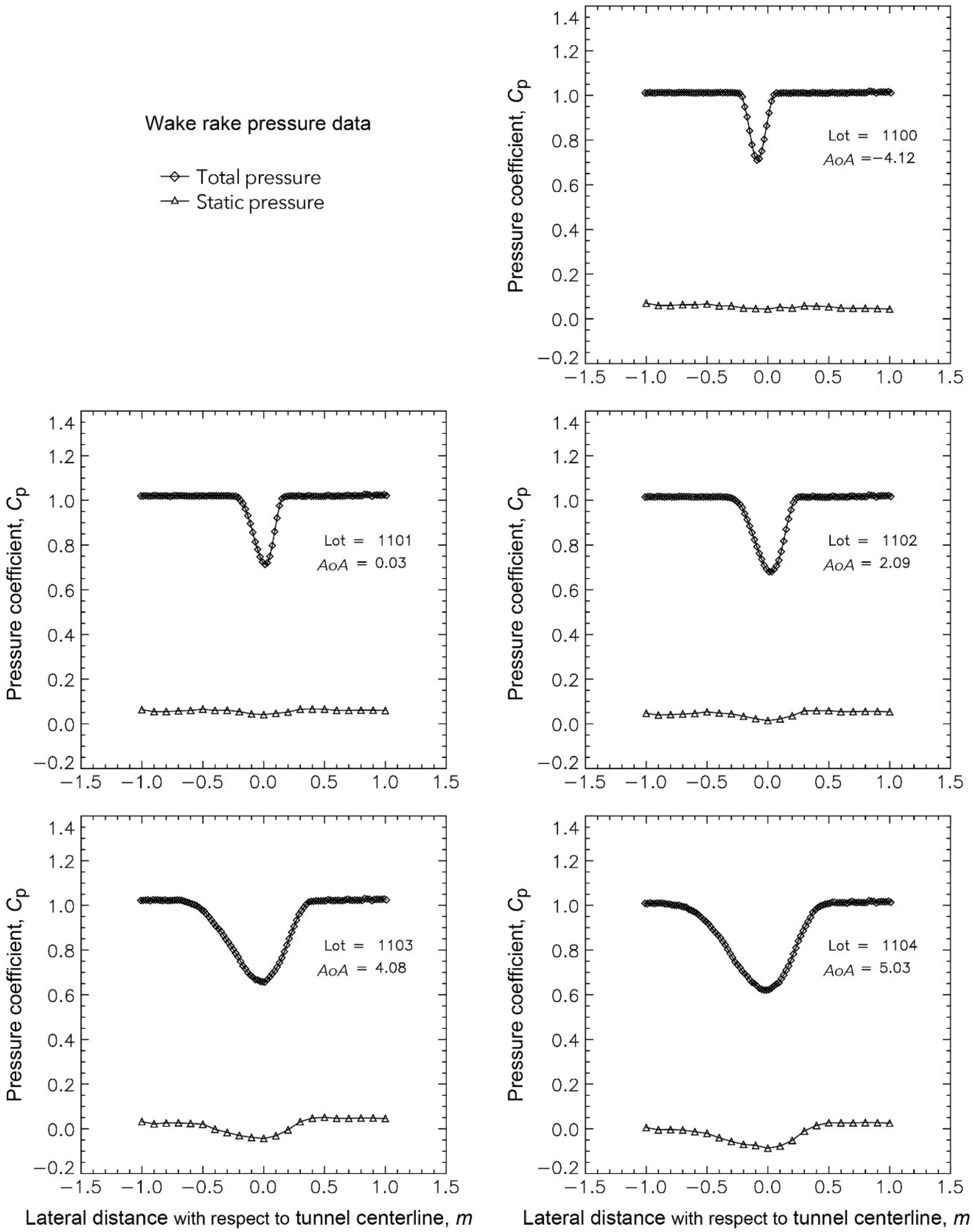

Spanwise Ridge Ice—Lot EG1159: M = 0.20 to 0.21 and Re = 12.1–12.3×10⁶

Appendix G.—F1 Full-Scale Model Tests

Spanwise Ridge Ice—Lot EG1159: M = 0.20 to 0.21 and Re = 15.8–16.0×10^6

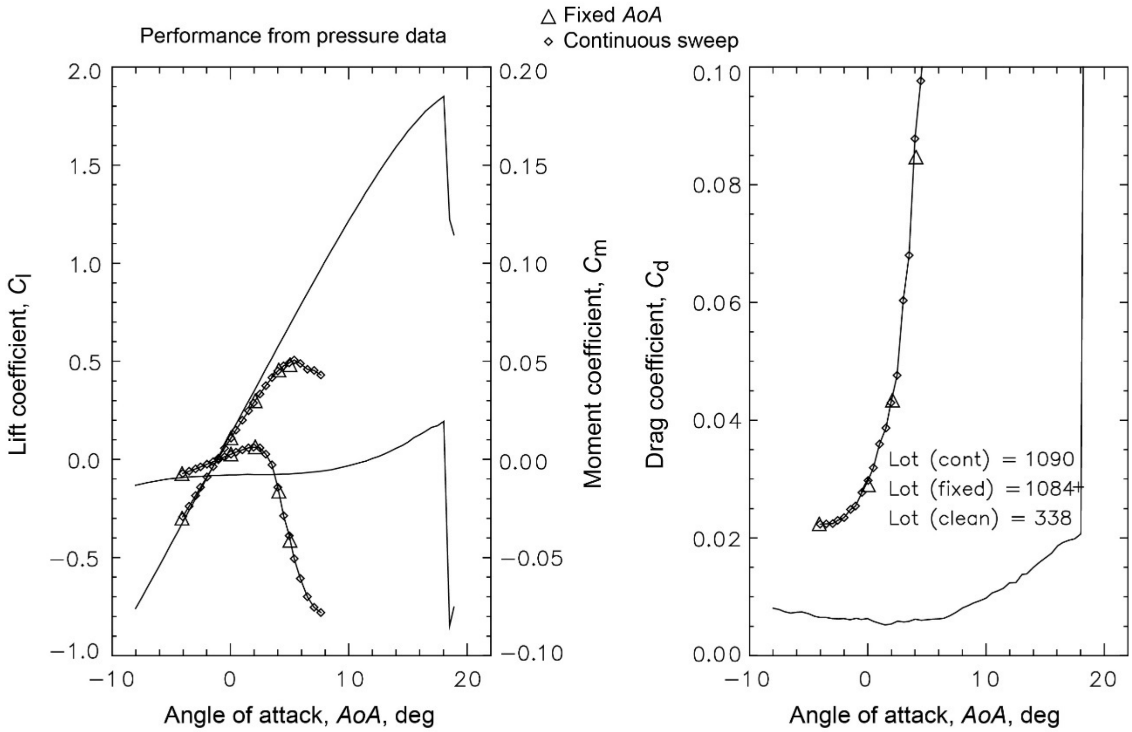

Spanwise Ridge Ice—Lot EG1159: M = 0.20 to 0.21 and Re = 15.8–16.0×10^6

Appendix G.—F1 Full-Scale Model Tests

Spanwise Ridge Ice—Lot EG1159: M = 0.20 to 0.21 and Re = 15.8–16.0×10[6]

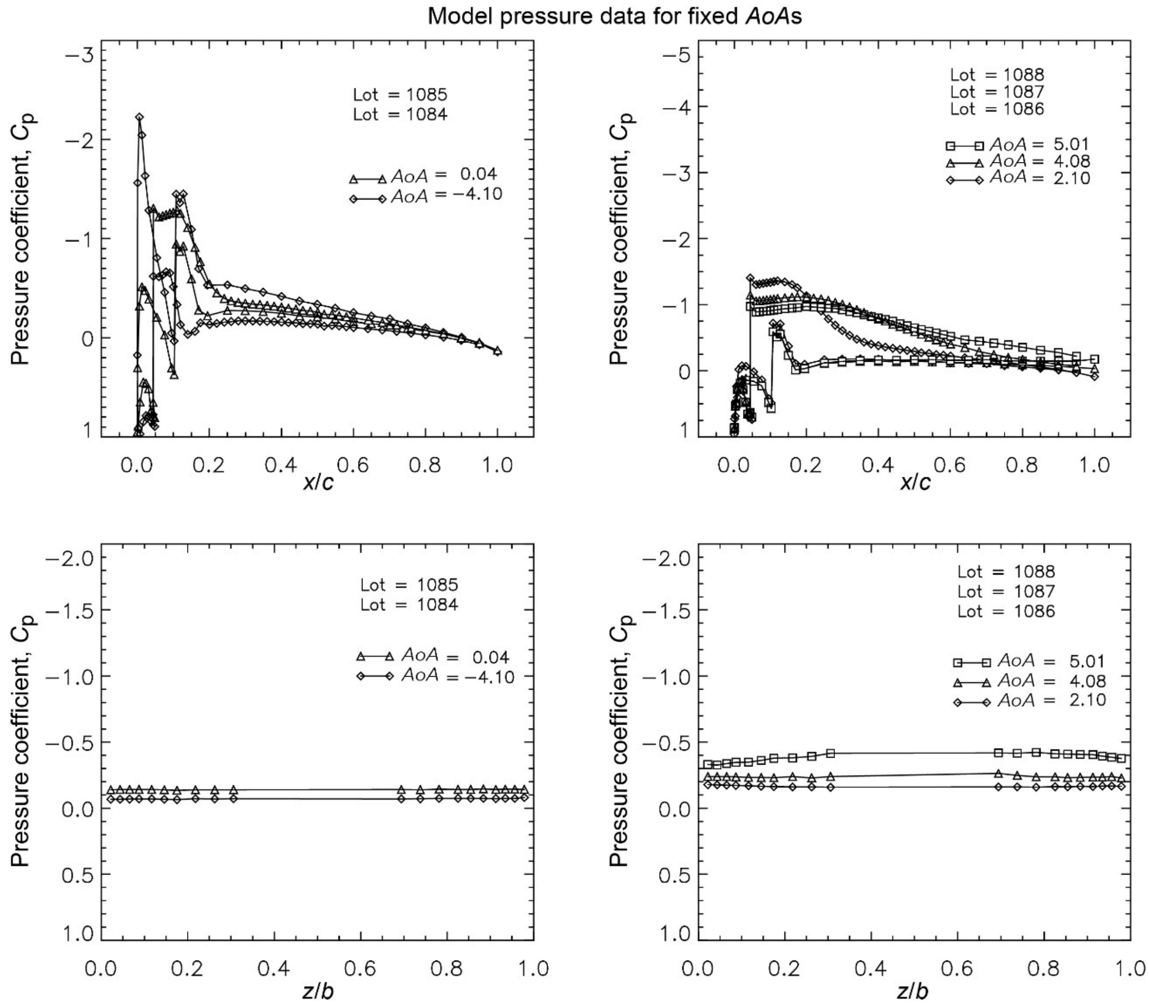

Spanwise Ridge Ice—Lot EG1159: M = 0.20 to 0.21 and Re = 15.8–16.0×10[6]

Appendix G.—F1 Full-Scale Model Tests

Spanwise Ridge Ice—Lot EG1159: M = 0.20 to 0.21 and Re = 15.8–16.0×10^6

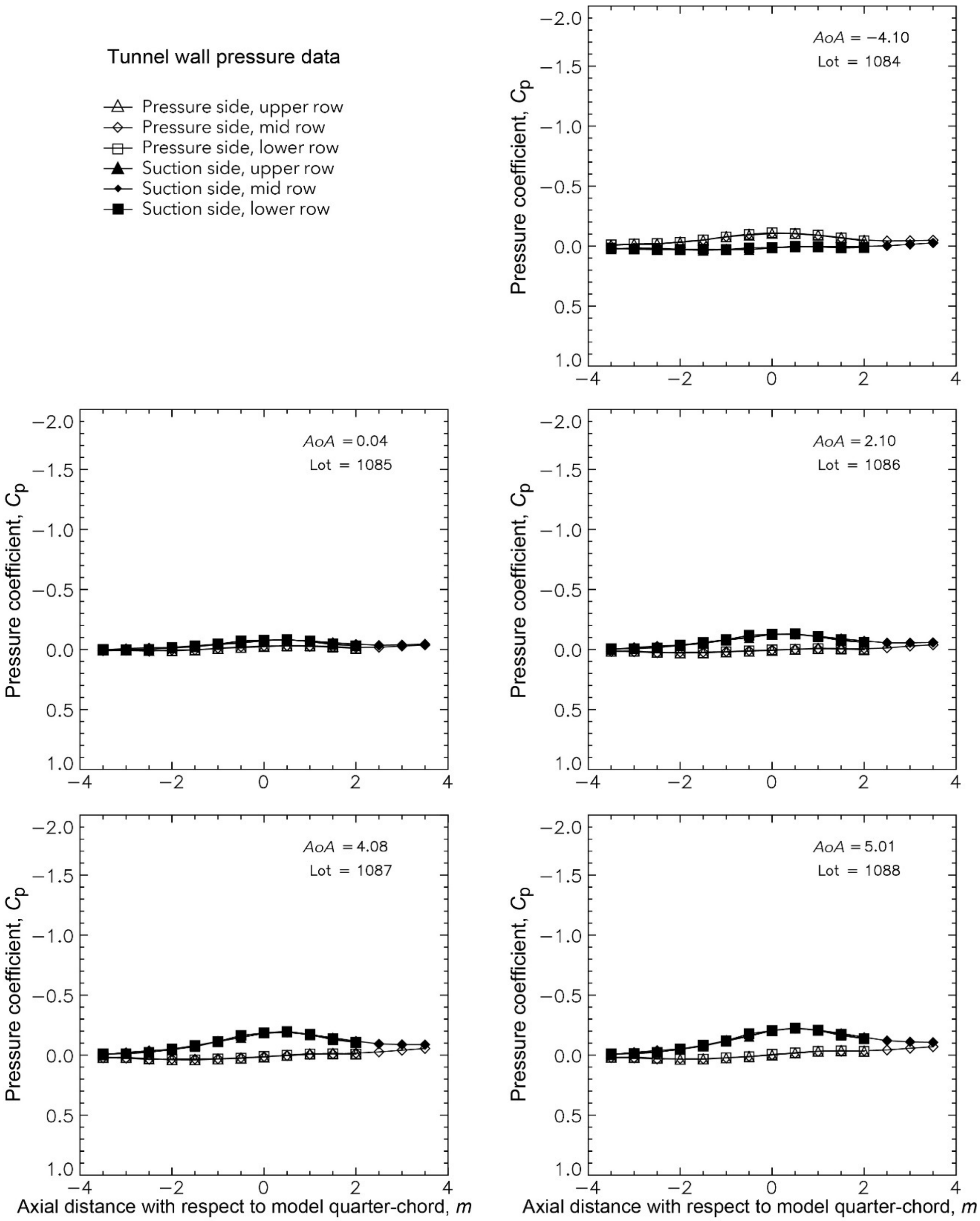

Spanwise Ridge Ice—Lot EG1159: M = 0.20 to 0.21 and Re = 15.8–16.0×10^6

Appendix G.—F1 Full-Scale Model Tests

Spanwise Ridge Ice—Lot EG1159: M = 0.20 to 0.21 and Re = 15.8–16.0×10⁶

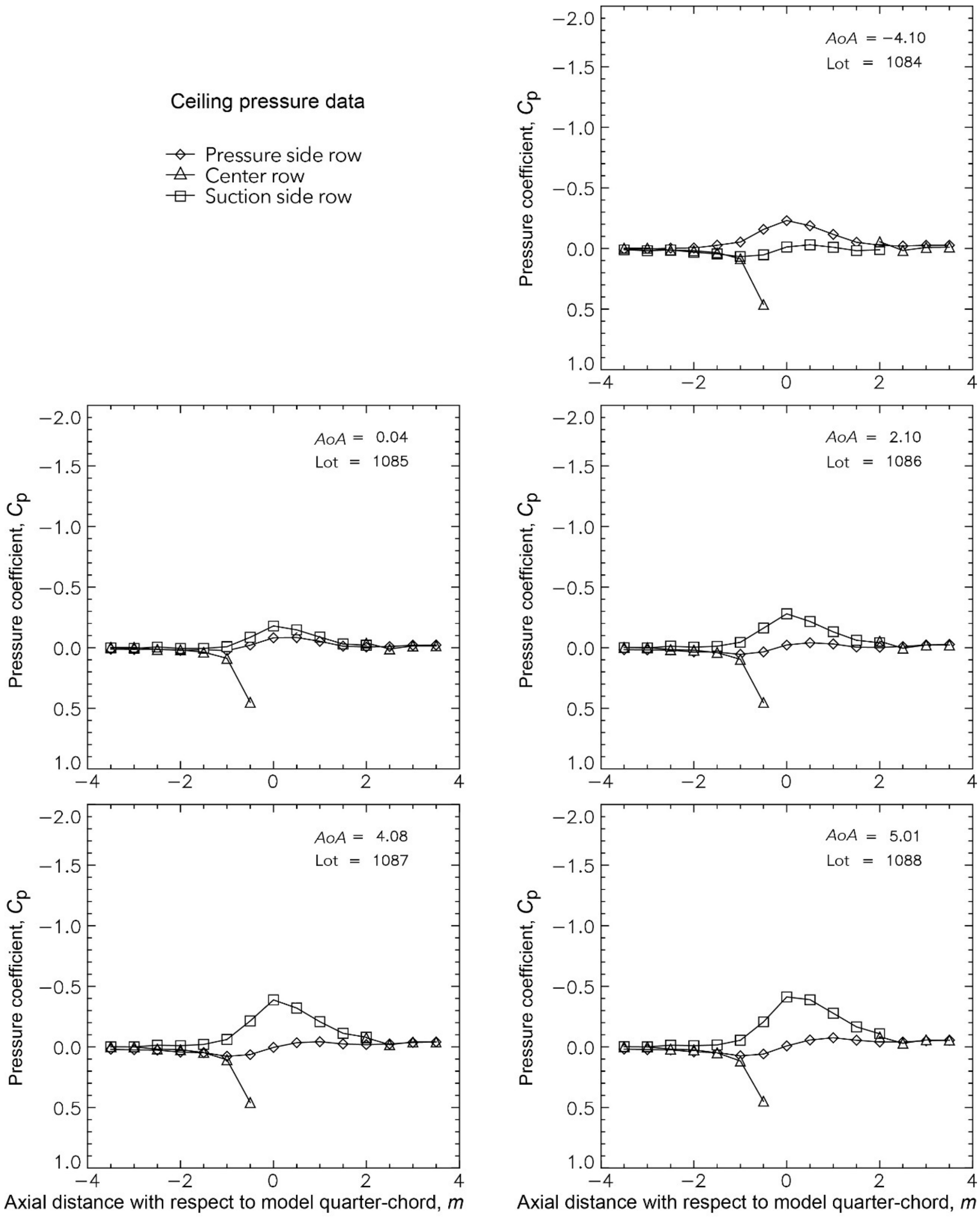

Spanwise Ridge Ice—Lot EG1159: M = 0.20 to 0.21 and Re = $15.8–16.0\times10^6$

Appendix G.—F1 Full-Scale Model Tests

Spanwise Ridge Ice—Lot EG1159: M = 0.20 to 0.21 and Re = 15.8–16.0×10^6

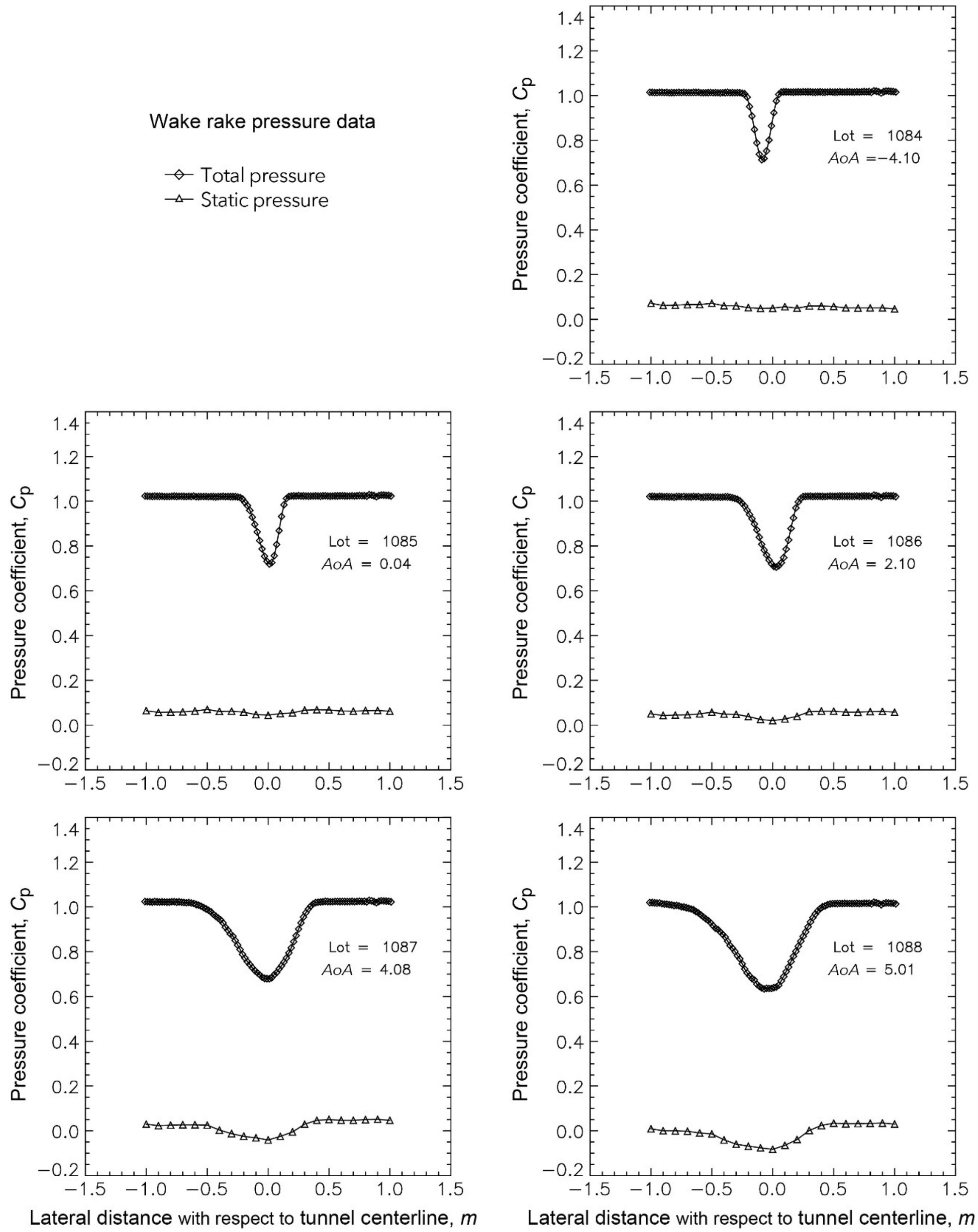

Spanwise Ridge Ice—Lot EG1159: M = 0.20 to 0.21 and Re = 15.8–16.0×10^6

Appendix G.—F1 Full-Scale Model Tests

Spanwise Ridge Ice—Lot EG1159: M = 0.29 and Re = 12.0–12.2×10^6

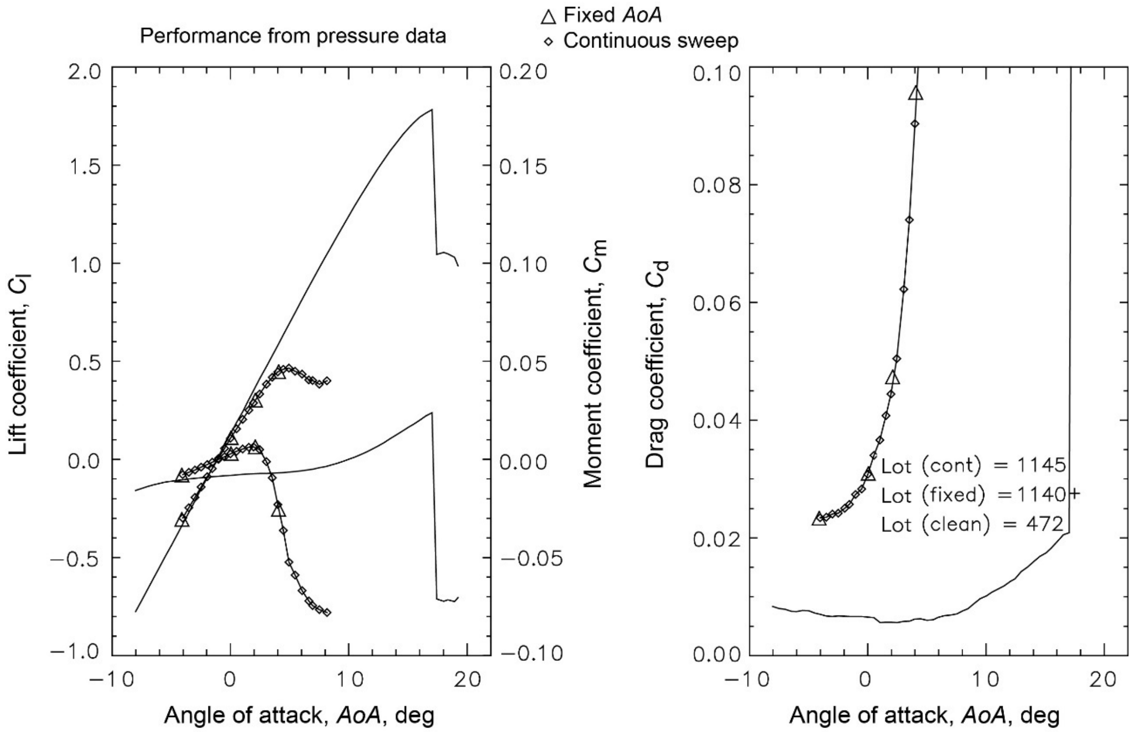

Spanwise Ridge Ice—Lot EG1159: M = 0.29 and Re = 12.0–12.2×10^6

Appendix G.—F1 Full-Scale Model Tests

Spanwise Ridge Ice—Lot EG1159: M = 0.29 and Re = 12.0–12.2×10^6

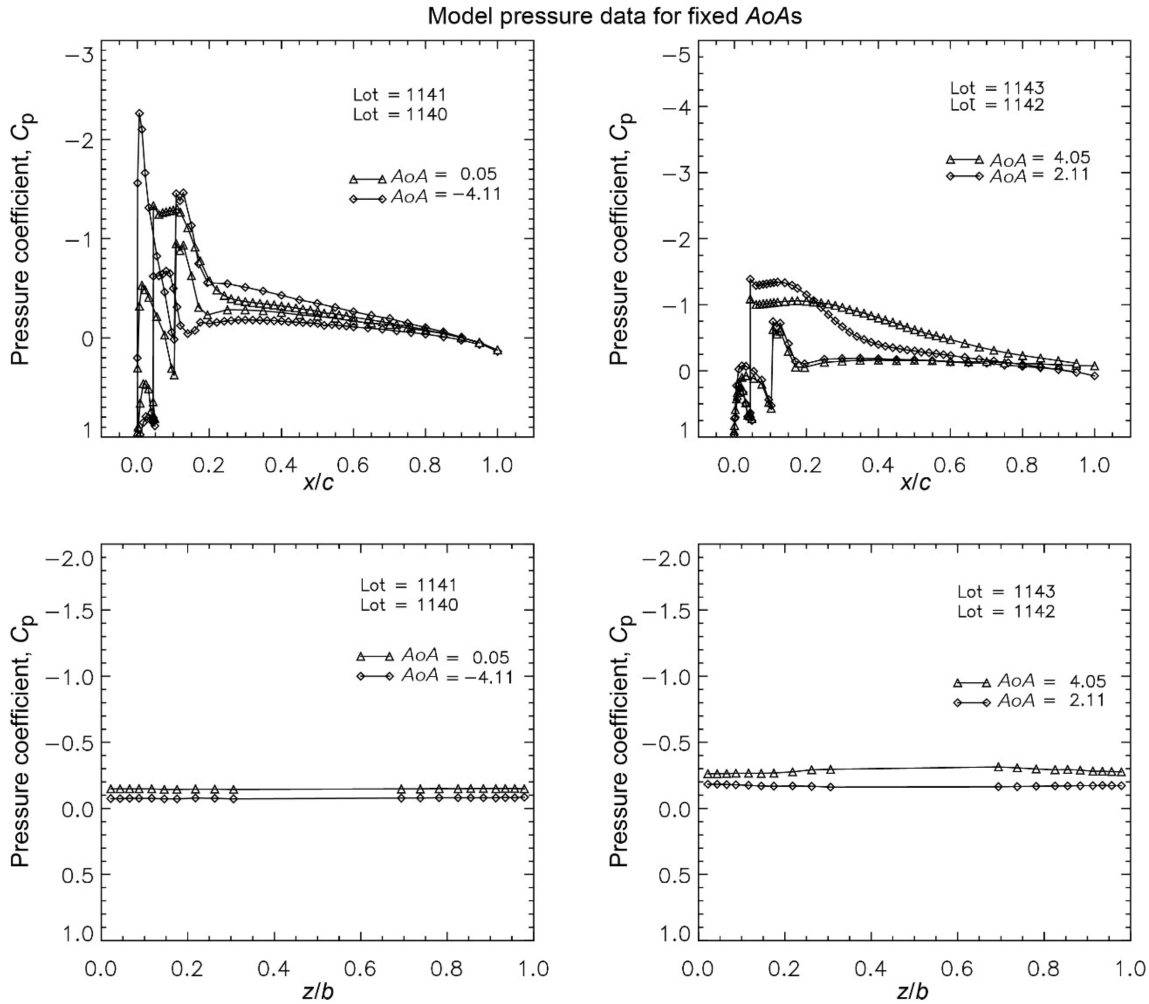

Spanwise Ridge Ice—Lot EG1159: M = 0.29 and Re = 12.0–12.2×10^6

Appendix G.—F1 Full-Scale Model Tests

Spanwise Ridge Ice—Lot EG1159: M = 0.29 and Re = 12.0–12.2×10^6

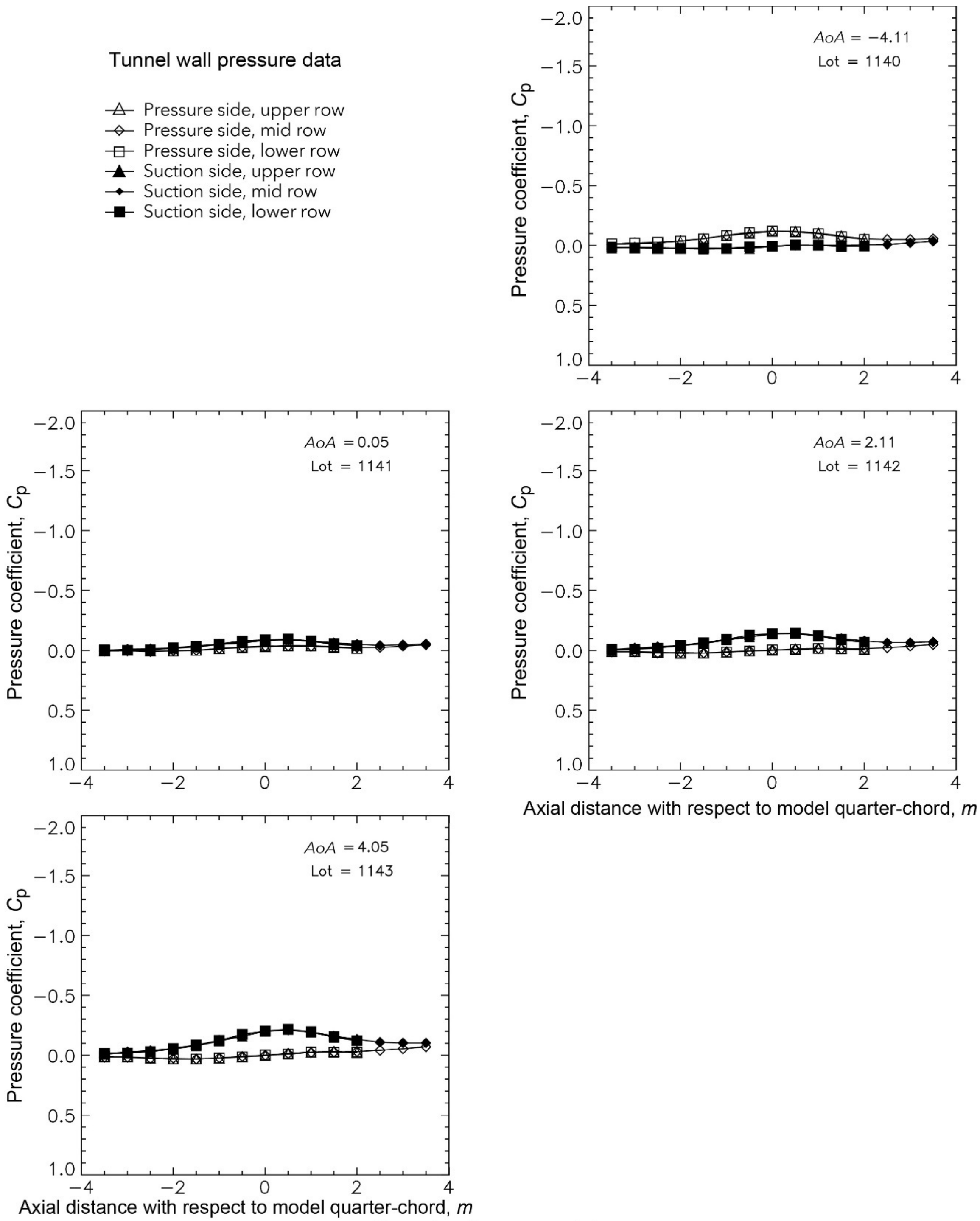

Tunnel wall pressure data

Spanwise Ridge Ice—Lot EG1159: M = 0.29 and Re = 12.0–12.2×10^6

Appendix G.—F1 Full-Scale Model Tests

Spanwise Ridge Ice—Lot EG1159: M = 0.29 and Re = 12.0–12.2×10^6

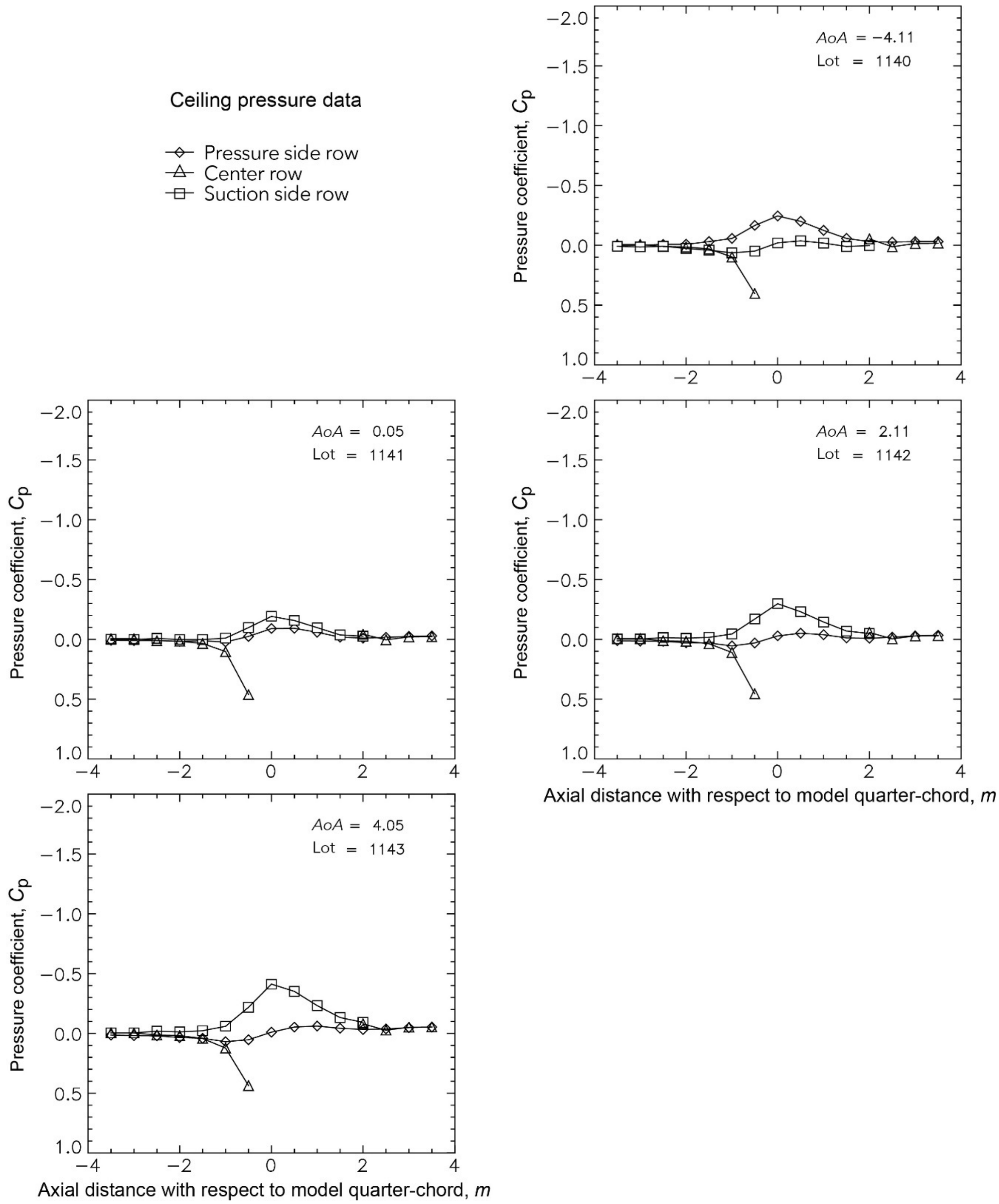

Spanwise Ridge Ice—Lot EG1159: M = 0.29 and Re = 12.0–12.2×10^6

Appendix G.—F1 Full-Scale Model Tests

Spanwise Ridge Ice—Lot EG1159: M = 0.29 and Re = 12.0–12.2×10^6

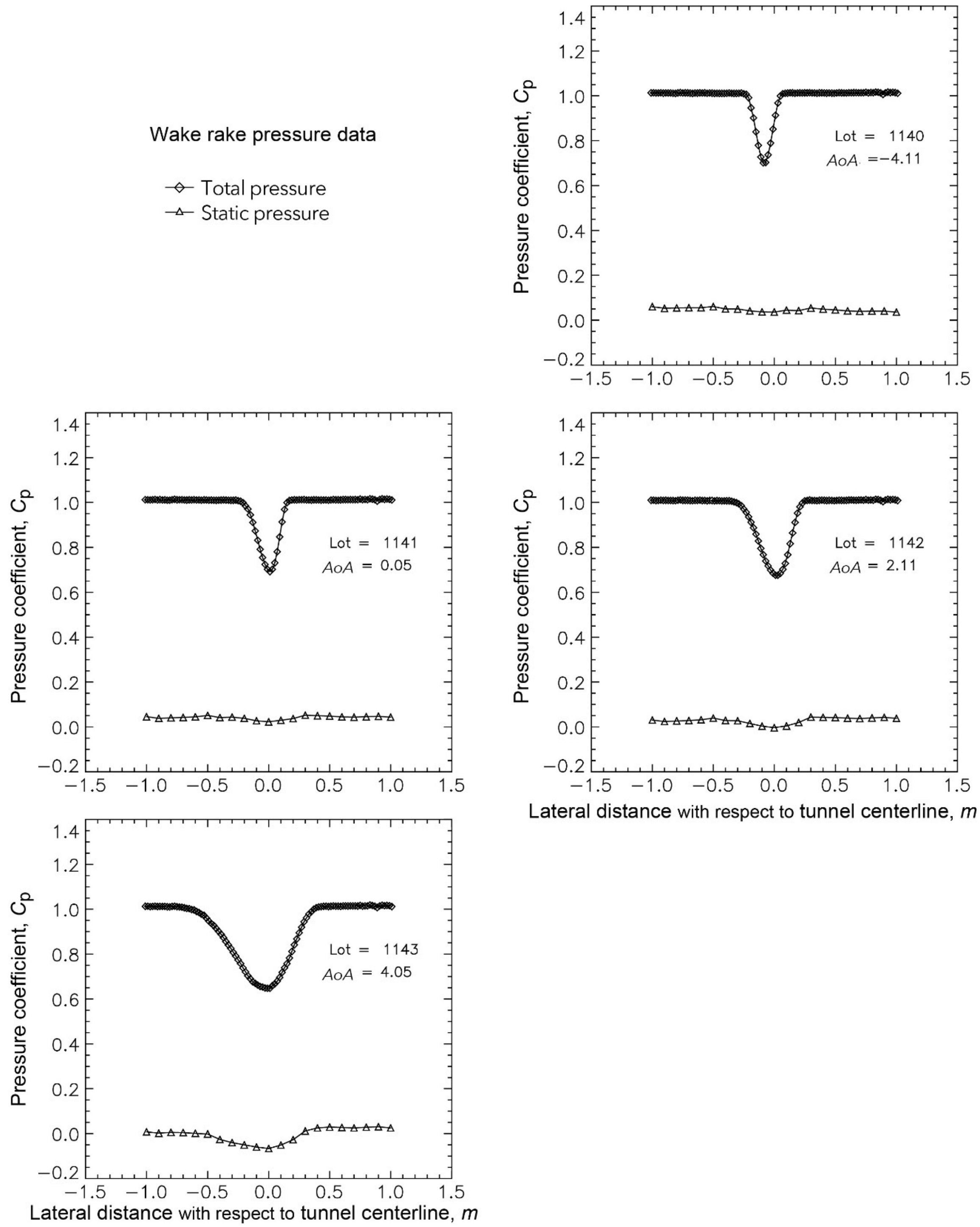

Spanwise Ridge Ice—Lot EG1159: M = 0.29 and Re = 12.0–12.2×10^6

Appendix G.—F1 Full-Scale Model Tests

Spanwise Ice 2—Lot EG1125: M = 0.10 and Re = 4.5×10^6

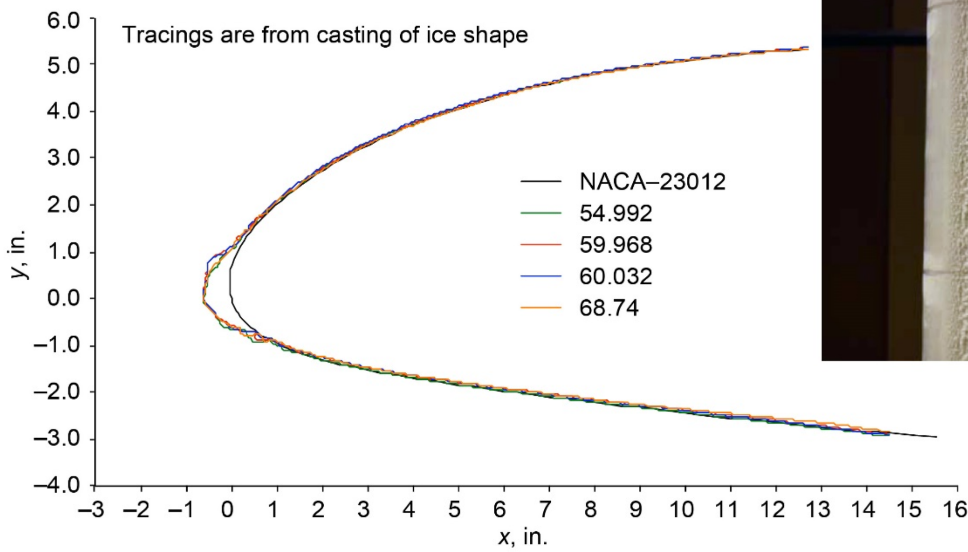

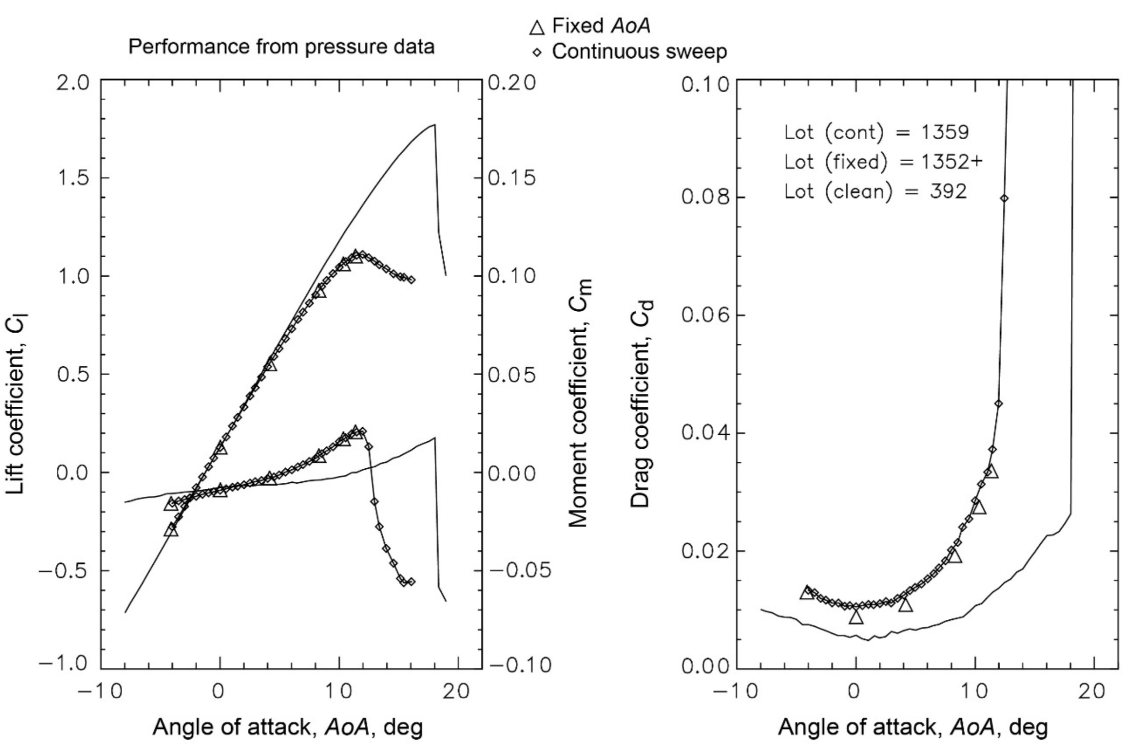

Spanwise Ice 2—Lot EG1125: M = 0.10 and Re = 4.5×10^6

Appendix G.—F1 Full-Scale Model Tests

Spanwise Ice 2—Lot EG1125: M = 0.10 and Re = 4.5×10^6

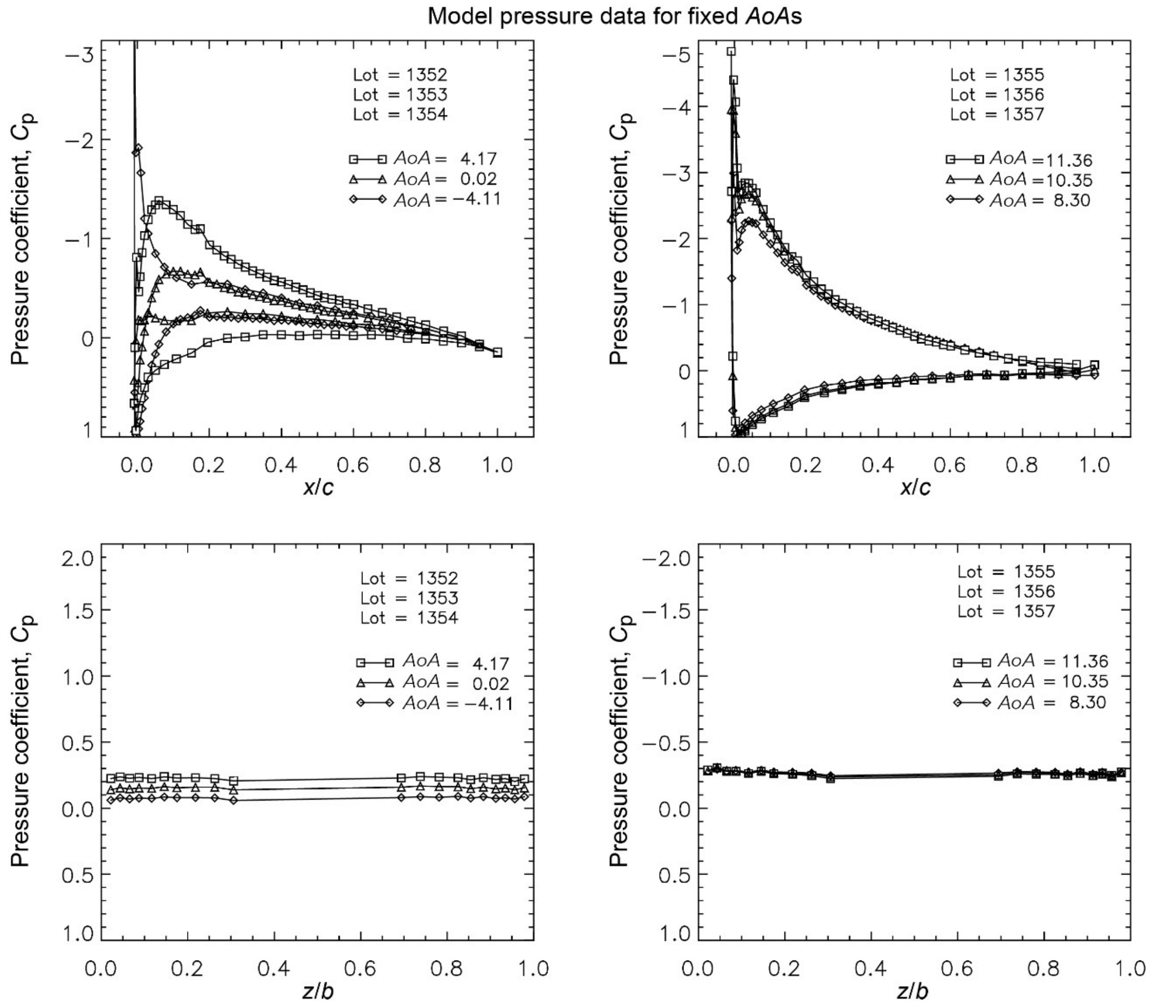

Spanwise Ice 2—Lot EG1125: M = 0.10 and Re = 4.5×10^6

Appendix G.—F1 Full-Scale Model Tests

Spanwise Ice 2—Lot EG1125: M = 0.10 and Re = 4.5×10^6

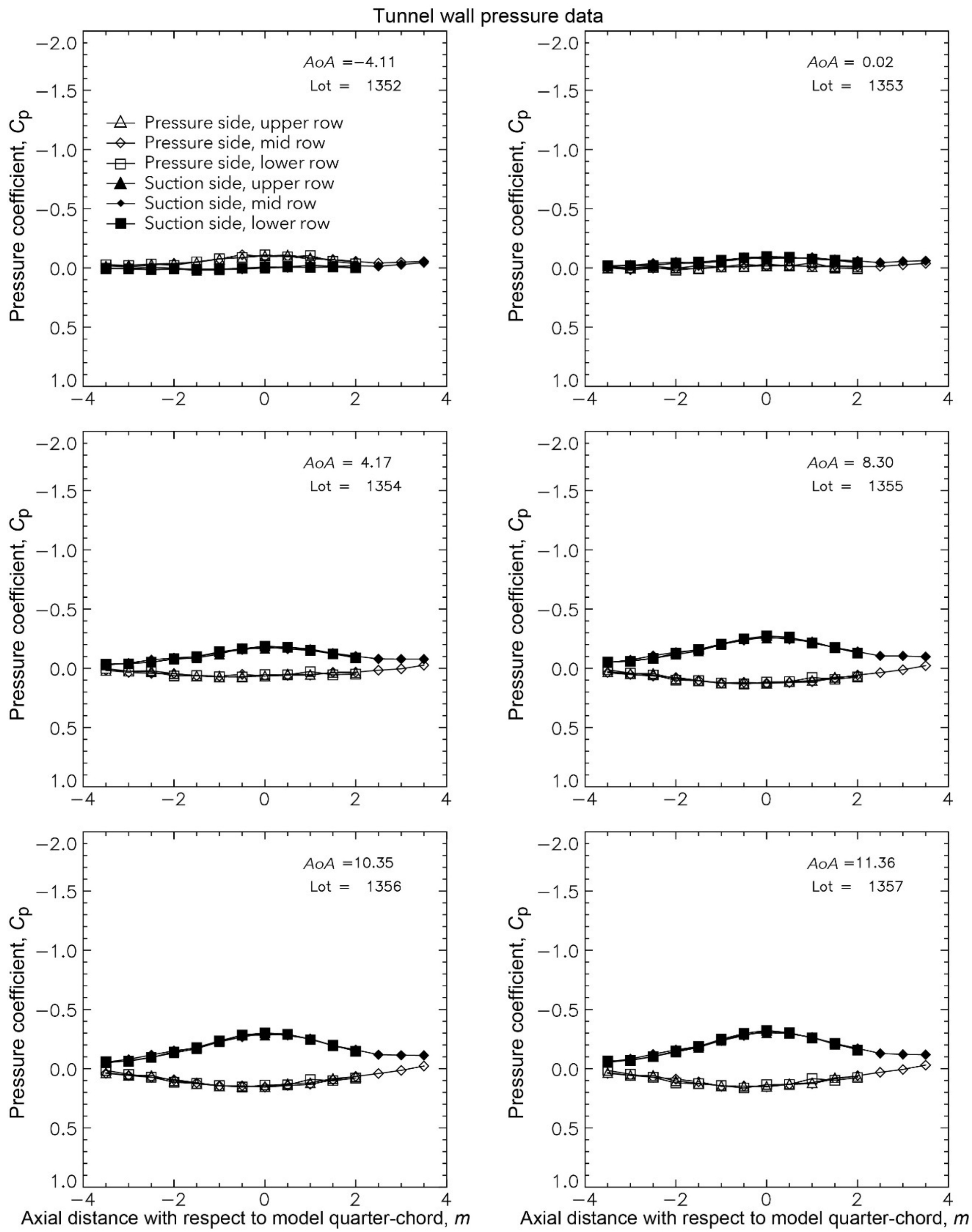

Spanwise Ice 2—Lot EG1125: M = 0.10 and Re = 4.5×10^6

Appendix G.—F1 Full-Scale Model Tests

Spanwise Ice 2—Lot EG1125: M = 0.10 and Re = 4.5×10^6

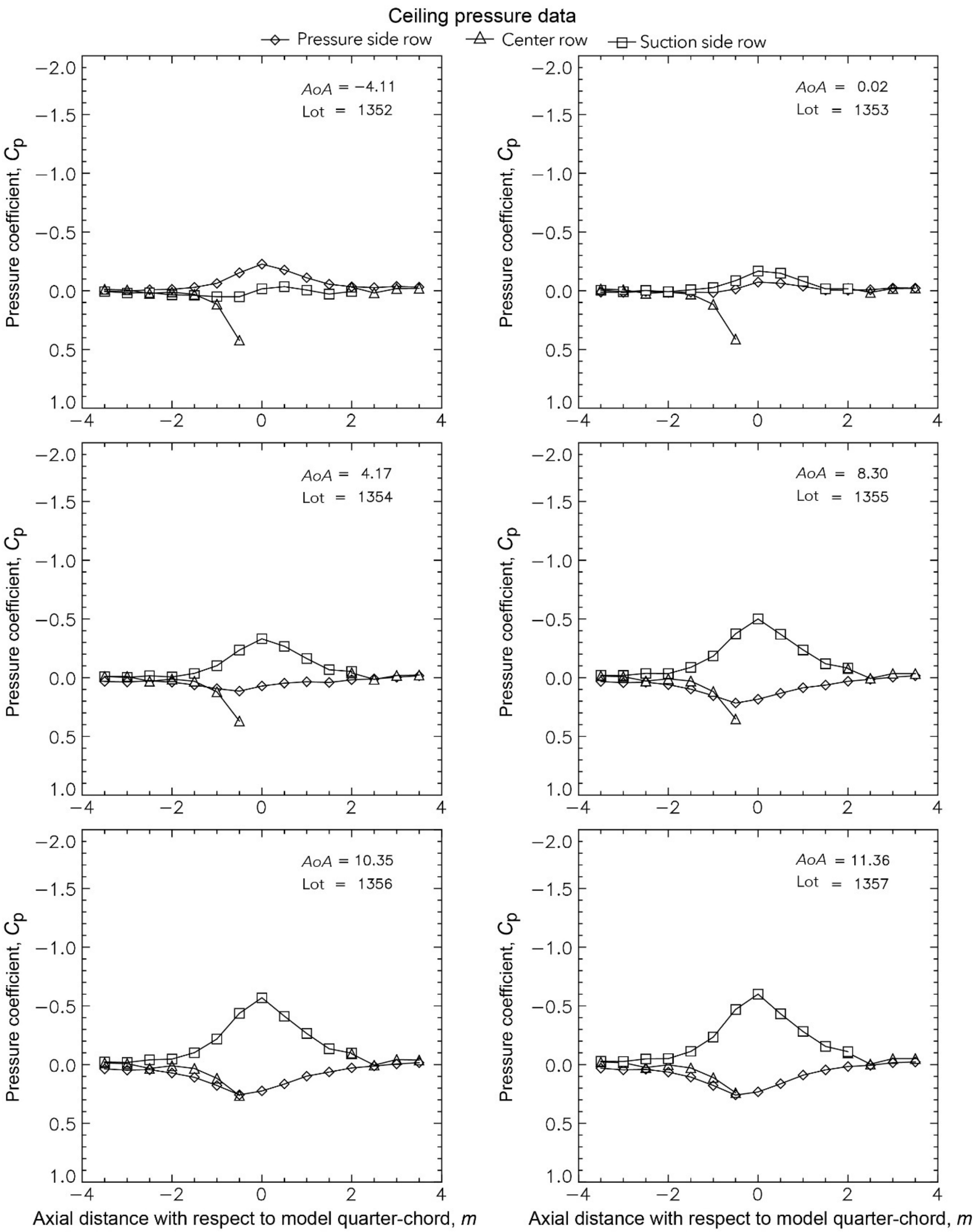

Spanwise Ice 2—Lot EG1125: M = 0.10 and Re = 4.5×10^6

Appendix G.—F1 Full-Scale Model Tests

Spanwise Ice 2—Lot EG1125: M = 0.10 and Re = 4.5×10^6

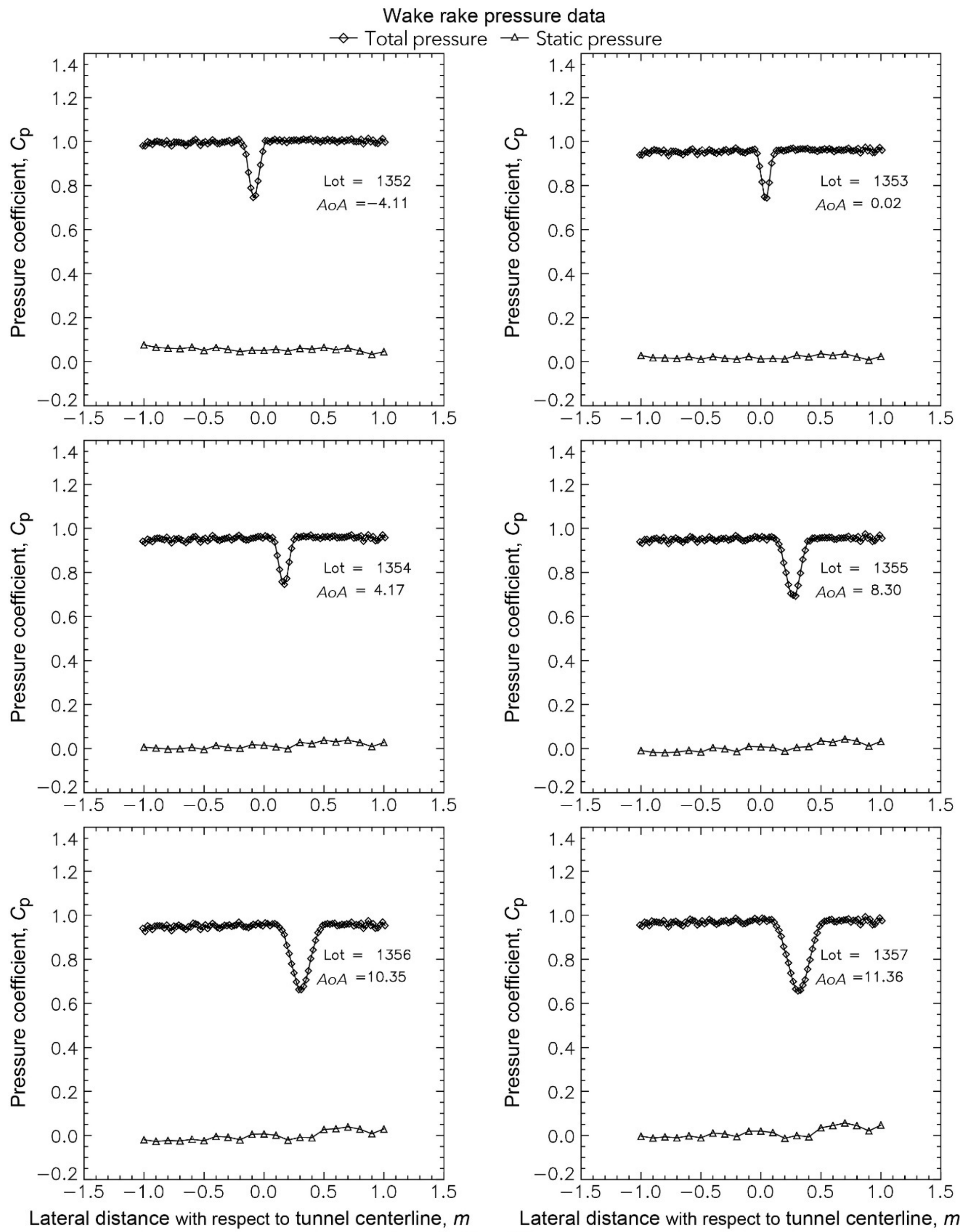

Spanwise Ice 2—Lot EG1125: M = 0.10 and Re = 4.5×10^6

Spanwise Ice 2—Lot EG1125: M = 0.10 and Re = 8.2–8.3×10^6

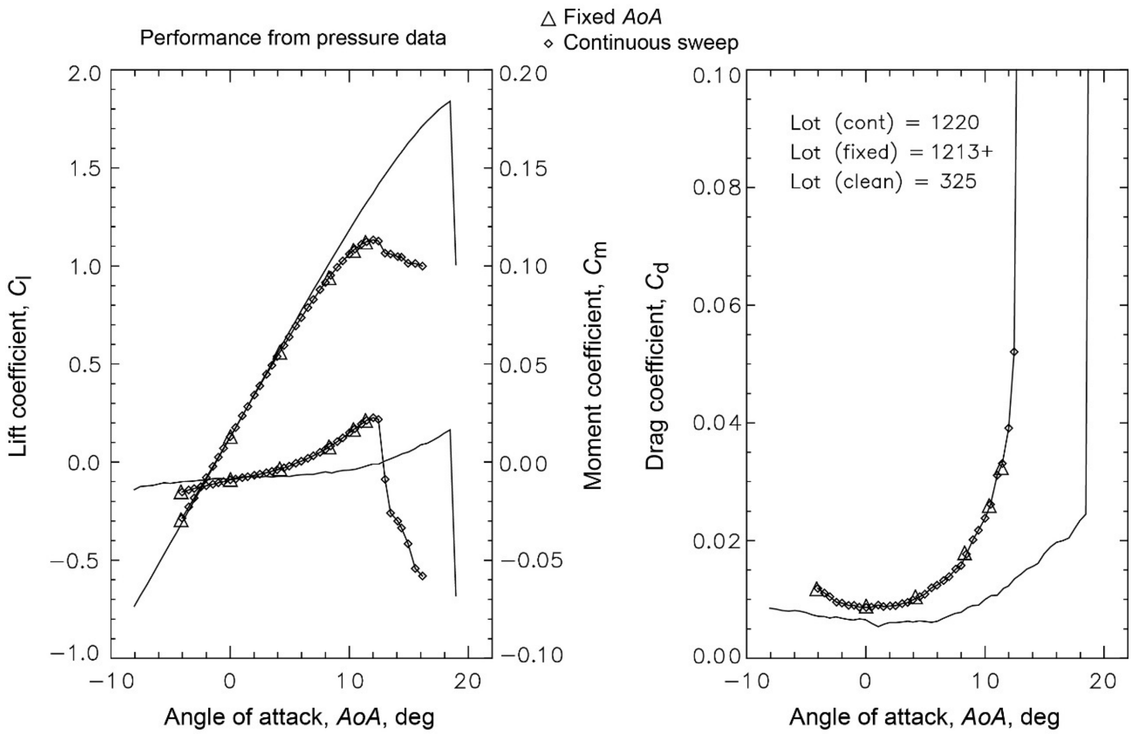

Spanwise Ice 2—Lot EG1125: M = 0.10 and Re = 8.2–8.3×10^6

Appendix G.—F1 Full-Scale Model Tests

Spanwise Ice 2—Lot EG1125: M = 0.10 and Re = 8.2–8.3×10^6

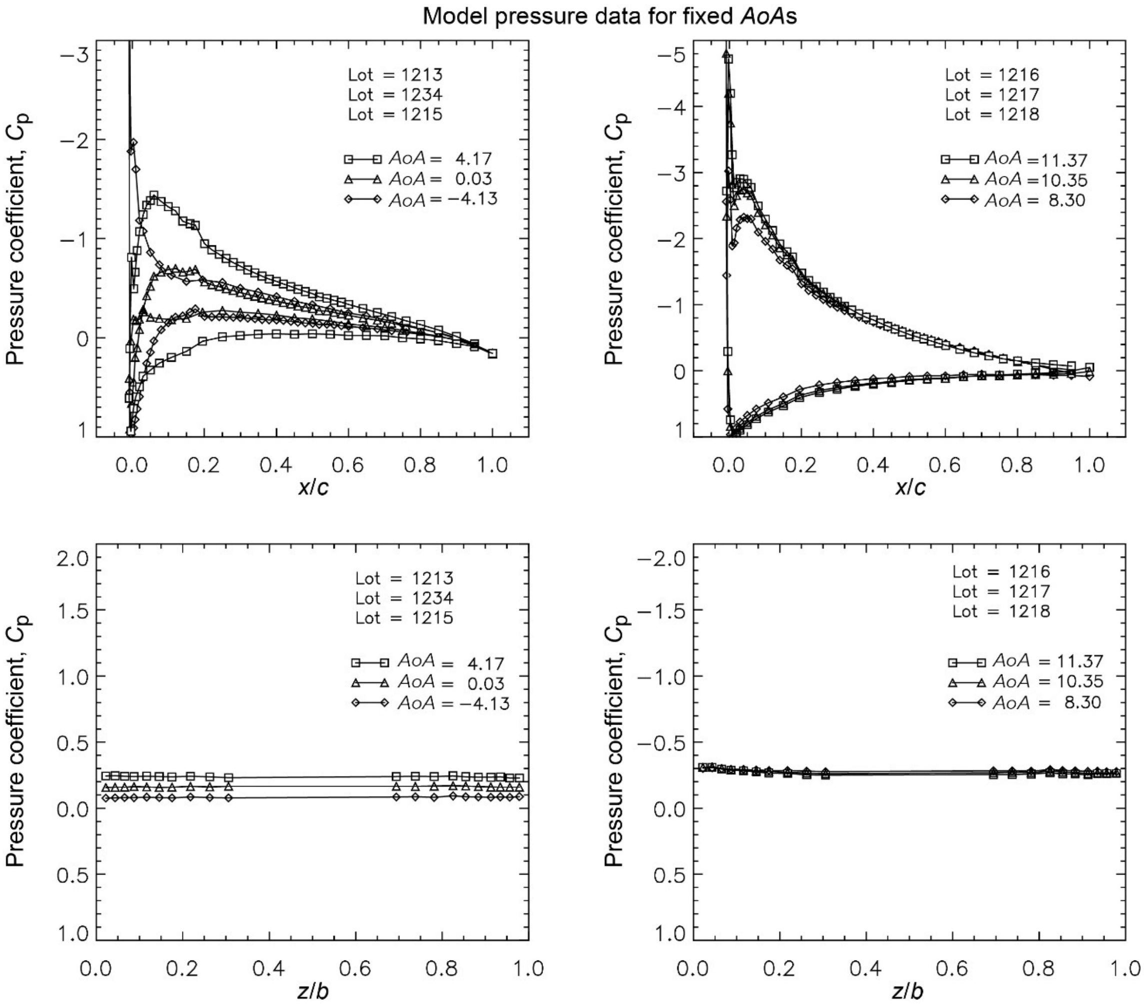

Spanwise Ice 2—Lot EG1125: M = 0.10 and Re = 8.2–8.3×10^6

Appendix G.—F1 Full-Scale Model Tests

Spanwise Ice 2—Lot EG1125: M = 0.10 and Re = 8.2–8.3×10^6

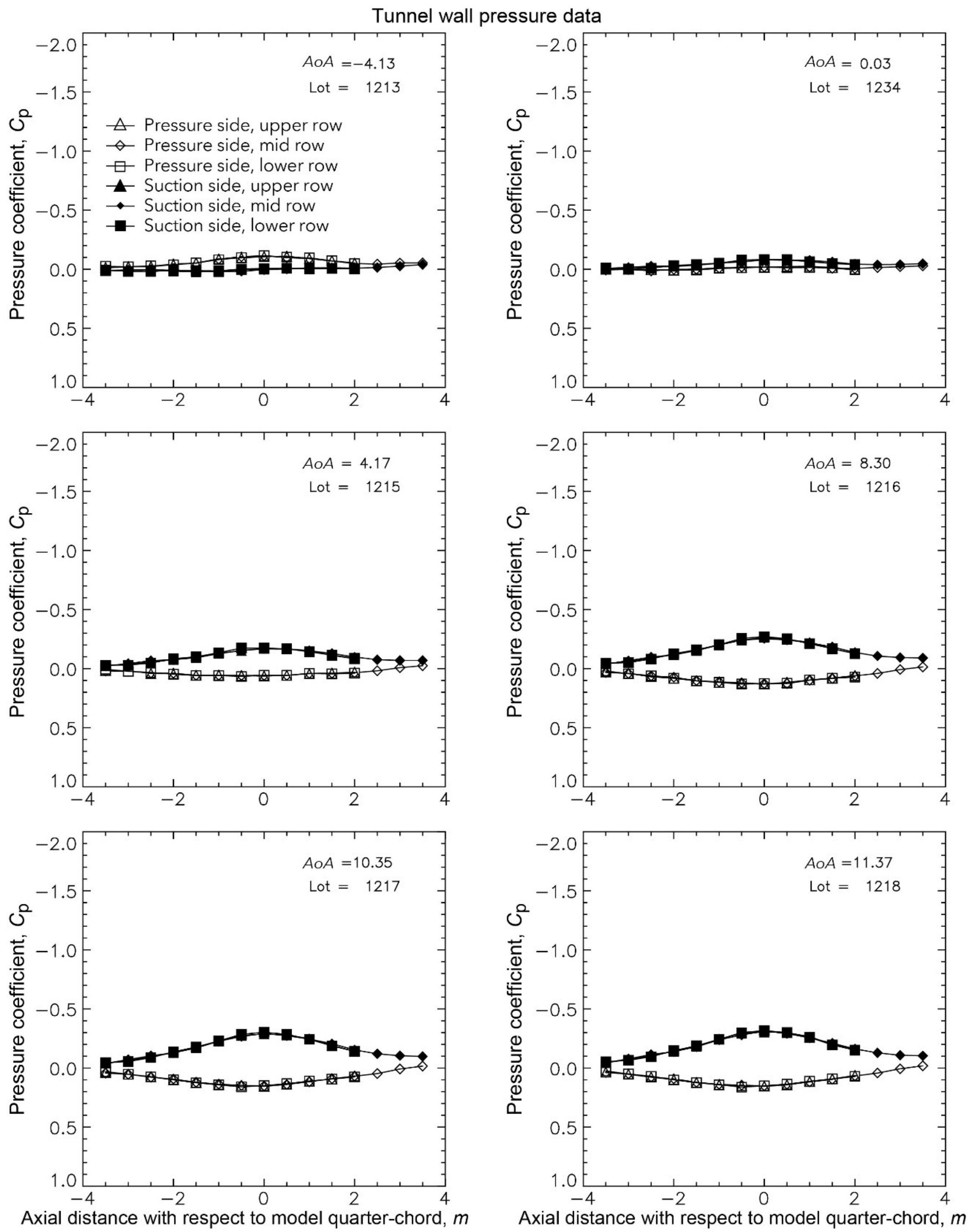

Spanwise Ice 2—Lot EG1125: M = 0.10 and Re = 8.2–8.3×10^6

Appendix G.—F1 Full-Scale Model Tests

Spanwise Ice 2—Lot EG1125: M = 0.10 and Re = 8.2–8.3×10^6

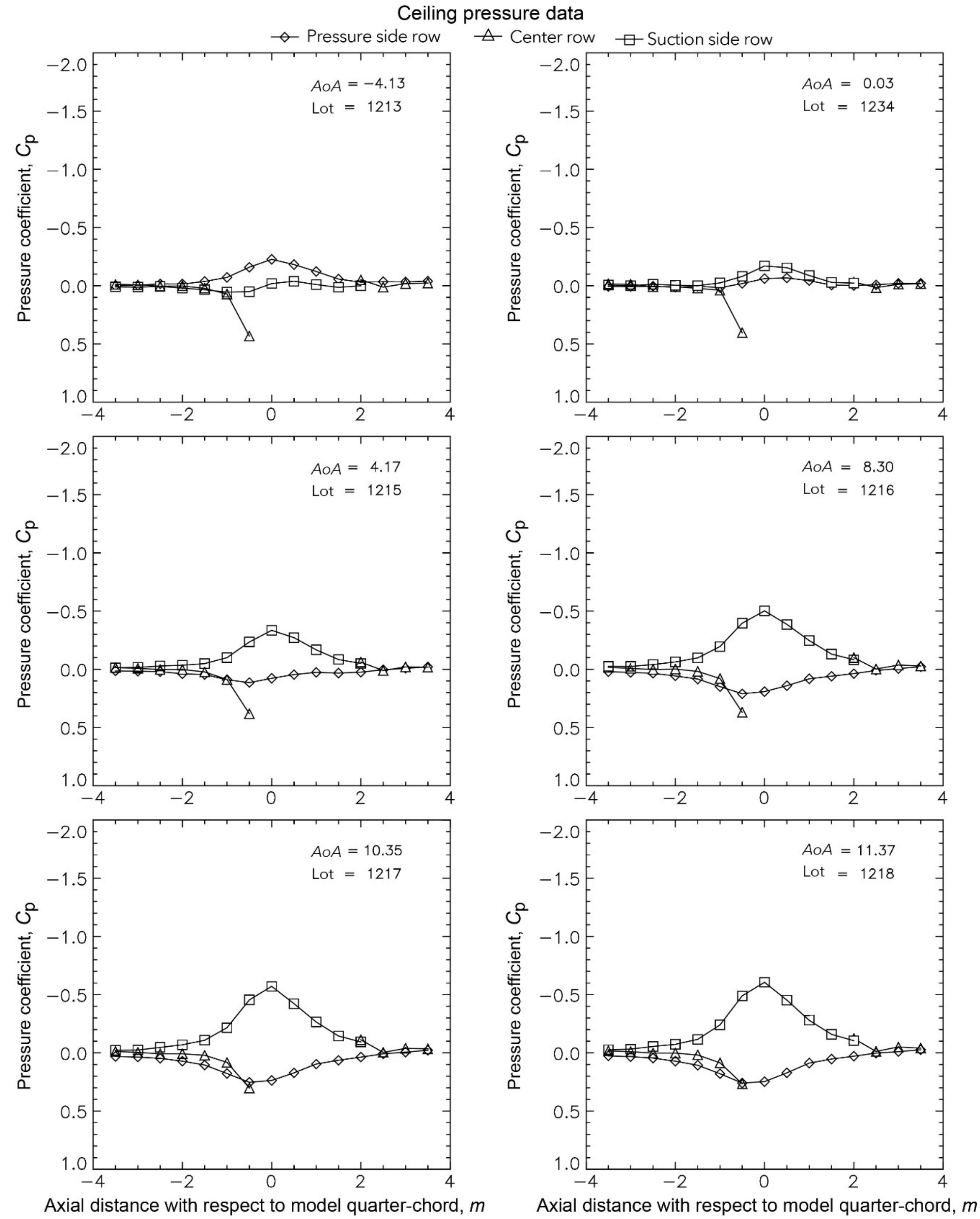

Spanwise Ice 2—Lot EG1125: M = 0.10 and Re = 8.2–8.3×10^6

Appendix G.—F1 Full-Scale Model Tests

Spanwise Ice 2—Lot EG1125: M = 0.10 and Re = 8.2–8.3×10^6

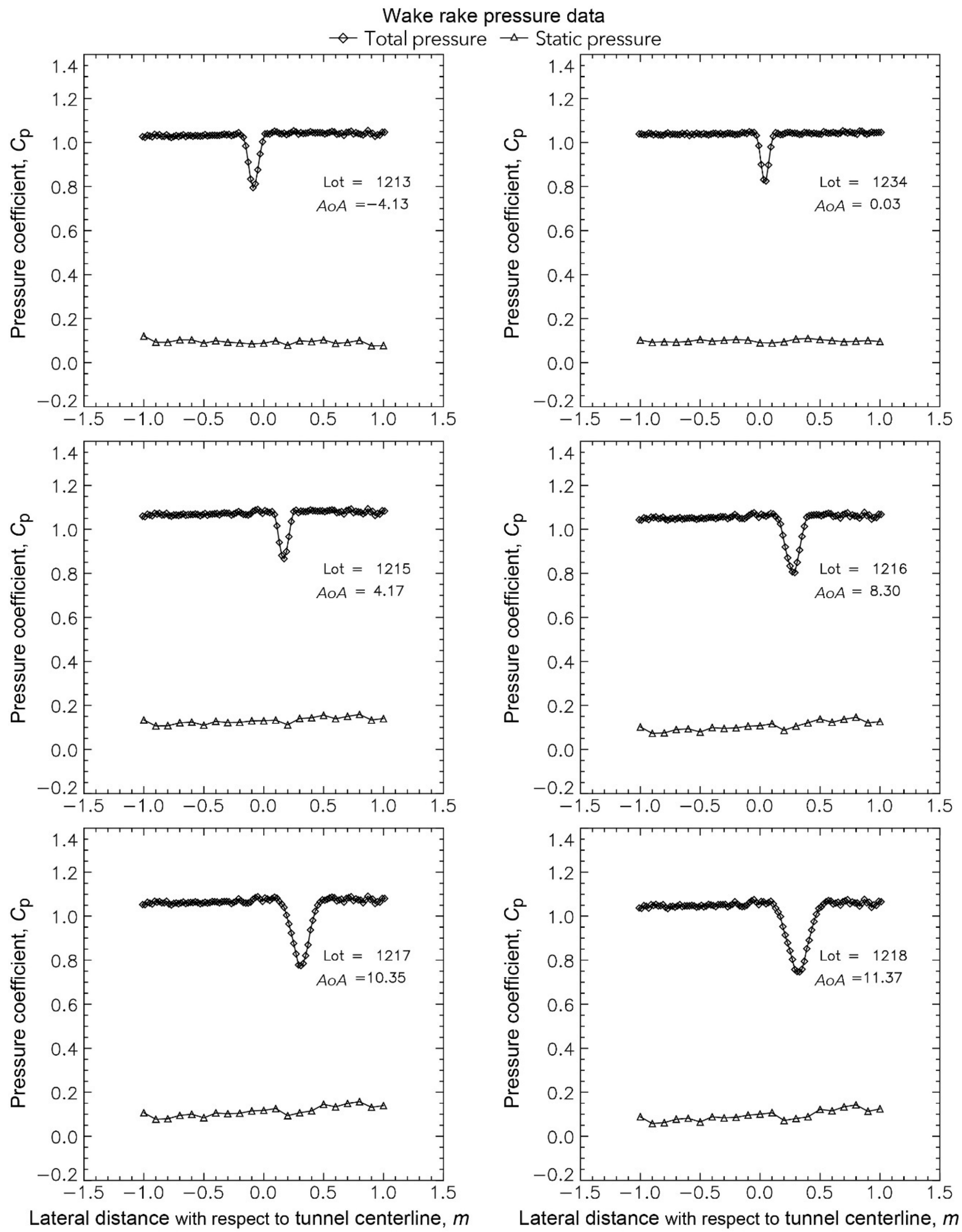

Spanwise Ice 2—Lot EG1125: M = 0.10 and Re = 8.2–8.3×10^6

Appendix G.—F1 Full-Scale Model Tests

Spanwise Ice 2—Lot EG1125: M = 0.10 and Re = 12.1–12.2×10^6

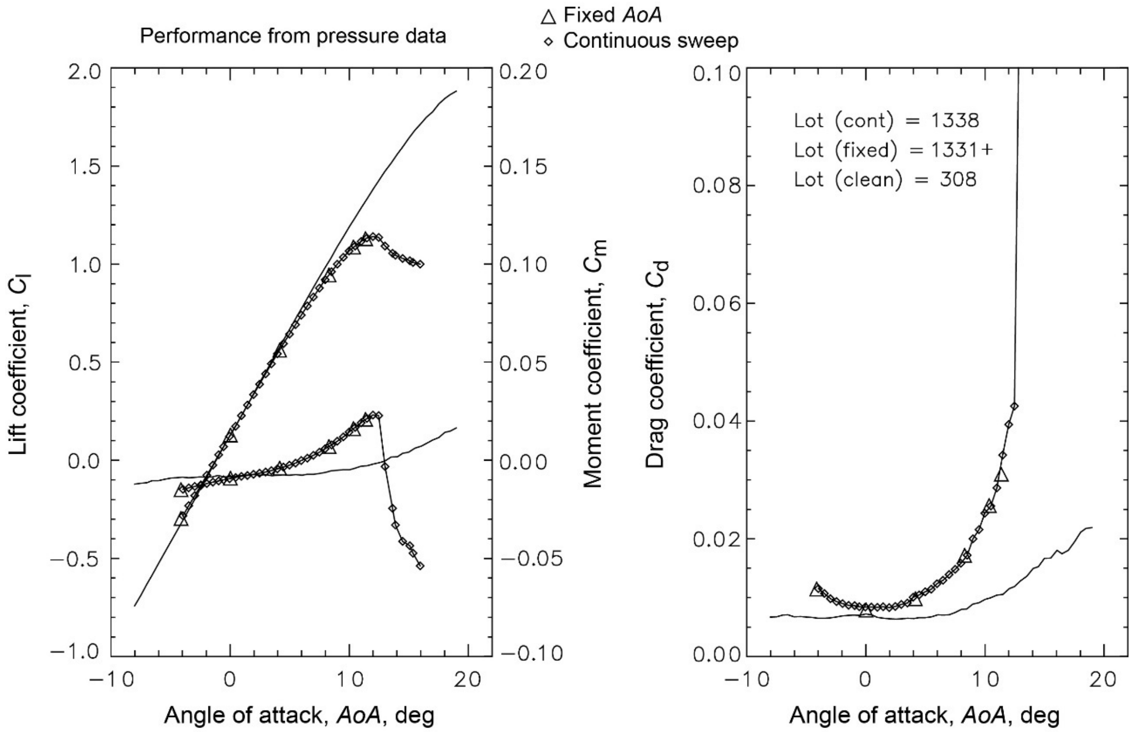

Spanwise Ice 2—Lot EG1125: M = 0.10 and Re = 12.1–12.2×10^6

Appendix G.—F1 Full-Scale Model Tests

Spanwise Ice 2—Lot EG1125: M = 0.10 and Re = 12.1–12.2×10^6

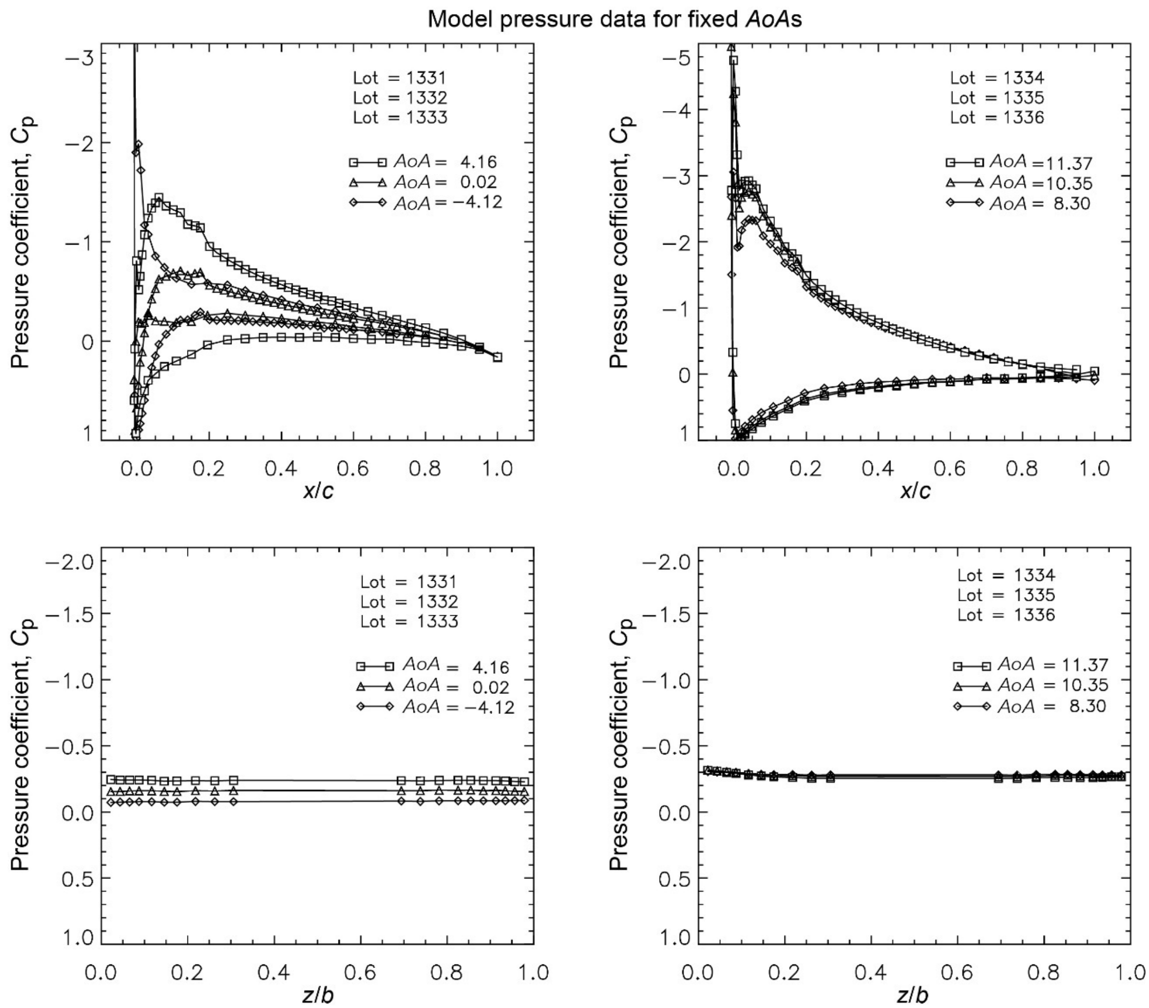

Spanwise Ice 2—Lot EG1125: M = 0.10 and Re = 12.1–12.2×10^6

Spanwise Ice 2—Lot EG1125: M = 0.10 and Re = 12.1–12.2×10[6]

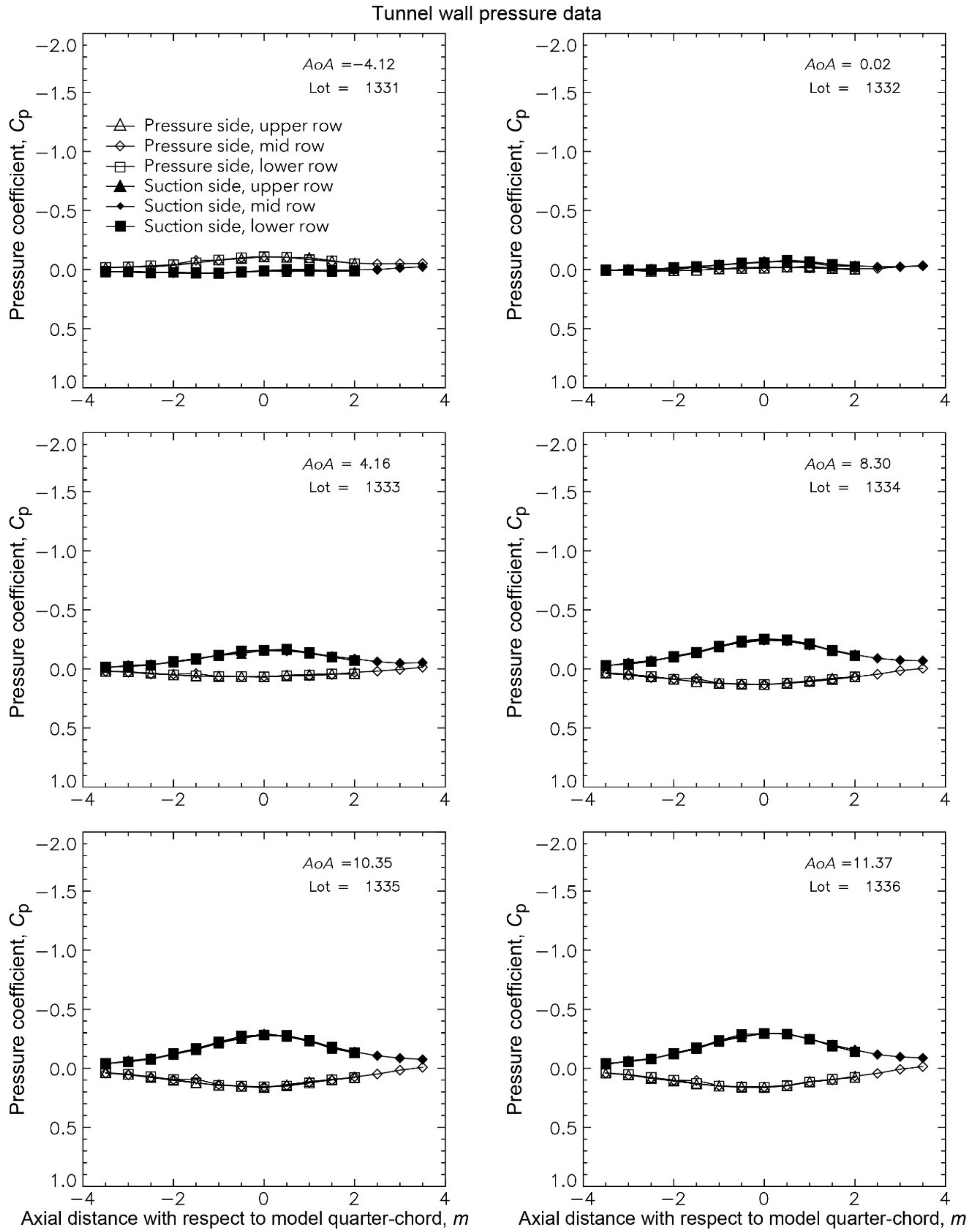

Spanwise Ice 2—Lot EG1125: M = 0.10 and Re = 12.1–12.2×10[6]

Appendix G.—F1 Full-Scale Model Tests

Spanwise Ice 2—Lot EG1125: M = 0.10 and Re = 12.1–12.2×10^6

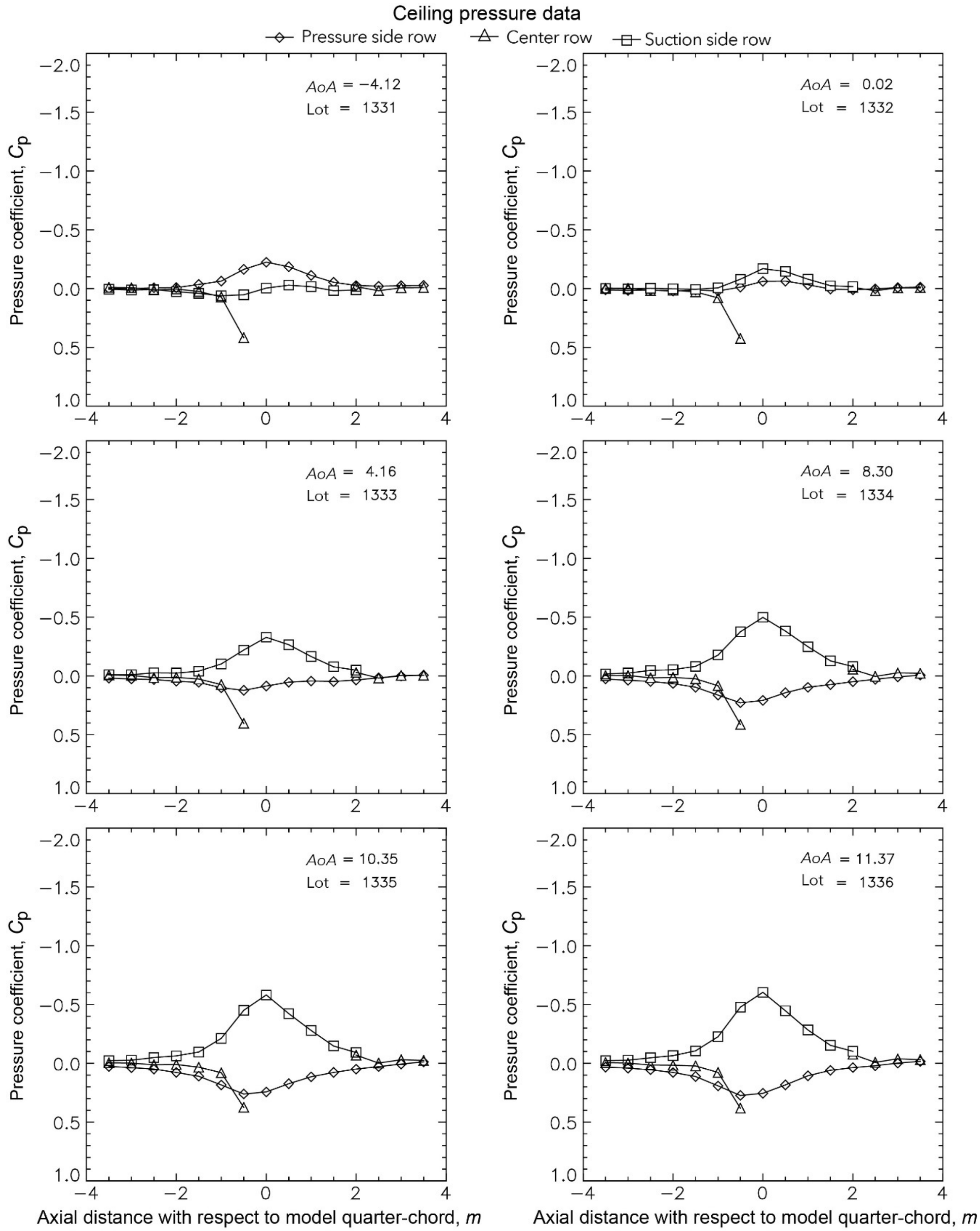

Spanwise Ice 2—Lot EG1125: M = 0.10 and Re = 12.1–12.2×10^6

Appendix G.—F1 Full-Scale Model Tests

Spanwise Ice 2—Lot EG1125: M = 0.10 and Re = 12.1–12.2×10[6]

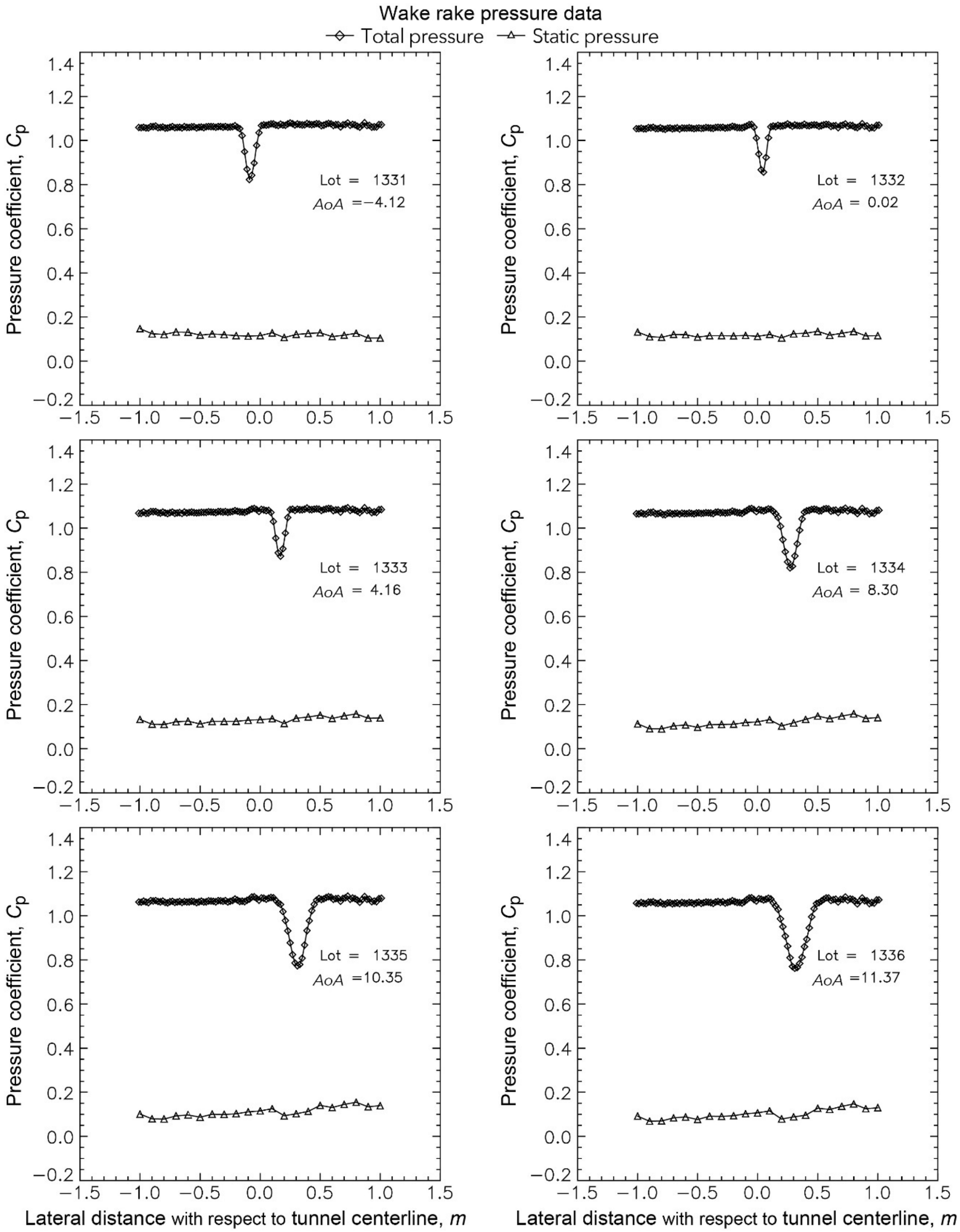

Spanwise Ice 2—Lot EG1125: M = 0.10 and Re = 12.1–12.2×10[6]

Appendix G.—F1 Full-Scale Model Tests

Spanwise Ice 2—Lot EG1125: M = 0.20 to 0.21 and Re = 8.9–9.0×10^6

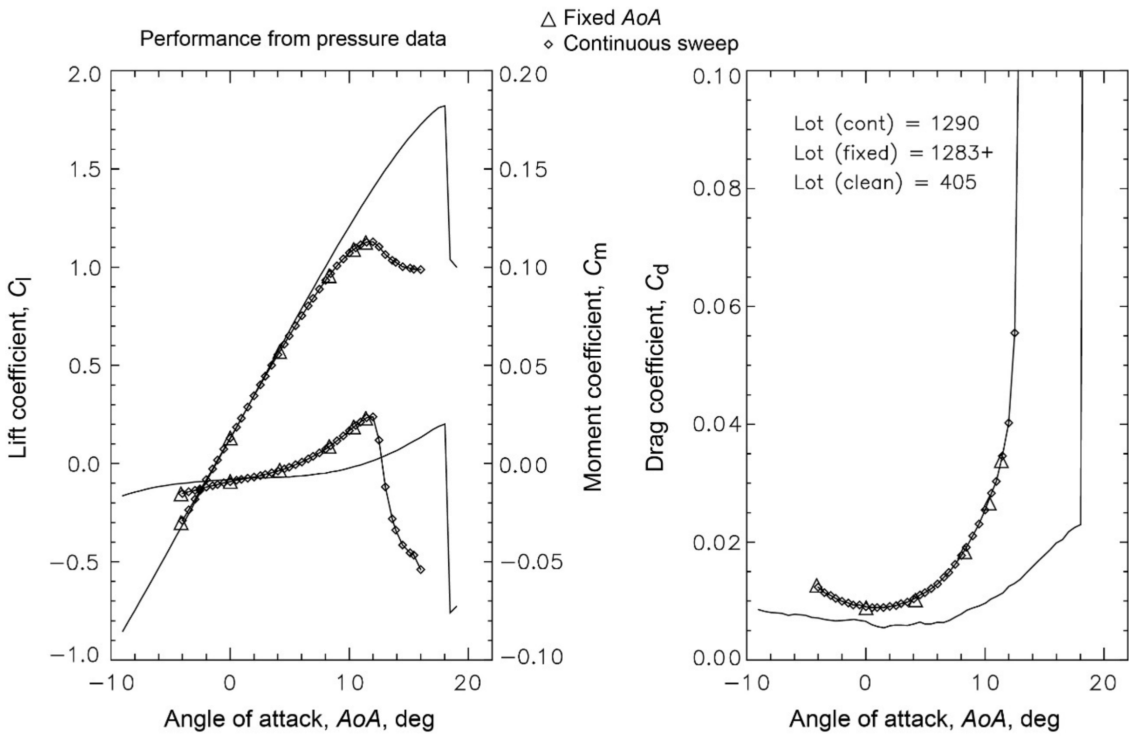

Spanwise Ice 2—Lot EG1125: M = 0.20 to 0.21 and Re = 8.9–9.0×10^6

Appendix G.—F1 Full-Scale Model Tests

Spanwise Ice 2—Lot EG1125: M = 0.20 to 0.21 and Re = 8.9–9.0×10[6]

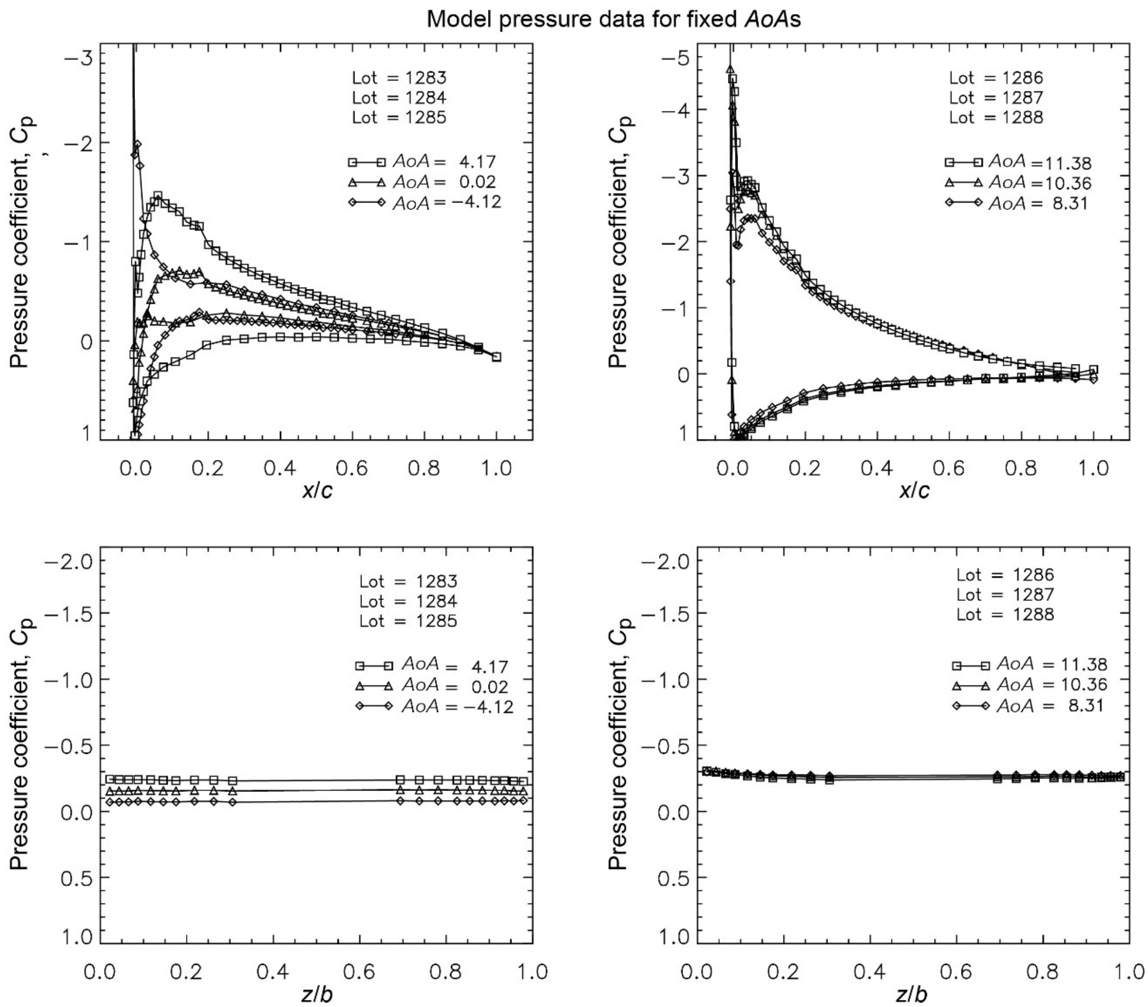

Spanwise Ice 2—Lot EG1125: M = 0.20 to 0.21 and Re = 8.9–9.0×10[6]

Appendix G.—F1 Full-Scale Model Tests

Spanwise Ice 2—Lot EG1125: M = 0.20 to 0.21 and Re = 8.9–9.0×10^6

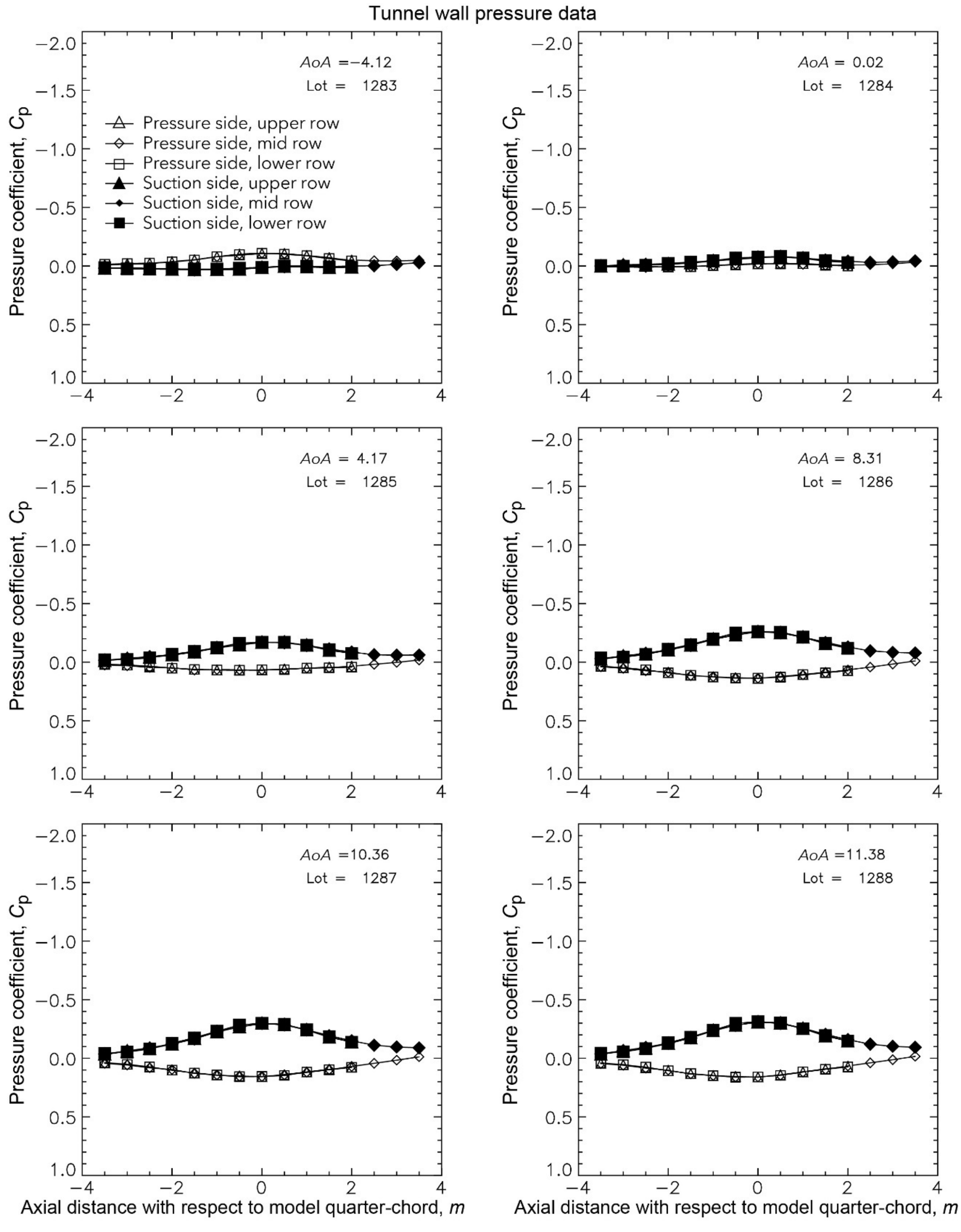

Spanwise Ice 2—Lot EG1125: M = 0.20 to 0.21 and Re = 8.9–9.0×10^6

Appendix G.—F1 Full-Scale Model Tests

Spanwise Ice 2—Lot EG1125: M = 0.20 to 0.21 and Re = 8.9–9.0×10⁶

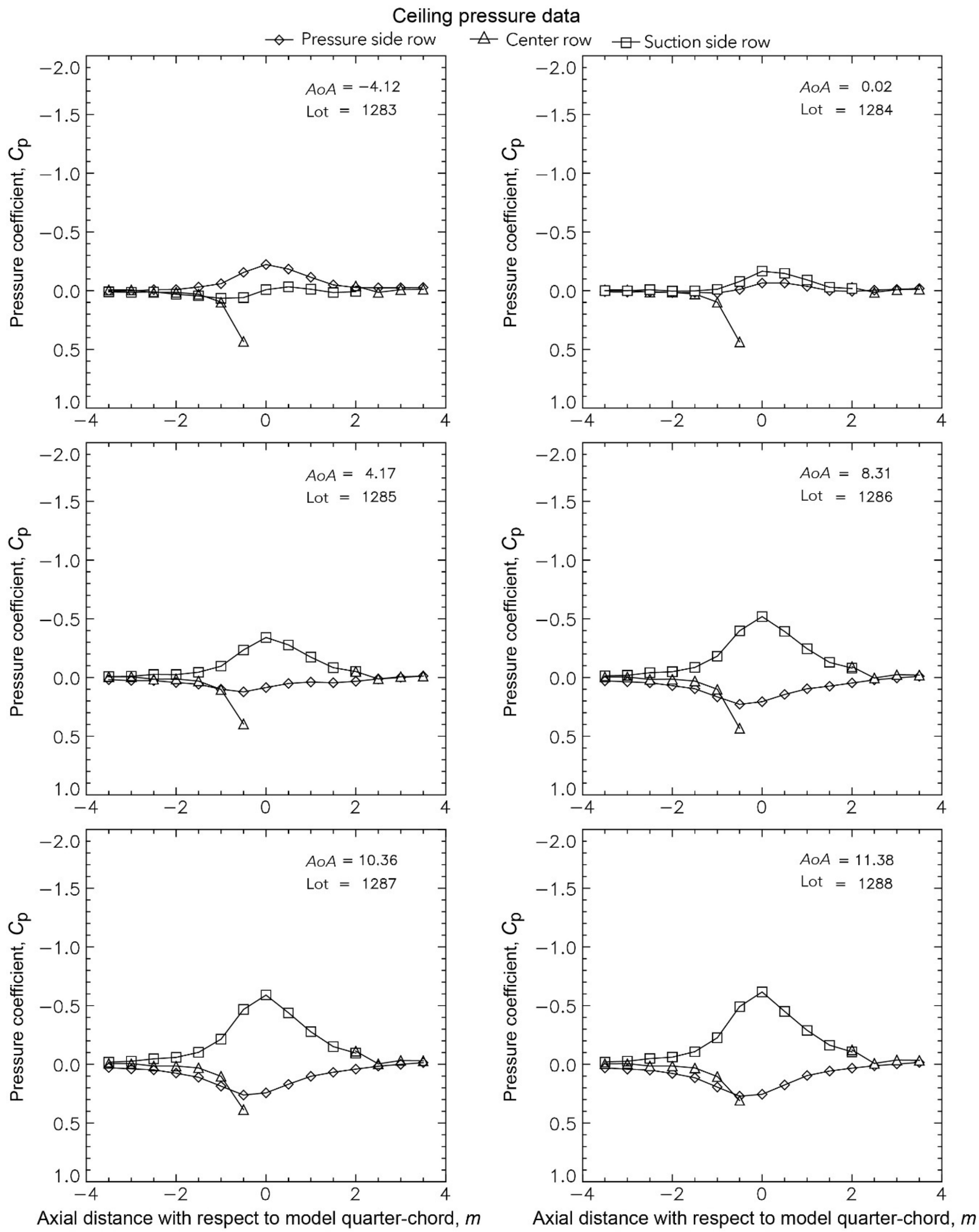

Spanwise Ice 2—Lot EG1125: M = 0.20 to 0.21 and Re = 8.9–9.0×10⁶

Appendix G.—F1 Full-Scale Model Tests

Spanwise Ice 2—Lot EG1125: M = 0.20 to 0.21 and Re = 8.9–9.0×10⁶

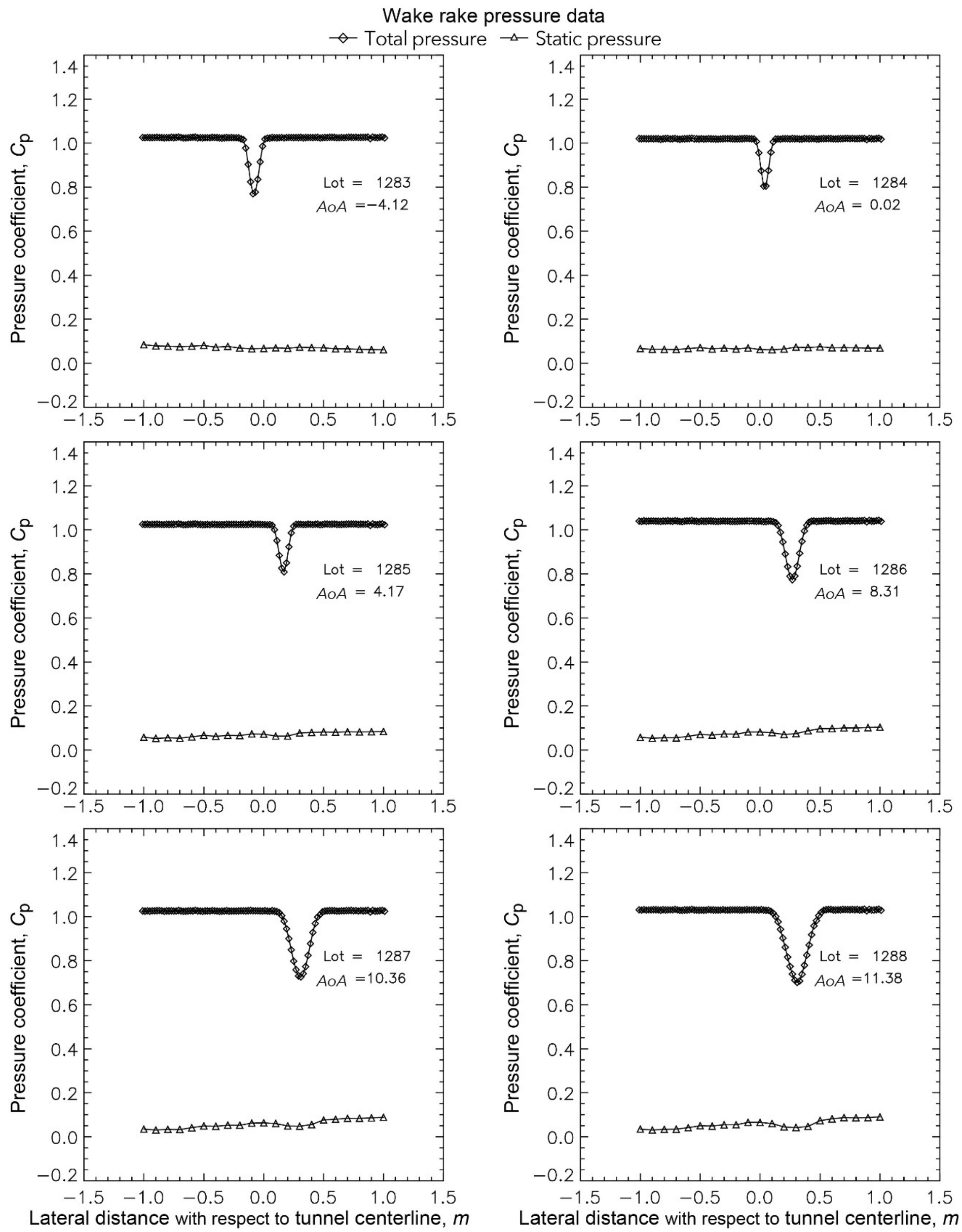

Spanwise Ice 2—Lot EG1125: M = 0.20 to 0.21 and Re = 8.9–9.0×10⁶

Appendix G.—F1 Full-Scale Model Tests

Spanwise Ice 2—Lot EG1125: M = 0.21 and Re = 12.1×10^6

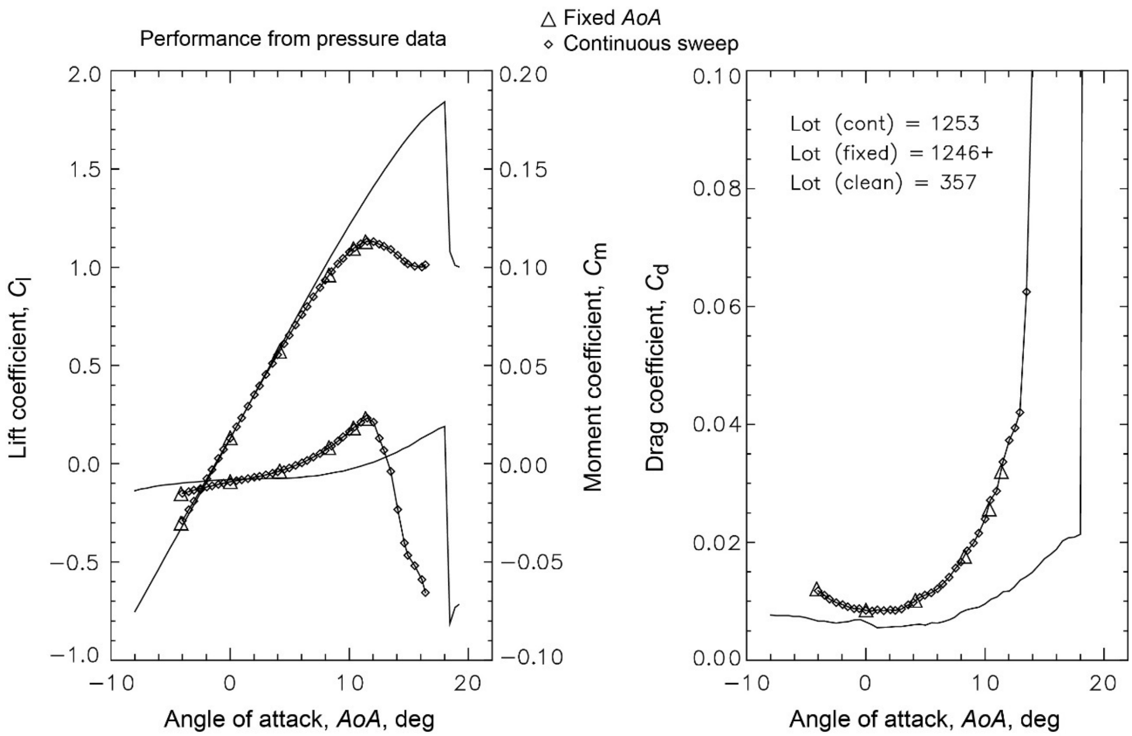

Spanwise Ice 2—Lot EG1125: M = 0.21 and Re = 12.1×10^6

Appendix G.—F1 Full-Scale Model Tests

Spanwise Ice 2—Lot EG1125: M = 0.21 and Re = 12.1×10^6

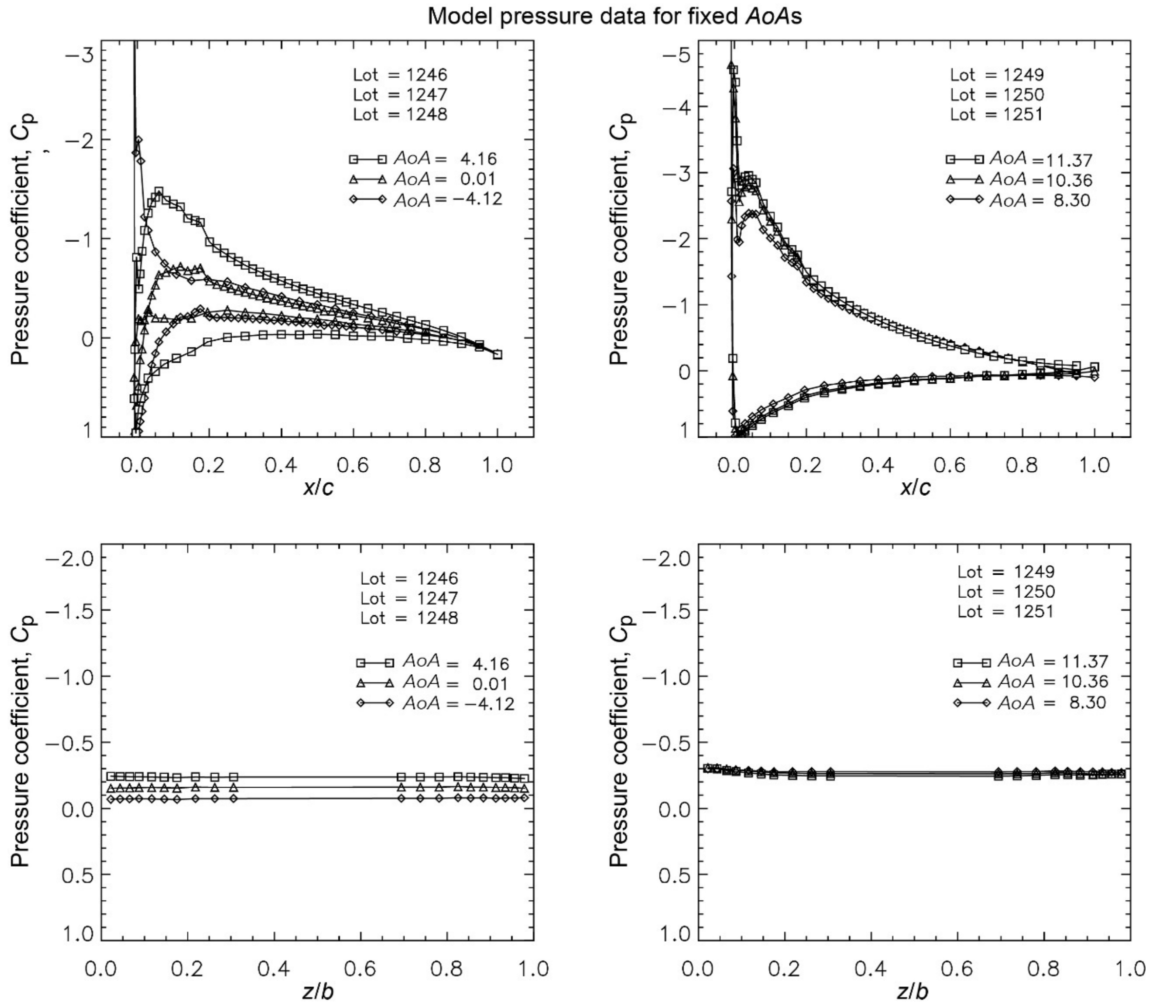

Spanwise Ice 2—Lot EG1125: M = 0.21 and Re = 12.1×10^6

Appendix G.—F1 Full-Scale Model Tests

Spanwise Ice 2—Lot EG1125: M = 0.21 and Re = 12.1×10^6

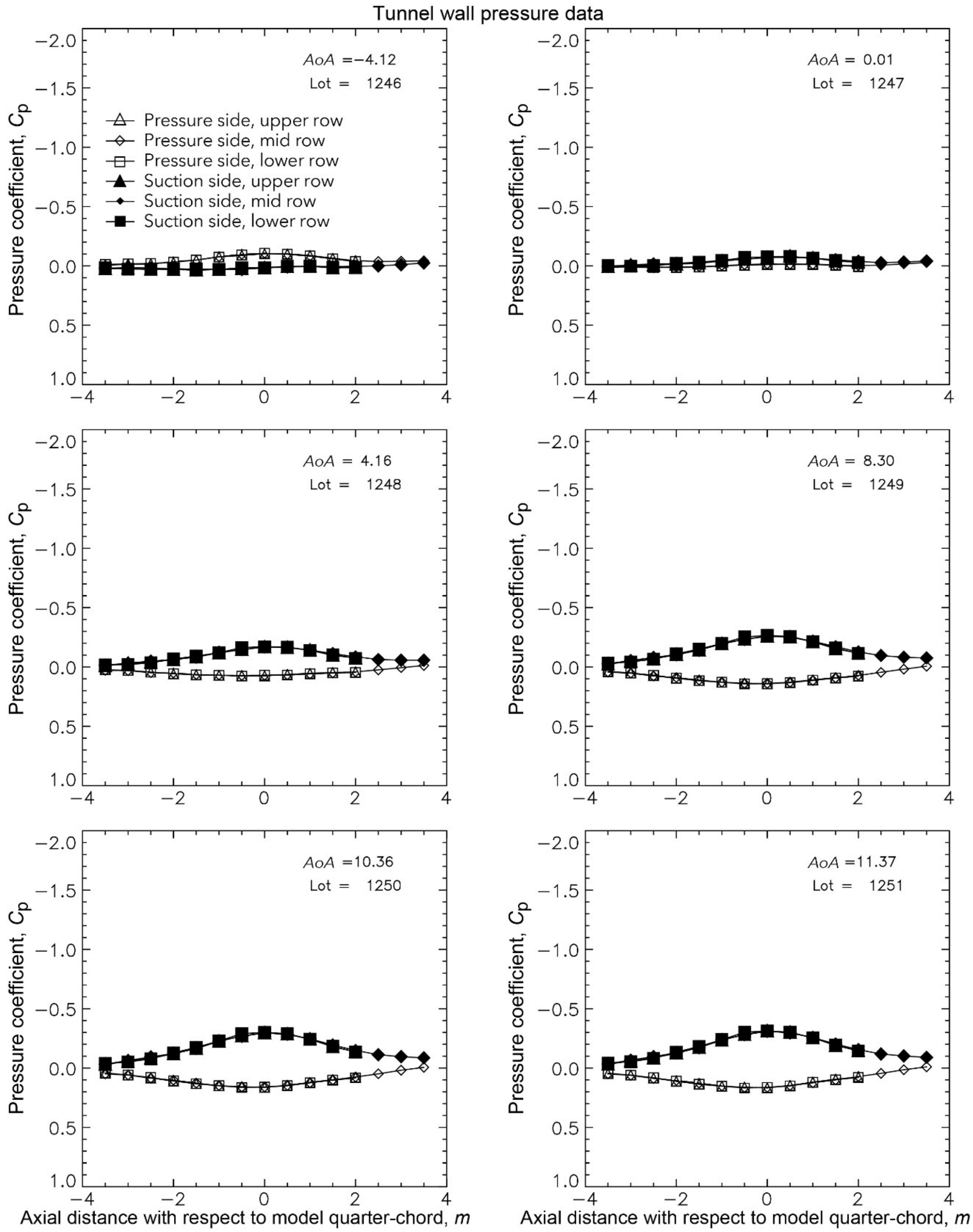

Spanwise Ice 2—Lot EG1125: M = 0.21 and Re = 12.1×10^6

Appendix G.—F1 Full-Scale Model Tests

Spanwise Ice 2—Lot EG1125: M = 0.21 and Re = 12.1×10^6

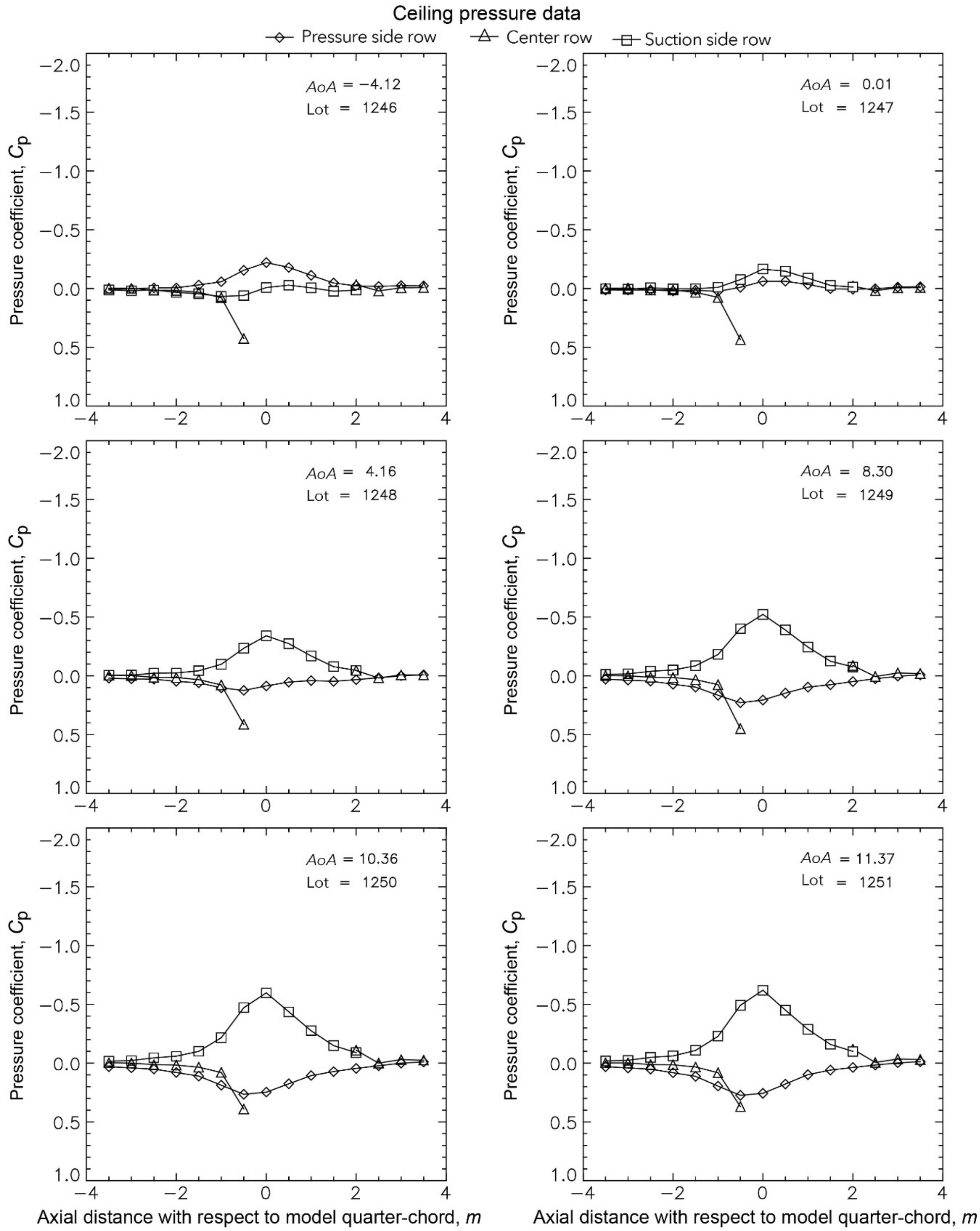

Spanwise Ice 2—Lot EG1125: M = 0.21 and Re = 12.1×10^6

Appendix G.—F1 Full-Scale Model Tests

Spanwise Ice 2—Lot EG1125: M = 0.21 and Re = 12.1×10^6

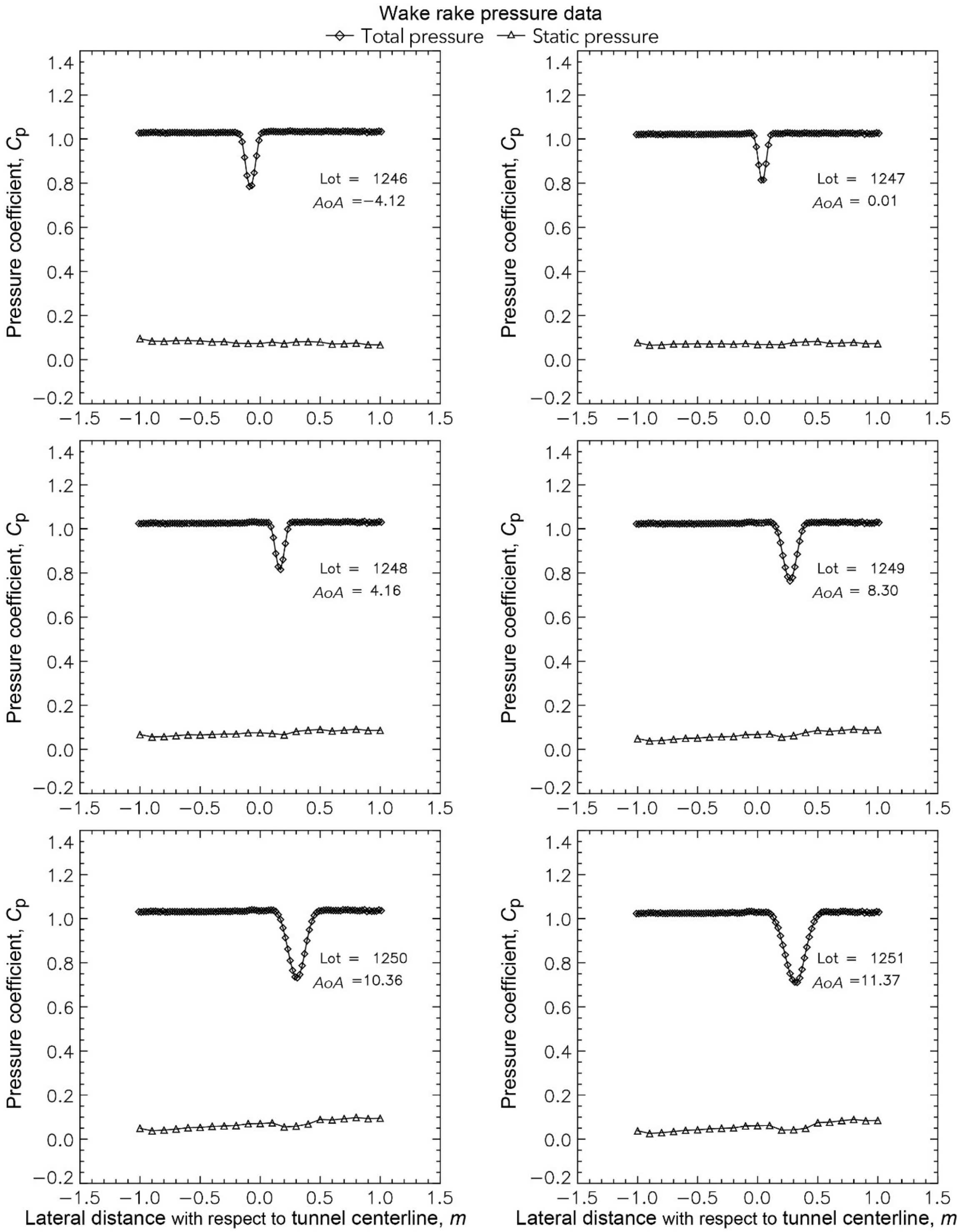

Spanwise Ice 2—Lot EG1125: M = 0.21 and Re = 12.1×10^6

Appendix G.—F1 Full-Scale Model Tests

Spanwise Ice 2—Lot EG1125: M = 0.20 to 0.21 and Re = 15.9–16.0×10^6

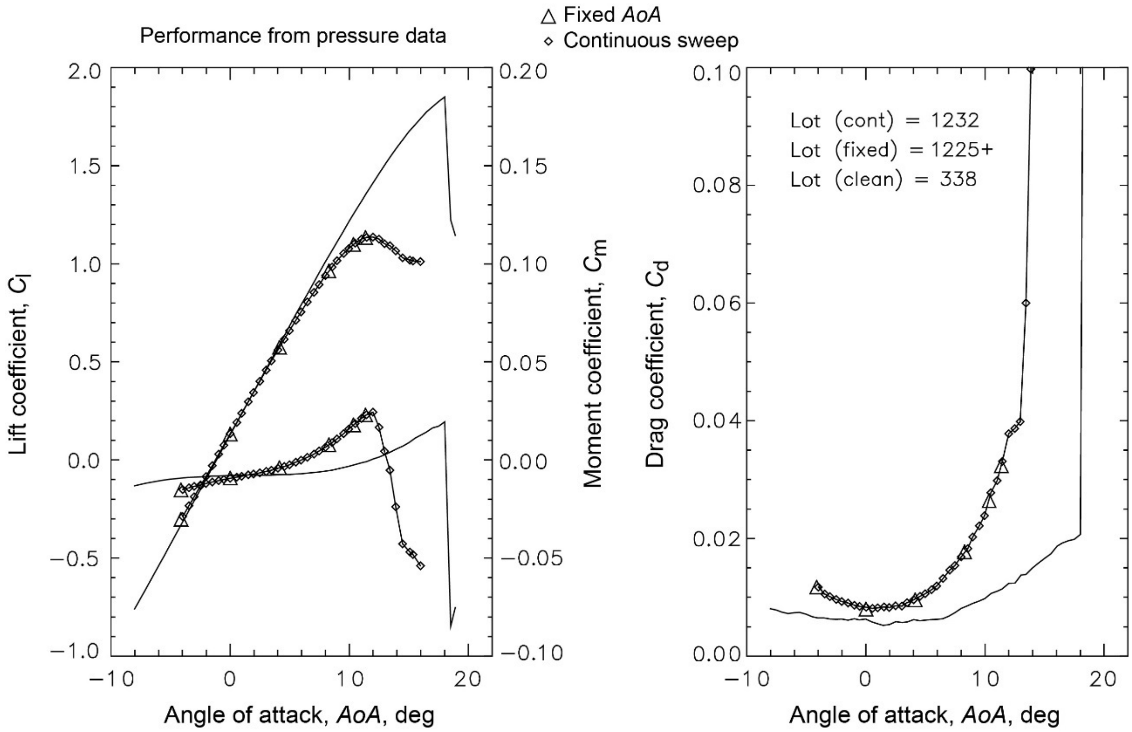

Spanwise Ice 2—Lot EG1125: M = 0.20 to 0.21 and Re = 15.9–16.0×10^6

Appendix G.—F1 Full-Scale Model Tests

Spanwise Ice 2—Lot EG1125: M = 0.20 to 0.21 and Re = 15.9–16.0×10[6]

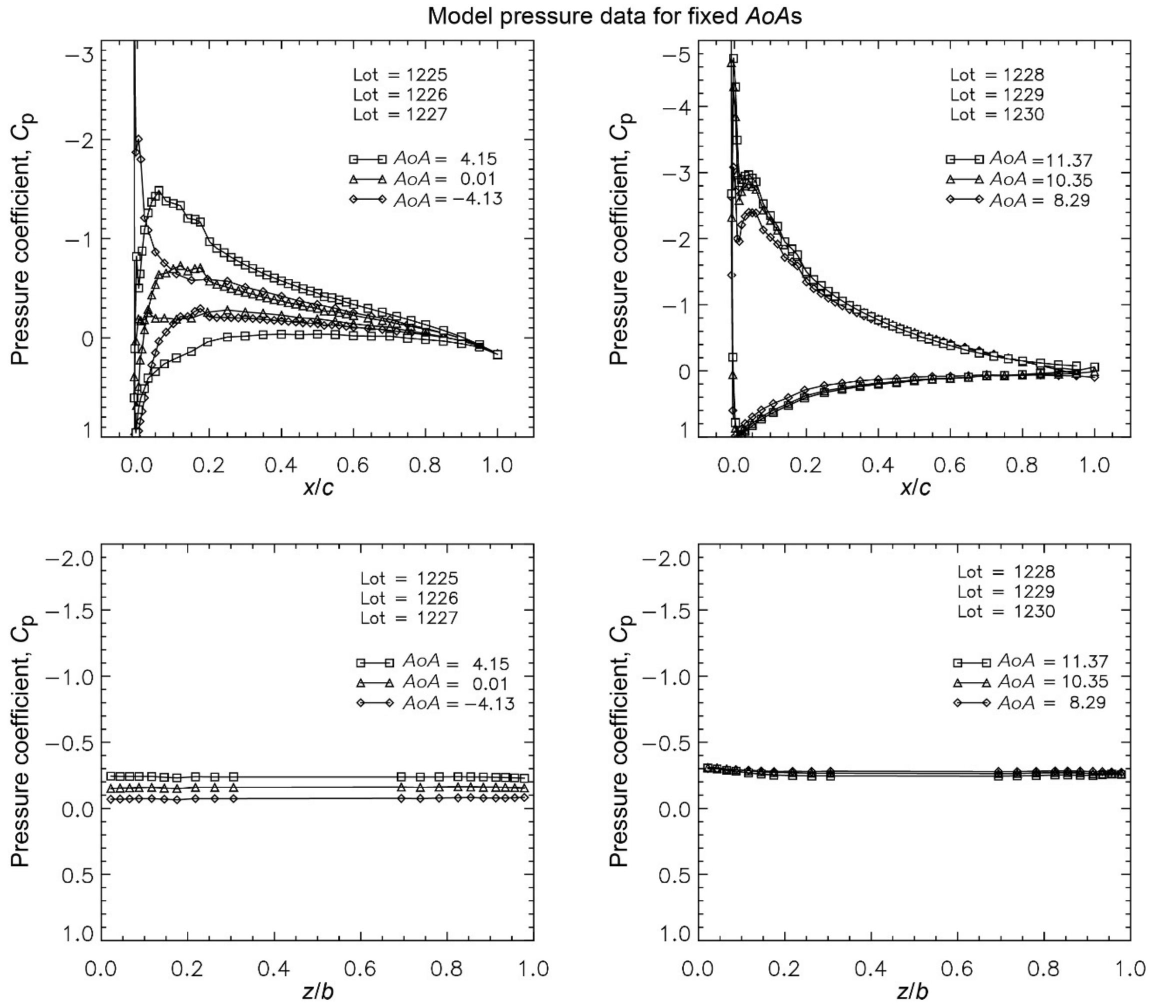

Spanwise Ice 2—Lot EG1125: M = 0.20 to 0.21 and Re = 15.9–16.0×10[6]

Appendix G.—F1 Full-Scale Model Tests

Spanwise Ice 2—Lot EG1125: M = 0.20 to 0.21 and Re = 15.9–16.0×10^6

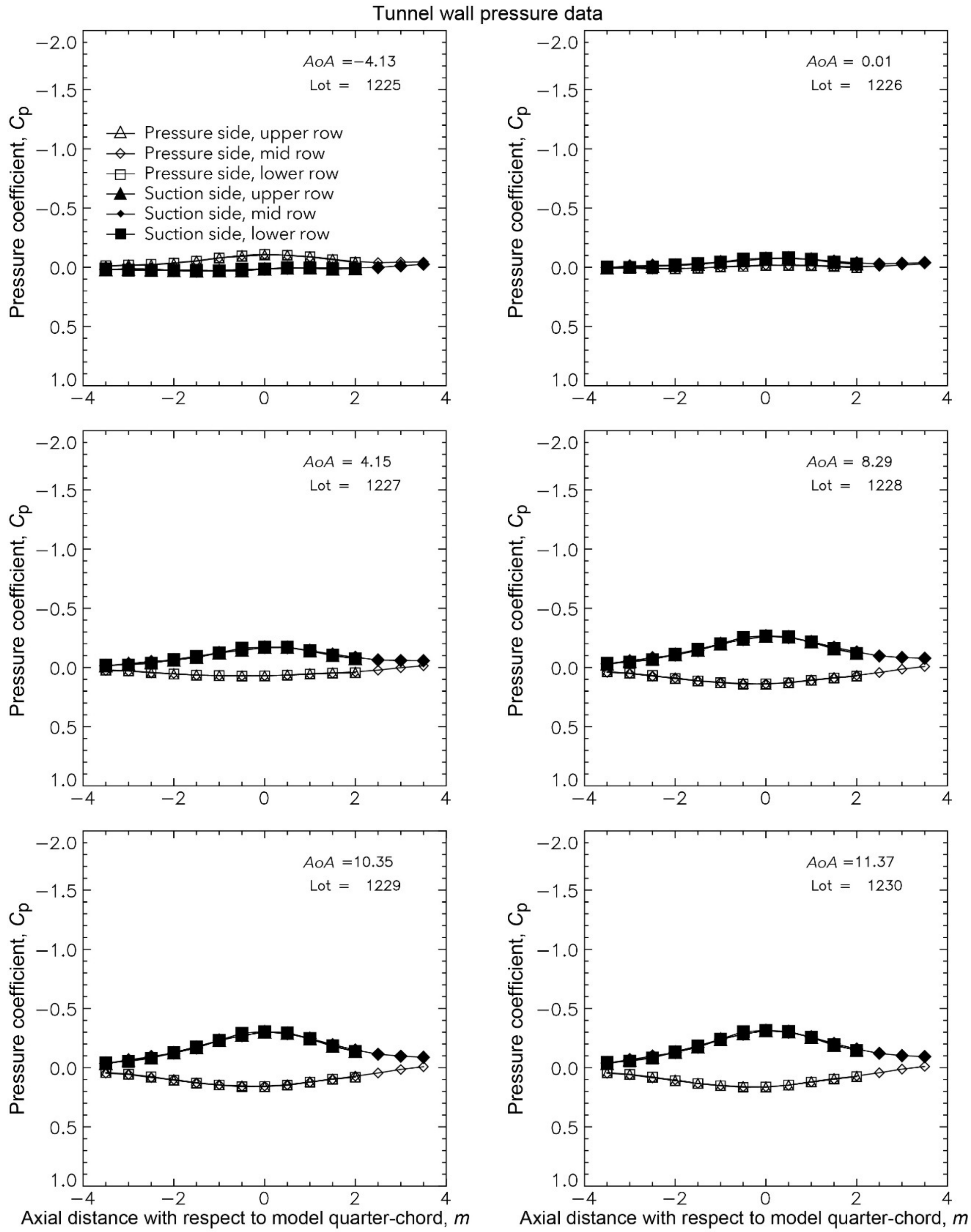

Spanwise Ice 2—Lot EG1125: M = 0.20 to 0.21 and Re = 15.9–16.0×10^6

Appendix G.—F1 Full-Scale Model Tests

Spanwise Ice 2—Lot EG1125: M = 0.20 to 0.21 and Re = 15.9–16.0×10^6

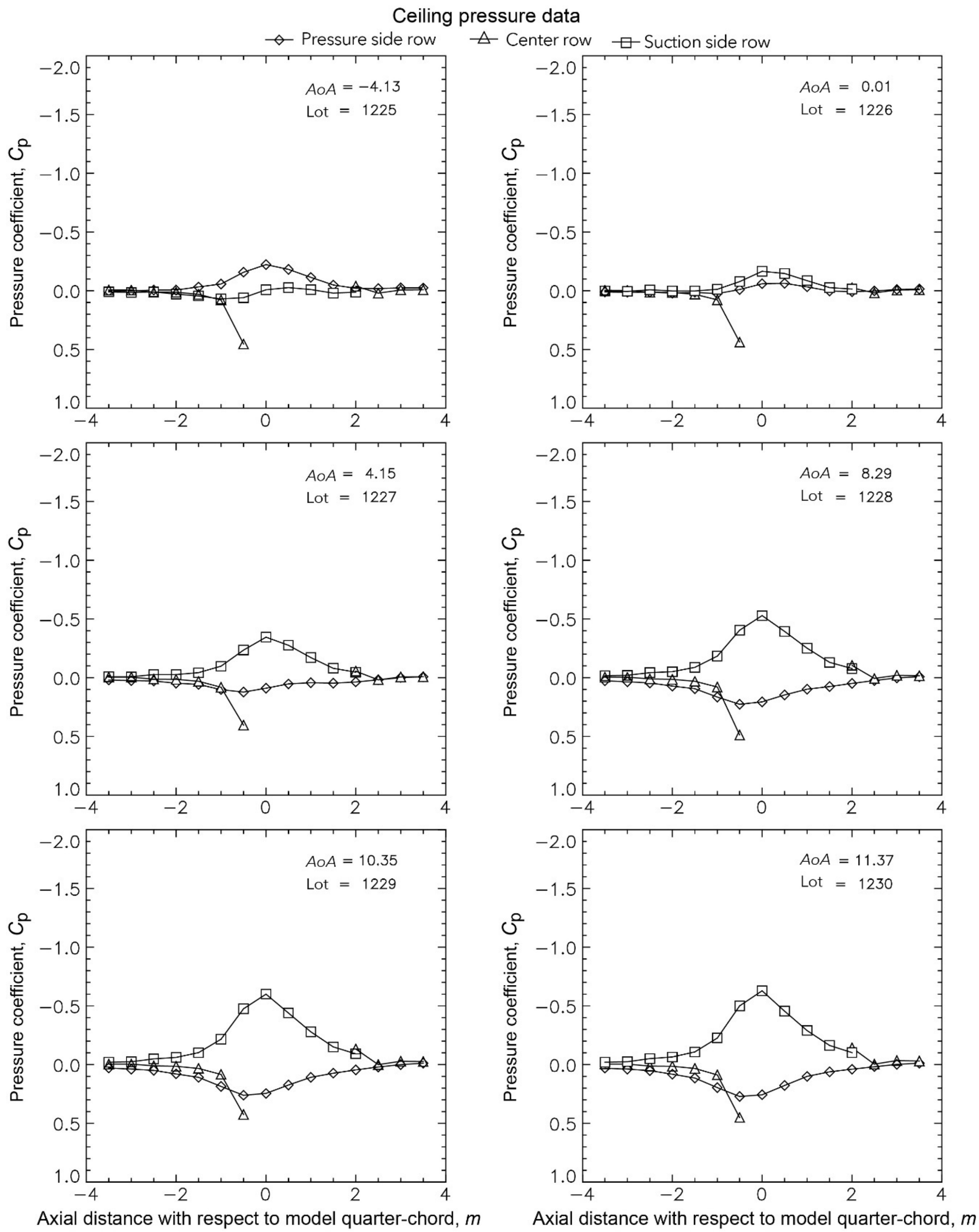

Spanwise Ice 2—Lot EG1125: M = 0.20 to 0.21 and Re = 15.9–16.0×10^6

Appendix G.—F1 Full-Scale Model Tests

Spanwise Ice 2—Lot EG1125: M = 0.20 to 0.21 and Re = 15.9–16.0×10^6

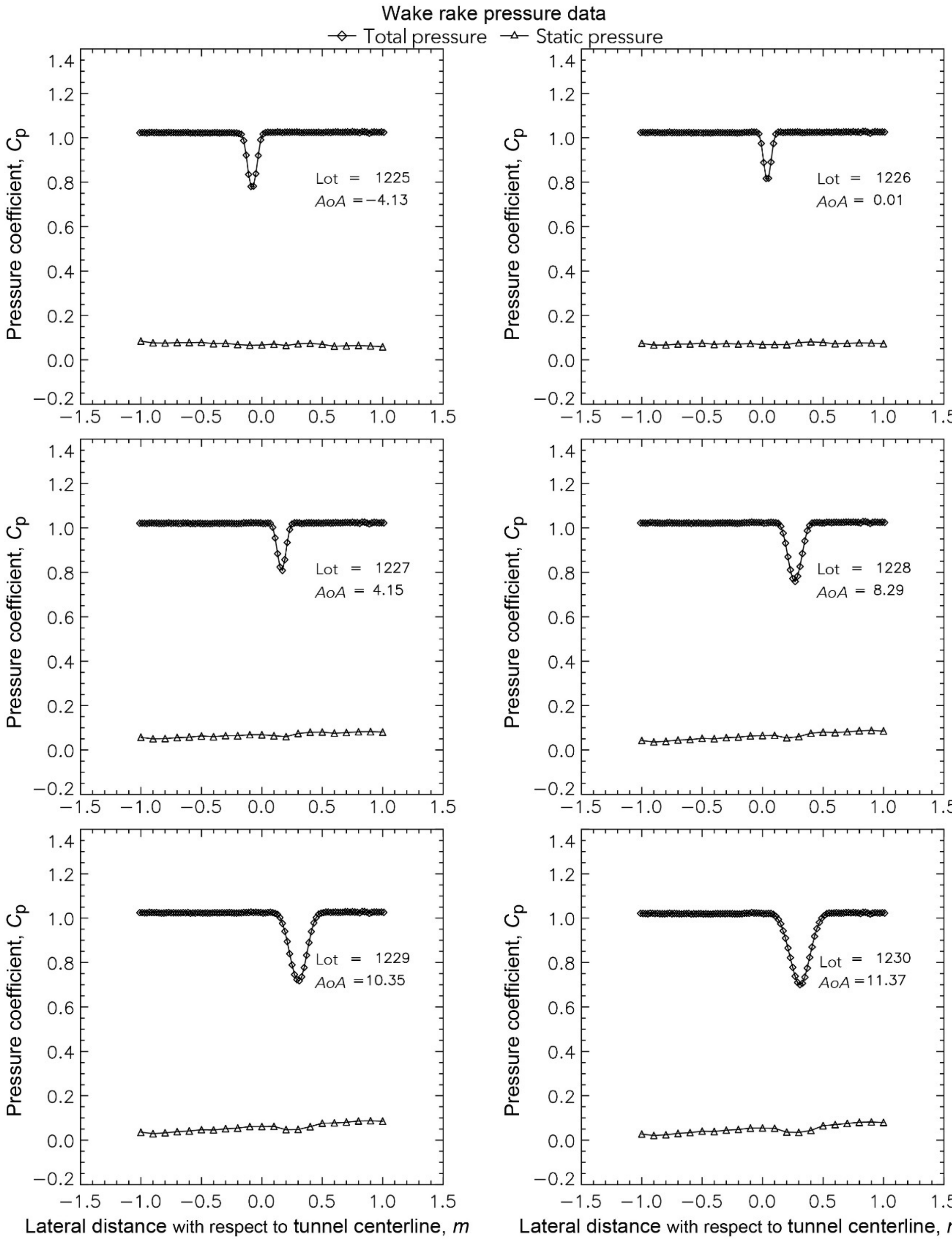

Spanwise Ice 2—Lot EG1125: M = 0.20 to 0.21 and Re = 15.9–16.0×10^6

Appendix G.—F1 Full-Scale Model Tests

Spanwise Ice 2—Lot EG1125: M = 0.29 and Re = 12.2×10^6

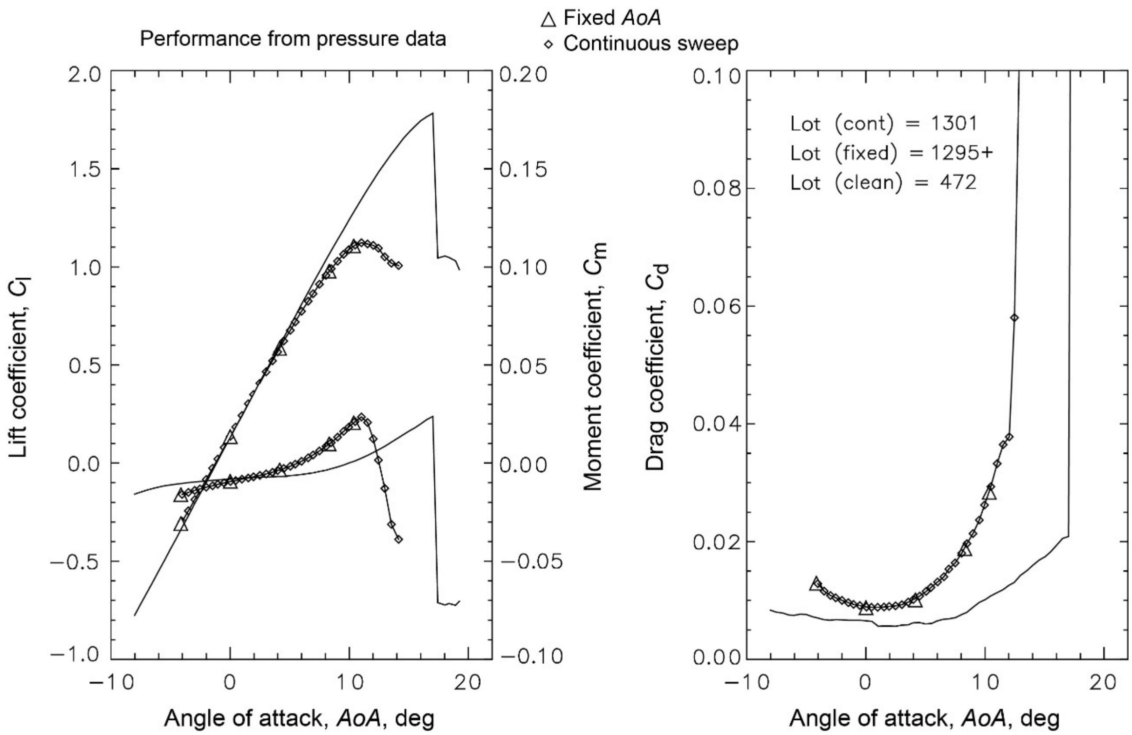

Spanwise Ice 2—Lot EG1125: M = 0.29 and Re = 12.2×10^6

Appendix G.—F1 Full-Scale Model Tests

Spanwise Ice 2—Lot EG1125: M = 0.29 and Re = 12.2×10^6

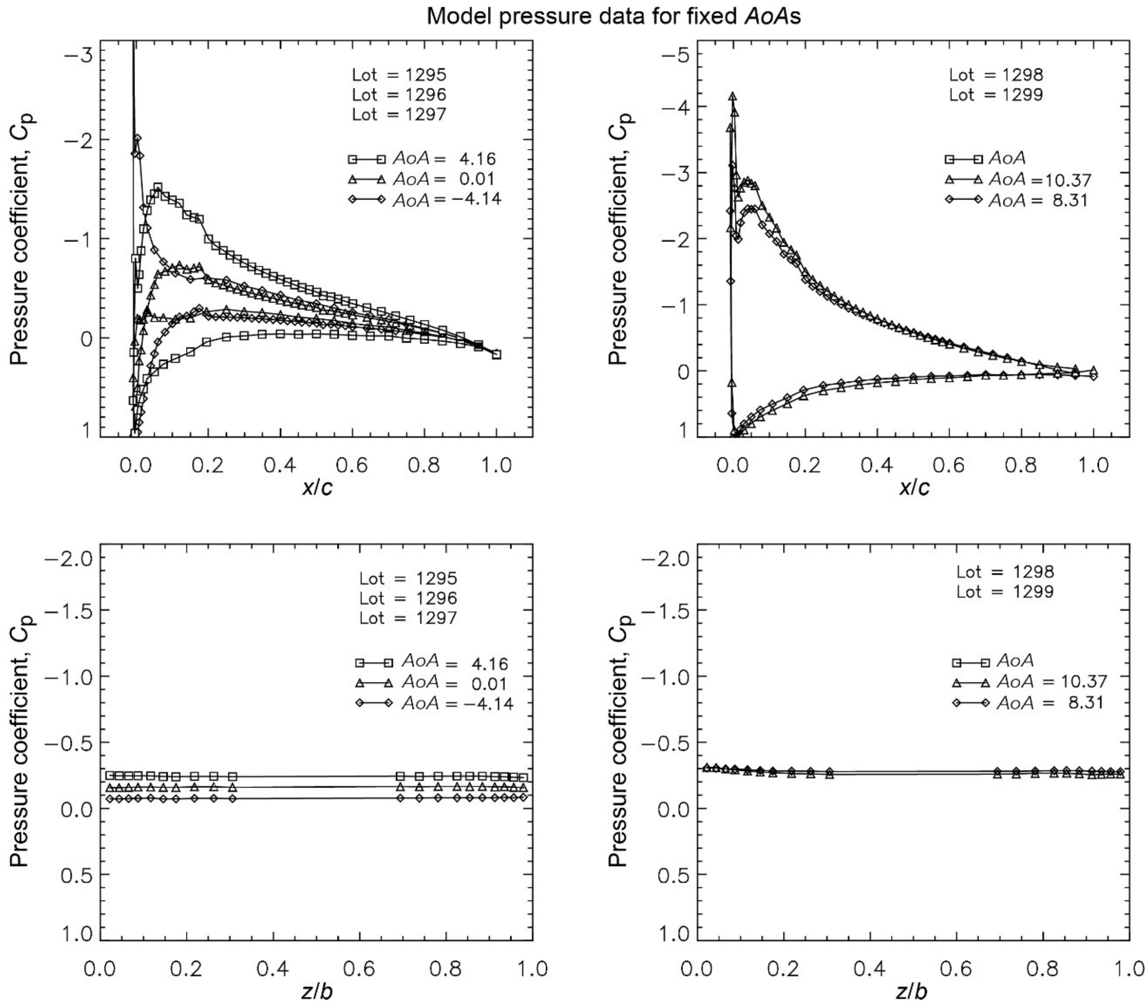

Spanwise Ice 2—Lot EG1125: M = 0.29 and Re = 12.2×10^6

Appendix G.—F1 Full-Scale Model Tests

Spanwise Ice 2—Lot EG1125: M = 0.29 and Re = 12.2×10^6

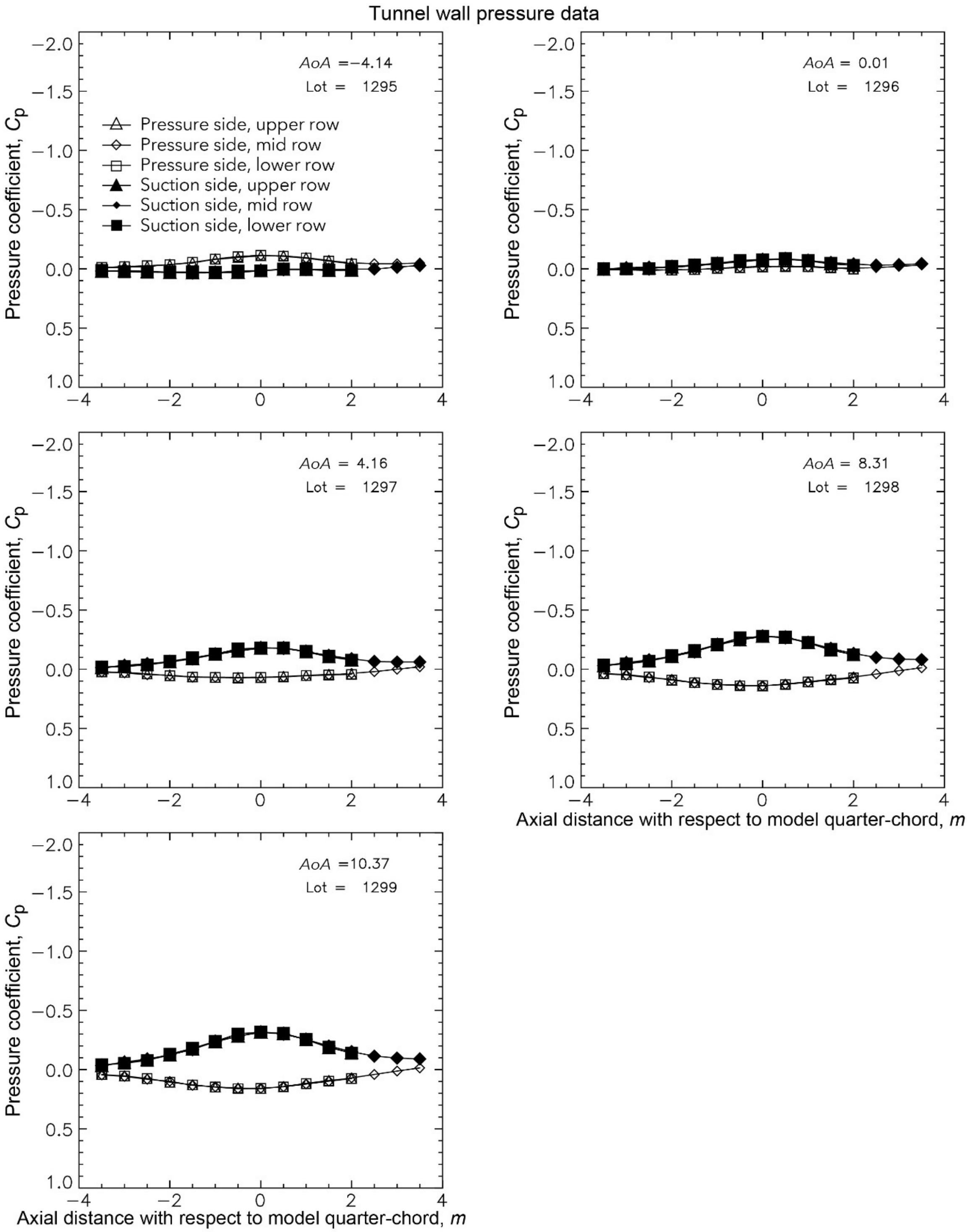

Spanwise Ice 2—Lot EG1125: M = 0.29 and Re = 12.2×10^6

Appendix G.—F1 Full-Scale Model Tests

Spanwise Ice 2—Lot EG1125: M = 0.29 and Re = 12.2×10^6

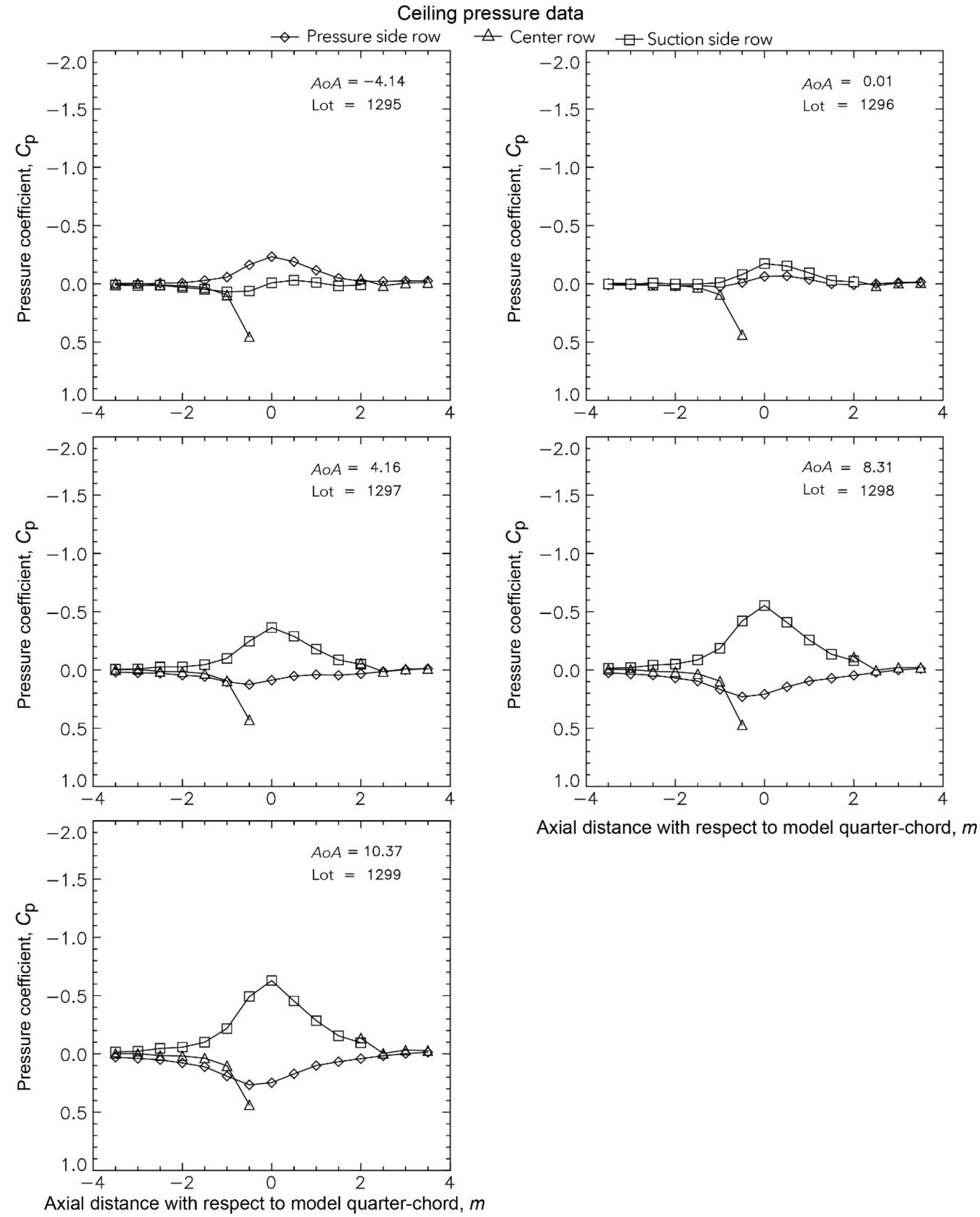

Spanwise Ice 2—Lot EG1125: M = 0.29 and Re = 12.2×10^6

Appendix G.—F1 Full-Scale Model Tests

Spanwise Ice 2—Lot EG1125: M = 0.29 and Re = 12.2×10^6

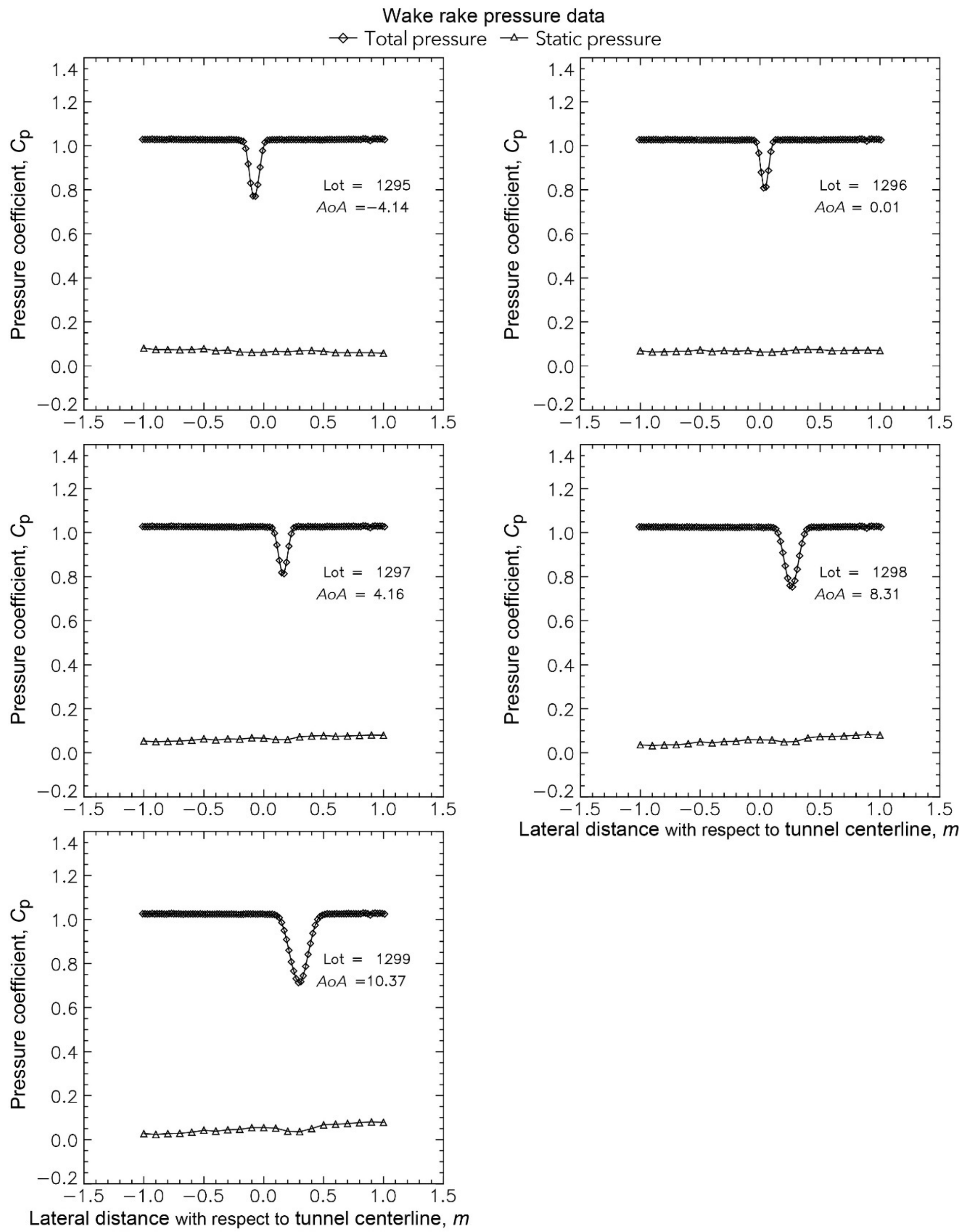

Spanwise Ice 2—Lot EG1125: M = 0.29 and Re = 12.2×10^6

Appendix G.—F1 Full-Scale Model Tests

Roughness Ice 2—Lot EG1134: M = 0.11 and Re = 4.6–4.7×10^6

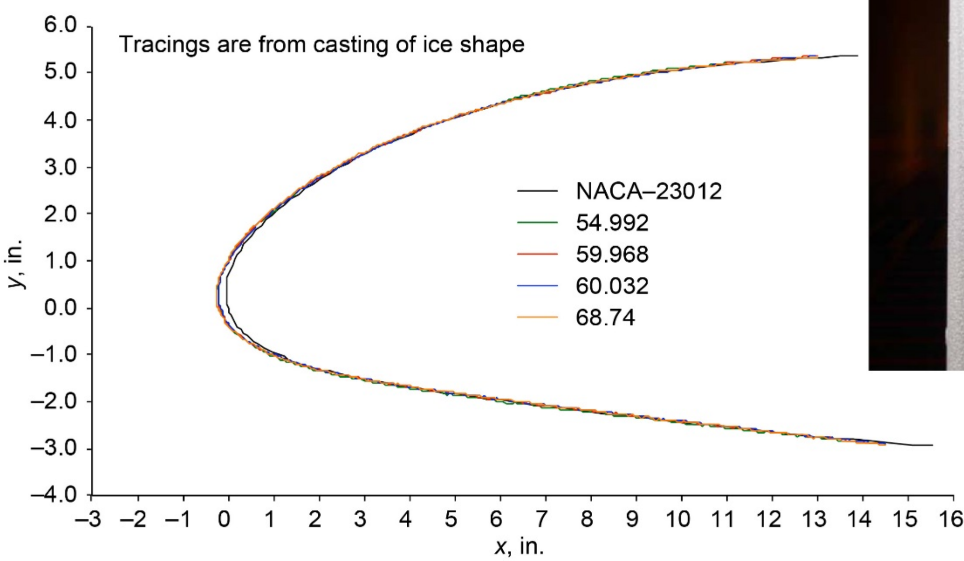

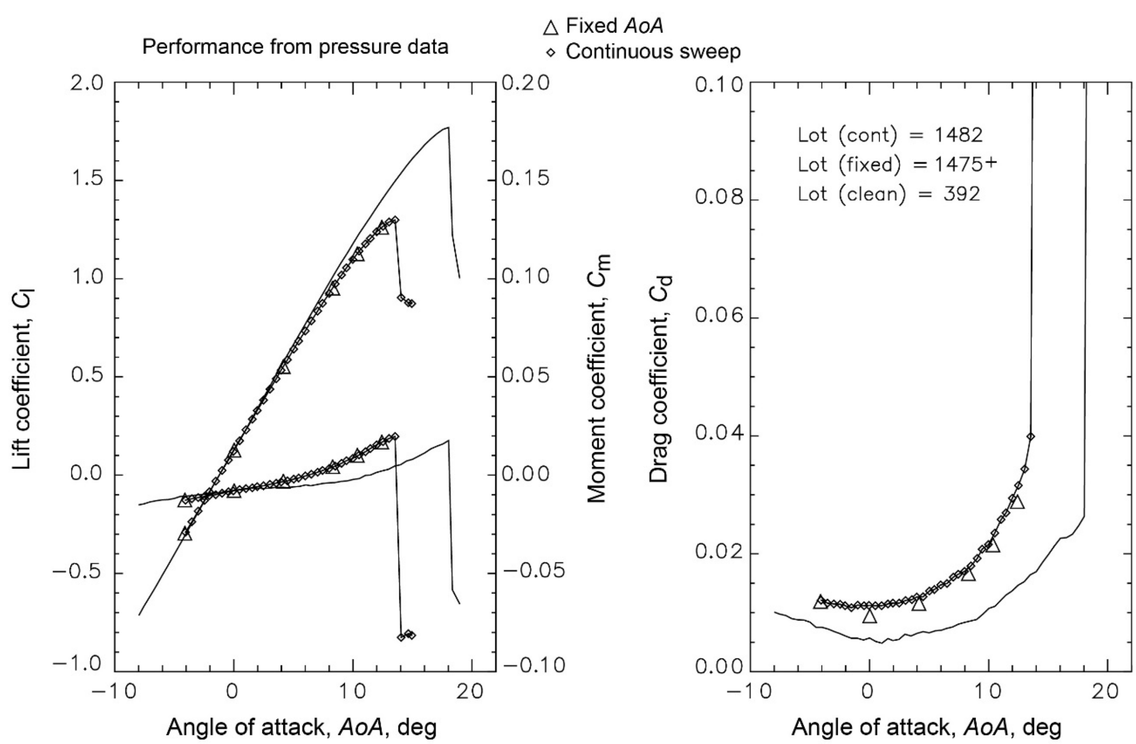

Roughness Ice 2—Lot EG1134: M = 0.11 and Re = 4.6–4.7×10^6

Appendix G.—F1 Full-Scale Model Tests

Roughness Ice 2—Lot EG1134: M = 0.11 and Re = 4.6–4.7×10^6

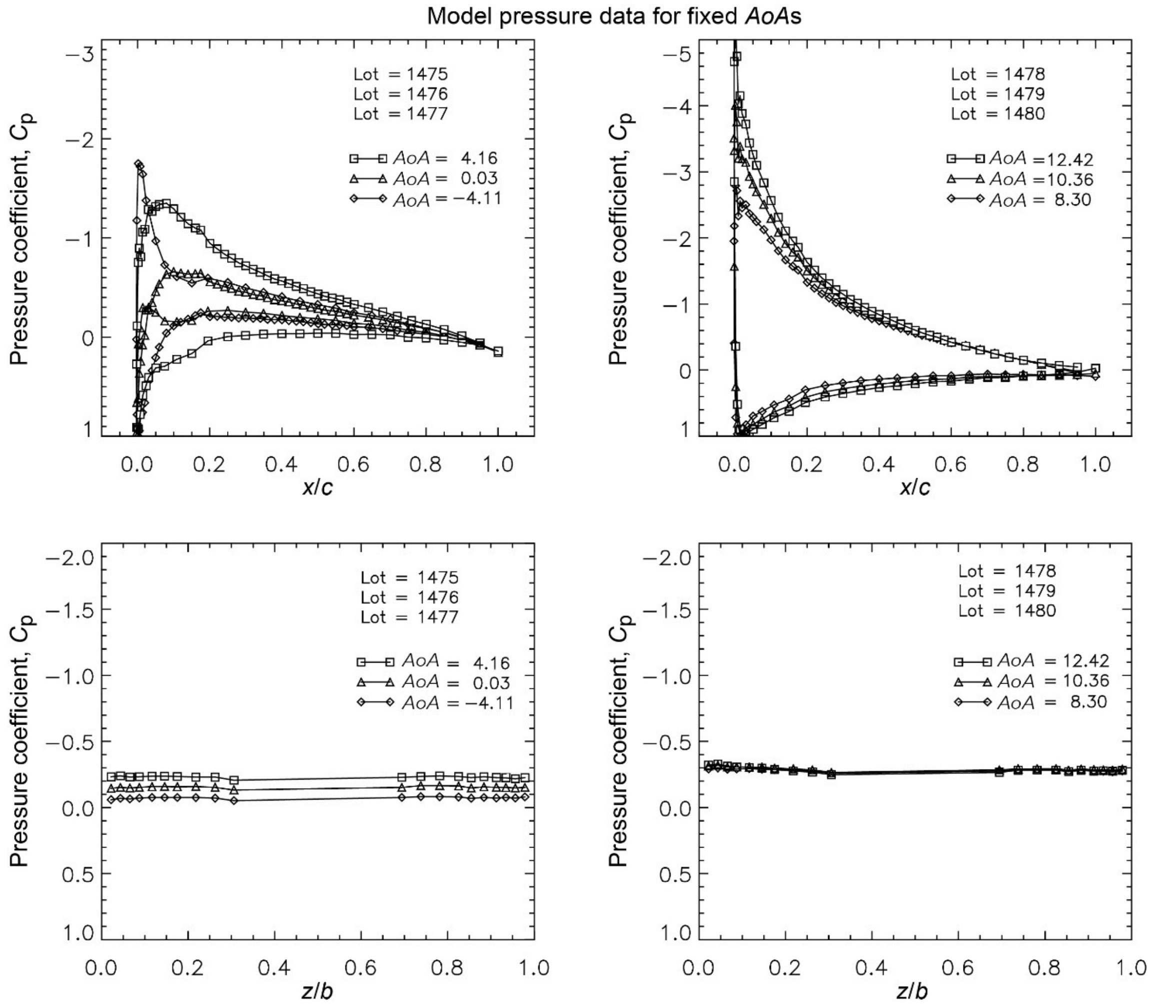

Roughness Ice 2—Lot EG1134: M = 0.11 and Re = 4.6–4.7×10^6

Appendix G.—F1 Full-Scale Model Tests

Roughness Ice 2—Lot EG1134: M = 0.11 and Re = 4.6–4.7×10^6

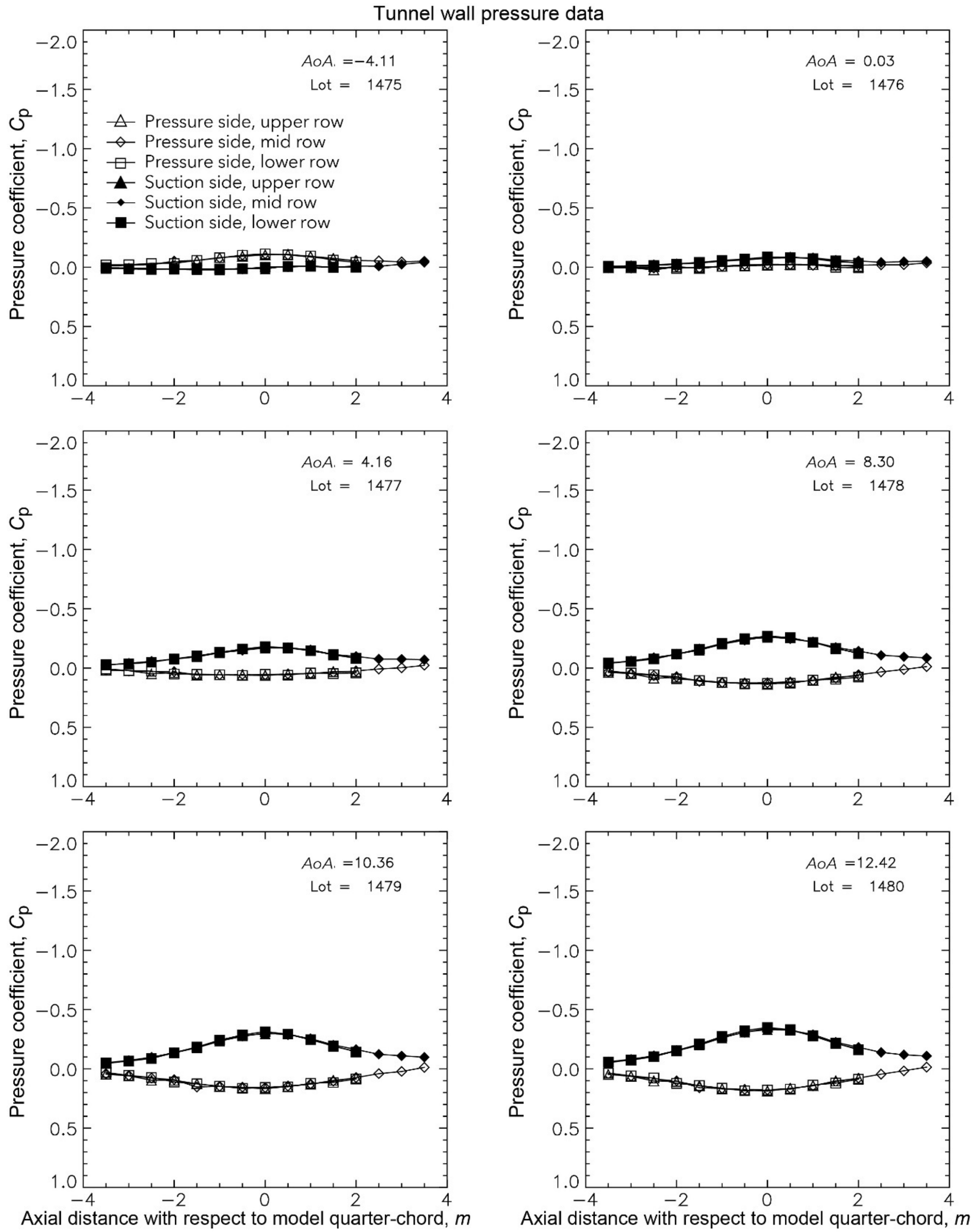

Roughness Ice 2—Lot EG1134: M = 0.11 and Re = 4.6–4.7×10^6

Appendix G.—F1 Full-Scale Model Tests

Roughness Ice 2—Lot EG1134: M = 0.11 and Re = 4.6–4.7×10^6

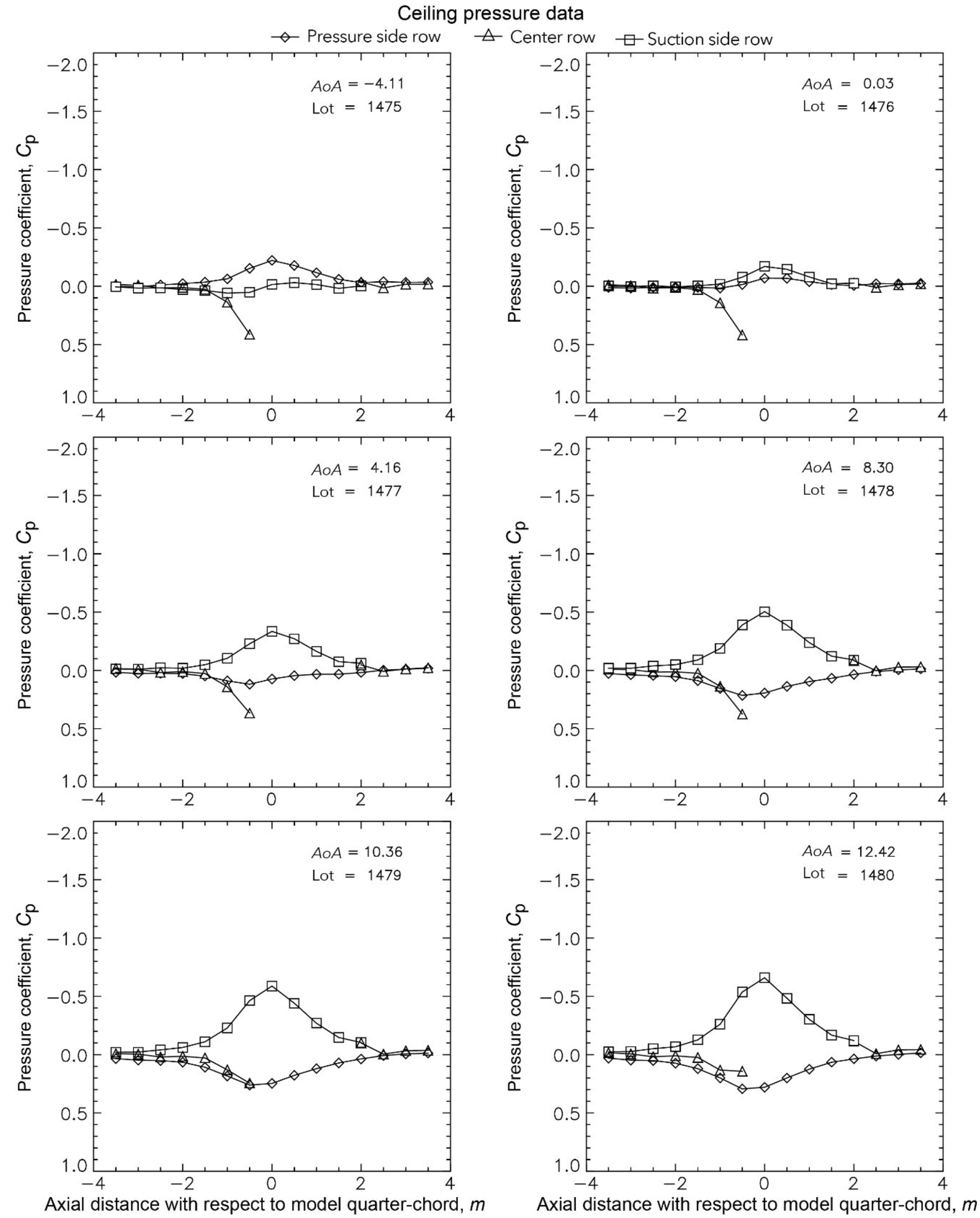

Roughness Ice 2—Lot EG1134: M = 0.11 and Re = 4.6–4.7×10^6

Appendix G.—F1 Full-Scale Model Tests

Roughness Ice 2—Lot EG1134: M = 0.11 and Re = 4.6–4.7×10^6

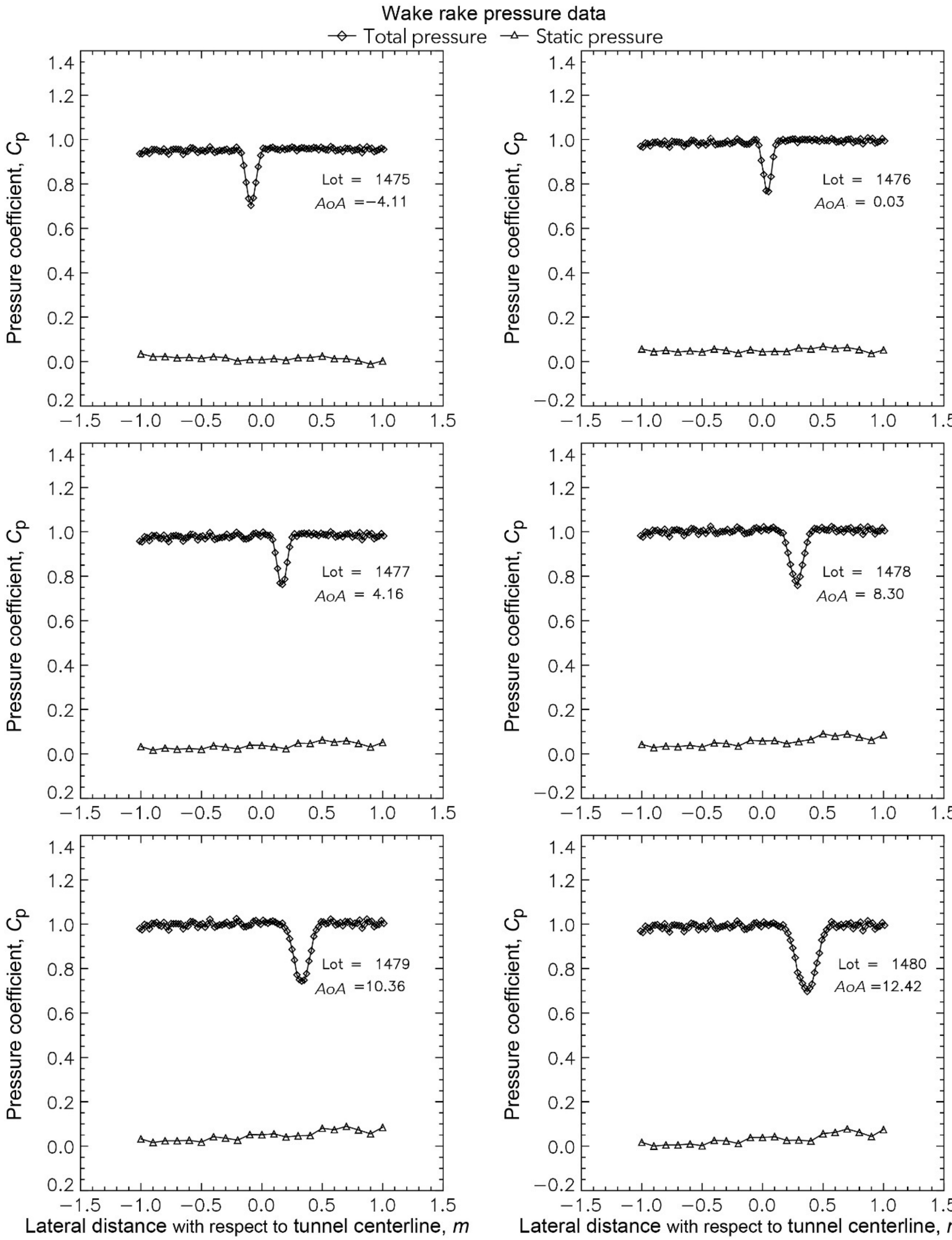

Roughness Ice 2—Lot EG1134: M = 0.11 and Re = 4.6–4.7×10^6

Appendix G.—F1 Full-Scale Model Tests

Roughness Ice 2—Lot EG1134: M = 0.10 to 0.11 and Re = 8.3–8.4×10^6

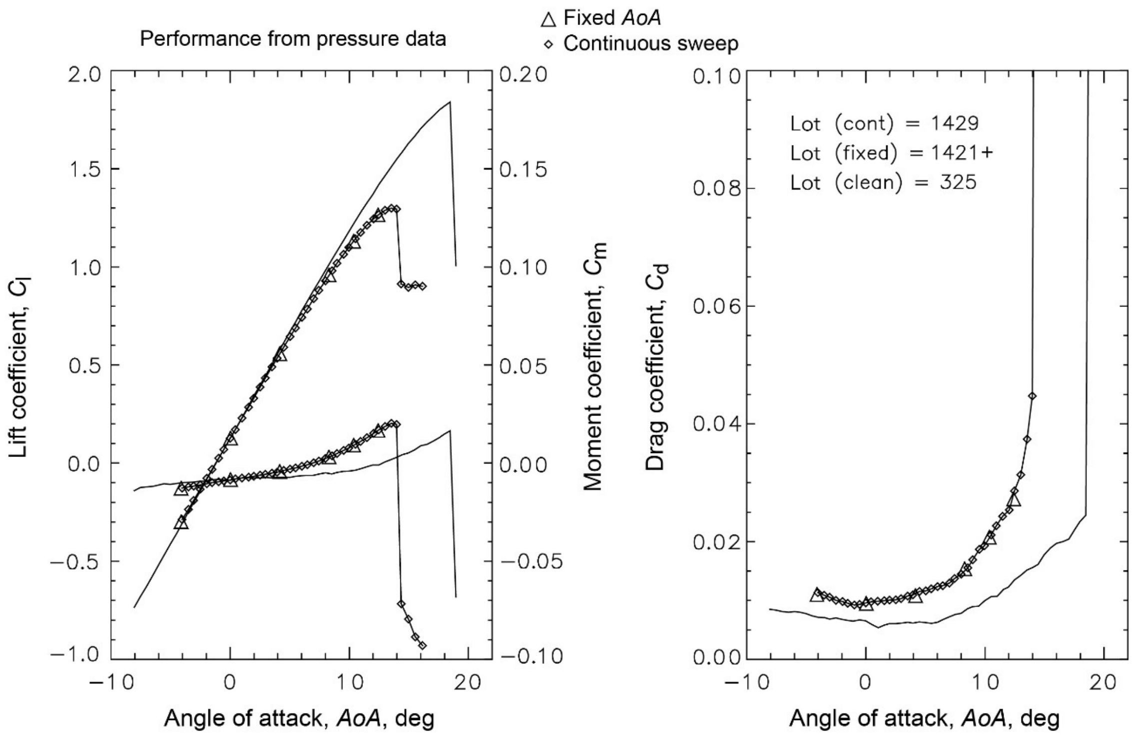

Roughness Ice 2—Lot EG1134: M = 0.10 to 0.11 and Re = 8.3–8.4×10^6

Appendix G.—F1 Full-Scale Model Tests

Roughness Ice 2—Lot EG1134: M = 0.10 to 0.11 and Re = 8.3–8.4×10^6

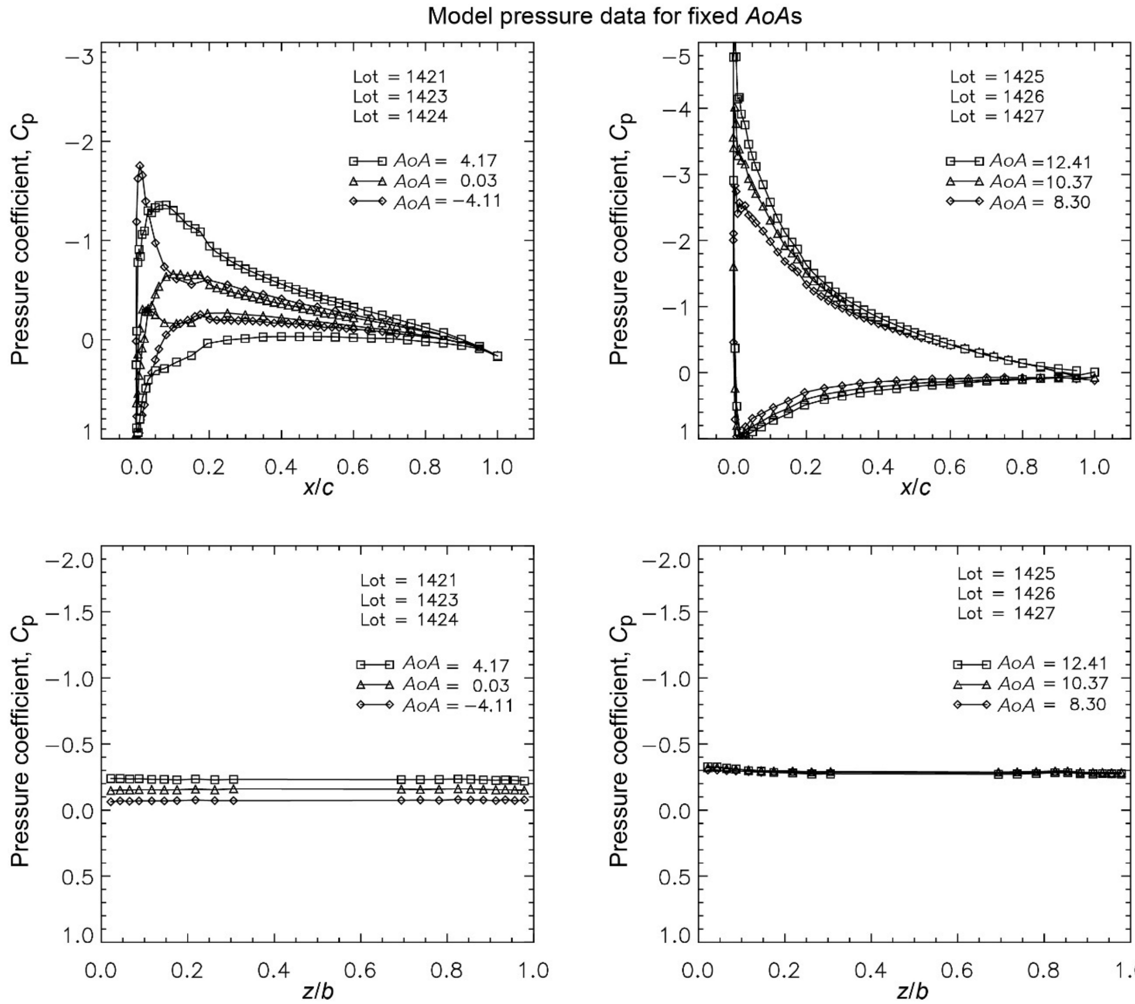

Roughness Ice 2—Lot EG1134: M = 0.10 to 0.11 and Re = 8.3–8.4×10^6

Appendix G.—F1 Full-Scale Model Tests

Roughness Ice 2—Lot EG1134: M = 0.10 to 0.11 and Re = 8.3–8.4×10[6]

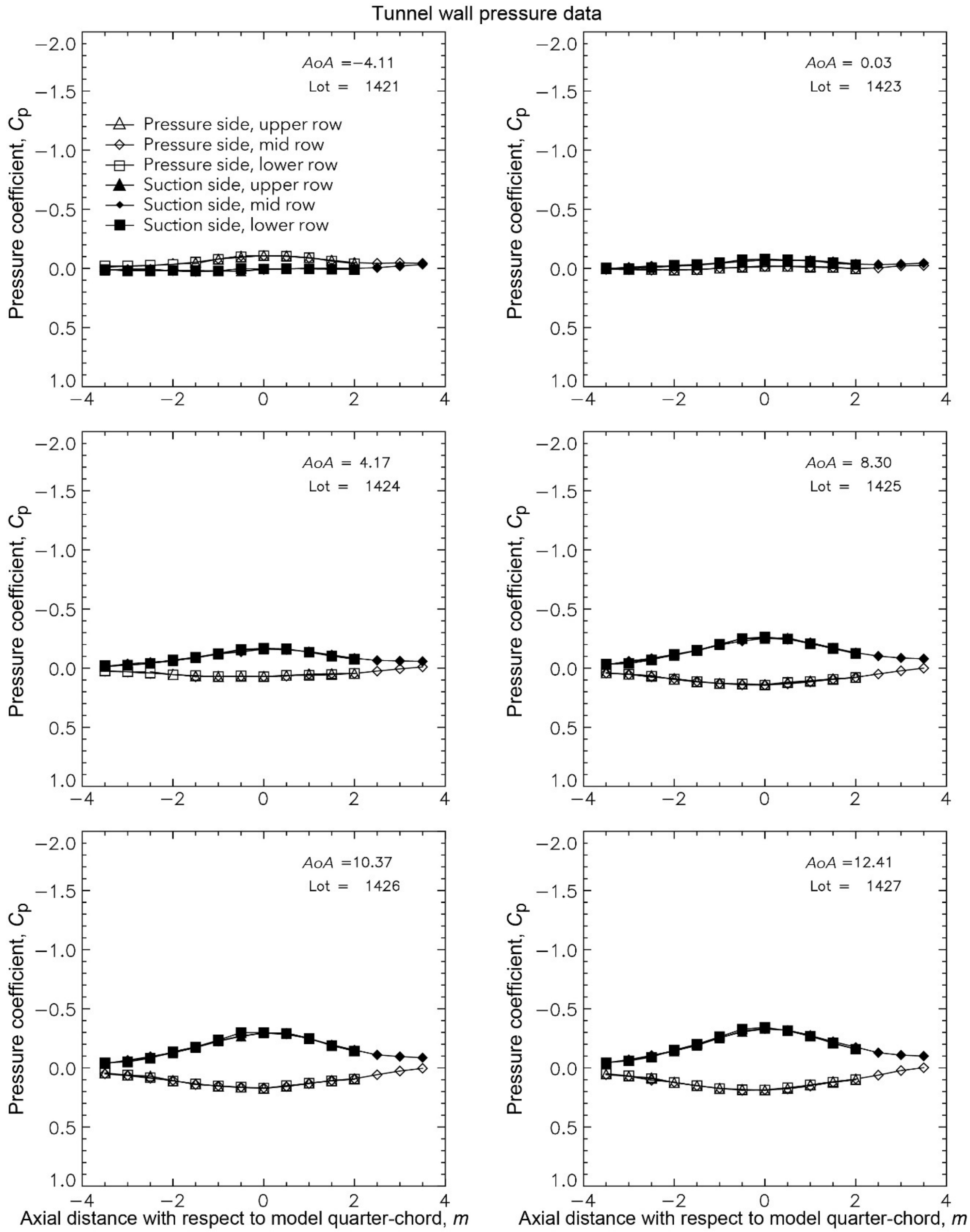

Roughness Ice 2—Lot EG1134: M = 0.10 to 0.11 and Re = 8.3–8.4×10[6]

Appendix G.—F1 Full-Scale Model Tests

Roughness Ice 2—Lot EG1134: M = 0.10 to 0.11 and Re = 8.3–8.4×10^6

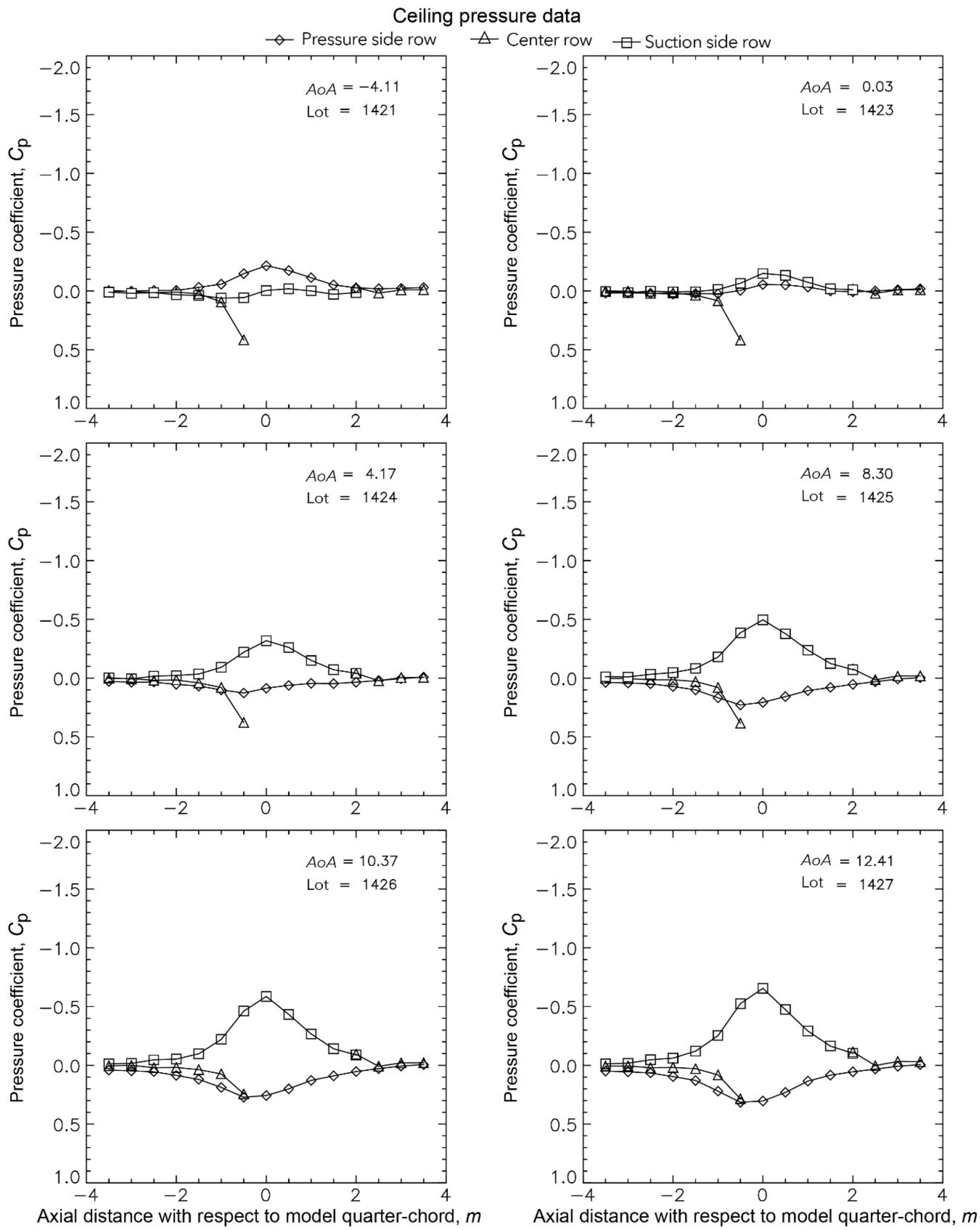

Roughness Ice 2—Lot EG1134: M = 0.10 to 0.11 and Re = 8.3–8.4×10^6

Appendix G.—F1 Full-Scale Model Tests

Roughness Ice 2—Lot EG1134: M = 0.10 to 0.11 and Re = 8.3–8.4×10[6]

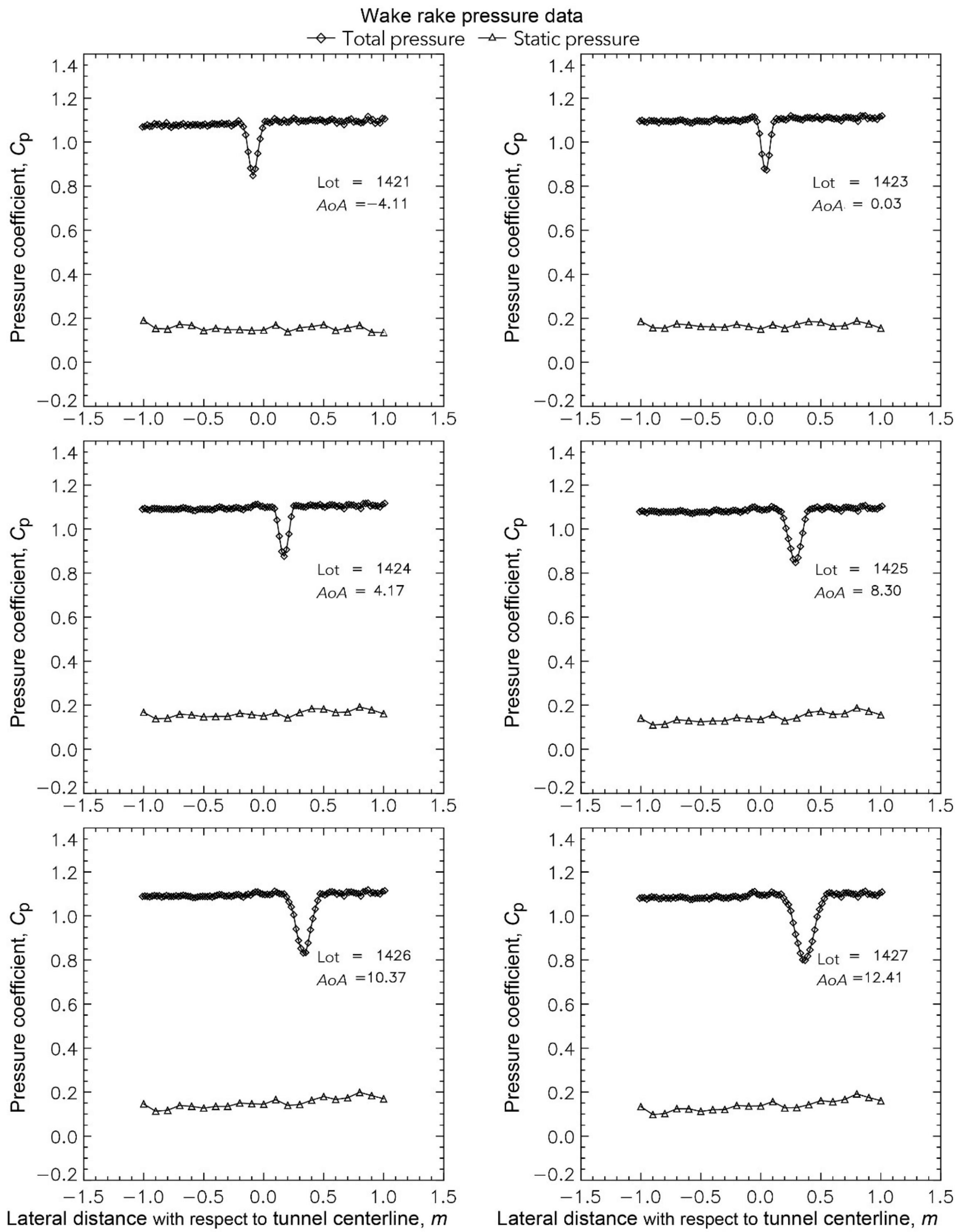

Roughness Ice 2—Lot EG1134: M = 0.10 to 0.11 and Re = 8.3–8.4×10[6]

Appendix G.—F1 Full-Scale Model Tests

Roughness Ice 2—Lot EG1134: M = 0.10 and Re = 12.1–12.3×10⁶

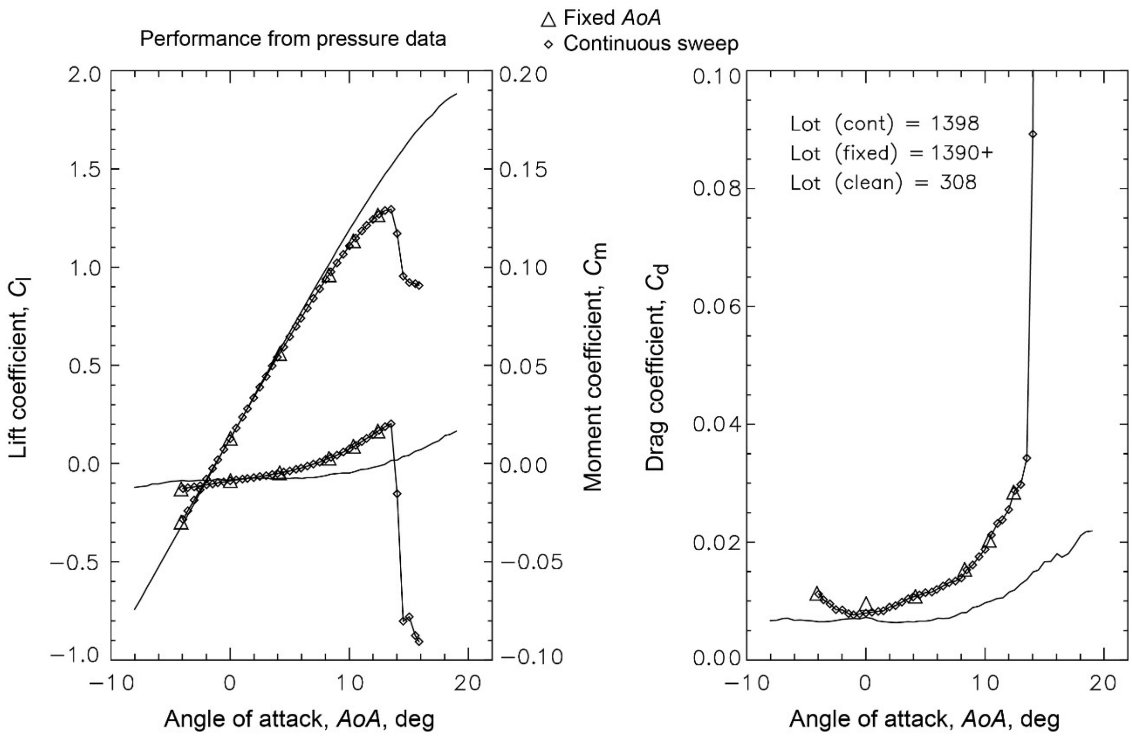

Roughness Ice 2—Lot EG1134: M = 0.10 and Re = 12.1–12.3×10⁶

Appendix G.—F1 Full-Scale Model Tests

Roughness Ice 2—Lot EG1134: M = 0.10 and Re = 12.1–12.3×10^6

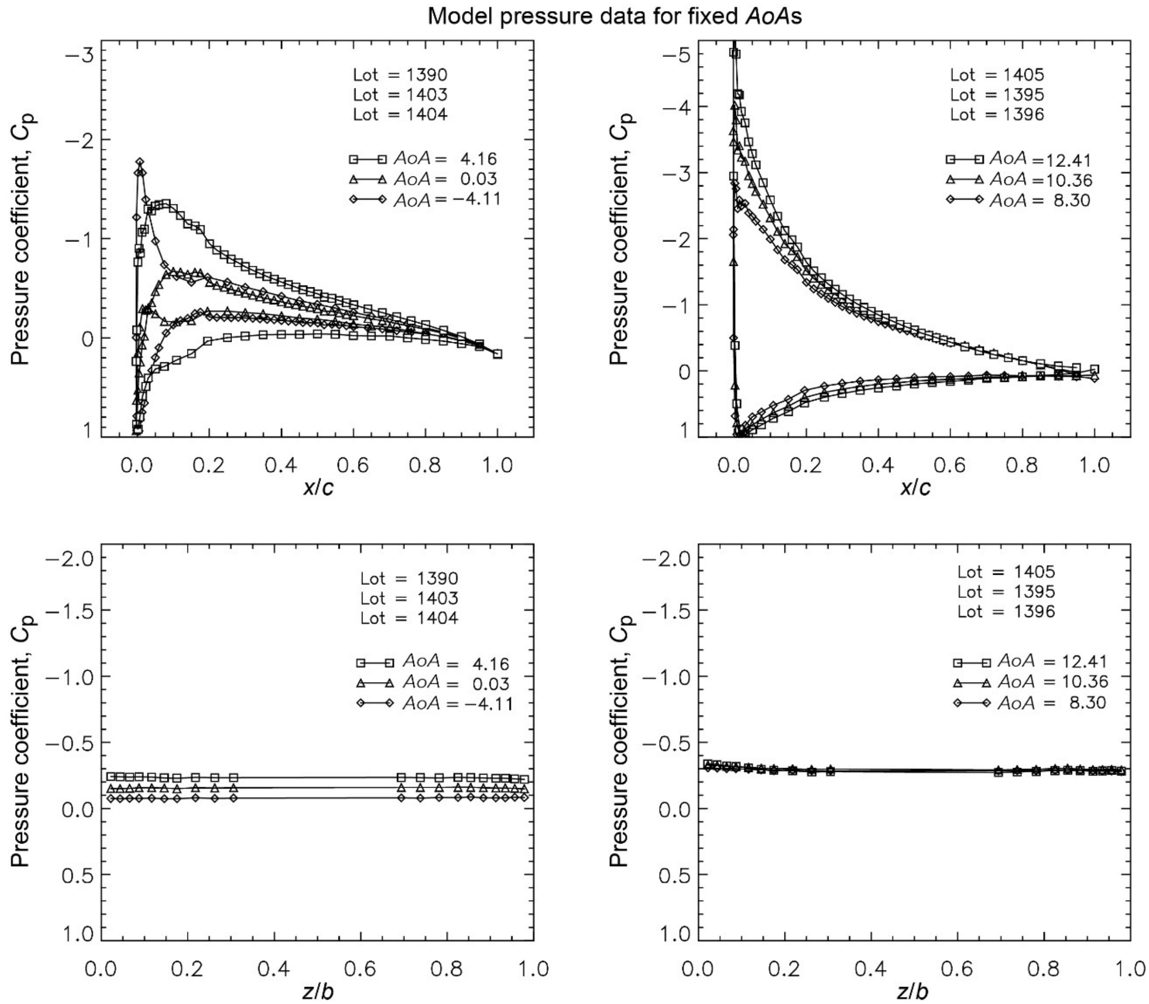

Roughness Ice 2—Lot EG1134: M = 0.10 and Re = 12.1–12.3×10^6

Appendix G.—F1 Full-Scale Model Tests

Roughness Ice 2—Lot EG1134: M = 0.10 and Re = 12.1–12.3×10^6

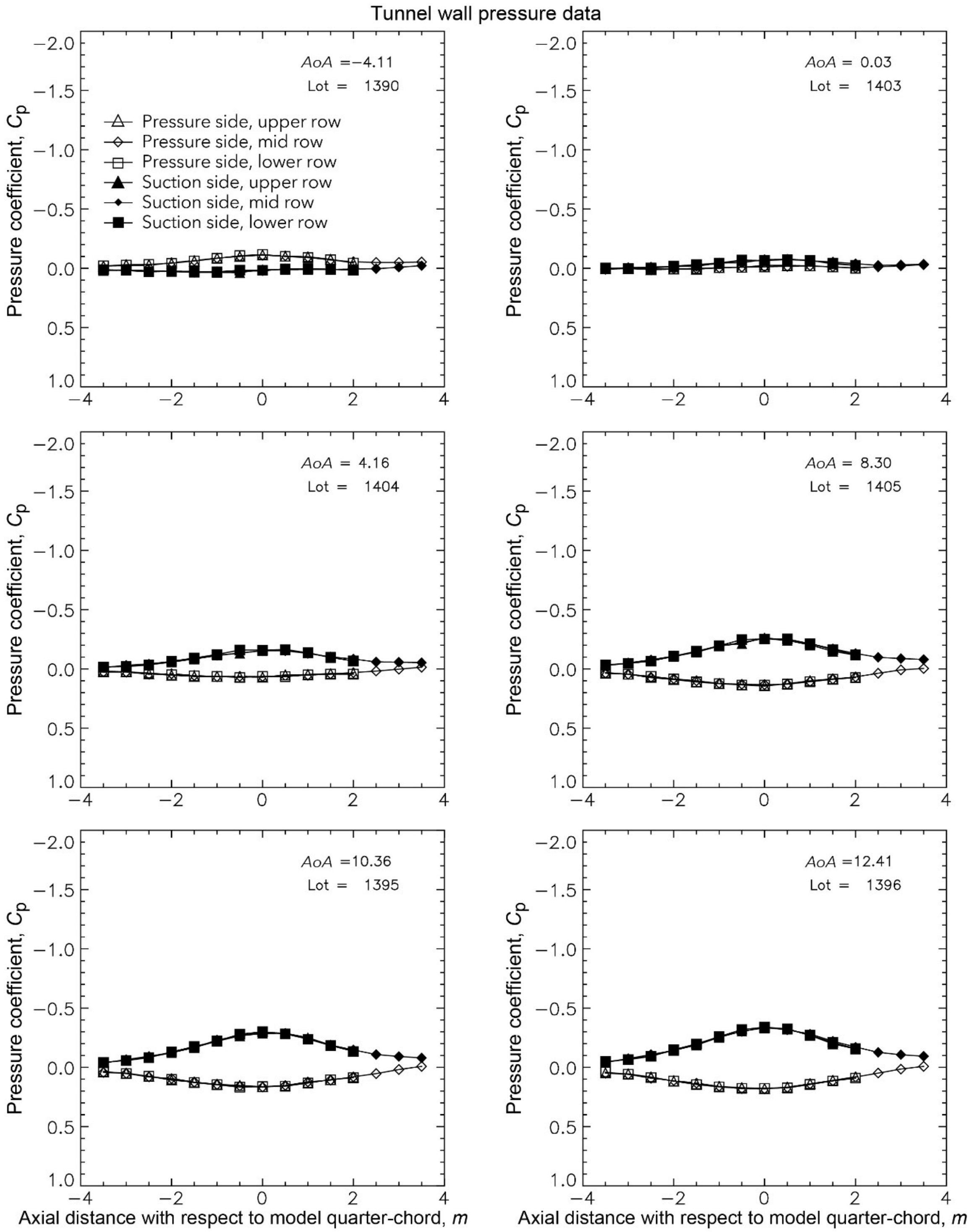

Roughness Ice 2—Lot EG1134: M = 0.10 and Re = 12.1–12.3×10^6

Appendix G.—F1 Full-Scale Model Tests

Roughness Ice 2—Lot EG1134: M = 0.10 and Re = 12.1–12.3×10^6

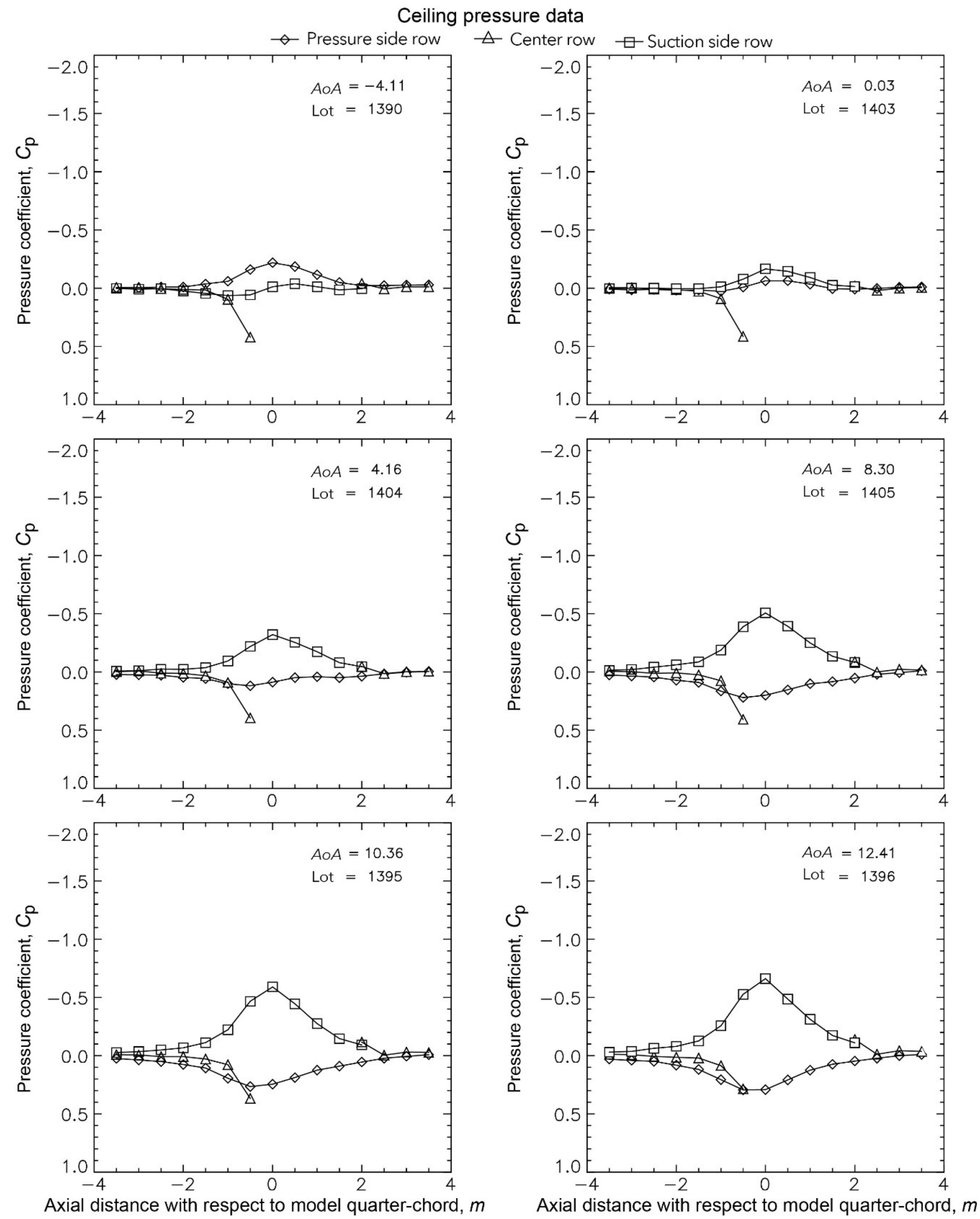

Roughness Ice 2—Lot EG1134: M = 0.10 and Re = 12.1–12.3×10^6

Appendix G.—F1 Full-Scale Model Tests

Roughness Ice 2—Lot EG1134: M = 0.10 and Re = 12.1–12.3×10^6

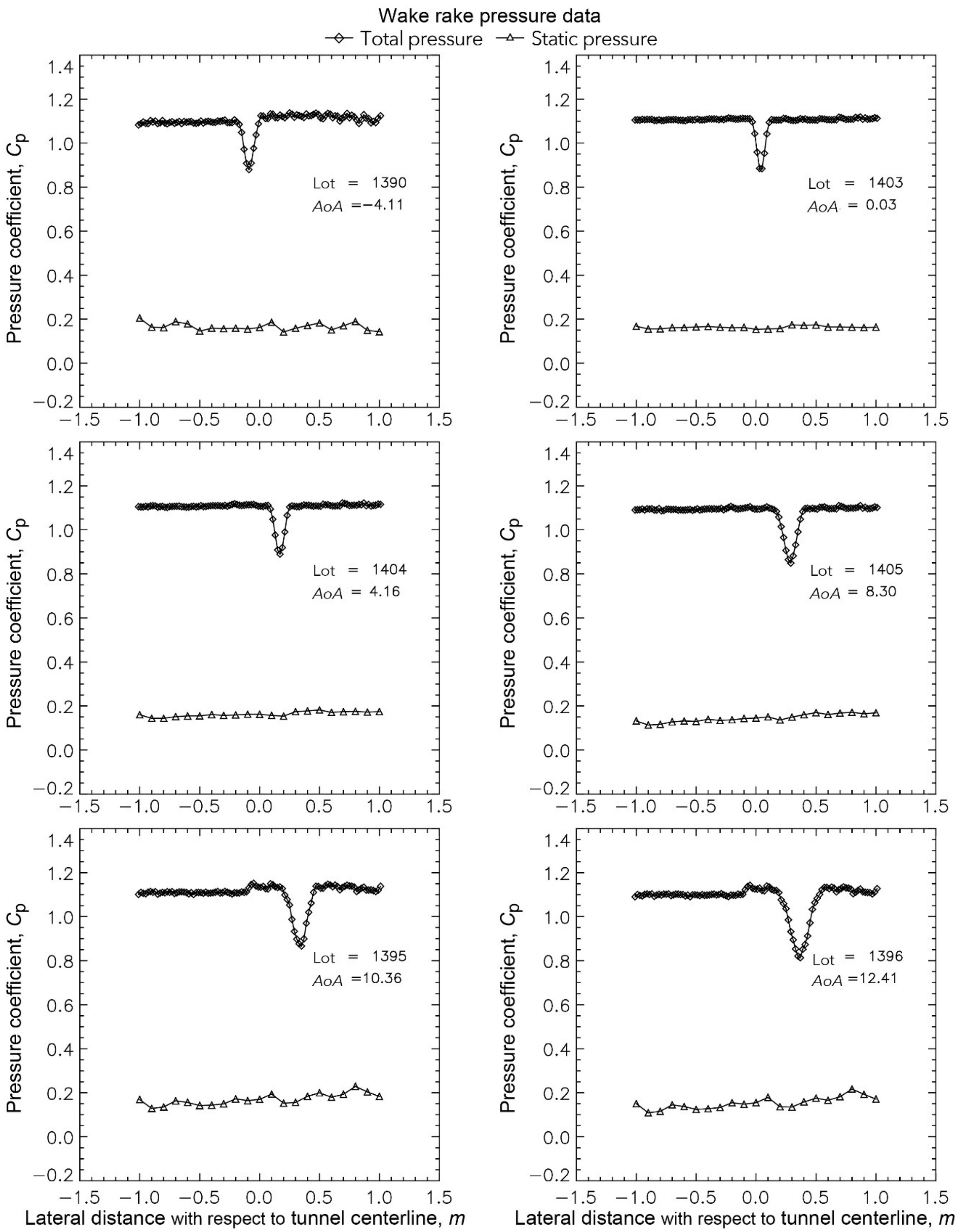

Roughness Ice 2—Lot EG1134: M = 0.10 and Re = 12.1–12.3×10^6

Appendix G.—F1 Full-Scale Model Tests

Roughness Ice 2—Lot EG1134: M = 0.20 to 0.21 and Re = 9.0×10^6

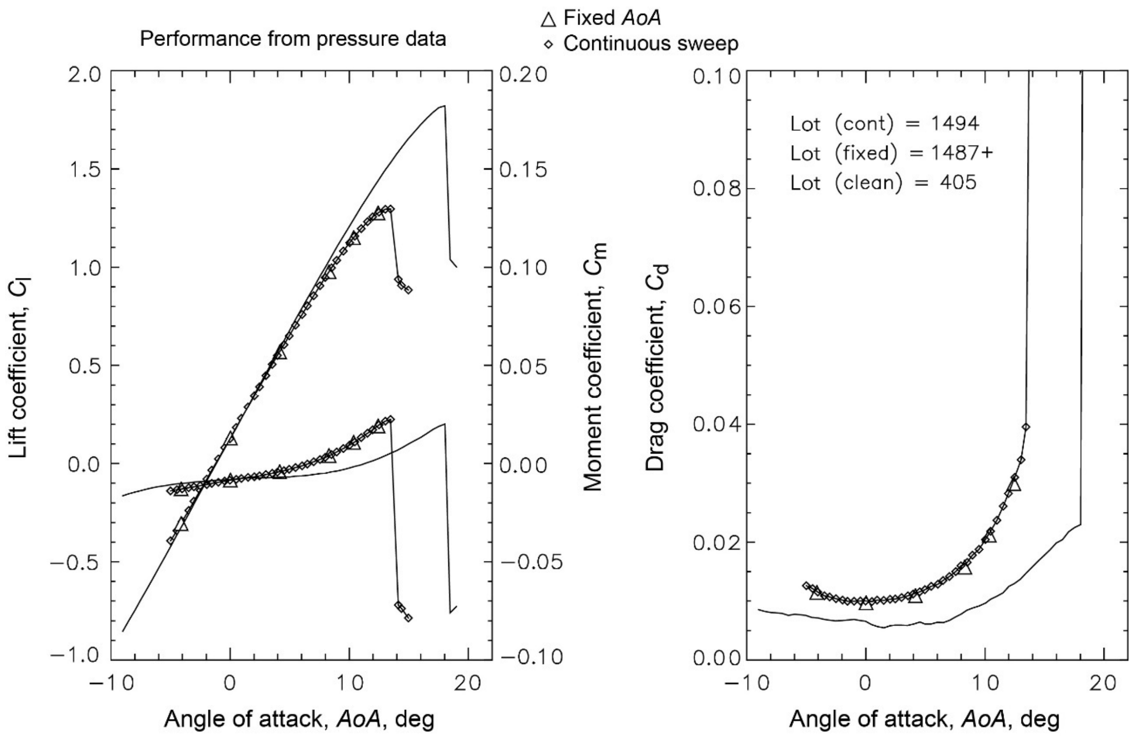

Roughness Ice 2—Lot EG1134: M = 0.20 to 0.21 and Re = 9.0×10^6

Appendix G.—F1 Full-Scale Model Tests

Roughness Ice 2—Lot EG1134: M = 0.20 to 0.21 and Re = 9.0×10[6]

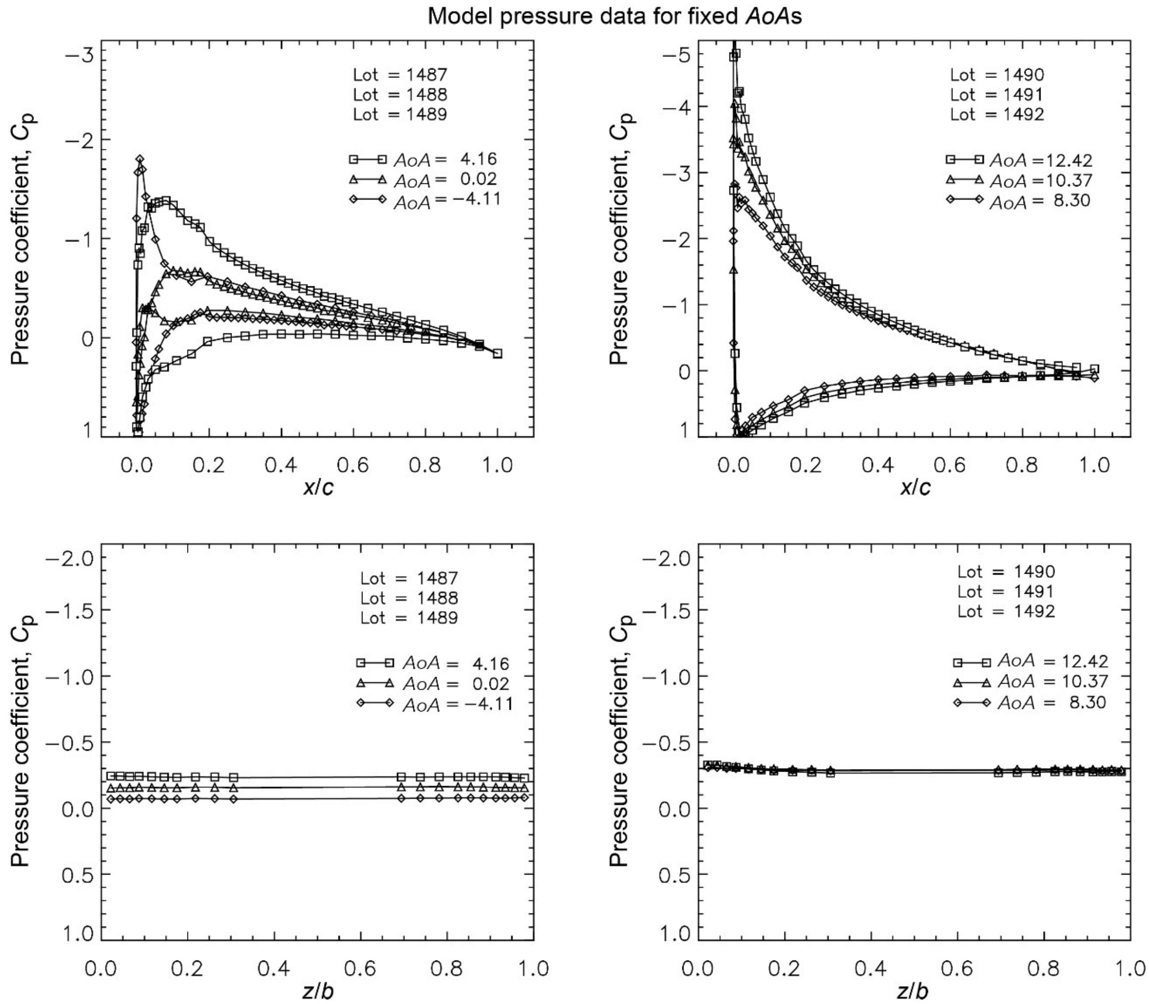

Roughness Ice 2—Lot EG1134: M = 0.20 to 0.21 and Re = 9.0×10[6]

Appendix G.—F1 Full-Scale Model Tests

Roughness Ice 2—Lot EG1134: M = 0.20 to 0.21 and Re = 9.0×10^6

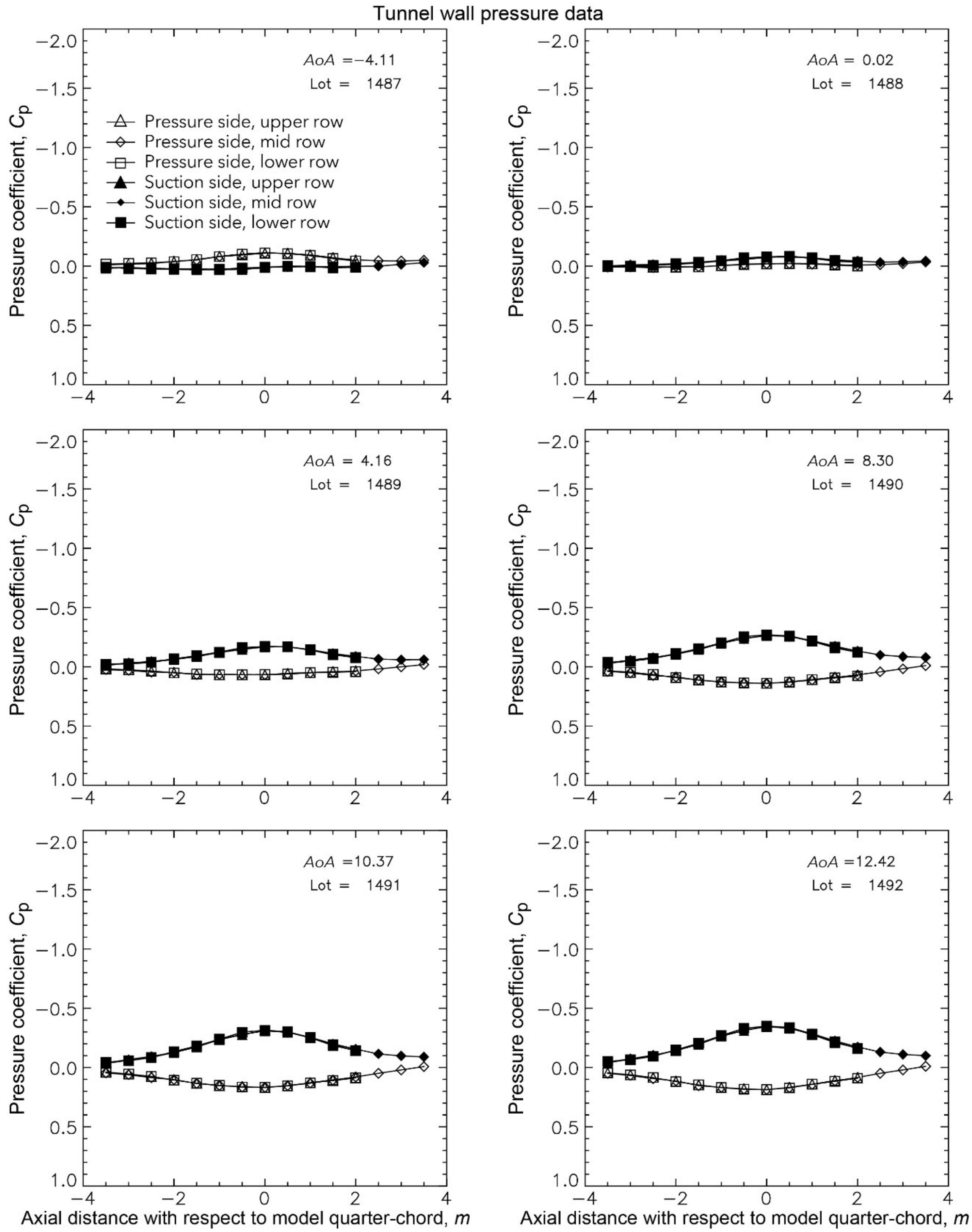

Roughness Ice 2—Lot EG1134: M = 0.20 to 0.21 and Re = 9.0×10^6

Appendix G.—F1 Full-Scale Model Tests

Roughness Ice 2—Lot EG1134: M = 0.20 to 0.21 and Re = 9.0×10^6

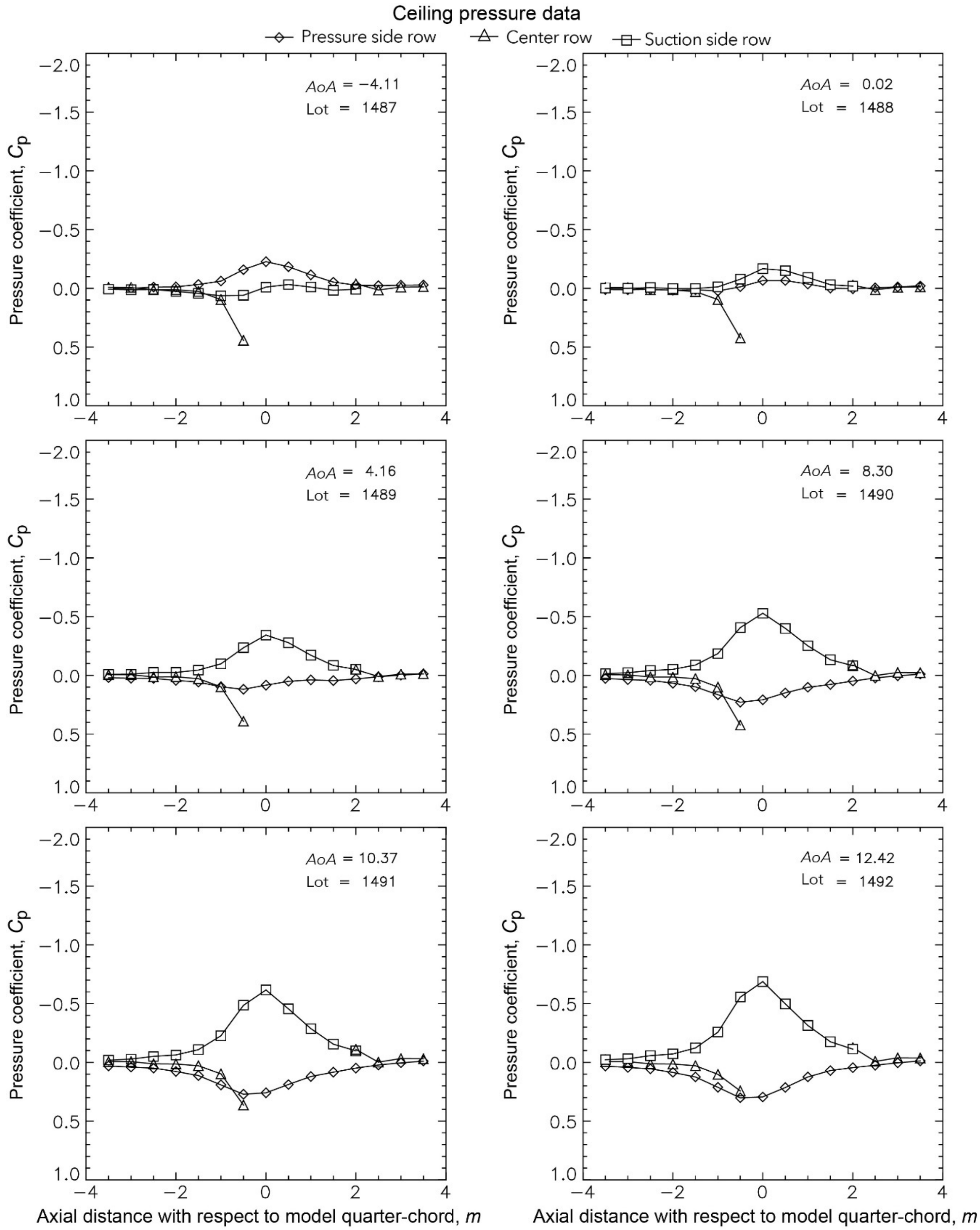

Roughness Ice 2—Lot EG1134: M = 0.20 to 0.21 and Re = 9.0×10^6

Appendix G.—F1 Full-Scale Model Tests

Roughness Ice 2—Lot EG1134: M = 0.20 to 0.21 and Re = 9.0×10⁶

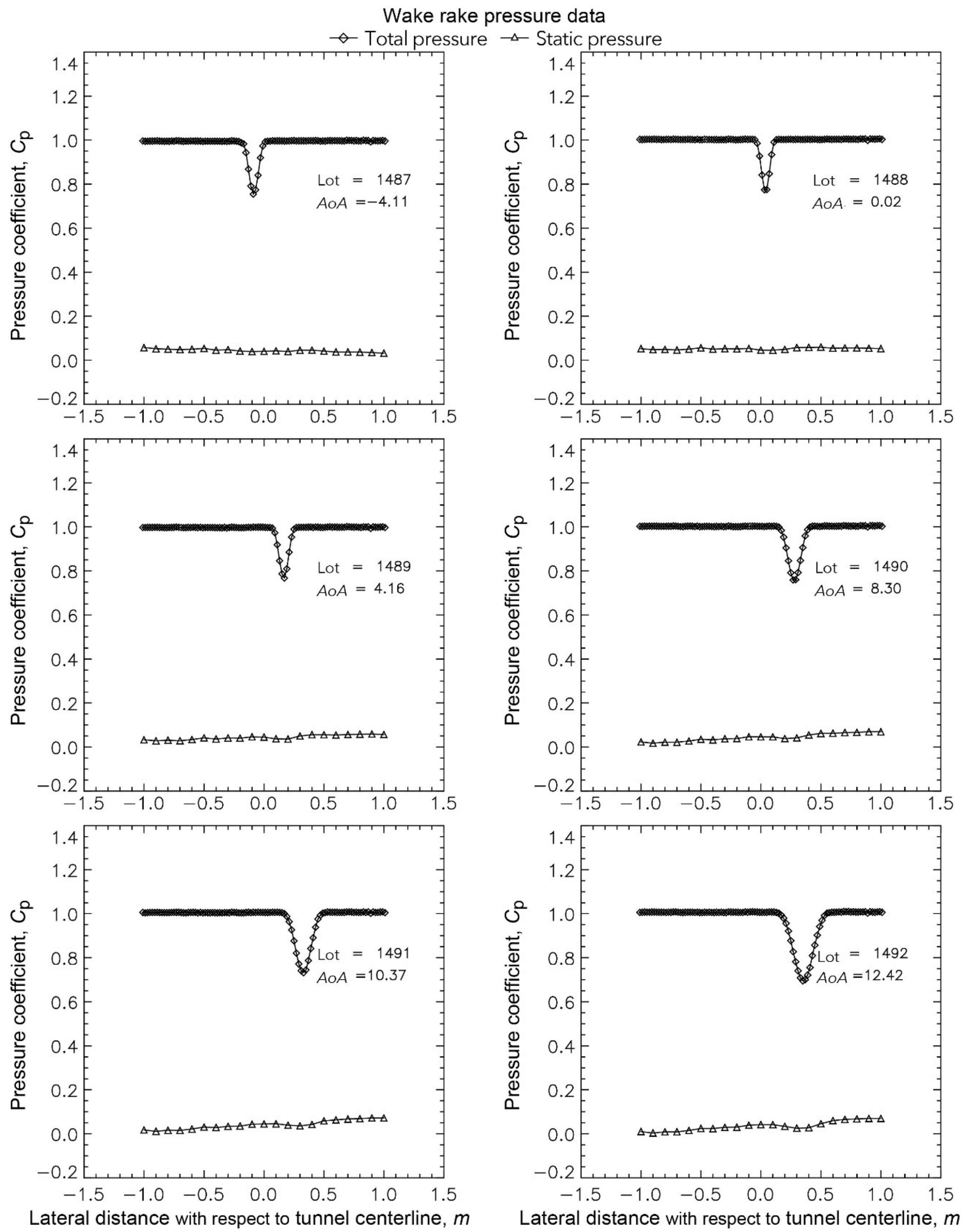

Roughness Ice 2—Lot EG1134: M = 0.20 to 0.21 and Re = 9.0×10^6

Appendix G.—F1 Full-Scale Model Tests

Roughness Ice 2—Lot EG1134: M = 0.20 to 0.21 and Re = 12.2–12.3×10[6]

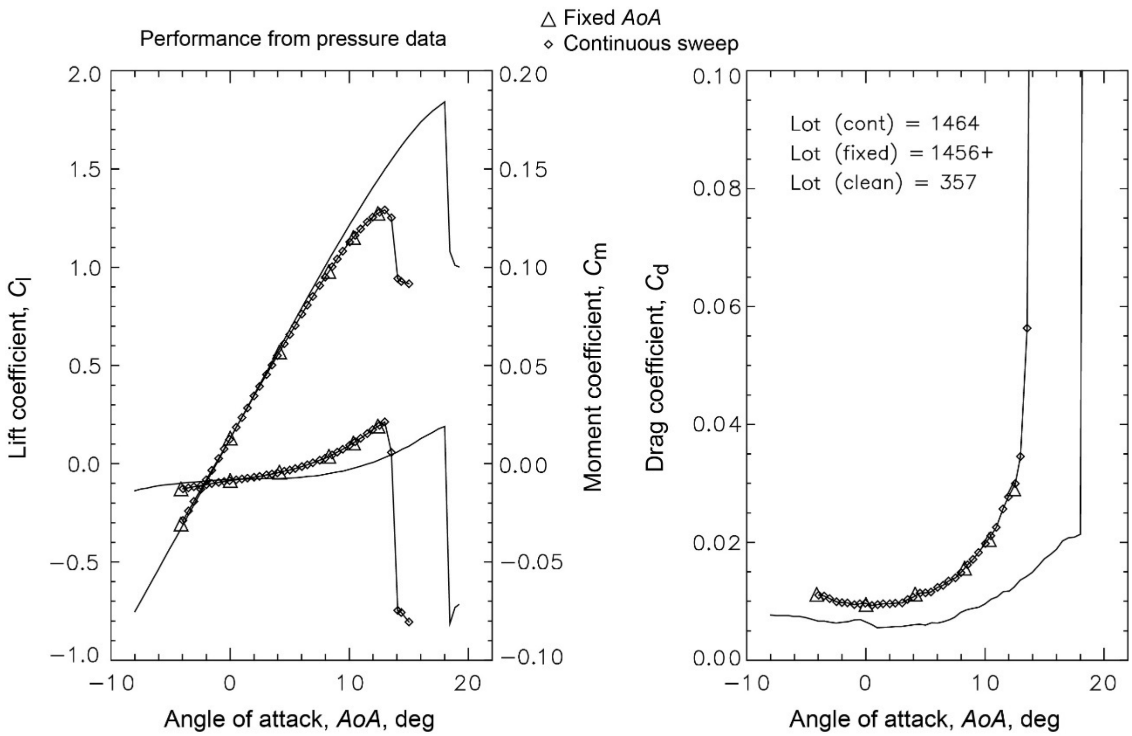

Roughness Ice 2—Lot EG1134: M = 0.20 to 0.21 and Re = 12.2–12.3×10[6]

Appendix G.—F1 Full-Scale Model Tests

Roughness Ice 2—Lot EG1134: M = 0.20 to 0.21 and Re = 12.2–12.3×10^6

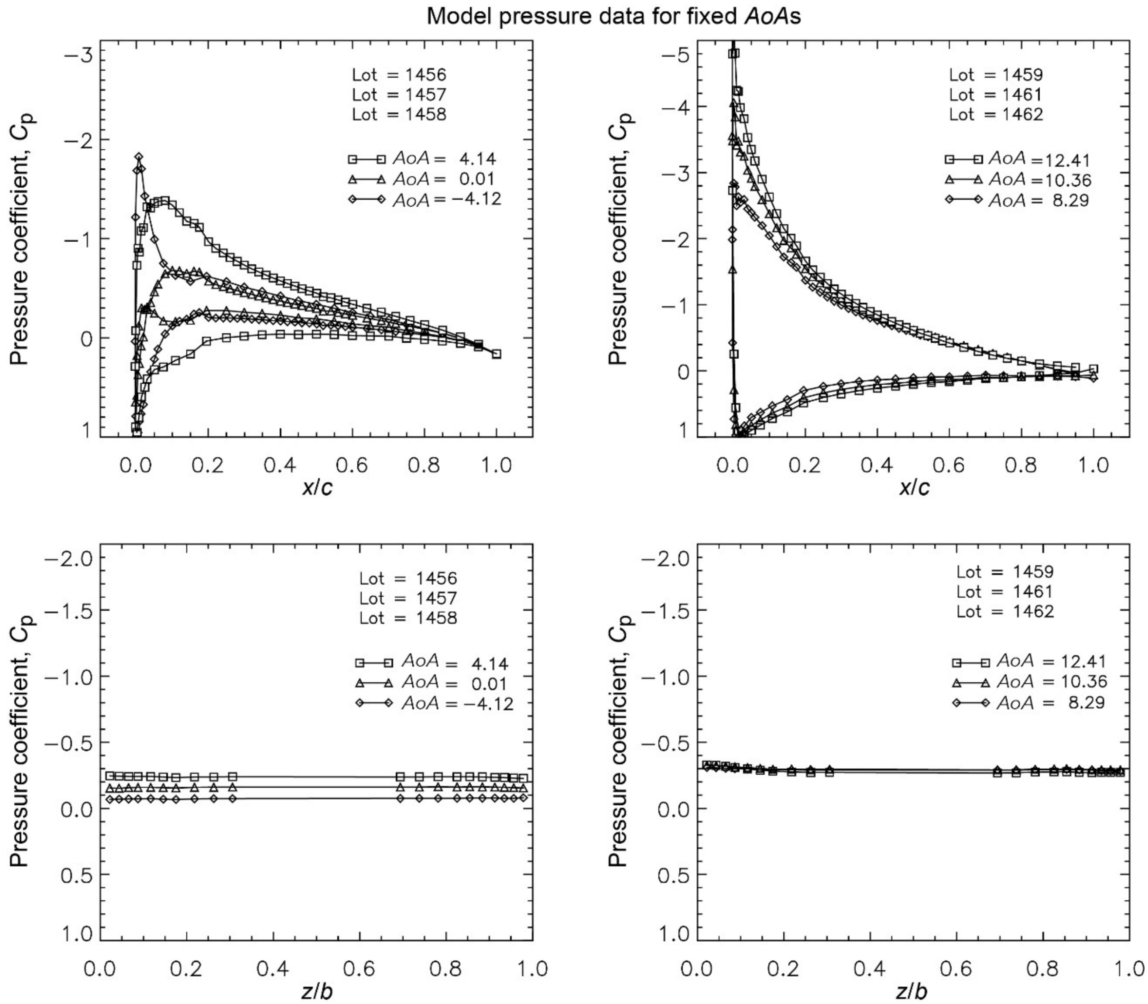

Roughness Ice 2—Lot EG1134: M = 0.20 to 0.21 and Re = 12.2–12.3×10^6

Appendix G.—F1 Full-Scale Model Tests

Roughness Ice 2—Lot EG1134: M = 0.20 to 0.21 and Re = 12.2–12.3×10^6

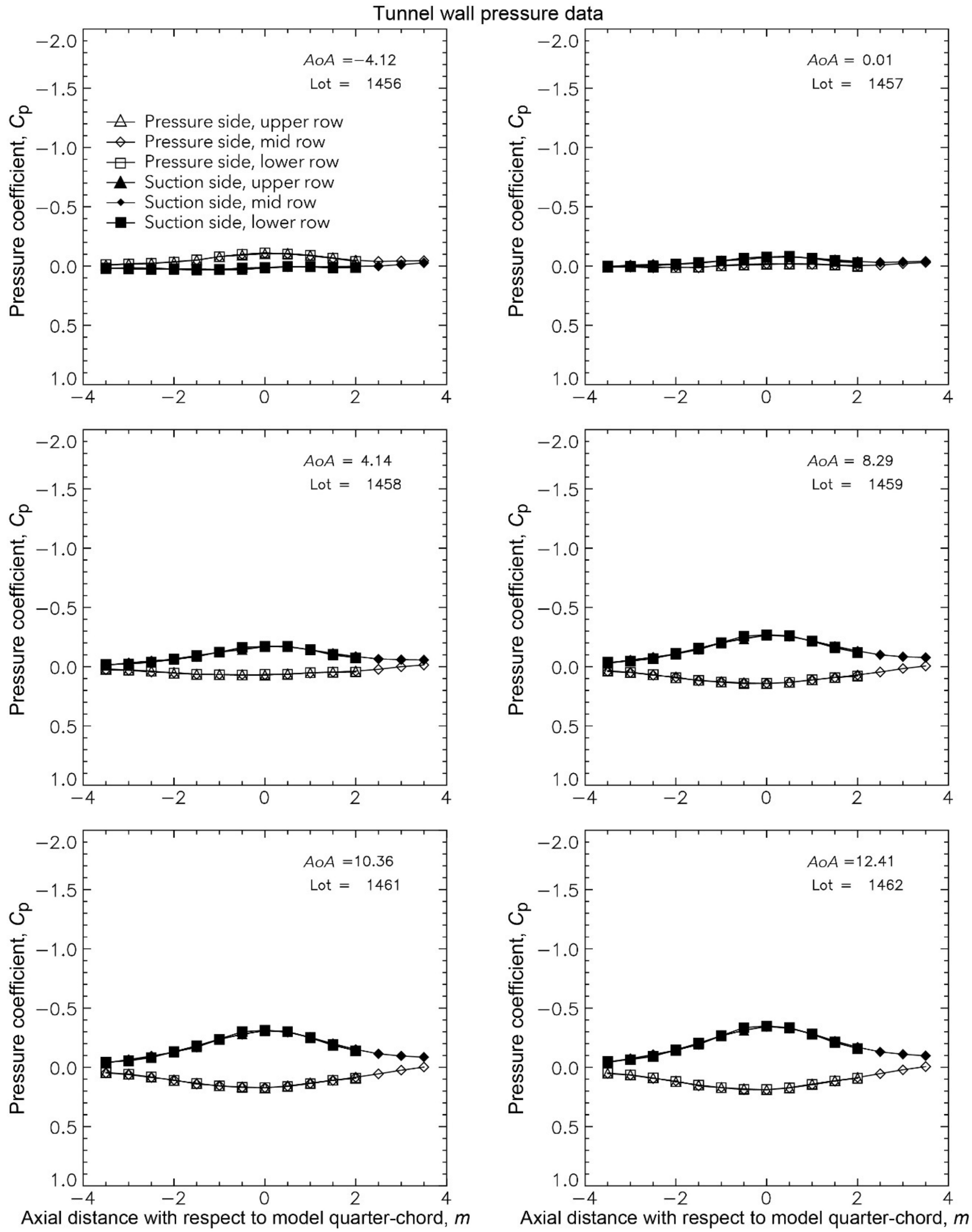

Roughness Ice 2—Lot EG1134: M = 0.20 to 0.21 and Re = 12.2–12.3×10^6

Appendix G.—F1 Full-Scale Model Tests

Roughness Ice 2—Lot EG1134: M = 0.20 to 0.21 and Re = 12.2–12.3×10^6

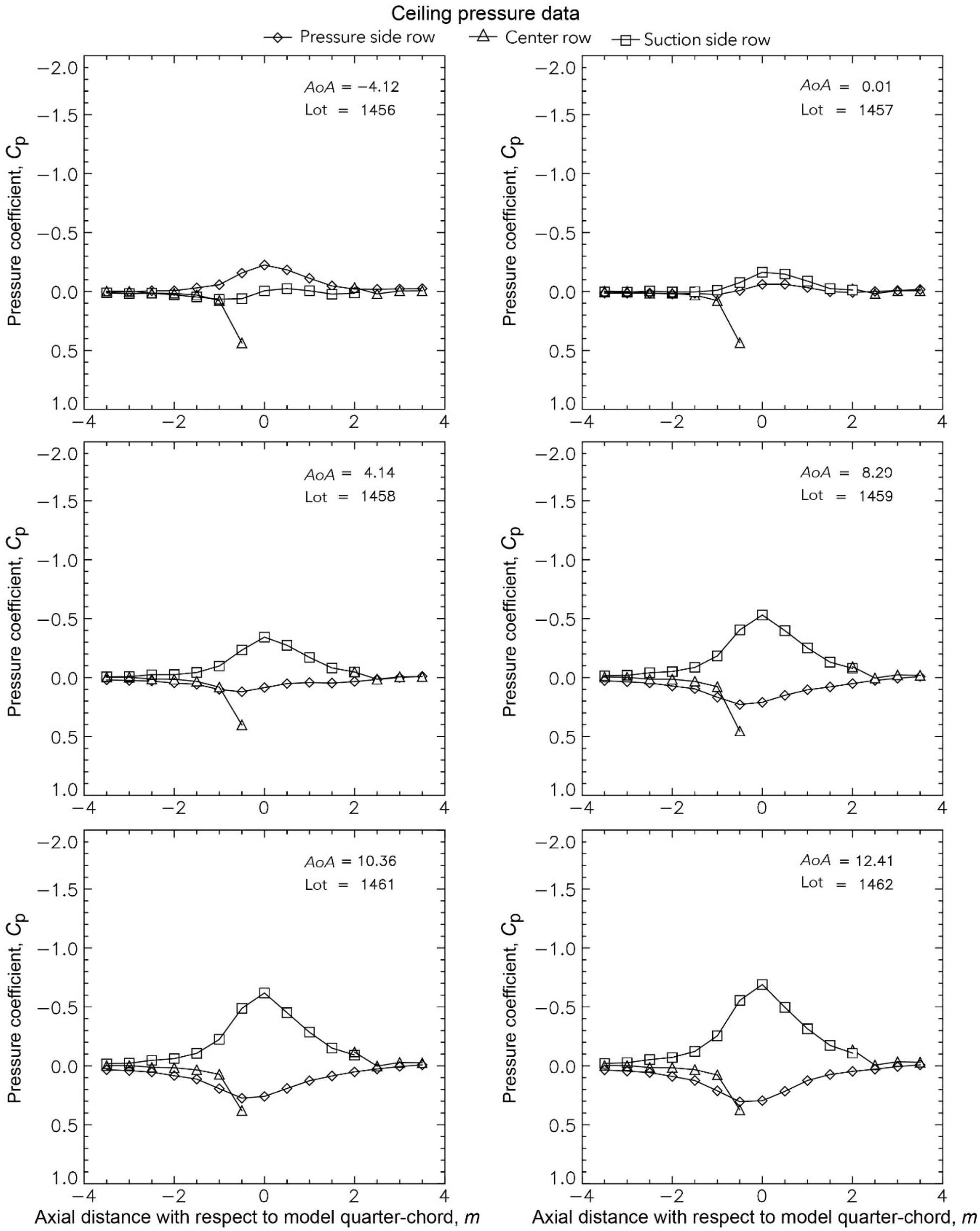

Roughness Ice 2—Lot EG1134: M = 0.20 to 0.21 and Re = 12.2–12.3×10^6

Appendix G.—F1 Full-Scale Model Tests

Roughness Ice 2—Lot EG1134: M = 0.20 to 0.21 and Re = 12.2–12.3×10^6

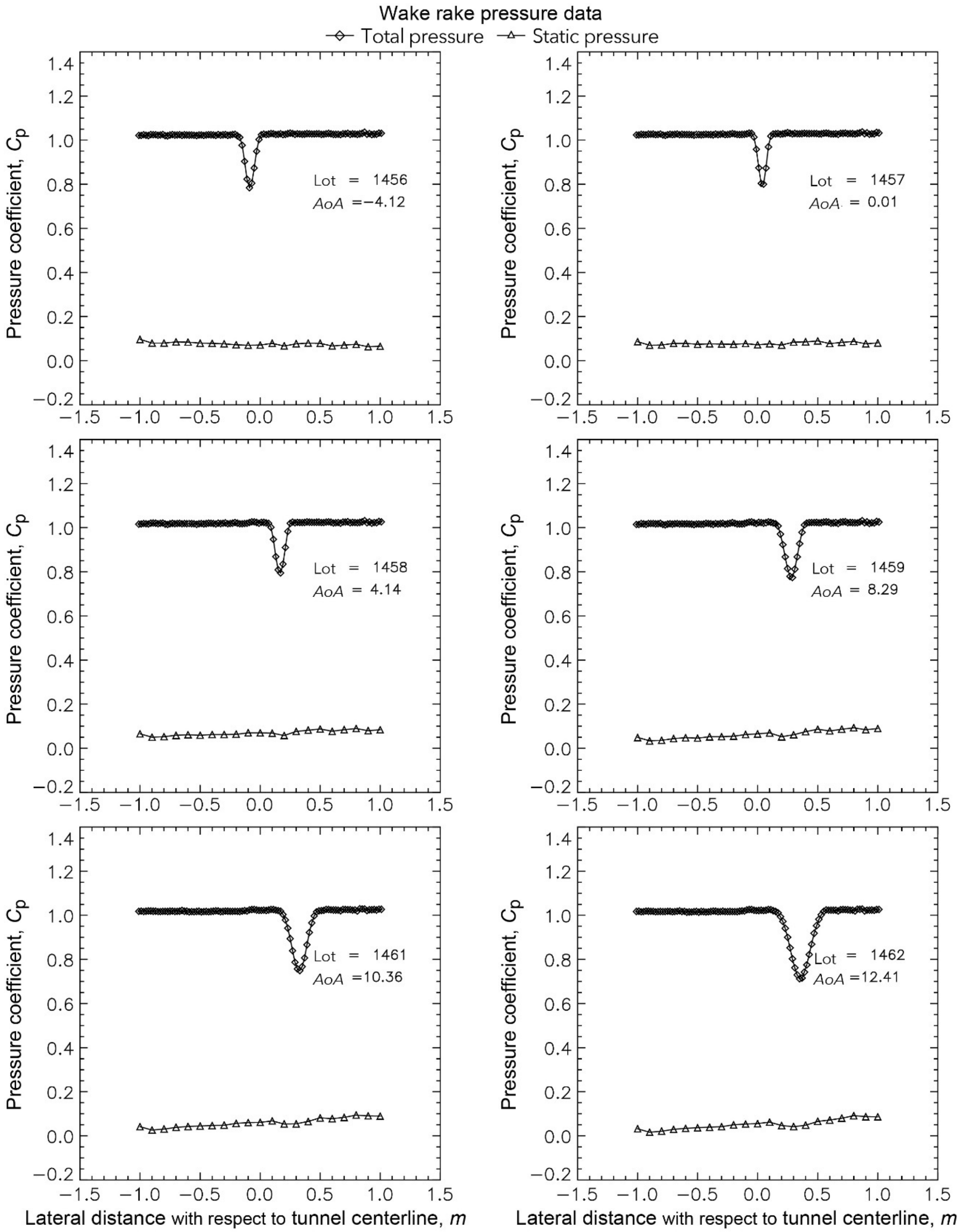

Roughness Ice 2—Lot EG1134: M = 0.20 to 0.21 and Re = 12.2–12.3×10^6

Appendix G.—F1 Full-Scale Model Tests

Roughness Ice 2—Lot EG1134: M = 0.20 to 0.21 and Re = 15.8–16.0×10^6

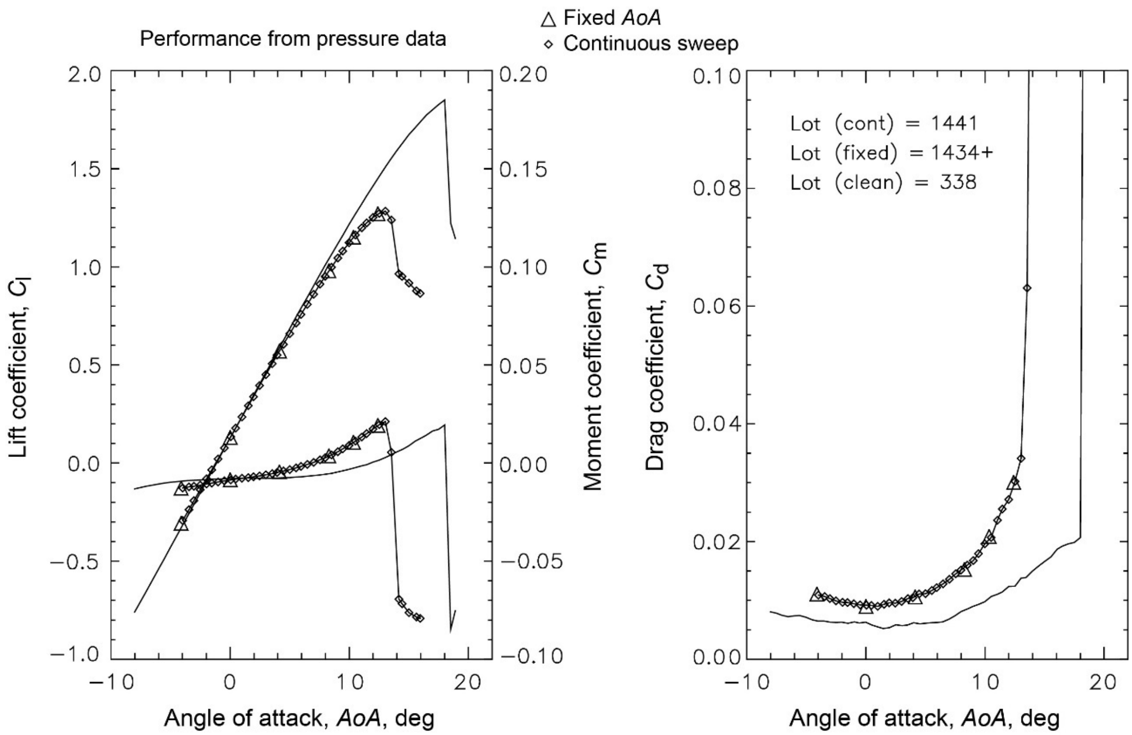

Roughness Ice 2—Lot EG1134: M = 0.20 to 0.21 and Re = 15.8–16.0×10^6

Appendix G.—F1 Full-Scale Model Tests

Roughness Ice 2—Lot EG1134: M = 0.20 to 0.21 and Re = 15.8–16.0×10[6]

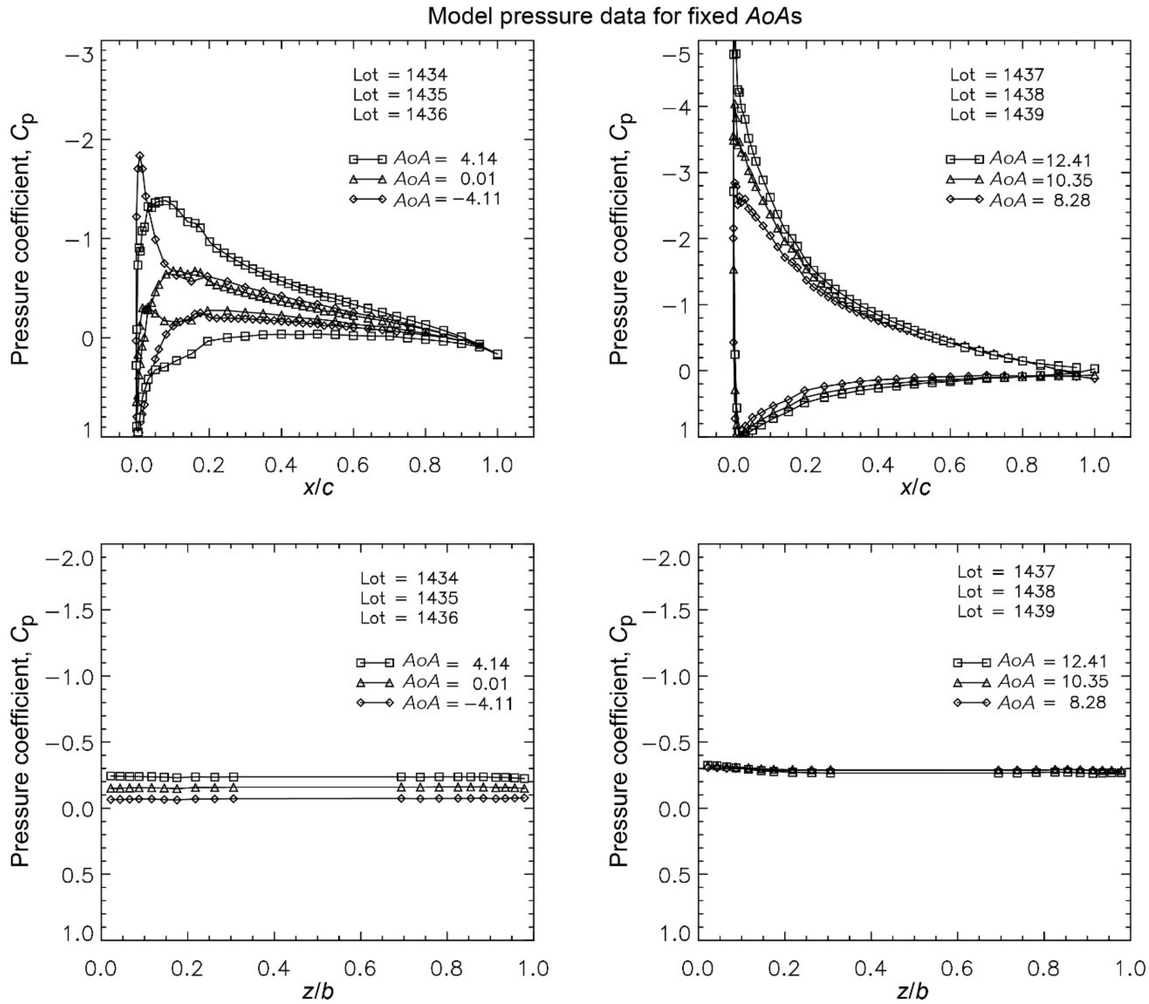

Roughness Ice 2—Lot EG1134: M = 0.20 to 0.21 and Re = 15.8–16.0×10[6]

Appendix G.—F1 Full-Scale Model Tests

Roughness Ice 2—Lot EG1134: M = 0.20 to 0.21 and Re = 15.8–16.0×10[6]

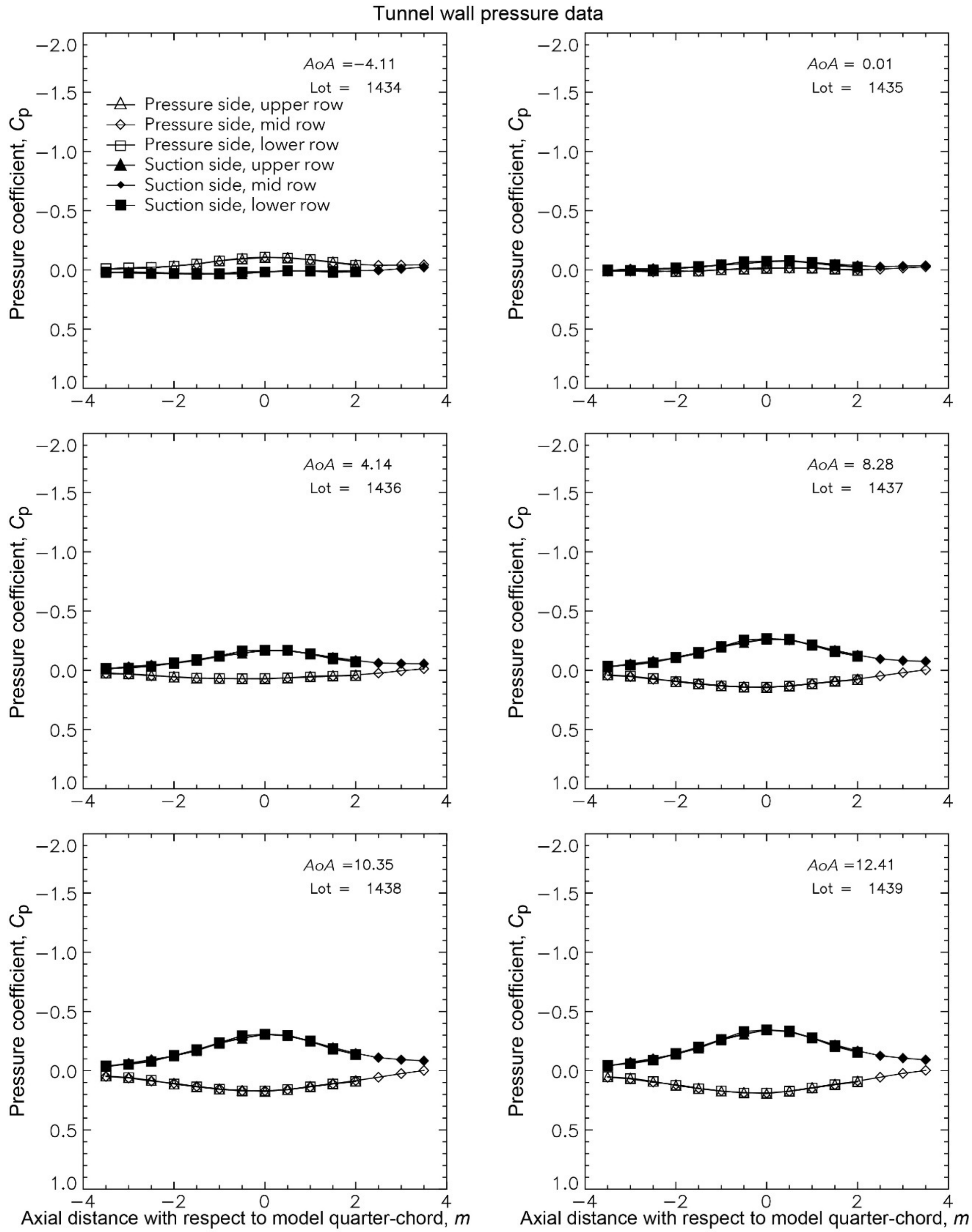

Roughness Ice 2—Lot EG1134: M = 0.20 to 0.21 and Re = 15.8–16.0×10[6]

Roughness Ice 2—Lot EG1134: M = 0.20 to 0.21 and Re = 15.8–16.0×10^6

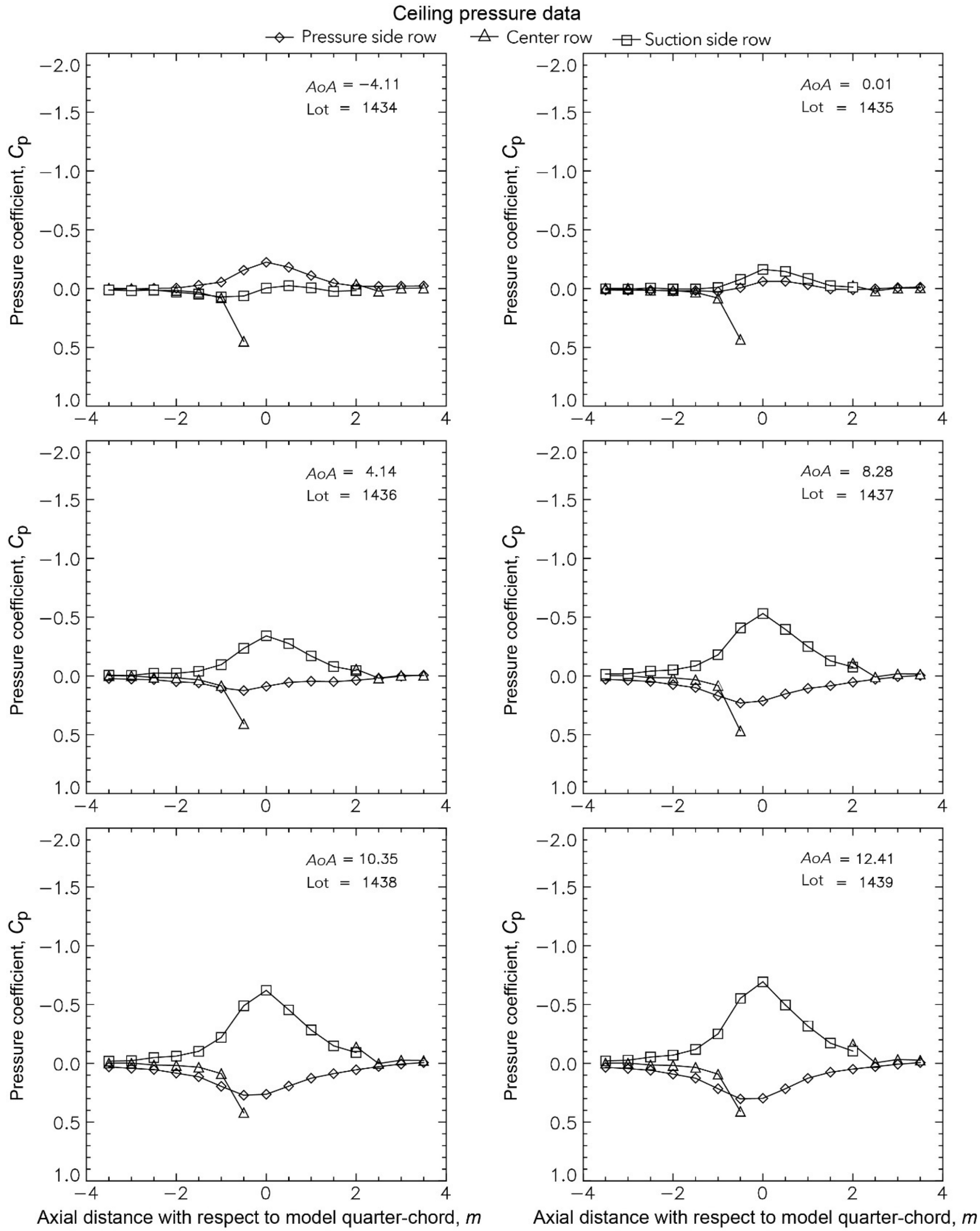

Roughness Ice 2—Lot EG1134: M = 0.20 to 0.21 and Re = 15.8–16.0×10^6

Appendix G.—F1 Full-Scale Model Tests

Roughness Ice 2—Lot EG1134: M = 0.20 to 0.21 and Re = 15.8–16.0×10^6

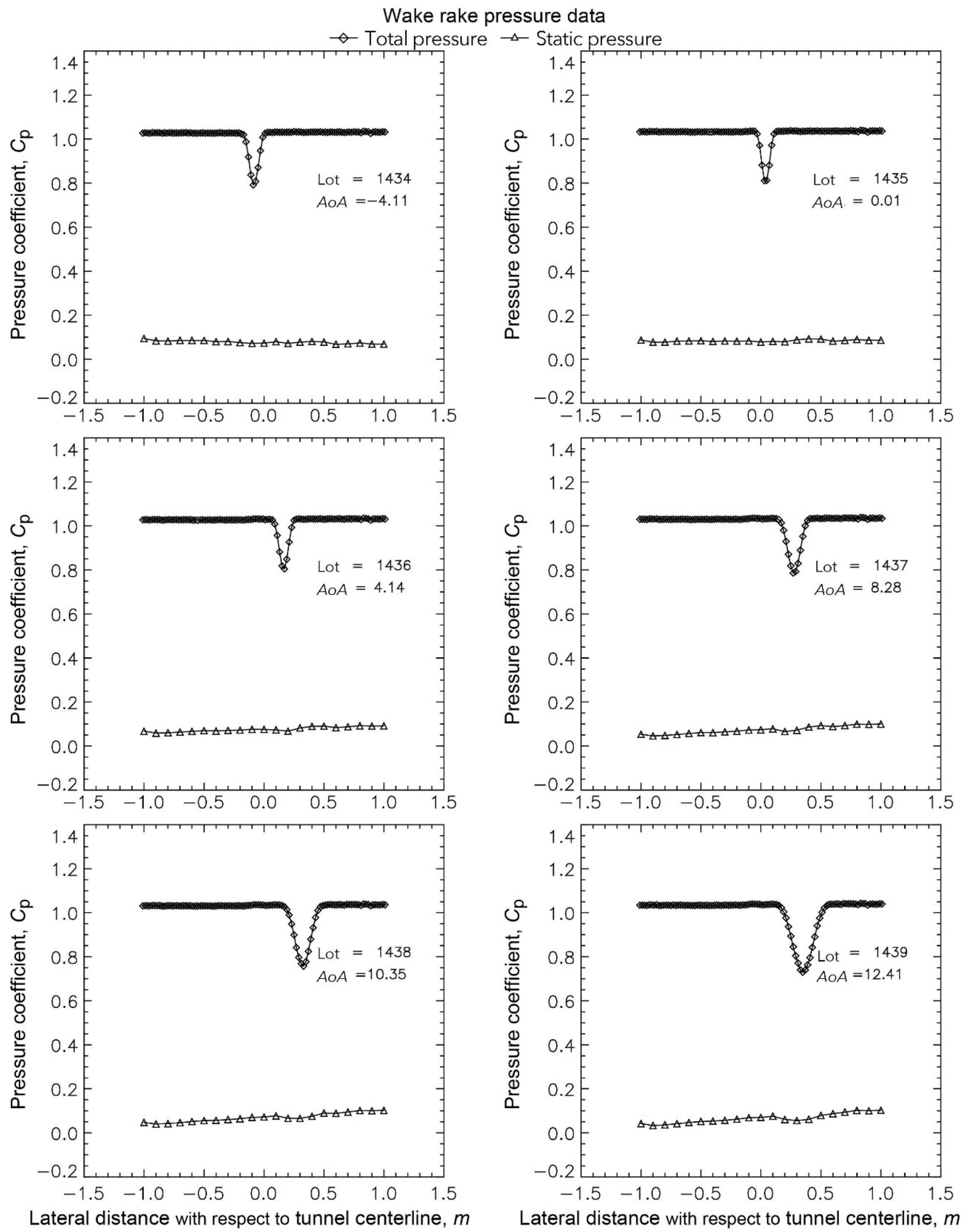

Roughness Ice 2—Lot EG1134: M = 0.20 to 0.21 and Re = 15.8–16.0×10^6

Roughness Ice 2—Lot EG1134: M = 0.29 and Re = 12.1–12.2×10[6]

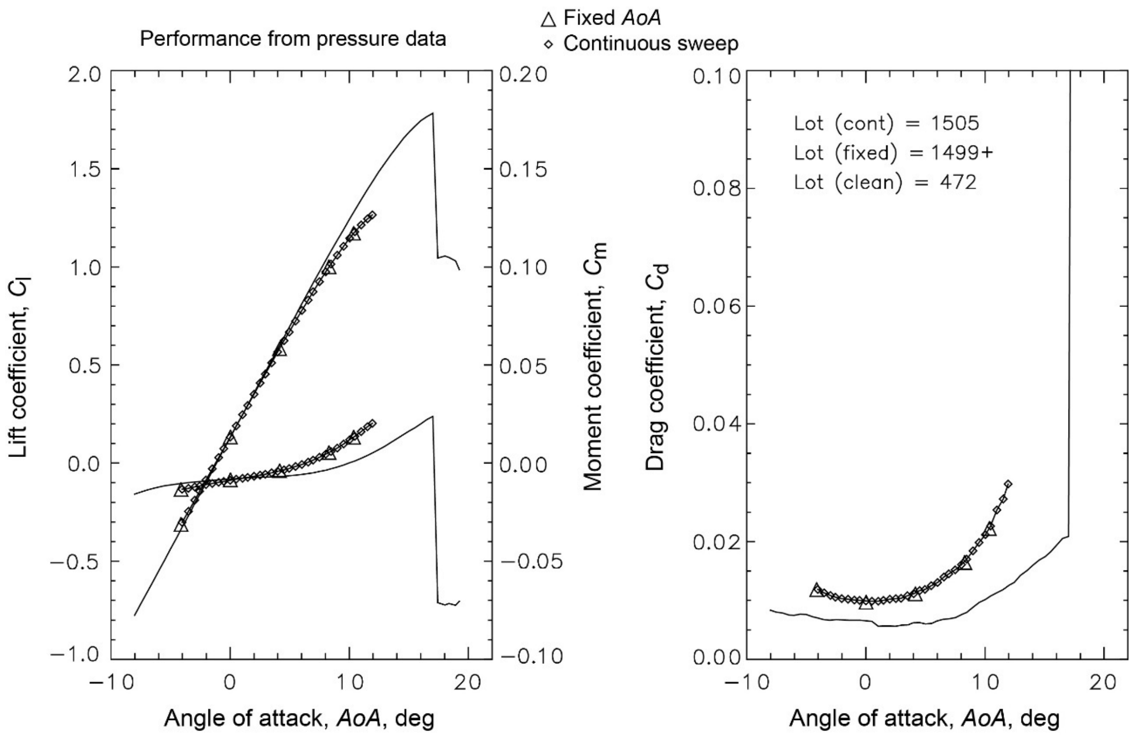

Roughness Ice 2—Lot EG1134: M = 0.29 and Re = 12.1–12.2×10[6]

Appendix G.—F1 Full-Scale Model Tests

Roughness Ice 2—Lot EG1134: M = 0.29 and Re = 12.1–12.2×10^6

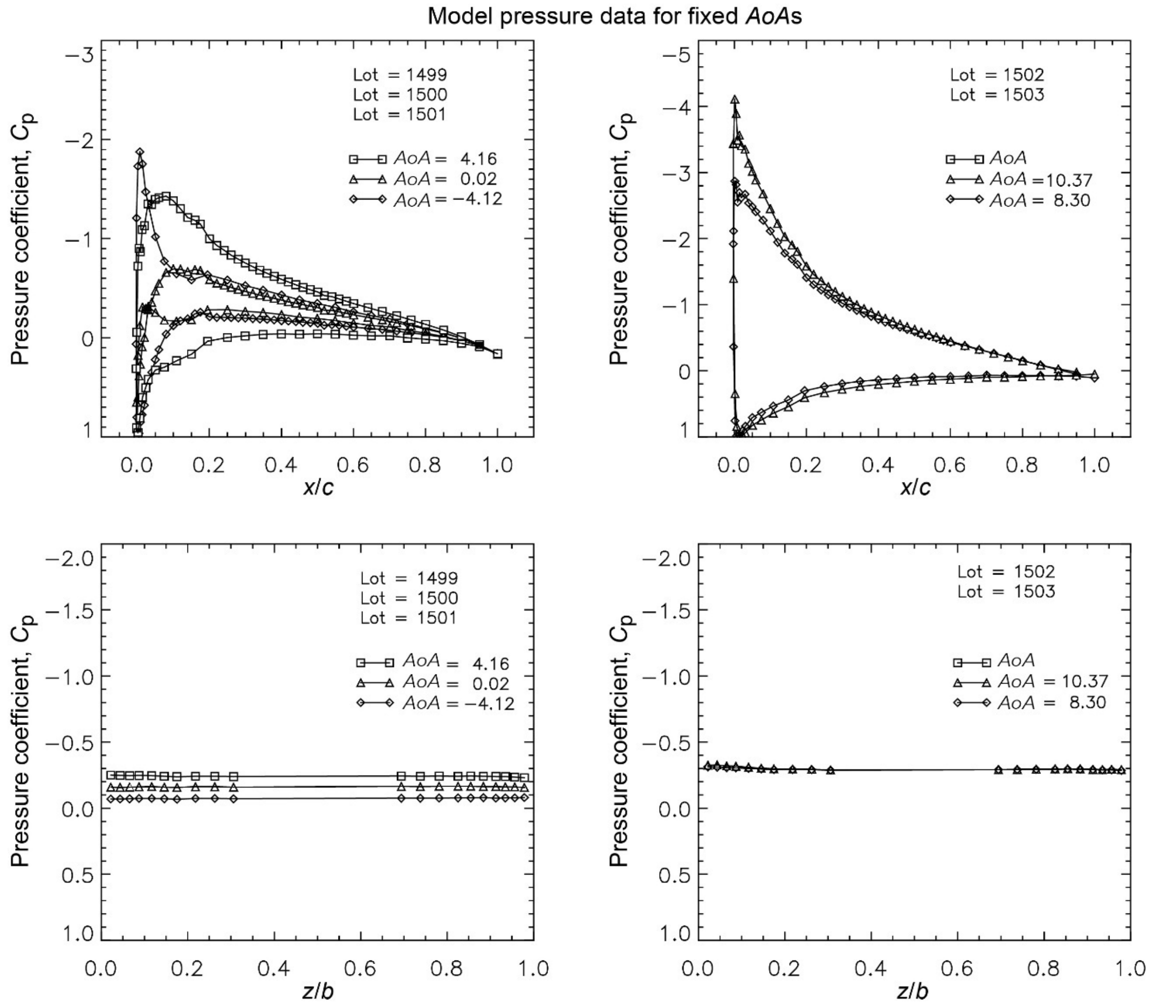

Roughness Ice 2—Lot EG1134: M = 0.29 and Re = 12.1–12.2×10^6

Appendix G.—F1 Full-Scale Model Tests

Roughness Ice 2—Lot EG1134: M = 0.29 and Re = 12.1–12.2×10^6

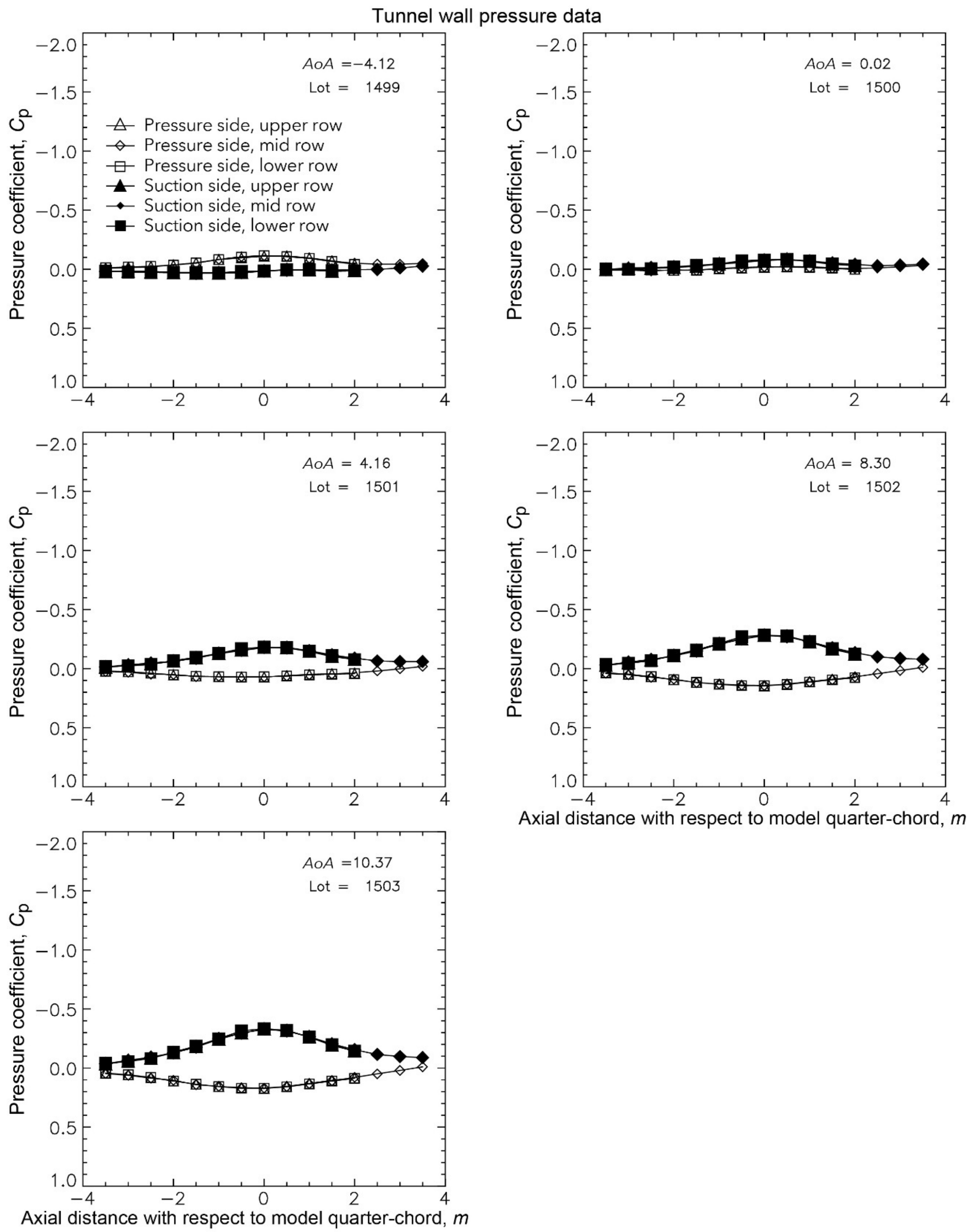

Roughness Ice 2—Lot EG1134: M = 0.29 and Re = 12.1–12.2×10^6

Roughness Ice 2—Lot EG1134: M = 0.29 and Re = 12.1–12.2×10[6]

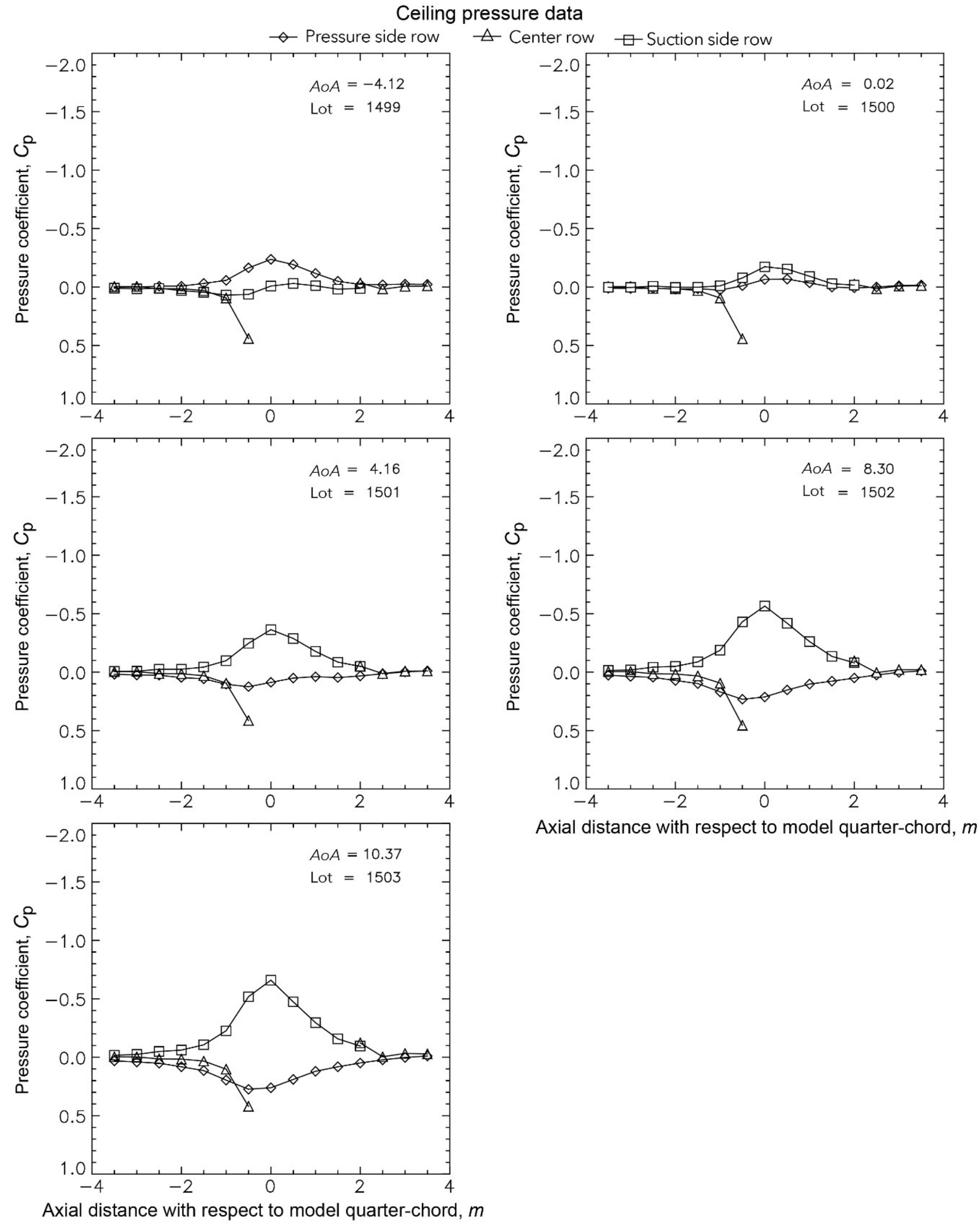

Roughness Ice 2—Lot EG1134: M = 0.29 and Re = 12.1–12.2×10[6]

Appendix G.—F1 Full-Scale Model Tests

Roughness Ice 2—Lot EG1134: M = 0.29 and Re = 12.1–12.2×10^6

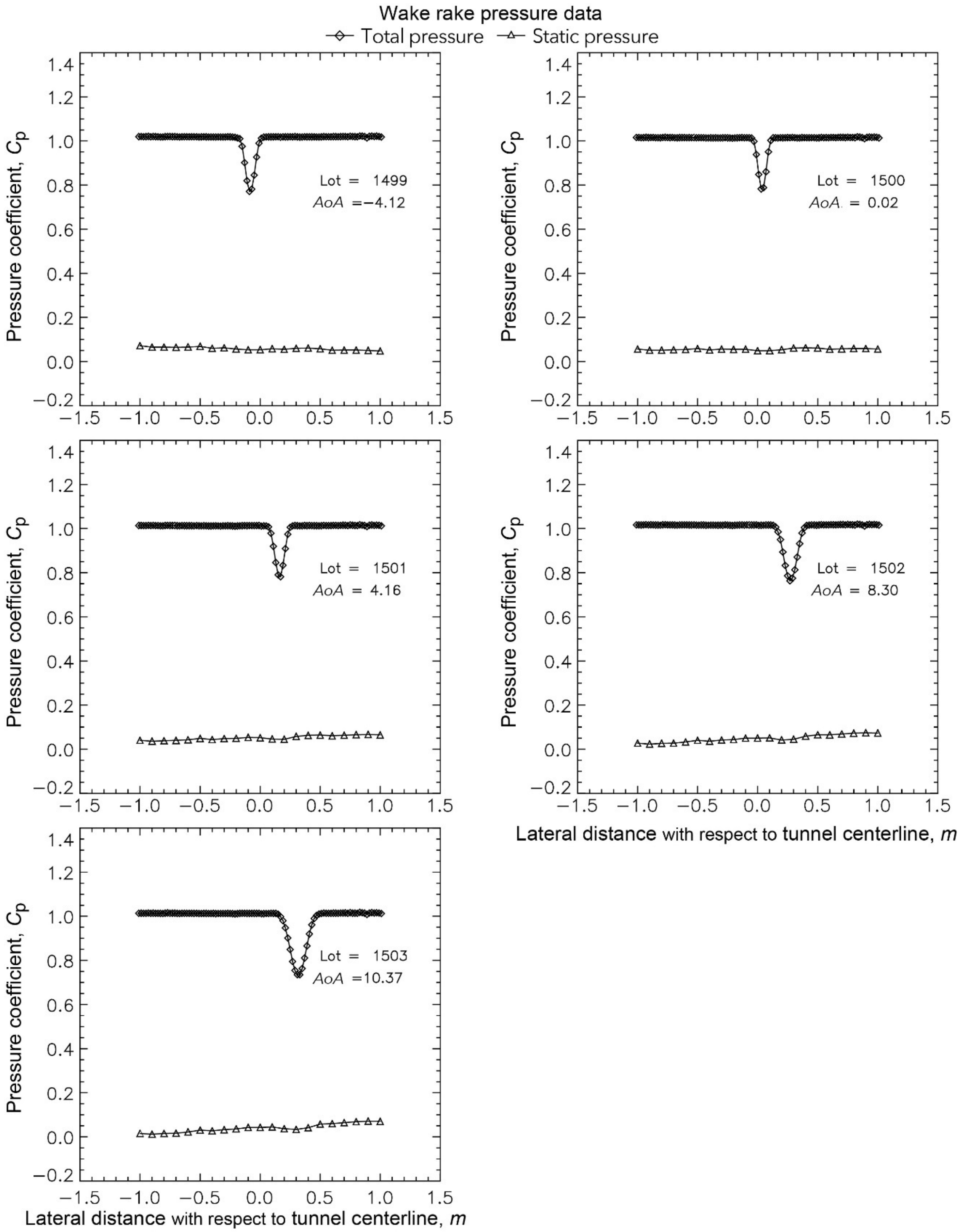

Roughness Ice 2—Lot EG1134: M = 0.29 and Re = 12.1–12.2×10^6

References

1. Bragg, M.B.; Broeren, A.P.; and Blumenthal, L.A.: Iced-Airfoil Aerodynamics. Prog. Aerosp. Sci., vol. 41, 2005, pp. 323–418.
2. Blumenthal, Leia A., et al.: Issues in Ice Accretion Aerodynamic Simulation on a Subscale Model. AIAA 2006–262, 2006.
3. Busch, Greg T.: Ice Accretion Aerodynamic Simulation on a Subscale Model. M.S. Thesis, Univ. of Illinois, 2006.
4. Busch, Greg; Broeren, Andy; and Bragg, Michael: Aerodynamic Simulation of a Horn-Ice Accretion on a Subscale Model. AIAA 2007–87, 2007.
5. Broeren, A.P.; Busch, G.T.; and Bragg, M.B.: Aerodynamic Fidelity of Ice Accretion Simulation on a Subscale Model. SAE Paper 2007–01–3285, 2007.
6. Busch, Greg T.; Broeren, Andy P.; and Bragg, Michael B.: Aerodynamic Simulation of a Horn-Ice Accretion on a Subscale Model. J. Aircraft, vol. 45, no. 2, 2008, pp. 604–613.
7. Busch, Greg; Broeren, Andy; and Bragg, Michael: Aerodynamic Fidelity of Sub-scale Two-Dimensional Ice Accretion Simulations. AIAA 2008–7062, 2008.
8. 1. Broeren, Andy P., et al.: Effect of High-Fidelity Ice-Accretion Simulations on Full-Scale Airfoil Performance. J. Aircraft, vol. 47, no. 1, 2010, pp. 240–254.
9. Soeder, Ronald H., et al.: NASA Glenn Icing Research Tunnel User Manual. NASA/TM—2003-212004, 2003. Available from the NASA Center for AeroSpace Information. http://ntrs.nasa.gov
10. Irvine, Thomas B., et al.: Overview of the Icing and Flow Quality Improvements Program for the NASA Glenn Icing Research Tunnel. AIAA–2001–0229, 2001.
11. Aircraft Inflight Icing Terminology. SAE Aerospace Recommended Practices, SAE ARP5624, 2013, p. 21.
12. Ide, Robert F.; and Oldenburg, John R.: Icing Cloud Calibration of the NASA Glenn Icing Research Tunnel. AIAA–2001–0234, 2001.
13. Gonsalez, Jose C.; Arrington, E. Allen; and Curry III, Monroe R.: Flow Quality Surveys of the NASA Glenn Icing Research Tunnel (2000 Tests). AIAA–2001–0232, 2001.
14. Desplas, P.: F1 Pressurized Subsonic Wind Tunnel User's Guide. ONERA, Mauzac, France, 1998.
15. Desplas, Ph., et al.: Test of the A400 Motorized Model in the ONERA Modernized F1 Wind Tunnel. AIAA 2006–3645, 2006.
16. Reehorst, Andrew L.; and Richter, G. Paul: New Methods and Materials for Molding and Casting Ice Formations. NASA TM–100126, 1987. http://ntrs.nasa.gov
17. CassouDeSalle, D.; and Gilliot, A.: SUNSET (Studies on Scaling Effects Due to Ice) Tests at High Reynolds Number in F1 Wind Tunnel. ONERA Report No. PV 4: 12361, 2008.
18. Barlow, Jewel B.; Rae, William H.; and Pope, Alan: Low-Speed Wind Tunnel Testing. Third ed., Wiley-Interscience, New York, NY, 1999.
19. Allen, H. Julian; and Vincenti, Walter G.: Wall Interference in a Two-Dimensional-Flow Wind Tunnel, With Consideration of the Effect of Compressibility. NACA Report 782, 1944.
20. Moens, F.: SUNSET Project: Numerical Investigations for the Preparation of the F1 Test Campaign. ONERA Report No. RT 1: 12405, 2007.